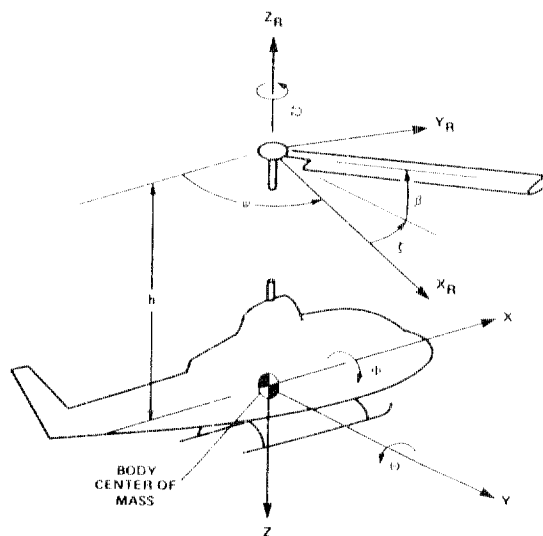


# NASA/Army Rotorcraft Technology

## *Volume I—Aerodynamics, and Dynamics and Aeroelasticity*



*Proceedings of a conference held at  
Ames Research Center  
Moffett Field, California  
March 17-19, 1987*



*NASA Conference Publication 2495*

# **NASA/Army Rotorcraft Technology**

## *Volume I—Aerodynamics, and Dynamics and Aeroelasticity*

Proceedings of a conference sponsored by  
the Department of the Army and the National  
Aeronautics and Space Administration and held at  
Ames Research Center  
Moffett Field, California  
March 17–19, 1987



National Aeronautics  
and Space Administration

Scientific and Technical  
Information Division

1988



## CONTENTS

### Volume I

Introduction.....	1
-------------------	---

#### Aerodynamics

Summary.....	5
--------------	---

Accomplishments at NASA Langley Research Center in Rotorcraft Aerodynamics Technology.....	7
John C. Wilson	

The Developmeny of CFD Methods for Rotor Applications.....	34
F.X. Caradonna and W.J. McCroskey	

#### Dynamics and Aeroelasticity

Summary.....	69
--------------	----

A Summary of Recent NASA/Army Contributions to Rotorcraft Vibrations and Structural Dynamics Technology.....	71
Raymond G. Kvaternik, Felton D. Bartlett, Jr. and John H. Cline	

A Review of Research in Rotor Loads.....	180
William G. Bousman and Wayne R. Mantay	

Comprehensive Rotorcraft Analysis Methods.....	312
Wendell B. Stephens and Edward E. Austin	

Rotorcraft Aeroelastic Stability.....	353
Robert A. Ormiston, William G. Warmbrodt, Dewey H. Hodges, and David A. Peters	

### Volume II

#### Materials and Structures

Summary.....	533
--------------	-----

Review of Fatigue and Fracture Research at NASA Langley Research Center.....	535
R.A. Everett, Jr.	

Delamination Durability of Composite Materials for Rotorcraft....	573
T. Kevin O'Brien	

Helicopter Crashworthiness Research Program.....	606
Gary L. Farley, Richard L. Boitnott, and Huey D. Carden	

## Contents (continued)

### Materials and Structures (continued)

Advanced Composite Airframe Program - Today's Technology.....	656
Danny E. Good and L. Thomas Mazza	

### Propulsion and Drive Systems

Summary.....	681
Technology Developments for a Compound Cycle Engine.....	683
G.A. Bobula, W.T. Wintucky, and J.G. Castor	
Small Gas Turbine Engine Technology.....	698
Richard W. Niedzwiecki and Peter L. Meitner	
The Convertible Engine: A Dual-Mode Propulsion System for Advanced Rotorcraft.....	737
Jack G. McArdle	
Results of NASA/Army Transmission Research.....	769
John J. Coy, Dennis P. Townsend, and Harold H. Coe	
NASA's Rotorcraft Icing Research Program.....	802
Robert J. Shaw, John J. Reinmann, and Thomas L. Miller	

### Flight Dynamics and Control

Summary.....	835
Helicopter Mathematical Models and Control Law Development for Handling Qualities Research.....	837
Robert T.N. Chen, J. Victor Lebacqz, Edwin W. Aiken, and Mark B. Tischler	
Rotorcraft Flight-Propulsion Control Integration.....	900
James R. Mihalow, Mark G. Ballin, and D.G.C. Rutledge	
Helicopter Human Factors Research.....	929
David C. Nagel and Sandra G. Hart	
Rotorcraft Handling-Qualities Design Criteria Development.....	948
Edwin W. Aiken, J. Victor Lebacqz, Robert T.N. Chen, and David L. Key	

### Acoustics

Summary.....	1001
Recent Langley Helicopter Acoustics Contributions.....	1003
H.G. Morgan, S.P. Pao, and C.A. Powell	

## Contents (continued)

### Acoustics (continued)

Identification and Proposed Control of Helicopter Transmission Noise at the Source.....	1045
John J. Coy, Robert F. Handschuh, David G. Lewicki, Ronald G. Huff, Eugene A Krejsa, and Allan M. Karchmer	
A Decade of Aeroacoustic Research at NASA Ames Research Center...	1066
F.H. Schmitz, M. Mosher, C. Kitaplioglu, J. Cross, and I. Chang	
Aeroacoustic Research Programs at the Army Aviation Research and Technology Activity.....	1091
Yung H. Yu, Fredric H. Schmitz, and H. Andrew Morse	

### Volume III

#### Systems Integration

Summary.....	1117
Status of NASA/Army Rotorcraft Research and Development Piloted Flight Simulation.....	1119
Gregory W. Condon and Terrence D. Gossett	
System Analysis in Rotorcraft Design - The Past Decade.....	1154
Thomas L. Galloway	
An Integrated Approach to Rotorcraft Human Factors Research.....	1167
Sandra G. Hart, E. James Hartzell, James W. Voorhees, Nancy M. Bucher, and R. Jay Shively	
Avionics Systems Integration Technology.....	1189
George Stech and James R. Williams	
Integrated Diagnostics.....	1211
Roger J. Hunthausen	

#### Research Aircraft

Summary.....	1233
Rotorcraft Flight Research with Emphasis on Rotor Systems.....	1234
W.J. Snyder	

#### Industry

Summary.....	1277
--------------	------

## Contents (continued)

### Industry (continued)

An Overview of Key Technology Thrusts at Bell Helicopter Textron.....	1279
Jim Harse, Jing G. Yen, and Rod Taylor	
Rotorcraft Technology at Boeing Vertol: Recent Advances.....	1341
John Shaw, Leo Dadone, and Robert Wiesner	
Recent Sikorsky R&D Progress.....	1395
Sikorsky Aircraft Division, United Technologies Corporation	
McDonnell Douglas Helicopter Company Independent Research and Development - Preparing for the Future.....	1450
A.C. Haggerty	
List of Conference Attendees.....	1485

## INTRODUCTION

Planning for the 1987 NASA/Army Rotorcraft Technology Conference was launched during the NASA/Army 20th Anniversary Celebration at the Ames Research Center, Moffett Field, California in September, 1985. The Ames Research Center is the lead center for NASA rotorcraft research and also the location of the U. S. Army Aviation Research and Technology Activity headquarters.

At the conclusion of his prepared remarks during the anniversary ceremonies, Dr. Raymond S. Colladay, NASA Associate Administrator for Aeronautics and Space Technology, called for a joint NASA/Army rotorcraft conference, as a follow-up to the twentieth anniversary, that would focus on the status of rotorcraft technology resulting from research progress over the previous five to ten years. The last major conference of this type had been held at the Langley Research Center in 1974 in cooperation with the American Helicopter Society. Prior to 1974 there had been a series of helicopter and V/STOL conferences sponsored by the U. S. Army and by NASA, and NACA, on a periodic basis.

The objective of conferences of this type is to provide a forum where summary technical papers are presented by invited researchers to key technical management staff representatives from government and industry. The conferences provide a milestone event to address the technology base contributions of ongoing research efforts. These conferences emphasize advancements in technical knowledge, while programmatic overviews and future plans are left to other routine briefings, meetings, workshops, and symposia that normally occur on a more frequent basis.

The Army and NASA have been conducting rotorcraft research under a very successful collocated laboratory arrangement since the 1960's. As a result, the joint sponsorship of a major technology conference was a natural outgrowth of this partnership a three aeronautical research centers: the Ames Research Center, Moffett Field, California; the Langley Research Center, Hampton, Virginia; and the Lewis Research Center, Cleveland, Ohio.

To an ever increasing degree, the government rotorcraft research effort is closely coordinated with the in-house research conducted by the U. S. helicopter industry. In recognition of this relationship, the industry, through the participation of the American Helicopter Society, was invited to present highlights of notable technology accomplishments resulting from industry-funded research efforts.

This three-volume conference proceedings document contains over thirty technical papers which were summarized in oral presentations on March 17-19, 1987. The organization of the proceedings is similar to the conference agenda. That is, Volume I contains technical papers addressed on March 17, 1987 covering the two disciplinary session topics of Aerodynamics, and Dynamics and Aeroelasticity. Volume II, the March 18 material, includes the four session topics of Materials and Structures, Propulsion and Drive Systems, Flight Dynamics and Control, and Acoustics. Volume III contains the material from the third and final day of the conference, March 19, 1987. This third volume contains papers that were addressed in the three concluding sessions: Systems Integration, Research Aircraft, and the Industry Session.

## AERODYNAMICS

### Session Cochairmen:

William G. Warmbrodt, NASA

William J. McCroskey, Department of the Army

## AERODYNAMICS SESSION

### SUMMARY

The first paper from the Aerodynamics Session, "Accomplishments of NASA Langley Research Center in Rotorcraft Aerodynamics Technology" by John C. Wilson, described noteworthy accomplishments in rotorcraft technology in the areas of rotor design, airfoil research, rotor aerodynamics, and rotor/fuselage interaction aerodynamics. The paper focused on key Langley Research Center facilities including the 14- by 22- Foot Subsonic Tunnel, the Transonic Dynamics Tunnel, and a 6- by 28- Inch Transonic Facility.

The second presentation, "The Development of CFD Methods for Rotor Applications" by F. X. Caradonna and W. J. McCroskey, outlined the recent developments in computational fluid dynamics (CFD) methodology as a new tool for the prediction of advancing blade transonic flow aerodynamics and the application of these methods to investigate this persistent limitation to high-speed rotor performance.

PRECEDING PAGE BLANK NOT FILMED



ACCOMPLISHMENTS AT NASA LANGLEY RESEARCH CENTER  
IN ROTORCRAFT AERODYNAMICS TECHNOLOGY

John C. Wilson

U.S. Army Aerostructures Directorate,  
Langley Research Center

## SUMMARY

In recent years, the development of aerodynamic technology for rotorcraft has continued successfully at NASA LaRC. Though the NASA Langley Research Center is not the lead NASA center in this area, the activity has been continued due to the unique facilities and individual capabilities which are recognized as contributing to helicopter research needs of industry and government. Noteworthy accomplishments which contribute to advancing the state of rotorcraft technology in the areas of rotor design, airfoil research, rotor aerodynamics, and rotor/fuselage interaction aerodynamics are described. New rotor designs have been defined for current helicopters and evaluated in wind tunnel testing. These designs have incorporated advanced airfoils defined analytically and also proven in wind tunnel tests. A laser velocimetry system has become a productive tool for experimental definition of rotor inflow/wake and is providing data for rotorcraft aerodynamic code validation.

## INTRODUCTION

Since the time that NASA Ames was designated as the lead Center for rotorcraft technology, the activity in rotorcraft aerodynamic technology has been carried on by the U.S. Army Aerostructures Directorate at Langley. Though at a reduced level because of less manpower and resources, significant work has been accomplished in analyses and experimentation for rotorcraft aerodynamics. For the latter activity there are two key facilities at Langley--the 14- by 22-Foot Subsonic Tunnel shown in figure 1 (formerly the 4- by 7-Meter Tunnel - and earlier the V/STOL Tunnel) and the Transonic Dynamics Tunnel shown in figure 2. At the 14- by 22-Foot Subsonic Tunnel, the Rotorcraft Aerodynamics Office comprised of a group of Army aerospace engineers has been performing pioneering work in rotor aerodynamic and acoustic analyses and experimentation. At the Transonic Dynamics Tunnel, another group of Army engineers, the Rotorcraft Aeroelasticity Group, pursues similar interests in rotor dynamics as well as in aerodynamics.

Both facilities have unique capabilities for helicopter technology developments. The 14- by 22-Foot Subsonic Tunnel can be operated with either an open- or closed-throat test section by raising or lowering the side walls, ceiling and floor. Typically, for laser velocimetry measurements of rotor inflow or for rotor acoustic measurements, the open-throat configuration, with floor in place, is used. Wind speeds of up to 200 knots can be generated in the 14.5 ft. high by 21.75 ft. wide test section. Acoustic reverberations in the open-throat test section are reduced by use of sound-absorbing panels on the test chamber walls surrounding the test section. A specially designed laser-velocimeter ("LV") laboratory for set-up (beam alignment and operation) and maintenance of a dedicated LV system is adjacent to the test section and

affords efficient preparations for testing. A new rotor model preparation area near the tunnel provides the capability to assemble and test rotor models in hovering conditions prior to actual entry into the tunnel test section.

In 1985, modifications (figure 3) to the 14- by 22-Foot Subsonic Tunnel were completed and have improved and expanded its aerodynamic and acoustic test capability (refs. 1 and 2). One of the more significant aerodynamic improvements was achieved through the use of flow deflectors installed downstream of the first corner of the tunnel circuit to improve the performance of the tunnel fan. The deflectors resulted in a more uniform velocity distribution into the tunnel drive system and eliminated regions of large-scale flow separation in the return leg of the tunnel circuit. A new turbulence reduction system consisting of a grid, a honeycomb, and four fine-mesh screens dramatically reduced the level of longitudinal turbulence intensity in the tunnel test section. The turbulence in the closed test section was reduced from nominally 0.2% to 0.1% as shown in figure 4. In the open test section, turbulence of nominally 10% was reduced to a level of only 1% (figure 5). The 10% level in the unmodified tunnel was caused by periodic flow pulsations which were eliminated by installing a new flow collector in the open test section.

The Transonic Dynamics Tunnel (TDT) is also unique (refs. 3 and 4) in its capabilities for model rotor testing as is illustrated in figure 6. It can use "Freon-12," a heavy gas with a low speed of sound, as the test medium. The tunnel was originally designed to test large dynamic models for the simulation of important aeroelastic structural properties of fixed-wing aircraft at transonic speeds. The TDT is a continuous flow tunnel and can be operated with freestream Mach numbers up to 1.2 and dynamic pressures ranging up to 550 psf. The present capability (figure 7) of the tunnel is the result of modifications completed in 1985. Model rotor testing for performance and rotor-system dynamics takes advantage of these flow characteristics to provide scale simulation of rotor tip Mach number and high Reynolds number. Using Freon 12 as the test medium allows this simulation to be accomplished with substantially reduced requirements for model power and rotor blade spar strength as compared to testing in air (figure 8). Another feature of the tunnel which is useful for rotor research is an airstream oscillator system. A simulated gust field may be applied to the flow through the test section in the form of a sinusoidal oscillation of the flow direction. The oscillating flow is generated by a biplane arrangement of vanes on either side of the entrance to the test section. Both frequency and amplitude of vane motion can be varied to generate a wide range of gust characteristics. These features of TDT have made it an extremely useful tool for aerodynamic and dynamic research for helicopter technology.

A very specialized facility for rotor airfoil development is the Langley 6- by 28-Inch Transonic Tunnel (ref. 5 and 6). This facility is a blowdown tunnel with a slotted floor and ceiling and is generally operated at stagnation pressures from about 30 psia to 90 psia at Mach numbers from 0.35 to 0.90. At a stagnation pressure of 90 psia, the maximum Reynolds number, based on a 6.0 inch chord, varies from about  $7.2 \times 10^6$  at a Mach number of 0.35 to about  $14.3 \times 10^6$  at a Mach number of 0.90.

The facilities just described are key to the experimental work in rotorcraft aerodynamic technology developments at Langley, and they are complemented by

model rotor test systems especially suited to the special capabilities of each of the facilities. The "General Rotor Model System" (GRMS) shown in figures 9 and 10 (ref. 7), and the "Two Meter Rotor Test System" (2MRTS) shown in figure 11 (ref. 8), are used in the 14- by 22-Foot Subsonic Tunnel; in the TDT, the "Aeroelastic Rotor Experimental System" (ARES) (figure 12) is used. The GRMS has been used to test rotors with diameters of 10 to 13 feet and rotor diameters for the 2MRTS have ranged from 5 feet to 6.5 feet. Both systems test rotors at full-scale tip speeds. On the ARES, the rotors are generally 9 feet in diameter. All three systems have been "work horses" and have been used in many experimental programs described in this paper.

Aerodynamic analyses are conducted as an essential adjunct to the experimental activity. These analyses are used to guide the experimental work in setting test objectives, and are themselves evaluated by the experimental results. The analyses treat the many aspects of helicopter design such as airfoils, rotor performance, rotor blade loads, and the interaction of rotor, airframe, and rotor inflow/wake. Computational codes developed by other research organizations are being used, but, code development is being carried on at Langley as well. Some of the codes in common use include the UTRC Free Wake, CAMRAD, VSAERO, HESS, AMI HOVER, C-81, Langley momentum hover program, and Langley DO 865. A variety of computers, from desktop personal computers to highly sophisticated mainframes such as the Control Data VPS-32, are available and used in rotorcraft aerodynamic analyses.

The following discussion is a review of some of the results of experimental and analytical work in rotorcraft aerodynamics which has been accomplished using the various capabilities at the NASA Langley Research Center.

## DISCUSSION

### Rotor Design

Over the past seven years, rotor design efforts have been directed toward an optimum combination of airfoils, planform, and twist (ref. 9) to provide advanced rotor designs for possible use on the UH-1 (figure 10, ref. 10), the AH-64 (figure 13, ref. 11), and the UH-60 (figure 12). The designs were evaluated in wind tunnel tests of models of the proposed rotors. The most distinctive feature of these rotor designs is the use of substantial taper of the rotor tip as much as 50 percent for the UH-1 design. Analyses by Gessow (ref. 12) many years ago showed that rotor hover performance could be improved by blade taper; this design philosophy was implemented with a rotor design for the UH-1 helicopter. Tests of a 25-percent scale model of the tapered rotor were conducted along with a model of the standard rotor in the 14- by 22-Foot Subsonic Tunnel using the GRMS. The test results validated the analytic prediction in that rotor performance for the advanced rotor was superior to that of the standard rotor, from hover up to 110 knots as shown in figures 14 and 15. Unfortunately the rotor hub (a 25%-scale model of the UH-1 hub) broke due to a fabrication flaw before the advanced design could be tested at a high thrust level (substantially higher than that for level flight at the design gross weight).

This specific approach to testing, in which one design is compared to another during the same test program under the same test conditions provides

confidence in the results. By comparing rotor measurements obtained with the same rotor drive system, and data acquisition and reduction system, incremental effects (i.e. performance benefits) are more reliably defined. This approach was used for tests of AH-64 and UH-60 advanced designs.

The advanced AH-64 design shown in figure 13 also used an analytically defined optimum combination of taper, airfoils, and twist. Model rotors were fabricated at 27-percent scale for both the baseline (rectangular with swept tip) and advanced designs, and both rotors were tested with models of the AH-64 hub and fuselage at the same scale. All components were mounted to the GRMS and tested in the Langley 14- by 22-Foot Subsonic Tunnel. As was the case for the UH-1, the advanced design resulted in improved performance throughout most (ref. 11) of the normal operating envelope of the rotor (See figures 16 and 17). At high thrust coefficient in hover, the improvement in figure of merit may decrease to zero. The taper of the original advanced design was 5 to 1, starting at 80 percent radius and it was suspected that reducing the amount of taper to 3 to 1 would improve hover performance. The blade tips were altered to the reduced taper, and hover tests were conducted in the new rotor test cell at the 14- by 22-Foot Subsonic Tunnel. The reduced taper resulted in a hover performance improvement as can be seen in figure 16. It should be realized that the improvement due to reduced taper may be the result of Reynolds number effects and not just taper. Evaluation of forward flight performance for the 3 to 1 taper will be conducted at a future time.

The change of taper for the AH-64 was based on results of exploratory tests which had been conducted on smaller scale tapered blades using the 2MRTS system. Hover tests of three different four-bladed rotors were conducted in the tests of reference 13 to evaluate whether a prescribed wake code could properly predict trends for tapered blades. The three were a swept-tip design based on the UH-60 rotor design, a configuration with 3-to-1 taper over the outboard 20 percent of the blade span, and a configuration with a 5-to-1 taper over the outboard 20 percent of the blade span. The investigation covered a range of tip speeds and thrust levels. The two tapered configurations had better hover performance than the baseline swept-tip configuration, and the 3-to-1 taper configuration was somewhat better than the 5-to-1 configuration as shown in figure 18. The test results were compared with predictions made by using a prescribed wake analysis, a momentum strip-theory analysis and a simplified free-wake analysis. The performance of the baseline blade was in fair agreement with predictions from both momentum strip-theory analysis and the prescribed-wake analysis when appropriate low Reynolds number airfoil data were used. The performance of the two tapered-blade configurations was in fair agreement with the prediction of the momentum strip-theory analysis; however, the prescribed-wake analysis incorrectly predicted performance that was much worse than was measured for the two tapered configurations.

The art of designing "advanced" rotor blades was next applied to the UH-60. A new design incorporating wide blade chord, tip taper, new airfoils, and different twist was defined and tested with the ARES in the TDT tunnel as shown in figure 12. As expected, the advanced rotor design demonstrated better performance than did the baseline UH-60 design. The test results will be published. These three experimental programs of wind-tunnel testing of advanced designs for the UH-1, AH-64, and UH-60 have demonstrated that rotor

blades incorporating substantial planform taper, advanced airfoils, and substantial twist will provide significant performance improvements in hover and forward flight.

Designing of advanced rotors such as those described has involved a tedious exercise of rotor performance codes as the three basic design variables of planform, airfoil, and twist were varied to home in on a "best" combination to meet specified performance requirements. But the efforts have paid off in the improved rotor thrust capability available in hover and increased efficiency in forward flight as demonstrated in the model test programs for the UH-1, AH-64 and UH-60. It should be realized that the percentage improvement in thrust is multiplied by a factor of 3 to 5 when useful load capability improvement is considered. In the last couple of years a more systematic approach for the design process has been initiated at Langley (Ref. 14). The Interdisciplinary Research Office has been tasked with the responsibility of integrating the computer codes into a formal optimization procedure for helicopter rotor blade designs. The proposed approach is to couple hover and forward flight analysis programs with a general purpose optimization procedure. The time and cost of designing rotor blades can then be significantly reduced to gain improvements such as demonstrated for the UH-1, AH-64, and UH-60.

A cooperative wind-tunnel test program was recently conducted at the Glenn Martin Wind Tunnel (figure 19) by the Aerostructures Directorate and the University of Maryland to investigate in more detail the effect of tapering of rotor blades on rotor forward flight performance. Analysis with the C-81 code indicated that taper beginning at about 94% blade span resulted in the lowest power required and, therefore, rotor performance improvements seen in earlier programs were, perhaps, attributable only to advanced airfoils and twist variations (ref. 15). However, the tests provided results which were contrary to the C-81 analysis that is, for high speeds as well as hover, tapering of blades inboard of 94% blade span is beneficial.

### Rotor Airfoils

The advanced design rotors have incorporated modern airfoils (ref. 16 through 22) designed for rotor applications and tested at the Langley Research Center in the 6- by 28-Inch Transonic Tunnel. A great deal of airfoil design work over many years has been conducted at Langley for fixed wing aircraft, but interest in rotorcraft applications has been relatively recent (in the last 15 years). Of course, designing airfoil sections for a helicopter rotor is more complex than that for a fixed wing aircraft since a rotor airfoil can experience lift coefficients from negative values to the maximum positive value, and Mach numbers from low subsonic to transonic values all in one rotor revolution. Further, since the ranges of lift coefficients and Mach numbers depend on the radial location along the rotor blade and the helicopter flight condition, different airfoils need to be identified for specified ranges of radial positions along the rotor blades. Designing airfoils within the plethora of constraints is an art which has reached a high level of sophistication. At Langley two notable airfoil families for helicopter rotor application have been patented (ref. 21 and 22).

## Rotor Inflow and Wake Studies

Defining the inflow to a rotor is a key element in predicting the performance, blade loads, and acoustic characteristics of a rotor. Also, defining the wake generated by the rotor is important in estimating helicopter fuselage aerodynamics. Unfortunately for helicopter designers, the analyses for definition of inflow and wake effects have little experimental data to validate them. Though some work in rotor inflow and wake measurement has been accomplished by Heyson (ref. 23), Landgrebe (ref. 24), De Sopper (ref. 25) and McMahon (ref. 26), much more is needed to provide a comprehensive database describing the time dependent and azimuth dependent flow characteristics. In the last several years the experimental capability needed to acquire such data has been built up at the Langley 14- by 22-Foot Subsonic Tunnel and centers around the use of a high powered laser velocimeter (LV) system (ref. 27). The LV system shown in figure 20 is dedicated to the facility, and was built up by personnel of the Rotorcraft Aerodynamics Office.

The LV is a dual-color four-beam fringe type system operating in a back scatter mode. Positioning of the measurement point within a cube of approximately 2 meters on a side is accomplished with a combination of rotation of mirrors and movement of the entire LV system enclosure within the large traverse apparatus shown in figure 20. Rather complex subsystems for remotely controlling the measurement point, acquiring the data, and reducing the data to engineering units have been developed by the researchers, and they functioned extremely well in recent test programs (ref. 28) to obtain measurements of rotor inflow. Because the LV system is dedicated to research, there is an ongoing program of system enhancements to accelerate the data acquisition process. For example, the flow seeding system presently requires manual translation of a large spray array located in the tunnel settling chamber. Even with this limitation, however, it provided excellent data rates (number of particles passing through the measurement point per unit time) with 1.7 micron particles. The manual system will be replaced with a remote positioning system which will speed up the process of obtaining high data rates. Also, the Langley Instrumentation Research Division which has contributed to the development of the current LV system has been provided funding for the definition of modifications to obtain a third velocity component.

In its current state the LV system has made it possible to begin mapping the inflow of generic research rotors, and to assess the effect of blade geometry (such as rectangular and tapered planforms) on rotor inflow characteristics (figure 21). Two programs have been conducted this past year and a sampling of the data obtained is shown in figure 22. The data include a full mapping of the rotor disc at approximately 1 blade chord above the rotor tip-path plane. Figure 22 provides a three-dimensional view of average inflow normal to the rotor disk. The time-varying inflow at a point is shown in figure 23. With each model entry, system enhancements have been made and will continue to be made with a view toward investigating the effects of variations of the many parameters such as advance ratio, thrust coefficient, blade number, blade planform, and proximity to the rotor. The early data obtained have already been compared with some of the many coded predictions of inflow for validation of the codes (ref. 28).

## Rotor/Fuselage Aerodynamic Interaction

The rotor and fuselage interact aerodynamically in a very complex way and there is presently a paucity of test data to validate the analyses currently used to quantify the interaction effects (refs. 26 and 29). To remedy the situation two helicopter models with generic fuselage shapes have been instrumented with miniature transducers and in recent tests at the Langley 14-by 22-Foot Subsonic Tunnel, time dependent pressures were measured to investigate the influence of the rotor wake. In the most recent program a two bladed rotor with over 100 miniature pressure transducers on the blades (figure 24) provided high quality data which are being used to evaluate wake/fuselage interaction codes. Simultaneous measurements of pressures on the blades and fuselage were obtained, along with measurements of blade loads.

Flow distortions caused by the fuselage affect rotor inflow, and the rotor wake in turn affects fuselage pressure distributions. Both average and time-dependent distortions are the result of these mutual perturbations. The extent to which interactional aerodynamics can influence helicopter vibrations was not sufficiently appreciated until recent years when the new series of military helicopters (AH-64, UH-60) began to experience more pronounced aerodynamically excited vibrations. Analytical methodology to predict and study the interactional causes and effects, particularly those related to the time-dependent excitations effecting vibrations, has not yet been fully developed, although, in recent years significant progress has been made toward the development of computerized methods which can take into account the large array of variables which need to be considered.

Two analytic approaches are being studied at Langley. One of these is a contractual effort with UTRC which is leading to a method for a first-order treatment for vibration purposes as represented in figure 25. In this approach, a rotor aeroelastic analysis ("G400" code) for predicting rotor aeroelastic response characteristics, a rotorcraft wake analysis ("RWA" code) for predicting rotor blade and wake induced airflow velocities, and an analysis predicting fuselage pressure distribution ("WABAT" code) are being integrated to predict interactional excitations for vibration analysis. The separate codes are being extended where necessary to model blade, wake, and fuselage surface pressures (including empennage surfaces). It should be recognized that the aerodynamic interactions are very complex and are influenced by features such as hub/pylon separated wake and tail rotor interactions which are beyond the scope of the initial study. It is not a complete treatment, by any means, but it is providing a framework for future refinements.

A second approach to modeling analytically the rotor/fuselage interactive aerodynamics is being developed in which an existing general panel method ("HESS" code) for calculation of flow about arbitrary shapes is being combined with a model ("Crispin" code, ref. 30) of the rotating blade system. The geometry of the rotor wake is computed with the Crispin code and allowed to contribute to the flow field of the total configuration. The integration of the two codes has required substantial changes to both. The capabilities of the Crispin code have been extended by providing for a two-bladed rotor and including a means of accounting for cyclic pitch variations. The wake

prediction of the code is shown in figure 26. Both analytic codes are being developed with the objective of being validated by experimental data obtained in the Langley 14- by 22-foot Subsonic Tunnel.

Interactional aerodynamic problems of helicopters are sometimes of a comparatively minor nature and involve separated flows so that experimental methods are the most effective means of study. One such problem is identified in references 31 through 33, and a simple solution is proposed in reference 34. A single-main-rotor helicopter being flown at low speeds has the tail boom immersed in the rotor wake. When flown in right sideward flight, the aerodynamic pressures on the tail boom resulting from the high downwash velocities of the wake can result in adverse side loads on the boom. The side loads contribute a yawing moment which may be beyond the capability of a tail rotor to counteract since it is already burdened by the need to counteract the main rotor torque. Such a limitation has been experienced by the AH-64, AH-1S, and the British Sea King helicopter. A spoiler (or strake) mounted on the upper left shoulder of a tail boom as shown in figure 27 has been shown to be effective in reducing the tail boom yawing moment, thereby improving heading control in sideward flight as shown in figure 28 for the SH-3.

#### Diagnostic Testing Activities

In addition to the fundamental research studies discussed so far, Army researchers at the Aerostructures Directorate are occasionally asked to investigate the causes of aerodynamic problems encountered in Army helicopter operations, or to develop solutions to problems whose causes have been identified in field operations. The availability of several helicopter modeling systems and full-scale components, along with the wind tunnels and computational capability at the NASA Langley Research Center have made it possible for Aerostructures Directorate researchers to respond quickly to Army needs. Two recent experimental efforts illustrate typical diagnostic testing conducted by researchers at the 14- by 22-Foot Subsonic Tunnel. One of these efforts addressed a concern regarding the AH-64 and the other focused on the UH-60 stabilator.

The AH-64 "Apache" is vulnerable, as many helicopters are, to being blown over by high winds when it is parked but not tied down, but the extent to which the Apache was subject to this danger was not known. A large AH-64 model was tested in the 14- by 22-Foot Subsonic Tunnel as shown in figure 29 to study this problem in detail. The model was yawed through a range of -20 to +160 degrees, and the wind loading which could tip the helicopter over was evaluated. Figure 30 shows tests results in terms of the combination of critical wind speed and azimuth for which tipover could be expected to occur.

A second study used a full scale UH-60 stabilator to measure the airloads which can occur at a combination of high flight speeds and high tail incidence. If the large UH-60 stabilator is inadvertently deflected to high incidence at high flight speed, the resulting pitching moment about the center of gravity would be beyond the capability of the pilot to counteract through rotor cyclic control. A flightworthy stabilator was installed in the tunnel (figure 31), and the airloading on the basic stabilator was measured. Various small spoilers were attached near the leading edge to reduce the lift load at high incidence. Though spoilers were not very effective at angles of attack



near 45°, they were very effective at angles of attack of between 10 and 20° where the problem of uncontrollable pitching moment is more likely to occur. Figure 32 summarizes the results of the tests on the UH-60 stabilator.

#### CONCLUDING REMARKS

The Aerostructures Directorate of USAARTA (AVSCOM) has continued to utilize capabilities in facilities, equipment, and personnel at Langley to make significant contributions to rotorcraft technology. These contributions cover a broad range of research in several areas, including rotor design, rotor airfoils, and rotor/fuselage interactional aerodynamics. Additional testing activities are also conducted to address operational needs on a quick response basis. Key facilities which aid in accomplishments in these facets of helicopter aerodynamics are NASA Langley's 14- by 22-Foot Subsonic Tunnel, the Transonic Dynamics Tunnel, and the 6- by 28-Inch Transonic Tunnel.

#### REFERENCES

1. Applin, Zachary T.: Modifications to the NASA Langley 4- by 7-Meter Tunnel for Improved Rotorcraft Aerodynamics and Acoustics. AHS National Specialists Meeting on Helicopter Testing Technology, Williamsburg, VA. Oct. 29, 1984.
2. Applin, Zachary T.: Flow Improvements in the NASA Langley 4- by 7-Meter Tunnel. AAIA 13th Aerodynamic Testing Conference, San Diego, California. March 5, 1984.
3. Staff of the Aeroelasticity Branch (NASA Langley Research Center): The Langley Transonic Dynamics Tunnel. LWP-799, September 23, 1969.
4. Mantay, Wayne R.; Yeager, William T.; Hamouda; M-Nabil, Cramer; Maj. Robert G.; and Langston, Chester W.: Aeroelastic Model Helicopter Rotor Testing in the Langley TDT. NASA TM 86440. June 1985.
5. Ladson, Charles L.: Description and Calibration of the Langley 6- by 28-Inch Transonic Tunnel. NASA TN D-8070, 1975.
6. Sewall, William G.: Description of Recent Changes in the Langley 6- by 28-Inch Transonic tunnel. NASA TM 81947, May 1981.
7. Wilson, John C.: A General Rotor Model System for Wind-Tunnel Investigations. J. Aviation, Vol. 14, No. 7, July 1977, pp. 639-643.
8. Phelps, Arthur E. III. and Berry, John D.: Description of the U.S. Army Small-Scale 2-Meter Rotor Test System (2MRTS). NASA TM-87762, January 1987.
9. Bingham, Gene J.: The Aerodynamic Influences of Rotor Blade Taper, Twist, Airfoils and Solidity on Hover and Forward Flight Performance. 37th Annual Forum of the American Helicopter Society, New Orleans, Louisiana, May 1981.

10. Berry, John D.: Quarter-Scale Testing of an Advanced Rotor System for the UH-1 Helicopter. 37th Annual Forum of the American Helicopter Society. New Orleans, Louisiana, May 1981.
11. Kelley, Henry L. and Wilson, John C.: Aerodynamic Performance of a 27-Percent-Scale AH-64 Wind-Tunnel Model with Baseline/Advanced Rotor Blades. 41st Annual Forum of the American Helicopter Society. Ft. Worth, Texas, May 1985.
12. Gessow, Alfred: Effect of Rotor-Blade Twist and Planform Taper on Helicopter Hover Performance, NACA TN 1542, 1947.
13. Phelps, Arthur E. III, and Althoff, Susan L.: Effects of Planform Geometry on Hover Performance of a 2-Meter-Diameter Model of a Four-Bladed Rotor. NASA TM 87607. March 1986.
14. Walsh, Joanne L., Bingham, Gene J., and Riley, Michael F.: Optimization Methods Applied to the Aerodynamic Design of Helicopter Rotor Blades. AIAA 26th Structural Dynamics and Materials Conference. Orlando, Florida. April 1985.
15. Noonan, K. W.: Aerodynamic Design of a Helicopter Main Rotor Blade with Consideration of Flap-Lag Flutter in Hover. Masters Thesis (University of Maryland), Dec. 1985.
16. Noonan, Kevin W.; and Bingham, Gene J.: Two-Dimensional Aerodynamic Characteristics of Several Rotorcraft Airfoils at Mach Numbers from 0.35 to 0.90. NASA TM X-73990. 1977.
17. Bingham, Gene J.; Noonan, Kevin W.; and Jones, Henry E.: Results of an Investigation of Several New Rotorcraft Airfoils as Related to Airfoil Requirements. Advanced Technology Airfoil Research, Volume II, NASA CP-2046, 1979, pp. 109-119.
18. Bingham, Gene J.; and Noonan, Kevin W.: Experimental Investigation of Three Helicopter Rotor Airfoils Designed Analytically. NASA TP-1396, AVRADCOM TR 79-11, 1979.
19. Bingham, Gene J.; Noonan, Kevin W.; and Sewall, William G.: Two-Dimensional Aerodynamic Characteristics of an Airfoil Designed for Rotorcraft Application. NASA TP-1965, AVRADCOM TR 81-B-6, 1981.
20. Bingham, G. J.; and Noonan, Kevin W.: Two-Dimensional Aerodynamic Characteristics of Three Rotorcraft Airfoils at Mach Numbers 0.35 to 0.95. NASA TP-2000. May 1982.
21. Bingham, Gene J.: Shapes for Rotating Airfoils. United States Patent 4,459,083. July 10, 1984.
22. Noonan, Kevin W.: Family of Airfoil Shapes for Rotating Blades. United States Patent 4,412,664, November 1, 1983.
23. Heyson, Harry H. and Katzoff, S.: Induced Velocities Near a Lifting Rotor With Nonuniform Disk Loading. NACA TR-1319. 1957.

24. Landgrebe, A. J., and Johnson, B. V.: Measurement of Model Helicopter Rotor Flow Velocities with Laser Doppler Velocimeter. Journal of the American Helicopter Society. pp. 19-21, July 1974.
25. De Sopper, A.: Rotor Wake Measurements for a Rotor in Forward Flight. International Conference on Rotorcraft Basic Research, Research Triangle Park, North Carolina, February 1985.
26. McMahon, H. M.; Komerath, N. M.; and Hubbardt, J. E.: Studies of Rotor-Airframe Interactions in Forward Flight. AIAA 3rd Applied Aerodynamics Conference. (AIAA-85-5015) October 1985.
27. Hoad, D. R.; Rhodes, D. B.; and Meyers, J. F.: Preliminary Rotor Wake Measurements with a Laser Velocimeter. NASA TM 83246. March 1983.
28. Berry, John D.; Hoad, Danny R.; Elliott, Joe W.; and Althoff, Susan L.: Helicopter Rotor Induced Velocities, Theory and Experiment. Proceedings of the AHS Specialists Meeting on Aerodynamics and Acoustics, Fort Worth, Texas, February 25, 1987.
29. Freeman, Carl E. and Wilson, John C.: Rotor Wake Effects on Helicopter Fuselages-Analysis and Test. Proceeding of the 34th Annual Forum of American Helicopter Society. Washington D.C. May 1979.
30. Crispin, Y.: Unsteady Rotor Aerodynamics Using a Vortex Panel Method. AIAA 9th Atmospheric Flight Mechanics Conference. AIAA-82-1348, Aug. 9-11, 1982.
31. Amer, K. B.; Prouty, R. W.; Walton, R. P.; and Engle, J. E.: Handling Qualities of Army/Hughes YAH-64 Advanced Attack Helicopter. Proceeding of the 34th Annual Forum of the American Helicopter Society Washington DC. May 1978.
32. Todd, Loren L.; et al: Preliminary Evaluation of the AH-1S (Modernized Cobra) with the Hellfire, TOW, and Stinger Missiles Installed. US AAEFA Project No. 84-11. October 1984.
33. Brocklehurst, Alan: A Significant Improvement to the Low Speed Yaw Control of the Sea King Using a Tail Boom Strake. Proceeding of the Eleventh European Rotorcraft Forum (Paper No. 32). September 1985.
34. Wilson, John C. and Kelley, Henry L.: Aerodynamic Characteristics of General Helicopter Tail Boom Cross Sections Including the Effect of Spoilers. NASA TP 2506.

ORIGINAL PAGE IS  
OF POOR QUALITY



Figure 1. The 14- by 22-Foot Subsonic Tunnel.



Figure 2. Transonic Dynamics Tunnel.

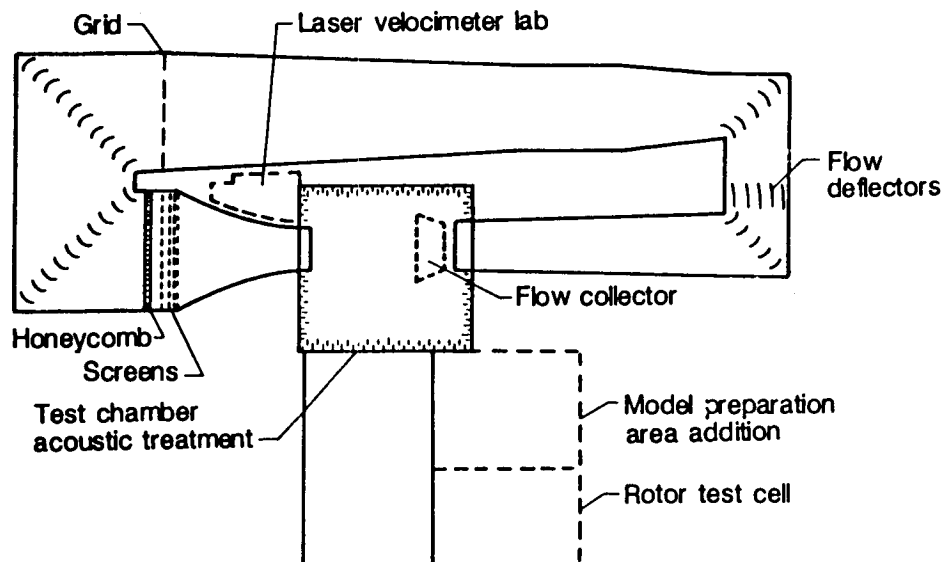


Figure 3. Modifications of the 14- by 22-Foot Subsonic Tunnel.

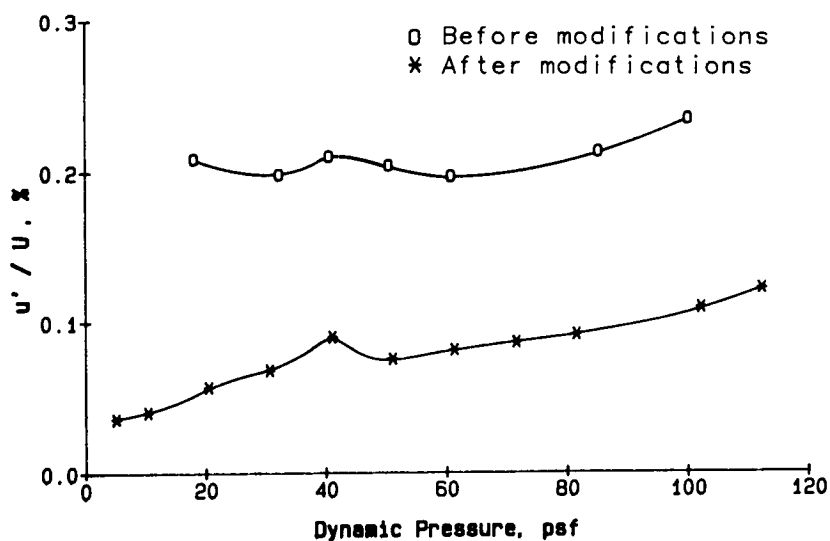


Figure 4. Turbulence intensity in the closed test section of the 14- by 22-Foot Subsonic Tunnel.

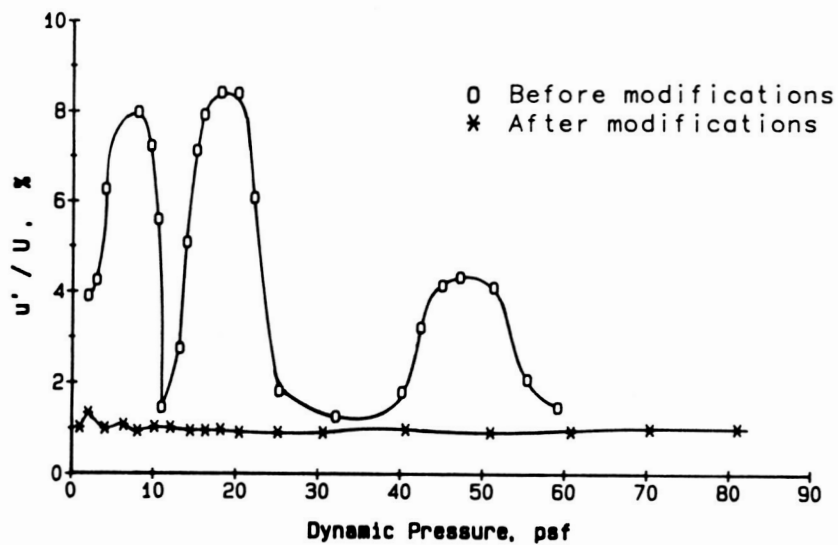


Figure 5. Turbulence intensity in the open test section of the 14- by 22-Foot Subsonic Tunnel.

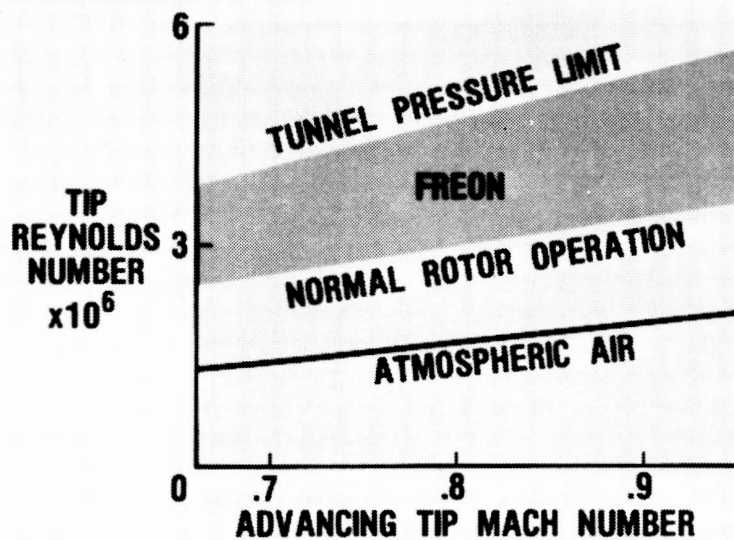


Figure 6. Rotor performance modeling improved at the Transonic Dynamics Tunnel.

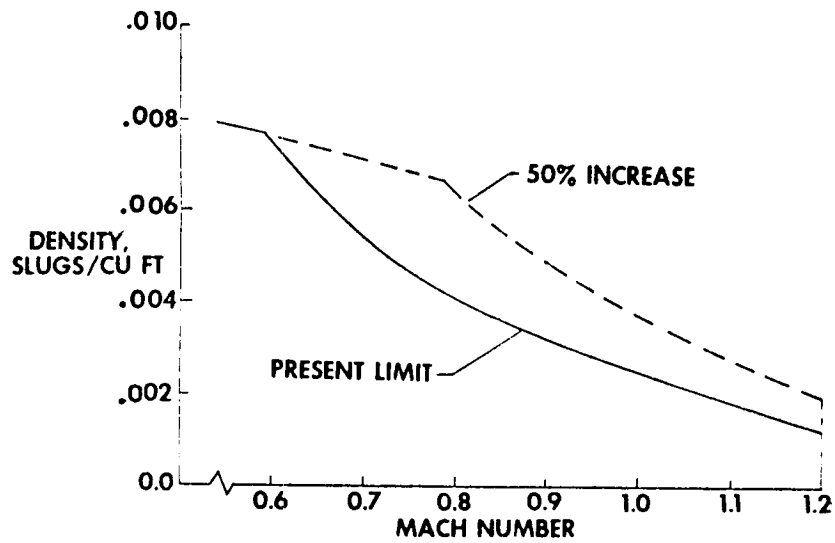


Figure 7. Increased test capability at the Transonic Dynamics Tunnel.

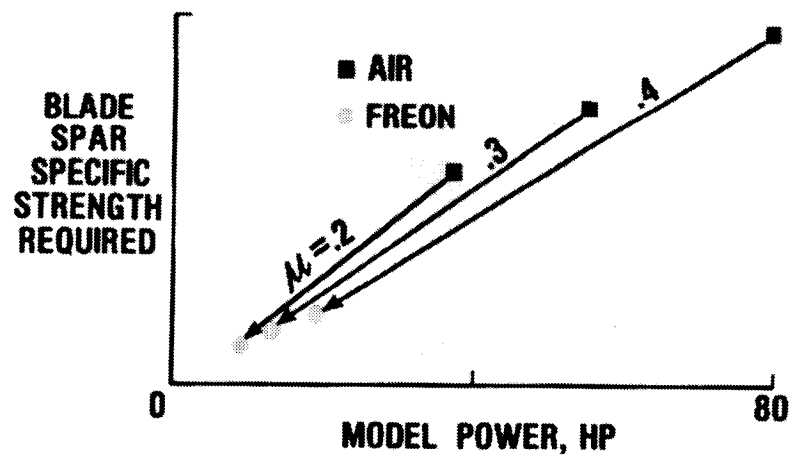


Figure 8. Rotor model torque and required strength reduction in the Transonic Dynamics Tunnel.

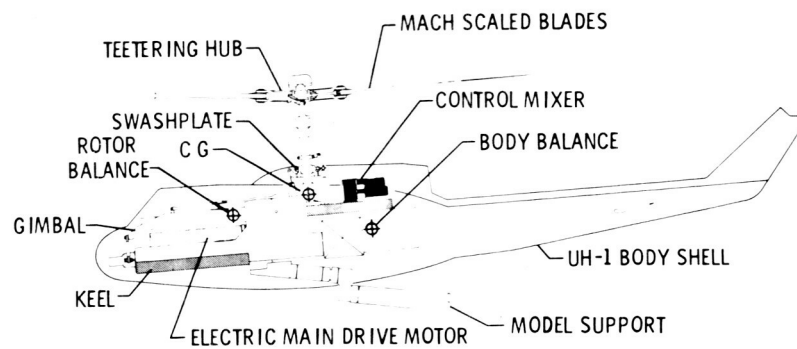


Figure 9. General Rotor Model System.

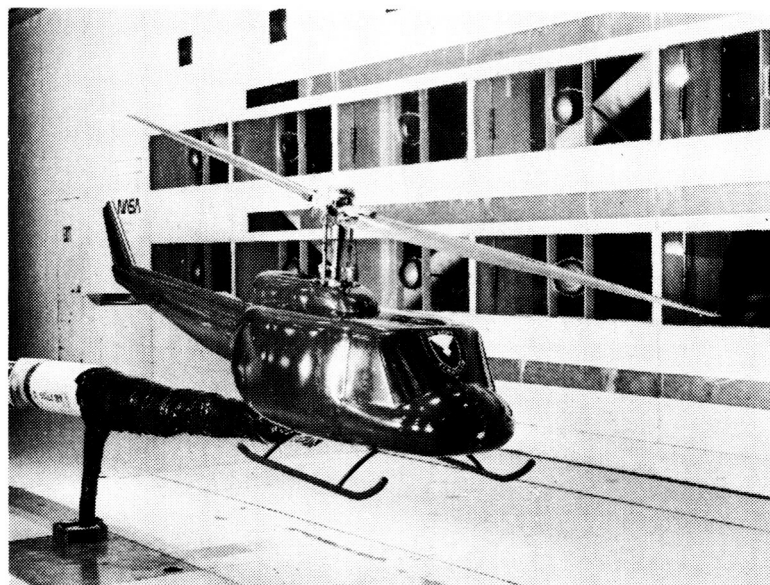


Figure 10. Installation of 1/4 scale UH-1 on the GRMS in the 14- by 22-Foot Subsonic Tunnel.



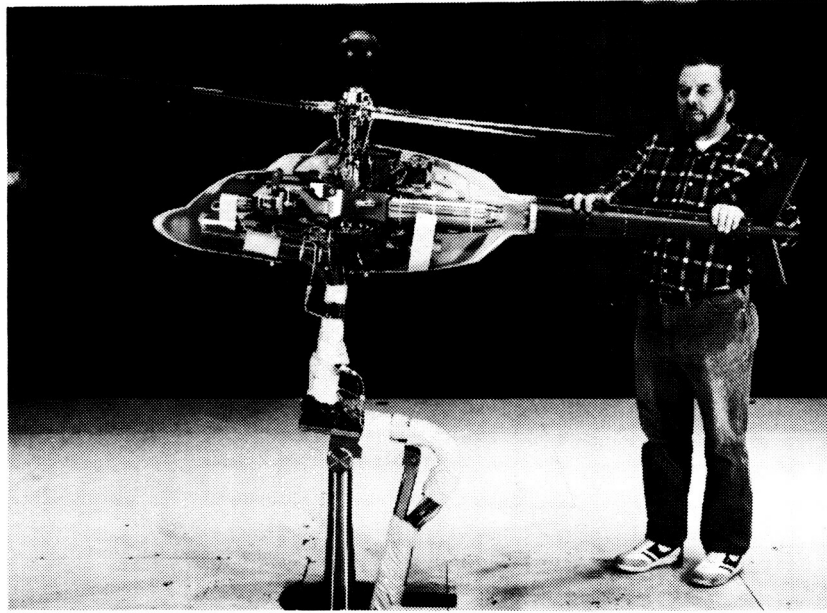


Figure 11. Installation of AHIP model on the 2MRTS in the  
14- by 22-Foot Subsonic Tunnel.

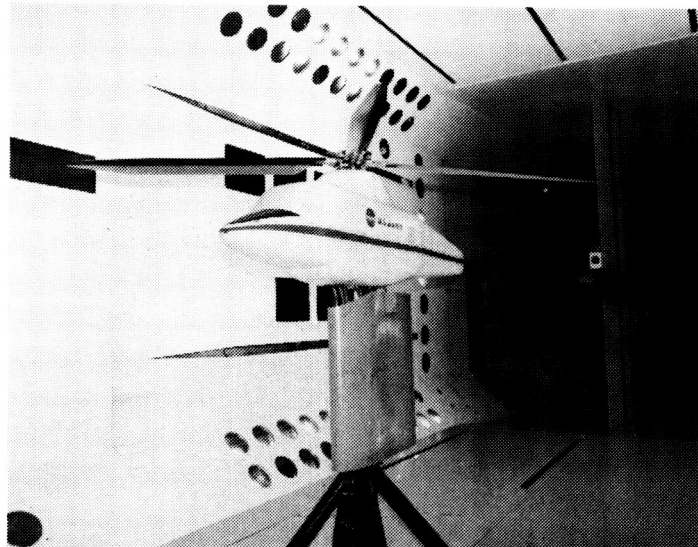


Figure 12. Installation of ARES with advanced design UH-60 rotor  
blades in the Transonic Dynamics Tunnel.

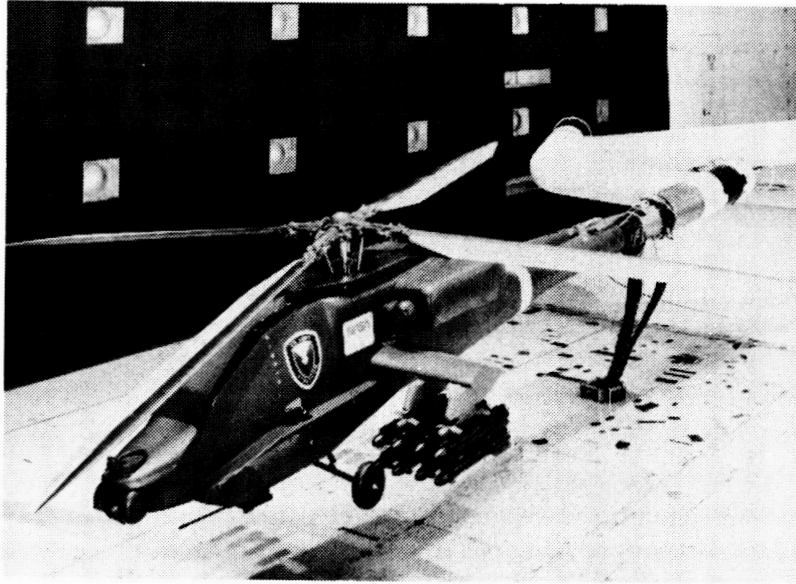


Figure 13. 27-percent scale AH-64 model on the GRMS in the 14- by 22-Foot Subsonic Tunnel.

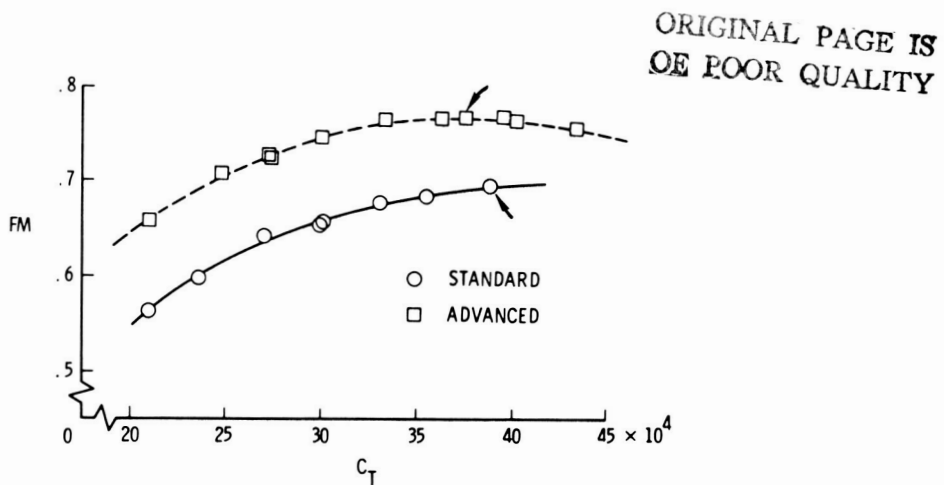


Figure 14. Hover performance (figure of merit) improvement for the advanced design UH-1 rotor.

IN HOVER (O. G. E.)

	STANDARD	ADVANCED	CHANGE	%
FIGURE OF MERIT	0.695	0.766	0.071	10.2
SHAFT HORSEPOWER*	1100	1003	97	8.8
GROSS WEIGHT, LBS*	9336	10000	664	7.1

IN FORWARD FLIGHT

	SPEED, KNOTS		
POWER REDUCTION	60	90	110
SHAFT HORSEPOWER*	137	164	222
PERCENT (%)	19.3	19.7	20.6

\*SEA LEVEL STANDARD ATMOSPHERE

Figure 15. Summary of model UH-1 rotor test results  
(converted to full scale)

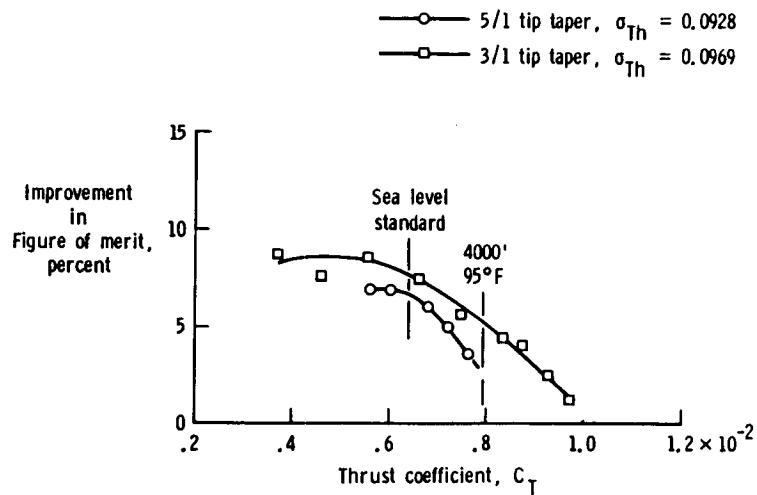


Figure 16. Hover performance improvement for the advanced  
design AH-64 rotor.

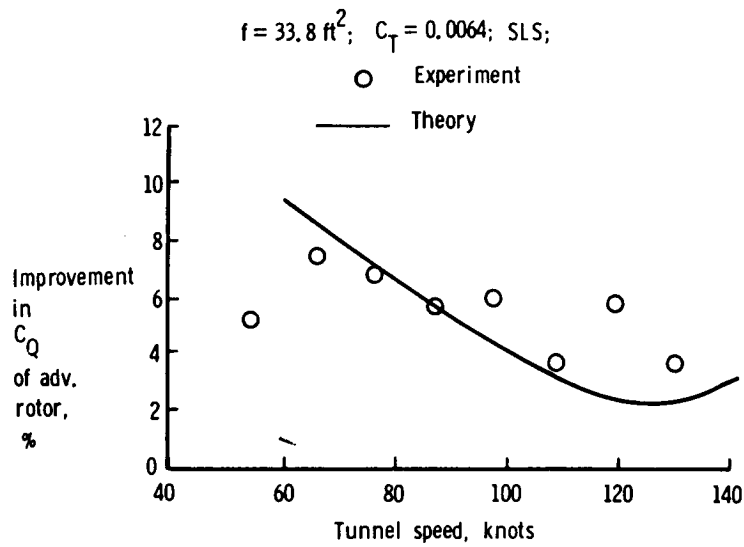


Figure 17. Forward flight performance improvement for the advanced design (5/1 tip taper) AH-64 rotor.

#### PLANFORMS TESTED

NACA 0012 AIRFOIL

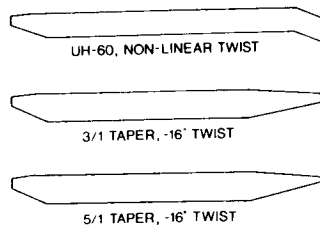


FIGURE OF MERIT

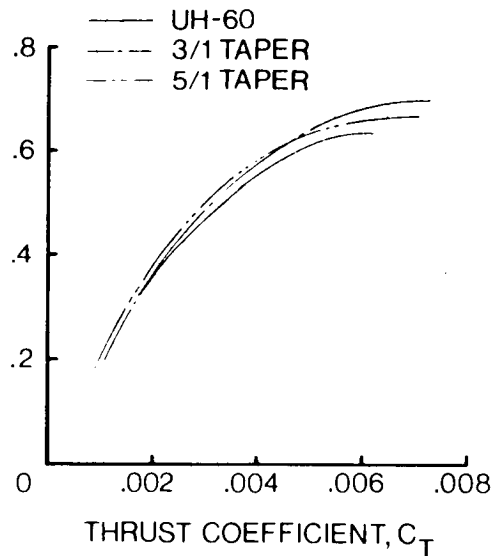


Figure 18. Effect of tip taper ratio on hover performance as measured with the 2MRTS.

ORIGINAL PAGE IS  
OF POOR QUALITY

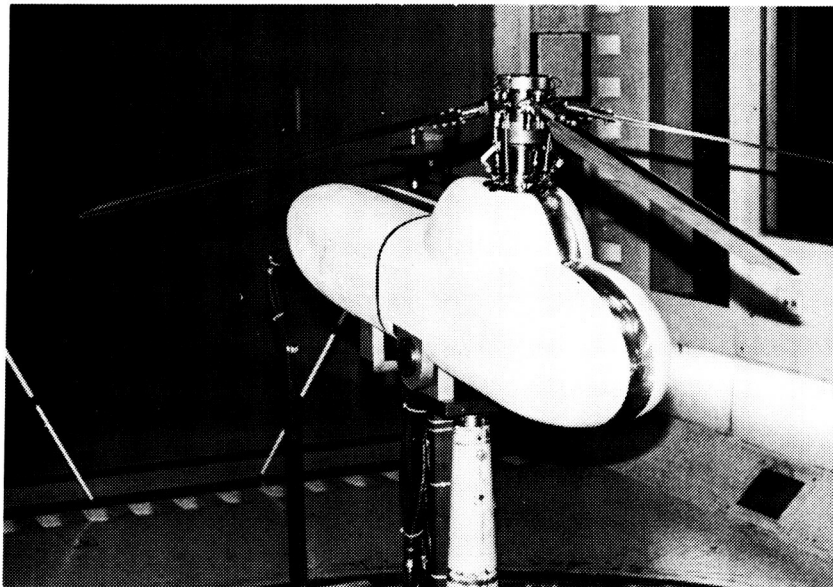


Figure 19. Tapered rotor blade test installation in the University of Maryland wind tunnel.

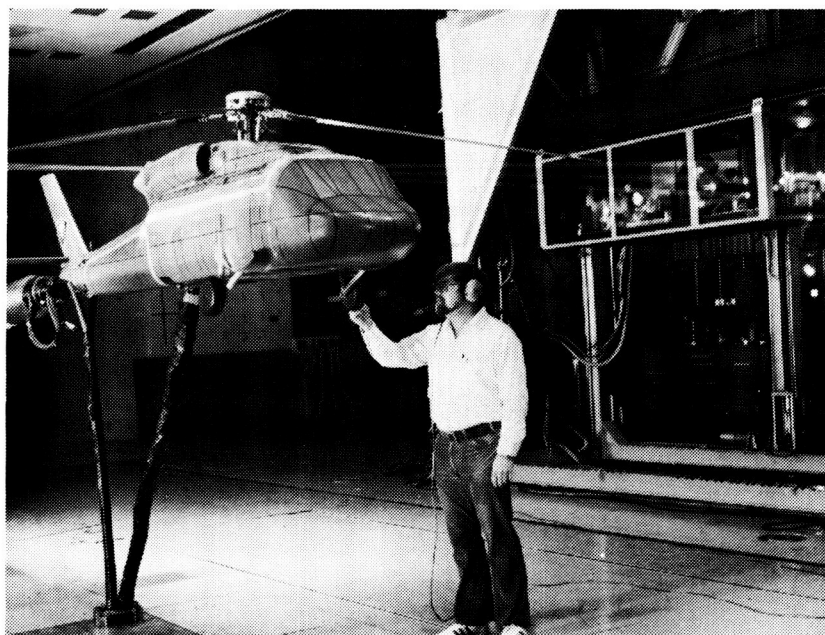
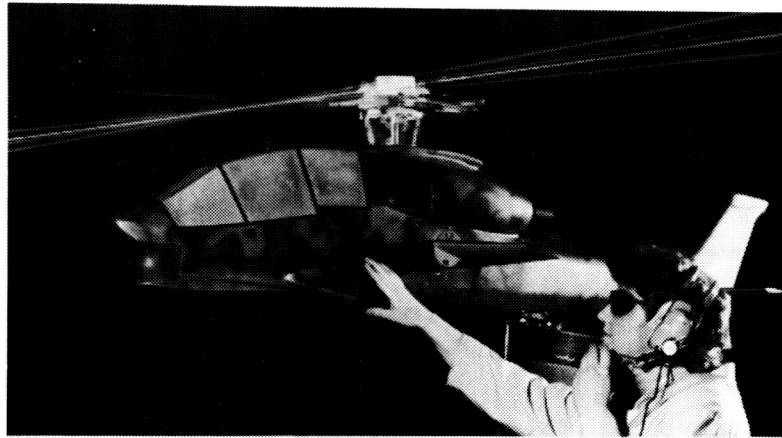
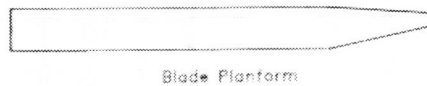


Figure 20. Laser velocimetry installation in the 14- by 22-Foot Subsonic Tunnel.



Rotor System With Laser Velocimeter



Blade Planform

Figure 21. Rotor inflow measurement installation.

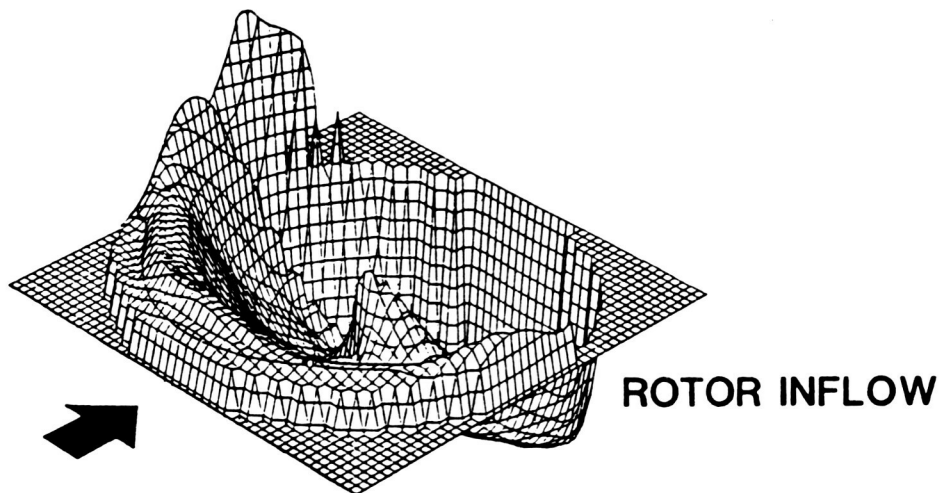


Figure 22. Three-dimensional plotting of measured average inflow velocities normal to rotor tip path plane.

ORIGINAL PAGE IS  
OF POOR QUALITY

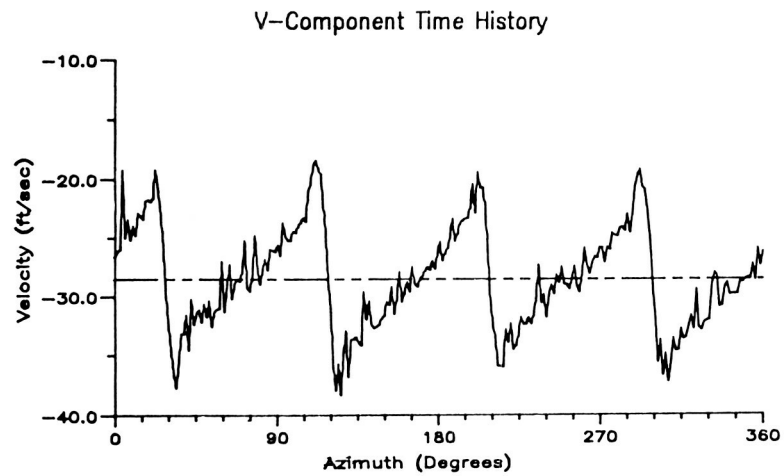


Figure 23. Inflow velocity at a point above the rotor disc  
varying with time.

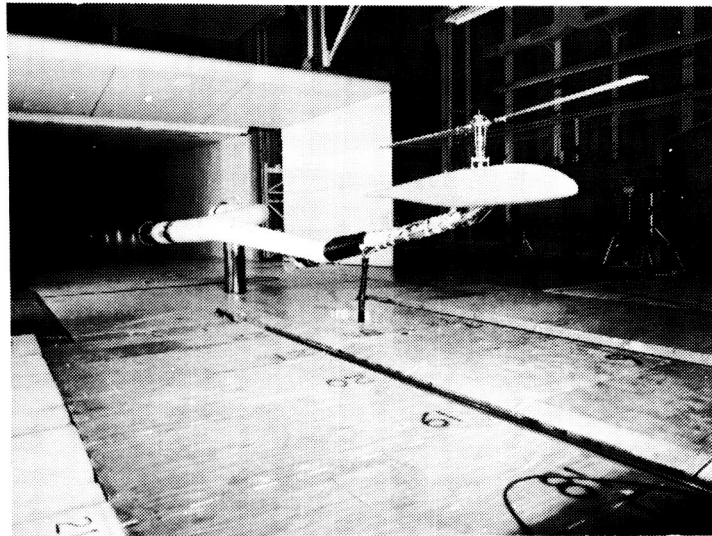


Figure 24. Pressure instrumented rotor installation in the  
14- by 22-Foot Subsonic Tunnel.

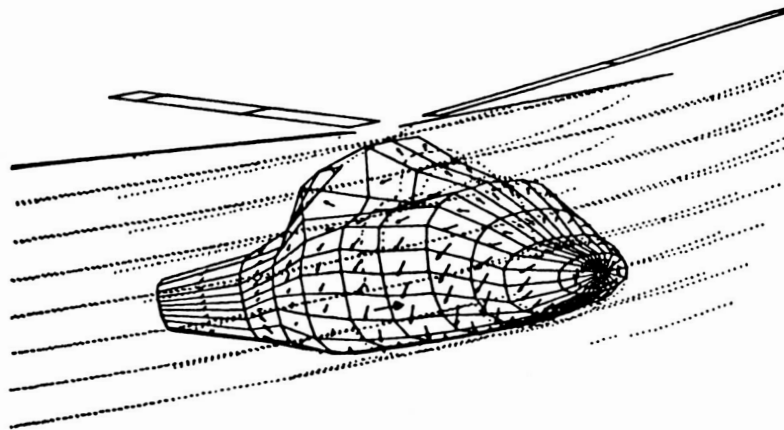


Figure 25. Interactive aerodynamics code development.

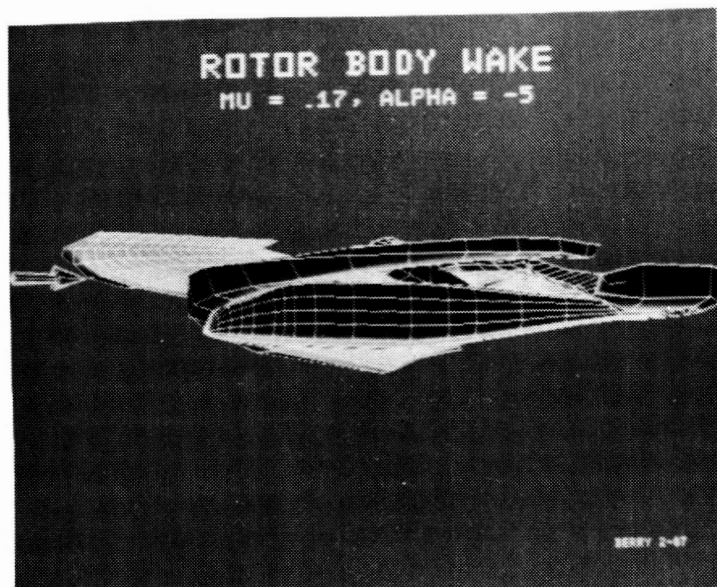


Figure 26. Wake prediction code development.



ORIGINAL PAGE IS  
OF POOR QUALITY

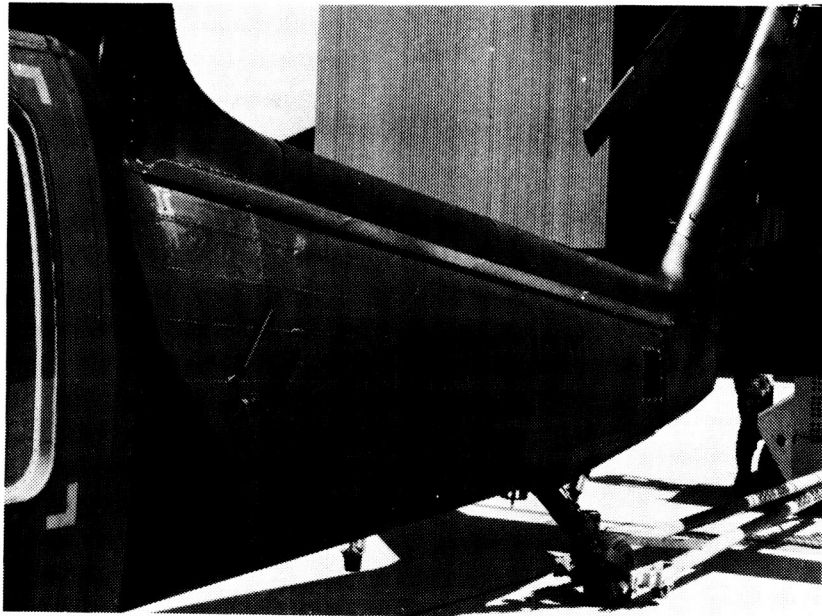


Figure 27. Strake installation on the UH-60 tail boom.

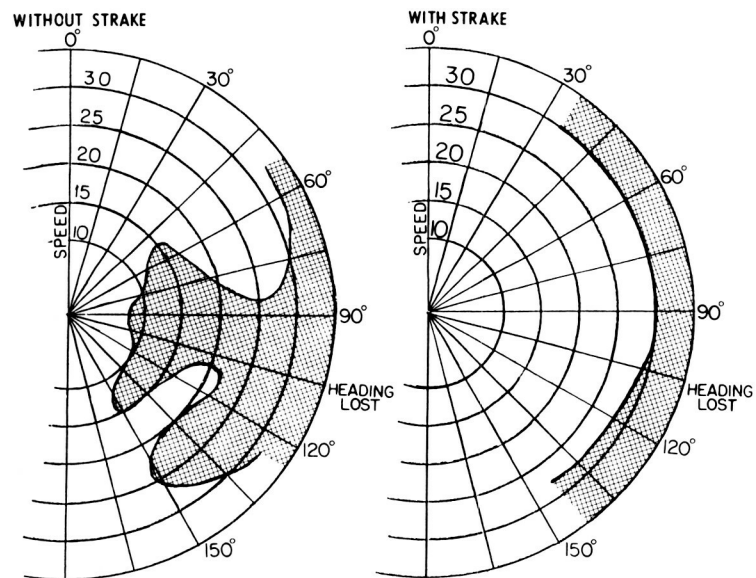


Figure 28. Sideward flight limitation of the SH-3  
alleviated with a strake.

ORIGINAL PAGE IS  
OF POOR QUALITY



Figure 29. AH-64 "tipover" test installation in the  
14- by 22-Foot Subsonic Tunnel.

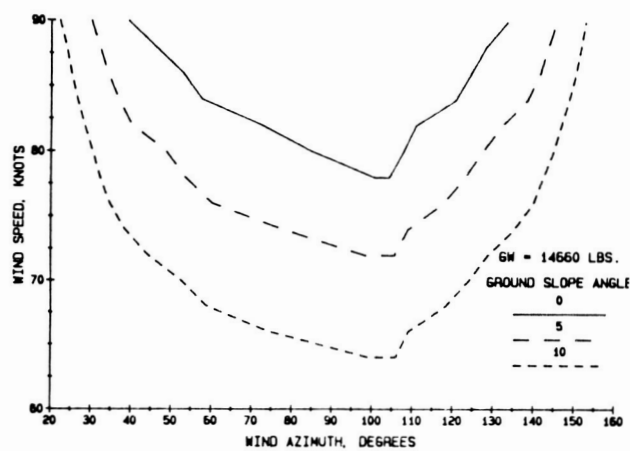


Figure 30. Critical wind velocities and azimuth for a  
parked AH-64.

ORIGINAL PAGE IS  
OF POOR QUALITY

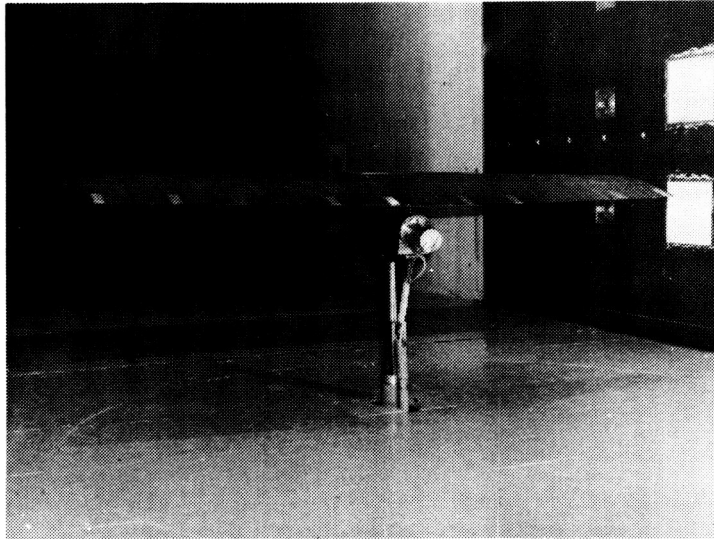


Figure 31. UH-60 stabilator installation in the 14-  
by 22-Foot Subsonic Tunnel.

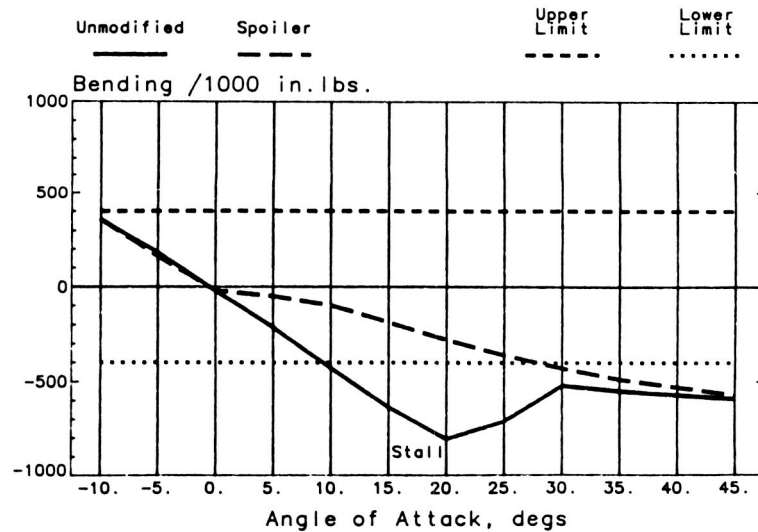


Figure 32. UH-60 stabilator contribution to rotor shaft bending  
moment at a flight speed of 120 knots.

## THE DEVELOPMENT OF CFD METHODS FOR ROTOR APPLICATIONS

F. X. Caradonna and W. J. McCroskey

U.S. Army Aeroflightdynamics Directorate (ARTA)  
Ames Research Center  
Moffett Field, CA 94035-1099

The optimum design of the advancing helicopter rotor for high-speed forward flight always involves a tradeoff of transonic and stall limitations. However, the preoccupation of the rotor industry was primarily concerned with stall until well into the 1970s. This emphasis on stall resulted from the prevalent use of low-solidity rotors with rather outdated airfoil sections. The use of cambered airfoil sections and higher-solidity rotors substantially reduced stall and revealed the advancing transonic flow to be a more persistent limitation to high-speed rotor performance. Work in this area was spurred not only by operational necessity but also by the development of a new tool for the prediction of these flows--the methods of computational fluid dynamics (CFD). The development of CFD for these rotor problems has been a major Army and NASA achievement--accomplished mainly via the original joint Army/NASA agreement at Ames Research Center. This work is now being extended to other rotor flow problems. These developments are outlined in the following discussion.

Development of Rotor Flow Codes

The first Army research on transonic flow began at NASA Ames Research Center in 1970 and closely followed the rapid developments in CFD work at NASA--most notably the work of Steger and Lomax (ref. 1). The first transonic rotor computations, those of Caradonna and Isom (ref. 2), came from this Army research. These computations involved the casting of the potential equation in blade-fixed rotating coordinates and then invoking the classical small perturbation approximation. Solutions were obtained by using the recently developed mixed differencing approach. These were steady, three-dimensional relaxation solutions of nonlifting hovering rotors with rectangular planforms. These computations revealed the onset and development of shocks with increasing radius. The tip relief of these shocks was also shown to be strongly affected by the aspect ratio (fig. 1). This work was extended by Ballhaus and Caradonna (ref. 3) to the treatment of nonrectangular planforms. This work had significant design implications in that it demonstrated that the proper choice of profile and planform are strongly interdependent on one another (fig. 2). The Army computational program was extended by Caradonna and Isom (ref. 4) to the treatment of unsteady flows in 1975. In this work the unsteady three-dimensional, small-disturbance-potential equation was solved. This work was unusual for unsteady solutions in that it used relaxation methods, that is, each time step was solved iteratively. It was shown by this means that transonic flows

are intrinsically unsteady and even a nonlifting transonic rotor flow displays considerable unsteadiness due to the varying incident Mach number that an advancing rotor encounters (fig. 3).

These unsteady computations demonstrated the importance of unsteadiness to the transonic rotor problem. However, the solution method was not very efficient. A more promising approach to unsteady transonic computations was soon developed by Ballhaus and Steger (ref. 5). Their approach was to perform a time linearization of the small perturbation equations. This linearization obviated the need for iteration because the nonlinear coefficients were completely determined by the previous time-step. They further streamlined the method by replacing the relaxation solution with an approximate factorization (AF) algorithm which was applied to the low frequency form of the transonic small-perturbation equations. The AF approach was much faster than relaxation because it imposed no limits on the speed of propagation of numerical information. This approach was soon applied to rotor problems by Caradonna and Philippe (ref. 6). This paper was significant on two accounts: (1) It described rotor computations which simulated the full unsteady-rotor environment, that is, with unsteadiness caused by both Mach number and angle of attack variation (fig. 4). (2) Actually, the most important facet of this paper is that it contained the first experimental confirmation of the unsteady transonic computations (fig. 5). By 1980, this work had been extended to three dimensions (refs. 7, 8) and the development of small perturbation algorithms had essentially reached its present state. Further computational algorithm developments required more exact flow models.

The obvious next step was the development of a full-potential rotor code. This was first accomplished by Arieli and Tauber (ref. 9), who cast the nonconservative, steady full-potential equation in rotating coordinates and modified the fixed wing code, FLO22, to obtain solutions. The resulting code, called ROT22, is probably the most-used finite-difference code in the rotor industry. Its limitation to quasi-steady solutions has not diminished its usefulness to various comparative design studies. However, unsteady full-potential codes have since been developed. One of these codes, developed by Chang, is the outgrowth of a quasi-steady code, TFAR1 (ref. 10), which solves the same nonconservative equation as in the ROT22 code. However, whereas ROT22 used a relaxation procedure, TFAR1 uses an approximate factorization approach. Not only is the AF scheme more efficient, but it is readily extended to include the unsteady terms. This has been done in the code TFAR2 (ref. 11, 12). All of the above full-potential treatments have been nonconservative, that is, mass conservation cannot be guaranteed at shocks. This problem was solved in 1980 by Steger (ref. 13) with the development of an AF algorithm to solve the unsteady, conservative full-potential equations. This algorithm was subsequently developed into the fixed wing code, TUNA, by Bridgeman in 1982 (ref. 14). This code was finally developed into the full-potential rotor code, FPR, by Strawn (ref. 15) in 1986. The code FPR represents the latest and most complete of all the potential rotor codes. Its main limitation (like all potential methods) is an inability to treat shock-induced vorticity or very strong (involving separation) blade/vorticity interactions. For these problems Euler and Navier-Stokes methods are necessary.

Euler rotor codes are still in their infancy. However, a very promising beginning is to be seen in the work of Chang (ref. 16). He has used a centered finite-volume approach to solve the Euler equations in the blade-fixed coordinate frame.

To summarize rotor code development, one must say that it has followed the fixed wing work and has progressed unabated for the past fifteen years. As a result, there are several available codes. The small disturbance code, FDR, which is the simplest and most efficient, models the essential unsteady physics and is accurate for high-Mach-number low-lift solutions. The ROT22 and TFAR1 codes (quasi-steady nonconservative) are the best codes to handle high lift solutions where unsteady effects are not dominant. As TFAR2 is an unsteady code, it has no such limitation; it has produced excellent unsteady results in spite of its nonconservative formulation. The problem of nonconservative formulation has been rectified in the code FPR, which is the most general full-potential code, and is readily available. These potential codes are by far the fastest approach to predict transonic flows. However, for problems entailing very strong shocks or requiring detailed modeling of the near wake, Euler and Navier Stokes methods are required and are under advanced development. TFAR3 (ref. 16) is an outstanding example of this line of development. There is now no lack of available codes. What is required now is the development of the techniques to use these codes in the overall rotor-flow-prediction process.

#### Prediction and Verification of Operational Rotor Flows

The early nonlifting rotor computations could be easily handled by simple grids designed to resolve flow features in the immediate vicinity of the blade surface (fig. 6). At present, all available codes still use such blade-localized grids. Nevertheless, any lifting rotor flow is dominated by a wake system which cannot be contained in such a grid. Figure 7 illustrates the problem for a simple hover flow--the first flow for which this problem was rigorously treated. As indicated in figure 7, several vortices from the wake system may pass through the finite difference grid, but the wake system outside of the grid is significant and must be accounted for. This problem was treated by finding (and including in the boundary conditions) the blade-surface normal velocity induced by this outer wake and then solving the local rotor flow in a manner which includes near-blade vortices. These near vortices have been included in several ways. In reference 17, these vortices were treated by imposing branch cuts, the edges of which were at the required vortex locations. A more general approach (ref. 15) is to reformulate the problem so as to find a blade-induced perturbation about a known vortex-induced velocity distribution. These approaches have been validated by comparison with the hover data of reference 18, which is presently the only supercritical rotor surface-pressure data for which simultaneous wake data are also available. The imposition of this measured wake in these codes has resulted in the excellent comparisons shown in figure 8. Subsequent to these comparisons, excellent comparisons (ref. 16) with these hover data have been obtained solely by the use of an inflow boundary condition. This approach is especially useful in a forward flight computation where the use of a near-field vortex model becomes quite tedious due to the time- and

space-varying vortex geometry relative to the blade. This approach was initially employed in the first true self-trimming, finite-difference rotor computation of Tung, Caradonna and Johnson (ref. 19). This computation was performed by combining the small disturbance code (ref. 8), FDR, with CAMRAD (ref. 20) a complete rotor comprehensive code which employs a detailed vortex wake representation. These codes were coupled by using CAMRAD to determine the blade motion and inflow (in the form of an effective angle of attack) resulting from all of the wake except for the vortex sheet contained in the FDR grid (fig. 9). The loads thus obtained by FDR then determined the vortex filament strengths. This coupling was also marked by an iterative scheme which obviated the need to compute the blade dynamics at every finite-difference time step. The resulting scheme is very efficient and will probably form the basis of future high-speed rotor computations. The above coupling procedure has since been applied using several of the NASA and Army codes including FPR and TFAR2. Figure 10 shows a comparison (ref. 21) of several codes with model operational loads survey (OLS) pressure data. Comparisons of CAMRAD/FPR computations with pressure data from an ONERA three bladed rotor are shown in figure 11. These and many other computations have demonstrated the effectiveness of this approach. Similar comparisons with full-scale flight test data are due for release within the year. It is clear that this analysis method should be highly effective for high-speed-rotor design.

It should be understood that these advancing computations use an approximate vortex model (that is, the use of a surface inflow induced by the wake vorticity). This approximation seems to work well for high advance-ratio conditions in which the wake of previous blades is well removed from the rotor. However, a sizable number of relatively high advance-ratio cases are known where the rotor wake is close and strong enough to induce considerable vibratory airloading. This problem has spurred a number of recent efforts to perform more exact computational treatments of blade vortex interactions (BVI).

### Blade Vortex Interaction

The strong interaction between a segment of a rotor blade and concentrated tip vortices in the wake is an important source of noise and vibration at low and moderate flight speeds. The limiting case of a vortex intersecting a rotor blade with its axis parallel to the leading edge of the blade, while fundamentally unsteady, is relatively simple for theoretical and numerical analysis, and it has been the subject of several recent investigations. These studies, which were reviewed recently in more detail by Srinivasan and McCroskey (ref. 22), have established the basic features of blade-vortex interactions, and they provide a choice among alternative methods that range from transonic small-disturbance to Navier-Stokes formulations for calculating such interactions.

Within this hierarchy of equations and solution algorithms, three basic methods of introducing a concentrated vortex into a computational domain have been employed. The most straightforward approach is (1) to specify initially the complete velocity and pressure field produced by the vortex when it is some distance upstream of the

blade, and then (2) to rely on the properties of the numerical method to maintain the correct vortex structure, and (3) to compute the subsequent interaction as the solution advances in time. Unfortunately, most numerical methods include artificial, numerical dissipation to improve their stability and convergence properties. As a result, the steep gradients within the vortex are diffused more rapidly by the numerics than by physical viscosity, unless excessively fine computational grids are used, and the computed blade-vortex interaction is seriously weakened and in error. Only within the past few months has a numerical scheme emerged that overcomes this difficulty, that of Rai (ref. 23), which is described later.

Consequently, two alternate methods were developed in previous years, in which the vortex is modeled to some extent. (1) The first of these was the branch-cut method (ref. 17), which can be used for potential flows. In addition to the usual branch cut that extends downstream of the trailing edge of the airfoil, a second branch cut is introduced between the vortex and an outer boundary of the flow field, and a jump in velocity potential equal to the strength of the vortex is prescribed across this second branch cut. The flow remains irrotational outside the airfoil and vortex branch cuts, and the governing equation and boundary conditions remain unchanged. However, if the vortex moves through the flow field, the logic of the numerical code must allow its branch cut to move accordingly. The numerical calculations seem to be sensitive to this motion, especially for strong interactions.

(2) The second approach is the prescribed-disturbance method, sometimes called the dual or split-potential method, although it is not restricted to potential flow. In this approach, the velocity field is split into a prescribed part, which represents the "free stream" plus an isolated vortex moving through the flow field, and the remainder that is to be determined and which results from the interaction of the vortex and the airfoil or blade. The resulting finite-difference equations are slightly more complicated, and the entire vortex field must be computed at every grid point and at every time step, thereby increasing the CPU time slightly. However, the method is stable and accurate, and an arbitrary vortex-core structure can be prescribed. The principal limitation of both modeling methods is that they ignore any changes in the structure of the vortex caused by the encounter with the blade. Rai's method (ref. 23) has no such restriction, and, as will be shown later, he has been able to compute a head-on collision between a vortex and an airfoil.

Representative two-dimensional results from References 22 and 25 are shown in figures 12 and 13 for a symmetrical airfoil section at transonic speeds. Figure 12 shows the distortions in the chordwise pressure distributions on the airfoil as the vortex passes underneath, computed by a thin-layer Navier-Stokes code with a solution-adaptive grid, which greatly improves the resolution by placing the most grid points in the regions of highest gradients. The changes in the grid with time are shown in the middle of the figure, and the Mach contours at the bottom help to delineate the flow-field details. These results illustrate that strong gradients in pressure occur with respect to both time and space, because of the vortex encounter. These gradients can be especially significant in the leading-edge region of a thin airfoil.



Figure 13 compares the fluctuating lift on the airfoil computed by transonic small-disturbance (ref. 22) (George, A. R. and Lyrantzis, A., private communication, Moffett Field, CA), full-potential (ref. 25), Euler (Sankar, N. L., Tang, W., and Hsu, T., private communication, Moffett Field, CA) and thin-layer Navier-Stokes codes (ref. 24) at Ames and elsewhere (refs. 22, 25, 26). This is a case with strong nonlinear and unsteady effects, but not severe enough to include boundary-layer separation. The various results are approximately the same for lift, although the instantaneous pressure distributions and shock-wave positions differ more (ref. 22).

The aforementioned head-on encounter, computed by Rai (ref. 23) with a Navier-Stokes code, is shown in figure 14. The vorticity contours indicate the vortex itself and the viscous boundary layer next to the airfoil, and the splitting of the vortex above and below the airfoil is clearly evident. Although there is no shock wave in this subsonic case, this kind of head-on interaction can currently be treated only by this code. The main disadvantage of this code is that it takes about two or three times as much CPU time than the prescribed-disturbance Navier-Stokes code on a comparable grid, and at least 50 times more than the transonic small-disturbance code.

The computational efficiency of the small-disturbance codes means that many more calculations can be performed on a given computational grid, or that much finer grids can be used without excessive CPU costs. This, in turn, has led to their use in exploring the radiating pressure field several chord-lengths away from the airfoil, i.e., BVI noise. Baeder et al. (ref. 26) combined CFD and aeroacoustics concepts in studying this problem, producing the results shown in figure 15. These disturbance-pressure contours exhibit a fidelity unmatched in other investigations. Their results indicate a dramatic sensitivity of the radiated sound to Mach number, but a surprising insensitivity to airfoil shape. Continuing research on this subject is employing other codes and computational grids.

The step from two dimensions to three is enormous, but it must be made for practical rotorcraft problems. The first efforts were by Strawn and Tung (ref. 27), who used a full-potential code to examine special experimental cases run at the Aeroflightdynamics Directorate (ref. 28). Figure 16 shows the rotor-vortex experiment, and figure 17 is a comparison of computed and measured pressure distributions for a difficult, highly-transonic case. Although the agreement is not perfect, the essence of the phenomenon is clearly captured by the numerical results. Extensions to the pressure field off the blade are under way.

### Viscous Transonic Airfoil Characteristics

The NASA-Ames code ARC2D (ref. 29) has been used in reference 30 to calculate the transonic viscous flow of helicopter profiles, based on the thin-layer Reynolds-averaged Navier Stokes equations, with an algebraic eddy-viscosity model to approximate boundary-layer turbulence. Figure 18 shows representative results for combinations of Mach numbers and angles of attack that produce significant nonlinear behavior and shock-wave/boundary-layer interaction. The numerical results reproduce

the experimentally observed airfoil behavior across the transonic regime. Also, the details of the computed flow fields provide new insights into transonic airfoil behavior under conditions for which accurate measurements are difficult to obtain and are often tainted by wall-interference effects.

Figure 18 shows the lift behavior at low angles of attack, including the loss of lift that occurs when significant separation is induced by the shock wave in the Mach number range,  $0.83 < M < 0.93$  for the NACA 0012 airfoil. The drag rise in the transonic regime is also shown. The abrupt change in pitching-moment behavior, known as "Mach tuck," is illustrated in figure 19. In all cases, the numerical results seem to be as reliable as wind tunnel data. However, the accurate prediction of maximum  $C_L$  remains a formidable challenge.

### Tip Vortex Formation

The importance of blade-vortex interactions for rotorcraft has led to many ad hoc attempts to alter the structure of the tip vortices. With the recent advent of several three-dimensional Navier-Stokes pilot codes, computational fluid dynamics offers a new tool for this problem. Preliminary results seem very promising.

Srinivasan et al. (ref. 31) recently examined four planforms of nonrotating wings and computed the details of their tip vortex formation. Fair agreement was obtained with the limited available experimental data, e.g., figure 20, although questions remain concerning the grid resolution and the validity of the turbulence model used.

Figure 21 shows the pressure distributions computed on a swept rotor-blade tip in a nonrotating environment. The beneficial effects of leading-edge sweep were demonstrated by comparisons with the same blade with a straight leading edge and the same taper distribution; this blade had a much stronger shock wave and considerable boundary-layer separation. However, it was found that the tip vortex on the swept-tip blade was much more concentrated and had higher peak velocities than the straight leading-edge blade. Therefore, there appears to be much room for planform optimization when both aerodynamic performance and tip-vortex structure are involved.

### Aerodynamics of Complete Rotorcraft Configurations

Computational fluid dynamics is incapable today of treating realistic combinations of rotors and bodies. However, algorithms are constantly improving, the rotorcraft industry is beginning to use and gain valuable experience with modern CFD codes, and supercomputer technology is advancing at a dazzling pace. The principal pacing items are algorithm improvements and adaptations to the peculiar features of rotorcraft, turbulence modeling, vortex wake modeling, grid generation; memory size and speed of current supercomputers, user familiarity in the rotorcraft industry, and management acceptance of the potential of CFD, notwithstanding the substantial investment required in manpower, software, and hardware.

In anticipation of future supercomputer capabilities, the Army and NASA have already begun laying the foundation for eventual computational analysis of complete configurations. A first step is creating computational grids on a combination of rotating blades and a nonrotating body, such as a fuselage or tail fin. Figure 22 shows the most promising grid topology that has emerged so far. Here a zonal, or block, grid strategy is employed, in which body-conforming grids are embedded within rotating and nonrotating cylindrical blocks. The cylinders provide the simplest and most accurate topology for passing computed information across the boundary between the rotating and nonrotating solid bodies, whereas other block topologies are more appropriate for computing the flow near the surfaces and in the near wakes.

Finally, the rotorcraft industry stands to benefit enormously from NASA's investment in computational aerodynamics and supercomputer technology in the National Aerodynamic Simulation program (NAS). This multimillion-dollar large-scale computer system, indicated schematically in figure 23, will provide a national computational capability for NASA, the Department of Defense, industry, other government agencies, and universities. Several rotorcraft projects have already been accepted for the NAS program. The vigorous pursuit of computational aerodynamics for rotorcraft applications will benefit all segments of our industry.

#### Concluding Remarks

Over the past fifteen years, the Army and NASA research groups at Ames Research Center have developed a wholly new approach to rotor flow prediction. This work has included the development of a number of rotary wing computational fluid dynamics (CFD) codes, which are now seeing extensive industrial use. With these codes it is now practical to perform many complete rotor computations which include transonic unsteady and three-dimensional effects without recourse to empiricisms and extensive data libraries. These tools permit a new level of high-speed-rotor design capability.

Although the high-speed-flow methods are now becoming operational, there are a number of significant flow problems which remain and can best be treated by CFD. Stall is one of the foremost of these problems. Although this problem has been neglected of late, it remains the primary limiter to rotor lifting capability. New Navier-Stokes codes will ultimately permit an understanding of three dimensional stall effects. Another area which requires much work concerns interactional aerodynamics, including various blade-vortex, main-rotor/tail-rotor and rotor-fuselage interactions. A developing understanding and ability to predict these effects will enable substantial control and design for vibratory loading.

The potential payoff for future rotor CFD developments remains high. As in the past, however, these developments will require the combination of computational, experimental, and operational capabilities which are found in the Army and NASA rotor research organizations.

## References

1. Steger, J. L.; and Lomax, H.: Transonic Flow About Two-Dimensional Airfoils by Relaxation Procedures. AIAA J., vol. 10, no. 1, Jan. 1972, pp. 49-54.
2. Caradonna, F. X.; and Isom, M. P.: Subsonic and Transonic Potential Flow Over Helicopter Rotor Blades. AIAA J., vol. 10, Dec. 1972, pp. 1606-1612.
3. Ballhaus, W. F.; and Caradonna, F. X.: The Effect of Planform Shape on the Transonic Flow Past Rotor Tips. Aerodynamics of Rotary Wings, AGARD CP-111, Feb. 1973.
4. Caradonna, F. X.; and Isom, M. P.: Numerical Calculation of Unsteady Transonic Potential Flow Over Helicopter Rotor Blades. AIAA J., vol. 14, no. 4, Apr. 1976.
5. Ballhaus, W. F.; and Steger, J. L.: Implicit Approximate Factorization Schemes for the Low-Frequency Transonic Equation. NASA TM X-73082, Nov. 1975.
6. Caradonna, F. X.; and Philippe, J. J.: The Flow Over a Helicopter Blade Tip in the Transonic Regime. Vertica, vol. 2, 1978, pp. 43-60.
7. Caradonna, F. X.; and Steger, J. L.: Implicit Potential Methods for the Solution of Transonic Rotor Flows. Proceedings of the Army Numerical Analysis and Computers Conference. ARO Rep. 80-3, Aug. 1980.
8. Chattot, J. J.: Calculation of Three-Dimensional Unsteady Transonic Flows Past Helicopter Blades. NASA TP-1721, 1980.
9. Arieli, R.; and Tauber, M. E.: Computation of Subsonic and Transonic Flow About Lifting Rotor Blades. AIAA Paper 79-1667, Aug. 1979.
10. Chang, I-Chung: Transonic Flow Analysis for Rotors - Part I. Three-Dimensional, Quasi-Steady, Full-Potential Calculation. NASA TP-2375, 1984.
11. Chang, I-Chung: Transonic Flow Analysis for Rotors - Part II. Three-Dimensional, Unsteady, Full-Potential Calculation. NASA TP-2375, 1985.
12. Chang, I-Chung; and Tung, C.: Numerical Solution of the Full-Potential Equation for Rotors and Oblique Wings Using a New Wake Model. AIAA Paper 85-0268, Jan. 1985.
13. Steger, J. L.; and Caradonna, F. X.: A Conservative Implicit Finite Difference Algorithm for the Unsteady Transonic Full Potential Equation. AIAA Paper 80-1368, Snowmass, CO, 1980.

14. Bridgeman, J. O.; Steger, J. L.; and Caradonna, F. X.: A Conservative Finite-Difference Algorithm for the Unsteady Transonic Potential Equation in Generalized Coordinates. AIAA Paper 82-1388, Aug. 1982.
15. Strawn, R. C.; and Caradonna, F. X.: Numerical Modeling of Rotor Flows with a Conservative Form of the Full-Potential Equations. AIAA Paper 86-0079, Jan. 1986.
16. Chang, I. C.; and Tung, C.: Euler Solution of the Transonic Flow for a Helicopter Rotor. AIAA Paper 87-0523, AIAA 25th Aerospace Sciences Meeting, Jan. 1987.
17. Caradonna, F. X.; Desopper, A.; and Tung, C.: Finite Difference Modeling of Rotor Flows Including Wake Effects. J. Am. Hel. Soc., vol. 29, no. 2, Apr. 1984.
18. Caradonna, F. X.; and Tung, C.: Experimental and Analytical Studies of a Model Helicopter Rotor in Hover. NASA TM-81232, 1981.
19. Tung, C.; Caradonna, F. X.; and Johnson, W. R.: The Prediction of Transonic Flows on an Advancing Rotor. AHS J., vol. 31, no. 3, July 1986, pp. 4-9.
20. Johnson, W.: A Comprehensive Analytical Mode of Rotorcraft Aerodynamics and Dynamics, Part 1, Analysis Development. NASA TM-81182, 1980.
21. Caradonna, F. X.; and Tung, C.: A Review of Current Finite Difference Rotor Flow Methods. AHS 42nd Annual Forum Proceedings. June 2-4, 1986, Washington, DC.
22. Srinivasan, G. R.; and McCroskey, W. J.: Numerical Simulations of Unsteady Airfoil-Vortex Interactions. Vertica, vol. 10, no. 5, 1986.
23. Rai, M. M.: Navier-Stokes Simulations of Blade-Vortex Interaction Using High-Order Accurate Upwind Schemes. AIAA Paper 87-0543, 1987.
24. Srinivasan, G. R.; McCroskey, W. J.; and Baeder, J. D.: Aerodynamics of Two-Dimensional Blade-Vortex Interaction. AIAA J., vol. 24, no. 10, pp. 1569-1576, Oct. 1986.
25. Jones, H. E.; and Caradonna, F. X.: Full-Potential Modeling of Blade-Vortex Interactions. 12th European Rotorcraft Forum, Paper no. 27, Sept. 1986.
26. Baeder, J. D.; McCroskey, W. J.; and Srinivasan, G. R.: Acoustic Propagation Using Computational Fluid Dynamics. AHS 42nd Annual Forum, Washington, June 1986.
27. Strawn, R. C.; and Tung, C.: The Prediction of Transonic Loading on Advancing Helicopter Rotors. AGARD CP-412, Paper no. 7, 1986.

28. Caradonna, F. X.; Tung, C.; and Laub, G.: An Experimental Study of the Parallel Blade Vortex Interaction. 10th European Rotorcraft Forum, The Hague, Netherlands, Aug. 1984.
29. Pulliam, T. H.; and Steger, J. L.: Recent Improvements in Efficiency, Accuracy, and Convergence for Implicit Approximate Factorization Algorithms. AIAA Paper 85-0360, 1985.
30. McCroskey, W. J.; Baeder, J. D.; and Bridgeman, J. O: Calculation of Helicopter Airfoil Characteristics for High-Tip Speed Applications. J. AHS, vol. 31, no. 2, pp. 3-9, Apr. 1986.
31. Srinivasan, G. R.; McCroskey, W. J.; Baeder, J. D.; and Edwards, T. A.: Numerical Simulation of Tip Vortices of Wings in Subsonic and Transonic Flow. AIAA Paper 86-1095, May 1986.

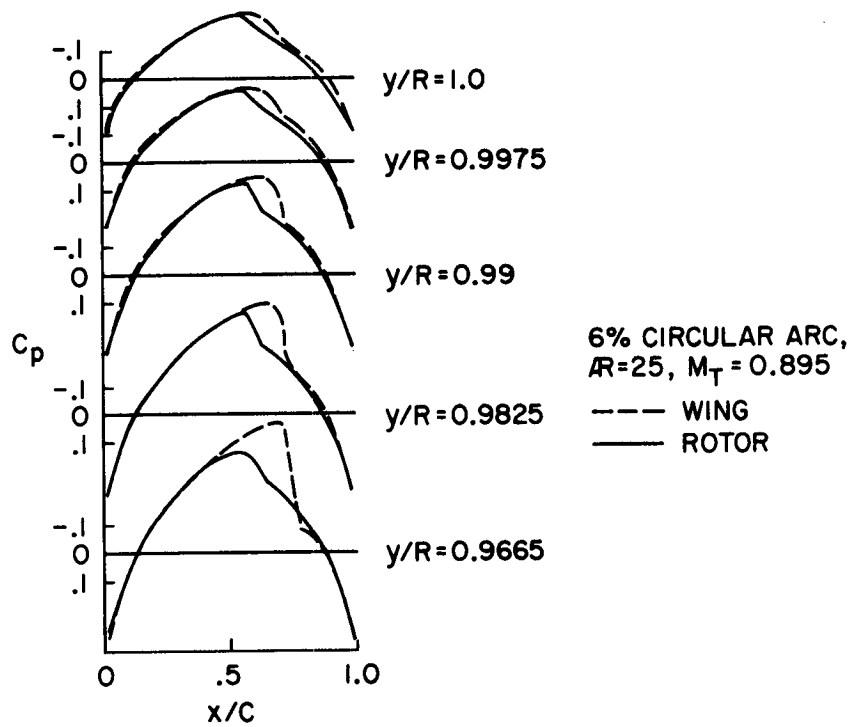


Figure 1(a).- Comparison of wing and rotor transonic flows. Such studies were first made possible by the development of CFD in the early 1970s.

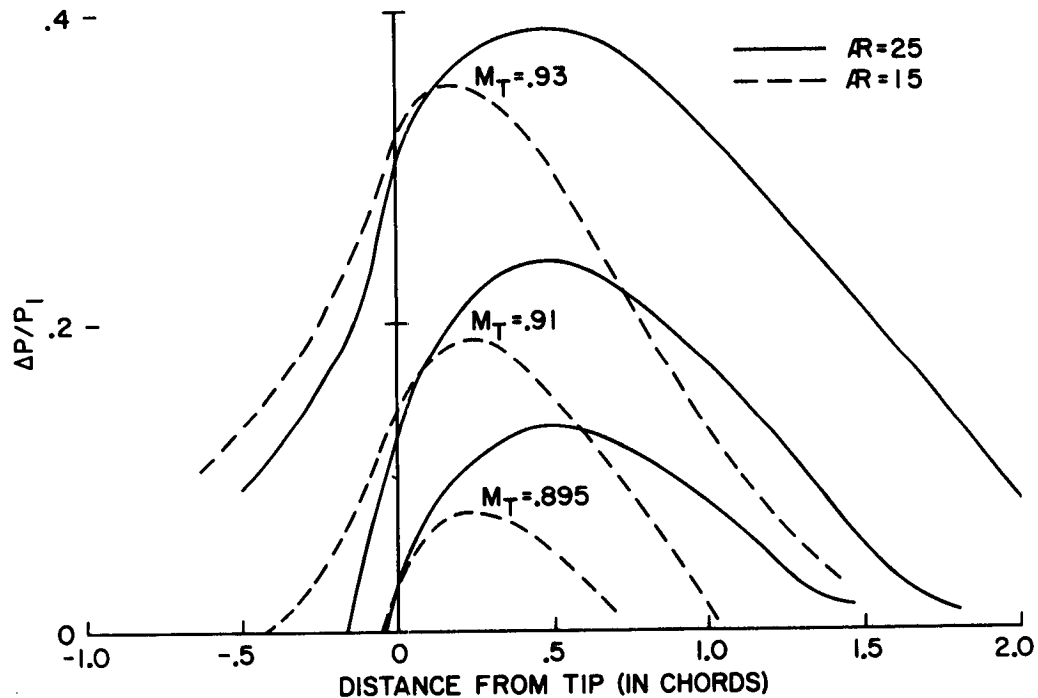


Figure 1(b).- Comparison of shock strength as functions of aspect ratio, rotor radius, and tip Mach number. The lower aspect ratios produce weaker shocks on the blade but stronger shocks off the blade. This early computational result has performance and acoustic implications which are not yet fully realized today.

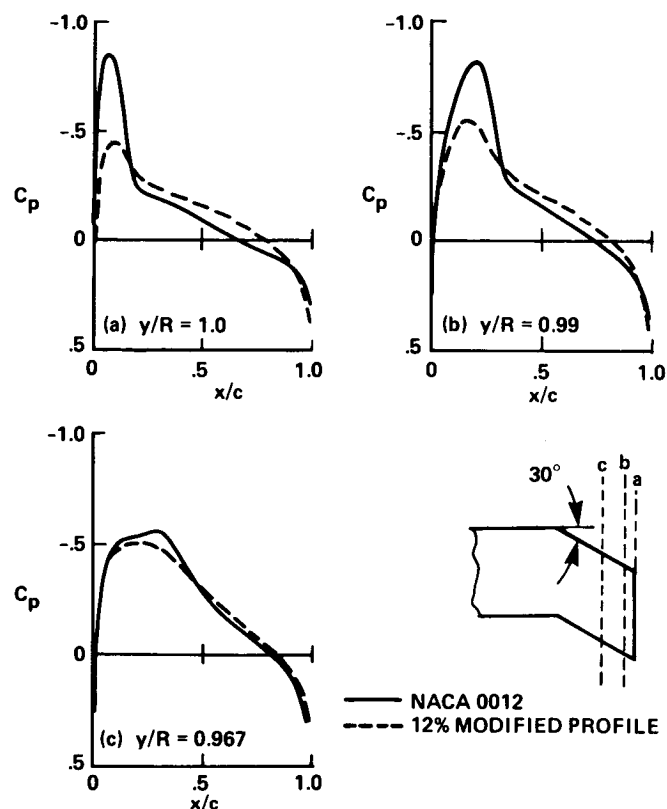


Figure 2.- Computed pressure distributions for a swept-tip planform. The NACA 0012 is seen to be unsuitable at the tip of this planform. Moving the maximum thickness point rearward at a point near the tip removes the strong shock there.

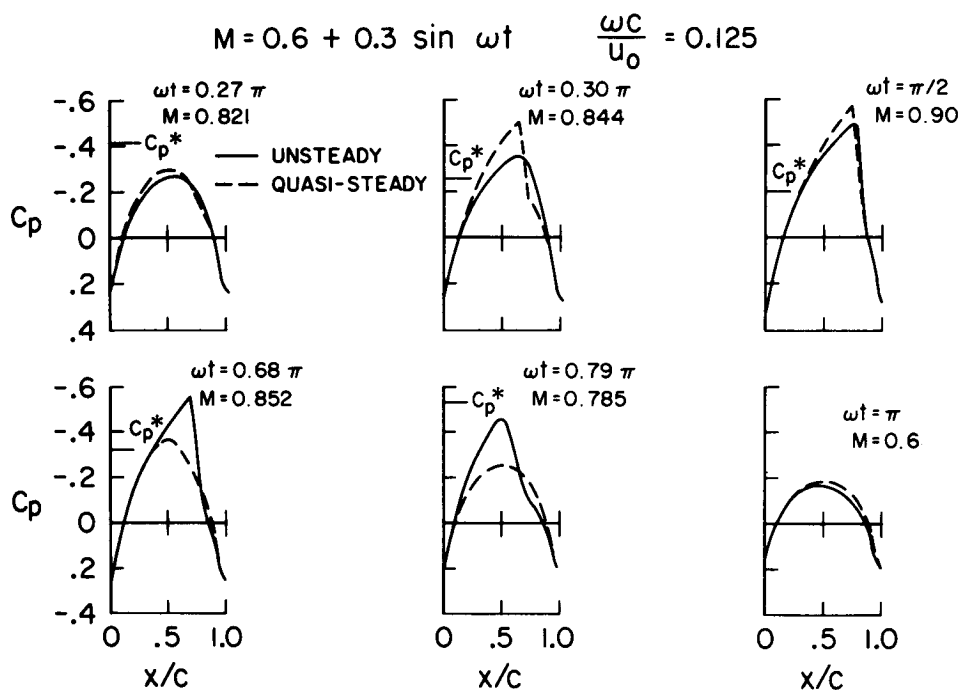


Figure 3.- The first computations of three-dimensional, unsteady rotor flows in the mid-70s showed a pronounced difference between steady and unsteady results.



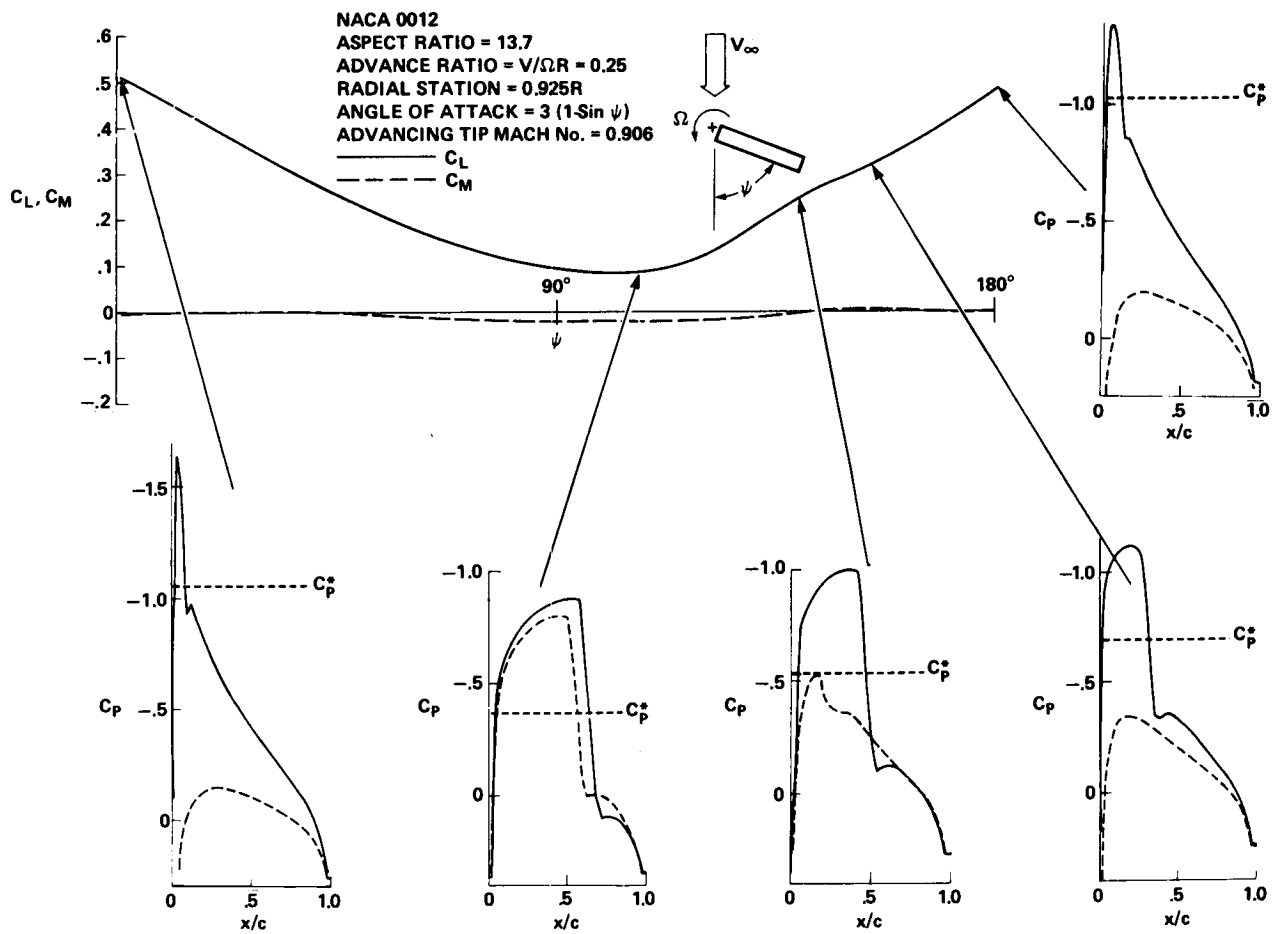


Figure 4.- A computed load variation on a helicopter rotor. By the later 1970s, hypothetical computations included both the effects of varying Mach number and lift. These computations further demonstrated the importance of unsteadiness.

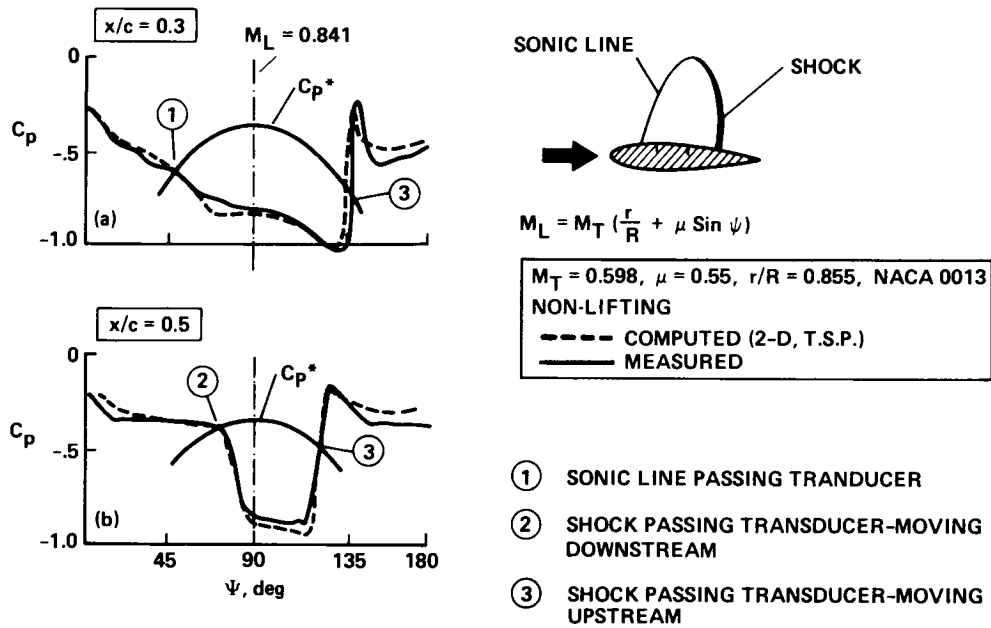


Figure 5.- The first experimental verification of computed transonic rotor flows. This nonlifting comparison further demonstrates transonic unsteadiness in the asymmetric shock motion about  $\psi = 90^\circ$ .

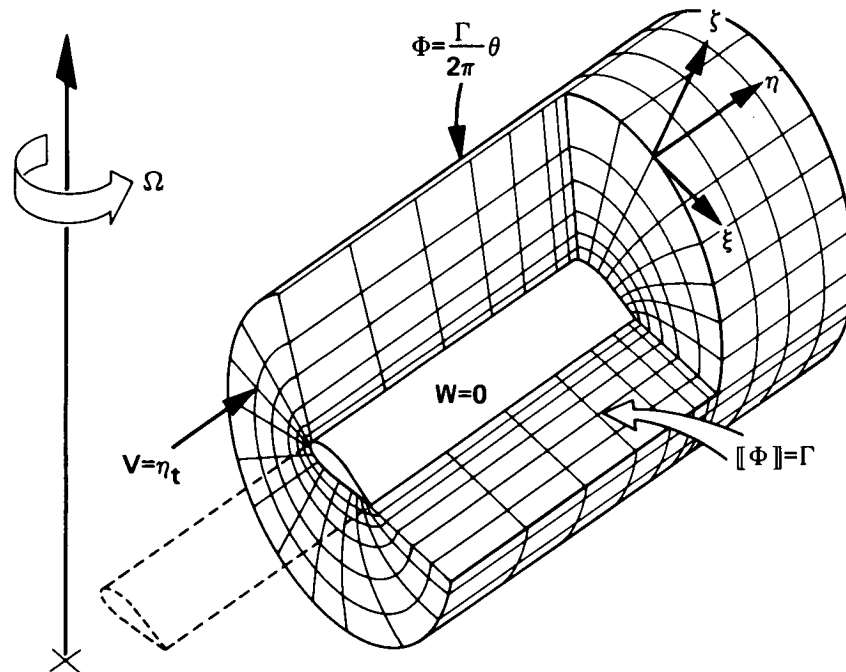


Figure 6.- Grid and boundary conditions for a local rotor computation. Up to the present all rotor CFD computations use a grid topology which is designed only to resolve flows near the blade surface.

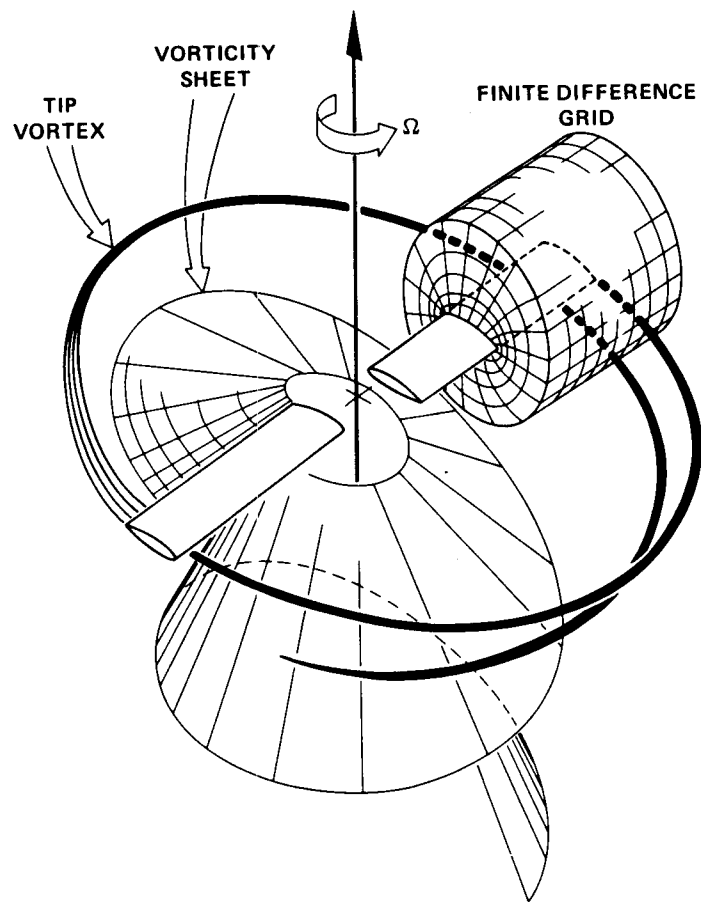


Figure 7.- A finite-difference grid embedded in a global flow region. The local blade grid can resolve only the most immediate wake features. These features must be accounted for by means other than grid resolution.

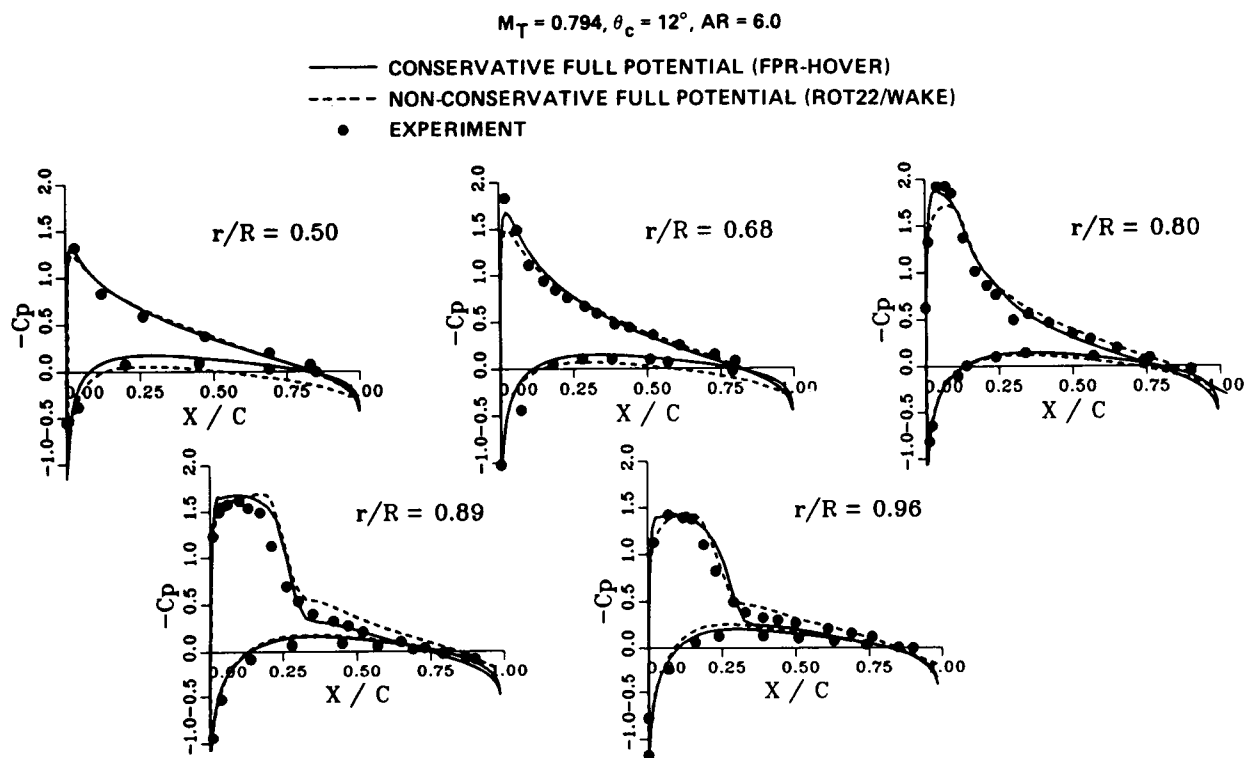


Figure 8.- Experimental verification of transonic computations for a hovering rotor. These computations employ various schemes to model the near and far wake details.

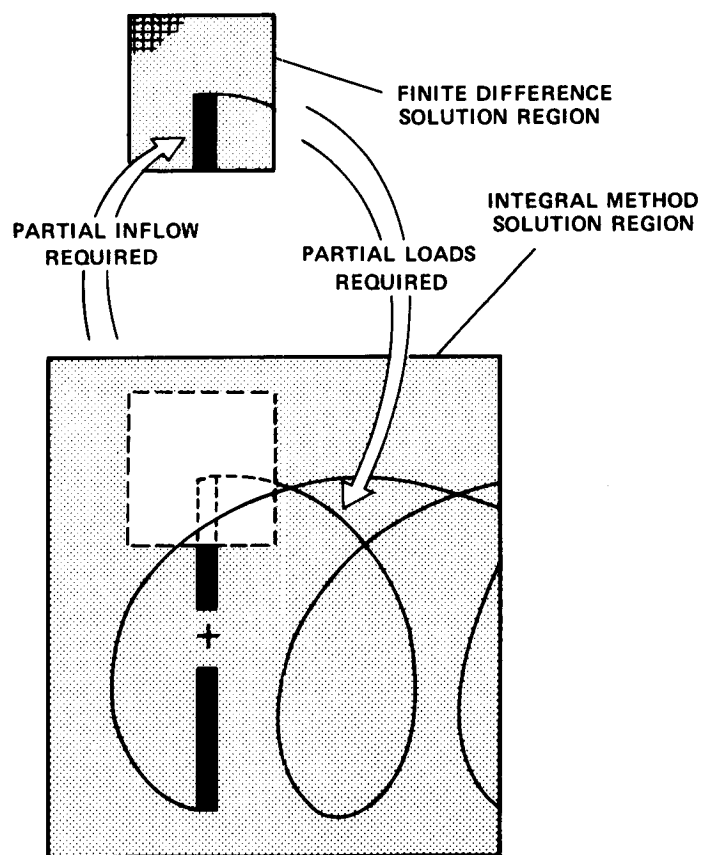


Figure 9.- Matching of local grids with advancing rotor wake system.

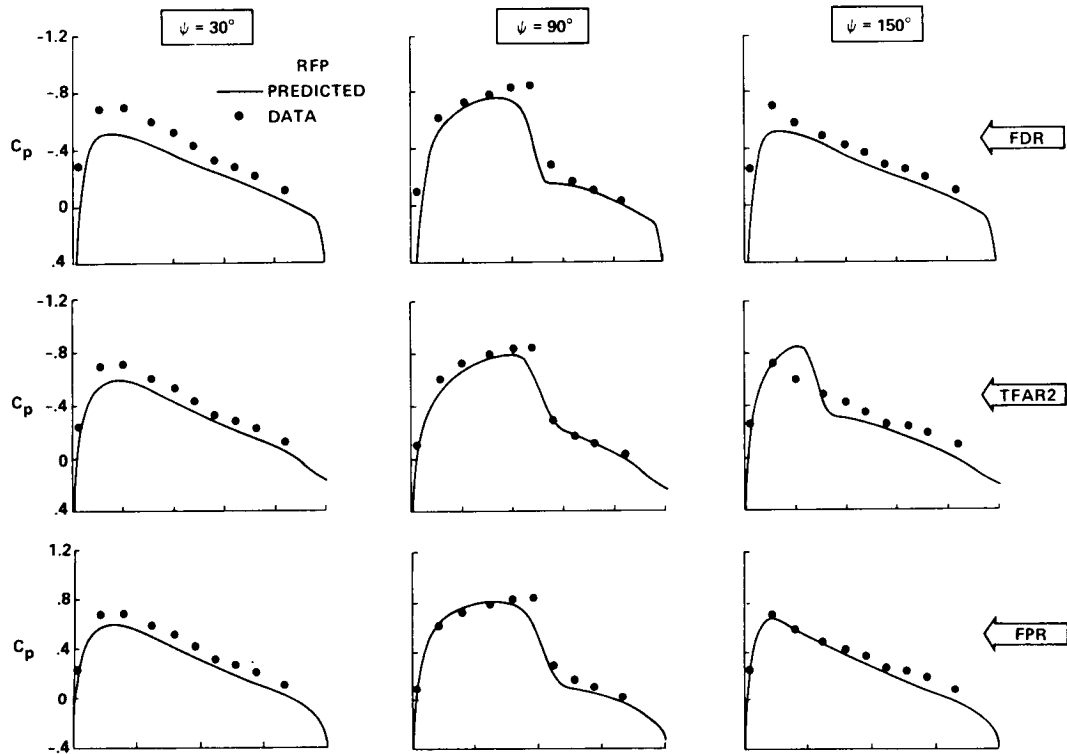


Figure 10.- A comparison of various computations with nonlifting rotor data.

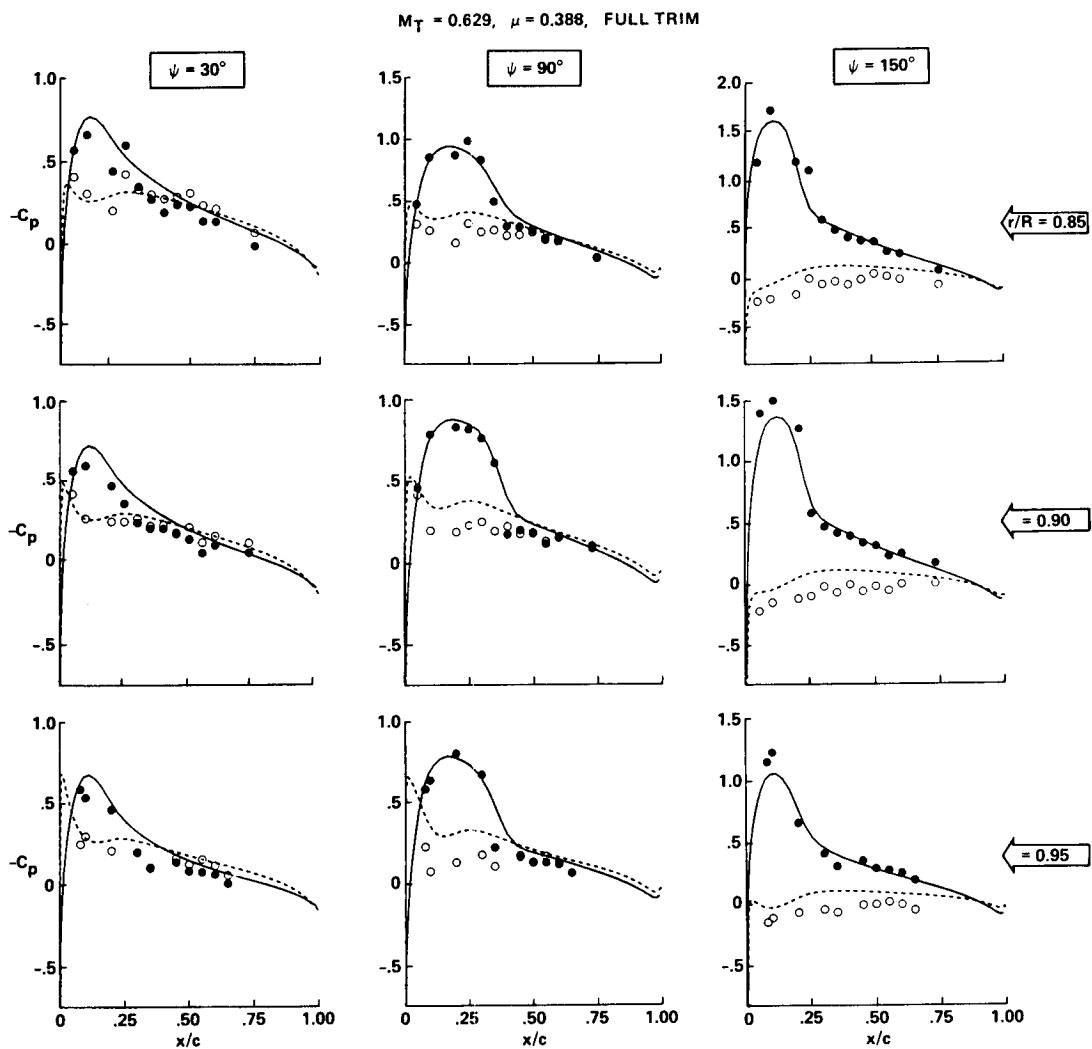


Figure 11.- A comparison of CAMRAD/FPR computations with lifting rotor data--ONERA 3-blade model.

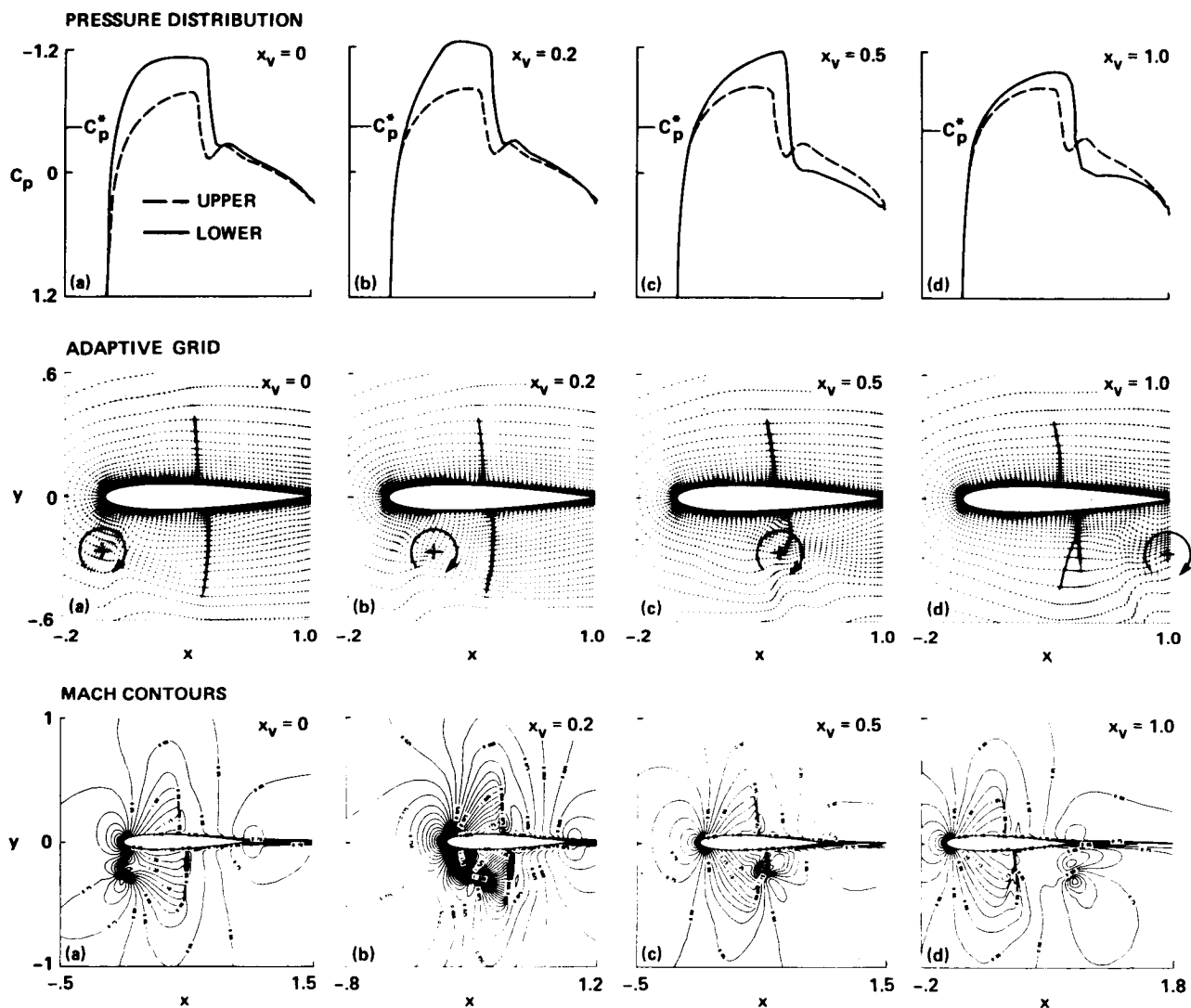


Figure 12.- Instantaneous surface pressure distributions, adaptive grid, and pressure contours for airfoil-vortex interaction; NACA 0012,  $M_\infty = 0.80$ ,  $\alpha = 0$ ,  $\Gamma_v = 0.20$ ,  $y_v = -0.26$ .



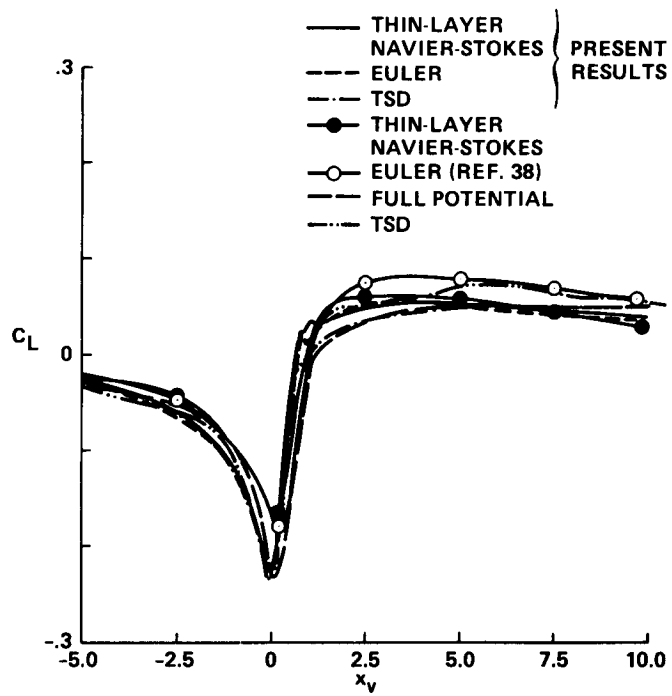


Figure 13.- Comparison of calculated lift coefficients from different methods for the case of figure 12.

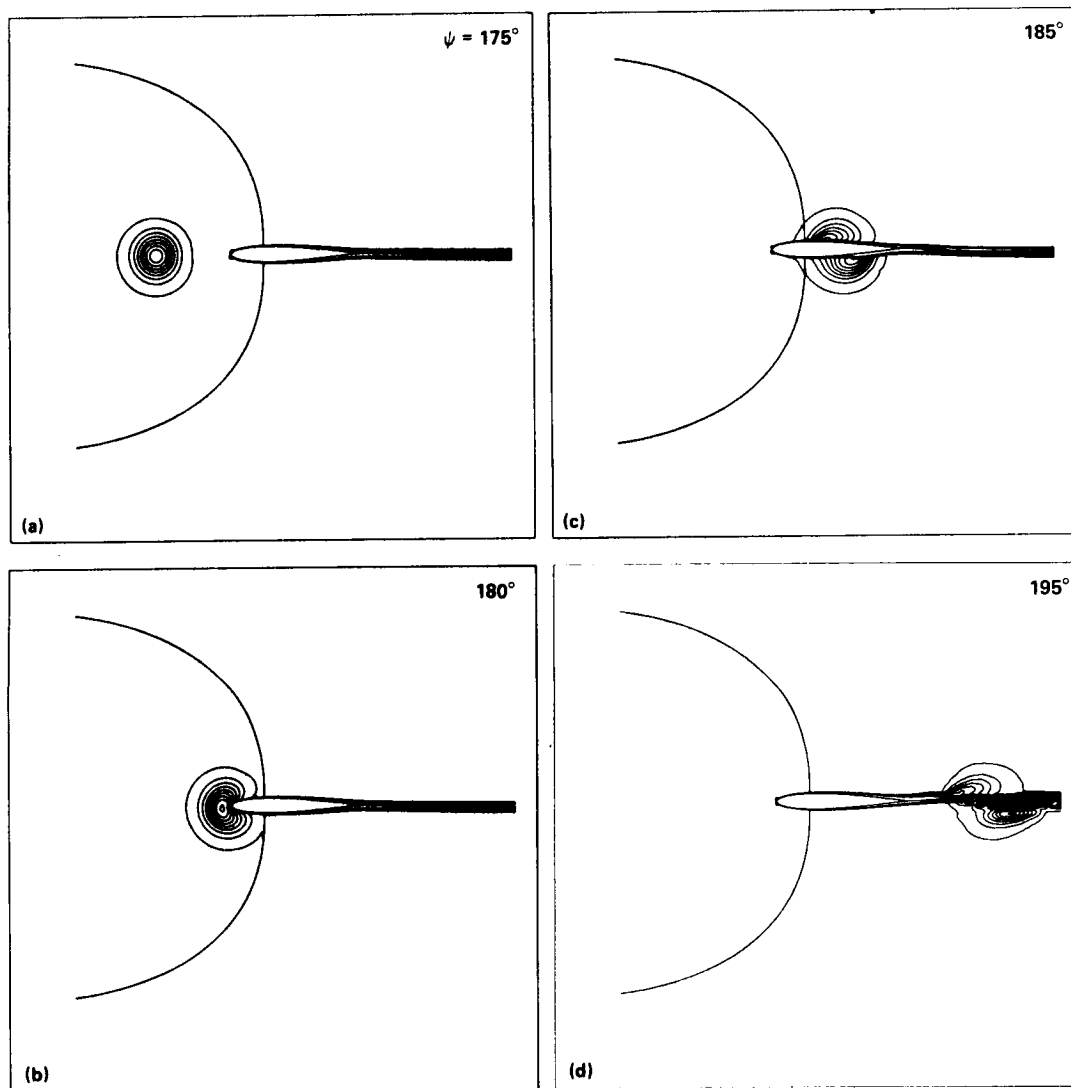


Figure 14.- Vorticity contours at various azimuthal angles for the case  $y_v = 0.0$  in. and  $M_\infty = 0.536$ . (a)  $\psi = 175.00^\circ$ ; (b)  $\psi = 180.00^\circ$ ; (c)  $\psi = 185.00^\circ$ ; (d)  $\psi = 195.00^\circ$ .

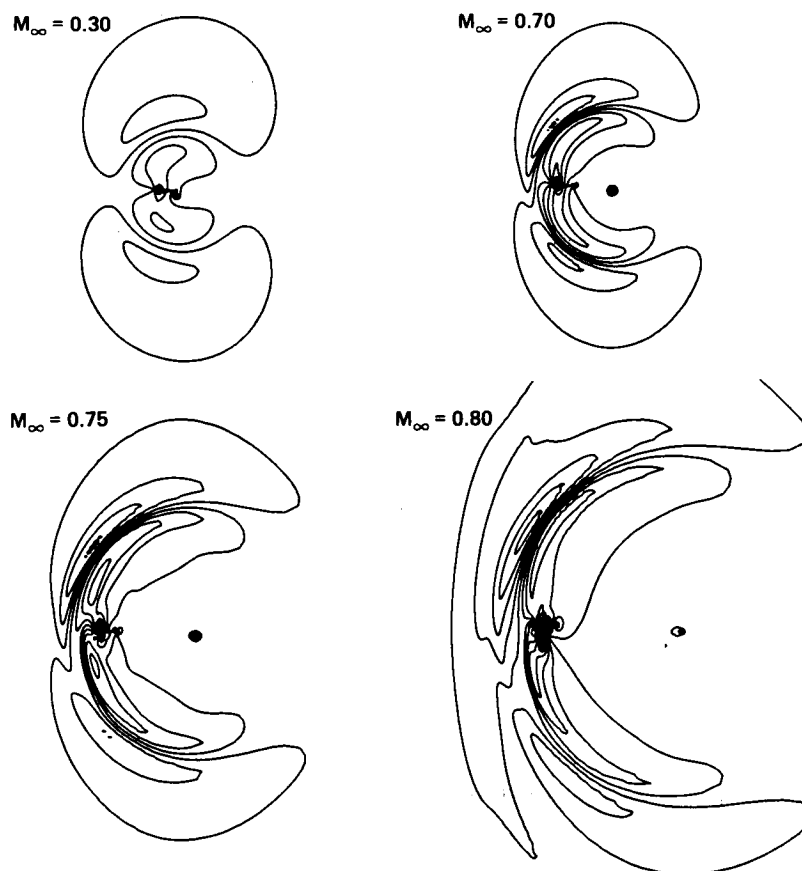


Figure 15.- Disturbance pressure contours,  $(C_p - C_{pi}) \cdot \sqrt{R}$ .  
 NACA 0012 airfoil,  $y_v = -0.26$ ,  $r_v = 0.20$ .

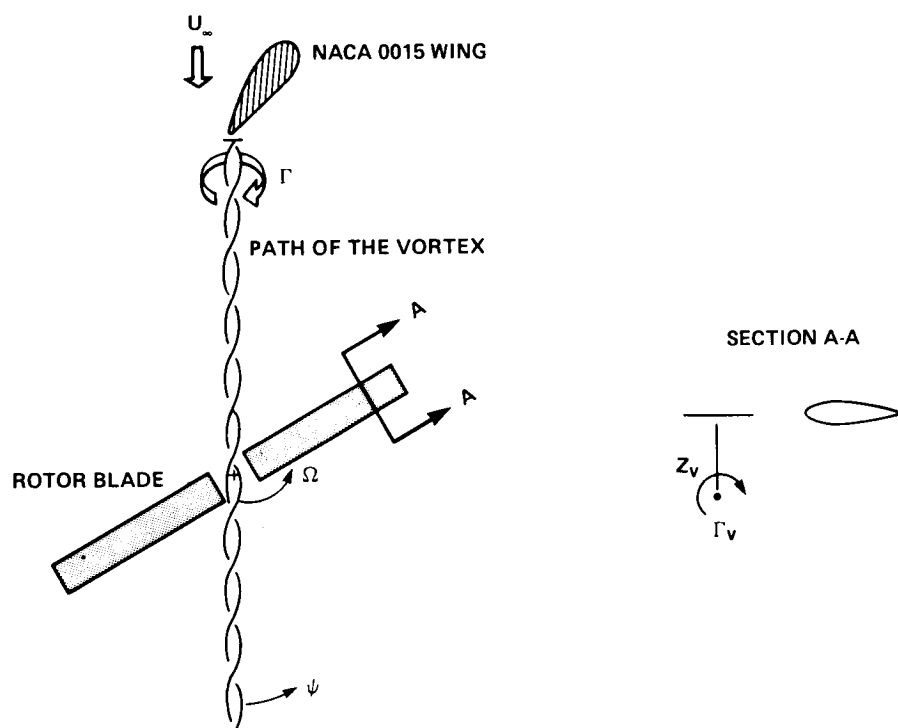


Figure 16.- Rotor-vortex interaction experiment described in reference 30.

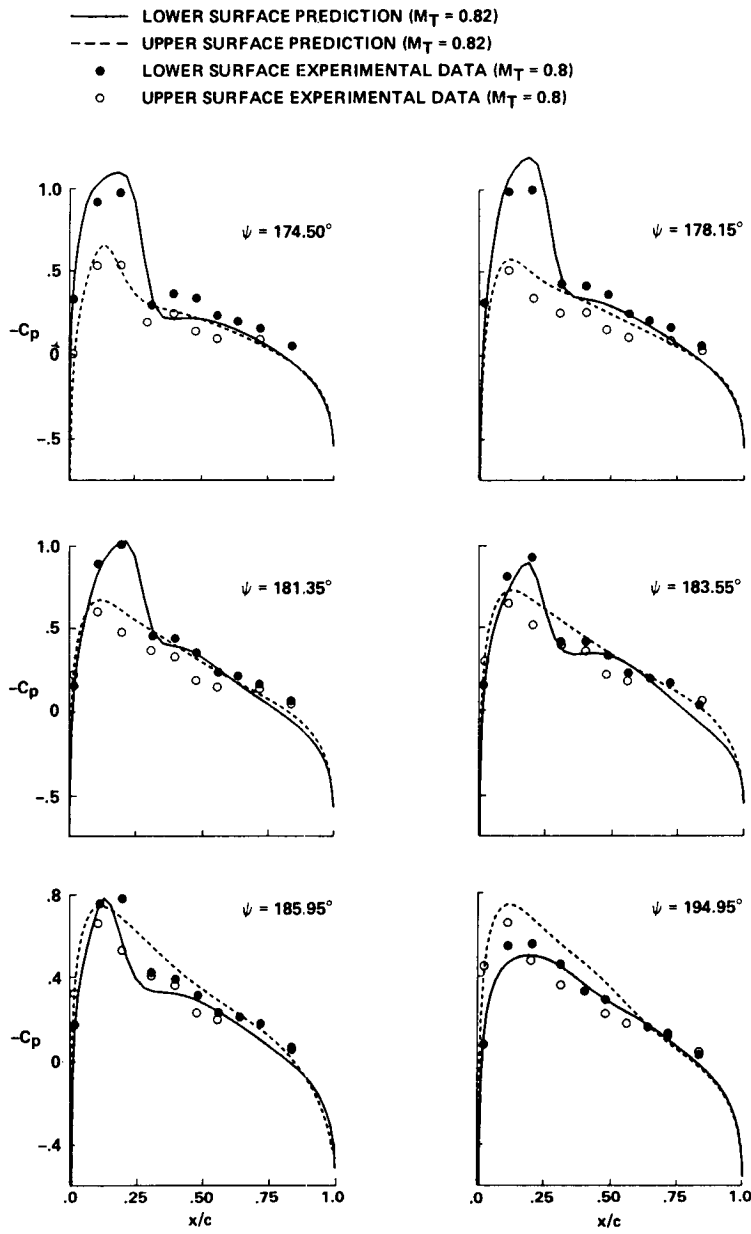


Figure 17.- Surface pressure results for a three-dimensional blade-vortex interaction,  $r_v = 0.177$ ,  $z_v/c = 0.4$ ,  $\mu = 0.2$ ,  $AR = 7.0$ ,  $r/R = 0.893$ ,  $\alpha = 0$ , untwisted, untapered, NACA 0012 blade. Data have  $M_T = 0.8$ , prediction is for  $M_T = 0.82$ .

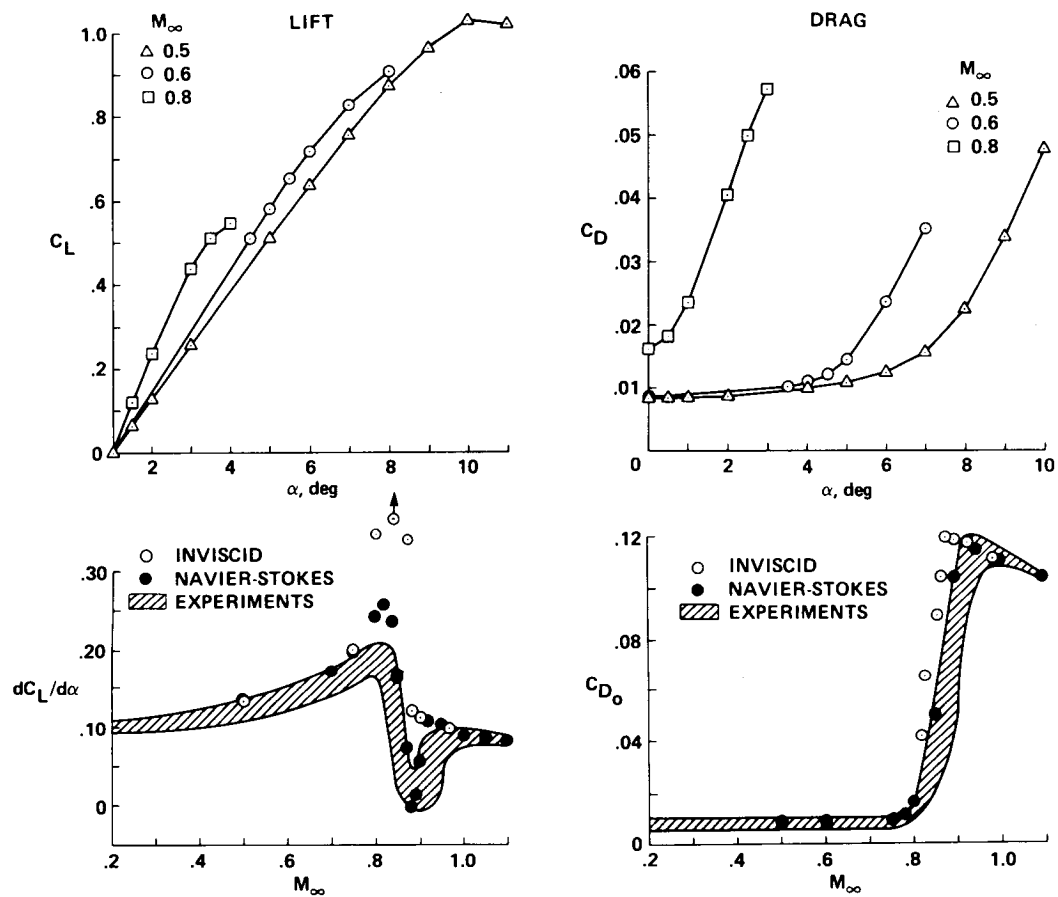


Figure 18.- Two-dimensional airfoil characteristics.

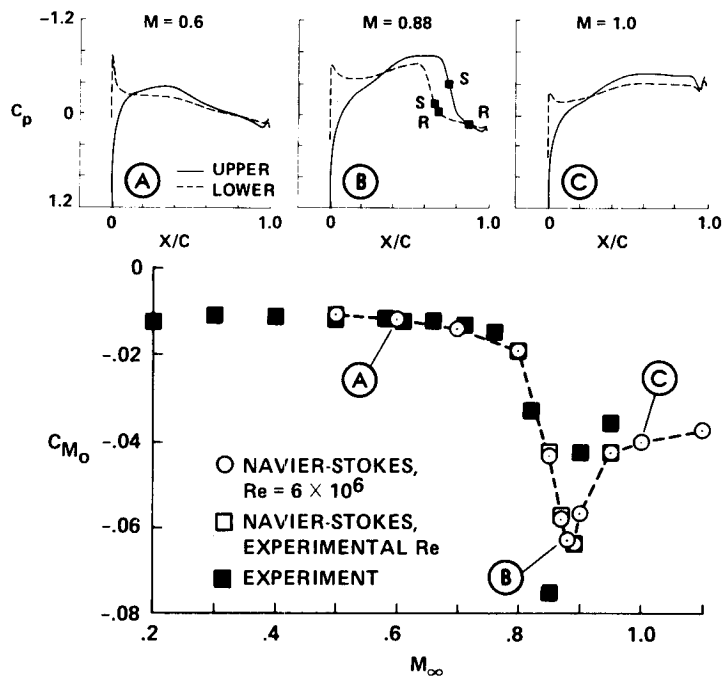


Figure 19.- Pitching moment vs. Mach number for the VR-8 airfoil at  $C_L = 0$ .

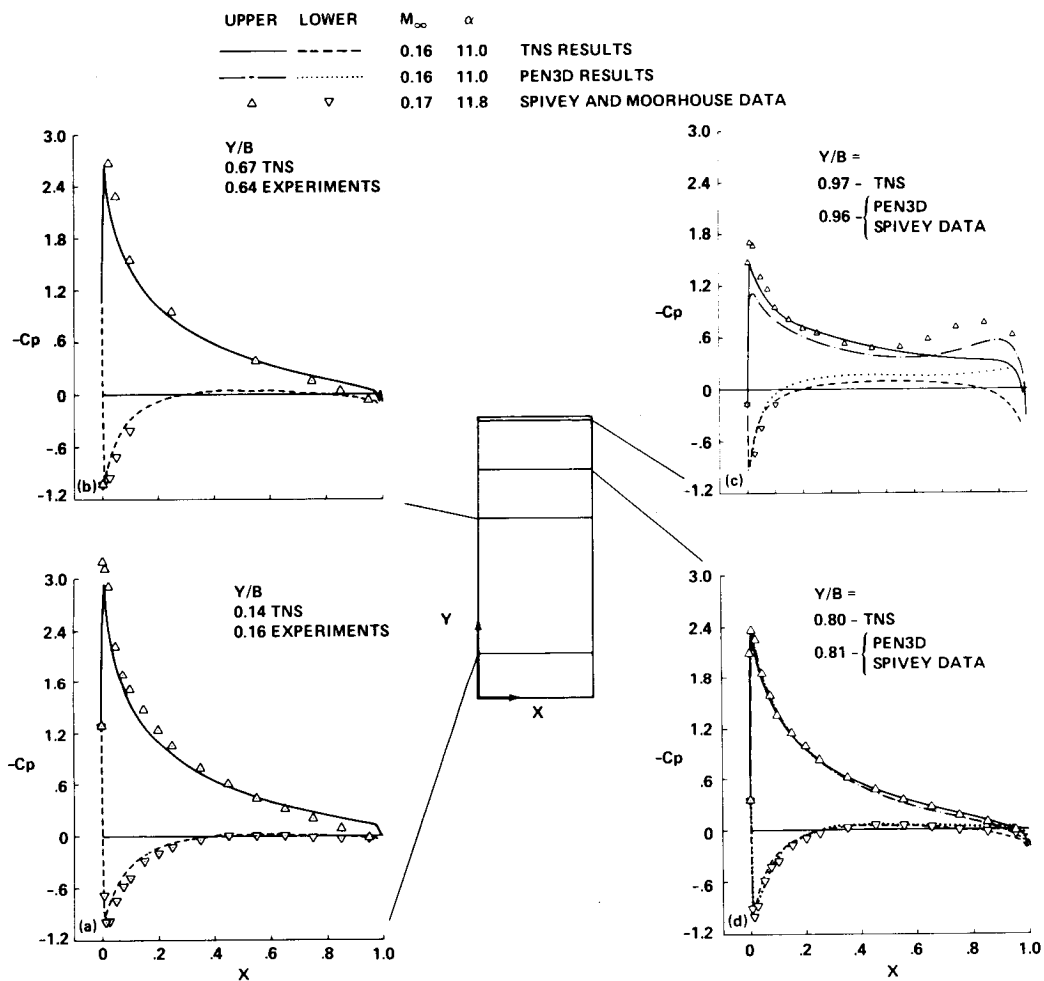


Figure 20.- Surface-pressure distributions for several spanwise stations and comparison with experimental data (refs. 16, 17) for NACA 0015 wing.  $M_\infty = 0.16$ ,  $\alpha = 11^\circ$ , and  $Re = 2$  million.



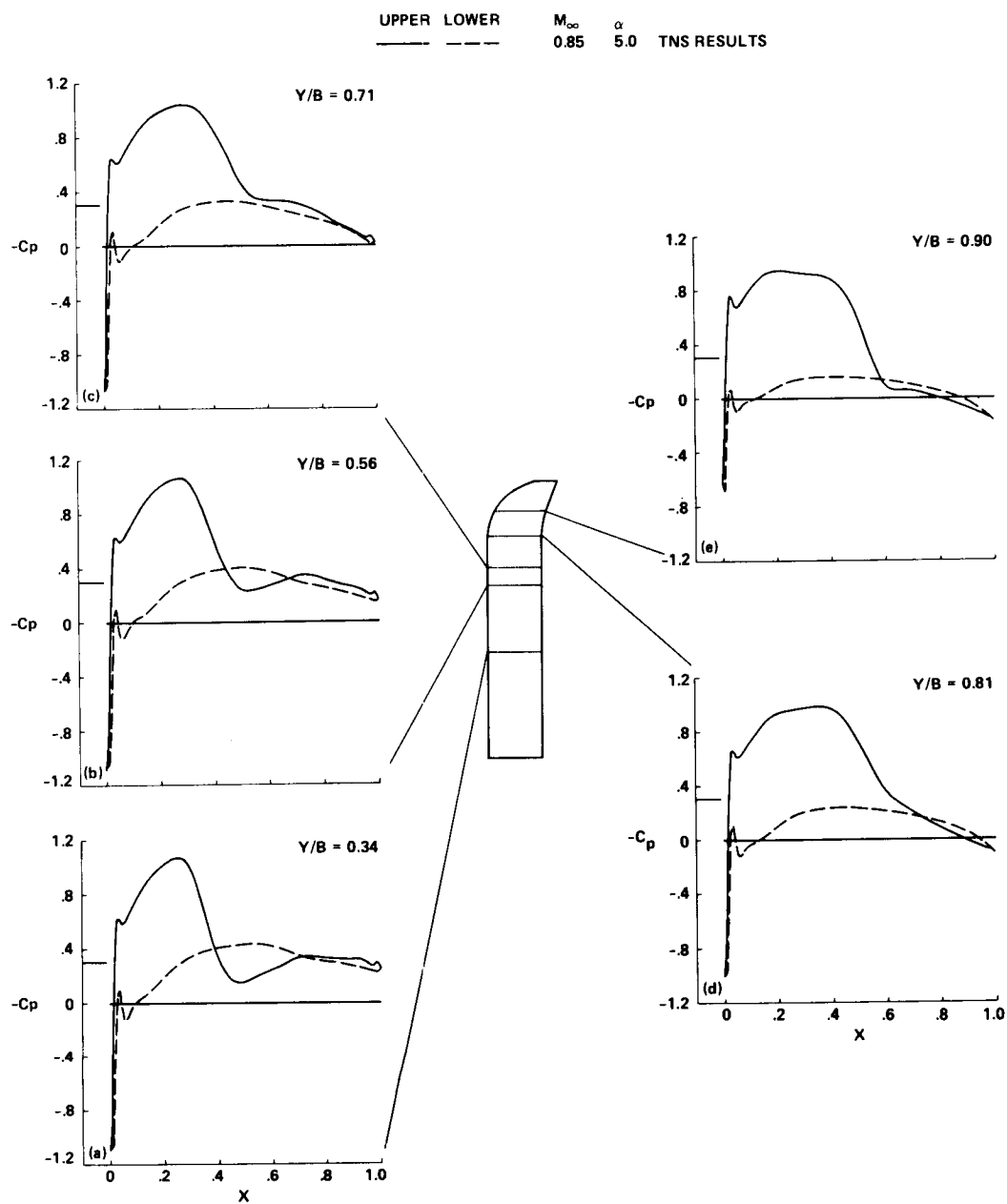


Figure 21.- Surface pressure distributions for the ONERA wing.  $M_\infty = 0.85$ ,  $\alpha = 5^\circ$ , and  $Re = 8.5$  million.

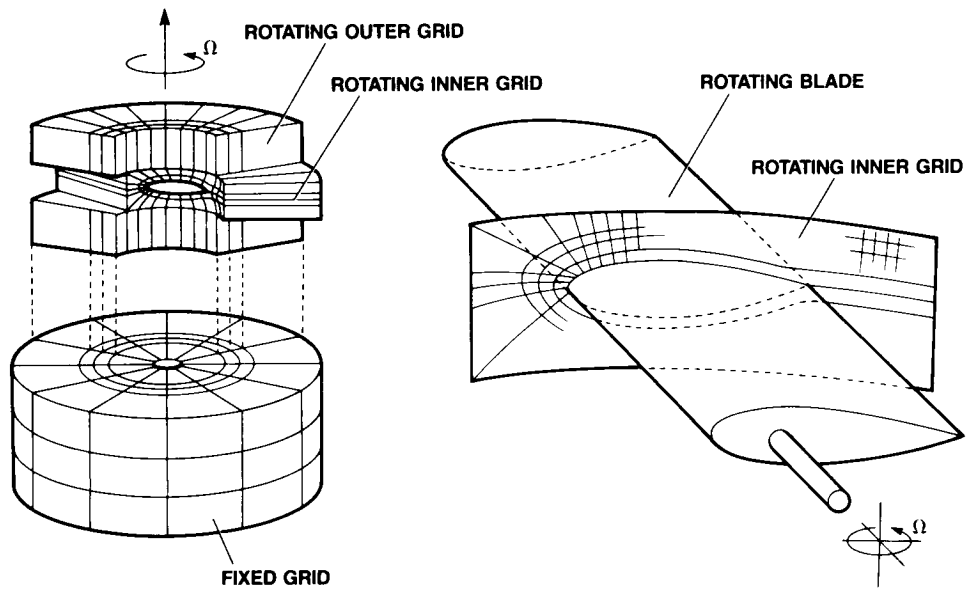


Figure 22.- Grid configuration for the computation of a complete helicopter.

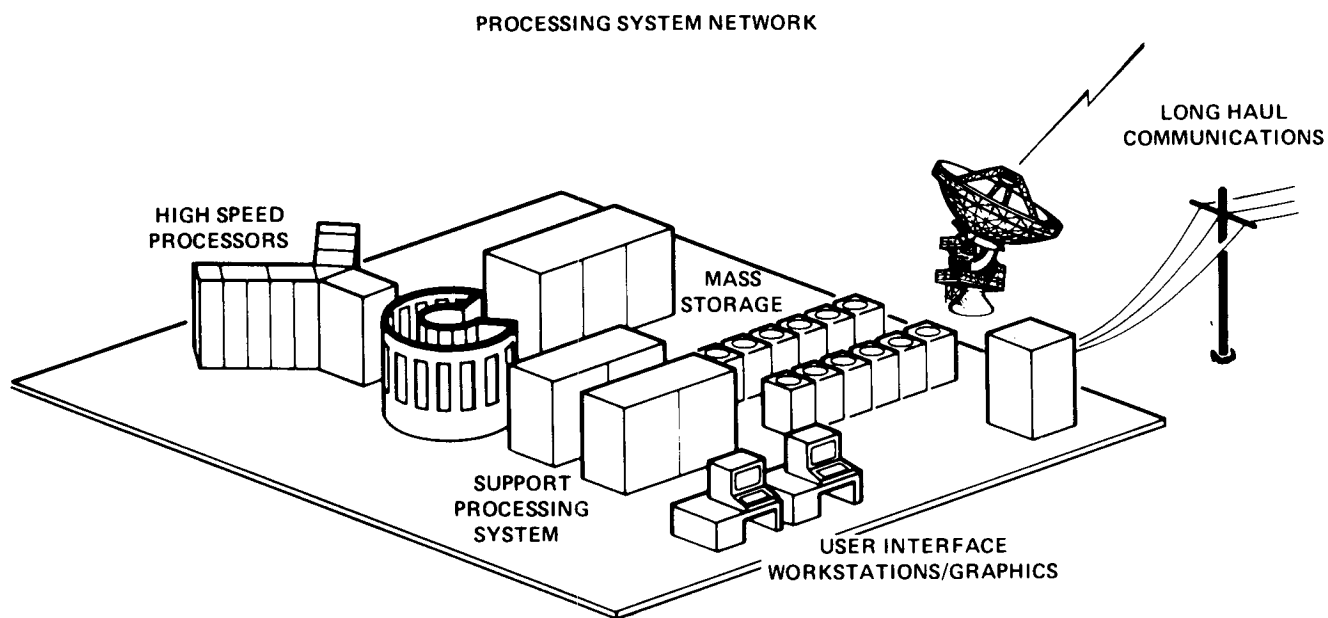


Figure 23.- NASA numerical aerodynamic simulation supercomputer project.

DYNAMICS AND AEROELASTICITY

Session Cochairmen:

Raymond G. Kvaternik, NASA

Robert A. Ormiston, Department of the Army

PRECEDING PAGE BLANK NOT FILMED

## DYNAMICS AND AEROELASTICITY SESSION

### SUMMARY

Four papers summarizing a broad spectrum of NASA and Army contributions to rotorcraft dynamics and aeroelastic technology over the last decade or so were presented in the Dynamics and Aeroelasticity Session. The first paper, "A Summary of Recent NASA/Army Contributions to Rotorcraft Vibrations and Structural Dynamics Technology," by R. G. Kvaternik, F. D. Bartlett, Jr., and J. H. Cline, summarized accomplishments in airframe finite-element modeling for dynamic analysis, analysis of coupled rotor-airframe vibrations, optimization of airframes subject to vibration constraints, active and passive control of vibrations in both the rotating and fixed systems, and the integration of testing and analysis in such guises as experimental modal analysis, system identification, structural modification, and vibratory loads measurement. The second paper, "Rotorcraft Loads Research - A Review," by W. G. Bousman and W. R. Mantay, summarized the progress which has been made in the areas of rotor loads prediction, the reduction of loads through the exploitation of blade structural tailoring, load modification through blade/control coupling, and aerodynamic tuning devices. Rotor loads research conducted with small-scale models and flight test were also described. The third paper, "Comprehensive Rotorcraft Analysis Methods," by W. B. Stephens and E. E. Austin, summarized advances which have been made in the development and application of large-scale, multidisciplinary rotorcraft analysis codes that can treat the entire aircraft in such diverse disciplines as dynamics and aerodynamics, performance, stability and control, loads, vibrations, and aeroelastic stability. Six such codes were reviewed with respect to their processing structures, analysis capabilities, mathematical models, and executive features. Selected comparisons with test data were shown. The last paper, "Rotorcraft Aeroelastic Stability" by R. A. Ormiston, W. G. Warmbrodt, D. H. Hodges, and D. A. Peters, summarized the theoretical and experimental developments in aeroelastic and aeromechanical stability of helicopter and tiltrotor aircraft, with emphasis on advanced hingeless and bearingless rotor configurations. The stability of both isolated rotors and coupled rotor-fuselage systems were considered. Correlation of theory with experimental data from small and large-scale wind-tunnel and flight test were also shown.

A SUMMARY OF RECENT NASA/ARMY CONTRIBUTIONS TO ROTORCRAFT  
VIBRATIONS AND STRUCTURAL DYNAMICS TECHNOLOGY

Raymond G. Kvaternik  
NASA Langley Research Center

and

Felton D. Bartlett, Jr.  
and

John H. Cline  
Aerostructures Directorate  
U.S. Army Aviation Research and Technology Activity (AVSCOM)

ABSTRACT

The requirement for low vibrations has achieved the status of a critical design consideration in modern helicopters. There is now a recognized need to account for vibrations during both the analytical and experimental phases of design. Research activities in this area have been both broad and varied and notable advances have been made in recent years in the critical elements of the technology base needed to achieve the goal of a "jet smooth" ride. The purpose of this paper is to present an overview of accomplishments and current activities of government and government-sponsored research in the area of rotorcraft vibrations and structural dynamics, focusing on NASA and Army contributions over the last decade or so. Specific topics addressed include: airframe finite-element modeling for static and dynamic analyses, analysis of coupled rotor-airframe vibrations, optimization of airframes subject to vibration constraints, active and passive control of vibrations in both the rotating and fixed systems, and integration of testing and analysis in such guises as modal analysis, system identification, structural modification, and vibratory loads measurement.

INTRODUCTION

Since the first U.S. helicopter went into production over four decades ago (fig. 1), excessive vibrations have plagued virtually all new rotorcraft developments. The problem transcends national boundaries and is not unique to the U.S. helicopter community. An account of the vibration problems encountered in the development of an early Soviet helicopter (fig. 2) is given by Alexander Yakovlev in reference 1. Yakovlev's account was popularized when excerpts from his book appeared in the magazine Aviation Week (December 28, 1959). The frustration of trying to solve an elusive vibration problem became so intense that, as the designer writes, "It got to the point where, instead of calling greetings when we met in the morning, we shouted at each other: 'How is it going - still shaking?' 'It's shaking; it's shaking!' 'When will this damned shaking stop?'" More recent accounts of the impact of vibrations on Army helicopter developments

are given in references 2 and 3 in which problems experienced during initial flight testing of the UH-60 Black Hawk (fig. 3) and AH-64 Apache (fig. 4) are described. The problems encountered on these helicopters included: higher than expected rotor vibratory loads, unanticipated rotor-airframe interactions, airframe resonances near excitation frequencies, excessive empennage vibrations, and ineffective vibration control devices. As a result, vibration levels on the prototype aircraft were significantly above Army specifications throughout the flight envelope.

Helicopters are susceptible to vibrations due to the inherent cyclic nature of the airloads acting on the rotors. The vibrations normally pervade both the rotor and the airframe and can seriously degrade both service life and ride qualities. Vibrations also frequently limit the maximum speed in forward flight. Considerable progress has been made over the past 40 years in reducing the level of vibration in helicopters as indicated in figure 5. While improvements have been significant, it should be noted that the procurement specifications have consistently been for levels of vibration lower than could usually be achieved on production helicopters. In the case of the Army UTTAS (Utility Tactical Transport Aircraft System) and AAH (Advanced Attack Helicopter) development programs in the mid-1970s, for example, the specifications originally required vibration levels not exceeding 0.05g. Because none of the competitors could meet this specification, it had to be increased to 0.10g. However, even with this relaxed requirement, the vibration levels in the UH-60 and AH-64 (the winning designs in the two competitions) were reduced to 0.10g only after making numerous structural and configuration changes which included raising main rotors, adding aerodynamic fuselage fairings, modifying hub absorbers, installing airframe absorbers, changing local stiffnesses, modifying crew seats, and isolating stabilators. (It should be pointed out that the 0.10g levels achieved are for the delivered aircraft and that structural changes which occur during normal aircraft operations tend to degrade vibration characteristics. Levels of 0.20g are more typical of fielded Army helicopters). The dramatic reduction in the level of vibration noted in figure 5 has, for the most part, been achieved through the use of add-on vibration control devices of one type or another. These devices, while quite effective in reducing vibrations, have tended to cost an increasing percentage of the design gross weight. The weight penalty associated with the addition of absorbers to reduce vibration levels to 0.10g can be as high as 2.5 percent of design gross weight. For a fixed design gross weight, this represents a reduction of from 10 to 15 percent in primary mission payload. Isolation systems have also gained popularity in recent years. These mechanisms, which are designed to uncouple the rotor dynamic system from the fuselage, appear to have somewhat reduced weight penalties with respect to other passive vibration control devices.

Even though excessive vibrations have always been prevalent in new helicopter developments, until recently, helicopter manufacturers have not addressed vibrations as part of the regular structural design process. The UTTAS RFQ in 1971 was the first instance when a procuring agency specified the level of vibration to be addressed in

a competitive design. With only a few exceptions, helicopters have been designed to performance requirements while relying on past experience to account for vibrations. Excessive vibrations (which invariably occur) are "tinkered out" during ground and flight testing. The vibration levels to be regarded as acceptable are usually negotiated during this tinkering process (recall the UTTAS and AAH experience). Oftentimes modifications to reduce vibrations to acceptable levels continue well into the operational phase of a helicopter.

The cost required to solve vibration problems during the development cycle is qualitatively illustrated in figure 6 which shows the trend of engineering manpower requirements dedicated to vibration reduction. During the design phase, effort increases gradually until first flight. At this point an abrupt increase occurs (the beginning of the so-called "crisis period") that extends well into the development cycle. This increase significantly raises development costs and leads to slipped delivery schedules. Operational costs are also increased both due to the attendant weight penalties associated with vibration treatments and due to the increased maintainability requirements for vibration control devices. Clearly, the payoff from minimizing crisis engineering and eliminating overruns is significant. As previously mentioned, helicopter companies have relied little on analysis during design to limit vibrations. However, because of the vibration problems encountered in the UTTAS and AAH development programs, there has emerged a consensus within the industry on the need to account for vibrations more rigorously during both the analytical and experimental phases of design. This need has resulted in the subject of helicopter vibrations receiving considerably increased attention in recent years (see, for example, refs. 4 to 9). The goal (unofficially) set down by the industry is to achieve the vibration levels associated with fixed-wing aircraft, the so-called "jet smooth" ride. To achieve this goal will require the development of advanced vibration design methodologies (ref. 10).

Vibration design can be broadly classified into three interdependent activities: (1) passive design to select rotor and airframe parameters which yield low inherent vibrations; (2) design of vibration control devices to minimize rotating and fixed-system vibratory loads; and (3) vibration testing to verify design concepts and to compensate for any deficiencies in analytical capabilities. The interactive nature of these activities is depicted in figure 7 which shows one representation of the helicopter vibration design cycle. The diagram indicates that the problem involves analytical and experimental considerations of the rotor, the airframe, and the coupling between the rotor and the airframe. The primary sources of high vibrations are cyclic loads transmitted to the airframe by the main and tail rotors as well as aerodynamic excitation of the tail boom and empennage by the main rotor wake. For the most part, passive vibration design combines past experience with rudimentary analysis. Special and general-purpose aeroelastic analyses are used to design for minimum blade vibratory loads. Large-scale finite-element models are used to verify adequate placement of airframe natural frequencies with respect to operating frequencies. Comprehensive rotor-airframe



coupling analyses which account for flexible hub structural dynamics and interactional aerodynamics have only become available recently and have not yet been validated. Correlation with test and comparative studies of these state-of-the-art helicopter rotor and airframe vibration analyses have confirmed what the Black Hawk and Apache experiences have demonstrated, namely, the inadequacies of existing passive vibration design methods.

Underlying all considerations related to vibrations and serving as a unifying element is structural dynamics. Every consideration of a helicopter system includes dynamic phenomena in some form (fig. 8), and the importance of structural dynamics is well recognized (ref. 11). The key role played by structural dynamics in the broader context of aerospace vehicle design as well as an assessment of structural dynamics needs are given in references 12 and 13. However, while structural dynamics clearly plays a principal role in determining the vibration characteristics of modern rotorcraft, it is not regarded as a sufficiently mature discipline by the helicopter industry on which to base vibration design decisions. (It is interesting to note that such is not the case for stability, with analytical predictions often influencing design decisions). Good structural dynamic characteristics are essential for the success of any rotorcraft. The modern helicopter is more susceptible to high vibrations because of increased operational demands for high-speed and nap-of-the-earth flight, high maneuverability and agility, improved crew effectiveness, advanced weapons delivery, increased structural integrity, high reliability, and low maintenance. As a result, vibrations has achieved the status of a critical design consideration in modern helicopters. The challenge is now, more than ever, passed on to the dynamicist. Indeed, it may well emerge that the success or failure of future rotorcraft developments will rest on the dynamicist.

Research activities in the U.S. in the area of rotorcraft vibrations and structural dynamics have been both broad and varied. Notable advances have been made in recent years in the critical elements of the technology base needed to achieve the goal of a "jet smooth" ride. The purpose of this paper is to present a management overview in the style of an executive summary of accomplishments and current activities of government and government-sponsored research in the area of rotorcraft vibrations and structural dynamics. The overview focuses on NASA and Army contributions over the last decade or so. Both in-house and contracted research and development efforts pertaining to design analyses for vibrations, vibration control, and vibration testing are described. Emphasis throughout is placed on the airframe. Rotorcraft aeroelastic stability, rotor blade vibratory airloads, rotor dynamics, and associated wind-tunnel testing are not addressed except if needed to provide for continuity. This separation between the rotor and the airframe is primarily a separation between aerodynamics and structural dynamics. In practice, this separation is not possible because of the interaction between the rotor and the airframe in producing vibrations. Specific topics addressed include: airframe finite-element modeling for static and dynamic analyses, analysis of coupled rotor-airframe vibrations, optimization of airframes subject to vibration constraints, active and passive con-

trol of vibrations in both the fixed and rotating systems, and integration of testing and analysis in such guises as modal analysis, system identification, structural modification, and vibratory loads measurement. NASA and Army funded efforts with the university community are also included. The information used as a basis for the overview was obtained by reviewing the material identified in a computerized literature search and from the extensive personal libraries of the authors. Of the hundreds of potentially relevant reports and papers reviewed those that were judged to be significant for the purposes of the paper are cited as references.

#### PREPARATORY REMARKS

With a view toward providing a better perspective of NASA and Army vibrations research, some material of a background nature is given in this section.

Current NASA rotorcraft research has evolved from the autogyro research begun by NACA in the 1930's. Valuable contributions to rotorcraft development have resulted from NACA/NASA research since that time. While there has always been a close association between NACA/NASA and the military rotorcraft research and development agencies, particularly with the Army, the relationship with the Army was strengthened in 1965 when the Army Aeronautical Research Lab was established at the Ames Research Center. In 1970 the Army established research labs at the Langley Research Center and the Lewis Research Center and formed what is currently called the Aviation Research and Technology Activity (ARTA) of the U.S. Army Aviation Systems Command (AVSCOM). These labs represented an important adjunct to the NASA organization and sparked a resurgence in NASA rotorcraft research activities aimed at strengthening and exploiting the joint research which was made possible by the collocated Army labs.

The first major NASA program addressing vibrations was the Civil Helicopter Technology Program (refs. 14 and 15). Although the primary goal of this program was ride quality research aimed at civil acceptance of helicopters for transports, vibrations was of interest because it was a major factor contributing to public acceptance of helicopters. In March 1978, NASA's Office of Aeronautics and Space Technology formed a special Rotorcraft Task Force to review rotorcraft technology needs and to prepare an appropriate rotorcraft research program aimed at advancing technology readiness. The Task Force solicited inputs from the rotorcraft industry, NASA research centers, and other government agencies. The National Research Council (NRC) and the Rotorcraft Subcommittee of the NASA Aeronautics Advisory Committee conducted independent reviews of the proposed NASA program. As a result of counsel received from all quarters, a plan was finalized and published in October 1978 (ref. 16). The review conducted by the NRC was published under separate cover (ref. 17). The Task Force proposed a 10-year, \$398 million (FY 78 dollars) program with four major elements: aerodynamics and structures, flight control and avionic systems, propulsion, and vehicle configurations.

Each of the four major elements was divided into two or more specific areas of emphasis. Vibrations was cited as one of three key areas under aerodynamics and structures. As enunciated in the Task Force Report, the focus was to be on providing the technology and design methodology for accurate prediction and substantial reduction of airframe vibrations. The Task Force Report was the catalyst for the NASA Langley Research Center to begin formulating a rotorcraft structural dynamics program to meet the needs of the helicopter industry with respect to airframe vibrations. The overall objective of the proposed program, which was defined in close cooperation with the industry and coordinated with the Army, was to establish in the U.S. a superior capability to utilize airframe finite-element analysis to support the design of helicopter airframe structures. Viewed as a whole, the program includes efforts by NASA, universities, and the helicopter industry. In the initial phase of the program, teams from the major manufacturers of helicopter airframes would formulate finite-element models of selected airframes of both metal and composite construction and carry out ground vibration tests and correlations to evaluate the analysis models. To maintain the necessary scientific observation and control, emphasis throughout these activities would be on advance planning, documentation of methods and procedures, and thorough discussion of results and experiences, all with industry-wide critique to allow maximum technology transfer between companies. The finite-element models formed in this phase would then serve as the basis for the development, application, and evaluation of both improved modeling techniques and advanced analytical and computational techniques to enhance the technology base which supports design of helicopter airframe structures. Here again, procedures for mutual critique have been established which call for a thorough discussion among the program participants of each method prior to the applications and of the results and experiences after the applications. Because of the emphasis on design methodology, the aforementioned rotorcraft structural dynamics program was given the acronym DAMVIBS (Design Analysis Methods for VIBrations).

In 1979, primarily because of the problems experienced during the UTTAS and AAH development programs, the Director of what is now the U.S. Army Aviation Research and Technology Activity requested that an assessment of helicopter vibration research be made. Information for this assessment was obtained by surveying the helicopter industry, Army research labs, and appropriate NASA research centers. This review addressed the status of past, present, and planned research efforts within the Army as well as joint Army/NASA programs. The results of this assessment were published in 1982 (ref. 18). The five major disciplines which were critically reviewed included: rotor vibratory loads, airframe structural dynamics, rotor-airframe coupling, vibration control devices, and vibration testing. As a result of this comprehensive review, and with a consensus of the rotorcraft community, significant technology voids were identified and areas for future research were recommended. The technology deficiencies can be summarized into two areas of concern relative to helicopter vibrations. First, the inability of present design methods to accurately predict rotor vibratory loads and coupled rotor-airframe vibrations. Hence, the need to resort to add-on vibration control devices. Sec-

ond, a lack of definitive procedures which make maximum use of vibration test data, instead of trial-and-error testing, to resolve vibration problems. To address these technical concerns, Army vibration research in recent years has been directed to rotor-airframe coupling analysis, advanced active and passive vibration control demonstration, and improved vibration testing methodology development.

The Army program (ref. 18) was reaffirmed and the proposed NASA DAMVIBS program was formally presented to the helicopter industry at a finite-element modeling workshop focusing on rotorcraft structures which was held at Langley Research Center in February 1983 (refs. 19 and 20). Because of the complementary nature of the two programs, industry consensus was to proceed with both programs. Army funding for the contracted activities envisioned under their program did not materialize so only the in-house work was initiated. NASA funding for the DAMVIBS program was approved and the program was implemented in April 1984 with the awarding of task-type contracts to each of the four primary helicopter airframe manufacturers (Bell Helicopter Textron, Boeing Vertol, McDonnell Douglas Helicopter Company (at that time Hughes Helicopters, Inc.), and Sikorsky Aircraft). Work completed to date under the NASA and Army programs as well as the status of current activities and near-term plans are also discussed in appropriate sections of the paper.

## DESIGN ANALYSIS FOR VIBRATIONS

As discussed in the Introduction, designing a helicopter for low vibrations may be viewed as consisting of essentially three interdependent activities: (1) design technology, wherein the use of analysis during design (i.e., design analysis) is employed to establish dynamically passive or vibration-benign rotors and airframes; (2) control technology, whereby vibration control devices are designed to further reduce rotating and fixed-system vibratory loads; and (3) test technology, wherein vibration testing is used to verify design concepts and to compensate for any deficiencies in analytical capabilities. This section is concerned with the first of these activities, namely, the use of vibration analysis to support design of airframe structures. Three specific areas are discussed: (1) airframe finite-element modeling; (2) analysis of coupled rotor-airframe vibrations; and (3) airframe structural optimization.

### Airframe Finite Element Modeling

Structural analysis methods employed in the aerospace industry today are based mostly on the finite-element method. The finite-element method is a numerical matrix technique for obtaining approximate solutions to a wide variety of engineering problems. Although originally developed about 25 years ago to analyze complex aircraft structures, it has since been extended and applied to a wide variety of problems spanning many fields of engineering. In particular, the finite-element method has assumed a premier role in the design and analysis of aerospace structures both in this country and abroad.

The idea of the finite-element method is to provide a library of structural elements (rods, beams, shear panels, plates, etc.) which can be connected together so as to model any structure of interest. A computer then automatically carries out the computations necessary to determine specified categories of behavior of the structure under specified loads. Finite-element analysis is the standard method for airframe structural analysis in the U.S. and is now routinely used as a design tool to calculate static internal loads on each airframe element to permit sizing and stress analysis. Within the U.S. helicopter industry, finite-element analysis as embodied in the NASTRAN computer code is used exclusively. NASTRAN (ref. 21) is the very widely emplaced, general-purpose computer code for finite-element analysis of structures originally developed under NASA sponsorship in the late 1960s. (Several commercial versions of the code have become available since that time, with the version developed by the MacNeal-Schwendler Corporation (ref. 22) being the most widely used). The remarkable collection of terms and symbols referring to various entities of the code has become a highly effective universal vocabulary. The increased accuracy of finite-element-analysis based methods (such as NASTRAN) over earlier strength-of-materials based methods of analysis for prediction of internal load distributions has contributed significantly to the ability to design more efficient (lighter weight) aircraft structures.

The major fixed-wing aircraft manufacturers developed their own special-purpose finite-element codes soon after the emergence of the finite-element method in the late 1950's and well in advance of the introduction of NASTRAN in 1970. Hence, the use of NASTRAN in this industry, while extensive, has been generally no more than supplemental to their own well-established codes in airframe design work. The U.S. helicopter industry, on the other hand, lagged the fixed-wing industry in the development of their own finite-element analysis codes for design so when NASTRAN became available in 1970 it was promptly adopted by the helicopter industry. NASTRAN is now used exclusively in this industry to support both static and dynamic design.

Some early accounts of the use of NASTRAN in the helicopter industry are contained in references 23-26. The integration of NASTRAN into the airframe design process at Bell Helicopter is described in reference 23. The reference outlines pre-processing procedures for automatic generation of the airframe finite-element model and distribution of non-structural weight to the three-dimensional model and a post-processing procedure for reformatting the output so that it is more directly useful to the stress analyst. Initial experiences at Bell with the use of the various options in NASTRAN for static and dynamic analysis are described in reference 24. A brief historical perspective of the adoption and subsequent application of NASTRAN for analysis of helicopter airframes at Sikorsky Aircraft are given in reference 25. With respect to the ability of a finite-element analysis to design a lighter weight aircraft, Sikorsky credits the use of NASTRAN during the design of the UH-60 Black Hawk with reducing the structural weight by about ten percent. Some additional industry accounts of the early use of

NASTRAN in design may be found in reference 26. As NASTRAN became more firmly established in the helicopter industry, analytical and experimental investigations based on the use of finite-element models began to become more common. Some of the more noteworthy of these finite-element modeling applications are summarized in the remainder of this section.

Combined experimental/analytical investigations conducted on Army OH-58A and OH-6A helicopters are reported in references 27 and 28, respectively. Those studies were some of the earliest aimed at determining engine response to airframe vibrations. The objective was to provide the data needed to establish a set of improved engine vibration specifications for engine manufacturers. The finite-element models developed as part of those studies are shown in figures 9 and 10, respectively. In each case, the finite-element model of the airframe was coupled to a model of the engine based on mobility data supplied by the engine manufacturer. Analytical predictions were reported to have agreed reasonably well with test data in both studies.

Some early modeling and correlation work conducted by Sikorsky on the CH-53A is reported in references 29 to 31. The initial finite-element model, described in reference 29, was based on an in-house code originally developed for civil engineering structures. The model was rather simple, with the forward and aft portions of the fuselage modeled as beams cantilevered from a detailed three-dimensional model of the center fuselage section. A companion simplified NASTRAN model (ref. 30) was later used to develop a complete, three-dimensional finite-element model of the CH-53A used in the NASA Civil Helicopter Program (fig. 11). This program (refs. 14 and 15), which was directed at evaluating helicopters for short-haul transportation, utilized a CH-53A modified to incorporate an airline passenger compartment. The modified CH-53A underwent an extensive shake test program and a detailed comparison was made between test results and NASTRAN results (ref. 31). Good agreement was noted for the fundamental airframe bending and transmission pitch frequencies, but poor agreement resulted for the lateral/torsion modes and the higher frequency transmission modes. The predominant vibratory loads imposed on an airframe by the rotor occur at the blade passage frequency which equals  $N$  times the rotational frequency, where  $N$  is the number of blades. It is customary to refer to this frequency as  $N$ -per-rev or  $N/\text{rev}$ . For the six-bladed CH-53A this frequency is 18.5 Hertz. Since the higher frequency transmission modes control the 6/rev vibratory response in the CH-53A airframe, the analysis was judged to be an unreliable design tool for predicting even the primary vibration levels. It was thus concluded that further development of finite-element modeling techniques was required before such analyses could reliably predict  $N/\text{rev}$  response at critical stations on an airframe.

The role of NASTRAN in the design of the Rotor Systems Research Aircraft (RSRA) is discussed briefly in reference 32. The RSRA (fig. 12) was intended to serve as a flying test bed for a variety of advanced rotors for helicopters. The requirement to mount different

rotors posed several unique vibration design problems for the airframe. NASTRAN was used extensively to provide the structural dynamics representations for the usual analytical checks on vibrations. An upgraded version of the original finite-element model of the RSRA in a compound configuration is shown in figure 12.

In 1973 the Army initiated a program to evaluate NASTRAN as a tool for vibration analysis of helicopter airframes. The first part of the program was to develop a NASTRAN model of the AH-1G helicopter that would represent the low-frequency (below 30 Hertz) vibration characteristics of the airframe. The documentation of the model was required to be clear and complete so that government personnel could independently make changes to the model and use it for in-house analyses. Following development of the NASTRAN model, the validity of the model was assessed by comparing the model with static and dynamic tests. References 33 to 37 describe the results obtained under this program. The NASTRAN finite-element model, which was developed under the technical direction of a NASA/Army team, is shown in figure 13 and described in detail in reference 33. Figure 14 illustrates the type of documentation which was provided for the stiffness modeling under the contract. The figure shows a drawing of the actual structure (with skins removed) of the fuselage portion of the airframe. An exploded view of the finite-element model corresponding to the aft (shaded) part of the fuselage is depicted in the middle of the figure. This sketch is the familiar "wire-frame" diagram that is customarily shown when graphically illustrating a finite-element model. The sketch at the bottom of the figure is an exploded view of one of the bulkheads in the model and shows the individual rods and shear panels which represent that particular bulkhead. Detailed sketches of this type appear for every bulkhead, frame, panel, etc. in the airframe. Each sketch is also accompanied by a set of tables which describes the structural elements, constraints which need to be imposed on the model, and an explanation of the basis for omitting degrees of freedom not employed for the dynamic analysis. Reference 34 contains the results of static and dynamic tests and comparisons of results from those tests with results from NASTRAN analysis. Some frequency response comparisons which are typical of those obtained from the ground vibration test are given in figure 15. In general, measured frequency response characteristics were found to be in fair to good agreement with NASTRAN predictions only through about 15-20 Hertz (This corresponds to about 4/rev for the two-bladed AH-1G). A report (ref.38) recently generated under the DAMVIBS program in support of an industry-wide coupled rotor-airframe vibrations activity (to be described in the next section) summarizes all the modeling and testing which has been conducted on the AH-1G, including some recent testing conducted by Kaman Aerospace Corporation. As a consequence of these well-documented activities on the AH-1G, the AH-1G is probably the best known airframe of any aircraft described in the open literature. This has resulted in the AH-1G finite-element model being used extensively throughout government, industry, and academia.

The vibrations portion of the rotorcraft research program plan laid out in 1978 by the Rotorcraft Task Force (ref. 16) contained an airframe modeling/test assessment activity. This proposed task area

was to involve participation by NASA and industry in a workshop environment to assess and document industry design procedures, difficulties with software, modeling techniques, and shake test procedures. All work was to be conducted on a production aircraft. NASA funding for that activity was approved and, as a result of a competitive procurement, a contract was awarded Boeing Vertol in 1980. The subject vehicle was to be the CH-47D. An unusual requirement of the contract was that each major step of the program be presented to and critiqued by the other three primary helicopter airframe manufacturers. Also unique was the requirement that plans for the modeling, testing and correlation be formulated and submitted to both NASA and industry representatives for review prior to undertaking the actual modeling and testing. Boeing was also required to make a study of current and future uses of finite-element models and to keep meticulous records on the manhours required to form the vibrations model. The latter "time and motion" study was intended to provide a basis on which to schedule finite-element modeling for any new helicopter development program. The contract also called for thorough documentation of the model, but not to the level of detail which had been required for the AH-1G. References 39-43 constitute the formal documentation of all work done under the contract. A concise summary of the program may be found in reference 44. The finite-element model developed under the program is shown in figure 16. An example of the type of modeling guides required as part of the modeling plan is given in figure 17, which shows static and mass modeling guides for a typical frame in the CH-47D. Figure 18 illustrates the types of comparisons which were obtained between measured and computed frequency responses. In general, the agreement between test and analysis was acceptable only through about 15-20 Hertz (3/rev for the 3-bladed CH-47D corresponds to 11.25 Hz). The modeling activity demonstrated that a finite-element model suitable for internal loads, structural member sizing, and vibrations can be developed, and that there is no need to form separate static and dynamic models as has usually been the practice. The study further showed that the cost of such a combined static and dynamic model is about five percent of the manhours of a typical airframe design effort. Of the five percent, four percent is already typically expended in most companies to form the internal loads model; the vibrations model is another one percent. The "time and motion" study showed that a vibrations model could be formed early enough in a new helicopter development program to influence the airframe design. A number of items were identified during the modeling and correlation effort which have the potential for improving the correlation. These include: consideration of nonuniformly distributed modal damping, the inclusion of secondary effects such as stringer shear area, assumptions on stringer continuity across splice joints, and the inclusion of suspension system effects. An example of the type of improvement which could be achieved by better treatment of damping is indicated in figure 19. Usual practice is to use the same (assumed) value of damping for each mode in forced response analyses. The figure shows the results of a preliminary exercise in which modal damping has been adjusted in some of the more important modes in an effort to improve correlation with test results. In the case shown the damping has been varied to obtain the best match away from the response peaks.



As a consequence of the CH-47D modeling and correlation activities, it became clear that the key to engendering in the industry the needed confidence to use finite-element models for vibration design was more industry hands-on experience along the lines of the CH-47D program. Also identified as being essential was a workshop environment which fostered the discussion of modeling details and the interchange of ideas. Prior to the CH-47D program, finite-element modeling work conducted by the industry was fragmented for the most part with each company going its own way and (sometimes) preparing a report (which wasn't always available to competitors). The transfer of technology related to modeling was minimal at best. The NASA rotorcraft structural dynamics program, known as DAMVIBS, was defined with a view toward providing the necessary focus and environment of shared experiences for the common good of all. As previously mentioned, the DAMVIBS program was implemented in April 1984 with the award of contracts to the four primary helicopter airframe manufacturers. The industry participants, working under task-type contracts, have already been issued several tasks for the modeling and testing of both metal and composite airframes. Three NASA/industry meetings have already been held under the DAMVIBS program (September 24-25, 1984; October 1-3, 1985; December 2-4, 1986) at which industry participants have either presented their plans for conducting an activity or the results and experiences of a completed activity. Draft final reports for the completed tasks have been submitted and are in various stages of NASA review. Finite-element modeling and correlation activities have been completed on the McDonnell Douglas AH-64A (fig. 20). Modeling of the Sikorsky UH-60A and Bell D-292 (ACAP) are complete and correlations are under way (figs. 21 and 22). The ground vibration test of the Boeing Model 360 (fig. 23) has been completed; modeling is nearing completion at which time correlation studies will begin. The results of the unfinished studies will be presented at the next DAMVIBS meeting (tentatively scheduled for late 1987). From the modeling and correlation results obtained to date under the DAMVIBS program, metal airframes continue to exhibit acceptable agreement through only about 15-20 Hertz. Preliminary results also show that the dynamics of composite airframes are essentially the same as metal airframes. While correlations are not yet completed, preliminary results indicate that agreement between test and analysis for composite airframes is similar to that obtained for metal airframes (still a problem above about 15-20 Hz). Preliminary results also indicate that damping levels in composite airframes are about the same as in metal airframes (2-4 percent critical).

The CH-47D modeling activities and attendant industry critique demonstrated that all companies are using essentially the same techniques to model metal aircraft. The DAMVIBS program has demonstrated that the same is true for composite airframes. In the basic modeling studies being conducted under the DAMVIBS program only the primary (major load carrying) structure is represented fully (stiffness and mass) when forming the finite-element model. This is consistent with usual modeling practice. There are many components (e.g., transmissions, engines, and stores) and secondary structure (e.g., fairings, doors, and access panels) which are represented in the model only as

lumped masses. This may be a major contributing factor to the disagreement noted between analysis and test at the higher frequencies. In an attempt to answer this question, a DAMVIBS activity called "Finite-Element Modeling of Difficult Components" has been recently initiated. The aim of the "difficult components" activity is to isolate the effects of modeling assumptions and to develop improved modeling guides for components which require more detailed modeling representation. The first study is being conducted by Bell utilizing an AH-1G helicopter. The airframe will be stripped down to primary structure and sequentially built back up to its full configuration, as suggested by figure 24. At each stage, a ground vibration test and an analysis based on a suitably modified finite-element model will be performed and the results compared. The end results will be the identification of modeling procedures which need to be improved. Current plans are to conduct a similar type activity on a composite airframe.

Effects of support systems and excitation systems on airframe elastic responses measured in a ground vibration test are typically assumed to be negligible. However, if there are differences between test and analysis, the question of possible extraneous effects associated with these systems often arises. It is clear that correlations would be interpreted with more confidence if these effects were included in the analysis. NASA has devised a scheme for including the effects of support systems and excitation systems in the finite-element dynamic analysis while taking into account the prestiffening effects due to gravity. Boeing Vertol applied this method to the CH-47D. While only minor effects were noted for the CH-47D (refs. 42 and 43) the effects may not be negligible for other configurations. The method appears promising but additional investigation is needed before the method can be routinely applied. The work of fully developing and verifying the method is continuing at Langley using the finite-element model of the CH-47D airframe. In connection with this latter effort, several areas in which the finite-element model could be improved have recently been identified. These latter refinements are to be done by a joint NASA/Boeing team.

Steady-state vibration response analyses are currently being used in evaluating the dynamic response of structures to cyclic excitation forces. An undocumented vibration response analysis based on modal superposition was developed at Langley about 13 years ago in support of RSRA dynamic studies. (This program was used to do the forced response analyses for the CH-47D contained in references 42 and 43). Recently, several enhancements were made to the program making it interactive for rapid evaluation and plotting of responses. The improved version of this computer program is thoroughly documented in reference 45.

There are two in-house Army activities of note relating to finite-element modeling of composite structures. One activity, recently completed, was aimed at examining the modeling and testing complexities of composite structures. A prototype composite tail boom of the type installed on several OH-58A helicopters for environmental evaluation purposes was selected as the test specimen. The

Engineering Analysis Language (EAL) finite-element computer program (ref. 46) was used to model the tail boom (fig. 25). Interest was focused on studying the effect of graphite fiber-volume fraction on static and dynamic behavior because material tests had indicated that the volume varied by as much as ten percent. Results (refs. 47 and 48) indicated that there was improved agreement with test if measured values of material properties were used in the analysis. The other composite modeling activity relates to a blade rather than an airframe but it seems appropriate to include it because the blade is being modeled as a three-dimensional structure. The interest here is to investigate the potential for improving the dynamic and aerodynamic performance characteristics of composite rotor blades through the exploitation of structural coupling associated with ply orientation. Extension-torsion coupling is currently being studied. A three-dimensional model of a highly twisted blade such as might be employed for a tilt rotor is being formed, both to support the design of a model blade and to support subsequent comparisons with both static and dynamic tests. A preliminary model of the D-spar of an untwisted blade as well as of a more recent twisted blade which includes the trailing edge are shown in figure 26. The model is being refined and work is under way to include the proper rotational effects.

### Analysis of Coupled Rotor-Airframe Vibrations

There are four technical factors that should be recognized when dealing with vibrations of a helicopter: (1) vibratory loads induced by the rotor actions; (2) response of the rotor; (3) coupling of the rotor and airframe; and (4) response of the airframe. The major source of vibrations arises from the cyclic loads acting on the rotor blades due to their interactions with the airstream. The dynamic characteristics of the rotor and the airframe and the coupling of these two systems determine the manner in which the helicopter responds to this excitation. As mentioned in the Introduction, the purpose of this paper is to present an overview of accomplishments and contributions associated only with factors (3) and (4) noted above. The response of airframe structures regarded as separate systems was addressed in the previous section. In this section attention is directed to factor (3), namely, the coupling of the rotor and the airframe to account for their interaction in producing vibrations. The emphasis here, as before, is on the response of the airframe as part of a coupled rotor-airframe system.

The analysis methods now employed by industry applicable to helicopter vibrations generally fall into two categories, namely, (1) methods for analysis of airframe behavior and (2) methods for analysis of rotor behavior. For nonrotating airframe components, the NASTRAN computer code, as discussed in the previous section, has become the standard finite-element analysis tool used throughout the helicopter industry for structural design. For rotating components, there has been extensive work on formulating and solving equations of motion of rotors (see, for example, refs. 49 to 57). These references include a number of existing computer simulations of the heli-

copter in flight. Such simulations, of course, incorporate representations of both the rotor and the airframe and the connections between the two and thus theoretically could be applied to calculate vibrations. However, there is little note in the literature of their use to calculate airframe vibrations. These simulations have been applied mainly to evaluate flight controls, to analyze rotor stability, and to calculate blade vibratory loads. As a rule, the current simulations incorporate only cursory, if any, treatment of the airframe elasticity, and are cumbersome to use for airframe structural design work.

It has long been recognized that the interaction or coupling of the rotor and the airframe is important in analysis of helicopter vibrations and there has been at least one early attempt at addressing the problem analytically (ref. 58). From a practical point of view, however, the complexity of the problem has been so overwhelming that it has been customary to separately compute rotor vibratory loads and then apply them to an analytical model of the airframe for determining airframe responses. In this method, a (usually) sophisticated aeroelastic rotor airloads program is employed to calculate the rotor vibratory forces and moments acting at the hub assuming the hub can not move (rotor rotation is, of course, permitted). These vibratory loads are then imposed on an airframe finite-element model to analyze vibrations. In an attempt to approximately account for the effect of the rotor, an "equivalent" rotor mass is usually included in the airframe finite-element model. Historically, most predictions of vibrations have been based on the approach which has just been described. It is clear that this approach can not account for interactions between the rotor and the airframe. A simplified view of how the rotor and the airframe interact to produce vibrations is depicted in figure 27. Due to the cyclic nature of the airloads acting on the blades of a turning rotor, the blades respond dynamically and the resulting vibratory loads are transmitted to the airframe causing it to respond. The resulting airframe motions cause the hub to vibrate which alters the aerodynamic loading on the blades and hence the loads transmitted to the airframe. Depending on the type and configuration of the hub, this interaction can substantially alter the loads which are transmitted to the airframe and hence its vibratory response. However, because of the complexity of such an analysis, the simplistic approach described above was adapted by industry as an early expedient to permit a rudimentary consideration of vibrations. In this regard the method has served the industry well. However, because of increasing demands for further reductions in vibrations to achieve the goal of a "jet smooth" ride, it is now recognized that the simplistic approach is no longer sufficient. Analysis methods which accurately account for rotor-airframe coupling must be employed in vibration design analysis.

Two of the earliest descriptions of practical methods for calculating vibrations of a helicopter as a single system may be found in references 59 and 60. The analyses described in these references are impedance coupling techniques which effect a solution in the frequency domain rather than in the time domain. The impedance coupling technique has been widely used for the vibration analysis of

mechanical systems which are composed of an assembly of point-connected components. In this approach each component is analyzed separately and then coupled together by requiring equilibrium and compatibility (i.e., matching forces and displacements) at each connection point. In its application to the solution of the coupled rotor-airframe problem (see, for example, ref. 60), the loads transmitted by the rotor to the airframe are given by the hub loads calculated assuming the hub is fixed and a (linear) correction term which accounts for small hub motions. The correction term is the so-called rotor hub impedance matrix and is obtained by prescribing small hub motions at the frequencies of interest and calculating the resulting constraint forces and moments at the hub. It should be pointed out that the gross vibratory forces exerted by the rotor on the airframe are given by the fixed-hub forces and that these forces are not, in general, computed by linear theory. The fixed-hub forces come from the solution of the underlying nonlinear rotor equations with the constraint that the rotor-airframe interface points are fixed. The rotor impedance matrix represents a correction to the gross rotor forces resulting from small displacements of the rotor from equilibrium. It is a tenet of design to avoid resonant conditions, and if such conditions are avoided, the displacements from equilibrium should be small. Thus, a rotor model linearized in the guise of a rotor impedance matrix should be nearly as good for vibration prediction as the underlying nonlinear model. The impedance matrix of the airframe at its interface with the rotor is calculated in a similar manner. Compatibility relations are then written for the interface forces and displacements leading to a set of coupled equations in terms of impedances. The resulting "harmonic balance" equations are a set of simultaneous linear algebraic equations which are solved for the hub motions, from which the airframe vibrations are computed.

Calculations based on the theory developed in reference 59 are compared with flight test data obtained on a Sikorsky H-34 rotor blade for several rotor-related quantities. However, only limited analytical results are shown for airframe vibrations and these are for a different helicopter. Reference 60 reports correlations for a tandem-rotor helicopter with three-bladed rotors. The correlations are reproduced in figure 28. While these results fall outside the period of time surveyed by this paper, they do represent some of the earliest published comparisons of a coupled rotor-airframe analysis with airframe vibrations measured in flight. Reference 61 reports a correlation for a different tandem-rotor helicopter using the analysis of reference 60. The relevant results are reproduced in figure 29. The rotor model was very crude. Specifically, only the fixed-hub forces obtained from the equilibrium solution were retained in the linearized rotor equations. The rotor impedance was ignored. Reference 62 reports correlations for a compound helicopter with a four-bladed hingeless rotor. Plots indicative of the correlations are reproduced in figure 30. Nonlinear rotor equations were used in that analysis, but the airframe was represented by impedances calculated using a simple stick model representation of the airframe. The results of an early application of the C-81 flight simulation analysis for computing airframe vibrations on a helicopter with a four-bladed hingeless rotor are reported in reference 63. Computed

results for the 4/rev hub vibrations are compared with measured flight vibrations in figure 31. The airframe was represented by only three modes: pitch and roll of the pylon about its focal point (the test vehicle was equipped with a "focused pylon" vibration isolation system) and a vertical rigid-body mode. A correlation performed for a helicopter with a two-bladed teetering rotor is reported in reference 37. In this case, the analysis did not incorporate a model of the rotor system. The procedure was to measure the flight vibratory accelerations at the rotor hub and then to impose the measured values of acceleration on a NASTRAN finite-element model of the airframe. The calculated response of the airframe was compared with the response measured in flight. Typical results for the major responses are shown in figure 32. Reference 64 describes procedures developed for correlating stresses derived from a NASTRAN finite-element model of the Bell 214A helicopter with stresses measured in flight. Although the flight tests were aimed at static structural qualification of the airframe in design maneuvers and not vibration, it seems appropriate to mention it here because C-81 was used to compute the external forces which were applied to the NASTRAN model. Analytical stresses were calculated by applying the internal loads calculated by NASTRAN to the effective cross-sectional area at each of the strain-gauge positions in the airframe as outlined in reference 64. Excellent correlation was noted.

In an analysis of helicopter vibrations based on a finite-element model of the airframe, the number of degrees of freedom in the finite-element model must be reduced. Two approaches are currently recognized for making this reduction and still preserving the essence of the finite-element model: (1) representing the airframe by forced responses (i.e., impedances) calculated at a few frequencies corresponding to the rotor harmonics of interest; and (2) representing the airframe by superposition of a few of the natural modes of vibration. Whichever approach is used, data needed to represent the airframe with a reduced number of degrees of freedom are calculated by using a finite-element model of the airframe alone. Modal representations can be used for reducing the number of degrees of freedom when calculating any of the linear structural responses of interest in practical flight dynamics. This includes problems of aeroelastic stability and transient response as well as the present problem of steady-state vibrations. This broad applicability has caused the modal representation of the airframe to be the choice of developers of computer simulations of the helicopter in flight (e.g., C-81, CAMRAD, REXOR). Modal representations of the airframe are also used in more specialized coupled rotor-airframe formulations (see, for example, refs. 49 and 65). However, for vibration analysis done to support design of airframe structures, there are several attendant advantages to representing the airframe by harmonic forced responses. Hence, developers of new codes specifically for computing coupled rotor-airframe vibrations have tended to represent the airframe in terms of harmonic forced responses.

There have been several research studies using simple math models of coupled rotor-airframe systems to gain physical insight into the helicopter vibrations problem and to identify governing param-

ters. References 66 to 74 contain solutions of such simplified rotor-airframe systems and relevant subsidiary analysis procedures. These and other studies have all shown that the coupling between the rotor and the airframe has a major effect on all aspects of vibration. In addition to studies using simplified models, there has been some work in developing equations of motion of coupled rotor-airframe systems which devotes particular attention to nonlinearities associated with the rotor contributions to the coupled equations of motion (refs. 75 to 78). Reference 75 addressed the problem of developing a general approach for the dynamic analysis of gyroscopic structures composed of point-connected substructures by a component mode synthesis technique. The resulting formulation was intended to permit the determination of the modal characteristics of a helicopter. The mathematical model underlying the formulation, as well as the simplified model of a helicopter used to illustrate the formulation, are shown in figure 33. A computational procedure for deriving explicit equations of motion for such dynamical systems using symbolic manipulation is described in reference 76. Reference 77 derived the governing equations of motion for a helicopter rotor with blades having freedom in flap, lag, and torsion coupled to an airframe modeled as a rigid body with three translational and three rotational degrees of freedom. The resulting differential equations are nonlinear and contain periodic coefficients associated with forward flight. Reference 78 derived the governing equations for rotor and airframe subsystems to use in an impedance matching approach to coupling. The reference also described a procedure for solving the resulting nonlinear equations for the coupled vibratory response by an iterative, combined harmonic-balance, impedance-matching method.

In recent years there have been several attempts to formulate a general method of vibration analysis suitable for airframe structural design work. These efforts have specifically addressed practical methods for calculating helicopter vibrations. Some of these endeavors are discussed below.

Dissatisfaction with first generation predictive capability for helicopter performance, loads, and vibrations motivated the Army to begin development of the Second Generation Comprehensive Helicopter Analysis System (2GCHAS). As a consequence of predesign studies related to 2GCHAS, several special-purpose codes have been developed by industry for solution of dynamics problems of coupled rotor-airframe systems, including vibrations. Two of these are RDYNE (ref. 79) and DYSCO (refs. 80 and 81). RDYNE (Rotorcraft System Dynamics Analysis) employs a time-history analysis for computing rotorcraft response (stability or vibrations). A substructures approach is employed to model the helicopter. The program has been applied to at least one flight vibrations analysis, which is discussed later. Another code that had its genesis in the 2GCHAS predesign studies is DYSCO (DYnamic System COupler). The DYSCO program has been under development since 1978 with both corporate (ref. 80) and government (ref. 81) funding. The program forms coupled equations of motion using the uncoupled equations of each component. Each component may contain periodic, nonlinear, and nonanalytic effects. Solutions can be effected in either the time or frequency

domain. There is no note in the literature of its use to calculate coupled rotor-airframe vibrations.

The SIMVIB (Simplified Vibration Analysis) code was developed under Army sponsorship to provide a design tool for predicting vibrations and for use in research studies (ref. 82). The analysis is based on a substructures approach and consists of a base program and a set of external programs (fig. 34). While emphasis is placed on obtaining solutions for steady-state vibrations by a harmonic balance method, other types of solutions are available. The results of limited correlations with data obtained from wind-tunnel tests of dynamically scaled models which include higher harmonic control effects are presented in that report. On the basis of these comparisons it was concluded that trends of vibration with airspeed could be predicted. A recent "application" of SIMVIB to the SH-60B Sea Hawk is reported in reference 83. In this case the rotor impedance was not calculated by the program. Instead, 4/rev vibratory hub loads measured on the UH-60 were scaled to the SH-60B and imposed (within SIMVIB) as known exciting forces on a six-mode representation of the airframe. Comparisons of predicted vibration levels with those measured in flight are given in figure 35.

Reference 84 is an outcome of recent efforts at the NASA Langley Research Center to establish foundations for adequate representation and treatment of the airframe structure in design analysis of helicopter vibrations. The report presents a body of formulations for coupling airframe finite-element analysis models to rotor analysis models and calculating airframe vibrations. The rotor is represented by a general set of linearized differential equations with periodic coefficients, and the connections between the rotor and airframe are specified through general linear equations of constraint. Coupling equations are derived and then applied to combine the rotor and airframe equations into one set of linear differential equations governing vibrations of the rotor-airframe system. These equations are solved by the harmonic balance method to yield the system steady-state vibrations. A key feature of the solution process is to represent the airframe in terms of forced responses calculated at harmonics of the rotor rotational frequency. A method based on matrix partitioning is presented for quick recalculations of vibrations in design studies when only relatively few airframe members are varied. A parallel development is given for the case in which the rotor is represented by impedances. All relations are presented in forms suitable for direct computer implementation. An illustration of this is given in figure 36 in which the coefficient matrix in the general harmonic balance equations retaining all the harmonics has been pulled out to show its structure. The explicit and practical nature of the formulation is illustrated by the example of the formula for the rotor contributions to the harmonic balance equations shown at the bottom of figure 36. Matrices appearing in the formula, such as KRLP, come directly from the linearized rotor equations and parameters, such as ULC, are computed by very simple algorithms which are provided. Such explicit formulas, FORTRAN-like notation, and the blueprint-like representation of matrices are used throughout the report to facilitate computer implementation.



Among the many activities being conducted under the DAMVIBS program is one aimed at evaluating existing analysis methods for calculating coupled rotor-airframe vibrations. In the initial effort in this area Bell, Boeing, McDonnell Douglas, and Sikorsky have applied in-house methods for coupled rotor-airframe analysis to calculate vibrations of the AH-1G helicopter. Comparisons were also made with existing Operational Loads Survey data (refs. 85 and 86). A finite-element model of the AH-1G airframe was adjusted by Bell to correspond to the aircraft configuration used in the loads survey. The updated model was furnished to the other participating manufacturers as part of the common data utilized for the subject study. Bell was also required to provide to the other companies a summary of all modeling, testing and correlation work conducted on the AH-1G (ref. 38). Bell was further required to assemble the flight vibration data to be used in the correlation and to describe the rotor system both mechanically and aerodynamically to the other participants (ref. 87). The aforementioned exercise on the AH-1G has been completed and the results have been presented at NASA/industry meetings held under the DAMVIBS program. Draft final reports have been submitted and are under NASA review. The comparisons shown in figures 37 and 38 are illustrative of the results obtained. Figure 37 shows a comparison of measured 2/rev and 4/rev vertical vibrations with predictions made by Bell using C-81. A summary of their results may be found in reference 88. Figure 38 shows a comparison of 2/rev vertical and lateral vibrations predicted by each of the four industry participants. These results were also compared with measurements at two locations in the airframe. The analytical results obtained by the four companies for the 2/rev vertical, lateral, and longitudinal vibrations are in fair to poor agreement with measured flight data. It should be noted that 2/rev is the primary main rotor excitation in the airframe. Best agreement was generally obtained for vertical vibrations; the worst for the lateral vibrations.

Boeing Vertol has recently implemented an impedance-based coupled rotor-airframe analysis (developed in-house) based on the concepts in references 60 and 61. The method (which was employed in the aforementioned AH-1G activity) is described in reference 89. Analytical results obtained for a wind-tunnel model and compared to test data showed, as had earlier studies, that results which include coupling differ significantly from results obtained without coupling. More important, however, their analyses also indicated that mechanical impedance effects predominate over aerodynamic effects for the scale model tested. If this result remains true for full-scale configurations, it would mean that a good approximation of rotor impedance for use in coupled rotor-airframe vibrations analyses could be obtained by neglecting (or at least drastically simplifying) the rotor aerodynamics. Because the computational effort required to compute rotor impedances which include aerodynamic effects is usually significant, any substantial reduction in the level of aerodynamic sophistication would greatly reduce these computations. This is an area that needs to be investigated further.

There are two NASA in-house activities of note related to

coupled rotor-airframe vibrations being conducted in support of the DAMVIBS program. The first activity is part of a continuing effort aimed at evaluating existing methods of analysis for coupled rotor-airframe vibrations. Work has been initiated toward the application of the SIMVIB analysis to the OH-6A helicopter (fig. 39) used in a recently completed NASA/Army Higher Harmonic Control flight test program (ref. 90). Analyses will be made with and without higher harmonic control and compared with similar results obtained in flight test. Current plans are to also evaluate the DYSCO analysis with respect to its applicability for computing coupled rotor-airframe vibrations. The other activity is aimed at developing new computational procedures for coupled rotor-airframe vibration analyses. The primary effort here will be to encode the computational procedures for coupled rotor-airframe analysis and reanalysis which are outlined in reference 84.

It is clear that further work is needed in analysis of coupled rotor-airframe vibrations. Current plans are to conduct another industry-wide coupled rotor-airframe vibrations analysis under the DAMVIBS program, this time utilizing a helicopter with a four-bladed articulated rotor. Also, in an attempt to identify the importance of aerodynamics in rotor impedance calculations, parametric studies will be conducted in-house by NASA to evaluate the effects of rotor aerodynamic and structural modeling assumptions on predicted airframe vibrations. Current Army plans call for some combined in-house and contractual efforts aimed at validating existing codes for coupled rotor-airframe vibrations analysis using both model and full-scale data.

### Airframe Structural Optimization

The design of aerospace vehicle structures to satisfy static and dynamic specifications is a complex process. This has become especially true for modern helicopters primarily because of increasingly stringent requirements for low vibrations. The structural design process involves the merging of an analysis procedure with a resizing and reanalysis procedure in which changes are made to the structure in an iterative process until a converged design that is best or optimum in some sense is obtained. With regard to the airframe structural design process, the selection of the best airframe that meets all the requirements, in particular the vibration requirements, is a difficult task. It would appear that structural optimization tools, properly brought to bear by the design engineer, could go a long way toward achieving the goal of a design analysis capability for vibrations. Indeed, even the automation of as much of the current design process as possible would clearly serve to reduce design time and hence cost.

The objective of structural optimization is to design a structure that minimizes a specified function while satisfying a set of restrictions imposed on the design. The function with respect to which the design is optimized is called the objective function (alternative names which are sometimes used are performance index and

merit function). For aircraft structures, weight is usually taken to be the objective function. However, the objective function can be any quantity of interest. The restrictions placed on the design that must be satisfied to produce an acceptable design are collectively called constraints. Typically, constraints impose upper or lower limits on quantities such as stresses, displacements, natural frequencies, and structural parameters which are varied. Optimization procedures start with an arbitrary (but usually feasible) initial design and proceed by varying structural parameters in stepwise fashion so that the value of the objective function is reduced. The search is terminated when no further reduction can be made in the objective function without violating some of the constraints. The parameters which are varied during the iterative design process are called design variables. Examples of design variables include member sizes such as thicknesses of panels and cross-sectional areas of stringers, ply thicknesses and fiber orientation angles in composite material laminates, and physical properties of materials. The optimization problem is nonlinear if either the objective function or any of the constraints are nonlinear functions of the design variables. This is the usual case for the class of structural optimization problems which are of interest here.

A design-optimization algorithm consists of an analysis of the structure and modification of the design variables at each iteration. The number of iterations depends on the number of design variables and on the nature and number of constraints. Analyses of most aerospace vehicle structures are based on some type of finite-element model. Modification of design variables can be achieved by employing an optimizer which is based on either a nonlinear mathematical programming method or an optimality criterion method. Optimality criteria methods have the longest history. The basis for this approach is the a priori specification, based either on intuition or rigorous mathematical considerations, of a set of conditions to be satisfied by the optimum design. The premise is that when the structure is sized to satisfy the condition, the objective function automatically attains an optimum value. The algorithm which is formulated to resize the structure is usually recursive in nature. The concept of a fully-stressed design, which has been widely used in static structural design, is perhaps the best example of these methods. Nonlinear programming (NLP) methods have their origins in the field of operations research. These rigorous methods are applicable to a wide range of problems, of which structural optimization represents only one particular application. NLP methods use derivatives to determine move directions in the design variable space. Their main drawback is that the derivatives may be costly to calculate, especially when the number of design variables is large. However, the capability to treat all types of objective and constraint functions makes these methods very versatile. This is the method of choice for most current work related to structural optimization.

Since the beginning of the "modern" field of structural optimization in 1960 (ref. 91), the published literature in the field has literally exploded with new papers. For example, reference 92, which summarizes aeronautical applications of formal optimization methods,

identified over 8000 aeronautically related titles (including 1381 on structural optimization) covering various periods between 1964 and 1980. However, despite its long history and continued widespread interest, as noted in reference 92, there have been few successful genuine applications to aeronautical problems. In so far as the helicopter community is concerned, interest in optimization as it might be employed in helicopter design goes back only a few years. A preliminary evaluation of optimization techniques as they relate to typical helicopter design problems is reported in reference 93. The paper describes the manner of combining nonlinear programming algorithms with conventional engineering analyses and summarizes the results of applying such algorithms to four different rotor design problems. The results obtained demonstrated that closed-loop design-oriented analyses can significantly reduce design time. The 39th American Helicopter Society Forum the following year featured a panel devoted to the subject (ref. 94) as well as two papers (refs. 95 and 96). The composition of the panel and the topics addressed are indicated in figure 40. References 95 and 96 treated the related topics of designing a rotor blade for minimum hub vibrations and of designing a blade for placement of natural frequencies, respectively. More recently in 1984, a NASA Symposium on Recent Experiences in Multidisciplinary Analysis and Optimization held at Langley Research Center (ref. 97) devoted an entire session to rotorcraft applications (fig. 41). Additional applications are reported in references 98 and 99. Two recent surveys of the application of structural optimization methods to helicopter design problems are given in references 100 and 101. All of the aforementioned references reporting on rotorcraft applications of structural optimization have addressed the rotor system. There has been very little published work within the rotorcraft community relating to structural optimization of the airframe subject to vibration response constraints. The remainder of this section will address work which has been done that is applicable to the airframe. The section concludes with a status report of related in-house work.

The basic idea of airframe structural optimization under vibration constraints is to design the airframe structure in a way that minimizes the vibratory response in the important areas. It is beyond the scope of current design-optimization codes to treat each element of a structure as a variable in the iterative process. Hence, it is necessary to identify those few elements in a structure that should be treated as variables and modified to effect a reduction in vibrations. This identification process constitutes a task in sensitivity analysis. In its formal implementation sensitivity analysis involves calculating changes in the structural response with respect to (small) changes in the design variables. Such sensitivity derivatives are used by all NLP-based optimization methods. As mentioned earlier, the computation of these derivatives may be costly when the number of design variables is large. Informal implementations of sensitivity analysis are usually based on considerations related to some physical characteristic or behavior of the system, such as the distribution of element strain energies. Hence, they are usually employed in optimality criteria based methods. To date, most applications of optimization to helicopter airframe structures have

employed optimality criteria type methods. Reference 102 considers two strain-energy methods for structural modification (detuning) to achieve vibration reduction. The first method is based on the modal strain energy concept wherein elements having the highest strain energy density in a mode are taken to be the best candidates for modification to obtain a maximum frequency change of that mode for a minimum weight penalty. The second method is an extension of the concept of modal strain energy to the case of damped forced response wherein the strain energy density is determined for all the structural elements under steady-state vibratory loading. The elements with the highest strain energy densities are taken as the best candidates for modification of the structural response condition under study. The damped forced response (DFR) method is an extension of the optimality criterion of uniform strain energy density proposed in reference 103 for modes to the case of forced response. Several applications of the DFR method are described in reference 102, one of which is reproduced in figure 42. The figure shows the results of using modal strain energy to tune the frequency of the fourth elastic mode of the CH-47A. Based on the calculated strain energies, the structure was stiffened (the thickness of ten elements in the forward pylon and main cabin side panels was increased with a weight penalty of 2.5 percent) to move a natural frequency (12.03 Hz) to a higher position (12.74 Hz) with respect to the excitation frequency (11.45 Hz), thereby reducing the dynamic response. As the table shows, only the single frequency of interest was significantly altered. A DFR analysis of the modified airframe confirmed that the vibration levels had been reduced with respect to those in the original structure in the area of interest. Based on the studies conducted in reference 102, it was concluded that the DFR method is more general and thus has a broader range of applicability than the modal strain energy method. However, the modal approach is appropriate if the structure is excited close to a resonance, as in the case of the CH-47A in figure 42. Application of the modal strain energy approach to the CH-47C is reported in reference 104.

As part of an investigation of structural optimization techniques for vibration reduction, reference 105 evaluated two techniques for vibration reduction through local structural modification, the forced response strain energy method of reference 102 and the Vincent Circle method (ref. 106). The latter method is based on a dynamic property of (damped) linear structures, first noticed by Vincent of Westland Helicopters, Ltd. Vincent observed that under sinusoidal excitation the response of a point removed from the point of excitation traces out a circular locus in the complex plane when any single structural element stiffness or mass parameter is continuously varied from minus infinity to plus infinity. The radius of the circle and the location of its center are indicative of the extent to which the parameter change can affect the response. Both methods were applied to an elastic line model of the AH-1G airframe (fig. 43). The objective was to reduce 2/rev vertical vibration at the pilot seat due to 2/rev vertical excitation at the main rotor hub. The results (fig. 43) indicated discrepancies between the two methods. The DFR method points to the tail boom as the area having the most potential for reducing vibrations at the pilot seat, while

the Vincent Circle method points to the pylon area. Based on the studies conducted in reference 105 it was concluded that the Vincent Circle method was appropriate as an identifier of important elements when considering local effects in relatively simple structures. However, for complex structures involving many elements the DFR method appeared to be preferable for indicating which structural elements are most responsible for the dynamic amplification.

Other approaches to local structural modification aimed at vibration reduction are described in references 107 and 108. Reference 107 describes a sensitivity analysis procedure based on taking derivatives of the stiffness matrix to identify the elements most influential on vibratory response. The method is demonstrated by using a modified version of the elastic line model used in reference 72 and by choosing as design variables Young's modulus of elasticity in each of the beam elements comprising the model. Reference 108 describes an approach for structural modification which utilizes not only the analytical model but also dynamically scaled models, optimization techniques (via optimality criteria) with frequency constraints, and system identification methods. The reference illustrates the approach by applying it to a simple cantilever beam structure.

The papers dealing with structural modification cited above are somewhat misleading. While the term "structural optimization" is used, none of the papers apply structural optimization in the usual way. Rather, the term is used to indicate that any local structural modifications which have been made are the best based on ad hoc considerations such as reduction of dynamic response or reduction of strain energy in a member. It should be recognized, however, that the methods described in those papers can be used as the first step in a procedure for formal optimization because they can identify the best few elements that can be treated as variables for reducing vibrations. Once the sensitive elements are identified a formal optimization procedure can be used to set the precise values of the parameters characterizing those elements.

There has been considerable research on structural optimization subject to dynamic constraints. Most of this work, however, is related to studies in which the only dynamic constraints are those imposed on natural frequencies. There is much less literature dealing with the problem of structural response under dynamic loading in which constraints are imposed on both dynamic responses and frequencies. References 109 to 111 are representative of work which is applicable to this more general problem. These papers discuss a phenomenon known as disjoint design space which complicates the structural optimization process for structures under harmonic excitation. The problem is associated with airframe natural frequencies which may move toward coincidence with a (fixed) forcing frequency as design variables are changed during iteration. These resonances form barriers which cause the feasible design space to be disconnected or disjoint.

The success of any optimization procedure rests primarily on the

efficiency of the analysis tool which is used to analyze the structure after every update to the design variables, and to a lesser extent on the efficiency of the optimizer. If the finite-element model is large (which is usually the case), the analysis step contributes significantly to the time for each iteration in the design process. There has been considerable effort directed toward means for reducing the time required for each iteration. Approximate mathematical models obtained from a first-order Taylor series expansion of the full finite-element model have been proposed to lessen the analysis time. Other expedients such as the use of design variable linking, reciprocal variables and constraint deletion have also been proposed. Such methods are described in reference 112, for example. There have also been attempts to develop algorithms for efficient reanalysis of structures which have been locally modified (see, for example, refs. 84, 113, and 114).

Motivated by participation in the initial planning stages of the DAMVIBS program in early 1983, Ames Research Center began building a breadboard structural optimization code for helicopter vibrations in late 1983. The resulting code, called NASOPT, combines MSC/NASTRAN (ref. 22) with the CONMIN optimization program (ref. 115) and is described in reference 116. A recent application of NASOPT to the problem of tuning a helicopter airframe for vibrations is described in reference 117. One case addressed in that paper was to minimize the vertical displacement at the pilot seat under 2/rev vertical forcing at the main rotor hub while subject to a frequency constraint on the first vertical bending mode. The design variables were taken to be the sectional area moments of inertia of each of the 22 beam elements comprising the longitudinal beam in the elastic line model. The resulting iteration history for three of the design variables is shown in figure 44.

The NASA Langley Research Center has a long history of research in structural optimization (see, for example, the summary of ref. 118). Most of this activity has, until quite recently, been centered in the Multidisciplinary Analysis and Optimization Branch (MAOB). In 1984 the Interdisciplinary Research Office (IRO) was formed, with optimization personnel from MAOB as its nucleus, to provide a more focused repository of optimization research. While most of the early Langley work on optimization has been directed to fixed-wing aircraft, it has been generic in nature and should be applicable to rotorcraft. Of particular interest in this regard is the method for decomposing large optimization problems into smaller subproblems described in reference 119. Some recent work directed to the dynamics of rotor blades are reported in references 120 and 121.

As part of the NASA/industry rotorcraft structural dynamics program, DAMVIBS, an in-house study was recently initiated at Langley on optimization of rotorcraft airframe structures for vibration reduction. The objective of the research is to evaluate and develop practical computational procedures for structural optimization of airframe structures subject to steady-state vibration constraints. One of the key ingredients to any approach based on a NLP method is design sensitivity analysis. A method for computing the sensitivity

coefficients for forced response behavior has recently been formulated and implemented in MSC/NASTRAN as a new solution sequence to complement the already available static and frequency sensitivity analyses. The results of an initial application of this design sensitivity analysis to a simplified elastic line model of the AH-1G helicopter are presented in reference 122. Some of the results from that study are reproduced in figure 45 which shows computed dynamic response sensitivities for the pilot seat with respect to elements in the tail boom. The forced response strain energies associated with the tail boom elements are also shown. The results show that elements in the tail boom would be likely candidates for modification to effect a favorable change in the response at the pilot seat. It should also be noted that elements with large sensitivities also generally have higher strain energies.

The Langley in-house work on airframe structural optimization described above is continuing. Current near-term plans are to include structural damping in the formulation for calculating forced response sensitivities, to study the implications of computing sensitivities of large finite-element models, and to interface the CONMIN optimizer with the sensitivity analysis. Long-term plans are to merge this airframe optimization activity with IRO activities on rotor blade optimization and establish a joint activity aimed at providing a rudimentary technology base for optimization of coupled rotor-airframe systems. Current plans are to also initiate some type of airframe optimization activities (as yet undefined) with industry under the DAMVIBS program. With respect to the NASOPT code developed at Ames Research Center, current plans are for Ames to maintain the code as a research tool for conducting basic research in structural optimization; long-term plans for the code are unclear at this time.

## VIBRATION CONTROL

The most significant vibration levels in a helicopter are caused by the cyclic airloads acting on the main rotor as it rotates. The resulting oscillating aerodynamic loads are transmitted to the fuselage as vibratory forces and moments of a frequency equal to the number of rotor blades  $N$  times the rotational frequency or  $N/\text{rev}$ . The character and magnitude of these vibratory loads have resulted in the design of vibration control devices to reduce or minimize these rotor-induced forced vibrations. Vibration reduction concepts may be separated into passive or active methods. Passive devices, as discussed in this paper, are absorbers in the rotating system, absorbers in the fixed system, or rotor isolation systems. Active systems sense vibration levels at one or more locations on the helicopter and attempt to minimize the sensed vibration levels by use of some type of active control feedback system. A variety of passive vibration control systems have been developed and tested over the past 25 years. The Army and NASA have sponsored considerable research in rotor isolation systems, hub absorbers, and blade absorbers. References 8 and 123 provide an excellent historical and technical prospective of vibration control system development. Since 1975 the Army and NASA have funded major vibration control system demonstra-



tion efforts in total main rotor isolation and higher harmonic control. There have also been some contracted research efforts for the analysis and testing of hub-mounted and blade-mounted absorbers. As previously pointed out, only Army and NASA research conducted in the past decade will be specifically discussed.

### Rotating-System Passive Absorbers

One of the simplest passive mechanisms for reducing vibratory loads in the rotating system is the pendulum absorber. It consists of a simple mass attached at a distance  $R$  from the center of rotation by a mechanical linkage of smaller radius  $r$  (fig. 46). The spring rate of the pendulum is controlled by centrifugal forces on the mass. The pendulum natural frequency is proportional to the rotational speed and the ratio of radii  $R/r$ . Therefore, the pendulum acts as a vibration absorber when the pendulum natural frequency equals the excitation frequency. Both blade-mounted and hub-mounted pendulum absorbers have been used in production helicopter. Reference 124 describes a blade-mounted pendulum absorber system that was designed for the Army AH-64. A general analytical study of pendulum absorber dynamics is reported in reference 125. This analysis was later extended to a frequency response analysis in which the spanwise airload distribution was varied harmonically to excite the rotor (ref. 126). The response of this absorber is shown in figure 47. Another type of rotating-system vibration absorber, the bifilar absorber, is a centrifugally tuned, pendulum-like device mounted to the main rotor hub. A bifilar absorber is shown in figure 48. Components of a bifilar absorber consist of a support arm and sets of bifilar masses each of which is comprised of a dynamic mass, and two cylindrical tuning pins. These pins constrain the mass radially and, together with the circular tracking holes in the support arm and mass, define the pendular radius of the mass (ref. 127). The bifilar rotor hub absorber has been used since the late 1960s. In support of the bifilar development, a coupled rotor-bifilar-airframe analysis was used to study the dynamic characteristics. This analysis was validated by correlation with UH-60 and S-76 helicopter flight test data as shown in figure 49 (ref. 128). In addition to industry-sponsored bifilar research, the Army funded research to develop advanced hub absorber concepts. A two degree-of-freedom rotating system absorber, the monofilar (fig. 50), was analyzed and tested in the early 1980's (refs. 129 and 130). The advantages of this concept compared to the bifilar were reduced weight and the ability to provide vibration reduction at two frequencies. Coupled rotor-monofilar-airframe analyses were conducted to design a monofilar configuration for a four-bladed rotor under contract to the Army (ref. 131). The system was tuned to reduce 3/rev and 5/rev rotating-system forces. Ground test results showed a significant attenuation of 3/rev in-plane rotating-system hub forces. However, attenuation of the 5/rev loads was poor as a result of physical binding of the monofilar components (ref. 131).

## Nonrotating-System Vibration Isolation

Although no Army or NASA in-house research has been conducted to develop specific vibration reduction hardware, in the past ten years efforts have been funded to demonstrate company-developed systems. The most successful passive isolation systems have been based on the anti-resonant (nodalization) principle. A schematic of an antiresonant isolator is shown in figure 51. By proper selection of the tuning weight and arm length, the inertial force can be made equal and opposite to the spring force, and therefore no N/rev vibratory forces are transmitted to the fuselage. Several antiresonant vibration reduction concepts have been investigated. One concept, described in reference 132, is the Dynamic Antiresonant Vibration Isolator or DAVI which was implemented by the Kaman Aerospace Corporation. The Kaman DAVI is a passive isolator that provides a high degree of isolation at low frequencies with low static deflections. Research and development has been conducted on one-dimensional, two-dimensional, and three-dimensional DAVIs (fig. 52). A two-dimensional DAVI system was tested on a modified Army UH-1H helicopter to provide isolation in the vertical, pitch, roll, and fore-and-aft degrees of freedom. This test demonstrated that the DAVI-modified UH-1H had substantially lower vibration levels (over 70 percent) when compared to the unmodified vehicle (fig. 53). The results of this test also demonstrated that the use of the DAVI could, without affecting flying qualities, reduce aircraft weight and lower operating costs due to lower maintenance requirements (ref. 132). In a parallel development, Bell tested a DAVI-type system called the NODAMATIC isolation system (ref. 133). The NODAMATIC system consists of a focused pylon to isolate rotor inplane hub shears and moments and a nodal beam to isolate rotor vertical shears (fig. 54). Boeing Vertol improved the DAVI by replacing the elastomeric springs with metal springs to reduce inherent damping. This new system, called the Improved Rotor Isolation System (IRIS), also provided isolation at twice N/rev (refs. 134-136) (fig. 55). The IRIS was designed and tested on a Boeing-owned BO-105 (fig. 56).

To demonstrate the full potential of passive isolation, the Army in 1979 initiated a program for total (six degree-of-freedom) main rotor isolation. The program was conducted in several phases which included predesign studies, design and bench test, and flight test. Predesign studies were conducted of two different mechanical isolation system concepts (refs. 137 and 138). Both designs were derivatives of the Kaman DAVI. A third concept, which used hydraulic isolator units to achieve antiresonance, was also evaluated (ref. 139). This hydraulic isolator is called the Liquid Inertia Vibration Eliminator (LIVE) and is depicted in figure 57. The LIVE unit consists of an inner cylinder which is bonded to an outer cylinder with a layer of rubber. The inner cylinder cavity is filled with a high-density fluid (mercury). Isolation is achieved when the dynamic pressures create inertial forces which cancel the spring forces associated with deformations of the rubber. Reference 140 describes an application of LIVE. As a result of the predesign effort, the LIVE concept was selected for detail design and bench testing of total main rotor isolation. The success of this phase resulted in an Army-funded con-

tract to install a Total Rotor Isolation System (TRIS) on the Bell 206LM helicopter. The testbed aircraft and the LIVE unit installation are shown in figure 58. The flight test data indicated that over 95 percent reduction of hub 4/rev (26.3 Hz) vibration levels had been achieved. Pilot seat vibrations were reduced to 0.04g throughout the flight envelope, including the transition region which traditionally has high vibration levels (fig. 59). The prototype TRIS installation had a weight penalty of 1.7 percent of the aircraft maximum gross weight. It was projected that the weight penalty could be reduced to less than 1 percent (ref. 141) by manufacturing the LIVE units out of lightweight material, instead of the stainless steel used for the proof-of-concept test.

The Rotor Systems Research Aircraft (RSRA), which is shown in figure 60, incorporated a passive isolation system. The system was designed to provide a satisfactory aircraft vibration environment for "any" rotor system installed on the aircraft. Although labeled the "RSRA Active Isolation/Rotor Balance System" or AIBS, this system is not "active" in the conventional sense. The AIBS (fig. 61) consists of four piston-in-cylinder units which combine the effects of an air spring for 4/rev passive isolation with a low frequency centering action (for active control of transmission alignment). The effective spring rate of the passive isolation system is controlled and set prior to flight by the precharge pressure of the system accumulators. Thus, the AIBS does not sense and react to changing flight vibration levels in the normal sense of "active" control. The hydropneumatic isolation system is described in reference 142. Although the reduced vibration levels measured during the RSRA isolation system shakedown flight test program were encouraging, the isolation system was not optimized for minimum cockpit vibrations and the potential for additional improvement exists (ref. 142).

### Active Vibration Suppression

Active vibration suppression systems, as discussed in this section, sense vibration levels at one or more locations on the airframe and actively minimize the sensed vibration levels by the use of an automatic feedback system (fig. 62). Because the primary source of helicopter vibrations is the rotor, it is logical to use the feedback system to manipulate the rotor blades to modify the aerodynamic excitation forces, thus reducing the airframe vibrations. The potential of direct rotor control to minimize vibrations has been studied since the 1960's. The early work, however, was limited to analytical studies because adequate hardware did not exist to implement a system (ref. 143). The use of active means for suppressing vibratory loads transmitted to the airframe in flight has become feasible with advances in high-speed, lightweight microcomputers and with advances in hydraulic servo-actuator technology.

One promising method of active vibration control, called Higher Harmonic Control or HHC, superimposes nonrotating swashplate sinusoidal motions at the blade passage frequency upon the basic collective and cyclic flight control inputs. This approach to control

vibratory loads has been the subject of several analytical studies by both NASA Ames and the Army (refs. 144 and 145) and wind-tunnel tests by both government and industry (refs. 146-148). These investigations, conducted on significantly different types of rotor systems, all showed that HHC produced substantial reductions in vibration levels transmitted to the airframe. Furthermore, the results indicated that the amplitude of HHC blade pitch inputs required to achieve the desired reductions was small, on the order of one degree.

In 1976, NASA Langley and the Army began some preliminary research into applications of HHC. This work resulted in two major activities which included: (1) wind-tunnel tests; and (2) a flight test demonstration. The initial wind-tunnel tests were conducted open-loop using trial-and-error for setting the amplitudes and phases of the HHC inputs. While these open-loop tests validated the concept, computerized control was needed to achieve optimum control of all vibratory forces and moments. The open-loop and closed-loop HHC test results on a dynamically scaled wind-tunnel model rotor were reported in references 149 and 150. The HHC method for reducing vibrations was demonstrated under contract using an OH-6A helicopter. The preliminary design work, control law development, and flight test results were reported in references 151 to 153. The open-loop and closed-loop flight testing of the OH-6A showed conclusively that HHC can reduce vibration levels in helicopters (fig. 64). Reference 90 constitutes a summary report for that program. Research has continued on HHC with Sikorsky flying the concept, open-loop, on an S-76 (ref. 154) and the Army funding two preliminary design studies for implementation of HHC on current and future generation helicopters.

Although individual blade control has been promoted for vibration reduction using HHC, the complications of moving any control system into the rotating system have slowed down advances in this area. Several concepts of direct rotor control with individual blades have been studied earlier (ref. 155) but to date none have been tested. Higher Harmonic Control shows much promise for reducing helicopter vibrations, especially for the next generation helicopters that may have a fly-by-wire/light control system and a variable speed rotor. The Army plans to extend HHC technology by sponsoring a flight demonstration program using a modern, four-bladed, high-speed helicopter. This program has been given the acronym SOFVIBS (Suppression Of Flight VIBRationS).

The helicopter vibration problem is complex and much time, effort, money, and man-power have been expended to reduce vibrations. Nevertheless, the problem has not been completely solved and a great deal more work remains for the helicopter community before the "jet smooth" ride is achieved. The vibration reduction systems discussed in this section only reduce vibrations that are transmitted mechanically to the fuselage from the rotor. While the helicopter industry has been able to significantly reduce these "mechanically-transmitted" vibrations in the last 30 years, another source of rotor-induced vibrations still must be addressed, in particular, wake impingement on the airframe. Blade tip vortices create pressure fluctuations on the fin and stabilizer that cause significant fuse-

lage vibrations. These rotor downwash induced vibrations need to be controlled or isolated from the fuselage before vibrations in the helicopter fuselage can ever be totally eliminated (ref. 132).

## VIBRATION TESTING

Vibration testing of helicopters involves experimental investigations to establish and to verify airframe dynamics, flight vibrations, and rotor-induced vibratory loads. Ground and flight vibration testing along with wind-tunnel testing are used to guide helicopter design and to evaluate vibration problems. For the most part, wind-tunnel testing is conducted to verify rotor performance and basic stability and control characteristics for straight and level flight. In recent years, wind-tunnel testing has been conducted to investigate the effects of main rotor wake geometry and aerodynamic interactions on control surface effectiveness and vibration. As mentioned in the Introduction, rotor aeroelastic research and associated wind-tunnel testing will not be specifically addressed in this paper. What will be addressed in some detail is progress in helicopter ground and flight vibration testing methodology. The emphasis of this paper is on the fixed system, i.e., from the rotor hub through the airframe.

Most structural dynamicists would probably agree that helicopter vibration testing requirements are much more critical than corresponding fixed-wing requirements. Vibration testing serves two valuable purposes in helicopter development. First, these tests provide loads and vibrations data to verify design concepts. Second, vibration testing compensates for voids in existing analytical capabilities. Helicopter vibration problems have been extremely difficult to quantify and, as a result, have been solved during the development cycle by trial-and-error testing. A major reason for these cut-and-try methods has been a lack of definitive procedures which make maximum use of vibration test data. As conventionally practiced, most helicopter ground and flight vibration tests provide limited information for resolving vibration issues. However, techniques have evolved over the past decade from combined Army and NASA research that provide systematic, as opposed to trial-and-error, procedures for testing, correlating, and evaluating helicopter vibrations. For the purposes of this paper, vibration testing is separated into four categories, namely: (1) modal analysis; (2) system identification; (3) structural modification; and (4) vibratory loads measurement. Many scientists and engineers are engaged in rotorcraft vibration research, and vibration testing research in the categories listed above has increased substantially over the past ten years. The majority of references listed in this paper emphasizes in-house and contractual work conducted by the Army and NASA.

### Modal Analysis

Modal analysis is the name given to techniques which extract from test data the natural frequencies, orthonormal modes, and modal

dampings of a structure. These modal parameters are most often used to verify analytical models and to determine which parts of a structure contribute to a given mode of excitation. The theory of modal analysis dates back to the 1940's (ref. 156). There have been some methods which use time domain data (refs. 157 and 158) but structural dynamicists traditionally perform modal analysis using frequency domain data (refs. 159 to 167). The most common frequency domain approach uses complex plane data (the so-called Kennedy and Pancu plots or Nyquist circles). Figure 65 shows an example of these frequency domain circles. The rate of change of arc length around the circle and the diameter of the circle are used to determine the modal parameters. Reference 168 presents a complete derivation and application of this modal analysis methodology. The availability of Fast Fourier Transform signal analyzers in the early 1970's provided the means to apply the Kennedy and Pancu theory (ref. 156) with speed, accuracy, and fidelity. Modal analysis accuracy is typically verified by comparing measured frequency responses with synthesized frequency responses which are calculated using the identified modal parameters. Figure 66 shows a comparison between test and analysis for frequency response measurements on an AH-1G helicopter. The ordinate shift evident in the real part of the response is caused by the rigid-body contribution which was not included in the synthesized curve. The rigid-body part is normally calculated from weights and geometry information.

In the past twenty years helicopter designers have used sophisticated finite-element computer programs for sizing the structure to meet static load requirements and to provide for the normal analytical checks on vibrations. Accurate dynamics models of airframes are necessary not only to assess vibration design against specifications but to evaluate the vibration effects of configuration changes. Numerous researchers have conducted correlation efforts of finite-element model predictions with vibration test measurements (refs. 29-31, 34, 38, 42, 47 and 48). From a dynamics perspective, natural frequencies and mode shapes have been used as fundamental parameters for verifying the accuracy of analytical models. For example, figure 67 compares calculated and measured mode shapes of an OH-58 composite tail boom. Elaborate correlation efforts of Army CH-47D, UH-60A, AH-64, and ACAP airframes have also been conducted by the helicopter industry under contract to NASA (the DAMVIBS program) to evaluate the state of the art in finite-element modeling. Besides comparing the fundamental modal parameters, frequency response comparisons between shake test and analysis were used to assess the airframe modeling accuracy. The results of these correlation programs have much in common. First, the presence of modes in analysis which are not present during test and vice versa. Second, good accuracy on natural frequencies (less than 5 percent) but correspondingly poor accuracy on frequency response. And finally, the frequency range of acceptable correlation is only from 5 Hertz to about 20 Hertz. Detailed discussions of these correlation efforts were presented in the vibration analysis section of this paper.

Extensive ground vibration testing of an AH-1G helicopter (fig. 68) was conducted about seven years ago to obtain data for ver-

ifying shake test methods and modal analysis techniques. A significant finding from this shake test program was the measurement of complex modes (modes that have real and imaginary components) in the frequency range of interest (fig. 69). Reference 163 provides an excellent description of the cause and effect of complex modes. In short, complex modes can result when damping is not uniformly distributed throughout the structure. As a result, the phase between response and excitation is not constant and the mode shapes change with time. In the case of the AH-1G, this "nonproportional" damping was more than likely caused by the highly damped elastomeric mounts used to attach the transmission to the airframe. For classical modes the real part of the frequency response has two turning points near resonance while the imaginary part has one turning point. The first mode of figure 66 is an example of a classical mode. However, the character of the real and imaginary frequency responses can reverse for complex modes. Figure 69 illustrates this effect for an almost pure imaginary complex mode at 45 Hertz. As a consequence of this research, improved shake test methods have been developed in terms of both frequency response measurement and modal analysis accuracy (refs. 169 to 173). These improved measurement techniques include criteria for determining response linearity, reciprocity, complex modes, local modes, and frequency resolution. The improved modal analysis techniques which are now available provide a more accurate and consistent data base for system identification and finite-element correlation of complex helicopter structures.

### System Identification

Uncertainties inherent with analytical modeling techniques have made experimental modeling a viable approach for augmenting structural dynamics analysis (refs. 168, 174 to 192). The process of obtaining structural dynamics equations of motion or improving existing mathematical models using ground vibration data has been termed system identification. System identification deals with finding impedance-type matrices which are abstract inverses of measurable natural properties of a structure. The objective of system identification is to use these mathematical abstracts for estimating structural response characteristics. The origin of system identification goes back to the 1960's (ref. 174), but most of the theoretical development and validation work was performed in the mid to late seventies. The data required to experimentally derive the equations of motion are the natural frequencies, orthonormal mode shapes, and modal dampings which characterize the frequency spectrum of interest. These parameters are used to determine mass, stiffness, and damping matrices which define the equations of motion. The model which is formulated from this system identification process is called a "truncated model" because there are fewer modes used to determine the model than degrees of freedom in the structure (ref. 175). Multiple regression is used to solve for the constant coefficient matrices which make up the equations of motion. The regression parameter is the difference between the actual frequency response and the approximated frequency response obtained by using a finite number of modes. The primary application of this truncated model is to predict the

effects of mass and stiffness changes on natural frequencies and mode shapes. Computer experiments have verified the accuracy and limitations of the method (refs. 176 and 177). In addition, the truncated model methodology has been applied using AH-1G airframe modal test data. Predicted changes in natural frequencies and mode shapes were compared with test results to assess its usefulness (ref. 168).

Another system identification technique which provides a capability for improving an existing analytical model is the so-called "incomplete model" theory (refs. 178 to 181). This method uses natural frequency and mode shape test data to update or improve mass and stiffness matrices. The approach which is used to create the incomplete model assumes that the measured modal data are correct and forces the analytical mass matrix to be orthogonal with the measured modes. Multiple regression is used to solve for the smallest possible changes (in a least-squares sense) that satisfy the specified conditions. In a similar manner, the modal data and improved mass matrix are combined to improve the stiffness matrix. The requirement for small changes is not necessary and is only assumed so that the improved model still represents the physical structure. Engineering judgement is required to determine acceptable values for these small changes. A measure of accuracy of the improved analytical model is obtained by comparing predicted frequency responses with test data. It should be pointed out that current finite-element models do not incorporate nonproportional damping and hence can not account for the effects which lead to complex modes. There has been some research to develop methods for converting complex modes obtained from test into classical (or real) modes for model improvement purposes (ref. 182). The usefulness of these procedures is questionable if the improved model cannot be used to calculate frequency response for the structure being tested. Another criterion for evaluating the usefulness of the incomplete model is its ability to predict the effects of a change. Figure 70 illustrates how the incomplete model predicts mode shape changes due to mass and stiffness configuration changes. The solid curves represent the original mode shapes for a simply supported beam. The new mode shapes, shown by the dashed curves, were calculated using the exact beam equations. The data points in figure 70 were determined using the incomplete model. However, one of the major problems associated with system identification technology is the inability to physically interpret the changes which are identified by the analysis. Model improvement techniques must be developed such that mass and stiffness changes to the original models are physically meaningful as well as mathematically sound. There has been some research outside of the Army and NASA on methods which use test data to identify modeling errors (ref. 183). These techniques provide information to the analyst as to which model parameters are causing discrepancies between test and analysis. New ideas such as these may provide the means for implementing system identification as part of helicopter vibration design.

## Structural Modification

Research into techniques which predict changes in structural



dynamics or flight vibrations due to structural modifications has been under way for about fifteen years. One of the first concepts for evaluating vibration reduction through structural modification was reported in reference 193. The so-called Vincent Circle method (ref. 193) was described earlier in the Airframe Structural Optimization section. This methodology has been applied and extended by numerous researchers (refs. 105-108 and 194-202) over the past ten years. For the most part the Army requirement for these procedures was motivated by vibration problems which surfaced during helicopter development testing. More recent Army research has concentrated on combining structural modification methodology with ground and flight vibration data to evaluate the effects on vibration. This integration of structural modification with vibration testing has also been referred to as "analytical testing" (ref. 195). Unlike the typical finite-element modeling approach, there is no airframe math model that has to be created or modified such that it correlates with shake test results. The only analytical model required is the structural change as characterized by single-point or multi-dimensional impedance adjustments. These modifications include simple mass, absorber, isolator, and collinear stiffness changes as well as more elaborate skin, stringer, or component changes. The operational equations require only baseline vibration data and the impedance change dynamics. Computer experiments have been conducted to demonstrate the usefulness of this methodology (refs. 195 to 197). The method has also been applied using AH-1G ground and flight vibration test data (refs. 195 and 198). Figure 71 illustrates how the method can be used to predict changes in cockpit vibration due to an absorber located on the vertical fin. In this example, the "remote" absorber was tuned for both frequency and damping to produce zero vibration at the required flight condition. Additional work is under way by Army researchers to validate the analytical testing methodology. The approach taken is to analytically make a change, predict its effect, and then to physically make the change, test the change, and compare the test results with analysis. This methodology has been verified on a generic helicopter model (fig. 72). Further research is being conducted to validate analytical testing using OH-58A ground vibration data and simulated flight test data. Successful implementation of this structural modification methodology will provide a much needed capability to respond to Army field problems and to eliminate costly trial-and-error testing.

### Vibratory Loads Measurement

Higher than expected vibratory loading is a fundamental cause of high maintenance manhours and low component reliability. In general, the most critical vibratory loads are generated by the main rotor and occur at the blade passage frequency or  $N/\text{rev}$ . An accurate knowledge of these vibratory loads is needed to improve rotor design, to evaluate vibration control devices, and to establish fatigue characteristics. In particular, the helicopter industry spends substantial resources to reduce vibratory loads in an effort to increase reliability. If the vibratory loads were known, then "ground" flying could be performed on the complete helicopter using these loads to simulate

flight. Thus, around-the-clock fatigue testing could be used to evaluate system reliability. Besides reliability testing, ground flying can be used with structural modification testing to evaluate and implement potential fixes to vibration problems before failures occur in the fleet.

The most common approach for measuring vibratory rotor loads (both hub shears and moments) uses strain gages on the main rotor shaft. Slip rings are required to transmit signals from the rotating system to the fixed system. Because this method was costly, slow, and often unreliable, Army research began in the mid 1970's on a method called Force Determination which uses airframe response measurements and shake test calibration data to determine the main rotor hub vibratory loads (refs. 203 to 206). Force Determination is a multiple regression technique (least-squares curve fit) which minimizes the differences between measured responses and calculated responses. All instrumentation is located in the fixed system (no slip rings are needed). Accelerometers and strain gages are distributed throughout the airframe to introduce a high degree of measurement independence and redundancy. The method has been verified on a generic helicopter dynamic model and full-scale aircraft (refs. 203 and 205). Figure 73 compares flight test, Force Determination calculated, and ground flying vibration levels at several points along an AH-1G airframe. These results demonstrated that the calculated main rotor hub loads can be used to synthesize actual flight vibrations accurately and with the correct distribution. Force Determination was also applied to a UH-1 helicopter (fig. 74) to evaluate rotor isolation system effectiveness (ref. 203). In this case the calculated loads for the baseline aircraft were combined with forced response measurements obtained from shake testing the aircraft with the isolation system installed. The predicted "new" flight vibrations were consistent with flight measurements and gave credibility to the method. Additional work has been performed by other researchers to improve Force Determination (refs. 207 and 208). Army in-house research is being conducted to evaluate the limitations of the method and to develop a full-scale reliability testing capability. Several technical issues which are being investigated include shaker cross talk, load versus response linearity, phase shift sensitivity, and shaker attachment (boundary condition) effects on the frequency response calibration data. There are other applications of this technique which are planned through Army in-house research. For example, Force Determination will be used to study the vibration effects of main rotor downwash impingement and main rotor wake interactions on tail surfaces.

There is considerable Army and NASA research in vibration testing planned for the next five years. Most of the work emphasizes verification of current methodologies such as System Identification, Analytical Testing, and Force Determination. Emphasis will be placed on using these new vibration testing methods to develop systematic procedures for solving vibration-related problems. Research will also be performed to demonstrate the applicability of these new methods on composite rotorcraft. Finite-element modeling correlation of composite structures, in particular the Army ACAP airframes, is also

planned. Other research issues which will be addressed through combined Army and NASA research include standardization of vibration testing methodology. This standardization will include not only vibration testing procedures but also data acquisition and analysis methodology. The results of these efforts will identify how tests should be performed, what data should be taken to meet vibration testing objectives, and what data analysis procedures give the best results.

#### CONCLUDING REMARKS

Excessive vibrations have plagued virtually all new rotorcraft developments since the first U.S. helicopter went into production over forty years ago. The problem is pervasive and transcends national boundaries. The impact of excessive vibrations on new helicopter development programs is significant, both with respect to increased development costs and slipped delivery schedules. Helicopter companies have relied little on analysis during design to limit vibrations. With few exceptions, helicopters have been designed to performance requirements and excessive vibrations were then "tinkered out" during ground and flight testing. With continued expansion of flight envelopes and more stringent requirements for crew and passenger comfort and component reliability in modern helicopters, the requirement for low vibrations has achieved the status of a critical design consideration. It is clear that vibrations can no longer be addressed in an ad hoc fashion. There is now a recognized need to account for vibrations more rigorously in both the analytical and experimental phases of design. With this as a background, this paper has presented a summary of NASA and Army contributions, both in-house and contractual, to rotorcraft vibrations and structural dynamics technology over the last decade or so. Specific topics that were addressed include: airframe finite-element modeling for dynamic analysis, coupled rotor-airframe vibrations, airframe structural optimization, active and passive control of vibrations, and integration of testing and analysis in such guises as experimental modal analysis, system identification, structural modification, and vibratory loads measurement (force determination). The status of current activities being conducted under major NASA and Army programs, as well as near-term plans, were also described. Viewed as a whole, it is fair to say that the work described constitutes an important contribution to the critical elements of the technology base needed to achieve the goal of a "jet smooth" ride. However, much work still needs to be done before this goal can be reached. To this end, both NASA and the Army have substantial in-house and contractual research activities planned over the next five to ten years. The ultimate success of these efforts will depend not only on the development of more reliable vibration design tools but also on the practical implementation of these tools into the design process by industry. It is left for a status report ten years hence to judge whether we have been successful.

## REFERENCES

1. Yakovlev, A. S.: Notes of an Aircraft Designer. Arno Press, Inc., 1972. Translation of the 1960 reprint of the book Rasskozy Aviakonstruktora.
2. Schrage, D. P.; and Peskar, R. E.: Helicopter Vibration Requirements. Presented at the 33rd Annual Forum of the American Helicopter Society, Washington, D.C., May 1977.
3. Stevens, S. C.: AVRADCOM Research in Helicopter Vibrations. Keynote Address, 53rd Shock and Vibration Symposium, Danvers, MA, October 1982. Shock and Vibration Bulletin, Part 1, May 1983, pp. 3-20.
4. Rotorcraft Dynamics. Proceedings of the AHS/NASA Ames Specialists' Meeting on Rotorcraft Dynamics, NASA SP-352, Feb. 1974.
5. Doman, G. S.: Research Requirements for the Reduction of Helicopter Vibration. NASA CR-145116, Dec. 1976.
6. Rotorcraft Vibration Workshop. NASA Ames Research Center, Moffett Field, CA, Feb. 22-23, 1978.
7. Technology for the Jet Smooth Ride. AHS National Specialists' Meeting on Helicopter Vibration, Hartford, CT, Nov. 2-4, 1981.
8. Loewy, R. G.: Helicopter Vibrations: A Technological Perspective. J. American Helicopter Soc., vol. 29, no. 4, Oct. 1984, pp. 4-30.
9. Rotorcraft Dynamics 1984. 2nd Decennial Specialists' Meeting on Rotorcraft Dynamics, NASA Ames Research Center, Moffett Field, CA, Nov. 7-9, 1984. Proceedings available as NASA CP-2400, Nov. 1985.
10. Balke, R. W.: The Helicopter Ride Revolution. Presented at the AHS National Specialists' Meeting on Helicopter Vibration, Hartford, CT, Nov. 2-4, 1981,
11. Gaffey, T. M.: Status of Rotorcraft Dynamics Technology. Keynote Address, 39th Annual Forum of the American Helicopter Society, St. Louis, MO, May 9-11, 1983.
12. Amos, A. K.; and Goetz, R. C.: Research Needs in Aerospace Structural Dynamics. AIAA/ASME/ASCE/AHS 20th Structures, Structural Dynamics and Materials Conference, St. Louis, MO, Apr. 4-6, 1979.
13. Ad Hoc Study Committee, OAST, NASA: Structural Dynamics Technology Research in NASA - Perspective on Future Needs. NASA TM 80078, Apr. 1979.

14. Snyder, W. J.; and Schoultz, M. B.: Civil Helicopter Flight Research. AIAA Aircraft Systems and Technology Meeting, Dallas, TX, Sep. 27-29, 1976. (AIAA Paper 76-896).
15. Snyder, W. J.; Cross, J. L.; and Schoultz, M. B.: Vibration Investigation of a Large Transport Helicopter. Shock and Vibration Bulletin, Part 3, Sep. 1977, pp. 139-147.
16. Advanced Rotorcraft Technology Task Force Report. Office of Aeronautics and Space Technology, NASA, Oct. 15, 1978.
17. An Evaluation of NASA's Program for Advancing Rotorcraft Technology. A Report of the Ad Hoc Committee on Rotorcraft Technology, Aeronautics and Space Engineering Board, Assembly of Engineering, National Research Council, National Academy of Sciences, Washington, D.C. 1978.
18. Bartlett, F. D., Jr.; and Tomaine, R. L.: Vibration Research Development Plan. AVRADCOM TR-82-B-1, Feb. 1982.
19. Bartlett, F. D., Jr.: Army Research in Helicopter Vibrations. Finite Element Modeling Workshop, NASA Langley Research Center, Hampton, VA, Feb. 2-4, 1983.
20. Walton, W. C., Jr.: Program for a Superior Capability to Utilize Airframe Finite Element Models. Finite Element Modeling Workshop, NASA Langley Research Center, Hampton, VA, Feb. 2-4, 1983.
21. The NASTRAN User's Manual. NASA SP-222(08), 1986.
22. The MSC/NASTRAN User's Manual. MSC/NASTRAN Version 64, 1986.
23. Gallian, D. A.; and Wilson, H. E.: The Integration of NASTRAN into Helicopter Airframe Design/Analysis. 29th Annual Forum of the American Helicopter Society, Washington, D.C., May 1973.
24. Wilson, H. E.; and Cronkhite, J. D.: Static and Dynamic Helicopter Airframe Analysis with NASTRAN. NASTRAN: Users' Experiences. NASA TM X-2893, Sep. 1973, pp. 611-619.
25. Rich, M. J.: Finite Element Analysis of Helicopter Structures. Research in Computerized Structural Analysis and Synthesis. NASA CP-2059, 1978, pp. 51-61.
26. Application of Dynamics Technology to Helicopter Design. Panel 3: Integrating Dynamic Analysis and Helicopter Design. Rotorcraft Dynamics. NASA SP-352, 1974, pp. 327-338.
27. White, J. A.: OH-58A Propulsion System Vibration Investigation. USAAMRDL TR-74-47, Aug. 1974.

28. Sullivan, R. J.; Head, R. E.; Korkosz, G. J.; Neff, J. R.; Soltis, S. J.; and Gockel, M. A.: OH-6A Propulsion System Vibration Investigation. USAAMRDL TR-74-85, Jan. 1975.
29. Kenigsberg, I. J.: CH-53A Flexible Frame Vibration Analysis/ Test Correlation. Sikorsky Engineering Report SER 651195, Mar. 1973. Prepared for Department of the Navy, Naval Air Systems Command.
30. Kenigsberg, I. J.; Dean, M. W.; and Malatino, R. E.: Correlation of Finite-Element Structural Dynamic Analysis with Measured Free Vibration Characteristics for a Full Scale Helicopter Fuselage. Proceedings of the AHS/NASA Ames Specialists Meeting on Rotorcraft Dynamics, NASA SP-352, Feb. 1974, pp. 67-80.
31. Dean, M. W.: Correlation of an Extended CH-53 Helicopter NASTRAN Model with Full-Scale Aircraft Shake Test Data. NASA CR-145012, 1976.
32. Walton, W. C., Jr.; Hedgepeth, R. K.; and Bartlett, F. D., Jr.: Report on Rotor Systems Research Aircraft Design for Vibrations. 1976 SAE Aerospace Engineering and Manufacturing Meeting, San Diego, CA, Nov. 30 - Dec. 2, 1976. Paper No. 760895.
33. Cronkhite, J. D.; Berry, V. L.; and Brunken, J. E.: A NASTRAN Vibration Model of the AH-1G Helicopter Airframe. U.S. Army Armament Command Report No. R-TR-74-045, Jun. 1974.
34. Cronkhite, J. D.; and Berry, V. L.: Correlation of AH-1G Airframe Test Data with a NASTRAN Mathematical Model. NASA CR-145119, Feb. 1976.
35. Cronkhite, J. D.: Development, Documentation and Correlation of a NASTRAN Vibrations Model of the AH-1G Helicopter Airframe. NASTRAN: Users' Experiences. NASA TM X-3428, 1976, pp. 273-294.
36. Frericks, D. E., et. al.: Measurement of the Static Influence Coefficients of the AH-1G Cobra Fuselage. U.S. Army Armament Command Report No. R-TR-76-005, Feb. 1976.
37. Cronkhite, J. D.; Wilson, H. E.; and Berry, V. L.: Correlation of AH-1G Helicopter Flight Vibration Data and Tail Boom Static Test Data with NASTRAN Results. NASA CR-145120, 1978.
38. Cronkhite, J. D.; Berry, V. L.; and Dompka, R. V.: Summary of the Modeling and Test Correlations of a NASTRAN Finite Element Vibrations Model for the AH-1G Helicopter. NASA CR-178201, Jan. 1987.
39. Gabel, R.; Ricks, R. G.; and Magiso, H.: Planning, Creating and Documenting a NASTRAN Finite Element Vibrations Model of a Modern Helicopter, Planning Report. NASA CR-165722, Apr. 1981.

40. Gabel, R.; and Reed, D. A.: Planning, Creating and Documenting a NASTRAN Finite Element Vibrations Model of a Modern Helicopter, Test Requirements Report. NASA CR-165855, Apr. 1982.
41. Gabel, R.; Kesack, W. J.; and Reed, D. A.: Planning, Creating and Documenting a NASTRAN Finite Element Vibrations Model of a Modern Helicopter, Modeling Documentation Report. NASA CR-166077, Mar. 1983.
42. Gabel, R.; Reed, D. A.; and Ricks, R. G.: Planning, Creating and Documenting a NASTRAN Finite Element Vibrations Model of a Modern Helicopter, Ground Shake Test - Results and Correlation Report. NASA CR-166107, May 1983.
43. Gabel, R.; Kesack, W. J.; Reed, D. A.; and Ricks, R. G.: Planning, Creating and Documenting a NASTRAN Finite Element Vibrations Model of a Modern Helicopter, Summary Report. NASA CR-172229, Oct. 1983.
44. Gabel, R.; Reed, D. A.; Ricks, R. G.; and Kesack, W. J.: Planning, Creating and Documenting a NASTRAN Finite Element Vibrations Model of a Modern Helicopter. Proceedings of the Second Decennial Specialists' Meeting on Rotorcraft Dynamics, NASA CP-2400, Nov. 1985, pp. 307-324.
45. Bowman, L. M.: VIBRA - An Interactive Computer Program for Steady-State Vibration Response Analysis of Linear Damped Structures. NASA TM 85789 (AVSCOM TM 84-B-1), Jul. 1984.
46. Whetstone, W. D.: EISI-EAL Engineering Analysis Language Reference Manual. EISI-EAL System Level 2091. Engineering Information Systems, Inc., Jul. 1983.
47. Calapodas, N.; and Hoff, K.: Correlation of Results of an OH-58A Helicopter Composite Tail Boom Test with a Finite Element Model. USAAVSCOM TR-85-D-15, Sep. 1985.
48. Bowman, L. M.: Effect of Measured Material Properties on the Finite Element Analysis of an OH-58A Composite Tail Boom. NASA TM 86430 (AVSCOM TR-85-B-5), Oct. 1985.
49. Johnston, R. A.; and Cassarino, S. J.: Aeroelastic Rotor Stability Analysis. USAAMRDL TR-75-40, Jan. 1976.
50. Anderson, W. D.; Conner, F.; Kretsinger, P.; and Reaser, J. S.: REXOR Rotorcraft Simulation. Volume I- Engineering Documentation. USAAMRDL TR-76-28A, Jul. 1976.
51. McLarty, T. T.: Rotorcraft Flight Simulation With Coupled Rotor Aeroelastic Stability Analysis. Volume I - Engineer's Manual. USAAMRDL TR-76-41A, May 1977. (Contains a description of the C-81 computer code.)

52. Banerjee, D.; and Johnston, R. A.: Integrated Technology Rotor Methodology Assessment. Hughes Helicopter Report prepared under Contract NAS2-10871, Nov. 1981. (Contains a description of the DART computer code.)
53. Johnson, W.: A Comprehensive Analytical Model of Rotorcraft Aerodynamics and Dynamics. Part 1: Analysis Development. NASA TM 81182, AVRADCOM TR-80-A-5, 1980. (Contains a description of the CAMRAD computer code.)
54. Gabel, R.: Current Loads Technology for Helicopter Rotors. Proceedings of the AGARD Specialists' Meeting on Helicopter Rotor Loads Prediction Methods, Milan, Italy, Mar. 30-31, 1973. AGARD CP-122. (Describes the C-60 computer code.)
55. Phelan, P. G.; and Tarzanin, F. J., Jr.: Restructuring the Rotor Analysis Program C-60. Proceedings of the Second Decennial Specialists' Meeting on Rotorcraft Dynamics, NASA CP-2400, Nov. 1985, pp. 171-183.
56. Bielawa, R. L.: Aeroelastic Analysis for Helicopter Rotor Blades with Time-Variable, Nonlinear Structural Twist and Multiple Structural Redundancy - Mathematical Derivation and Program User's Manual. NASA CR-2638, Oct. 1976. (Describes the G400 computer code.)
57. Bielawa, R. L.: Aeroelastic Analysis for Helicopter Rotors with Blade Appended Pendulum Vibration Absorbers - Mathematical Derivations and Program User's Manual. NASA CR-165896, Jun. 1982. (Describes the G400PA computer code.)
58. Yeates, J. E., Jr.; Brooks, G. W.; and Houbolt, J. C.: Flight and Analytical Methods for Determining the Coupled Vibration Response of Tandem Helicopters. NACA Report 1326, 1957.
59. Gerstenberger, W.; and Wood, E. R.: Analysis of Helicopter Aeroelastic Characteristics in High-Speed Flight. AIAA J., vol. 1, no. 10, Oct. 1963, pp. 2366-2381.
60. Novak, M. E.: Rotating Elements in the Direct Stiffness Method of Dynamic Analysis With Extensions to Computer Graphics. Shock and Vibration Bulletin, Bull. 40, Pt. 4, Oct. 1969, pp. 41-46.
61. Staley, J. A.; and Sciarra, J. J.: Coupled Rotor/Airframe Vibration Prediction Methods. Rotorcraft Dynamics, NASA SP-352, 1974, pp. 81-90.
62. Anderson, W. D.; and Gaidelis, J. A.: Vibration Inputs and Response of a Hingeless Rotor Compound Helicopter. Report LR 26523, Lockheed-California Co., Rotary Wing Div., Jun. 1974.
63. Hughes, C. W.; and Wernicke, R. K.: Flight Test of a Hingeless Flexbeam Rotor System. USAAMRDL TR-74-38, Jun. 1974.



64. Howard, J. V.: NASTRAN Correlation for the Model 214A Helicopter. 32nd Annual Forum of the American Helicopter Society, Washington, D.C., May 1976.
65. Cassarino, S. J.; and Mouzakis, T.: Bifilar Analysis User's Manual - Volume II. NASA CR-159228, 1980.
66. Kunz, D. L.: Effects of Rotor-Body Coupling in a Linear Rotorcraft Vibration Model. 36th Annual Forum of the American Helicopter Society, Washington, D.C., May 1980.
67. Kunz, D. L.: Response Characteristics of a Linear Rotorcraft Vibration Model. J. of Aircraft, vol. 19, no. 4, Apr. 1982, pp. 297-303.
68. Hohenemser, K. H.; and Yin, S-K: The Role of Impedance in Vibration Analysis of Rotorcraft. Vertica, vol. 3, no. 3/4, 1979, pp. 189-204.
69. Yen, J. G.; and McLarty, T. T.: Analysis of Rotor-Fuselage Coupling and Its Effect on Rotorcraft Stability and Response. Vertica, vol. 3, no. 3/4, 1979, pp. 205-219.
70. Hsu, T-K; and Peters, D. A.: Coupled Rotor/Airframe Vibration Analysis by a Combined Harmonic-Balance, Impedance-Matching Method. J. American Helicopter Soc., vol. 27, no. 1, Jan. 1982, pp. 25-34.
71. Ming-Sheng, H.; and Peters, D. A.: Coupled Rotor-Body Vibrations with Inplane Degrees of Freedom. Proceedings of the Second Decennial Specialists' Meeting on Rotorcraft Dynamics. NASA CP-2400, Nov. 1985, pp. 325-339.
72. Rutkowski, M. J.: The Vibration Characteristics of a Coupled Helicopter Rotor-Fuselage by a Finite Element Analysis. NASA TP 2118 (AVRADCOM TR-82-A-15), Jan. 1983.
73. Peters, D. A.; and Ormiston, R. A.: Flapping Response Characteristics of Hingeless Rotor Blades by a Generalized Harmonic Balance Method. NASA TN D-7856, 1975.
74. Eipe, A.: Effect of Some Structural Parameters on Elastic Rotor Loads by an Iterative Harmonic Balance. Ph.D. Dissertation, Washington Univ., Sever Inst. of Tech., Dec. 1979.
75. Meirovitch, L.; and Hale, A. L.: Structural Dynamics, Stability, and Control of Helicopters. NASA CR-158909, Jul. 1978.
76. Meirovitch, L.; and Hale, A. L.: A Special Purpose Symbolic Manipulation Program for the Derivation of the Equations of Motion for Large Flexible Structures. Proceedings of the AIAA Symposium on Dynamics and Control of Large Flexible Spacecraft, Blacksburg, VA, Jun. 13-15, 1977, pp. 367-385.

77. Warmbrodt, W.: Coupled Rotor and Fuselage Equations of Motion. NASA TM 81153, Oct. 1979.
78. Kunz, D. L.: A Nonlinear Response Analysis and Solution Method for Rotorcraft Vibration. J. American Helicopter Soc., vol. 28, no. 1, Jan. 1983, pp. 56-62.
79. Sopher, R.; and Hallock, D. W.: Time-History Analysis for Rotorcraft Dynamics Based on a Component Approach. J. American Helicopter Soc., vol. 31, no. 1, Jan. 1986.
80. Berman, A.: A Generalized Coupling Technique for the Dynamic Analysis of Structural Systems. J. American Helicopter Soc., vol. 25, no. 3, Jul. 1980, pp. 22-28.
81. Berman, A.; Chen, S-Y; Gustavson, B.; and Hurst, P.: Dynamic System Coupler Program (DYSCO 4.0) - Theoretical Manual/ Users Guide. USAAVSCOM TR-85-D-24A,B, Sep. 1985.
82. Sopher, R.; Studwell, R. E.; Cassarino, S.; and Kottapalli, S. B. R.: Coupled Rotor/Airframe Vibration Analysis. NASA CR-3582, Nov. 1982.
83. Tsai, H. C.: Rotary Wing Structural Dynamics Analysis. Naval Air Development Center Report No. NADC 85020-60, Jan. 1985.
84. Kvaternik, R. G.; and Walton, W. C., Jr.: A Formulation of Rotor-Airframe Coupling for Design Analysis of Vibrations of Helicopter Airframes. NASA RP-1089, Jun. 1982.
85. Shockey, G. A.; Williamson, J. W.; and Cox, C. R.: AH-1G Helicopter Aerodynamics and Structural Loads Survey. USAAMRDL TR-76-39, Feb. 1977.
86. Van Gaasbeek, J. R.: Validation of the Rotorcraft Flight Simulation Program (C-81) Using Operational Loads Survey Flight Test Data. USAAVRADCOM TR-80-D-4, Jul. 1980.
87. Dompka, R. V.; and Cronkhite, J. D.: Summary of AH-1G Flight Vibration Data for Validation of Coupled Rotor-Fuselage Analyses. NASA CR-178160, Nov. 1986.
88. Dompka, R. V.; and Corrigan, J. J.: AH-1G Flight Vibration Correlation Using NASTRAN and the C-81 Rotor/Airframe Coupled Analysis. 42nd Annual Forum of the American Helicopter Society, Washington, D.C., Jun. 1986.
89. Gabel, R.; and Sankewitsch, V.: Rotor-Fuselage Coupling by Impedance. 42nd Annual Forum of the American Helicopter Society, Washington, D.C., Jun. 1986.

90. Straub, F. K.; and Byrns, E. V., Jr.: Application of Higher Harmonic Blade Feathering on the OH-6A Helicopter for Vibration Reduction. NASA CR-4031, Dec. 1986.
91. Schmit, L. A.: Structural Synthesis - Its Genesis and Development. AIAA J., vol. 19, no. 10, Oct. 1981, pp. 1249-1263.
92. Ashley, H.: On Making Things the Best - Aeronautical Uses of Optimization. J. Aircraft, vol. 19, no. 1, Jan. 1982, pp. 5-28.
93. Bennett, R. L.: Optimum Structural Design. Proceedings of the 38th Annual Forum of the American Helicopter Society, May 1982, pp. 398-407.
94. Optimum Design Panel. 39th Annual Forum of the American Helicopter Society, St. Louis, MO, May 1983.
95. Friedmann, P. P.; and Shanthakumaran, P.: Optimum Design of Rotor Blades for Vibration Reduction in Forward Flight. Proceedings of the 39th Annual Forum of the American Helicopter Society, May 1983, pp. 656-673.
96. Peters, D. A.; Ko, T.; Korn, A.; and Rossow, M. P.: Design of Helicopter Rotor Blades for Desired Placement of Natural Frequencies. Proceedings of the 39th Annual Forum of the American Helicopter Society, May 1983, pp. 674-689.
97. Symposium on Recent Experiences in Multidisciplinary Analysis and Optimization. NASA CP-2327, Apr. 1984.
98. Walsh, J. L.; Bingham, G. J.; and Riley, M. F.: Optimization Methods Applied to the Aerodynamic Design of Helicopter Rotor Blades. AIAA/ASME/ASCE/AHS 26th Structures, Structural Dynamics and Materials Conference, Apr. 15-17, 1985.
99. Davis, M. W.; and Weller, W. H.: Application of Design Optimization Techniques to Rotor Dynamics Problems. Presented at the 42nd Annual Forum of the American Helicopter Society, Washington, D.C., Jun. 1986.
100. Miura, H.: Application of Numerical Optimization Methods to Helicopter Design Problems. Vertica, vol. 9, 1985, pp. 141-154.
101. Friedmann, P. P.: Application of Modern Structural Optimization to Vibration Reduction in Rotorcraft. Vertica, vol. 9, no. 4, 1985, pp. 363-376.
102. Sciarra, J. J.: Use of the Finite Element Damped Forced Response Strain Energy Distribution for Vibration Reduction. Boeing Vertol Report D210-10819-1, U.S. Army Research Office - Durham, Durham, NC, Jul. 1974.

103. Venkayya, V. B.; Knot, N. S.; Tischler, V. A.; and Taylor, R.F.: Design of Optimum Structures for Dynamic Loads. Third Conference on Matrix Methods in Structural Mechanics, WPAFB, OH, Oct. 1971.
104. Ricks, R. G.; and Gabel, R.: Vibration Optimization of the CH-47C Helicopter Using NASTRAN. Symposium on Mathematical Modeling in Structural Engineering, NASA Langley Research Center, Hampton, VA, Oct. 24-26, 1979.
105. Hanson, H. W.: Investigation of Vibration Reduction Through Structural Optimization. USAAVRADCOM TR-80-D-13, Jul. 1980.
106. Done, G. T. S.: Reducing Vibrations by Structural Modification. Vertica, vol. 1, 1976, pp. 31-38.
107. Wang, B. P.; Kitis, L.; Pilkey, W. D.; and Palazzolo, A. B.: Helicopter Vibration Reduction by Local Structural Modification. J. American Helicopter Soc., vol. 27, no. 3, Jul. 1982, pp. 43-47.
108. Hanagud, S. V.; Meyyappa, M.; Cheng, Y. P.; and Craig, J. I.: Rotorcraft Structural Dynamic Design Modification. 10th European Rotorcraft Forum, The Hague, The Netherlands, Aug. 28-31, 1984,
109. Johnson, E. H.: Disjoint Design Spaces in the Optimization of Harmonically Excited Structures. AIAA J., vol. 14, no. 2, Feb. 1976, pp. 259-261.
110. Johnson, E. H.; Rizzi, P.; Ashley, H.; and Segenreich, S. A.: Optimization of Continuous One-Dimensional Structures Under Steady Harmonic Excitation. AIAA J., vol. 14, no. 12, Dec. 1976, pp. 1690-1698.
111. Mills-Curran, W. C.; and Schmit, L. A.: Structural Optimization with Dynamic Behavior Constraints. AIAA J., vol. 23, no. 1, Jan. 1985, pp. 132-138.
112. Schmit, L. A.; and Miura, H.: Approximation Concepts for Efficient Structural Synthesis. NASA CR-2552, Mar. 1976.
113. Wang, B. P.; and Pilkey, W. D.: Efficient Reanalysis of Locally Modified Structures. First Chautauqua on Finite Element Modeling. Sponsored by Schaeffer Analysis, Inc., Harwichport, MA, Sep. 15-17, 1980, pp. 37-61.
114. Bhatia, K. G.: Rapid Iterative Reanalysis for Automated Design. NASA TN D-7357, Oct. 1973.
115. Vanderplaats, G. N.: CONMIN: A FORTRAN Program for Constrained Function Minimization - User's Manual. NASA TM X-62,282, Aug. 1973.

116. Vanderplaats, G. N.; Miura, H.; and Chargin, M.: Large Scale Structural Synthesis. Finite Elements in Analysis and Design, Vol. 1, 1985, pp. 117-130.
117. Miura, H.; and Chargin, M.: Automated Tuning of Airframe Vibration by Structural Optimization. 42nd Annual Forum of the American Helicopter Society, Washington, D.C., Jun. 1986.
118. Rogers, J. L., Jr.: Combining Analysis with Optimization at Langley Research Center - An Evolutionary Process. Second International Computer Engineering Conference and Show, San Diego, CA, Aug. 15-19, 1982.
119. Sobieski, J.: A Linear Decomposition Method for Large Optimization Problems - Blueprint for Development. NASA TM 83248, Feb. 1982.
120. Pritchard, J.; Adelman, H.; and Haftka, R. T.: Sensitivity Analysis of Mode Shape Node Point Locations. NASA/VPI&SU Symposium on Sensitivity Analysis in Engineering, NASA Langley Research Center, Hampton, VA, Sep. 25-26, 1986.
121. Spain, C. V.: Application of a System Modification Technique to Dynamic Tuning of a Spinning Rotor Blade. NASA/VPI&SU Symposium on Sensitivity Analysis in Engineering, NASA Langley Research Center, Hampton, VA, Sep. 25-26, 1986.
122. Murthy, T. S.: Design Sensitivity Analysis of Rotorcraft Airframe Structures for Vibration Reduction. NASA/VPI&SU Symposium on Sensitivity Analysis in Engineering, NASA Langley Research Center, Hampton, VA, Sep. 25-26, 1986.
123. Reichert, G.: Helicopter Vibration Control - A Survey. Sixth European Rotorcraft and Powered Lift Aircraft Forum. Bristol, UK, Sep. 1980.
124. Gupta, B. P.; and Wood, E. R.: Low Vibration Design of AAH for Mission Proficiency Requirements. AHS National Specialists' Meeting on Helicopter Vibrations, Hartford, CT, Nov. 1981.
125. Murthy, V. R.; and Hammond, C. E.: Vibration Analysis of Rotor Blades with Pendulum Absorbers. J. Aircraft, vol. 18, no. 1, Jan. 1981, pp. 23-29.
126. Hamouda, M. H.; and Pierce, G. A.: Helicopter Vibration Suppression Using Simple Pendulum Absorbers on the Rotor Blade. NASA CR-3619, Sep. 1982.
127. Paul, W. F.: Development and Evaluation of Main Rotor Bifilar Absorber. Presented at the 25th Annual Forum of the American Helicopter Society, Washington, D.C., May 1969.
128. Miao, T.; and Mouzakis, T.: Bifilar Analysis Study, Vol-I. NASA CR-159227, Aug. 1980.

129. Mouzakis, T.: Monofilar - A Dual Frequency Rotorhead Absorber. AHS National Specialists' Meetings on Helicopter Vibrations, Hartford, CT, Nov. 1981.
130. Duh, J. and Miao, W.: Development of Monofilar Rotor Hub Vibration Absorber. NASA CR-166088, May 1983.
131. Jones, R.: Control of Helicopter Vibrations Using the Dynamic Antiresonant Vibration Isolator. National Aerospace Engineering and Manufacturing Meeting, Los Angeles, CA, Oct. 16, 1973.
132. Jones, R.; and McGarvy, J. H.: Advanced Development of a Helicopter Rotor Isolation System for Improved Reliability: Volume I - Summary. USAAMRDL TR-77-23A, Dec. 1977.
133. Gaffey, T. M.; and Balke, R. W.: Isolation of Rotor Induced Vibration with the Bell Focal Pylon-Nodal Beam System. National Aerospace Engineering and Manufacturing Meeting, San Diego, CA, Dec. 2, 1976.
134. Hooper, W. E.; and Desjardins, R. A.: Antiresonant Isolation for Hingeless Rotor Helicopters. National Aerospace Engineering and Manufacturing Meeting, San Diego, CA, Dec. 2, 1976.
135. Desjardins, R. A.; and Hooper, W. E.: Antiresonant Rotor Isolation for Vibration Reduction. Presented at the 34th Annual Forum of the American Helicopter Society, Washington, D.C., May 1978.
136. Desjardins, R. A.; and Hooper, W. E.: Helicopter Rotor Vibration Isolation. Vertica, vol. 2, pp. 145-149.
137. Sankewitch, V.: Total Main Rotor Isolation System Analysis. NASA CR-165666, Mar. 1981.
138. Eastman, L.: Main Rotor Six Degree-of-Freedom Isolation System Analysis. NASA CR-165665, May 1981.
139. Halwes, D. R.: LIVE - Liquid Inertia Vibration Eliminator. Presented at the 36th Annual Forum of the American Helicopter Society, Washington, D.C., May 1980.
140. Halwes, D. R.: Total Main Rotor Isolation System Analysis. NASA CR-165667, Jun. 1981.
141. Halwes, D. R.; and Cline, J. H.: Total Rotor Isolation System (TRIS) Flight Test Results. Presented at the 42nd Annual Forum of the American Helicopter Society, Washington, D.C., Jun. 1986.
142. Kuczynski, W. A.; and Madden, J.: The RSRA Active Isolation/Rotor Balance System. J. American Helicopter Soc., vol. 25, no. 2, Apr. 1980.

143. Shaw, J.: Higher Harmonic Blade Pitch Control for Helicopter Vibration Reduction: A Feasibility Study. MIT Report ASRL TR-150-1, Dec. 1968.
144. McCloud, J. L., III: An Analytical Study of a Multicyclic Controllable Twist Rotor. Presented at the 31st Annual Forum of the American Helicopter Society, Washington, D.C., May 1975.
145. Piziali, R. A.; and Tenka, A. R.: A Theoretical Study of the Application of Jet Flap Circulation Control for Reduction of Rotor Vibratory Forces. NASA CR-137779, 1975.
146. Sissingh, C. J.; and Donham, R. E.: Hingeless Rotor Theory and Experiment on Vibration Reduction by Periodic Variation of Conventional Controls. NASA SP-352, Feb. 1974.
147. McCloud, J.L., III; and Weisbireh, A. L.: Wind-Tunnel Test Results of a Full Scale Multicyclic Controllable Twist Rotor. Preprint No. 78-60, 34th Annual Forum of the American Helicopter Society, Washington, D.C., May 1978.
148. McHugh, F. J.; and Shaw, J., Jr.: Benefits of Higher Harmonic Blade Pitch: Vibration Reduction, Blade-Load Reduction and Performance Improvement. Proceedings of the American Helicopter Society Mid-east Region Symposium on Rotor Technology, Aug. 1976.
149. Hammond, C. E.: Helicopter Vibration Reduction via Higher Harmonic Control. Proceeding of Rotorcraft Vibration Workshop, NASA Ames Research Center, Moffett Field, CA, Feb. 22, 1978.
150. Hammond, C. E.; and Cline, J. H.: On the Use of Active Higher Harmonic Blade Pitch Control for Helicopter Vibration Reduction. Army Science Conference, West Point, NY, Jun. 1980.
151. Powers, R. W.: Application of Higher Harmonic Blade Feathering For Helicopter Vibration Reduction. NASA CR-159327, Jun. 1980.
152. Wood, E. R.; Powers, R. W.; Cline, J. H. and Hammond, C. E.: On Developing and Flight Testing a Higher Harmonic Control System. J. American Helicopter Soc., vol. 30, no. 1, Jan. 1985.
153. Molusis, J. A; Hammond, C. E.; and Cline, J. H.: A Unified Approach to the Optimal Design of Adaptive and Gain Scheduled Controllers to Achieve Minimum Helicopter Rotor Vibration. Proceedings of the 37th Annual Forum of the American Helicopter Society, May 1981.
154. Miao, W.; Kottapalli, S. B. R.; and Frye, H. M.: Flight Demonstration of Higher Harmonic Control (HHC) on S-76. Presented at the 42nd Annual Forum of the American Helicopter Society, Washington D.C., Jun. 1986.

155. Guinn, K. F.: Individual Blade Control Independent of a Swash-plate. J. American Helicopter Soc., Jul. 1982.
156. Kennedy, C. C.; and Pancu, C. D. P.: Use of Vectors in Vibration Measurement and Analysis. J. Aeronaut. Sci., vol. 14, no. 11, Nov. 1947.
157. Ibrahim, S. R.; and Mikulcik, E. C.: A Time Domain Modal Vibration Test Technique. Shock and Vibration Bulletin, no. 43, 1973.
158. Ibrahim, S. R.; and Mikulcik, E. C.: A Method for the Direct Identification of Vibration Parameters from Free Response. Shock and Vibration Bulletin, no. 46, part 5, Aug. 1978.
159. Bishop, R. E. D.; and Gladwell, G. M. L.: An Investigation into the Theory of Resonance Testing. Phil. Transactions, vol. 255, no. A 1055, 1963, pp. 241-280.
160. Richardson, M.; and Potter, R.: Identification of the Modal Properties of an Elastic Structure from Measured Transfer Function Data. ISA J., 1974, pp. 239-246.
161. Klosterman, A.; and Zimmerman, R.: Modal Survey Activity Via Frequency Response Function. SAE Paper no. 751068, 1975.
162. Brown, D. L.; Allemang, R. L.; Zimmerman, R.; and Mergeay, M.: Parameter Estimation Technique for Modal Analysis. SAE Transactions, vol. 88, 1976, pp. 828-846.
163. Flannelly, W. G.; and Lang, G. F.: Modal Analysis for Managers. Sound and Vibration, vol. 13, no. 11, Nov. 1979.
164. Giansante, N.; and Calapodas, N. J.: Modal Analysis Using Helicopter Dynamic Test Data. ASME Design Engineering Technical Conference, Paper No. 81-DET-30, Sep. 20-23, 1981.
165. Looser, W.: Accuracy of Modal Parameters from Modal Testing. 1st International Modal Analysis Conference Proceedings, 1982, pp. 201-207.
166. Chen, J. C.: Evaluation of Modal Testing Methods. AIAA Dynamics Specialists Conference, Paper No. 84-1071, May 1984.
167. Ewins, D. J.: Modal Test Requirements for Coupled Structure Analysis Using Experimentally-Derived Component Models. ASME/ASCE Joint Mechanics Conference, Jun. 24-26, 1985.
168. Giansante, N.; Berman, A.; Flannelly, W. G.; and Nagy E. J.: Structural System Identification Technology Verification. USAAVRADCOTR-81-D-28, Nov. 1981.
169. Nagy, E. J.: Improved Methods in Ground Vibration Testing. J. American Helicopter Soc., vol. 28, no. 2, Apr. 1983.



170. Nagy, E. J.: Non-linearities Encountered in the AH-1G Helicopter Ground Vibration Test. Second Flight Testing Conference, Paper No. 83-2765, Nov. 16-18, 1983.
171. Fabunmi, J. A.: Developments in Helicopter Ground Vibration Testing. J. American Helicopter Soc., vol. 31, no. 3, Jul. 1986.
172. Calapodas, N. J.: AATD's Vibration Testing Facility. Army RD&A Magazine, vol. 27, no. 2, Mar./Apr. 1986.
173. Chen, J. C.; and Wada, B. K.: Criteria for Analysis-Test Correlation of Structural Dynamic Systems. Applied Mechanics Western Conference, Paper No. 75-APMW-32, Mar. 25-27, 1975.
174. Rodden, W. P.: A Method for Deriving Structural Influence Coefficients from Ground Vibration Tests. AIAA J., vol. 5, no. 5, May 1967, pp. 991-1000.
175. Flannelly, W. G.; Berman, A.; and Barnsby, R. M.: Theory of Structural Dynamic Testing using Impedance Techniques. USAAVLABS TR-70-6A-B, Jun. 1970.
176. Giansante, N.; Flannelly, W. G.; and Berman, A.: Research on Structural Dynamic Testing by Impedance Methods. USAAMRDL TR-72 63A-D, Nov. 1972.
177. Flannelly, W. G.; and Giansante, N.: Experimental Verification of System Identification. USAAMRDL TR-74-64, Aug. 1974.
178. Berman, A.; and Flannelly, W. G.: Theory of Incomplete Models of Dynamic Structures. AIAA J., vol. 9, no. 8, Aug. 1971, pp. 1481-1487.
179. Berman, A.; and Wei, F. S.: Automated Dynamic Analytical Model Improvement. NASA CR-3452, Jul. 1981.
180. Berman, A.; and Nagy, E. J.: Improvement of a Large Analytical Model Using Test Data. AIAA J., vol. 21, no. 8, Aug. 1983, pp. 1168-1173.
181. Fuh, J.; and Berman, A.: Automated Dynamic Analytical Model Improvement for Damped Structures. NASA CR-177945, Sep. 1985.
182. Ibrahim, S. R.: Dynamic Modeling of Structures from Measured Complex Modes. AIAA J., vol. 21, no. 6, Jun. 1983, pp. 898-901.
183. Ojalvo, I. U.: Contrasts in Two Classes of Structural Dynamic Correlation Procedures. 4th International Modal Analysis Conference Proceedings, Feb. 3-6, 1986, pp. 81-87.

184. Young, J. P.; and On, F. J.: Mathematical Modeling Via Direct Use of Vibration Data. SAE National Aeronautic and Space Engineering and Manufacturing Meeting, Preprint 690615, Oct. 1969.
185. Raney, J. P.; and Howlett, J. T.: Identification of Structural Systems by Use of Near-Resonance Testing. NASA TN D-5069, Feb. 1969.
186. Ross, R. G., Jr.: Synthesis of Stiffness and Mass Matrices from Experimental Vibration Modes. SAE National Aeronautic and Space Engineering and Manufacturing Meeting, Paper no. 710787, Sep. 28-30, 1971.
187. Bowes, M. A.; and Berman, A.: Prediction of Vibration and Noise of a Transmission Using a Dynamic Model Partially Derived from Test Data. IES Twenty-Third Annual Technical Meeting, Apr. 25-27, 1977.
188. Baruch, M.: Optimization Procedure to Correct Stiffness and Flexibility Matrices Using Vibration Tests. AIAA J., vol. 16, no. 11, Nov. 1978, pp. 1208-1210.
189. Chen, J. C.; and Garba, J. A.: Matrix Perturbation for Analytical Model Improvement. 20th Structures, Structural Dynamics and Materials Conference, Paper No. 79-0831, Apr. 1979.
190. Berman, A.; Giansante, N.; and Flannelly, W. G.: Rotor Dynamic Simulation and System Identification Methods for Application to Vacuum Whirl Data. NASA CR-159356, Sep. 1980.
191. DuVal, R. W.; and Mackie, D. B.: Identification of a Linear Model of Rotor-Fuselage Dynamics from Nonlinear Simulation Data. Vertica, vol. 5, 1981, pp. 317-335.
192. Martinez, D. R.: Combined Experimental/Analytical Modeling of Dynamic Structural Systems. ASME/ASCE Joint Mechanics Conference, Jun. 24-26, 1985.
193. Vincent, A. H.: A Note on the Properties of the Variation of Structural Response with Respect to a Single Structural Parameter when Plotted in the Complex Plane. Westland Helicopters, Ltd., Report GEN/DYN/RES/010R, Sep. 1973.
194. Done, G. T. S.; and Hughes, A. D.: The Response of a Vibrating Structure as a Function of Structural Parameters. J. of Sound and Vibration, vol. 38, no. 2, 1975, pp. 255-266.
195. Flannelly, W. G.; Fabunmi, J. A.; and Nagy, E. J.: Analytical Testing. NASA CR-3429, May 1981.
196. Hanson, H. W.; and Calapodas, N. J.: Evaluation of the Practical Aspects of Vibration Reduction Using Structural Optimization Techniques. J. American Helicopter Soc., vol. 25, no. 3, Jul. 1980, pp. 37-45.

197. Nagy, E. J.: Vincent's Circle as a Tool for Machine Vibration Optimization Techniques. ASME Design Engineering Technical, Conference, Paper No. 81-DET-78, Sep. 20-23, 1981.
198. Bartlett, F. D., Jr.: Flight Vibration Optimization Via Conformal Mapping. J. American Helicopter Soc., vol. 28, no. 1, Jan. 1983, pp. 49-55.
199. Wang, B. P.; Kitis, L.; Pilkey, W. D.; and Palazzolo, A. B.: Structural Modification to Achieve Antiresonance in Helicopters. J. Aircraft, vol. 19, no. 6., Jun. 1982, pp. 499-504.
200. Okada, Y.; Wang, B. P.; and Pilkey, W. D.: Discrete Modifications to Continuous Dynamic Structural Systems. Shock and Vibration Bulletin, no. 54, part 3, Jun. 1984.
201. Wang, B. P.; Okada, Y.; and Pilkey, W. D.: Reanalysis of Continuous Dynamic Systems with Continuous Modifications. The Shock and Vibration Bulletin, no. 54, part 3, Jun. 1984.
202. Mays, W. D.: ATEST - An Interactive Computer Program for Predicting Changes in Flight Vibrations Due to Structural Modifications. USAAVSCOM TR-86-D-6, Jul. 1986.
203. Flannelly, W. G.; Bartlett, F. D., Jr.; and Forsberg T. W.: Laboratory Verification of Force Determination, A Potential Tool for Reliability Testing. USAAMRDL TR-76-38, Jan. 1977.
204. Bartlett, F. D., Jr.; and Flannelly, W. G.: Model Verification of Force Determination for Measuring Vibratory Loads. J. American Helicopter Soc., vol. 24, no. 2, Apr. 1979, pp. 10-18.
205. Jones, R.; Flannelly, W. G.; Nagy, E. J.; and Fabunmi, J. A.: Experimental Verification of Force Determination and Ground Flying on a Full-Scale Helicopter. USAAVRADCOM TR-81-D-11, May 1981.
206. Giansante, N.; Jones, R.; and Calapodas, N. J.: Determination of In-Flight Helicopter Loads. J. American Helicopter Soc., vol. 27, no. 3, Jul. 1982.
207. Fabunmi, J. A.: Effects of Structural Modes on Vibratory Force Determination by the Psuedo Inverse Technique. 26th Structures, Structural Dynamics and Materials Conference, Paper No. 85-0784, Apr. 15-17, 1985.
208. Fabunmi, J. A.: Modal Constraints on Structural Dynamic Force Determination. J. American Helicopter Soc., vol. 30, no. 4, Oct. 1985, pp. 48-54.

ORIGINAL PAGE IS  
OF POOR QUALITY



Figure 1.- The Sikorsky R-4, the first U.S. production helicopter.



Figure 2.- Soviet Yak-24.



Figure 3.- UH-60 Black Hawk.



Figure 4.- AH-64 Apache.

ORIGINAL PAGE IS  
OF POOR QUALITY

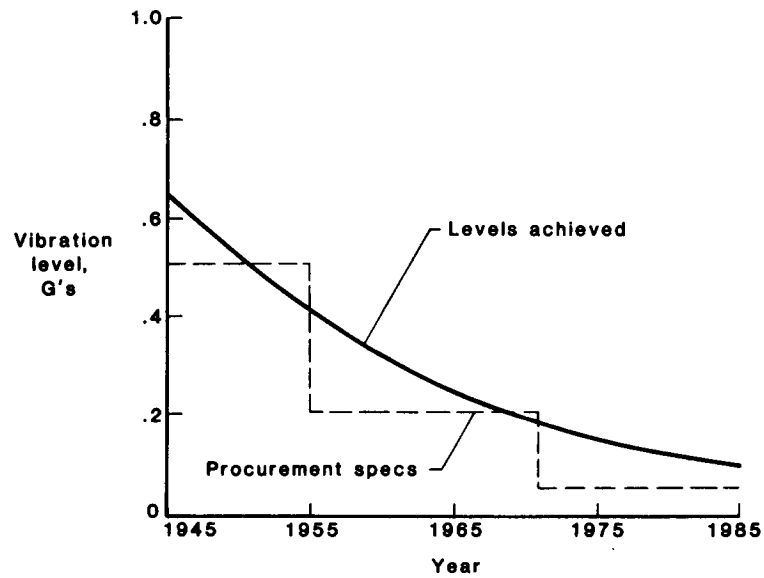


Figure 5.- Trend of helicopter vibration levels.

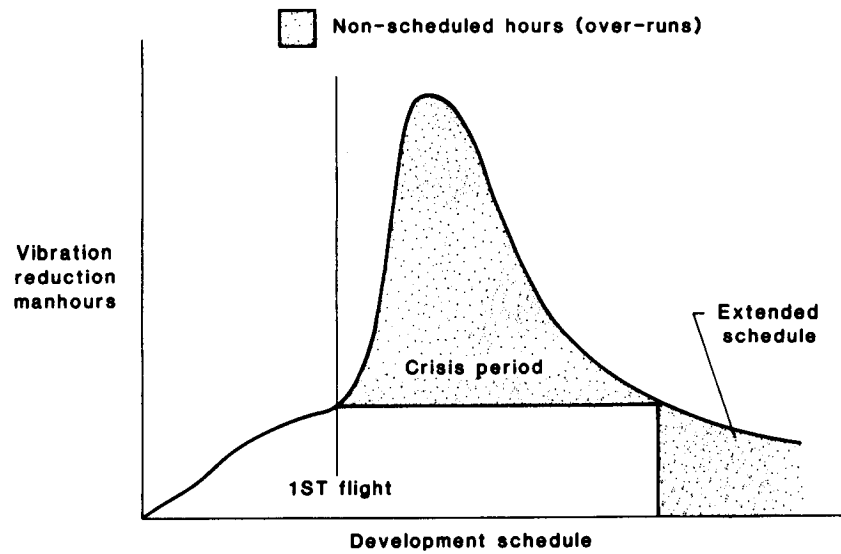


Figure 6.- Impact of vibrations on helicopter development.

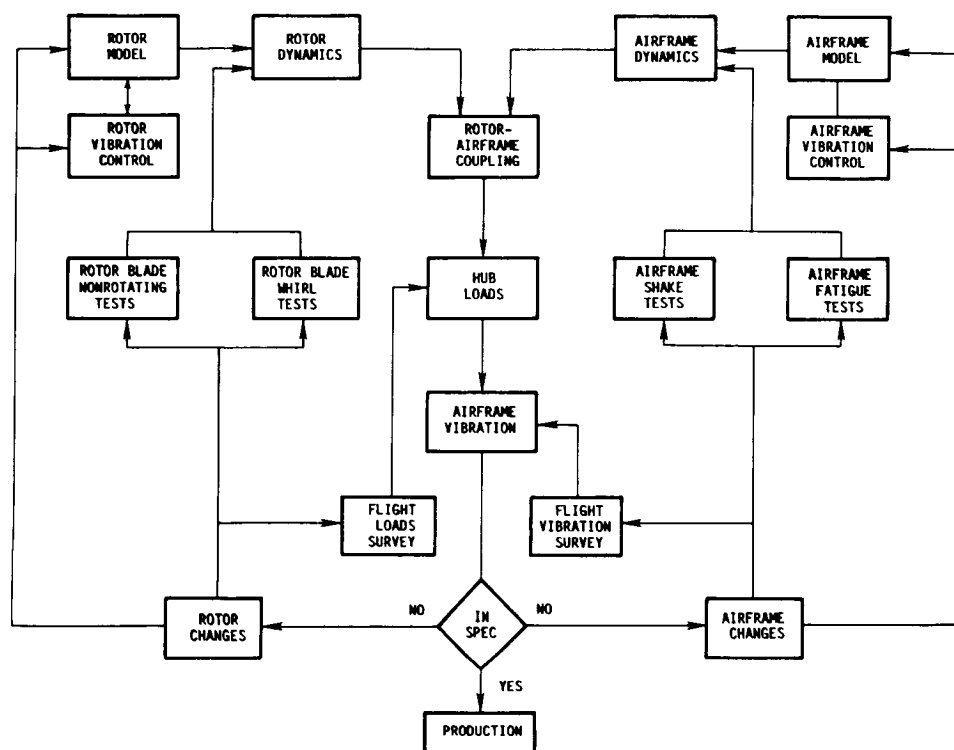


Figure 7.- Helicopter vibration design cycle.

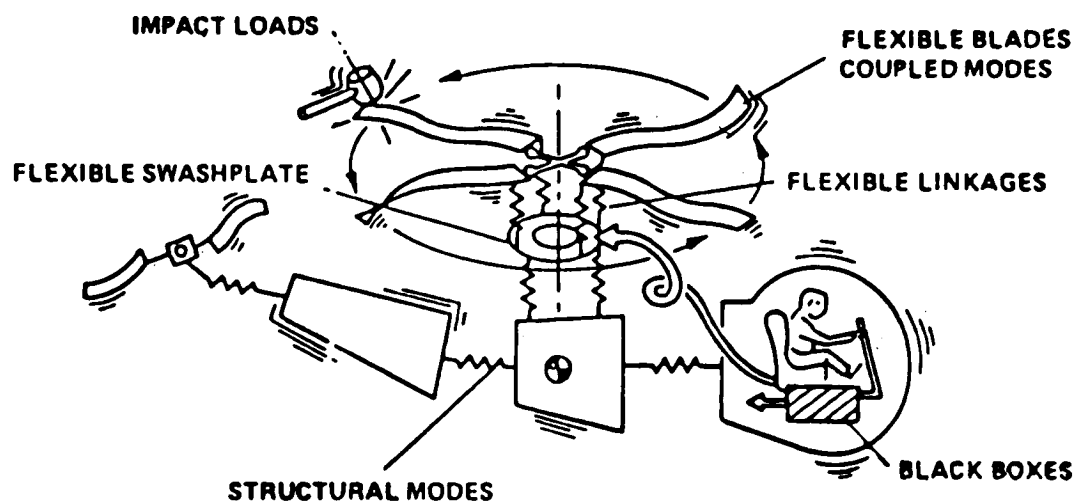


Figure 8.- The helicopter as might be viewed by a dynamicist.

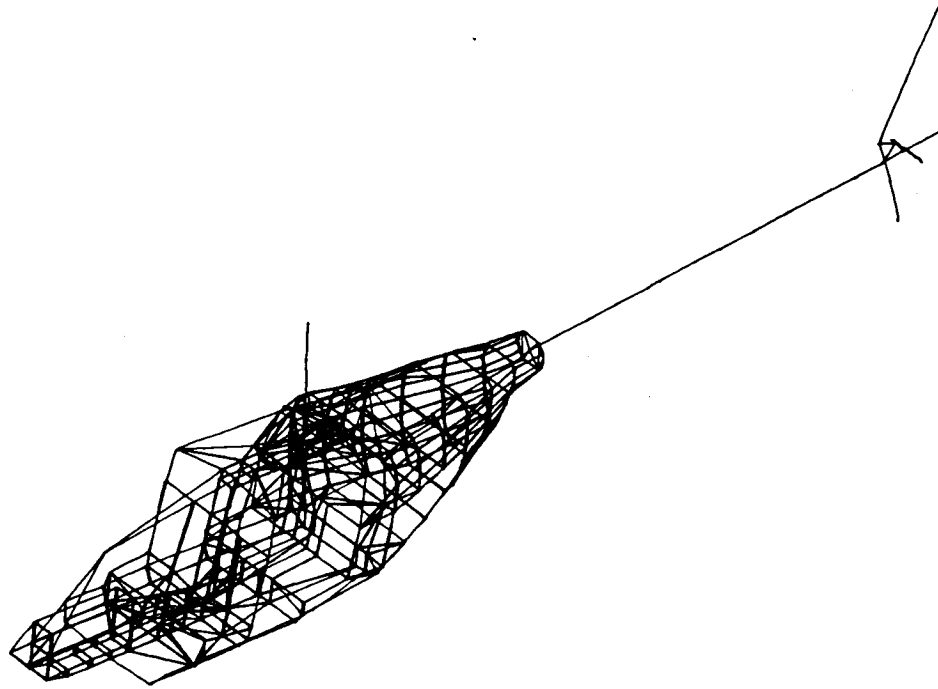


Figure 9.- NASTRAN finite-element model of OH-58A helicopter. (From ref. 27.)

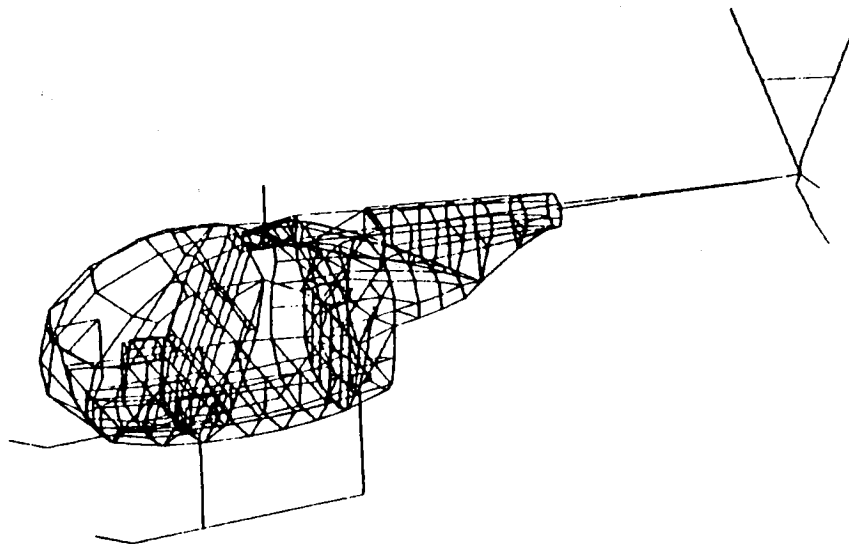


Figure 10.- NASTRAN finite-element model of OH-6A helicopter. (From ref. 28.)



ORIGINAL PAGE IS  
OF POOR QUALITY

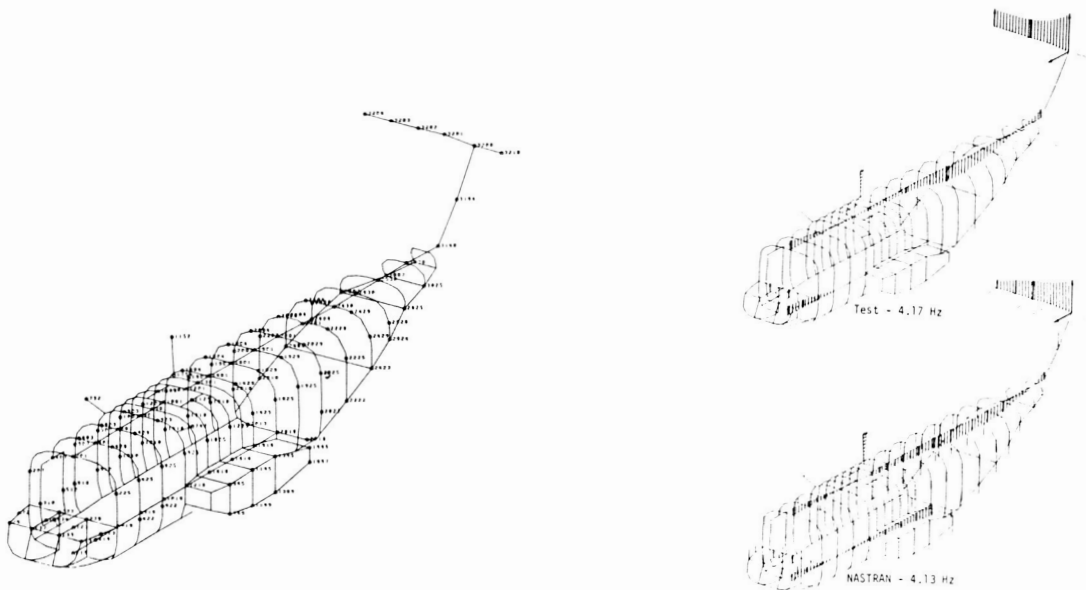


Figure 11.- NASA CH-53 Civil Helicopter Research Aircraft showing NASTRAN model with dynamic degrees of freedom indicated and correlation for the first vertical bending mode. (From ref. 31.)

ORIGINAL PAGE IS  
OF POOR QUALITY

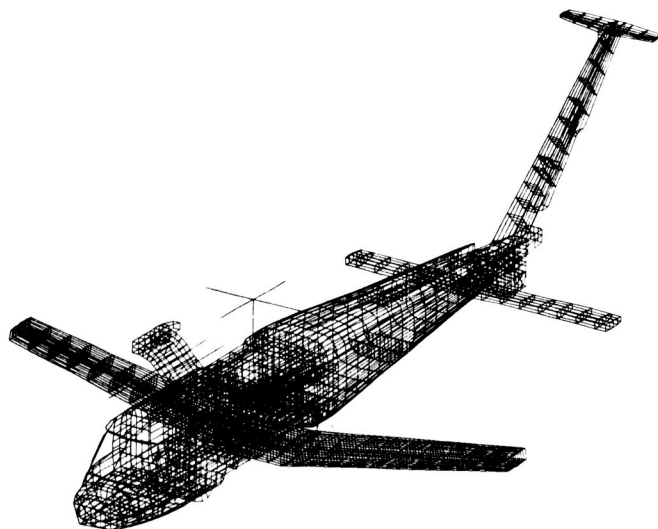


Figure 12.- Rotor Systems Research Aircraft (RSRA) in compound configuration and associated NASTRAN model. (Courtesy Sikorsky Aircraft.)

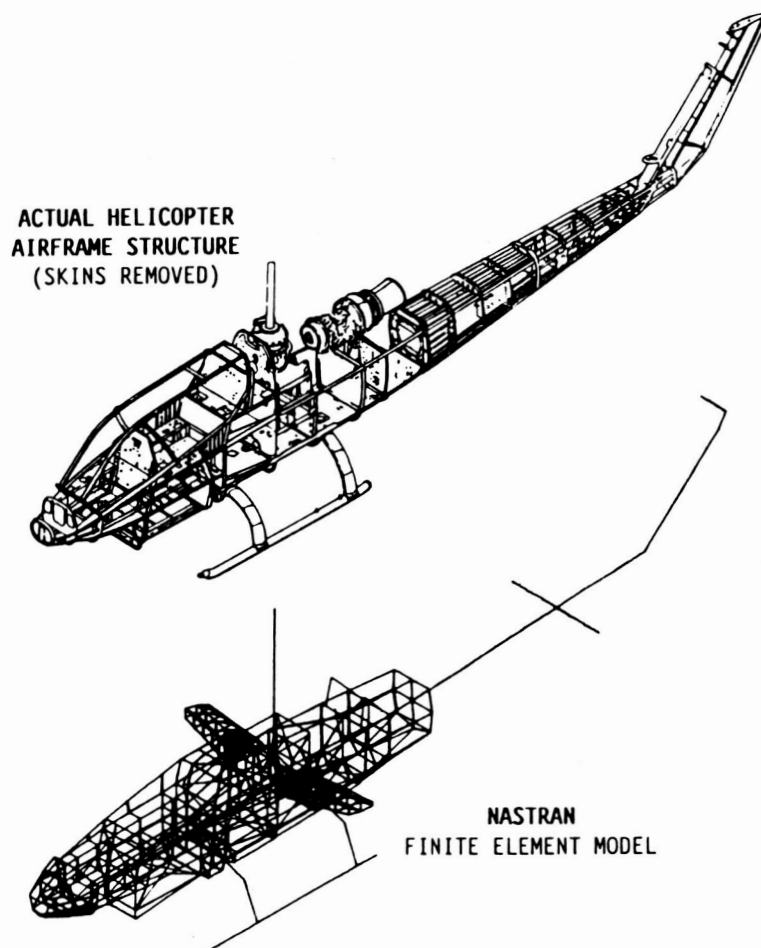
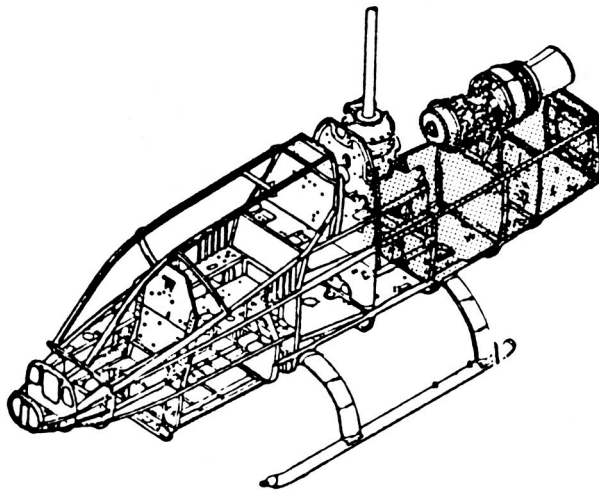
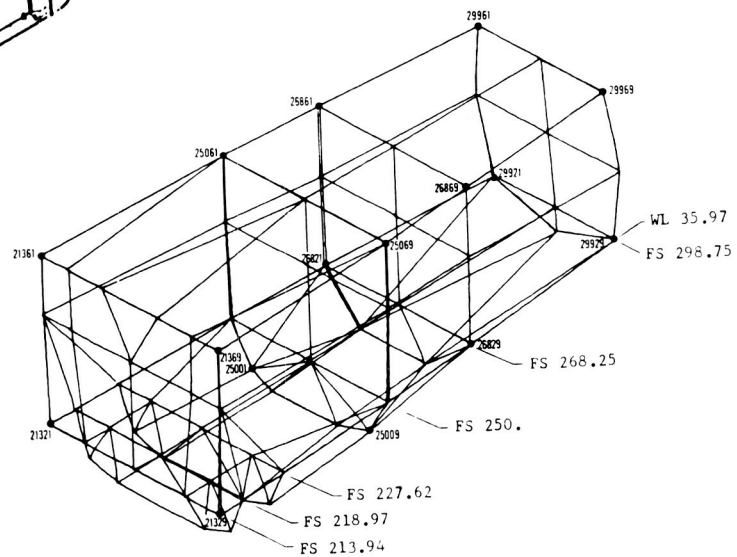


Figure 13.- AH-1G helicopter showing airframe structure with skins removed and NASTRAN finite-element model. (From ref. 33.)

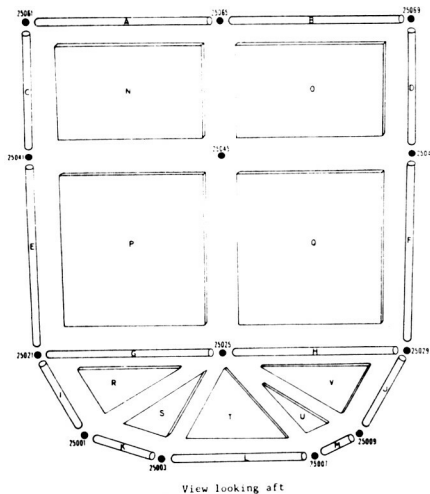
ORIGINAL PAGE IS  
OF POOR QUALITY



Actual Structure for Reference  
(Aft fuselage shown shaded)

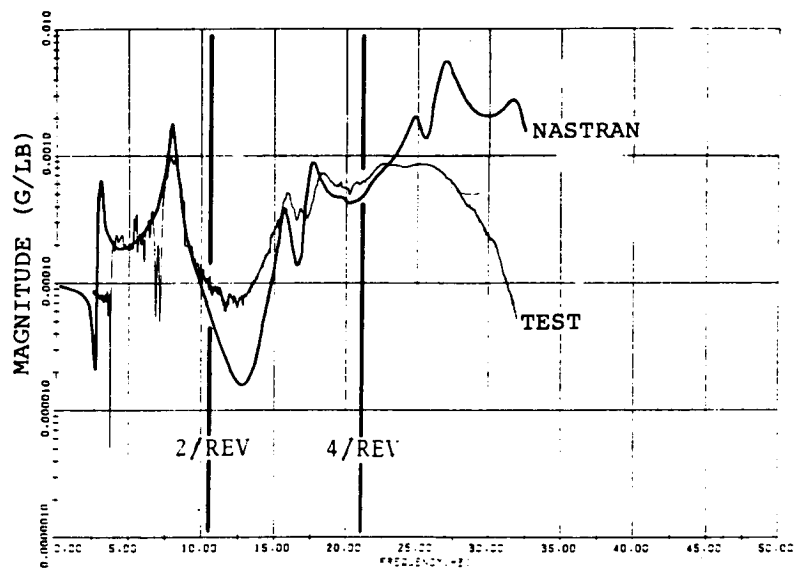


## Finite-Element Model of Aft Fuselage

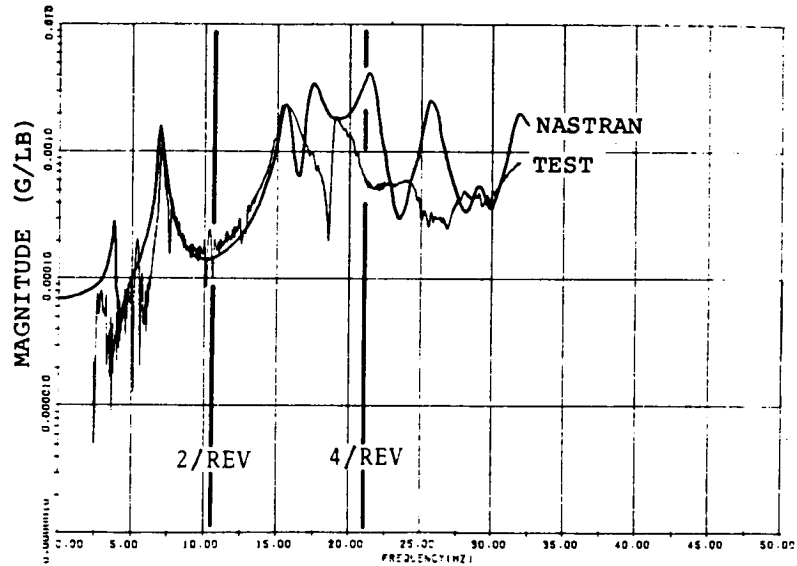


## Bulkhead Detail

Figure 14.- Typical sketches used in description of AH-1G NASTRAN model.  
(From ref. 33.)



Tailboom Vertical Shake (Clean Wing)  
Pilot Seat Vertical Response.



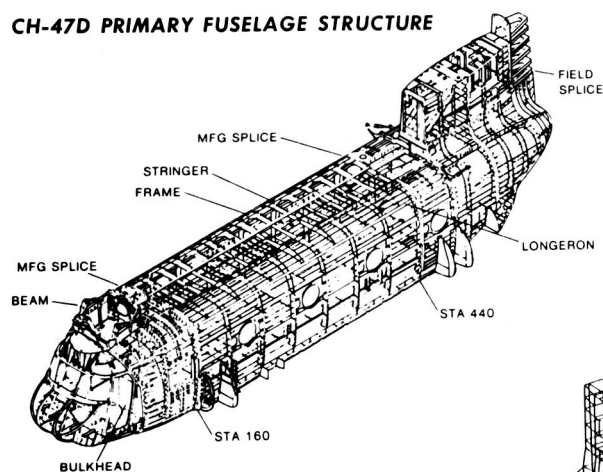
Tailboom Lateral Shake (Clean Wing)  
Pilot Seat Lateral Response.

Figure 15.- Comparisons of frequency response results for AH-1G.  
(From ref. 34.)

ORIGINAL PAGE IS  
OF POOR QUALITY



#### CH-47D PRIMARY FUSELAGE STRUCTURE

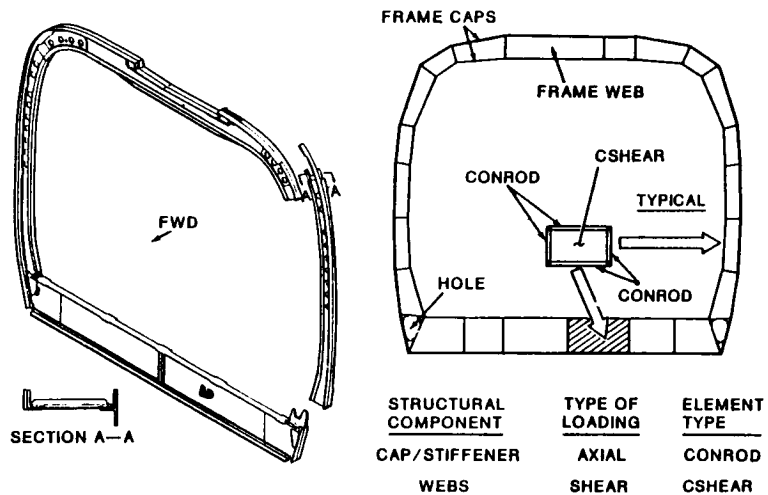


#### STATIC MODELING CH-47D NASTRAN STRUCTURAL MODEL

NASTRAN MODEL	
1,883 STRUCTURAL NODES	
5,758 STRUCTURAL ELEMENTS	
NO. OF ELEMENTS	TYPE
398	CBAR - BEAM
76	CELAS2 - SPRING
3,253	CONROD - AXIAL
1,707	CSHEAR - QUADRILATERAL SHEAR
156	CTRMEM - TRIANGULAR MEMBRANE
156	CQUAD1 - QUADRILATERAL SHELL
12	CTRIA1 - TRIANGULAR SHELL

Figure 16.- CH-47D helicopter showing primary fuselage structure and NASTRAN finite-element model. (From ref. 41.)

## STATIC MODELING GUIDES — FRAMES



## MASS MODELING GUIDES — FRAME STATION MASS TREATMENT

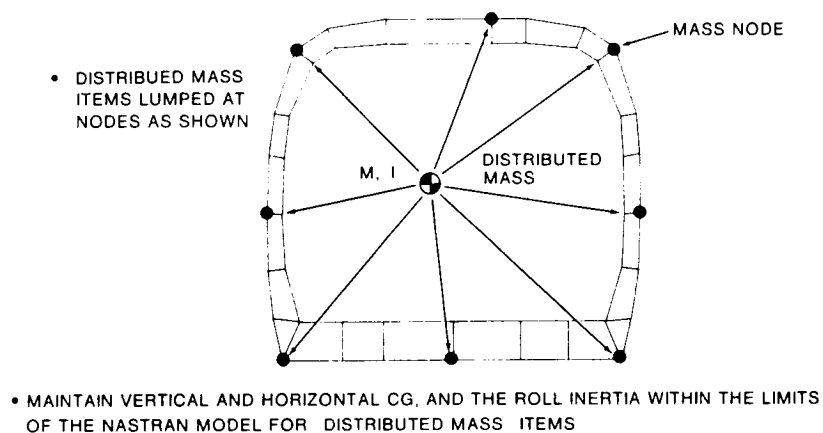
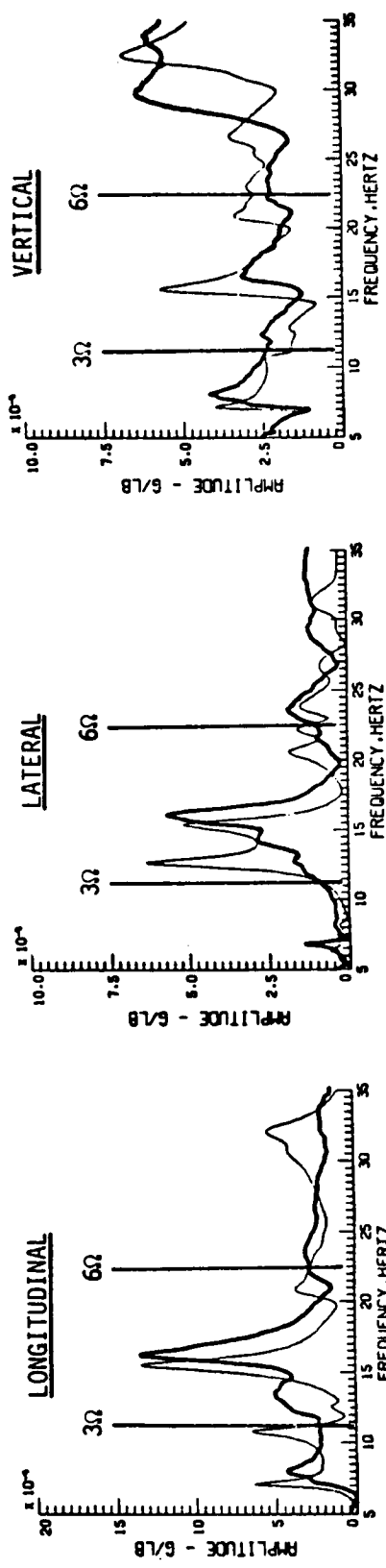


Figure 17.- CH-47D static and mass modeling guides for a typical frame.  
(From ref. 41.)

— TEST  
— SUSPENDED ANALYSIS  
(2.5% DAMPING)

FORWARD HUB - GRID POINT 7002 (LOC. 1)



COCKPIT STA. 52 R/H - GRID POINT 52 (LOC. 11)

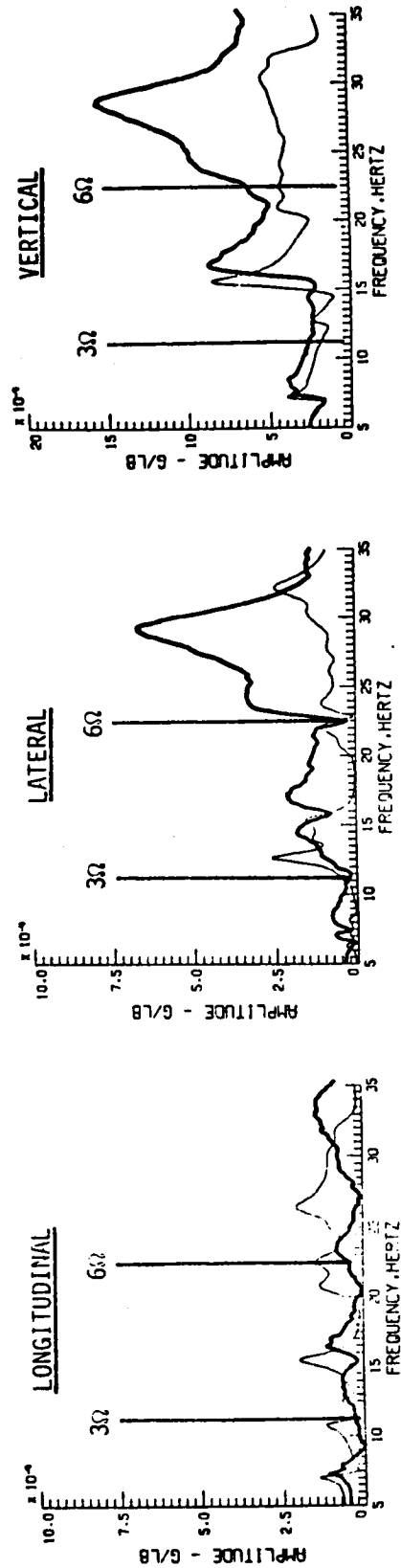


Figure 18.- Comparison of test and analysis for vertical excitation of CH-47D at forward hub.  
(From ref. 42.)



# SUGGESTED IMPROVEMENTS EFFECT OF VARIATION IN MODAL DAMPING

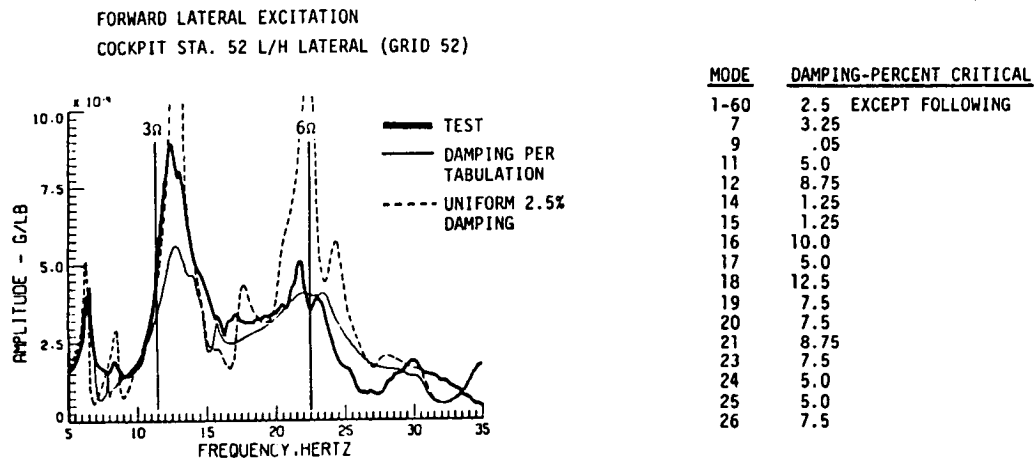


Figure 19.- Effect of variation in modal damping used in analysis on correlation for CH-47D. (From ref. 42.)

ORIGINAL PAGE IS  
OF POOR QUALITY



MODEL STATISTICS	
1635 GRID POINTS	
4461 ELEMENTS	
951 MASS ITEMS	
No OF ELEMENTS	TYPE
872	BAR
53	BEAM
2041	ROD
1302	SHEAR
80	TRIA3
28	RBAR
85	RBE

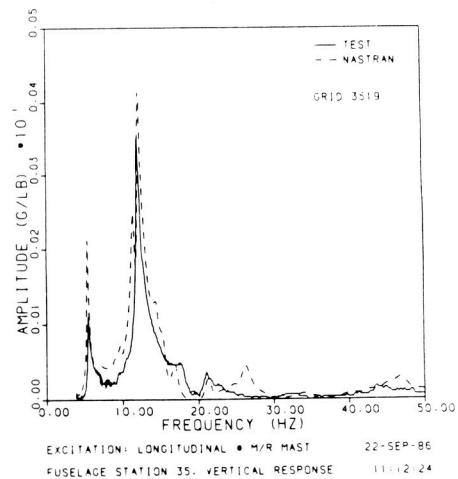
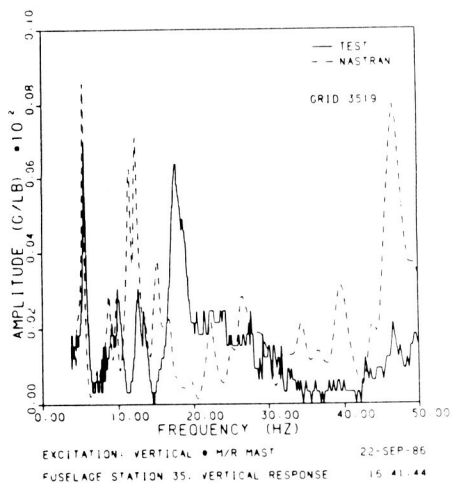
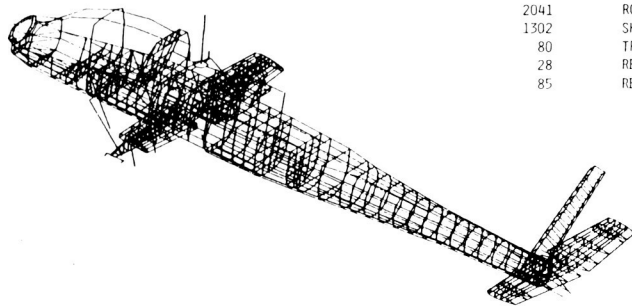
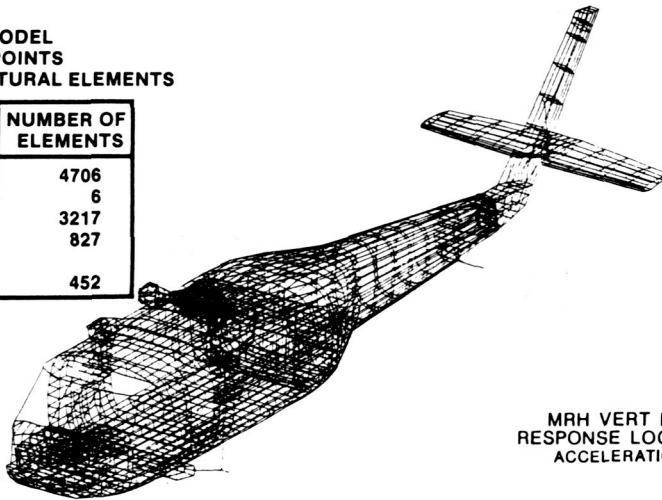


Figure 20.- AH-64A helicopter, NASTRAN finite-element model and typical frequency response comparisons. (From draft final report submitted under DAMVIBS program.)

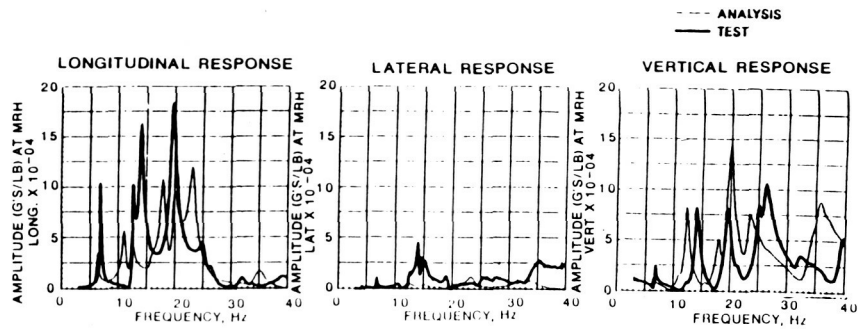
# UH-60A NASTRAN MODEL STATICS MODEL

NASTRAN MODEL  
4,341 GRID POINTS  
8756 STRUCTURAL ELEMENTS

ELEMENT TYPE	NUMBER OF ELEMENTS
BAR	4706
CONROD	6
QUAD4	3217
TRIA3	827
CONM2	452



MRH VERT EXCITATION  
RESPONSE LOCATION : MRH  
ACCELERATION VECTOR



MRH LAT EXCITATION  
RESPONSE LOCATION : MRH  
ACCELERATION VECTOR

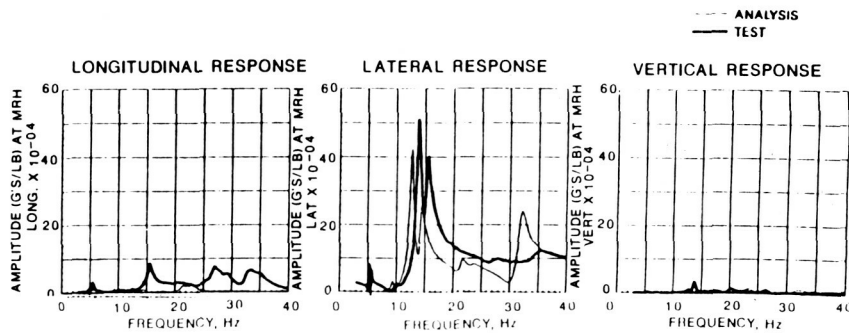


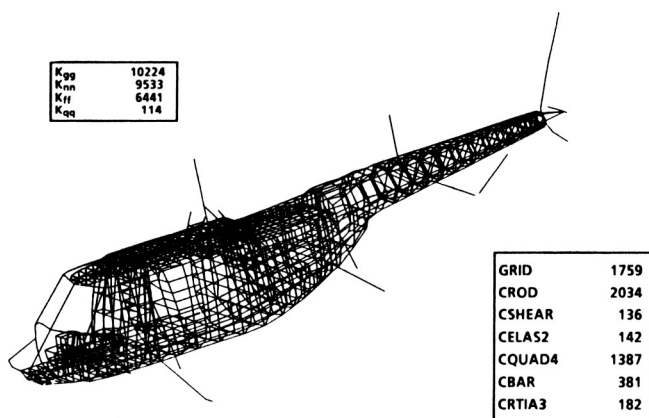
Figure 21.- UH-60A helicopter, NASTRAN finite-element model and typical frequency response comparisons. (From draft final report submitted under DAMVIBS program.)

The figure consists of two side-by-side line graphs. Both graphs plot Magnitude (G/LB) on a logarithmic y-axis against Frequency (Hz) on a linear x-axis from 0 to 30 Hz. Vertical lines at 10 Hz and 25 Hz mark 2/REV and 4/REV respectively.

**Left Graph: PILOT SEAT VERTICAL RESPONSE TO HUB VERTICAL EXCITATION**  
 The y-axis ranges from 0.000001 to 0.01. The solid line shows peaks at approximately 7 Hz (labeled '1st fus vert'), 10 Hz (labeled 'nodal beam sym'), 18 Hz (labeled 'elev sym'), and 25 Hz (labeled '2nd fus vert'). A dashed line shows a peak at 7 Hz (labeled 'pylon pitch').

**Right Graph: PILOT SEAT LATERAL RESPONSE TO HUB LATERAL EXCITATION**  
 The y-axis ranges from 0.0000001 to 0.001. The solid line shows peaks at approximately 7 Hz (labeled '1st fus lat'), 10 Hz (labeled 'pylon roll'), 18 Hz (labeled 'elev asym'), and 25 Hz (labeled 'm/r mast f/a'). A dashed line shows a peak at 7 Hz (labeled 'nodal beam asym').

LEGEND  
- - - - - NASTRAN  
————— Test



141

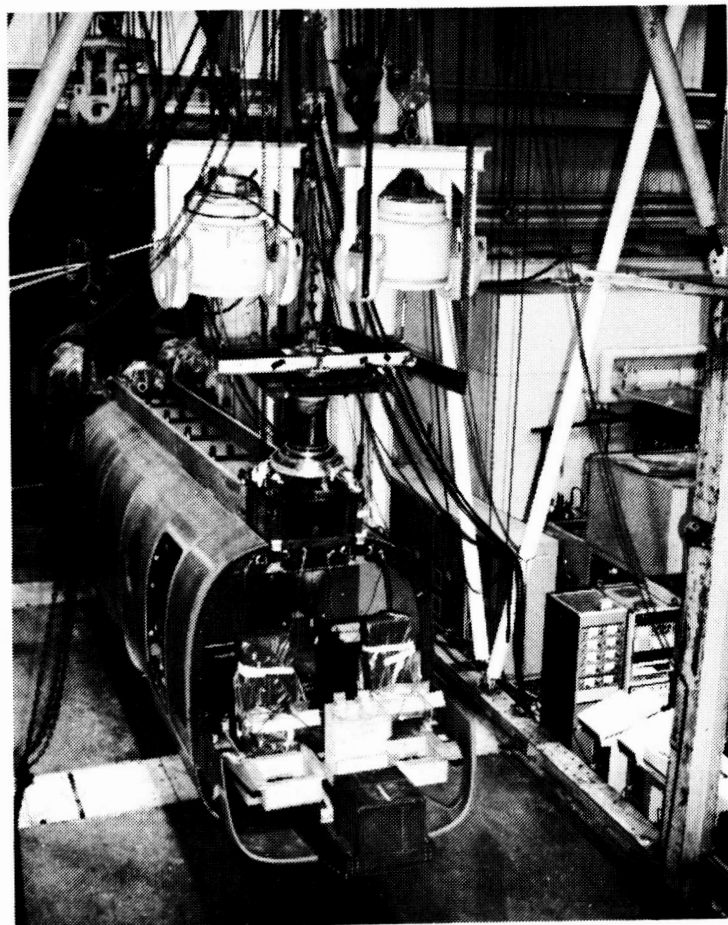
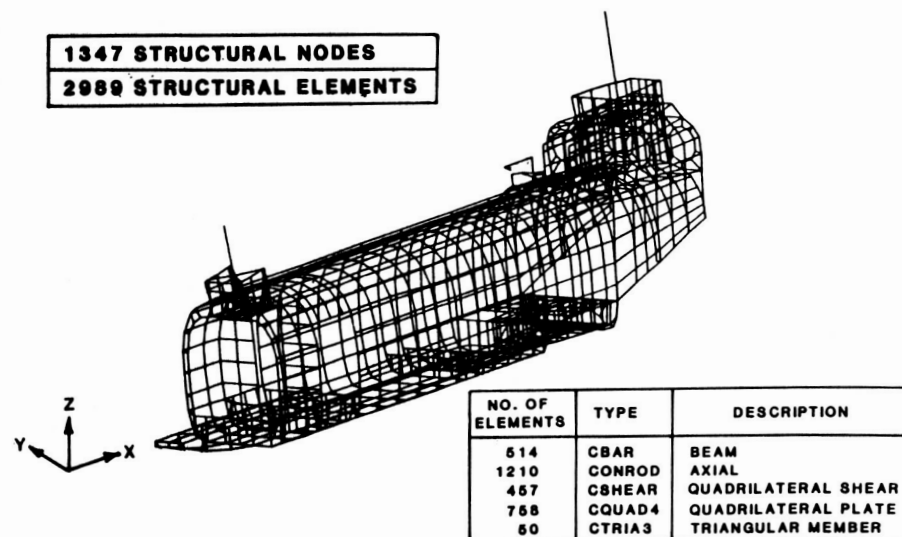


Figure 23.- NASTRAN finite-element model of Model 360 composite airframe and airframe during ground vibration test. (From draft final report submitted under DAMVIBS program.)

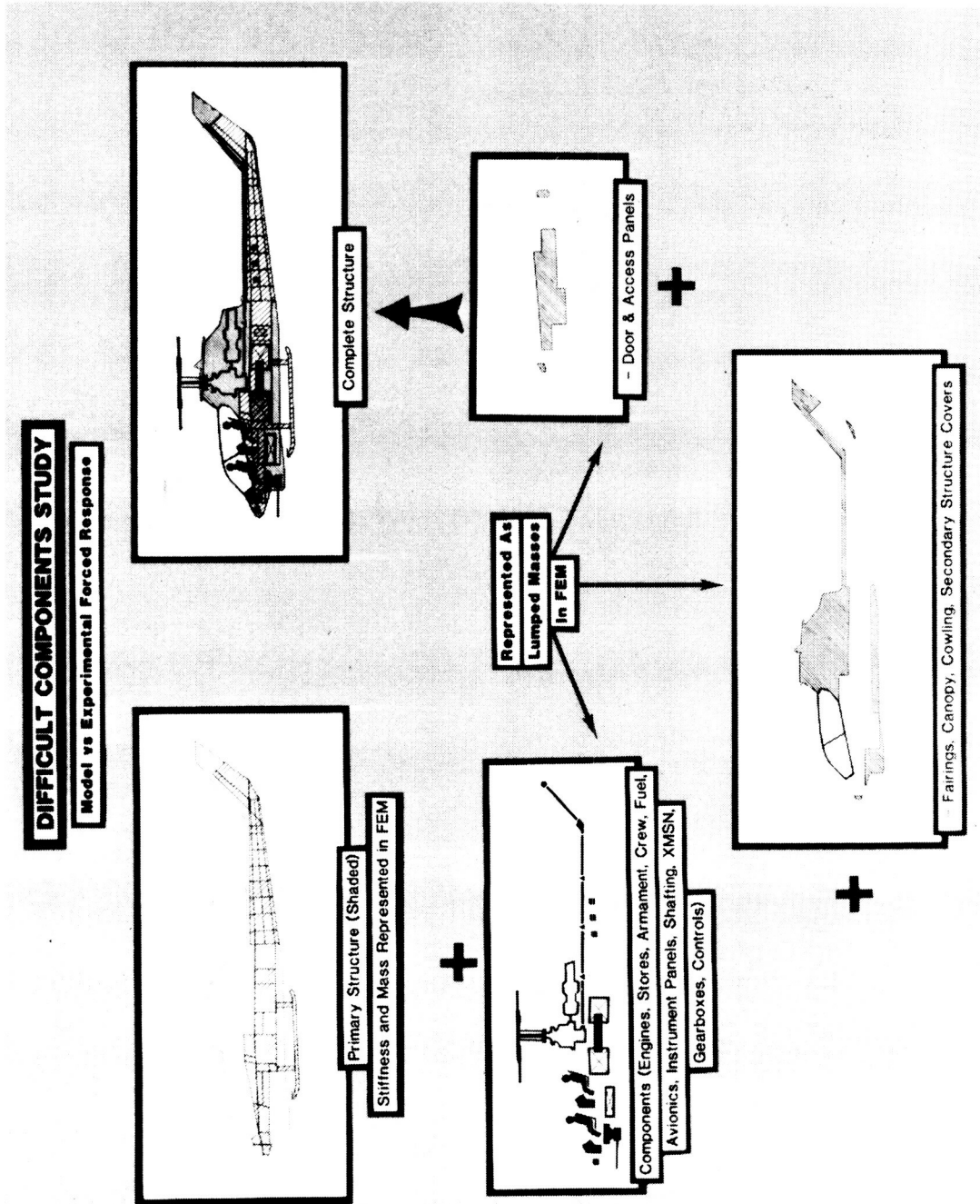


Figure 24.- Difficult components study being conducted on the AH-1G under DAMVIBS program.

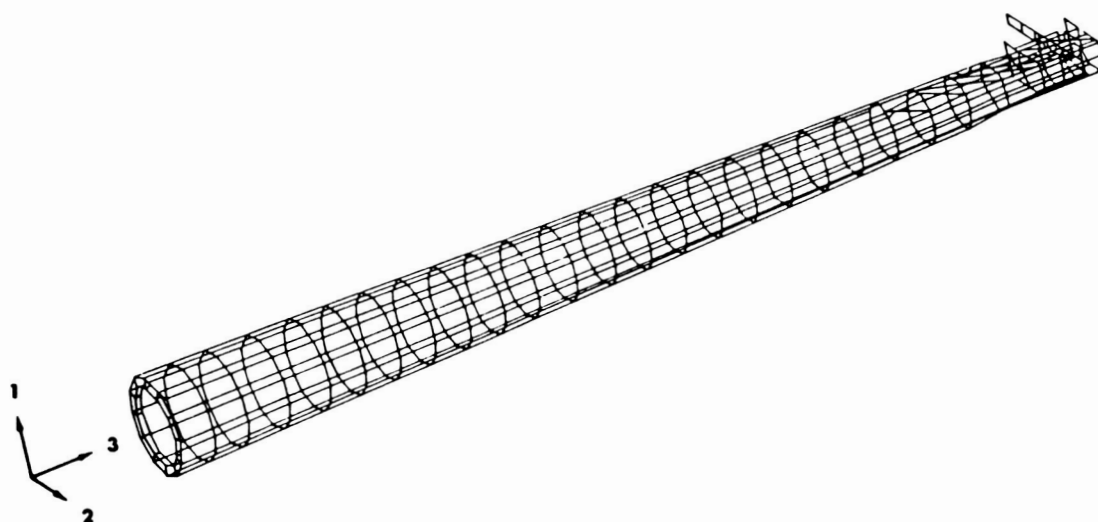
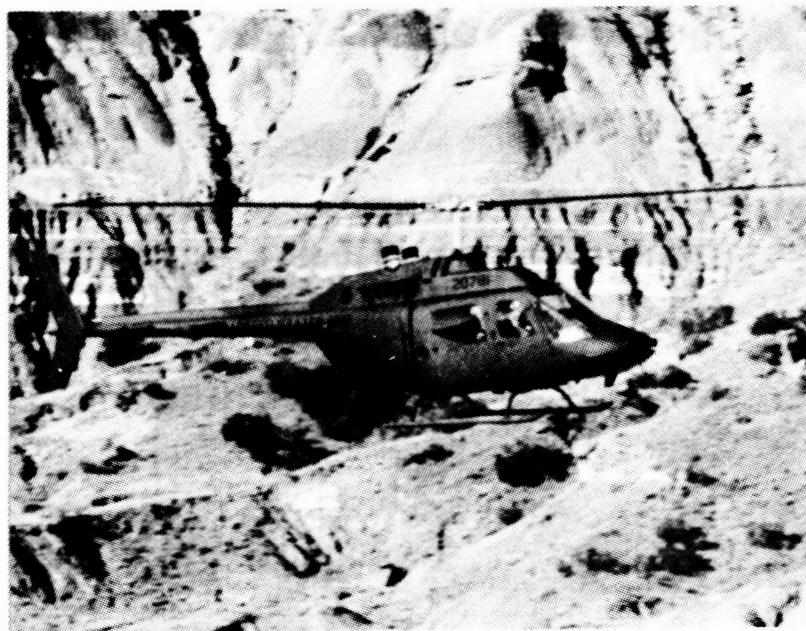


Figure 25.- OH-58A helicopter and EAL finite-element model of composite tail boom. (From ref. 47)

ORIGINAL PAGE IS  
OF POOR QUALITY.

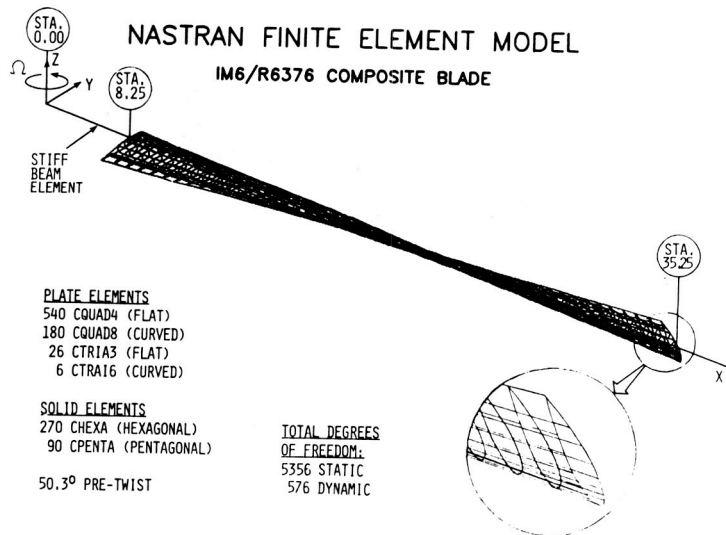
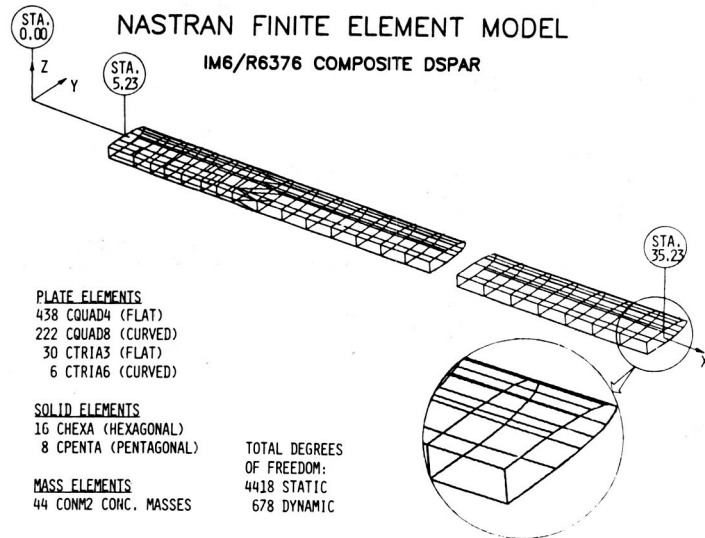


Figure 26.- NASTRAN finite-element models of composite model rotor blades.



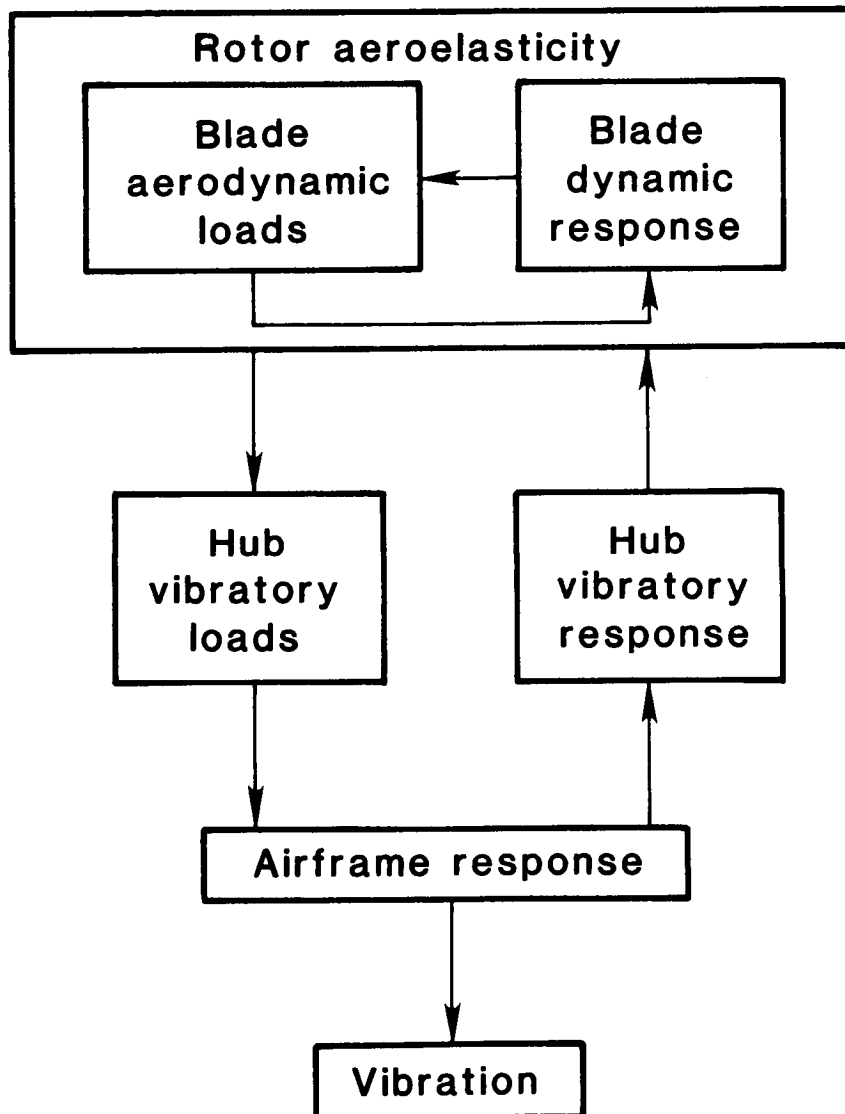


Figure 27.- A simplified view of rotor-airframe interaction in producing vibrations.

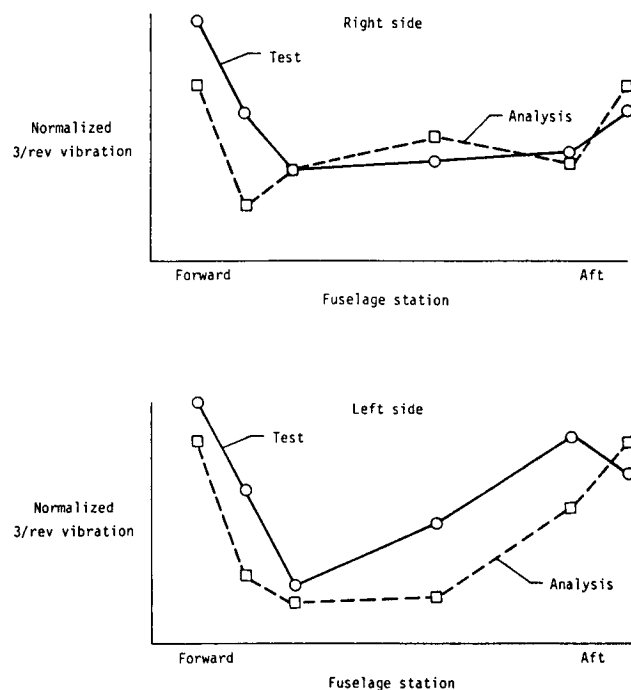


Figure 28.- Correlation of flight test data with a coupled rotor-airframe analysis for 3/rev vibration of a three-bladed tandem-rotor helicopter in high-speed level flight. (From ref. 60.)

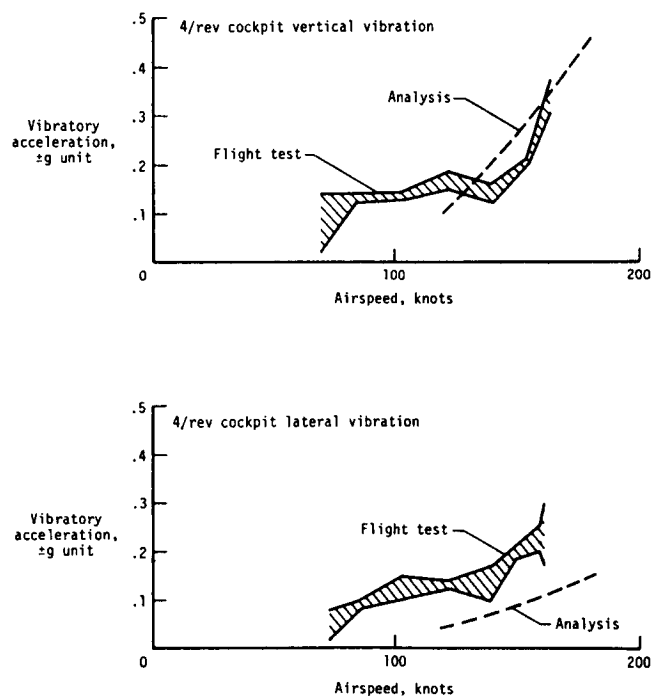


Figure 29.- Correlation of flight test data with an uncoupled rotor-airframe analysis for 4/rev vibrations of a four-bladed tandem-rotor helicopter. (From ref. 61.)

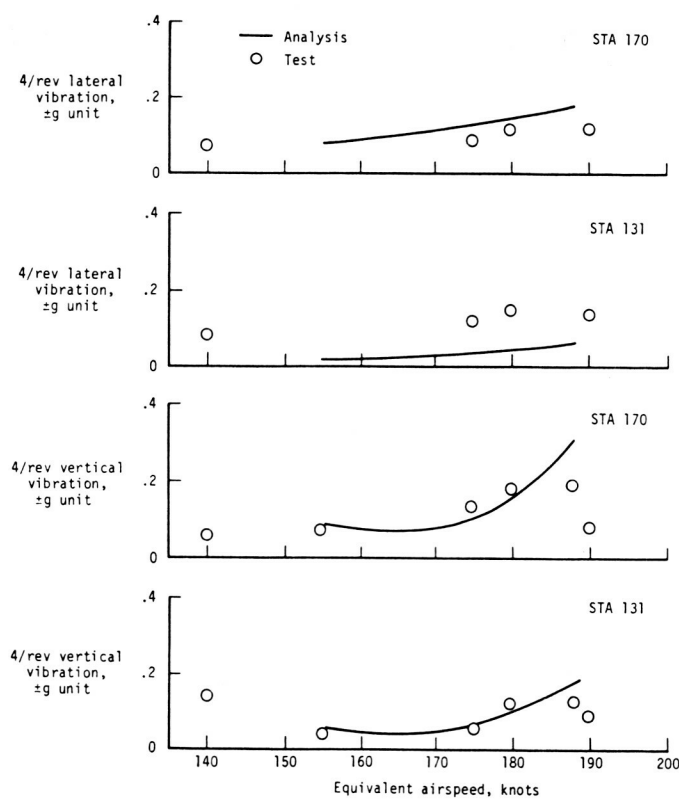
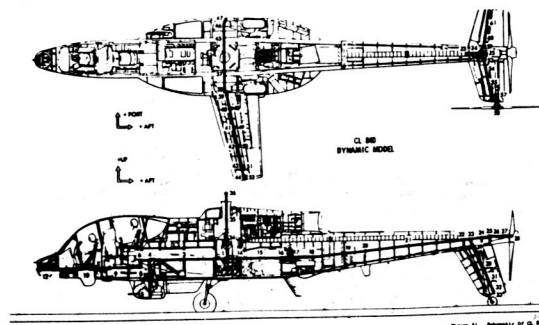


Figure 30.- Comparison of computed coupled rotor-airframe vibrations with measured data for a compound helicopter with four-bladed hingeless rotor. (From ref. 62.)

ORIGINAL PAGE IS  
OF POOR QUALITY

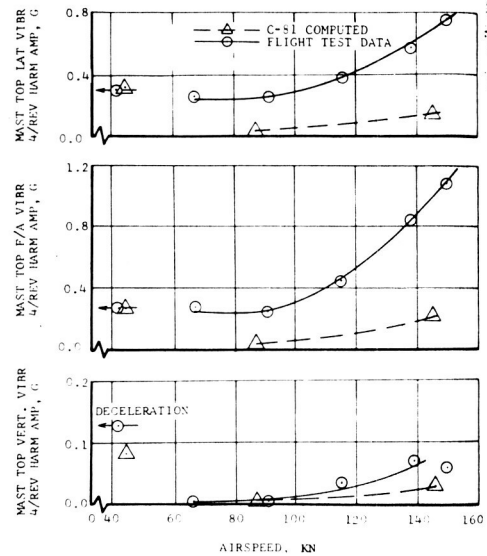


Figure 31.- Comparison of computed and measured hub vibrations for a helicopter with a four-bladed hingeless rotor. (From ref. 63.)

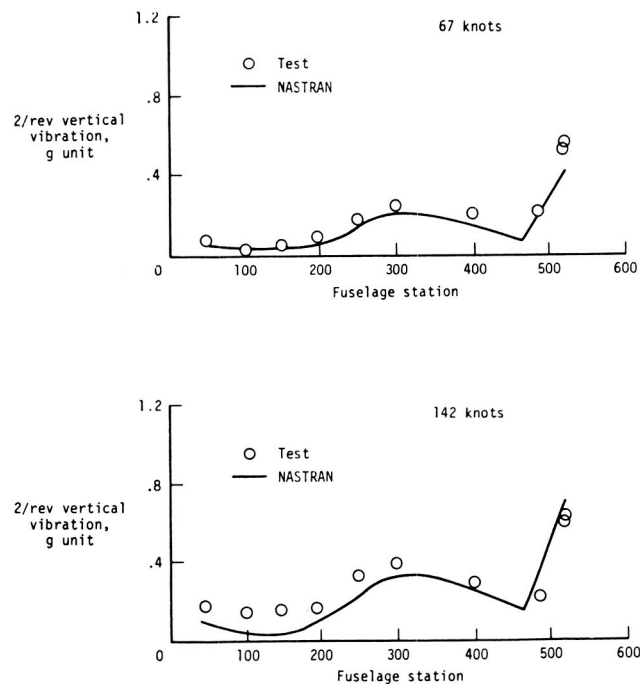
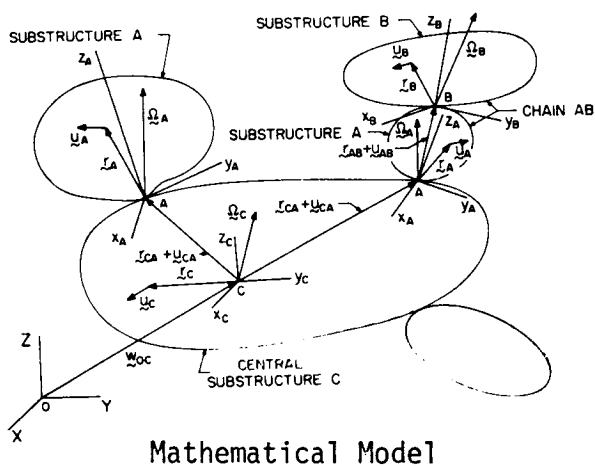


Figure 32.- Comparison of measured 2/rev vertical airframe vibrations with C-81 analysis using measured hub accelerations for a two-bladed teetering rotor helicopter. (From ref. 37.)



ORIGINAL PAGE IS  
OF POOR QUALITY

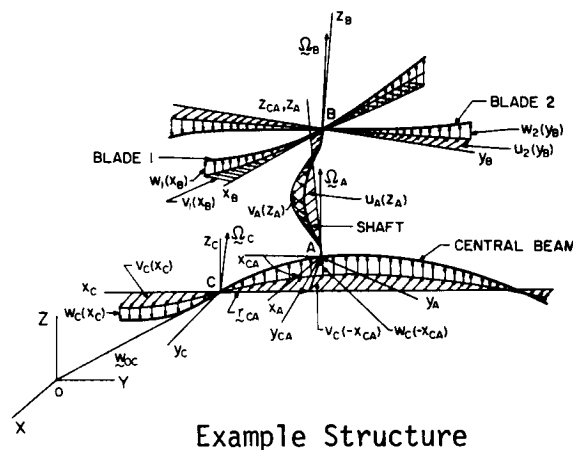


Figure 33.- A formulation for dynamic synthesis of gyroscopic structures consisting of point-connected substructures. (From ref. 75.)

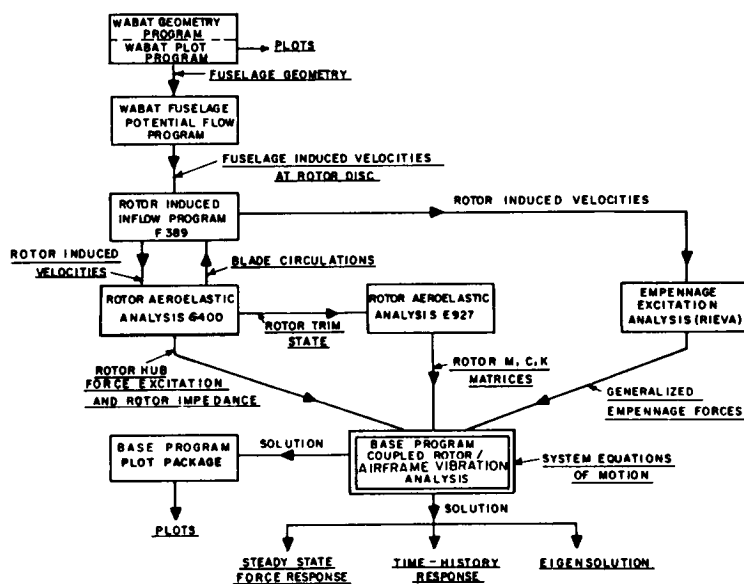


Figure 34.- Arrangement of program blocks in SIMVIB coupled rotor-airframe vibration analysis program. (From ref. 82.)

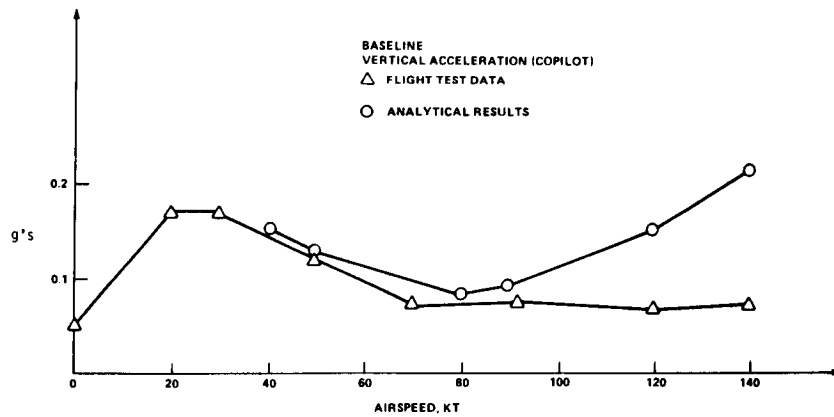
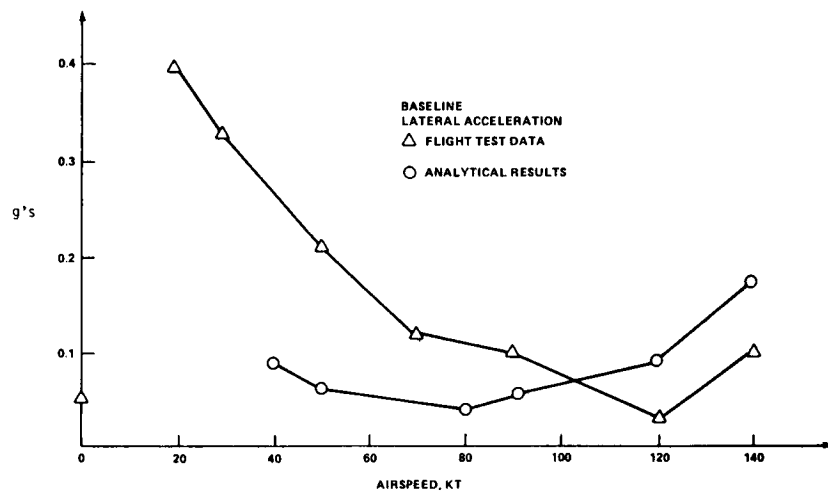
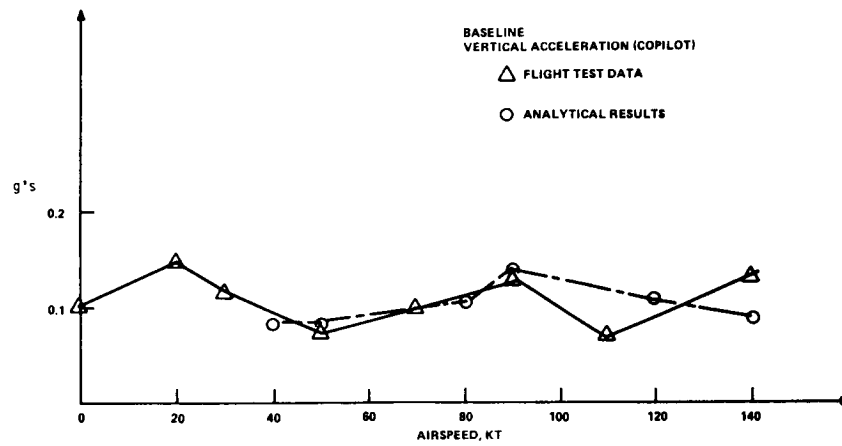
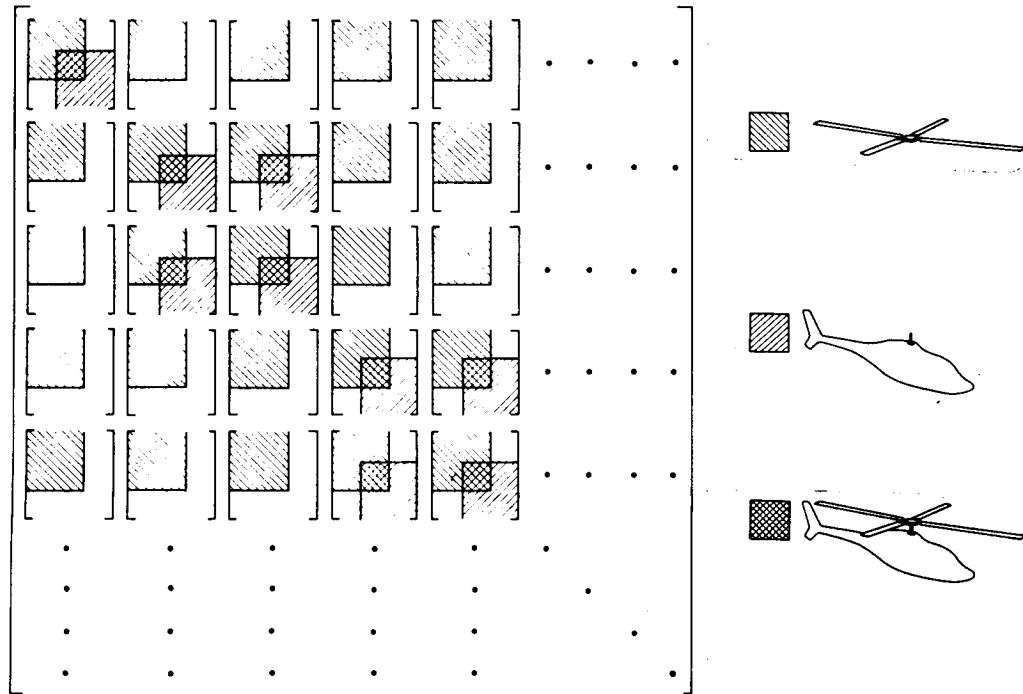


Figure 35.- Comparison of measured 4/rev vibrations for SH-60B with SIMVIB analysis using hub loads measured in flight. (From ref. 83.)

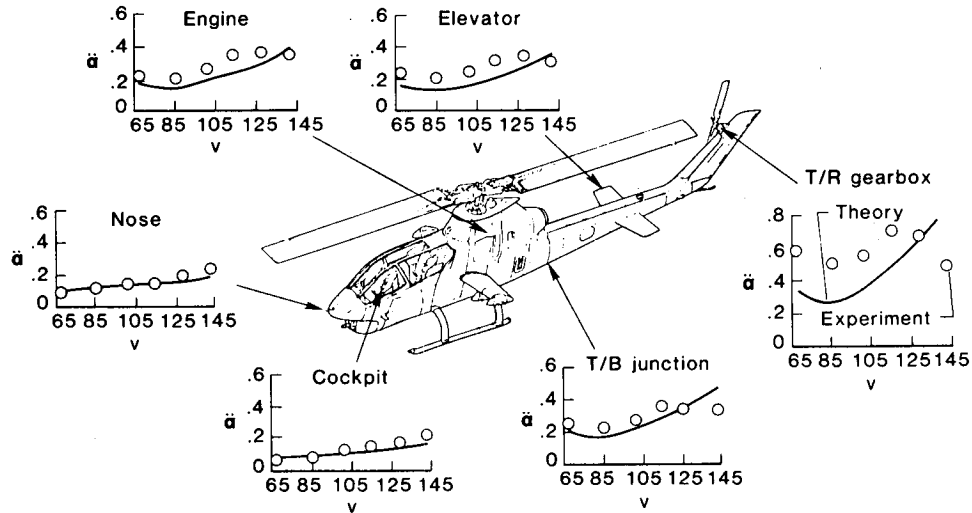


$$\begin{aligned}
 \boxed{\text{shaded}} &= (UOK) [KROC] + \frac{1}{2} (ULK) [KRLP] + \frac{1}{2} (UHK) [KRHP] \\
 &+ x_3 \Omega \left( (UOC) [CROC] + \frac{1}{2} (ULC) [CRLQ] + \frac{1}{2} (UHC) [CRHQ] \right) \\
 &- (x_3 \Omega)^2 \left( (UOM) [MROC] + \frac{1}{2} (ULM) [MRLP] + \frac{1}{2} (UHM) [MRHP] \right)
 \end{aligned}$$

Figure 36.- Illustrative example showing manner in which matrices and equations are depicted in a formulation of rotor-airframe coupling aimed at providing a basis for implementation of a design analysis capability for airframe vibrations. (Adapted from ref. 84.)

## AH-1G FLIGHT VIBRATION ANALYSIS/EXPERIMENT CORRELATION 2/REV VERTICAL RESPONSE

(Acceleration in g units versus airspeed in knots)



## AH-1G FLIGHT VIBRATION ANALYSIS/EXPERIMENT CORRELATION 4/REV VERTICAL RESPONSE

(Acceleration in g units versus airspeed in knots)

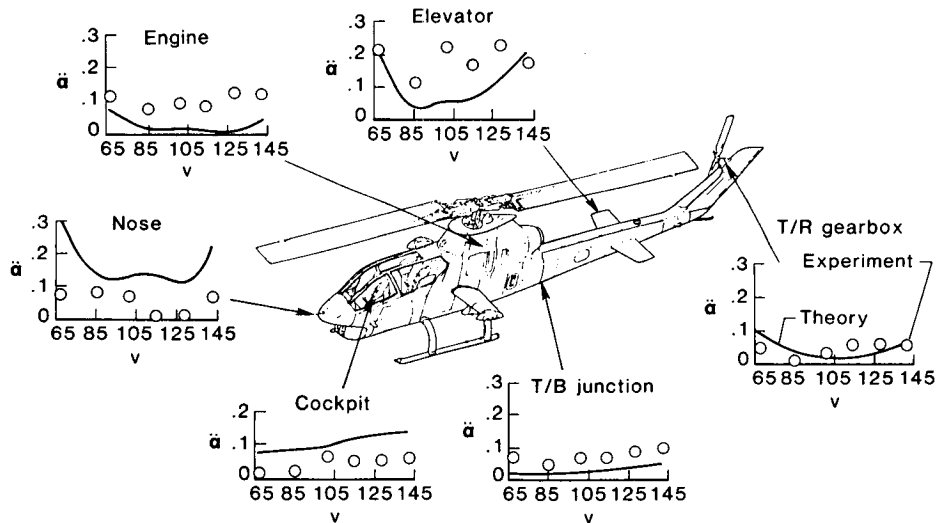


Figure 37.- Comparison of measured AH-1G 2/rev and 4/rev vertical vibrations with results of C-81 analysis. (Based on results presented in ref. 88)



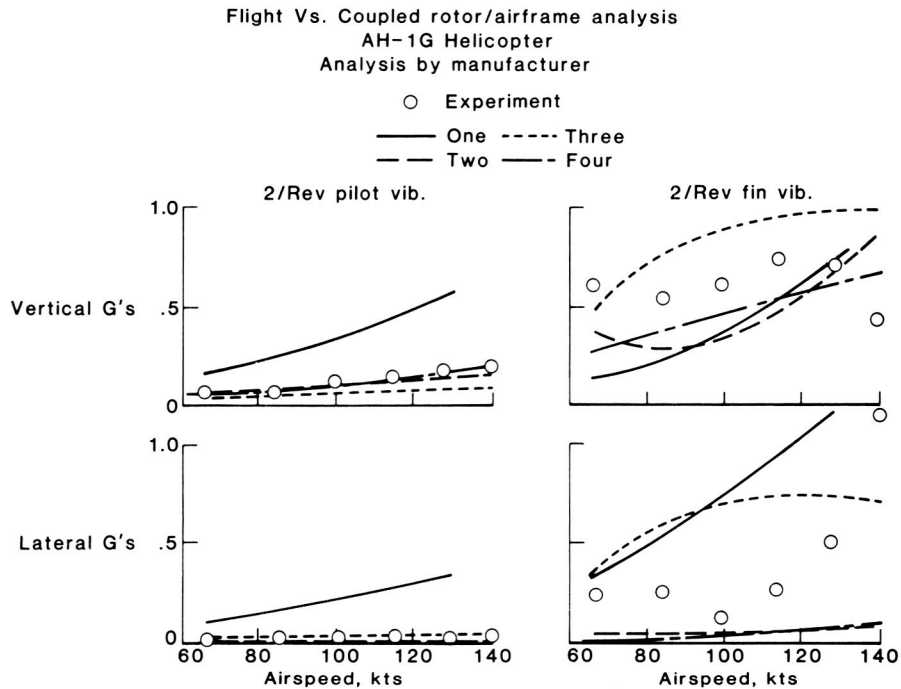


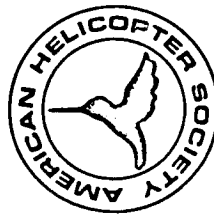
Figure 38.- Typical comparisons of measured AH-1G 2/rev vibrations with analysis by each of four manufacturers. (From results presented in draft final reports submitted under DAMVIBS program.)



Figure 39.- OH-6A helicopter used in NASA/Army higher harmonic control flight test program.

ORIGINAL PAGE IS  
OF POOR QUALITY

# OPTIMAL DESIGN



PANEL CHAIRMAN: Richard L. Bennett

*Introduction to Optimal Design*

*Numerical Optimization Concepts and Definitions —*  
G.N. Vanderplaats, Naval Postgraduate School

*Optimization in the Industrial Design Process —* J.A.  
Bennett, General Motors Research Laboratories

*Fixed Wing Aircraft Applications to Optimization —*

R.T. Haftka, Virginia Polytechnic Institute & State  
University

*Structural Optimization —* J.S. Arora, University of  
Iowa

*Future of Optimization —* J. Sobieski, NASA-Langley  
Research Center

Figure 40.- Panel on Optimal Design held at 39th Annual National Forum of the American Helicopter Society. (From ref. 94.)

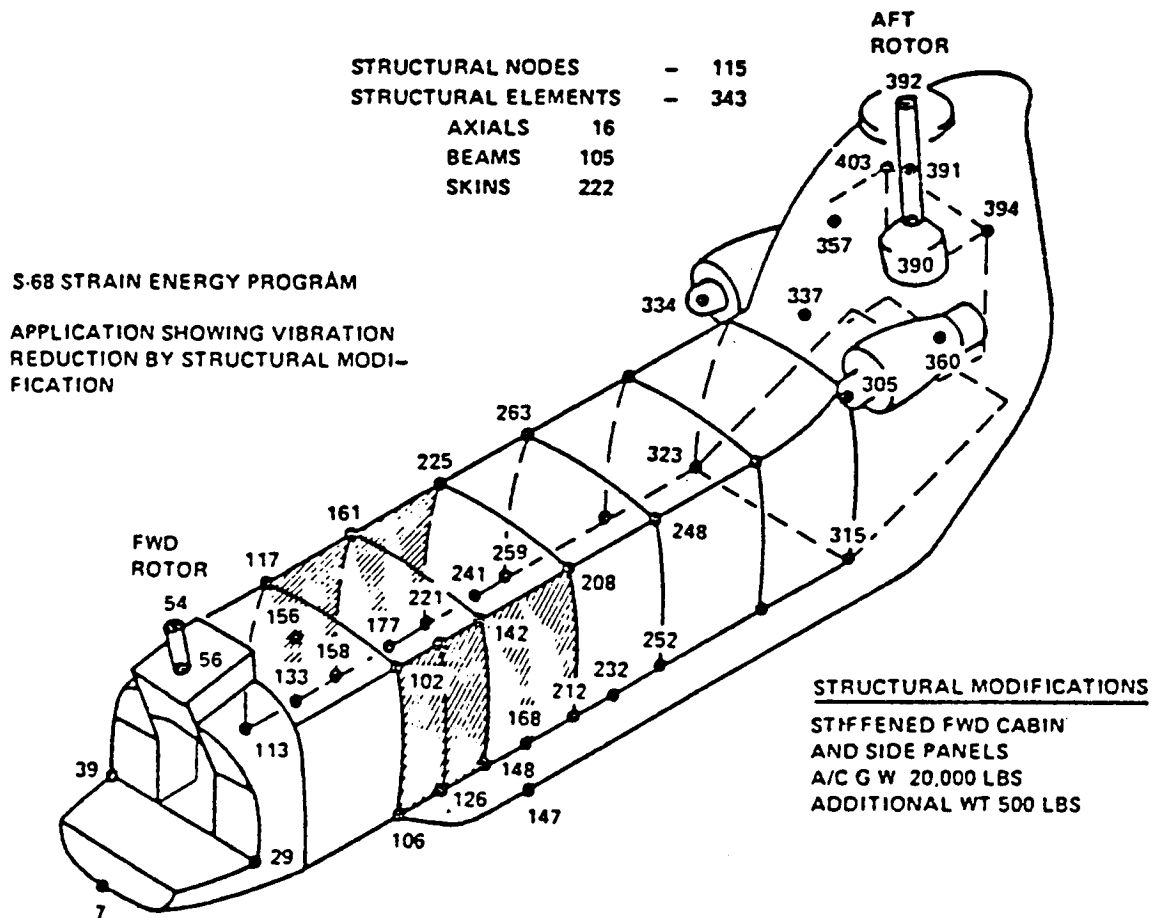
Part 2

SESSION 5A: ROTORCRAFT APPLICATIONS  
Co-Chairmen: C. E. Hammond and R. J. Huston

OVERVIEW: APPLICATIONS OF NUMERICAL OPTIMIZATION METHODS TO HELICOPTER DESIGN PROBLEMS . . . . .	539
H. Miura	
APPLICATION OF MODERN STRUCTURAL OPTIMIZATION TO VIBRATION REDUCTION IN ROTORCRAFT . . . . .	553
P. P. Friedmann	
HELICOPTER ROTOR BLADE AERODYNAMIC OPTIMIZATION BY MATHEMATICAL PROGRAMING . . . . .	567
Joanne L. Walsh, Gene J. Bingham, and Michael F. Riley	
REGRESSION ANALYSIS AS A DESIGN OPTIMIZATION TOOL . . . . .	579
Richmond Perley	
A ROTOR OPTIMIZATION USING REGRESSION ANALYSIS . . . . .	595
N. Giansante	
OPTIMIZATION OF HELICOPTER ROTOR BLADE DESIGN FOR MINIMUM VIBRATION . . . . .	609
M. W. Davis	
APPLICATION OF NUMERICAL OPTIMIZATION TO ROTOR AERODYNAMIC DESIGN . . . . .	627
W. A. Pleasants III and T. J. Wiggins	
AEROELASTIC/AERODYNAMIC OPTIMIZATION OF HIGH SPEED HELICOPTER/ COMPOUND ROTOR . . . . .	643
L. R. Sutton and R. L. Bennett	
THE STRUCTURAL OPTIMIZATION OF A SPREADER BAR FOR TWIN LIFT HELICOPTER OPERATIONS . . . . .	663
Alan Dobyns	
MULTIOBJECTIVE OPTIMIZATION TECHNIQUES FOR STRUCTURAL DESIGN . . . . .	675
S. S. Rao	

Figure 41.- Rotorcraft session at Symposium on Recent Experiences in  
Multidisciplinary Analysis and Optimization. (From ref. 97.)

ORIGINAL PAGE IS  
OF POOR QUALITY



Mode	Original Fuselage Hz	Modified Fuselage Hz	Excitation Frequency 11.45 Hz
7	6.687	6.703	Natural Frequency Changed (Mode No. 10, 4th Elastic Mode) - Mode Amplification Factor Down From 9.1 to 5.0
8	7.879	8.160	
9	8.442	8.494	
10	12.03	12.74	
11	12.52	12.79	
12	14.48	14.82	
13	15.69	16.02	
14	16.95	17.22	
15	18.94	19.06	

Figure 42.- CH-47A vibration reduction by structural modification based on modal strain energy. (From ref. 102.)

ORIGINAL PAGE IS  
OF POOR QUALITY

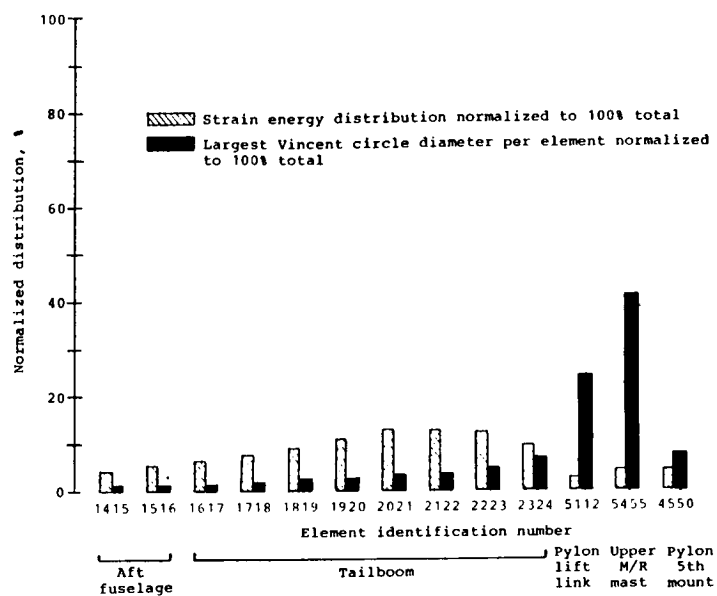
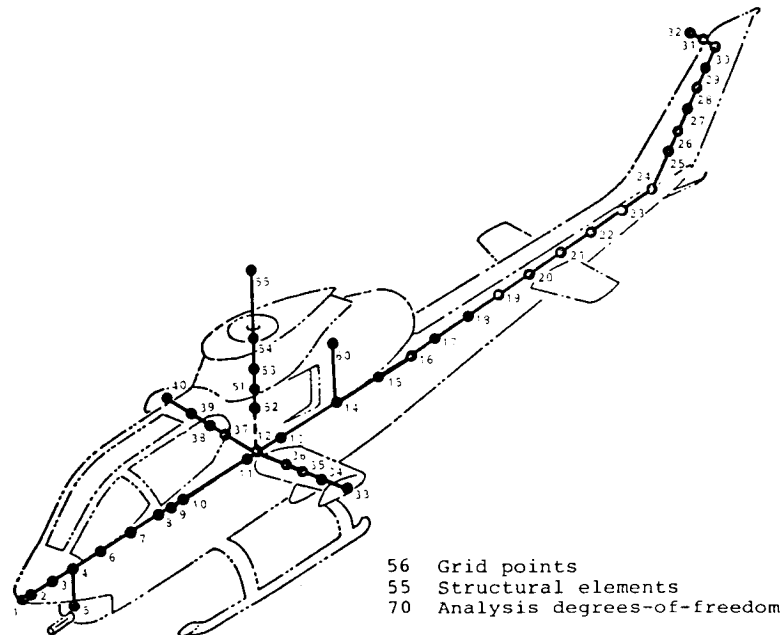
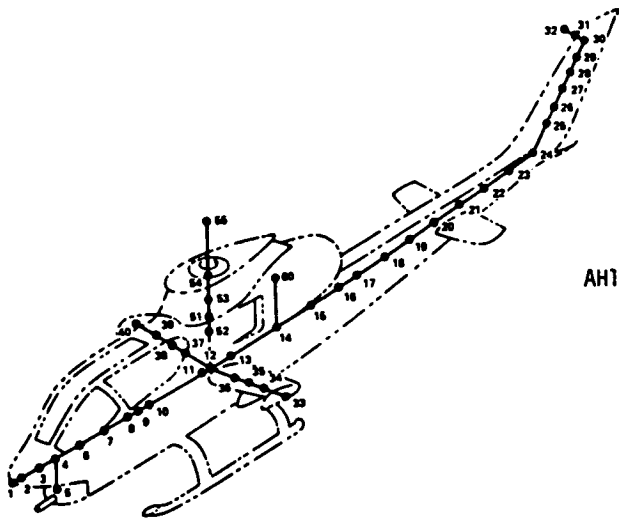


Figure 43.- Comparison of forced response strain energy and Vincent Circle methods as indicators of elements having the most potential for reducing vibrations. (From ref. 105.)

ORIGINAL PAGE IS  
OF POOR QUALITY



AH1G ELASTIC LINE MODEL

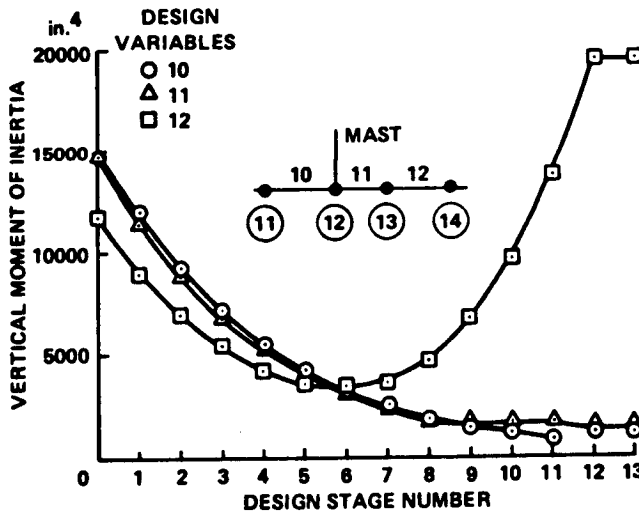
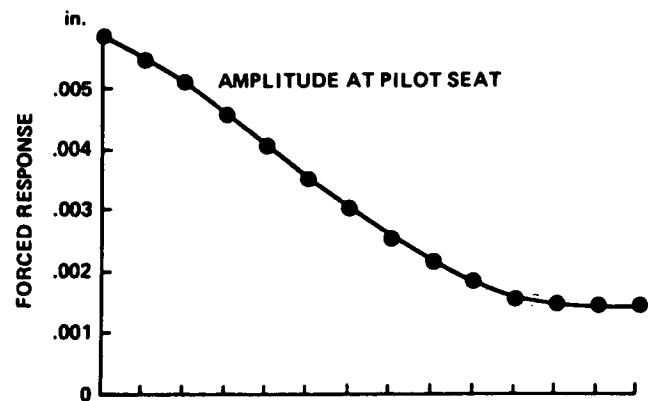
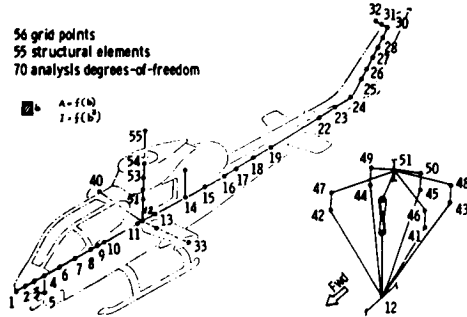


Figure 44.- Application of NASOPT code to minimization of pilot seat vibrations in AH-1G. (From ref. 117)

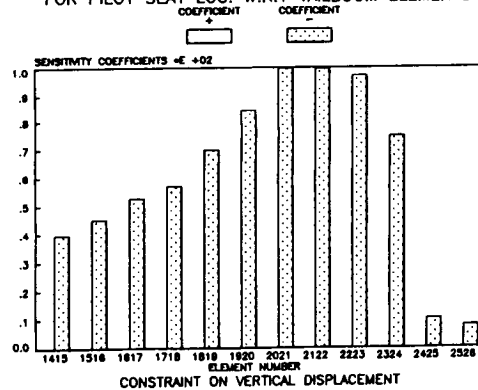
# ELASTIC LINE (STICK) MODEL OF THE AH-1G AIRFRAME

56 grid points  
55 structural elements  
70 analysis degrees-of-freedom

$\square = A = f(u)$   
 $\square = f(v)$



## SENSITIVITY OF DYNAMIC DISPLACEMENT FOR PILOT SEAT LOC. W.R.T TAILBOOM ELEMENTS



## ELEMENT STRAIN ENERGY DENSITIES IN TAILBOOM FOR FORCED RESPONSE

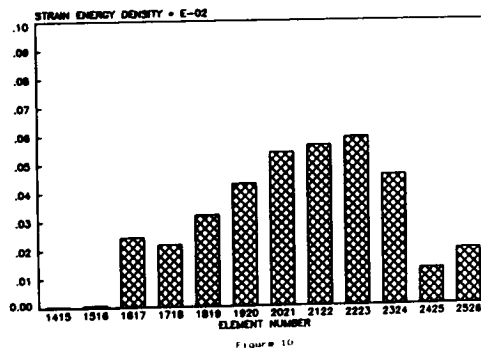


Figure 45.- Distribution of sensitivity of dynamic displacement and strain energy in tail-boom elements of AH-1G. (From ref. 122.)

ORIGINAL PAGE IS  
OF POOR QUALITY

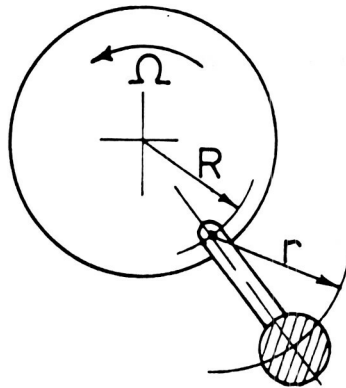


Figure 46.- Simple Pendulum Absorber.

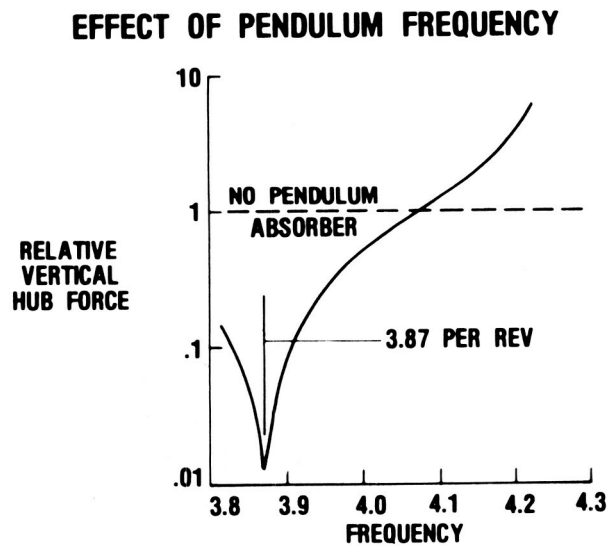
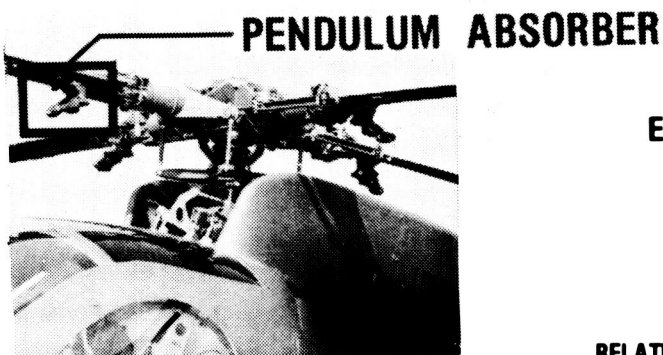


Figure 47.- Response of Blade Mounted Pendulum Absorber.  
(From ref. 126.)



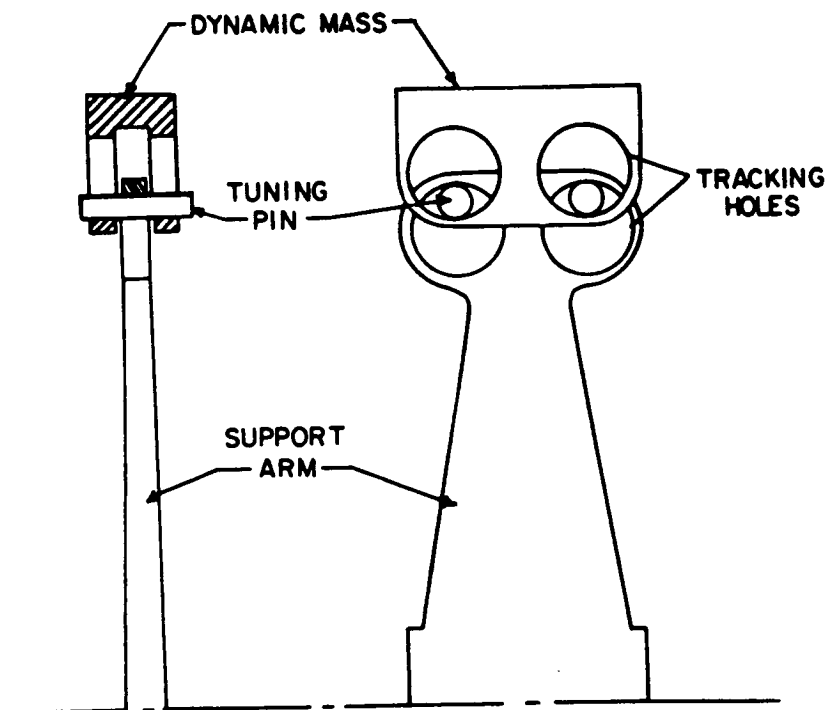


Figure 48.- Schematic of Bifilar Assembly. (From ref. 127.)

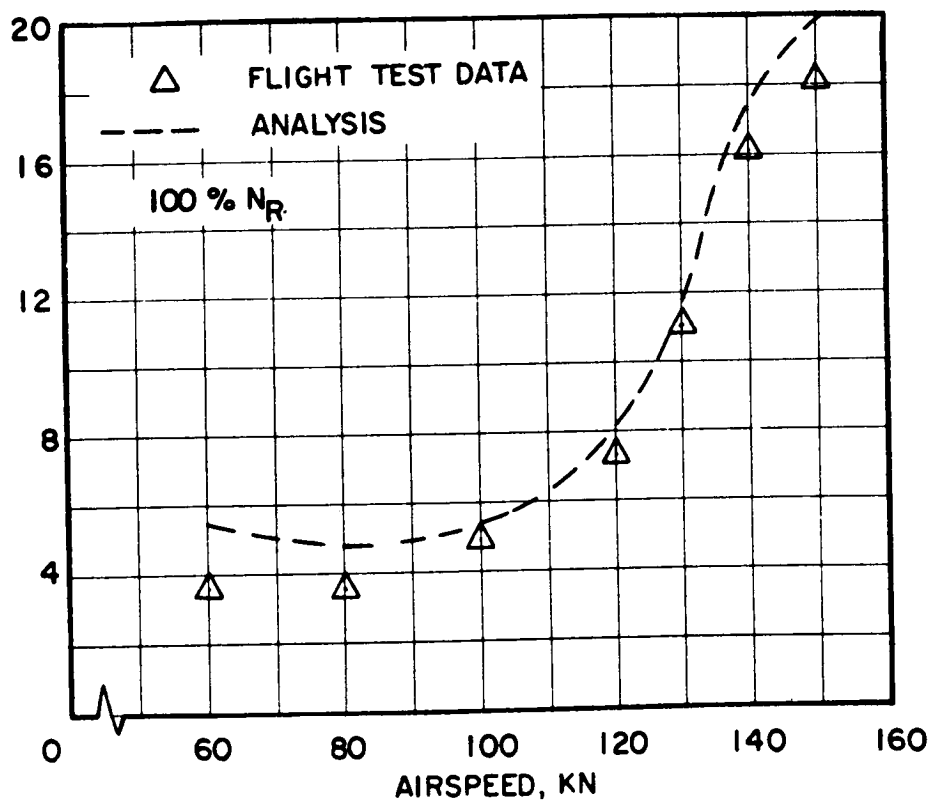


Figure 49.- Correlation of UH-60 Bifilar Absorber Flight Test Data and Analysis. (From ref. 128.)

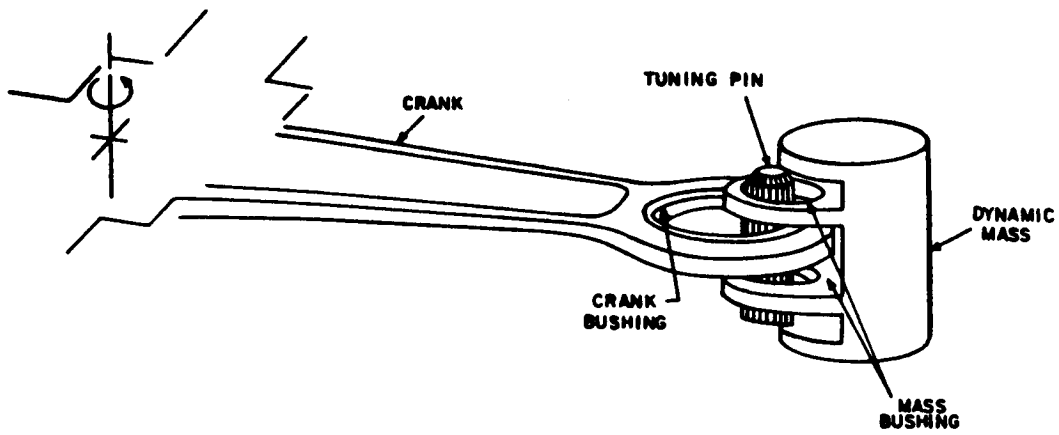


Figure 50.- Monofilar Schematic. (From ref. 129.)

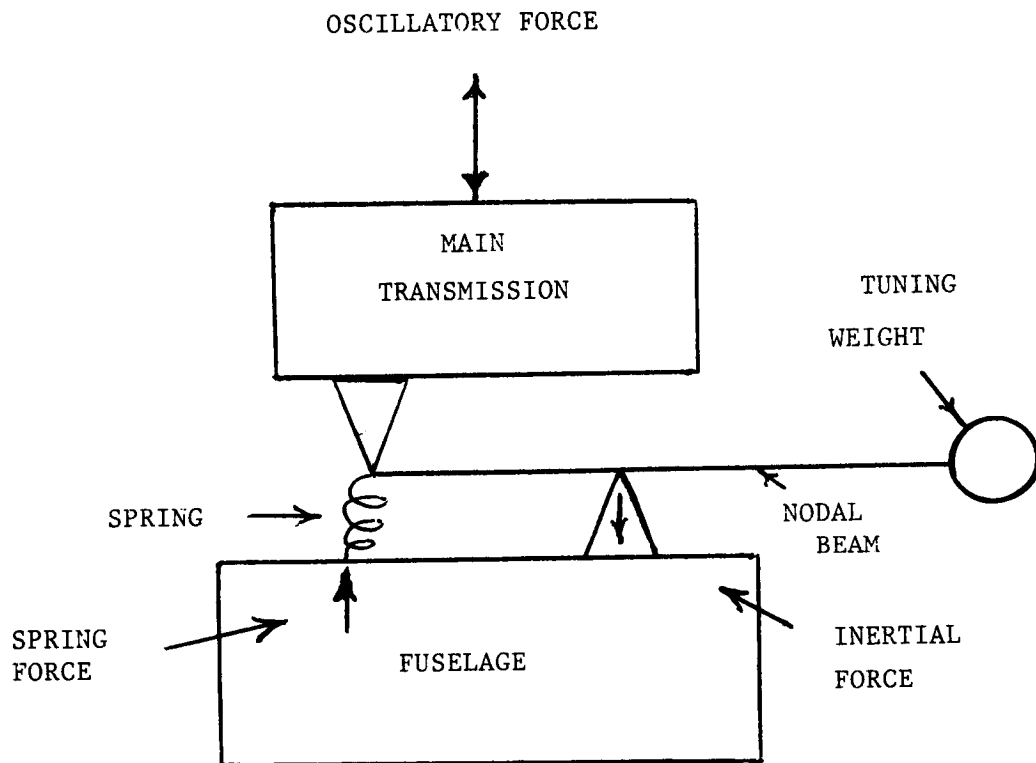


Figure 51.- Schematic of Conventional Fixed-System Vibration Isolator.

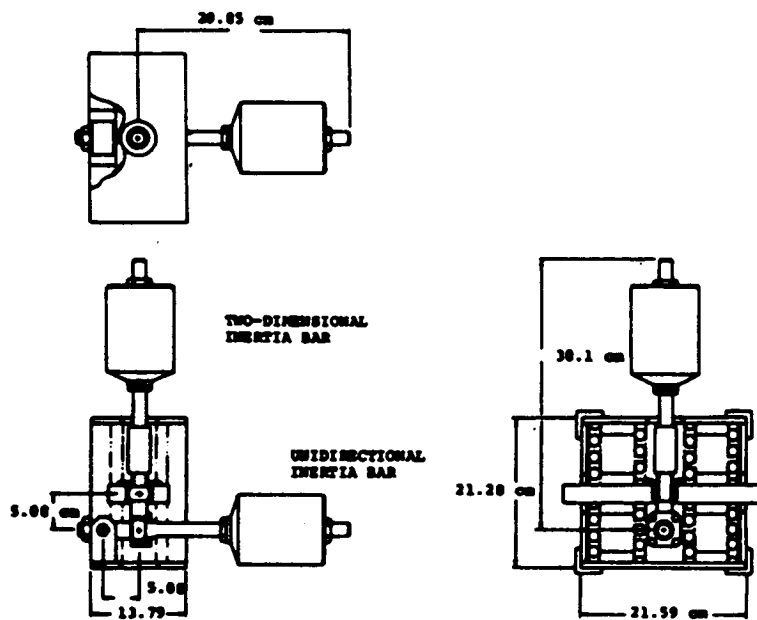


Figure 52.- Three-Dimensional DAVI. (From ref. 131.)

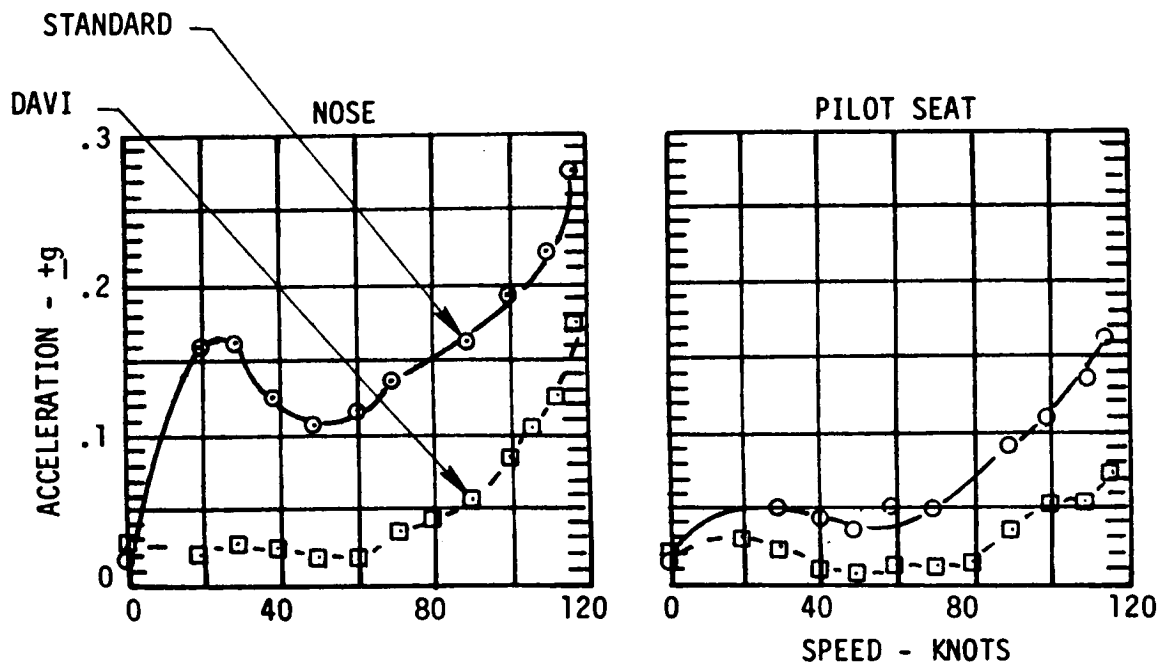


Figure 53.- DAVI Flight Test Data. (From ref. 132.)

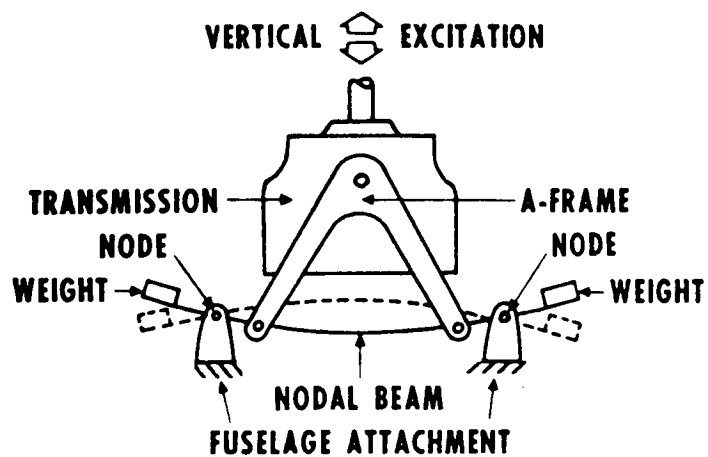


Figure 54.- Isolation by "Nodalized" Beam. (From ref. 133.)

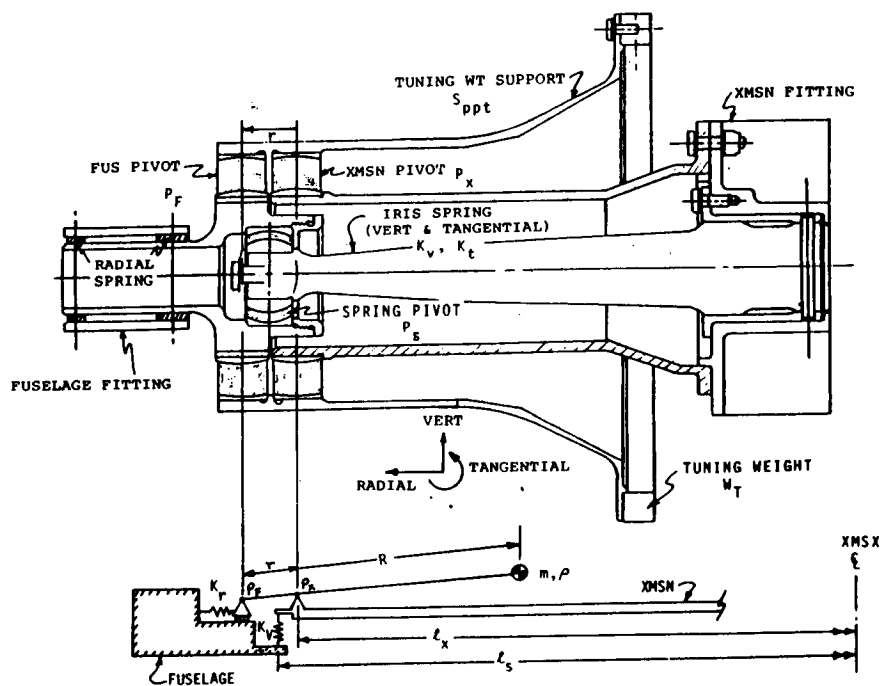


Figure 55.- Bidirectional IRIS Unit. (From ref. 136.)

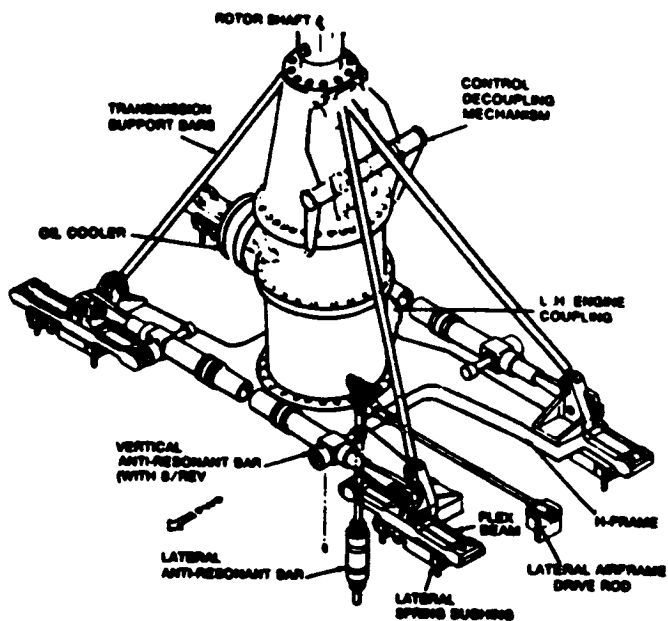


Figure 56.- BO-105 IRIS Installation. (From ref. 137.)

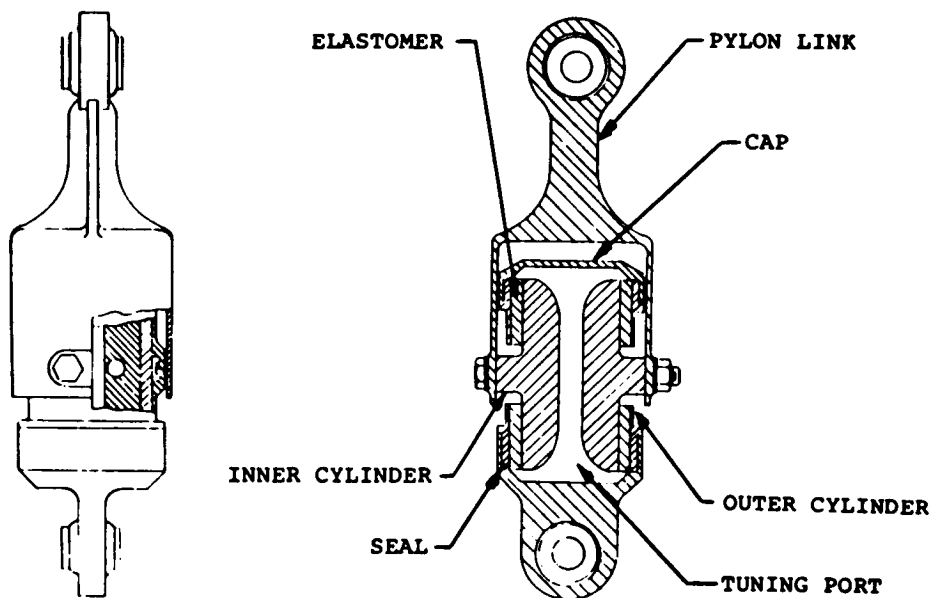
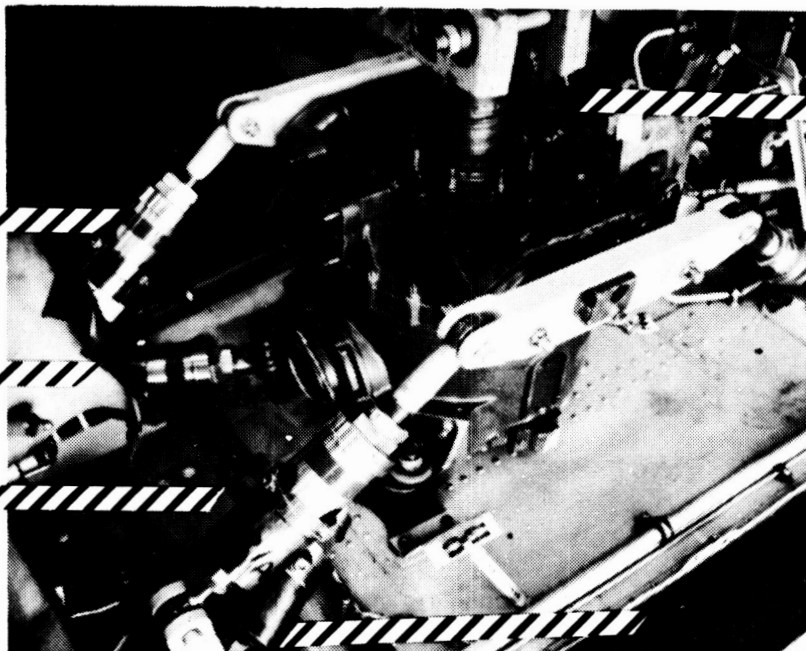


Figure 57.- Pinned-Pinned LIVE Unit. (From ref. 139.)

ORIGINAL PAGE IS  
OF POOR QUALITY



////// Six LIVE Units

Figure 58.- Total Rotor Isolation System Aircraft and LIVE Installation.

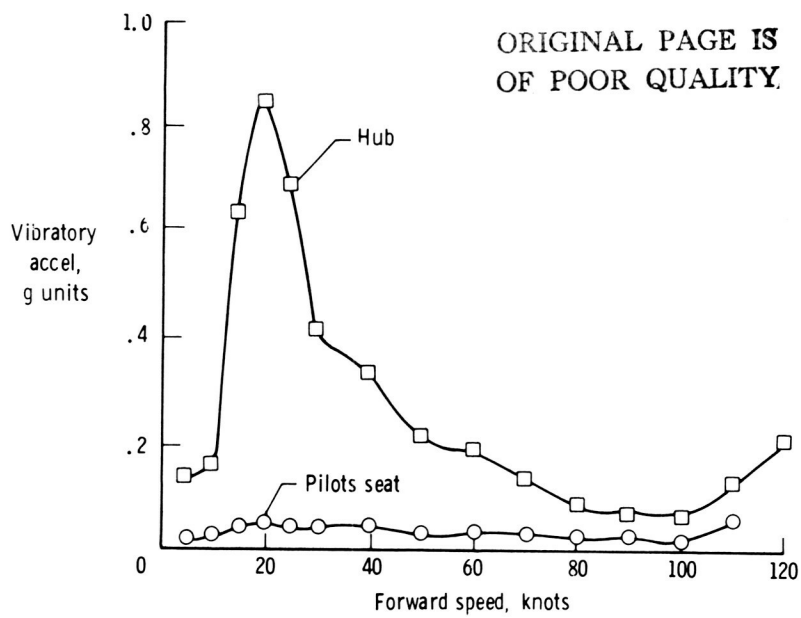


Figure 59.- TRIS Flight Test Data. (From ref. 141.)



Figure 60.- Rotor Systems Research Aircraft - RSRA.

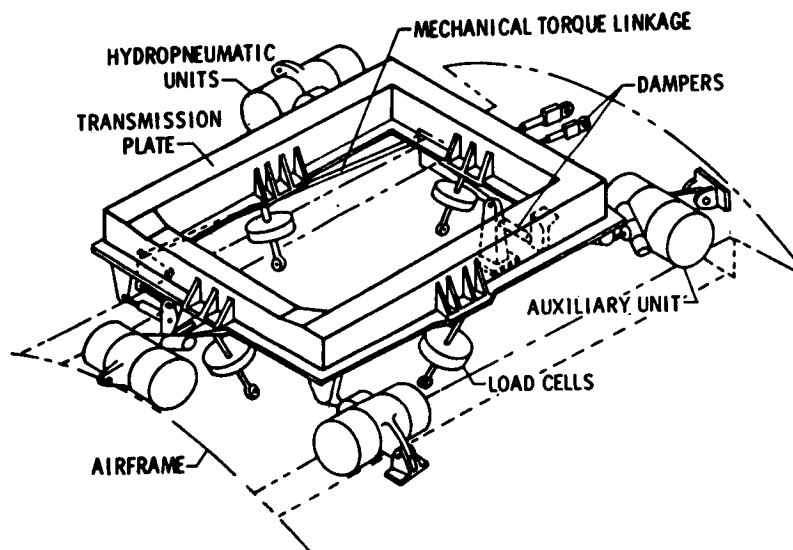


Figure 61.- RSRA Aircraft AIBS Schematic. (From ref. 142.)

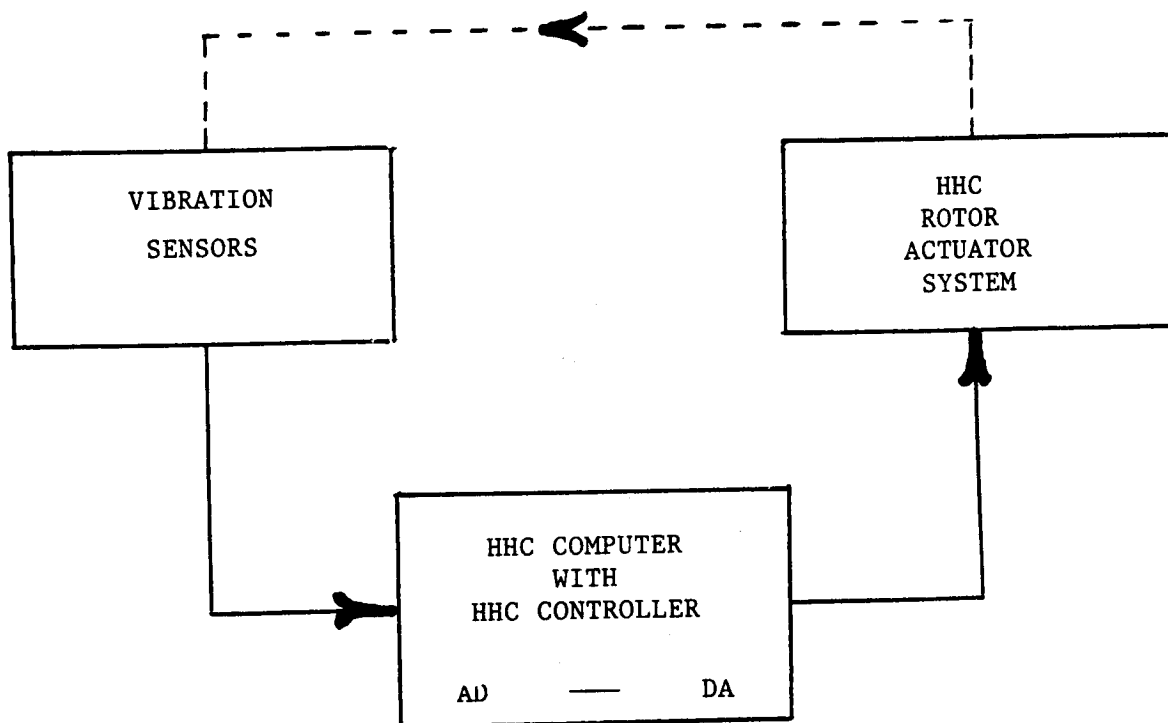


Figure 62.- HHC Feedback System.



ORIGINAL PAGE IS  
OF POOR QUALITY

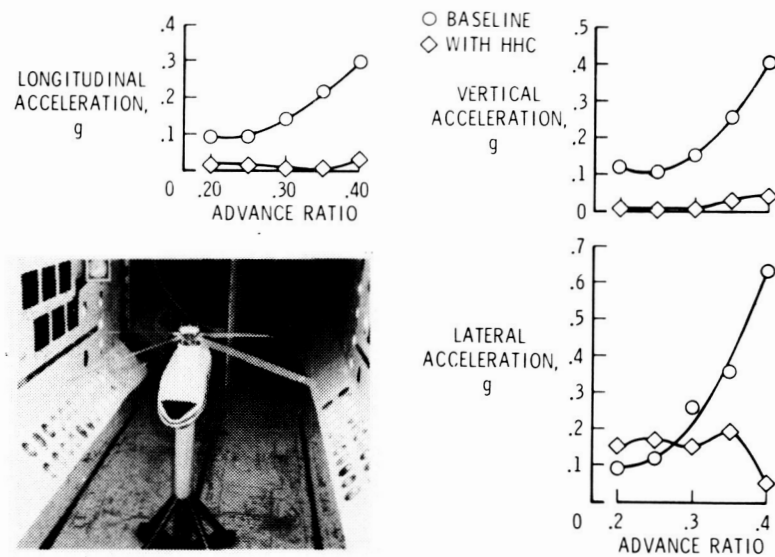


Figure 63.- Higher Harmonic Control Closed-Loop Wind Tunnel Test Results. (From ref. 150.)

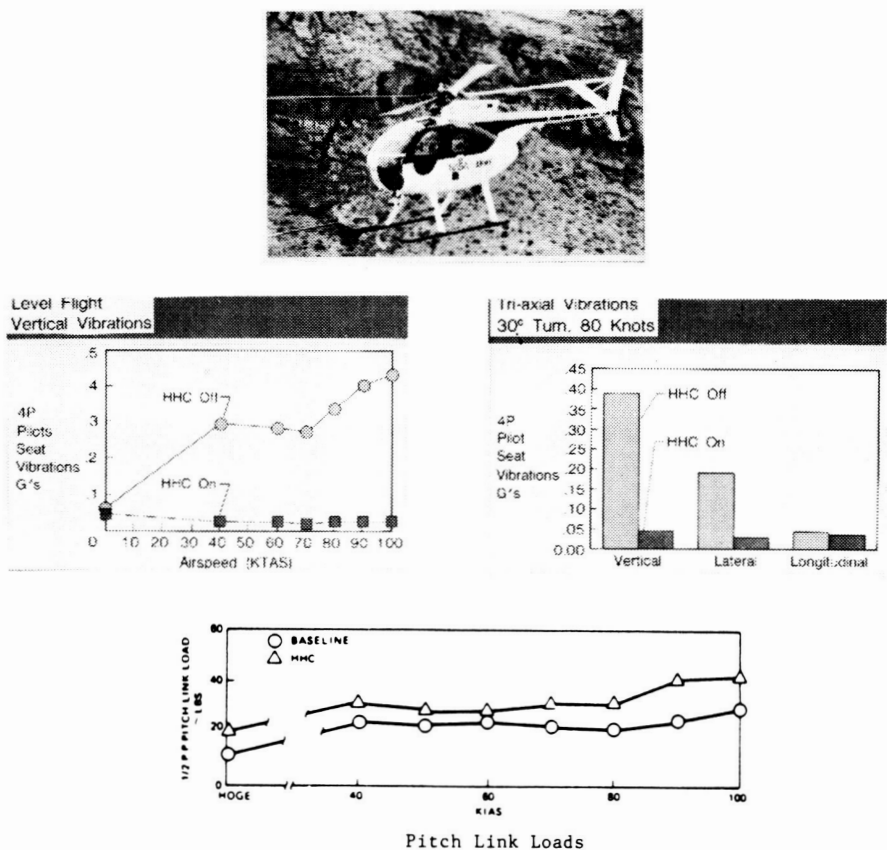


Figure 64.- OH-6A HHC Flight Test Results.

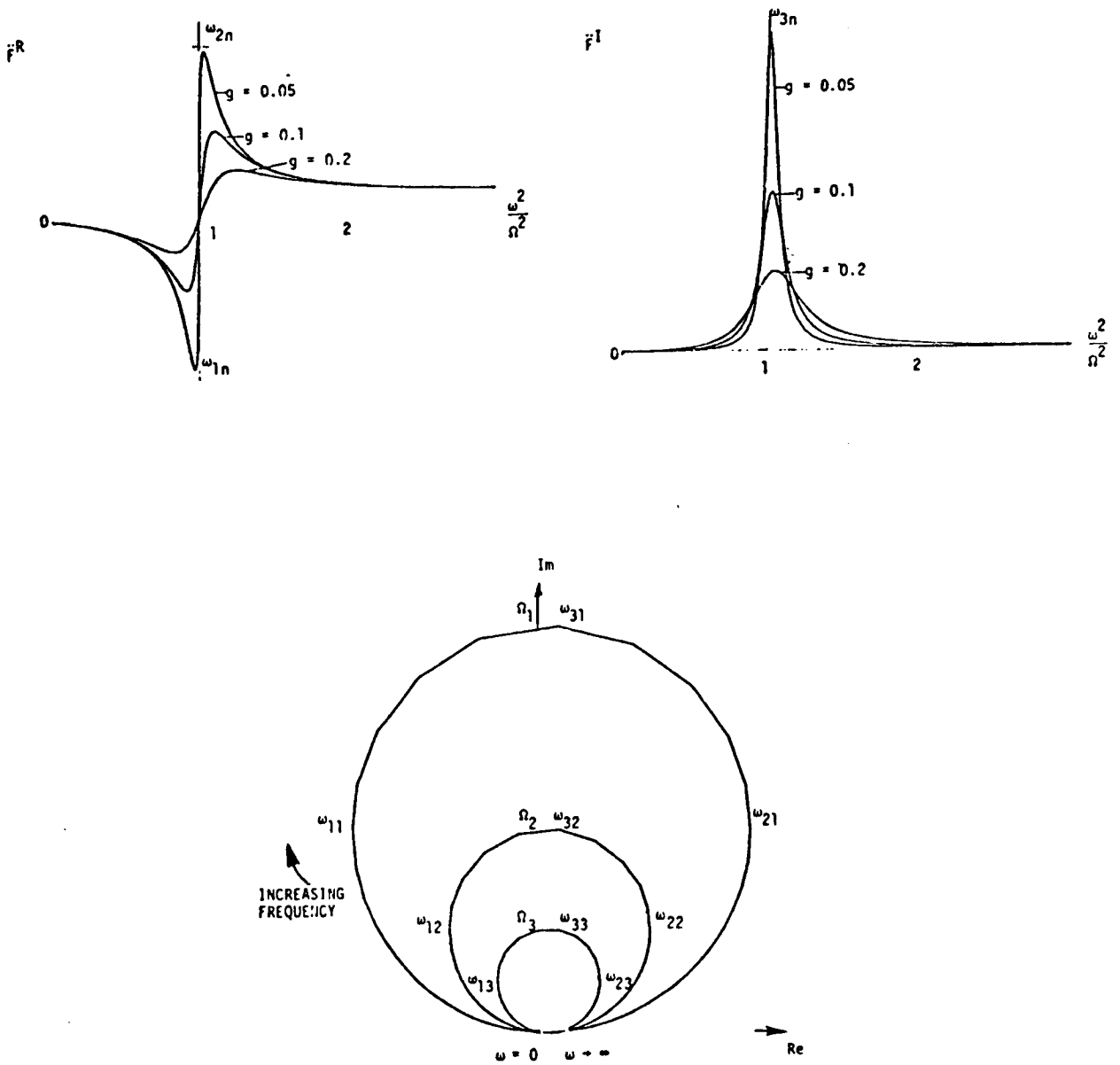
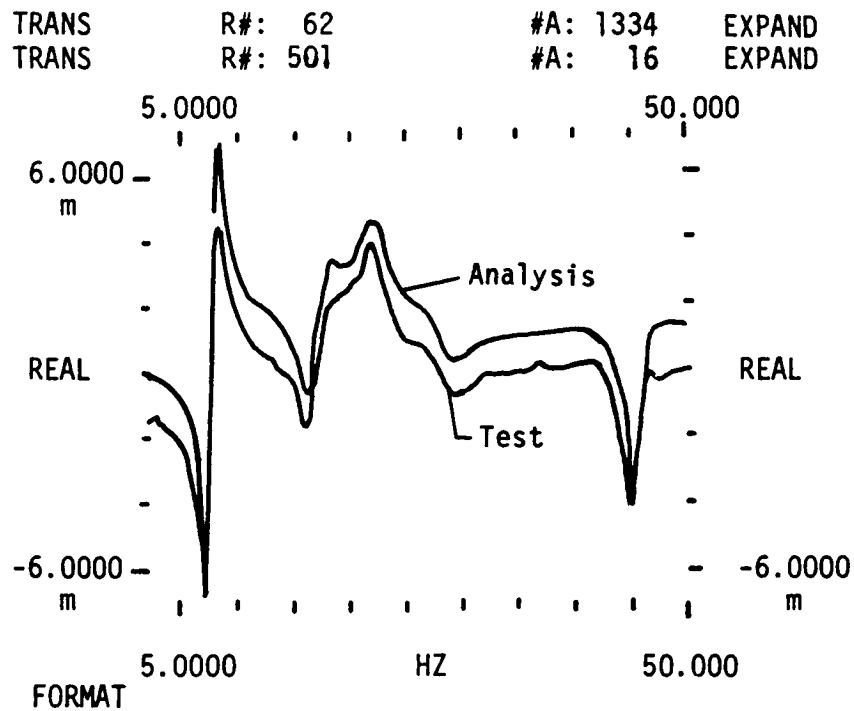
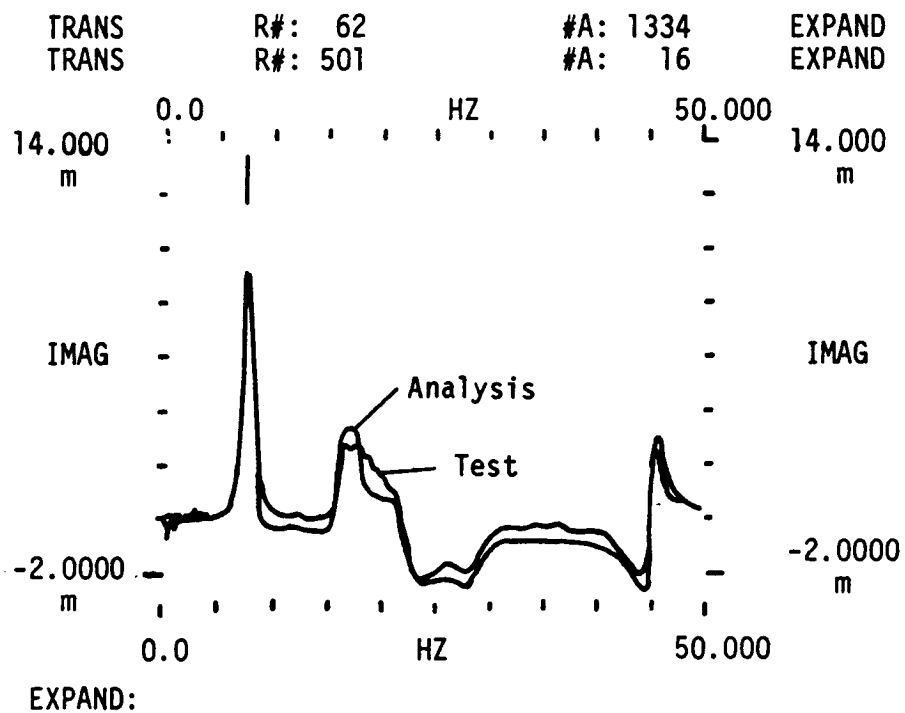


Figure 65.- Typical frequency domain representations of dynamic response. (From ref. 168.)



Real parts superimposed.



Imaginary parts superimposed.

Figure 66.- AH-1G modal analysis correlation. (From ref. 168.)

ORIGINAL PAGE IS  
OF POOR QUALITY

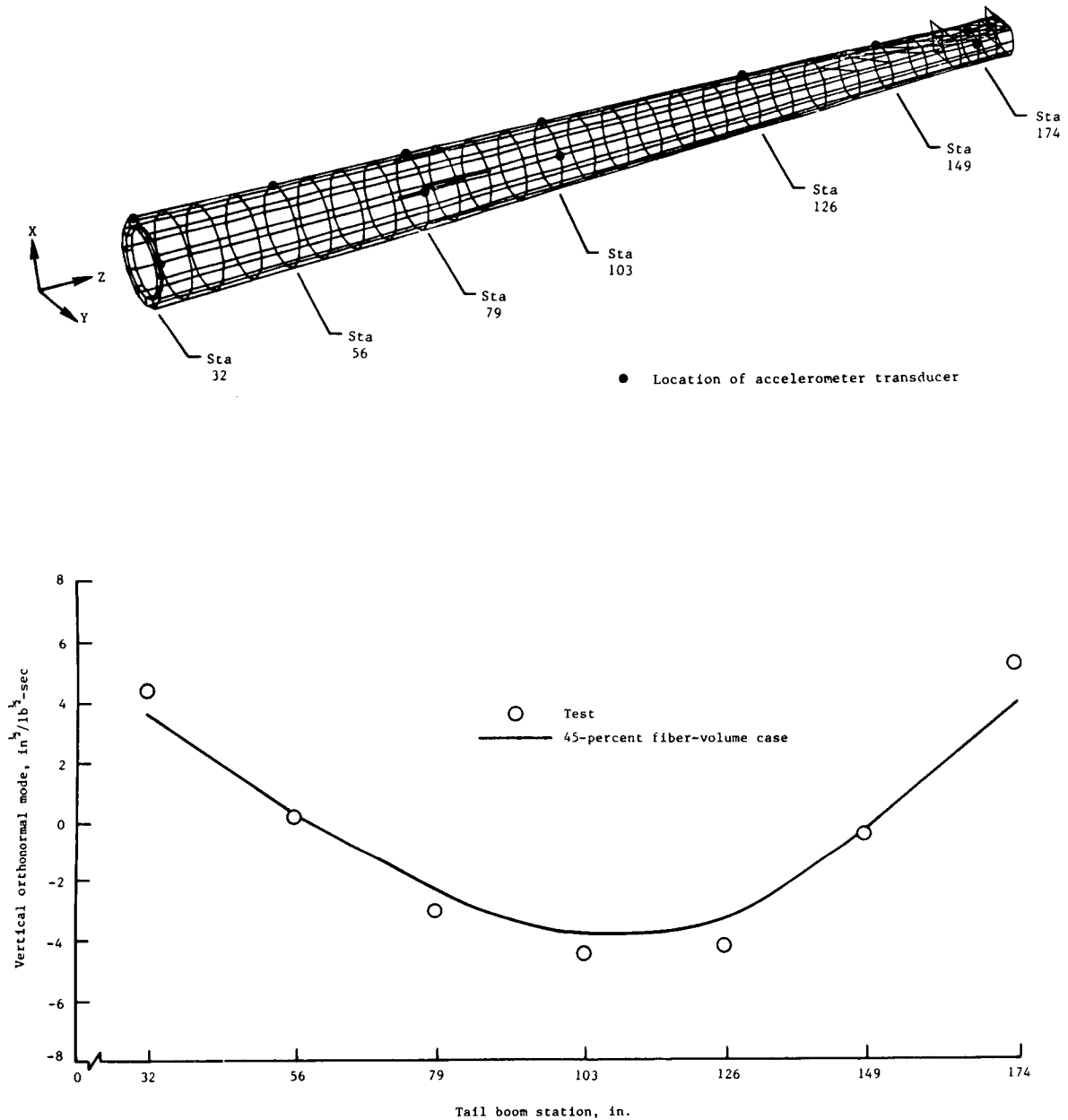


Figure 67.- OH-58 composite tail boom mode shape correlation.  
(From ref. 48.)

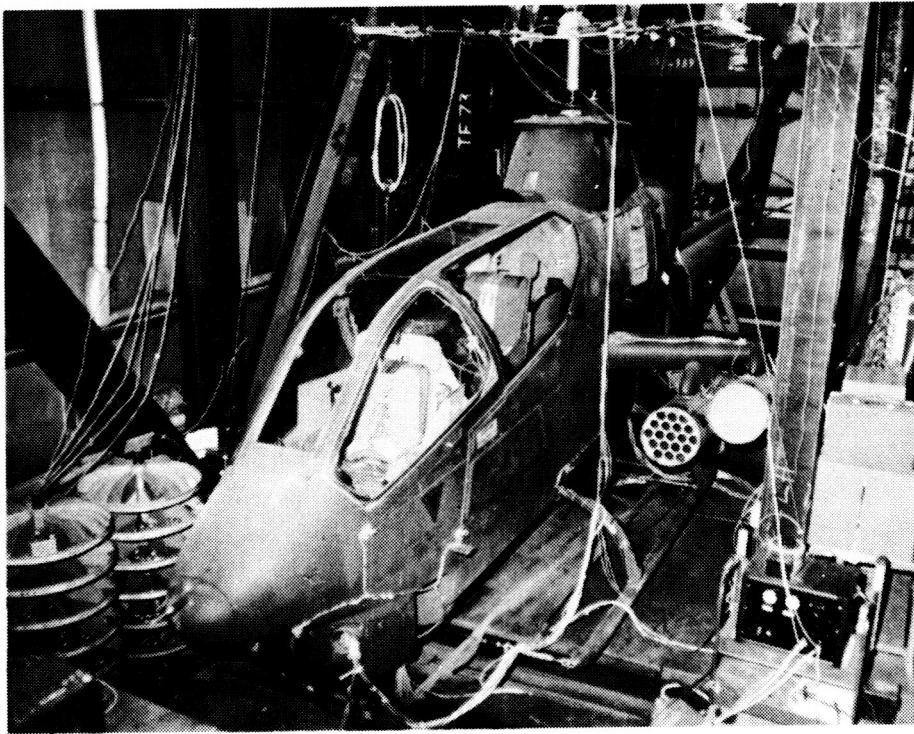


Figure 68.- AH-1G shake test configuration.

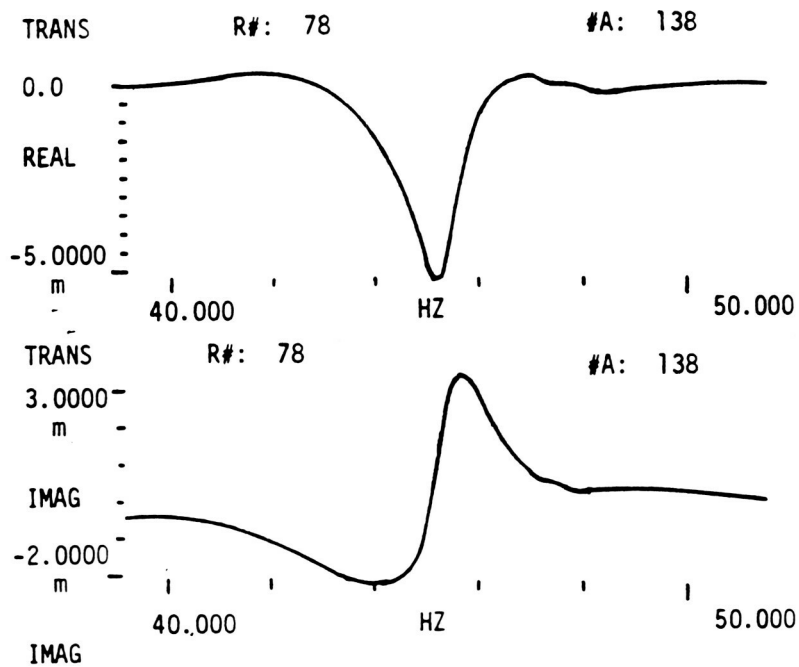


Figure 69.- Frequency response measurement of complex mode.  
(From ref. 168.)

ORIGINAL PAGE IS  
OF POOR QUALITY

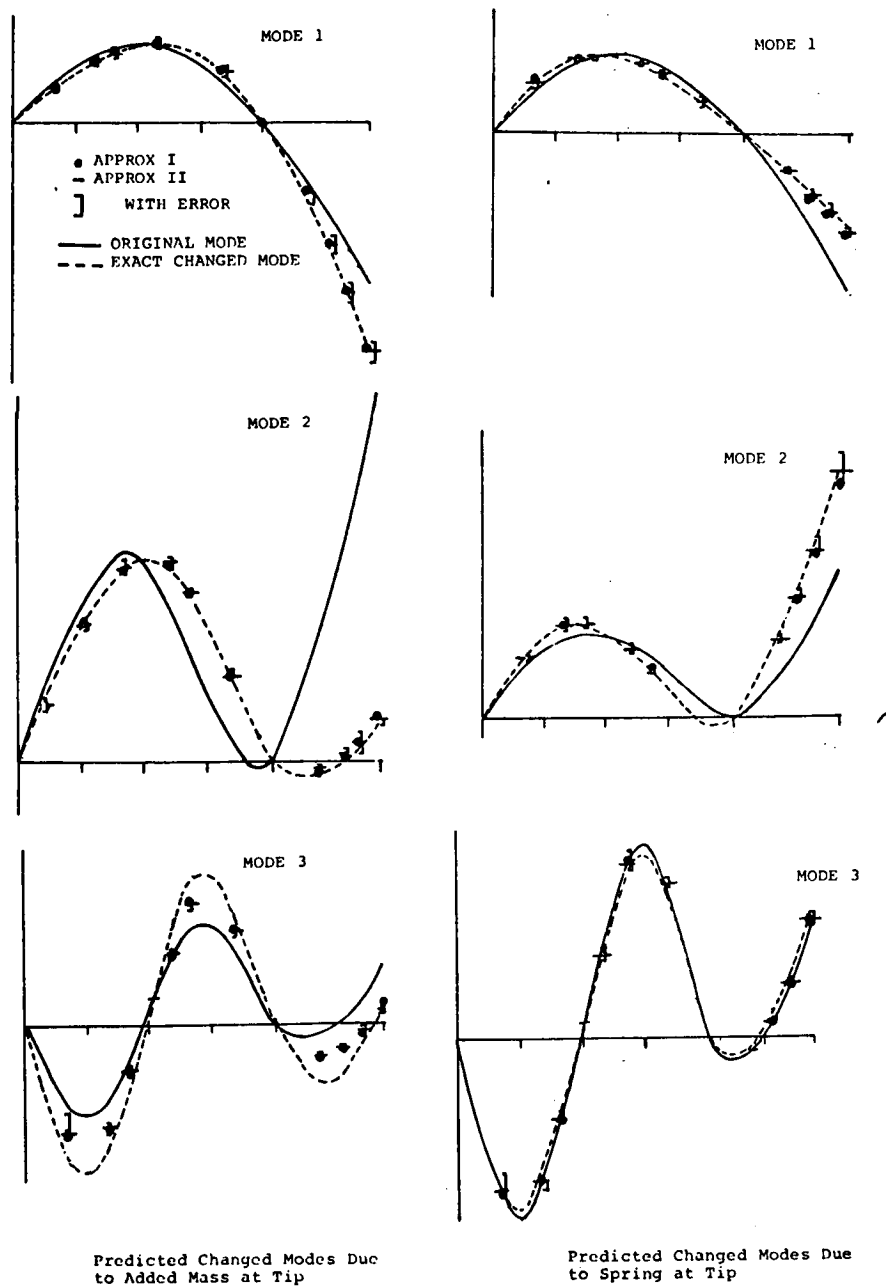


Figure 70.- Application of incomplete model theory. (From ref. 178.)

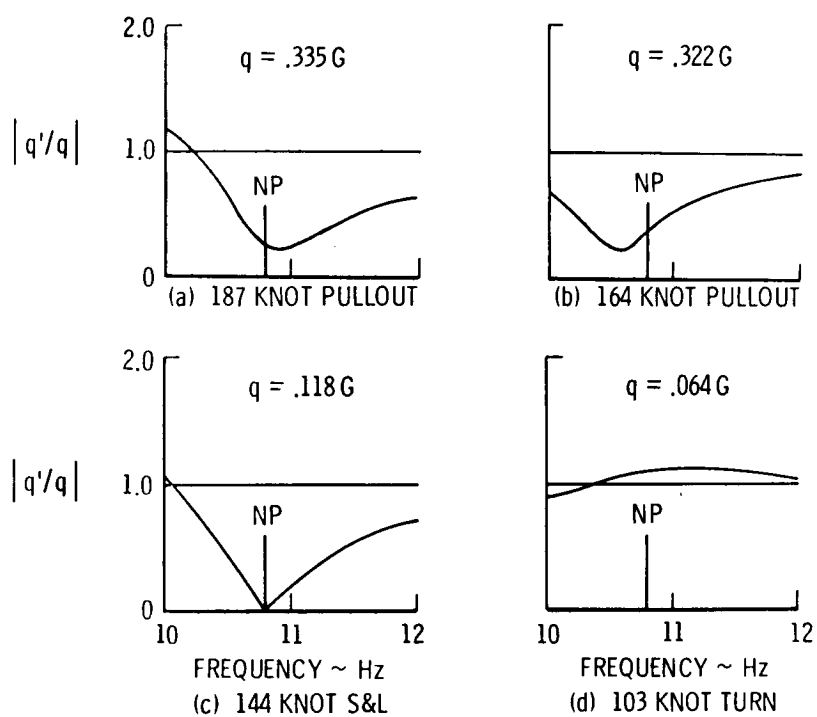
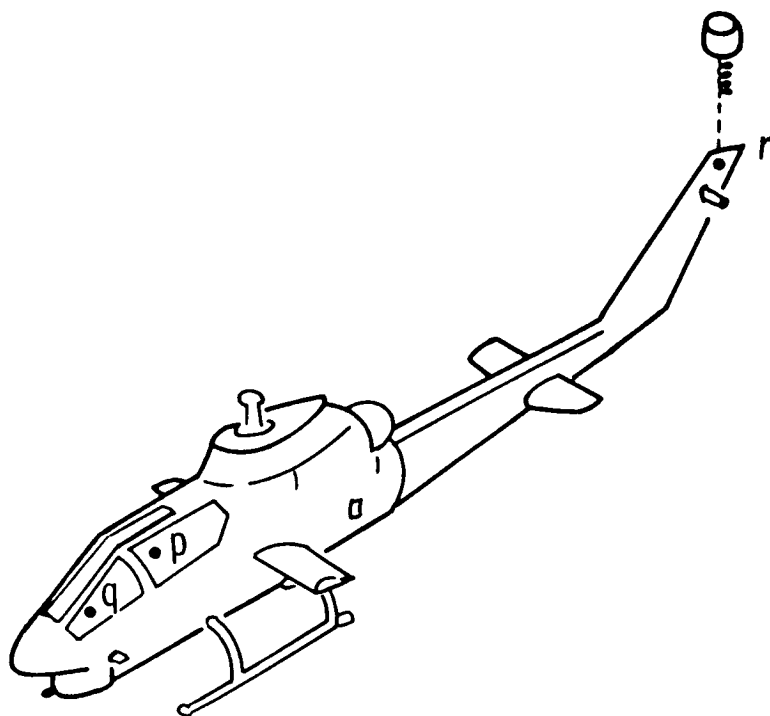
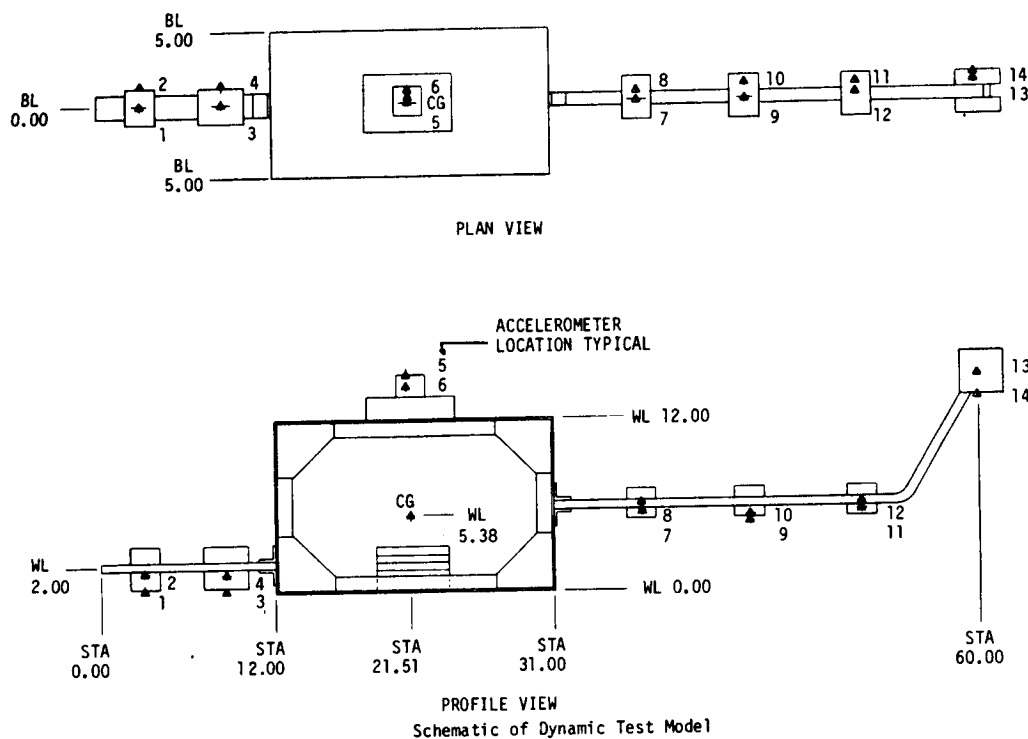


Figure 71.- Simulated effect of vertical fin absorber on cockpit vibration. (From ref. 198)



### DYNAMIC MODEL VIBRATIONS DUE TO LATERAL NOSE REMOTE ABSORBER

TUNING FREQUENCY = 19.2 HZ  
 ABSORBER WEIGHT = 0.50 LB  
 ABSORBER DAMPING = 2%

□—□—□ = BASELINE (TEST)  
 ◇—◇—◇ = CHANGE (TEST)  
 +—+—+ = PREDICTED

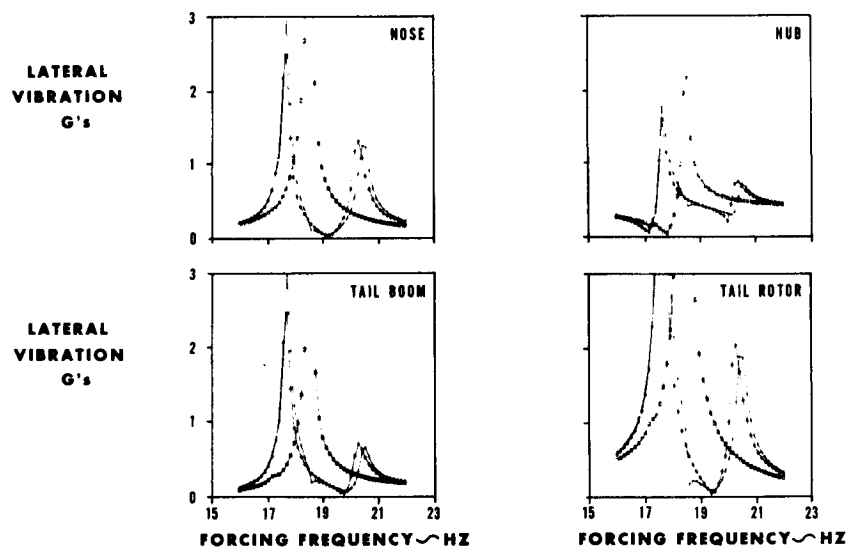
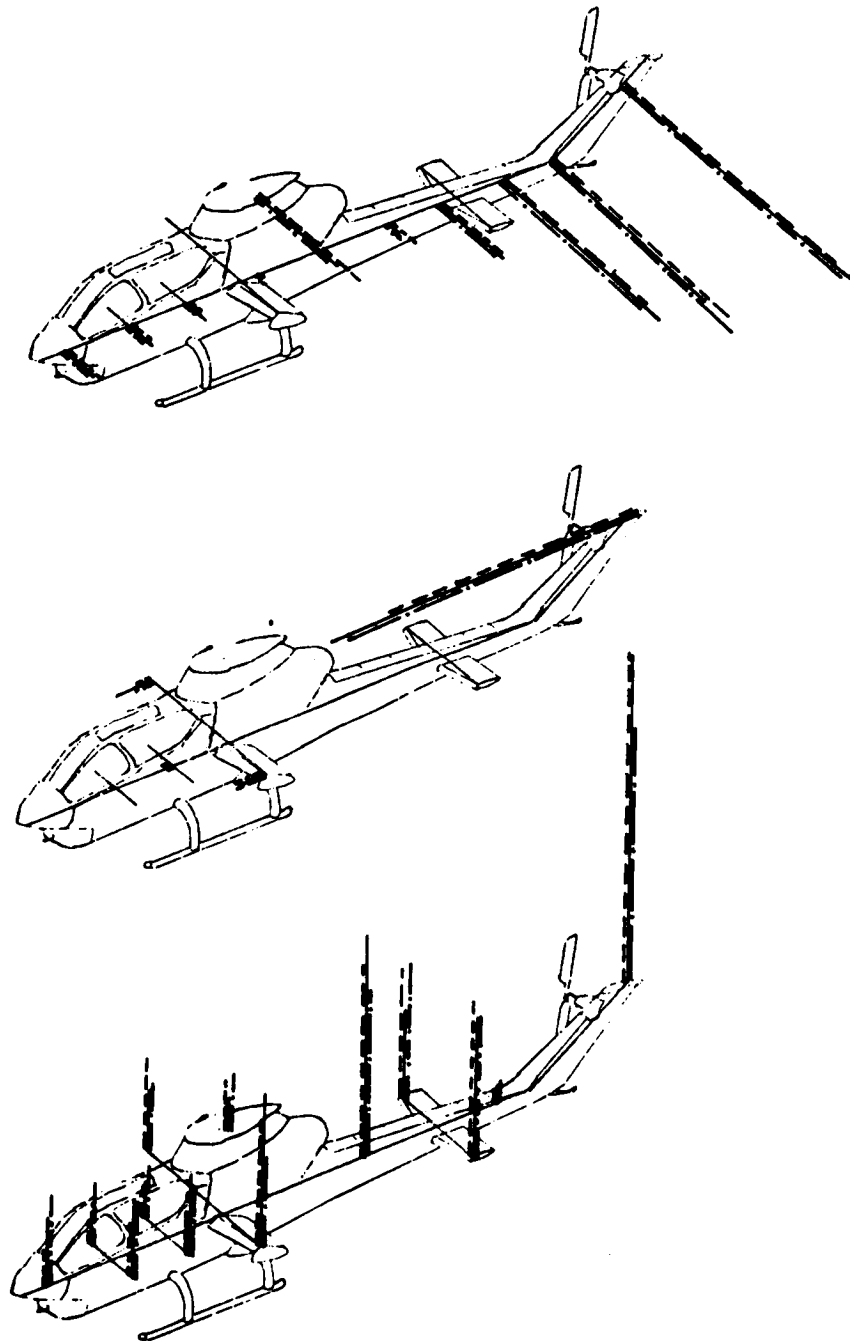


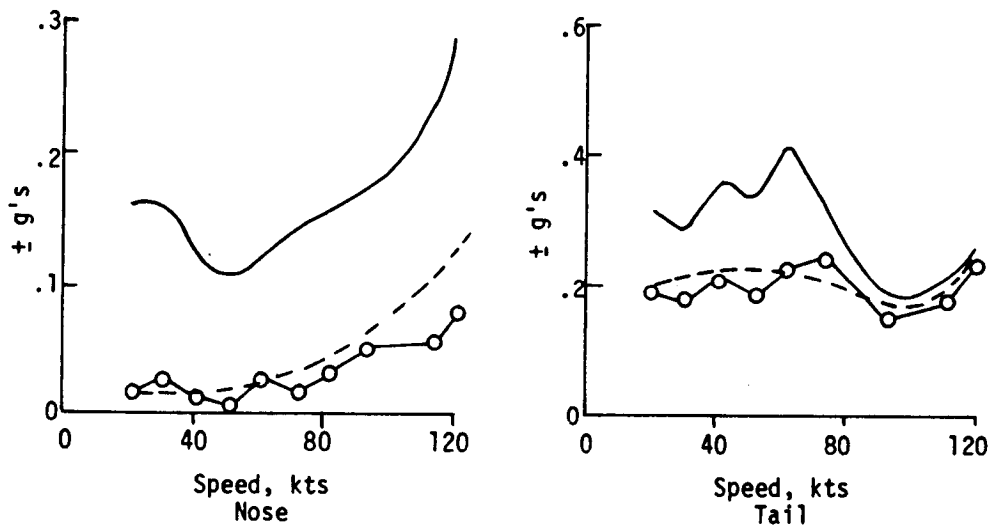
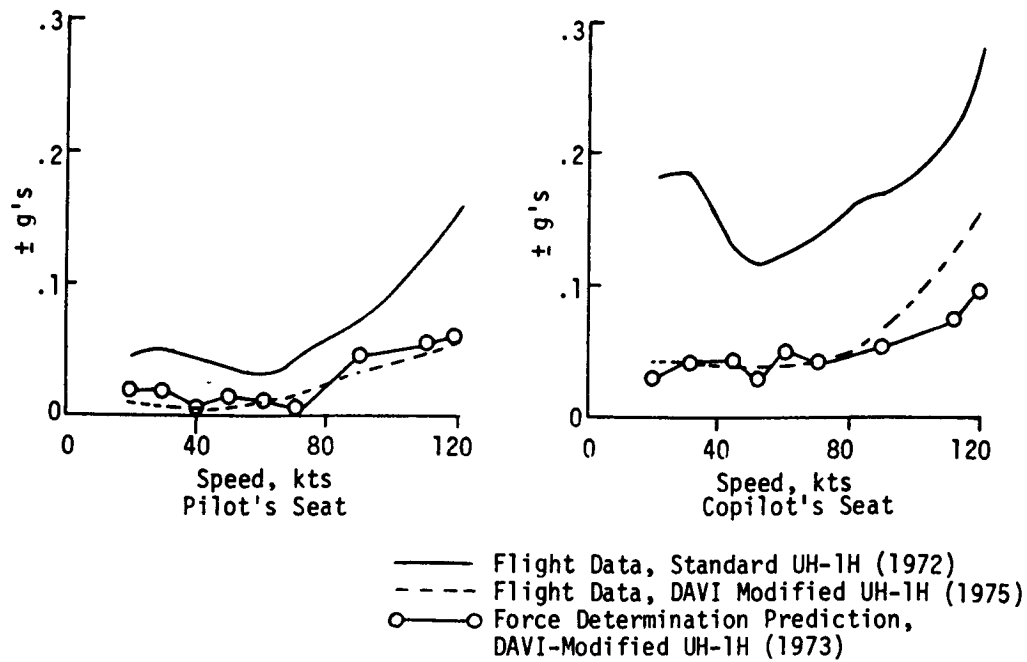
Figure 72.- Analytical Testing verification on generic helicopter dynamic model.





Left rolling pullout at a gross weight of 8465 pounds.

Figure 73.- AH-1G Force Determination results. (From ref. 205.)



Two-Per-Rev Vertical Vibration on the UH-1H

Figure 74.- Force Determination applied to DAVI-modified UH-1H.  
 (From ref. 203.)

## A REVIEW OF RESEARCH IN ROTOR LOADS

William G. Bousman  
Research Scientist  
U.S. Army Aeroflightdynamics Directorate  
Moffett Field, California 94035

and

Wayne R. Mantay  
Aeromechanics Division Chief  
U.S. Army Aerostructures Directorate  
Hampton, Virginia

## ABSTRACT

The research accomplished in the area of rotor loads over the last 13 to 14 years is reviewed. The start of the period examined is defined by the 1973 AGARD Milan conference and the 1974 hypothetical rotor comparison. The major emphasis of the review is research performed by the U.S. Army and NASA at their laboratories, and/or by the industry under government contract. Important independent work is included in the review to keep an appropriate perspective on the field. For the purpose of this review, two main topics are addressed: rotor loads prediction and means of rotor loads reduction. A limited discussion of research in gust loads and maneuver loads is included. In the area of rotor loads predictions, the major problem areas are reviewed including dynamic stall, wake induced flows, blade tip effects, fuselage induced effects, blade structural modeling, hub impedance, and solution methods. It is concluded that the capability to predict rotor loads has not significantly improved in the time frame of the paper. Future progress will require more extensive correlation of measurements and predictions to better understand the causes of the problems, and a recognition that differences between theory and measurement have multiple sources, yet must be treated as a whole.

The development of comprehensive models for rotor loads must be the first priority of the government, but this development should be the responsibility of the government laboratories instead of their contractors. There is a need for high-quality data to support future research in rotor loads, but the resulting data base must not be seen as an end in itself. It will be useful only if it is integrated into firm long-range plans for use of the data.

Research in reducing rotor loads has sometimes been successful in the time frame of this paper, but the reasons have not always been understood. This research area should be productive in the future. The major emphasis should be placed on understanding the fundamental mechanisms of vibration, and this should be accompanied by careful experimentation.

---

Presented at NASA/Army Rotorcraft Technology Conference, March 14-16, 1987, NASA Ames Research Center.

## INTRODUCTION

"Instead of running into unexpectedly high loads almost everywhere the first time the full flight envelope is explored, we now only run into them occasionally, at some extreme flight condition." - Loewy, 1973

### Rotor Loads Problem

The rotor of a vehicle in trimmed flight provides the necessary lift and propulsive force to sustain flight. The aerodynamic loads on the rotor will cause the blade to deform which will induce additional aeroelastic loads and deflections, and will affect the trim of the rotorcraft. The motions and deformations of the individual rotor blades will combine to impart shears and moments at the rotor hub. In turn, the fuselage will respond to these shears and moments, and modify the blade airloads and stresses. The complete problem of the loads and stresses on a helicopter is very complex; however, substantial progress has been made in the past by reducing the problem into smaller pieces. The aerodynamics of the rotor and its associated performance in forward flight can be understood to a substantial degree without considering the elastic deformation of the blades. In turn, the distribution of moments and stresses in the rotor blade and control system can normally be treated without considering the impedance of the rotor hub. And, lastly, the problem of the treatment of vibration within the fuselage can be approached even when the vibratory source in the rotor is not well understood. These three divisions--aerodynamics, rotor loads, and fuselage vibration--are useful in the design and analysis of a flight vehicle, but, to a degree, such divisions remain arbitrary. The scope of the present paper is the second division, rotor loads. For the purpose of this paper, rotor loads is meant to include both the aerodynamic loading of the rotor and its structural response.

The loads on a rotor include both a steady component and an oscillatory component that appears at harmonics of the rotor rotational frequency; that is, 1/rev, 2/rev, and so forth. The oscillatory component is sometimes referred to in the literature as the alternating load or half peak-to-peak load, but for this paper, the term oscillatory will be used to describe loads that have had the steady or mean value removed. In general, the rotor loads are dominated by the steady component and the first one or two harmonics. These are the loads that generally determine the fatigue life of the blade and controls, and are the primary interest of the rotor designer. At harmonics above the second, the loads become progressively smaller and often have little influence on the rotor structural design. However, it is these higher harmonic loads that are the source of vibration in the fuselage and their understanding is fundamental for progress in rotor loads predictive capability. For the purposes of this paper, the loads at the third harmonic and above will be termed the vibratory loads.

The characteristic behavior of rotor loads with increasing harmonic is illustrated in figure 1 using data obtained on a CH-34 rotor tested in the Ames 40-by 80-Foot Wind Tunnel (ref. 1). In this example, the airload at  $r/R = 0.85$  is largest in the first and second harmonics and decreases quite rapidly as the harmonic number is increased. The flap and chord bending moments measured at  $r/R = 0.375$  also decrease with the harmonic number, but show the influence of the blade elastic modes. This is particularly clear in this example for the chord bending moment, where the second chord mode is between 3 and 4/rev and the third chord mode is near 8/rev. In terms of blade design, what is of most interest is the fatigue loading and this is a function of the steady loads (which are not shown here) and the oscillatory loads, which in this case, are largely dominated by the first and second harmonics. In terms of vibratory loading, what is of most interest is the 3, 4, and 5/rev shears at the hub for this four-bladed rotor. The size of the steady component and first two harmonics of the rotor loads is such that it generally masks the behavior of the vibratory loads. Unfortunately, the vibratory loads are rarely shown by themselves and this has acted as an impediment to improved understanding.

#### Status of Technology in 1970s

The status of rotor loads prediction methodology in the early 1970s is best evaluated through two significant events. In March 1973 a "Specialists Meeting on Helicopter Rotor Loads Prediction Methods" was held in Milan under AGARD sponsorship (AGARD CP 122) and was attended by most of the major helicopter manufacturers who presented examples of correlation between their flight test data and their analytical methods. These same prediction methods were used again in February 1974 to predict the loads of a hypothetical helicopter rotor at the Specialists' Meeting on Rotorcraft Dynamics sponsored by NASA Ames Research Center and the American Helicopter Society (ref. 2).

Examples of correlation with flight test data from the Milan AGARD meeting are shown in figures 2 to 4 (refs. 3, 4, and 5, respectively). The predictions of the Boeing Vertol C-60 analysis (ref. 3) show quite good agreement for the pitch link waveform for the aft rotor of a CH-47C aircraft under stall conditions. The agreement for the oscillatory flap bending moment is not as good and it is not clear that the nonuniform downwash model is better than the uniform downwash model. Calculations using the Sikorsky Normal Modes Analysis, Y200, for an articulated single rotor show that a constant inflow model gives nearly the same results for oscillatory loads as the variable inflow model. However, when compared on a time-history basis, the variable inflow model shows better agreement with higher harmonics. On the basis of oscillatory loads, correlation of C81 with data from UH-1D flight test is quite good.

In his assessment of the prediction technology shown at the Milan meeting, Piziali expressed his belief that advances in the previous decade had been primarily in the scope of predictive capability and not accuracy (ref. 6). He felt that the structural problem was in hand, but that the analyses were limited by the

aerodynamic model. This view was not shared by other observers at the Milan meeting. Loewy, in his meeting summary (ref. 7), said that the major development problems of the previous decade had been in the area of structural dynamics. He also felt that major progress had been made in the predictive analyses, particularly in reducing the potential for surprises in new designs.

The importance of the 1974 hypothetical rotor comparison of Ormiston (ref. 2) was that it provided a test of the various comprehensive models for one hypothetical rotor configuration. Figure 5 shows that even for identical blade properties, the rotating natural frequencies calculated in a vacuum with the different math models showed significant differences. The range of variation for the oscillatory blade moments is shown in figure 6 (taken from ref. 8) and shows that the various analyses disagreed widely, especially for the torsional behavior. As a result of the comparison, it was apparent that there were significant problems in one or more of the competing analyses, but as there was no experimental data with which to compare, there was no obvious "right" or "wrong" answer. Ormiston's recommendations for future research were:

1. Continue to make standardized comparisons.
2. Assess in detail the assumptions and semi-empirical factors used in the analyses.
3. Perform fundamental experimental research in the areas of dynamic stall, blade/vortex interaction, and three-dimensional flow effects.
4. Compare the prediction methods (after some progress with items 2 and 3 above) with experimental data from the test of a full-scale rotor in a wind tunnel.

#### Survey Articles

In the years since the Milan AGARD meeting and the hypothetical rotor comparison of Ormiston, there have been a number of assessments of rotor loads prediction methodology. Arcidiacono and Sopher examined the United States progress in rotor loads predictive capabilities at the AGARD conference on the "Prediction of Aerodynamic Loads on Rotorcraft" held in London in 1982 (ref. 8). They concluded that a good deal of fundamental work had been done with regard to dynamic stall, blade/vortex interaction, and three-dimensional flow effects. In addition, they felt that the modeling of the structure had improved, both in terms of the physics of representing the rotor blade and in the design of structured computer programs. However, it was unclear at what point these analytical advances would be integrated into analyses. They noted that the older analyses were not easily modifiable without a substantial investment of time and money. They expressed optimism that with the development of the Second Generation Comprehensive Helicopter Analysis System (2GCHAS), these advances could be introduced in a controlled and efficient manner.

Johnson assessed the state of rotor loads prediction in a survey paper that covered the entire area of rotorcraft dynamics (ref. 9). He compared predictions

made at the 1973 Milan meeting with more recent calculations shown in the literature, and pointed out that, in general, the analyses are able to calculate the mean and oscillatory loads; but, that an examination of the time histories reveals that the fundamental phenomena are not being modeled correctly.

Friedmann addressed advances in rotorcraft aeroelasticity in a number of survey articles (refs. 10 and 11) and, although these do not deal with the predictive capabilities of the rotor loads analyses, they do provide useful summaries of advances in structural modeling and dynamic stall.

Johnson also provides a detailed survey of recent developments in rotary-wing aerodynamic theory (ref. 12). The survey pays particular attention to efforts in lifting surface theory, panel methods, transonic theory, and transonic blade-vortex interaction analyses. In his treatment, he makes a number of useful comparisons to the equivalent fixed-wing formulations. He concludes that lifting-line theory will remain the basis for rotor-aerodynamic calculations as long as it is the only theory that can accurately include viscous effects. He feels that work should continue toward the goal of turbulent Navier-Stokes calculations for the entire aircraft although there is no immediate expectation of success in this area.

A restricted class of survey articles (nonetheless very useful), are papers that summarize the application of rotor loads technology within a company. Gabel (ref. 3) has provided a useful discussion of how the rotor loads analyses are used at Boeing Vertol, and Yen and Glass (ref. 13) have done the same for Bell Helicopter Textron and included a historical perspective as well. Dadone (ref. 14) has discussed the application of the aerodynamics technology to the rotor design and has shown how it has evolved over the years at Boeing Vertol. Landgrebe (ref. 15) has discussed the evolution of the rotor-wake geometry representation at the United Technologies Research Center (UTRC) and at Sikorsky.

### Organization of Paper

This review of rotor loads research is divided into two main sections: research into understanding and improving the capability to predict rotor loads, and research into means of reducing rotor loads. Within the first section, the discussion is organized by breaking the loads problem into the aerodynamics model, the structural model, and solution methods. Within the section on rotor loads reduction, the major topics are investigations into effects of blade tailoring, control of blade loads through kinematic coupling or control system design, and aerodynamic tuning devices. Following these main sections, rotor loads in the presence of gusts and maneuvers is discussed. In the concluding part of the paper, an assessment is made of the progress that has occurred in the rotor loads area in the last 15 years. The role of the U.S. Army and NASA in this process is discussed and some conclusions and recommendations are made as to the major emphasis that should be taken in the years to come.

## Two Themes

Two themes will appear and reappear in this paper. The first of these themes deals with the balance between analysis and synthesis, and the second deals with the question of whether progress in controlling rotor loads can be made without understanding the basic mechanisms. The place of analysis in rotor loads research is well established, especially in the government laboratories and academia. This process of analysis, the breaking down of a problem into its constituent parts, examining each part in detail, and performing theoretical work and experiment to obtain improved understanding, has often been repeated. But, the process of putting the various pieces together again (which is referred to here as synthesis), is not so easy. To take the improved understanding, and to put the constituent parts back together again and understand their interrelationships, is not done well nor is it done often. When it is done, it is usually within the industry where the need is imperative. The balance between analysis and synthesis is the first of these themes.

The ultimate objective of research in rotor loads is not just the understanding of the fundamental mechanisms involved, but rather to be able to design improved rotor systems. The problem of rotor loads prediction is so intractable that to progress in this area, it is necessary to pursue not just the basic research into rotor loads, but to also pursue research in loads reduction even if the mechanisms to be used are only guessed at. A great deal of effort has been placed on experimentation in recent years--to parametrically vary major rotor properties and to measure the resulting improvement. This research has often been guided by a substantial amount of careful thought and the results have provided insight into the rotor loads mechanisms. The reduction of rotor loads through feedback control is the ultimate extension of this approach. But it must be recognized that the control of rotor loads, either through empiricism or feedback, is a complementary approach; it is not a substitute for research into the mechanisms of rotor loads. This is the second theme, the balance between reducing the rotor loads and understanding the physics.



## ROTOR LOADS PREDICTION

"For a good prediction of loads it is necessary to do everything right, all of the time. With current technology it is possible to do some of the things right, some of the time." - Johnson, 1985

Comparisons of measured rotor loads and prediction methods normally show both areas of agreement and places where things are not right. A number of approaches are made to understand the sources of disagreement and these can be generally categorized as: (1) fundamental investigations of the physics, (2) theoretical and experimental tests of simplified models, and (3) theoretical and experimental tests of the complete model, that is, of the rotor itself. Examples of all three of these approaches will be shown in this section.

For the purposes of this review, research into rotor loads prediction will be broken down into the aerodynamics model, the structural model, and solution methods. The aerodynamics model will be further broken down into dynamic stall, the wake-induced flow, blade-tip effects, and fuselage effects. The structural model discussion will include topics involving the blade structural properties and the influence of the fuselage impedance.

### Dynamic Stall

The work of McCroskey and Fisher (ref. 16) with a model rotor that had pressure transducers installed at  $r/R = 0.75$  and skin friction gages to characterize the boundary layer behavior, provided a clear description of the sequence of events involved in the dynamic stall of a rotor over the inboard section of the blade. To properly model the dynamic stall process, it is necessary to account for the lift overshoot and the large pitching moment changes that are related to the vortex that is shed from the blade leading edge. Johnson (ref. 17) used the Sikorsky Y200 analysis to test three of the early empirical models: the  $\alpha$ , A, B Method developed at UTRC (refs. 18 and 19); the MIT Method (refs. 20 and 21), and the Boeing Vertol Method (ref. 22). The elastic torsion angle for a highly loaded rotor at  $\mu = 0.333$  calculated with these models is shown in figure 7. As only one torsion mode was used, the blade-torsion moment is directly proportional to the elastic deflection. Even though the blade dynamics are identical for the three models, the predicted torsion behavior shows significant differences, particularly in the third and fourth quadrants of the rotor.

Sikorsky derived a simplified dynamic-stall model based on a universal nondimensional time constant,  $\tau = U_0 \Delta t / c$ , where  $\Delta t$  describes the start of a stall event determined from two-dimensional (2-D) measurements,  $U_0$  is the free-stream velocity, and  $c$  the chord length (ref. 23). They tested the predictive capability of this time delay model and the  $\alpha$ , A, B Method by comparing first with a simplified experiment, and second with flight-test data (refs. 23 and 24). The simplified

experiment was a test of a 2-D airfoil mounted on a torsion spring and oscillated in and out of stall at 1/rev. The torsion spring was sized to provide an appropriate torsional natural frequency with respect to the 1/rev of the primary oscillation and in this way to simulate stall flutter. These 2-D model tests were representative of full-scale, 3-D tests in ways that were not anticipated, including considerable cycle-to-cycle variation and unresolved ambiguities when the measurements were compared to theory. The time delay method tended to overpredict the 2-D test results and underpredict the 3-D, full-scale test results. Pitch-link loads predicted with the Y200 analysis using the two methods are compared with flight-test data in figure 8. The test data show that the blade stalls at an azimuth of about 190°, and this is not shown by the calculation. The  $\alpha$ , A, B Method predicts some stall on the second stall cycle at about 250° while both methods show substantial stall on the third stall cycle. The  $\alpha$ , A, B Method shows better agreement in terms of amplitude of the pitch link oscillation.

All of the dynamic stall models are empirically derived from experimental data, normally 2-D wind tunnel tests of oscillating airfoils. McCroskey (ref. 25) used data from an NACA 0012 airfoil tested in the U.S. Army's 7- by 10-Foot Wind Tunnel at Ames (ref. 26) to test the predictions of five empirical dynamic stall models. In addition to the three models that had been examined previously by Johnson, he also included two time delay methods (refs. 23 and 27) and a method derived by Lockheed (ref. 28). The methods were evaluated for their ability to predict the phase angles of lift and moment stall, and maximum values of the normal force and pitching moment coefficients. No single method was notably better than the others, and each was deficient in some area of prediction.

A new empirical model for dynamic stall that has been developed and integrated into the Sikorsky analyses is reported by Gangwani (refs. 29-31). As in the  $\alpha$ , A, B Method, this model uses the angle of attack and pitch rate as major parameters, but the angle of attack acceleration term, B, is replaced with a parameter that accounts for the time-history effects of changes in angle of attack and is based on the Wagner function. Lift, pitching moment, and drag are all determined as functions of these parameters where the functional behavior is determined from a least squares fit of 2-D oscillating airfoil data. The comparison of this empirical model and available 2-D oscillating airfoil data (ref. 30) is more extensive than for any of the other dynamic stall models. However, only limited comparisons with flight test data are shown. Gangwani (ref. 32) has also integrated this empirical model into a rotor loads analysis based on a model developed at Rochester Applied Science Associates (RASA) and described in reference 33, and has compared the results with data obtained from flight test of an AH-1G (ref. 34). The use of the synthesized-stall data does not improve the flap or chord bending moment correlation, but does show an improvement in the modeling of the torsion moment.

There have been no direct comparisons of the various dynamic stall models since Johnson (ref. 17), nor are there any extensive comparisons between any of these models and flight test data published in the literature. Future comparisons should include the ONERA dynamic stall model (ref. 35) with the extensions recommended by Peters (ref. 36). Any extensive correlation with flight test data may have to model

the fuselage induced flow as well. As shown by Wilby *et al.* (ref. 37) the upwash from the fuselage may increase the blade angle of attack sufficiently to cause stall over the nose of the aircraft. The stall-induced pitch-link load that is seen in figure 8 at a blade azimuth of about  $190^\circ$  for the CH-53A may be a result of this phenomenon.

The dynamic stall models in use today are empirically based on 2-D airfoil data. Near the blade tip, the blade stalling process will be 3-D and in some situations, the interaction of a previous blade's vortex will also induce a 3-D form of stall. Brotherhood and Riley (ref. 38) show the rotor blade of a Wessex helicopter in two different kinds of stall as visualized by pressure transducers mounted in the blade's leading edge. The pressure time histories are shown in figure 9 as a function of the blade azimuth. The first stall event appears at  $r/R = 0.90$  and is seen to move outboard. This event corresponds to the passage of the previous blade's vortex across the tip of the blade. The flow reattaches after the passage of the vortex, and then a second stall event is seen on the three outer blade stations, but this time the stall is simultaneous. How such complicated events can be modeled (or even if they need to be) is unclear. One useful approach has been taken by Costes (ref. 39) who has made experimental measurements on an oscillating half-span airfoil and compared the unsteady pressure measurements to calculations which were based on an extension of the ONERA dynamic stall model to three-dimensions. It appears that the blade lift can be estimated satisfactorily with this model, but the pitching moment cannot. This problem will become more important as variation in tip planform is used more frequently in the design of new rotors.

#### Wake-Induced Flow

In his seminal paper (ref. 40) Hooper has examined seven sets of airload measurements made on full-scale rotors using Cartesian, 3-D plots to visualize the data obtained in flight or wind tunnel tests. He has demonstrated that the low-speed (or transition) flight regime vibratory airloading is dominated by the interaction of the blade and the preceding blade's tip vortex first on the advancing side of the disk and then on the retreating side. This behavior is seen regardless of rotor type or blade number. At higher speeds, it appears that the greatest part of the vibratory airloads is caused by events on the advancing side of the disk, but in this case, there appear to be substantial differences which are due to rotor type or blade number. The low-speed or transition case will be discussed first as this has drawn the most attention of investigators in the past. The high-speed vibratory loading will be discussed at the end of this section on wake-induced flow.

An example of the low-speed vibratory loading is shown in figure 10 in the manner of Hooper using the data of reference 41. On the advancing side of the disk, there is a down-up pulse in the airload as the blade passes first through the downwash, and then the upwash, of the preceding blade's tip vortex as that vortex moves inward on the blade. On the retreating side, there is an up-down pulse as that same vortex moves radially outward on the blade. To properly calculate the wake induced

airload, it is necessary to correctly model the wake geometry, the vortex strength, and the blade-vortex interaction.

The advent of the digital computer has made feasible the calculation of the induced flow including the effects of a realistic wake representation. By the start of the time period covered in this paper, the use of a prescribed wake, that is, a wake where the tip and root vortices are assumed to follow a prescribed helical pattern, was well established. In addition, calculations using a free wake, where the wake geometry is modified by self-induced effects, had been developed and applied to a number of problems (refs. 15 and 42).

The free-wake calculations have shown that distortions of the wake geometry are primarily in the vertical or axial direction. In the plane of the rotor disk, the wake geometry lies very close to the cycloidal pattern of the prescribed wake. This has been shown from flight testing of pressure-instrumented rotors where the vortex passage can be identified from the characteristic up-down or down-up pulse in the measured pressure. Measurements obtained using a Puma helicopter (ref. 43) are compared with the cycloidal geometry in figure 11 and show little distortion in the disk plane from advance ratios of 0.11 to 0.35. Landgrebe and Bellinger (ref. 44) have compared their free-wake calculation to the measured axial geometries obtained by Lehman in a water tunnel (ref. 45) and have achieved good results. Johnson (ref. 46) has compared a free-wake analysis to the laser-velocimeter measurements of the wake geometry of a two-bladed rotor in a wind tunnel which were obtained by Biggers et al. (ref. 47) and has also demonstrated good agreement. However, he notes that in this case, the tip-path plane angle of attack was sufficiently large so that the difference in axial-wake position predicted with either the prescribed or free wake had no effect on the blade loading.

The predictions of wake geometry using free-wake analyses appear good in those cases where data are available, but the predictions of the airloads and blade bending moments have not been done as well. Egolf and Landgrebe (ref. 48, summarized in ref. 49) and Yamauchi et al. (ref. 50) have compared the analytical predictions of a rotor loads analysis that includes a free-wake model with measurements of blade airloads and structural loads obtained in flight. Figure 12 compares the blade airloads measured on the CH-34 rotor at the 0.90R radial station (the same case as was shown in fig. 10) with predictions using both prescribed and free-wake analyses (ref. 48). The data show the influence of the blade-vortex intersections on the advancing and retreating sides of the disk. The prescribed-wake calculation shows similar behavior, but the load is much reduced in strength. The free-wake calculation shows multiple tip-vortex intersections (that is, intersections with two or more tip vortices from the preceding blades), but these are not apparent in the test data. The analysis predicts very high blade airloads due to the initial intersection, much higher than those measured in the test, as these calculations show a direct intersection of the tip vortex and the blade. The resulting blade flap bending moments using the free-wake analysis, coupled to the Sikorsky Y200 rotor loads program, are shown in figure 13. The airload peak seen in figure 12 is highly localized so its impact on blade loading is not severe. Both the theoretical prediction and the measured loads are rich in higher harmonics, but except for the

loading at about 270° azimuth, the agreement in amplitude and phase is not particularly good.

Yamauchi et al. (ref. 50) compare predictions using the prescribed and free-wake analyses of CAMRAD with flight-test data for the Aerospatiale SA 349-2. Airloads data for this test program were obtained at  $r/R = 0.75, 0.88, \text{ and } 0.97$ . The CAMRAD predictions for lift coefficient are compared in figure 14 with the measurements made at  $0.88R$  and an advance ratio of  $0.14$ . As with the CH-34 results, the data show loads caused by the blade vortex interaction on both the advancing and retreating sides of the disk and the free wake provides a better prediction of the loading induced by the vortex wake. Again, as with the CH-34 case, the theoretical predictions show multiple vortex intersections that are not apparent in the data. The core size used in the CAMRAD free-wake prediction shown here has been determined after an a posteriori fitting of the data. Calculation of the flap bending moments for the SA 349-2 using the free-wake analysis show mixed results with good agreement at the blade midspan, but poor agreement elsewhere.

The influence of blade vortices at high speed is not as clear as for the low-speed transition case. Figure 15 shows the vibratory loading measured on the CH-34 rotor in the 40- by 80-Foot Wind Tunnel at an advance ratio of  $0.39$  (refs. 1 and 51). A strong, impulsive loading is seen on the advancing side of the disk, but unlike the low-speed case, the load is an up-down pulse, suggesting that the blade is encountering first an upwash and then a downwash. Miller (ref. 52) has proposed that, because the outer portion of the blade is negatively loaded for this case, that two vortices of opposite sign are trailed from the blade as shown in figure 16. An analysis of this case made using a number of simplifying assumptions, including fixing the position of the midspan or inboard vortex, shows good agreement with the measurements as shown in figure 17. This progress is encouraging, as Hooper has shown in reference 40 that neither the Boeing Vertol C-60 analysis nor CAMRAD show satisfactory agreement for this case. (However, note that Phelan and Tarzanin, ref. 53, have reported correcting a programming error in C-60 and now show much better agreement for the airloads in this case.)

The importance of the blade-vortex interaction studied in the CH-34 high-speed case is not entirely clear since it appears to be strongly related to the amount of negative lift on the advancing side of the disk. The CH-34 which was studied in the 40- by 80-Foot Wind Tunnel was operated at reduced lift (about 60-70% of the lift for normal flight), and data on the XH-51A and NH-3A compound aircraft studied by Hooper were obtained with some of the lift provided by the aircraft wing. Unfortunately, there are few high-speed data available for conventional rotors. The maximum speed case studied for the CH-53A aircraft was an advance ratio of  $0.32$  and the vibratory loading is quite different from that seen in figure 15. Measurements made on the outer blade stations of the SA 349-2 at an advance ratio of  $0.38$  do not show any clear evidence of vortex-induced loads (ref. 54). However, model-scale data acquired on the Boeing Vertol Model 360 rotor (ref. 55), show airloads that are remarkably similar to the CH-34 airloads as shown in figure 18.

Application of free-wake calculation techniques to rotor loads requires first, that the physics of the phenomena be correctly modeled and second, that the wake

calculations be efficiently integrated into the rotor loads calculation. It seems evident from the research with the free-wake models that the first step has not yet been achieved. It is not possible at this time to accurately model the free wake. However, some progress has been made in making the calculation more efficient. Egolf and Landgrebe (ref. 48) have approached this problem for their free-wake calculations by constructing an approximate or generalized model of the wake, and in this fashion, reduced the computational time by a factor of a thousand.

Young (ref. 56) has taken a different approach to the problem of an efficient wake calculation by starting with a simplified wake model that is very efficient and then modifying it step-by-step to see how much improvement is obtained and at what cost in computation time. Young models the near wake with rigid semicircles of constant vorticity whose radius varies as the blade moves around the azimuth, and the far wake as a series of vortex rings. As vortex rings will not give the same blade vortex intersection as a cycloidal path, the actual intersection geometry is used to fix the outer position of the wake vortex rings. Figure 19 compares the flap bending moments measured on a Puma with the original vortex ring model, and the vortex ring model with the improvements discussed by Young in reference 56. The representation of the higher harmonic loads appears reasonably accurate in both amplitude and phase.

Alternative approaches to the calculation of aerodynamic loading have been devised using the acceleration potential. Costes has demonstrated the feasibility of this method and compared his results to rotor measurements obtained in a wind tunnel (ref. 57). Runyan and Tai (ref. 58) have developed a similar approach and made limited comparisons with model rotor loads measurements. Pierce and Vaidyanathan (ref. 59) have applied the method of Van Holten (ref. 60) to the prediction of the airloads measured on the CH-34 in flight and in the wind tunnel. In general, the prediction of the oscillatory loads is good, but the prediction of harmonics beyond two is difficult to judge as they are masked by the first and second harmonics.

### Blade-Tip Effects

The calculation of rotor loads based on lifting-line theory normally accounts for the reduction of lift at the blade tip by introducing a tip-loss factor for the blade normal force, but the chordwise force is assumed to extend to the blade tip. When the wake-induced flow is calculated by a prescribed or free wake then the radial distribution of bound vorticity is determined as part of the solution. Johnson (ref. 46) has compared the calculated bound vorticity using a free-wake analysis to measurements obtained with a laser velocimeter on a model rotor in a wind tunnel (ref. 47) and these show fairly good agreement, particularly near the tip. This comparison was made at an advance ratio of 0.18 and it is expected that the calculation problem will become more difficult at higher speeds as transonic effects begin to dominate the loading.

A great deal of progress has been made in recent years in developing finite difference codes to analyse the flow over an advancing blade including the effects

of shocks and unsteadiness. Caradonna and Tung (ref. 61) have provided a comprehensive discussion of the present status of these codes and have compared a number of the code predictions with surface pressures measured in nonlifting and lifting rotor experiments. At the present time, the codes are being integrated into comprehensive analyses either in a partially coupled manner (ref. 62) or as a post-processor (ref. 55). In the former case, the comprehensive analysis (CAMRAD in ref. 62) is used to obtain the trim solution and then to provide the finite-difference code with a partial inflow distribution along the blade. The calculated inflow from the comprehensive analysis excludes the influence of the trailing vortex sheet that is calculated as a part of the finite difference grid. The finite difference program, in turn, provides the comprehensive analysis with an improved estimate of the blade lift. The solutions are matched when there is no change in lift from one iteration to the next. The blade pitching moment and drag are not coupled in this manner, and spanwise discontinuities in calculated properties are allowed at the grid inner boundary. There is great optimism as to the utility of these new methods, but the applications are in their infancy.

### Fuselage Flow Effects

The U.S. Army developed four prototype aircraft in the early 1970s to meet the needs of their utility and attack helicopter missions. All of these prototypes encountered severe vibration problems, and in each case, the rotor shaft was extended; as a consequence, the vibration was reduced. There was a great deal of intense activity at that time to understand the problem, but because of the competitive aspects of the developments little information was published. (An account of some of these problems was given by Gabel in a panel at the 2nd Decennial Specialists' Meeting on Rotorcraft Dynamics held at Ames in 1984, ref. 63.)

The effect of a fuselage on the air flow during flight will be to cause an upwash on the forward side of the disk and a downwash on the rearward side. This will cause a 1/rev variation in the induced flow at the rotor disk and will affect the rotor loads. The rotor wake may also impinge on the fuselage and cause vibratory excitations. Wilby *et al.* (ref. 37) have presented results from model tests with and without a fuselage. The flap bending moments measured at an advance ratio of 0.3 are shown in figure 20 for this model. Although the fuselage causes a 1/rev variation in the induced flow, the effect on the blade is to cause an increase in the 5/rev moments at 400 rpm and 4/rev moments at 600 rpm. In both cases, the increased loading corresponds to the second flap mode frequency. Similar effects are seen in experimental measurements reported by Freeman and Wilson (ref. 64).

Huber and Polz (ref. 65) have used an analytical model to examine the effect of the fuselage aerodynamics on the blade loads. Figure 21 shows that the calculated effect of the fuselage is to cause an upwash over the nose of the aircraft and a downwash over the tail. The greatest effect is seen in the 2 and 3/rev loads. Huber and Polz note that the upwash is a maximum at about 0.4R and that this corresponds to the antinode of the second flapping mode and explains why the second flap mode responds so strongly to the fuselage induced flow.

The effect of the fuselage on full-scale rotor loads has been studied by Jepson et al. (ref. 66) using flight test data, wind tunnel data, and calculation. Figure 22(a) shows flap bending moments measured at 0.70R on an S-76 rotor in flight and in the Ames 40- by 80-Foot Wind Tunnel (ref. 67). Figure 22(b) shows calculations using Y201 for the S-76 rotor alone and for the rotor with the aircraft fuselage. The calculations show that the effect of the fuselage is to cause a significant increase in the 3/rev flap bending moments. This same sort of increase is seen in comparing the flight-test results with the wind tunnel measurements. In the wind tunnel, the rotor was mounted on the Ames Rotor Test Apparatus (RTA). Calculations in reference 66 show that the S-76 fuselage increases the angle of attack about  $1^\circ$  over the fuselage nose compared to the predicted effect of the RTA.

The theoretical calculations discussed above have all represented the fuselage using potential flow-panel methods. Johnson and Yamauchi (ref. 68) have used a modification to slender body theory to represent the fuselage and have shown that this approach gives the same results as did a panel method for axisymmetric bodies at zero angle of attack, but at a much lower computational cost. Typically, the use of the modified slender body theory increases the computational run time (including a prescribed wake) by only 10-20% with respect to an isolated rotor calculation. Using this approach, the influence of the RTA on rotor loads has been estimated (ref. 69) and it was shown that the flap bending moments increase by 5-10% and the chord bending by 10-15%. The effect on pitch-link loads is negligible. The measurement of rotor loads on the RTA, therefore, is a reasonable approximation of isolated rotor conditions.

The measurements and calculations made in the last decade examining the effects of the flow induced by the fuselage have all shown a significant effect on higher harmonic loads. It seems clear from this perspective that testing future improvements to rotor loads prediction methods will be fruitless unless the effect of the fuselage induced flow is accounted for.

### Blade Response

A substantial amount of research has been performed in the last 10-15 years to understand the influence of the blade structural, inertial, and kinematic properties of the rotor loads. A great deal of this research has been directed toward loads reduction and this will be discussed in more detail below in the Rotor Loads Reduction section. The emphasis of the material covered here under the Blade Response heading is the improved understanding of how the rotor responds to the aerodynamic loading.

The understanding of rotor loads is greatly enhanced when the source of the blade loads can be identified by harmonic and blade mode. In the 1973 Milan AGARD meeting, McKenzie and Howell (ref. 70) compared the Westland rotor loads analysis with flight-test data from the Lynx; examples are shown in figures 23 and 24. In figure 23, the 4/rev rotor hub pitch and rolling moments are broken out by the proportion of the moment that occurs in the first three flapping modes. As the 4/rev hub moments are the primary source of vibratory loads on the Lynx, this



technique is valuable; first, in identifying which blade modes are most important for vibration reduction, and second, to judge how well these loads can be predicted. (Note that the modal contributions cannot be directly measured from flight test, but are obtained by using the blade-bending moment data to estimate the amplitudes of the modes as generalized coordinates. This technique has been used by other investigators (refs. 71 and 72), but none of these references discuss the technique or its limitations in any detail. It appears that the method is similar to the formalism of the Strain Pattern Analysis Method (refs. 73 and 74).) Figure 23 shows that the second-flap mode contribution is most important for the Lynx as determined from flight measurement, but that the theory predicts approximately equal effects from both the second- and third-flap modes. Figure 24 compares the theory and flight-test estimates for the second mode deflection for three harmonics of blade loading. The 1/rev deflection is overpredicted, while the 2 and 3/rev deflections are underpredicted. This approach to comparing measurement and prediction provides a better assessment of the rotor behavior and the validity of the prediction model than more typical approaches that are based on the comparison of oscillatory loads or azimuthal waveforms.

Blackwell and Commerford (ref. 24, summarized in ref. 75) have made an extensive theoretical investigation of the means of reducing stall-induced loads. One of the advantages of the theoretical approach is that it is relatively straightforward to break down the various components of a load to understand what is the primary cause and what can be done to reduce its influence. In that study they calculated that a reduction in torsion frequency would reduce the stall-induced pitch link loads. Figure 25 shows the torsion moment at the root caused by the aerodynamic pitch moment; the moment caused by the inertial loads; the moment caused by deflection and shear of the blade, and their sum. The plot shows one rotor revolution starting at  $180^\circ$  to better illustrate the stall-flutter behavior. For this articulated rotor, the effect of blade deflections in combination with shears has only a small effect; the largest effect is caused by the aerodynamic pitching moment and the inertial moment which are of opposite phase. The change in torsional frequency does not change the aerodynamic pitching moment very much, but does reduce the inertial load and this accounts for the calculated reduction in the root moment. It is expected that shear/deflection loading will be much more important for hingeless and bearingless rotor designs.

Extensive data have been obtained in the Langley Transonic Dynamics Tunnel (TDT) on the conformable model rotors and the data show that the tip design, blade camber, and torsional stiffness all have a substantial influence on the rotor loads (refs. 76 and 77). These data are discussed in detail in the Rotor Loads Reduction section, but mention is made here because the data have stimulated additional work by Blackwell and Kottapalli to understand the reasons for the observed changes in rotor loads.

Blackwell (ref. 72) has re-examined the data obtained in the TDT and has fitted the measured blade bending moments with calculated modal moments to identify the generalized coordinates. He states that the hub shears calculated in this fashion "trended directly" with the loads measured on the rotor balance, although no results

are shown. The major differences seen in comparing the rectangular- and swept-tip configurations are the reductions in the 3/rev vertical shears at the hinge, and the 3 and 5/rev inplane shears at the hinge for the swept tip. The generalized coordinate amplitudes show that most of this reduction is in the second flap mode.

Kottapalli (ref. 78) has taken a purely theoretical approach to better understand the changes in rotor loads that were seen as the model blade-tab deflection was changed in the TDT tests. Using the Sikorsky Y201/F389 family of programs he shows that the reduction in 4/rev vertical root shears is related to reductions in the blades' 4/rev angle of attack distribution. The angle of attack reduction is calculated to be due to reductions in elastic torsion (42%), elastic flapping (39%), and inflow (19%).

The complementary approaches of Blackwell and Kottapalli are useful in providing an improved understanding of rotor loads behavior, but both approaches have substantial limitations. The experimental approach of Blackwell can break the problem down to a certain level, but not to the individual terms of the equations of motion. Relationships between different properties can be demonstrated experimentally, but the cause and effect cannot necessarily be derived. The theoretical approach, however, can break the problem down to the level of the individual terms of the equations of motion and, in some cases, clearly demonstrate cause and effect. However, the inability of the analysis to predict rotor loads as measured in flight test makes the analysis untrustworthy.

Blackwell has also looked at the effects of spanwise mass distribution on vibratory loads in reference 72. Based on a simple analytical representation, he suggests that the distribution of spanwise mass should modify the blade-root shears which depend upon the product of the airload distribution and the mode shape. Taylor (ref. 79) has pursued this approach and examined the sum of the modal root shear contributions for all blades and derived a Modal Shaping Parameter which is defined as

$$\text{MSP} = \frac{(\text{Modal Shear Integral}) \times (\text{Generalized Force})}{(\text{Generalized Mass})}$$

Taylor assumes the airload can be represented as a polynomial in the radial coordinate and, once the loading is defined, that the modal shaping parameter provides a design method to seek a reduced vibratory load. Taylor extends this approach in reference 80. In this study he uses the G400 analysis to calculate the rotor loads and breaks down each component into essentially the terms of the equations of motion. Figure 26 shows an example of the calculation of 3/rev lateral shears where each component of shear is identified in terms of amplitude and phase. As changes are made to the blade design based on the modal shaping parameter, then the behavior of each component of the vibratory shear can be observed, and insight into the loads behavior obtained. This approach holds great promise once more reliable analyses are developed as the reduction in rotor loads will be accompanied by an understanding of the system behavior. This must be contrasted with the formal optimization

approach where an understanding of the physics is not necessary to the achievement of loads reduction.

Another approach to understanding the blade response problem has been taken by Esculier and Bousman (ref. 81) who have calculated the blade response for the CH-34 using measured airloads. This approach avoids the question of the adequacy of the aerodynamic model by substituting measurements, and in this way, the adequacy of the structural model can be evaluated. Figure 27 compares the measured moments from reference 1 with calculations for the first harmonic of blade loads. Two calculations are shown for the flap and chord bending moments: an uncoupled calculation and a coupled calculation assuming the flap and chord motions are coupled through the local pitch angle. The comparison of the flap bending moments show very good agreement between the measurements and the calculations based on measured airloads. This good agreement is, in general, obtained through the ninth harmonic. This means that for relatively simple rotors such as the CH-34, the flap bending loads can be calculated quite precisely if the aerodynamic model is correct.

This is not the case for the chord loads as neither the coupled or uncoupled calculations accurately predict the blade chord bending moments. Two reasons for this were identified in reference 81. First, the chord airloads are not measured directly, but are obtained from the flap airloads, and second, the CH-34 hydraulic damper is represented as a linear viscous damper, but the data suggest that it also acts as a relatively strong spring. The blade torsional moments appear fairly well predicted using the measured pitching moments, especially in phase, but as pointed out in reference 81 the calculation of torsional moments is sensitive to the control system stiffness and that was not measured in reference 1.

The adequacy of blade structural modeling has also been assessed by testing of rotors in a vacuum. Lee (ref. 82) measured modal frequencies and displacements of a rotating, cantilevered UH-1D blade in a vacuum chamber and obtained good agreement with prediction for the lower frequency modes as long as they were not strongly coupled. The mode shape prediction was not as good for the higher frequency and more strongly coupled modes. Srinivasan et al. (ref. 83) have made frequency and modal strain measurements of a torsionally soft model rotor spinning in a vacuum chamber. These measurements may become useful for validating the prediction of structural models because of the extensive model properties documentation that have been obtained for these blades (ref. 84).

### Fuselage Impedance

Rotor loads predictions are normally made assuming the rotor is mounted to an infinitely stiff structure. One exception to this is that Bell Helicopter Textron models the pylon flexibility in calculating the rotor natural frequencies and mode shapes used by the C81 analysis for their two-bladed rotor designs. Yen and McLarty (ref. 85) have shown the importance of modeling the pylon impedance for the calculation of rotor loads, and an example for the OH-58A is shown in figure 28. The effect of the pylon impedance on the oscillatory loads is clearly shown here and it has also been shown by measurements in wind tunnel tests (ref. 86).

Sopher et al. (refs. 87 and 88) have reported on the development of an analysis that couples the Sikorsky G400 rotor loads analysis to a fuselage model and allows the calculation of rotor loads and vibration. These calculations showed that the hub impedance has a large effect on the rotor loads when a rotor frequency is close to an N/rev. However, the predicted effect was very sensitive to the fuselage representation used and the reasons for this were not determined.

Gabel and Sankewitsch (ref. 89) have reported the development of a method to couple the Boeing Vertol C-60 rotor loads analysis to a fuselage representation through an impedance-matching technique. The fuselage impedance is shown to have a significant effect on the hub vibratory loads, but the effect on blade loads is not discussed.

### Solution Methods

The modal blade representation used for the solution of the rotor equations is usually based on a set of uncoupled or coupled rotating modes (ref. 2). In the case of coupled modes, the calculation is made for a representative blade pitch angle and the effects of variation in the geometric pitch angle around the azimuth are assumed negligible. Harvey (ref. 90) has examined this assumption using a rotor model that represents the actual pitch angle of each blade. He applied this analysis to a simplified model of a two-bladed rotor and compared the results of calculations with and without the cyclic variation. The effect on the blade harmonic loads is small when the pitch bearing is at 0.25R, but large when it is located at the rotor centerline.

Hansford (ref. 91) has also addressed this problem and has derived correction terms for the coupled modes that depend upon the cyclic pitch. Comparison with model and flight-test data show that the correction terms are not important for the calculation of the flap bending moments, but are important in some cases for the chord bending moments. Figure 29 compares flight-test measurements from the Lynx to rotor load predictions using the conventional modal representation and a modified theory that uses the cyclic correction terms. The modification does not appear important at the inboard station, but does have a significant effect outboard. For this case, it appears that the modified theory provides a better representation of the blade loads than does the conventional modal representation.

Once the modal solution is obtained, there are alternative approaches to the calculation of the rotor-bending moments. The normal approach is to sum the contribution of all of the modes. However, where there is a discontinuity in the loading, such as a load path split on a bearingless rotor design, then the modal-summation approach will not accurately model the load distribution at the discontinuity. Bielawa has examined this problem in reference 92 by comparing the modal-summation method with a force-integration technique where the bending moment at any location is obtained by calculating the balance of forces out to the blade tip. He shows that the force-integration method can properly represent the rotor loading at discontinuities, but the method is computationally more expensive. Hansford (ref. 93) has devised a method of unifying the two approaches by deriving correction terms to

the modal-summation method based on the force-integration expression. This unified method is applied to the Sea King where the lag damper causes a discontinuity in the load at the inboard end of the blade. The modal-summation method and the unified method are compared to Sea King flight-test data in figure 30. The unified formulation shows much better agreement with the data.

A related problem in obtaining a modal solution for rotor loads prediction is knowing how many modes are needed for accurate prediction. Yamauchi et al. (ref. 50) have examined the effect of the number of modes used in comparing CAMRAD with the SA 349-2 flight-test data. The analysis uses up to eight coupled flap and chord modes, and up to four torsion modes. A comparison with the flight-test data shows there is little effect on the flap bending moment correlation beyond the use of five coupled modes, and for the chord bending moment correlation little change is seen after seven coupled modes. For the blade torsional moment, it appears that two torsion modes are sufficient.

## ROTOR LOADS REDUCTION

"Compared to the volume of literature available concerning various devices which can reduce unacceptable vibration (absorbers, isolators, higher harmonic control systems, etc.) there appears to be a decided lack of information describing the origin of the vibratory loading and how the loads may be affected (reduced) through blade design. There may well be design procedures which will substantially reduce or eliminate the need for other vibration control treatment." - Blackwell, 1981

The aeroelastic environment of the rotor blade has several natural divisions used by researchers to modify blade loads. First, one may define a series of loads reduction concepts where the blade is aeroelastically tuned to avoid critical driving mechanisms such as severe aerodynamic loadings or frequency coalescence. A second classification of research reduces the loads through blade and control system coupling. Third, a substantial effort has been made to modify the blade's aerodynamics to provide less excitation to the aeroelastic response of the rotor. The following sections will address these three research areas through examples of research and design concepts.

### Blade Tailoring

Tuning the rotor blade to avoid critical driving mechanisms, both elastic and aerodynamic, has involved several different approaches. These have included non-structural mass placement, stiffness and mass distributions, and aeroelastic coupling parameters. An example of the latter is the aeroelastically conformable rotor (ACR) concept.

Conformable Rotor Research- Studies of conformable rotors at the beginning of the review period examined the effects of blade properties on stall-induced control loads. Blackwell and Commerford (ref. 24, summarized in ref. 75) examined the effects of a number of blade parameters on control loads and concluded that torsional frequency and inertia had a major influence on the loads (see fig. 25 and discussion in Rotor Loads Prediction section). A similar effort by Tarzanin and Ranieri (ref. 94, summarized in ref. 95) based on limited model test data and theoretical studies using C-60, also concluded that the torsion degree of freedom had a significant influence on control loads, showing substantial reductions on the retreating side as torsional frequency was reduced. However, they predicted that further reductions in torsional frequency would show increased loads on the advancing side.

Later studies suggested that careful attention to the blade design could reduce all blade vibratory loads and this has become known as the conformable rotor concept. Reference 96 included a study of airload and vibratory loads from flight

data. According to that reference, for three different rotor types ". . . the phase angles and spanwise distributions of the principal harmonics of airloads were remarkably similar . . . and the bending load distributions and phases were predictably related to the hub configurations and to the modal natural frequencies." This revealed a constancy in character for the forcing function and some hope of tailoring the blade to redistribute the loads. It was suggested that vibratory flap bending and lift deficiency be attacked using elastic twist distribution with such design parameters as camber, chordwise c.g. position, and blade sweep. Test results from a Mach-scaled hingeless rotor indicated that for a representative high speed cruise condition, introducing a nose-up pitching moment reduced mid-span flap bending (1 and 2/rev) by 40%. Furthermore, a 10° sweepback of the outer 35% of the rotor radius reduced midspan flap loads by 10% in 1/rev and by 30% in 2/rev. It was noted, however, that phasing of flap loading harmonics with blade sweep prevented unloading of the retreating blade and further inertial tuning would be required.

Studies such as the above encouraged a series of NASA/Army sponsored analyses and tests of the ACR concept. Blackwell and Merkley (ref. 97) analytically investigated time-varying elastic twist to improve performance and reduce loads, and then provided design guidelines for elastic twist by qualifying the potential of several blade parameters for producing favorable elastic twist. The impetus for this study was a maximum rotor efficiency for a given rotor class. The Y200 analysis with two inflow models was used to define the improvements possible with airload redistribution as shown in figure 31 using the elastic twist distribution shown in figure 32. Parametric sensitivity to rotor-design variables was investigated for a torsionally soft rotor during the study with encouraging results (figure 33). Recommendations for model designs were made which emphasized the predicted tradeoff between performance and blade loads for the ranges of conformable rotor design variables employed.

Testing of candidate ACR designs has included work in the Langley Transonic Dynamics Tunnel (TDT). Weller (ref. 98) tested a four-bladed articulated rotor with four different tip shapes. The blades had a high torsional stiffness ( $\omega_\theta \approx 11/\text{rev}$ ). It was found that aft sweep of the blade tip by itself decreased flap and chord oscillatory loads with respect to a rectangular tip as shown in figures 34(a) and 34(b). The addition of tip anhedral, however, increased these loads. Both sweep and anhedral in the tip region reduced torsional and control loads as shown in figure 34(c).

The above analytical and experimental results encouraged more comprehensive model testing of conformable concepts including that reported by Blackwell *et al.* (refs. 76 and 77). In that research effort two blade sets of different torsional stiffness were tested in the Langley TDT at four advance ratios and several hover tip Mach numbers. Three tip shapes were used as well as trailing-edge tab deflection variations. It is noted that in the search for load alleviation, several design parameters were incorporated for each model configuration. The elastic twist differences caused by configuration changes shown in figure 35 were significant, and an analysis of the resulting loads and blade response yielded several useful design guides. For example, for the configurations tested that reduced advancing blade

twist, blade loads were generally reduced as is shown in figure 36. It is of interest to note that the torsionally soft configurations provided both the best and the worst vibration environments with the highest vibratory loads on the rectangular ACR and the lowest on the ACR with sweep and camber change. The camber changes also generated the highest torsion moments at high blade loading.

Performance and rotor control sensitivity were evaluated for several configurations. A correlation study using the Y200 code resulted in good trend agreement for the elastic twist resulting from camber changes. However, the effects of sweep on steady and 1/rev elastic twist were overpredicted by the analysis. Wave form correlation was poor as is shown in figure 37, but the trend of oscillatory loads with rotor task was described as fairly good. The effect of configuration changes on performance and loads for the rotor tasks shown was predicted fairly well as is shown in figure 38. It should be noted that performance "rankings" changed significantly with rotor task. Several conclusions from this study are useful to loads reduction tailoring. The paper cites that a pitching moment coefficient change of +0.03 effected a much larger dynamic twist than did 20° of tip sweep, and that both sweep and camber reduced vibratory loads for the torsionally soft blade. However, the torsionally soft blade generated loads as high or higher than the baseline rotor.

The extensive work of reference 77 showed the potential of several design variables for loads reduction when used in several combinations, but the isolated sensitivity of each parameter and the effectiveness of each when used in combinations remained elusive.

In an effort to understand and explore the relationship between torsional loading and rotor performance, Yeager and Mantay (ref. 99) did an expanded test and analysis of the configurations tested by Weller (ref. 98) including additional tip configurations. For the baseline torsionally stiff ( $\omega_{\theta} \approx 11/\text{rev}$ ) model rotor used in that test, the parametric variations of tip sweep, taper, and anhedral measurably changed the elastic twist and integrated performance, but there did not appear to be a strong connection between the two phenomena. The oscillatory and mean torsional moment data of references 98 and 99 agreed with respect to configuration trends.

Yeager and Mantay (ref. 100) reported additional tests of the rotor originally used in references 76 and 77, but with extended tips. This reference presents data in tabular and graphic formats. Performance, harmonic blade and fixed system loads, and torsional deflection data were offered to the analyst for correlation purposes.

The Army contractual effort which initiated much of the above ACR analysis and testing also provided the impetus for the work described by Sutton *et al.* (ref. 101). In that study, a selection of primary ACR parameters was made. A series of codes providing predictions for performance, forced response, and stability were used to parametrically vary key aeroelastic parameters for a four-bladed rotor. The relative performance benefits of each parameter combination were assessed, with torsional stiffness and tip sweep being found to be the most effective. A model rotor was constructed and tested in the Langley TDT for four configurations. Figure 39 shows the measured variation in the flap bending moment for the



three four-bladed rotor models that were tested. A conclusion to this effort cited the potential of the ACR concept if the cause and effect relationships of the design variables could be well understood.

The ACR research effort reported on in references 76 and 77 was expanded in order to understand the effects of aeroelastic couplings on loads and performance. Mantay and Yeager have reported the results of a first stage of testing in reference 102 and the complete results in reference 103. Although the earlier work had demonstrated the importance of tab deflection on vibratory loads, the primary research emphasis of the new experiments was on the blade tip. Seven tips, incorporating single and combined sweep, taper, and anhedral, were tested for two different blade torsional stiffnesses at several advance ratios in the TDT. Twist and inertial properties were held to known values. Rotor loads were correlated with elastic twist magnitude and azimuthal activity while explanations were offered for the resulting rotor-control phenomena and substantial performance variations effected by the simple and controlled combinations of ACR tip parameters. The practical aspects of ACR track sensitivity were also addressed with significant differences in torsional loads and response characteristics for the ACR maverick blade. The conclusions offered in these references included the existence of a strong correlation between azimuthal variation of elastic twist and rotor performance and loads. The oscillatory flap bending moments are shown relative to performance rank in figure 40. The elastic twist variation with azimuth is shown in figure 41 for three configurations as the performance rank decreases from 1 to 5 to 13. In addition, there did not exist a strong correlation of elastic twist magnitude with performance as is shown in figure 42. Finally, fixed system and blade loads as well as rotor track for potential ACR candidates appeared very sensitive to parametric rotor changes as shown in figure 43.

A similar parametric effort was analytically accomplished by Tarzanin and Vlaminc (ref. 104). The goal of that study was to evaluate the effect of sweep parameters on vibratory hub, blade, and control system loads. Furthermore, the relative importance of flapwise and torsional stiffness was evaluated along with the aeroelastic mechanism which produces the reductions in loads. An analytical investigation was performed on a reference blade for which aft sweep was generally beneficial to oscillatory loading. The C-60 was used, which included coupled torsion and flap, planform sweep variations, shear center, neutral axis, chordwise c.g. and pitch axis location variations. Airloads were modeled using compressibility, stall, 3-D flow, unsteady aerodynamics, and nonuniform downwash. The reference rotor in this study was predicted to have its 4/rev loads significantly reduced by tip sweep over a wide range of airspeeds. It was found that although the blade torsional stiffness must not be too high and, thus, obviate the tip sweep effectiveness, specific blade frequency placement and flap/pitch coupling were not necessary for hub load reductions with sweep for the reference rotor. Reductions in 4/rev hub loads were predicted for forward mass and aft aerodynamic center configurations with respect to the blade's elastic axis. Elastic twist via c.g./ac distributions was quantified and the correlation between 4/rev elastic twist and vibratory loads strengthened. Several nonreferenced blade designs exhibited detrimental qualities with aft tip sweep, but could be further altered with the predicted parameter

sensitivities acquired in this study. The understanding of the hub load reduction method is illustrated in figure 44.

Modal Tailoring- The review of rotorcraft applications for design optimization by Miura (ref. 105) included an overview of government and industry research in loads reduction using new design methodologies. Several studies in loads tailoring have been undertaken using empirical modal techniques and automated design analyses. During these studies requirements to understand rotor loading mechanisms and design parameter sensitivity were addressed.

Peters et al. (ref. 106) have presented the results of a grant effort to investigate the potential of tailoring blade properties to achieve weight, inertia, and dynamic goals. A finite element model was used with the CONMIN code to solve 21 design problems. Simple beams as well as teetering and articulated rotor blades were tailored for frequency placement. Reference 106 states that the frequency placement formulation is a useful approach to vibration reduction for a prescribed airload distribution. Numerical procedures and preferred operation of the design method were defined. The achievement possible in the modal optimization process was defined in large part by the rotor's rotational speed.

Prescribed airloads were also used by Pritchard et al. (ref. 107) for a sensitivity analysis and optimization of nodal point locations for reduced vibratory loads. Lumped masses were chosen as the design variables to move a node where either low response is required, or to a point which makes a mode shape orthogonal to the force distribution while minimizing the total amount of added mass. Direct comparison with an optimization scheme that minimizes the generalized force indicated that nodal placement has essentially the same success.

Friedmann and Shanthakumaran (ref. 108) have used optimization techniques to directly minimize oscillatory vertical shears or roll moments at a specified advance ratio. Frequency placements and hover stability margins were used as constraints. Instead of prescribed airloads, a fully coupled flap-lag-torsion analysis was used. The example chosen was a soft inplane hingeless rotor which, when optimized, exhibited a 15-40% reduction in vibration, and was 20% lighter than the initial design (though mass was not an objective function). At a cruise condition ( $\mu = 0.30$ ) use of linear hub shears as an objective function produced both shear reductions at all advance ratios below 0.30 and hub rolling moment reductions. Nonstructural mass, used for blade tailoring, was best placed along the elastic axis for the outboard blade sections, since its impact on hub rolling moments and stability was not detrimental. The use of roll moment as the objective function with vibratory shear as the constraint proved less efficient and the optimization technique of this work offered little for a stiff inplane design in the proximity of an aeroelastic stability margin.

Empirical methods for modal tailoring have been advocated by several research organizations. Taylor (ref. 79) has presented a theoretical formulation which shows that consideration of blade mode shapes can be as important as frequency placement for vibration control. A modal shaping parameter (MSP) is derived that is a measure of blade modal vibration severity (as was discussed in the Rotor Loads Prediction

section above). When blade variables such as stiffness, mass, and mass distribution are changed to drive MSPs to low values for a prescribed loading, Taylor predicts that a lower vibration blade design will result. The Sikorsky analysis G400 was used to predict the effects of modifications to a baseline blade and calculated reductions in the root shears and the blade loads as shown in figures 45 and 46, respectively.

During a recent test of a Growth Black Hawk Rotor candidate in the Langley TDT, modal-shaping techniques were attempted on the model blade. This was done with nonstructural mass placement in an attempt to control the blade's second and third flap modes. Two independent analyses were used to alter the modal properties based on the predicted airload distributions and the predicted shears are shown in figure 47. The two analyses predict different locations for optimal mass placement and each analysis indicates that the other's prediction will be nonoptimal. An experimental program has been initiated at the U.S. Army Aerostructures Directorate and NASA Langley which will provide for parametric modal shaping tests to evaluate this passive technique further and provide a means for analysis verification.

A more complex approach to modal tailoring is presented by Yen (ref. 109) that stresses that the interaction of structural properties of a rotor with airloads distribution is a powerful tool for vibration reduction. In this approach, blade stiffnesses, as well as radial and chordwise mass distributions, are design variables. For a four-bladed hingeless rotor, for example, the primary blade modes for tailoring are cited as the second cyclic flap bending mode, which dominates the 3/rev blade root flap bending moment; the third collective flap bending mode, which drives the 4/rev blade root vertical shear; and the second cyclic chord bending mode, which influences the 5/rev blade root flap bending moment. Several design methodologies are advocated. One uses assumed airload harmonic distributions and a modal participation factor to lower the vibration contributions of offending modes. An optimum design approach is also offered with constraints on blade weight, rotational inertia, and bounds on stiffness and weight distribution. The objective function includes 4/rev shears and moments. A comparison of the reduction in root shear and moment obtained from prediction and a model test in a wind tunnel is shown in figure 48.

The feasibility of using this tailoring technique for advanced blade geometries, especially with unknown airload harmonics, provided the impetus for the Tailored Bearingless Rotor Program. This program provides for the design and fabrication of aeroelastically tailored model rotor blades for testing in the Langley TDT. The five sets of blades include two baseline rotors, one with government-designed advanced aerodynamic characteristics in terms of planform, airfoil selection, and twist. The three remaining rotors will have improved blade dynamics using the Bell "nodalization" method. One of the three "nodalized" blade sets will also have Bell-designed advanced aerodynamics characteristics. The primary purpose of this effort is to determine what effects, if any, the "nodalization" method has on rotor blades with advanced aerodynamic design. All five blade sets will be tested on the ARES model in the TDT using a Bell model bearingless rotor hub. Rotor

performance, as well as rotor and fixed-system loads, will be measured for all rotors over a wide range of test conditions.

Taylor (ref. 80) has conducted an analytical investigation to understand the importance of certain blade-design parameters on rotor response. Blade modal shaping, frequency placement, aerodynamic, structural, and intermodal couplings were examined systematically to identify vibratory sensitivity to these techniques. An example of how the various components of vibration combine has already been shown in figure 26. Taylor states several "obvious" and "nonobvious" results from his study. For example, the role of the lag mode in the 3/rev inplane shears and the canceling of the applied forcing by the inertial response is listed as an obvious result. The role of the flapping motion in forcing the example rotor's 3/rev edgewise mode is cited as a "nonobvious" result of the research effort. In looking for a consistent method to predict vibratory loads in rotor blades, Taylor concludes that nonuniform inflow is not needed in cruise to produce vibration; the rotor operating in uniform inflow is sufficient to induce vibratory loads.

#### Blade/Control Coupling for Loads Modification

Several research activities in the rotorcraft community have explored concepts which modify blade loads through direct couplings in the rotor system or decoupling devices in the rotating system. These concepts rely on prescribed blade motions effected by control designs or load alleviation attained by rotor load non-transmittal along the blade. An example of the first system, strongly supported by Army/NASA rotorcraft research, is higher harmonic control (HHC).

HHC Blade Loading- The results of wind tunnel testing of an HHC concept are described by Hammond (ref. 110). A dynamically scaled four-bladed model, incorporating harmonic pitch control, used an adaptive control system in a test in the Langley TDT. Reduced vibratory loads in the fixed system were sought by altering the loads at their source (the blade's aeroelastic environment). The vibratory forces and moments to be minimized provided inputs to the HHC algorithms being evaluated. The particular series of tests described by Hammond used the fixed-system model strain gage balance as the vibratory load sensor. The model was tested at advance ratios above 0.2, simulating 1g level flight, with the rotor trimmed to the shaft. Blade loads data obtained for  $\mu = 0.3$  were fairly consistent with previous open-loop testing in the TDT. Figure 49 shows a small reduction in the flap bending moment, a large increase in the oscillatory chord bending, and a moderate increase in the torsional moment. A possible explanation of the increase in the chord-bending moment was the close proximity of the chord-elastic mode to 6/rev which may have been aggravated by impurities in the 3/rev control inputs. Pitch link loads increased with HHC because of the 3, 4, and 5/rev input requirements as is shown in figure 50.

The goals of the wind tunnel program (reduced fixed-system vibratory loads) were largely met. This provided impetus for an HHC flight program on an OH-6A (ref. 111). In this test series, the HHC system was flown open and closed loop. In addition to the flight proof-of-concept program goals, the test scrutinized the

rotating system loads. An example is shown in figure 51 for a 70-knot level flight condition with  $\pm 0.33^\circ$  lateral blade pitch in the open-loop HHC mode. The flapwise harmonics follow the same trend with controller phase as the fixed-system vibratory loads. The chord 3 and 4/rev do also, but the 5/rev harmonic is above the baseline value, independent of controller phase.

Controllable Twist Rotor Loads- The controllable twist rotor (CTR) concept has been studied for multicyclic operation by McCloud (ref. 112). The required torsional deflections of the blade were driven by a servo flap as shown in figure 52. This theoretical work used a transfer-matrix technique with a general rotor-control code to explore the potential for altering loads. McCloud predicted that substantial reductions in fixed-system vibration could be achieved with four harmonics of servo flap control, with 2/rev controls providing most of the advantage. Adding 4/rev (instead of 3/rev excitation) reduced vibration at the expense of blade oscillatory bending loads.

Decoupler Concepts- Blade designs which prevent transmission of vibratory loads across blade stations have provided loads data for unconventional boundary conditions. An example of such a concept was tested in the Langley TDT by Hammond and Weller (ref. 113) as part of a teetering rotor, scale model investigation of stall flutter phenomena. Two sets of wide chord, 1/5 scale, teetering rotors were tested; one set had a midspan flapping hinge. As shown in figure 53 the hinge was effective in reducing the flapwise loads. This was accomplished without the blades exhibiting instability or excessive motion.

### Aerodynamic Tuning Devices

Modifying the relationship between blade aerodynamics and blade motion has been suggested as a means of altering loading mechanisms on the rotor. Several concepts have been advocated such as blade-tip shapes, vortex alleviation devices, prescribed tip motion, and blade/wake geometry variations. The vibratory loads which are impacted by such concepts are of research interest because of the (usually) controlled manner in which aerodynamic-design parameters are used.

Variable Geometry Rotor- A systematic design program was undertaken (as reported by Mantay and Rorke, ref. 114) to study the phenomena associated with blade/wake geometry, and to design a rotor which takes advantage of common aerodynamic and geometric relationships. The resulting design was the variable geometry rotor (VGR). Maneuver flight loads observed during vortex/blade interaction provided the motivation for a rotor-system design which could effect changes in the geometric relationship between a rotor and its wake. The test plan for the VGR included theoretical studies with a free wake (ref. 115), flow visualization, and model scale hover, and forward-flight wind tunnel tests (ref. 116). Further analyses simulating maneuvers (ref. 117) and a full-scale hover program (ref. 118) contributed to the design's ability to alter blade loads and performance. Parameters of interest in the above investigations are shown in figure 54.

Initial studies (ref. 115) on the VGR indicated that changes in azimuthal geometry and vertical spacing caused less excursions in harmonic loading between rotors than did other key aerodynamic parameters. Radii and collective pitch changes between rotors resulted in larger harmonic changes in certain rotor loads. These initial efforts provided the impetus for a model rotor experiment, though the driver was rotor performance, not the loads. Figure 55 shows a photograph of the VGR model in the UTRC wind tunnel. Inertial scaling for the model configurations was not matched to a representative full-scale rotor. In addition, forward-flight configurations were chosen based on hover-performance results. The measured vibration for the VGR configurations tested did not vary with  $\Delta\psi$ ,  $\Delta z$ , or with differences in blade pitch angle, and hence, provided no conclusive load-tailoring information to support the predictions made in reference 115.

When full-scale VGR hover tests (ref. 118) were conducted, no vibration or loads conclusions were drawn because of the hover mode. However, blade-tracking phenomena were observed for the configurations tested. Loads information for the VGR needed to be obtained while in forward flight on a dynamically scaled model. To prepare for this, a comprehensive analysis was conducted (ref. 117) at several advance ratios and for a symmetrical pullup condition. Blade shears, bending moments, and pitching moments were calculated using analytical tools similar to the reference 113 work.

An example of the predicted effect of VGR configuration on upper rotor-flap shear harmonics is shown in figure 56. The loading harmonics on the lower rotor were affected mainly by  $\Delta\psi$  variations. Reference 117 provided numerous examples of harmonic loadings for geometric parameter variations between the rotors and their wakes. In general, for a six-bladed VGR in a cruise condition, the lowest harmonic loads occurred for two rotors vertically separated by  $\Delta z = 1$  chord and azimuthally symmetric. In a pullup maneuver, the lowest flap shears were predicted to occur for  $\Delta\psi = 90^\circ$  for the same six-bladed rotor system.

Tip Planform- The rotor-tip region has long been recognized as critical for performance and acoustics phenomena. Many researchers have explored the effect of the blade tip's elastic, inertial, and aerodynamic characteristics on blade loads. The effects of four different tips on the performance and loads of a full-scale rotor have been studied in the Ames 40- by 80-Foot Wind Tunnel (refs. 67 and 119). The tip geometries used are shown in figure 57, and the blade layout and instrumentation are shown in figure 58. Performance and the first 10 harmonics of loads data are tabulated in reference 67. In studying the effects of the different blade tips, Rabbott and Niebanck (ref. 119) have concentrated on the control-loads information and observed that significant variations in the loads were caused by tip-planform changes. Major reductions in control-load harmonics were seen for one of the configurations (swept-tapered). In figure 59, the data show high-frequency content that was not predicted by the pretest aeroelastic analysis. Time histories of control and flap-bending moments are given in figure 60 and show that tip shape alters the advancing blade pitch-down moment and its effects on vibratory loads.

Prescribed Aerodynamic Devices- Imposing an aerodynamic loading at critical blade stations has been the impetus for several rotor designs. The free-tip rotor

is described in reference 120 and uses a tip-moment controller that applies a prescribed moment, driving the tip to a nearly constant lift. (A schematic is shown in fig. 61.) The concept was tested small scale (5.1 m diam) with interesting power and loads results. An example of inboard flap-bending moment is shown in figure 62. Harmonic analysis of these data cite 1 and 2/rev load reductions as the main cause for oscillatory load reductions, at the values of advance ratio where reductions occur. Figure 63, however, shows a substantial increase in inboard oscillatory chord moment. The free-tip concept prescribes a weathervane effect, which seems to generate lower control loads than does a fixed tip of the same (swept) planform as shown in figure 64.

Another prescribed aerodynamic concept tested for loads alleviation is the multicyclic jet-flap rotor (ref. 121). This 12 m diam, two-bladed teetering jet-flap rotor was subjected to experimental transfer functions in forward flight in the Ames 40- by 80-Foot Wind Tunnel. This was done to minimize either specific harmonic bending stresses, rms levels of those stresses, or to lower fixed-system vertical vibratory loads. It was shown that three harmonic controls could greatly reduce specific components of loads.

## GUST LOADING

Dave Brandt: ". . . to the best of your knowlege, has this analysis [for gust loading] or any analysis that's similar to this, ever designed so much as one rivet on any piece of flightworthy hardware in the helicopter industry?"

Peter Arcidiacono: "To the best of my knowledge, I think the answer is no."

- NASA SP-352, 1974

For design purposes, the effects of gusts are modeled by calculating an incremental load factor using a simplified quasi-steady theory and multiplying this incremental load factor by a gust-alleviation factor. For military aircraft, this gust-alleviation factor is specified in the helicopter structural-design specification, MIL-S-8698. The adequacy of this gust alleviation factor has been examined by comparing the predictions of the Bell Helicopter Textron analysis C81 (ref. 122) and the Sikorsky analysis Y200 (refs. 123 and 124) to simplified theory. Both the Bell and Sikorsky studies concluded that the structural specification was too conservative and that the gust-alleviation factor should be reduced. The Sikorsky study did note, however, that if blade stall was encountered, the appropriate gust-alleviation factor was increased, but the requirements of MIL-S-8698 were still considered unrealistic.

Arcidiacono et al. (ref. 124) have also summarized extensive measurements obtained on aircraft during military operations. These measurements included load factor and control positions. From the measurements it was possible to determine load factors induced by maneuvers, and load factors induced by turbulence. A comparison showed that incremental load factors caused by gusts were much less than those induced by maneuver, and the gust-induced loads represented only a small percentage of the flight experience. This is summarized in figure 65 which shows the frequency of occurrence for both gusts and maneuvers. This figure clearly shows that the rotor-design problem for military aircraft is one of specifying the maneuver loading, not the gust loading.

The emphasis of the research in gust loading over the period covered by this paper has been towards the development of calculation methods. Gaonkar (ref. 125) provides an extensive review of the gust response of helicopters and relates this to parallel work with fixed-wing models. Bir and Chopra (refs. 126 and 127) have developed a math model to represent the response of a helicopter to a deterministic gust field, and in their analysis, have included blade flap, chord, and torsional flexibility; fuselage degrees of freedom; and a dynamic inflow representation of the wake. They show that the rotor and fuselage response is sensitive to all of these parameters as well as the assumed gust field. Prussing, Lin, and their colleagues



have used a simplified rotor representation to examine the blade response to a gust where the equations are derived in stochastic form (refs. 128 and 129). This formulation, which is a more accurate representation of the physics, does not change the blade-gust response significantly.

Recent experimental research on gust loading has been limited to examining the response of a teetering helicopter to the vortex wake trailed from a fixed-wing aircraft (refs. 130 and 131). Limited correlation with the Bell C81 analysis shows fair agreement with the measurements. The analysis of Bir and Chopra (ref. 127) has been extended to treat this case as well in reference 132. The methods of extending rotor loads analyses to treat gust loads appear to be well in hand. However, the significant problems that remain in calculating rotor loads accurately under trimmed-flight conditions have prevented their extension to the problems of predicting loads or ride quality in the forward flight gust environment. It does not appear that gust loading is important in defining the vehicle load capacity. However, gust-induced loads may be important for some rotor components, especially when the rotor is stalled. Tarzanin (ref. 133) has pointed out that flight-test data used to compare with predictions are normally selected from smooth air tests and carefully checked for repeatability. If, however, data are used from flights which include turbulence, substantial load variations can be encountered. Figure 66 shows the scatter band of measured CH-47C pitch-link loads for five test flights. This is a case where the pitch-link loads are rising rapidly because of blade stall and represent a critical loading condition. Although there is no information on the actual flight conditions, the wide variation in loading suggests that the pitch link load is very sensitive to gust loading under stalled conditions.

## MANEUVER LOADING

"In the future, it may be possible to predict envelope loads completely by analytical means." - Gabel, 1973

The structural envelope for a new aircraft in terms of load factor and airspeed will look something like the sketch in figure 67. The problem of loads prediction discussed in this paper so far deals only with the loads on the rotor in trimmed, 1 g flight. In the figure, this is represented by the long dash line that extends from the maximum rearward flight speed to the forward speed at the 30-min rating of the engine,  $V_H$ . If a maneuver requirement is imposed, it might be something like maintaining a specified load factor for a specified number of seconds without losing too much airspeed. This is shown schematically in figure 67 by the heavy bar. The periphery of the envelope represents structural limits. There are other limits as well such as the engine power limit, and rotor aerodynamic limits. The power limit, which is not shown here, may be thought of as the additional load factor that could be obtained from excess power. For the case shown here, there is no excess power available at either  $V_H$  or hover; but in between, there is excess power, and the peak in excess power will correspond to the speed for minimum power. The rotor aerodynamic limit can be estimated from model tests reported by McHugh (refs. 134 and 135) where the blade lift was increased until it reversed sign and thus represents an aerodynamic limit, not a structural or actuator limit. Scaled to the V-n diagram of figure 67 the rotor lift limit is represented by the short dashed line. Operation of the rotor at any point outside these performance limits can only occur for short periods of time. For some aircraft, it may be possible to demonstrate compliance with the structural boundary only with the most extreme maneuvers. To calculate the loads for these conditions requires not only solving all the rotor load prediction problems that have been discussed previously in this paper, but also solving the transient problem, as opposed to the trimmed problem.

A number of the comprehensive analysis programs solve the equations of motions by time integration (ref. 2). Using these analyses, it is relatively straightforward to perform a transient-maneuver calculation starting from a trimmed steady state condition. Van Gaasbeek (ref. 136) has compared the C81 analysis with measurements made on an AH-1G during flight maneuvers. An example for a 2 g pull-up from autorotation is shown in figure 68. The C81 calculation shows good agreement in terms of the maximum level reached; however, there is some oscillatory behavior that is not seen in the flight-test data.

Despite the capability that exists in a number of the comprehensive analyses for calculation of maneuver loads, the normal procedure in the industry is to scale maneuver loads on the basis of previous flight-test experience (refs. 3 and 12). Gabel describes this process in considerable detail in reference 3.

The critical steps in rotor-blade design are the calculation of loads in trimmed, unaccelerated flight to insure that all loads are within material allowances for infinite fatigue life, and the assumed operational fatigue spectrum to

define what the fatigue life will be. Considering the uncertainty that remains in both of these critical areas, it is understandable that that the calculation of maneuver and gust loads has not received a great deal of attention.

## ASSESSMENT

"In fact, it can be argued that government and the helicopter industry have not optimized the basic helicopter blade design before resorting to exotic and sophisticated approaches and devices. The fundamentals of vibration have not been understood, and before radical planform changes, elastic couplings, and active control are implemented, there must be a basis of fundamental understanding based on analysis and experiment." - Taylor, 1984

This paper has reviewed the research performed in the last 13 to 14 years in the areas of rotor loads prediction and reduction. The assessment in this section seeks to put this research into perspective by addressing three topics: (1) how good are the present analyses in predicting rotor loads, (2) to what extent can rotor loads be reduced through design practice, and (3) what has the government contribution been in these areas. Inherent in this assessment is the identification of areas that require new or increased research effort.

The question of how good the present analyses are for predicting rotor loads is addressed below by examining the present predictive capability of the major rotor loads analyses as reported in the literature. In addition, the analyses are examined to identify where advances from rotor loads research have been incorporated or synthesized in the analyses. The question of the extent to which advances in rotor loads reduction have been transferred to design practice is addressed by summarizing the most productive research areas and discussing a limited number of applications that have been reviewed in the literature. Lastly, the contribution of the government is assessed indirectly in two ways. First, government support of research is estimated by tracing the number of papers and reports published. Secondly, the government development of public data bases is assessed by examining the use of these data bases.

### Rotor Loads Prediction

The 1973 AGARD meeting in Milan and the hypothetical rotor comparison of 1974 (ref. 2) provided a basis for assessing the capabilities of the rotor loads analyses of the early 1970s. The present assessment is made substantially more difficult as there has been no equivalent demonstration of the industry methods since that time. For that reason, the present judgments are based upon incidental results that have been published in the open literature. In some cases, there have been no calculations published since either the Milan meeting or the hypothetical rotor comparison.

The characteristics of present rotor loads analyses are shown in Table 1 (refs. 137-142) and this provides a useful framework for subsequent discussion. The format for the table is similar to that used in reference 2 although some of the

analyses shown in that reference are no longer in use and are not included here. The table is believed to be current as of 1986.

The history of the development of the Bell Helicopter Textron analysis C81 is covered by Bennett (ref. 5). Subsequent modification and documentation as of 1974 have been provided by Davis (ref. 143). The Army evaluated the capability of C81 to predict rotor loads for aircraft other than teetering rotors by contracting correlation studies for a hingeless rotor (ref. 144) and for articulated rotors (ref. 145). These studies revealed a number of significant limitations with C81, some of which were addressed by McLarty in the 1977 version of the analysis (ref. 146). Further modifications were made by Van Gaasbeek et al. (ref. 147) in 1979 including an option to provide the inflow distribution from a free-wake calculation as an input table. The inflow distribution is based on the free-wake analysis of Crimi (ref. 139). In reference 148 Van Gaasbeek has updated the analysis to provide an interface with DATAMAP.

Extensive comparisons have been made between the OLS measurements obtained on the AH-1G helicopter (ref. 34) and C81 (refs. 34, 149-153). In general, these show good prediction of the oscillatory loads; but the blade higher harmonics are not well-predicted, even using the free-wake analysis. Correlation with flight-test data for a prototype Model 222 with a teetering rotor (ref. 13) is shown in figures 69 and 70. The prediction of the distribution of the oscillatory flap-bending moments is good, but the oscillatory chord-bending moments are overpredicted. Figure 70 shows that the waveform behavior is not well predicted either with or without unsteady aerodynamics. This lack of C81 waveform correlation is typical for the OLS data for all blade loads (ref. 151).

The predictive capability of the C81 analysis for the four-bladed Model 412 rotor is shown in figures 71 and 72 (ref. 154). The comparison includes a configuration where a tab on the outer portion of the blade is used to provide a nose-up pitching moment. The prediction of the oscillatory blade bending moments is fairly good, although the flap-bending moments are over predicted over the middle of the span. Figure 72 shows that, although the analysis shows similar peak-to-peak levels in the pitch link load, the waveforms are different, especially in terms of higher harmonic content.

The Boeing Vertol analysis C-60 is not documented in the literature as the government has directly funded only a small part of its development. A good description of the program as it was used through the mid-1980s is given in reference 104. Recently the program has undergone two significant changes. First, it has been restructured to take advantage of current programming techniques and to make it more flexible for future use (ref. 53). Second, the blade representation is now fully coupled in flap, lag, and pitch where previously the lag degree of freedom was treated as uncoupled.

Correlation using the modified C-60 has not been published. Correlation using the older version is shown in reference 155 using data obtained during lift-limit tests of an articulated model rotor (refs. 134 and 135). Midspan flap bending and torsion moment data are compared with C-60 in figure 73. The oscillatory loads are

reasonably well predicted for both flap bending and torsion. For flap bending there is good agreement in the first harmonic, but surprisingly, the theory shows higher harmonic content that is not seen in the measurements. The torsion moment data show reasonable agreement on the advancing side of the disk in terms of amplitude and phase, but not on the retreating side.

The Kaman Aircraft Corporation presently uses three analyses: 6F, which was developed to model torsionally soft rotors with servo flaps; DYSCO, which has been designed using current structured software methods; and a version of C81 that has been modified to incorporate a servo flap (without a degree of freedom). The 6F analysis is described in reference 156. (There is no recent correlation published.) The DYSCO analysis (ref. 157) is designed as a general method to couple and analyse the dynamic behavior of individual components. No rotor loads correlation has been published.

McDonnell Douglas Helicopter Company has used three analyses in recent years: DART, which has evolved from the SADSAM analysis; RAVIB, which has evolved from analyses developed at Rochester Applied Science Associates (RASA) in the mid-1970s; and RACAP, which is an entirely new development. The DART analysis is not described in the literature, nor are there any recent published comparisons of DART predictions and measured rotor loads. RACAP is expected to become the primary loads analysis for McDonnell Douglas, but as of yet details of its development and comparisons with rotor loads measurements have not been published.

The RAVIB analysis has been described by Gangwani in reference 32 and correlation with the AH-1G OLS data (ref. 34) is shown in figure 74. For the correlation shown here the model uses a free-wake analysis based on Sadler (ref. 115). In the figure, the flight-test data are compared with a conventional aerodynamics model without dynamic stall and Gangwani's synthesized stall model (ref. 30). The flap-bending moment comparison shows good agreement with the 1/rev load, but does not show good agreement at the higher harmonics. The strong 3/rev loading seen in the chord bending is fairly well predicted regardless of the aerodynamic model used. The blade-torsion moments are only poorly predicted with the conventional aerodynamic model, but the dynamic stall results show much better agreement. Calculations with C81 for similar flight cases (ref. 151) show chord bending and torsion moment waveforms that bear little relationship to the measurements shown here.

Sikorsky Aircraft currently uses three analyses for rotor loads: the Normal Modes Analysis, Y201; G400 as part of the SIMVIB package; and RDYNE, which is a recent development. The Y201 analysis was used for the calculations at the 1973 Milan meeting and for the hypothetical rotor comparison. Modifications have since been made to the aerodynamic model to correct for yawed flow and swept tips. A panel method can be used to represent the fuselage and calculate inflow at the rotor disk which is induced by the fuselage. A new analysis, G400, was developed at the United Technology Research Center in the mid-1970s under government funding. This analysis was designed to model bearingless rotors and is described in references 158-160. It is now incorporated in the SIMVIB executive and can be used for the prediction of vibration as well as rotor loads (ref. 88). Although G400 uses numerical integration to solve the equations of motion, only the harmonic response

is used in the SIMVIB computations. The newest analysis at Sikorsky is RDYNE (ref. 161). It uses a component coupling structure that is the same as SIMVIB, but uses numerical integration to solve the equations. It appears that RDYNE will soon become the primary-loads analysis tool at Sikorsky, and Y201 and G400 will no longer be supported.

The Y201 analysis has been compared with flight-test data and wind tunnel data by Jepson et al. (ref. 66). The wind tunnel data are reported in reference 67. The flight-test and wind tunnel data are quite similar, although the higher harmonic loads are greater for the flight vehicle as was shown in figure 22. Figure 75 compares the radial distribution of the oscillatory flap and chord bending moments as measured in flight and as calculated with the Y201 analysis. The prediction using constant inflow is quite close to the measurements outboard of 0.30R for the flap-bending moment, but neither inflow model gives good results for the chord-bending moments. The variable inflow model is based on a prescribed wake and predicts the oscillatory bending moments quite poorly. It is both surprising and disappointing that increasing sophistication in the inflow model causes the correlation to degrade. The azimuthal time history for these moments, plus the pitch link load, is shown in figure 76. Even if the amplitude were to increase to match the flight test data, the harmonic character would not be matched.

The analysis G400 has been compared with model bearingless rotor data in reference 158. Limited comparisons of oscillatory bending moments have been made in reference 88 using G400 as a part of SIMVIB. However, there is no recent correlation that allows the azimuthal behavior of the analysis to be judged. No correlation has been published for rotor loads using RDYNE.

Johnson has described the development of a comprehensive rotorcraft analysis in references 162-164. The predictions of this analysis, now referred to as CAMRAD, are compared with flight test data obtained on the SA 349-2 in reference 50. Figure 77 compares the lift coefficient obtained from pressure measurements at 0.75R with the prediction of CAMRAD for a high-speed case. The predictions show good agreement with the measurements, except for some high frequency oscillations that are seen on the retreating side of the disk where the velocity is low. The calculations shown here were made with a prescribed wake. Calculation with a free wake showed little difference, but both gave better results than calculation using uniform inflow. The correlation for rotor loads is shown in figure 78 for this case. The predicted flap bending shows good agreement with the measurements for this station, but the chord bending shows a great deal of 5/rev response that is not seen in the data. The oscillatory pitch-link loads are overpredicted by CAMRAD, and the agreement in waveform is not particularly good.

The results presented in the 1973 Milan AGARD meeting and in the 1974 hypothetical rotor comparison indicated that the available rotor loads analyses could make reasonable predictions of oscillatory rotor-blade loads. These loads are important for the fatigue design of the rotor blade and control system. It seems to be generally accepted that the scatter in predictions that was calculated for the hypothetical rotor and is shown in figure 6 represents a worst case (or outer bound) on the prediction methods. Within each company, it is felt that the oscillatory loads can

be predicted with better accuracy if a new design does not differ too much from previous designs. However, the results shown here suggest that even for the prediction of oscillatory loads significant differences do occur and are not understood. It does not appear that oscillatory loads can be predicted with any more confidence now than in 1973.

An examination of the correlation for rotor load waveforms or time histories suggests that the basic physics of the problem are not accurately modeled by any of the rotor loads analyses. Even when the amplitude of the first harmonic load is reasonably well-predicted, the phase is not. The correlation for higher harmonics appears worse, but here it is difficult to make judgments as the waveform behavior is normally dominated by the first and second harmonics, and this obscures the higher harmonic behavior. There appears to have been some progress in the analysis of separate parts of the problem; a great deal has been learned about dynamic stall and wake induced velocities. But the various pieces of the problem have not gone back together correctly; there has been no improvement in the synthesis.

The major features of the present rotor loads analyses came into place in the early 1970s with the incorporation of dynamic stall and unsteady aerodynamics in most of the analyses. Since then, there have been minor improvements and upgrades to most of these analyses, but with the exception of the addition of the calculation of fuselage induced inflow to Y201 and CAMRAD, there has been no change to these analyses to improve their ability to represent the physics of the rotor loads problem.

Computation speed has increased by at least a factor of 50 over this time period and available computational capability does not appear to have hindered development of improved analyses. What does appear to have limited advances in the prediction of rotor loads is the twofold perception that, first, the prediction of oscillatory loads is adequate, and, second, vibratory loads cannot be predicted by anyone for the foreseeable future. That perception will not change until the accurate prediction of vibratory loads is demonstrated.

### Rotor Loads Reduction

The application of the conformable or compliant rotor has, to a degree, preceded the research into the ACR concept. The tip shape of the S-76 which first flew in March 1977, was selected in part to reduce the control loads (ref. 165). The S-76 swept/tapered tip does show a reduction in control loads for most thrust and airspeed conditions when compared to other blade tips, as was shown in tests in the 40- by 80-Foot Wind Tunnel (refs. 119 and 67). The research efforts that followed and that have been reviewed in this paper, examined blades that are, in general, much softer in torsion than the S-76. As yet, the best combination of tip design and torsional stiffness for reduced loads is unclear; what is necessary here are further experimental and theoretical efforts.

The ACR research has demonstrated that pitching-moment changes induced by a tab deflection can have a significant effect on the rotor loads and this approach has



been used during a number of recent development programs after high vibratory loads were encountered in initial flight tests. Yen and Weller (ref. 154) report the application of negative camber to reduce steady and oscillatory rotor loads encountered in the development of the Bell Model 412 rotor. During development flight testing, it was determined that the steady pitch-link loads were higher than predicted and this limited maximum up collective during boost-off operation. In addition, the oscillatory flap bending and torsion moments were higher than predicted. They examined the effects of negative camber on rotor loads using the C81 analysis based on the test experience with conformable rotors reported by Blackwell *et al.* (ref. 77). This work suggested that the loads could be reduced for the Model 412 rotor, and as a consequence, they added a 1.25 in. tab between 0.80 and 0.87R with the tab set to  $-12^\circ$  (trailing edge up). This resulted in approximately a 40% reduction in the steady pitch link loads, a 40% reduction in the oscillatory blade torsion loads, and a 15% reduction in the oscillatory flap-bending loads.

Gupta (ref. 166) has reported on vibration and loads problems that were encountered during the testing of a Composite Main Rotor Blade (CMRB) for the McDonnell Douglas AH-64. Unlike the Model 412 rotor, there was a steady positive torsion moment on the blade, and positive camber was used to reduce the steady torsion load, and this also reduced the vibration. It was also determined that the vibration could be reduced by reducing the tip thickness. Although it is stated that the DART analysis was used during this investigation, no examples of its predictive capability are given.

Yen and Tanner (ref. 167) discussed development tests of a Composite Main Rotor Blade (CMRB) for the UH-1 aircraft. The design goal was to significantly improve the performance of the blade without changing the dynamics. Design calculations using C81 showed that the CMRB 2/rev hub shears were substantially higher than on the metal blade. A number of design changes were examined and two were selected: a chordwise c.g. shift and a reduction in nonlinear twist. Calculation showed that this reduced the hub shears, but they were still higher than for the metal blade. When the CMRB was flight tested, the predictions of C81 were borne out as the cockpit vibration was significantly higher. To reduce the vibratory shears, a tab was added outboard and this was able to reduce the vibratory loads back to the level of the metal blades. It is not clear at this time whether the original performance goals of this rotor can be met following the modifications that have been made necessary by the high vibratory loads.

Research into the potential for loads reduction through mass and stiffness distribution changes has shown great promise. Yen (ref. 109) has described a number of approaches used at Bell including the classical frequency-separation approach, a preliminary design method that calculates root shears based on assumed airloads, and a formal optimization approach. The newer approaches have shown considerable promise for model-scale data (fig. 48) and these techniques will be applied on the next generation of rotors at Bell. Similar techniques have also been applied at Westland for the British Experimental Rotor Program (BERP) rotor as described by Hansford (ref. 168) and have shown a substantial reduction in vibratory loads. These

successes suggest that the design for vibratory load reduction will become more important in the preliminary and detail design process for new rotor developments.

The research into loads reduction using mechanical or electrical feedback has been relatively inconsequential over the last decade with the exception of higher harmonic control (HHC). The demonstration programs to date have shown that HHC is a very powerful means of loads control, but any future applications will be directed toward vibration reduction in the cockpit.

Recent research into new rotor configurations that include loads reductions as a benefit has been done in the period covered by this paper. This includes the jet-flap rotor, the variable geometry rotor, and the free-tip rotor. However, at this time only the latter concept is being pursued.

#### Government Support of Rotor Loads Research

The government support of rotor loads research is assessed in two ways. First, research funding is examined in terms of its output; that is, published papers and reports. Second, the value of government-supported data bases is assessed by examining their use in research. Neither of these measures is comprehensive nor exact; such a metric does not exist. However, they do provide a useful framework for a discussion of the government role in rotor loads research.

The results of government research funding can be assessed by tracking the number of research reports and papers published each year that were funded under government contract or grant. All papers examined as part of this review are included (not all cited) with the exception of survey or summary papers. The data are filtered using a 3-year running average and are shown in figure 79. The number of papers published tends to be cyclical depending on the technical meetings being held each year. In general, the number of papers or reports being published each year is holding constant and, hence, the funding for rotor loads is assumed to have been holding relatively constant. Research into load-reduction methods appears to use a quarter to a third of the resources applying the measure used here.

The government contribution to rotor loads research appears to have held fairly constant over the last decade. A major transition that has occurred, however, is that the government investment in comprehensive analyses is now largely restricted to programs that have been (or are being) developed internally, that is, CAMRAD and the Second Generation Comprehensive Helicopter Analysis System (2GCHAS). The government has made a major contribution in the past to the development of a number of the comprehensive models used by industry and has attempted to transform some of these analyses into well-documented, general-purpose analyses that could be used by both industry and the government. This effort to develop a public domain, comprehensive model based on an industry code has not been successful. As a consequence, the government is proceeding with the development of 2GCHAS with industry participation. Although CAMRAD was developed more by individual initiative than government plan, its continued development represents an essential part of research in the

rotor loads area at least until 2GCHAS is operational and has demonstrated that it can support future progress in this area.

The second measure that is used to gauge government support of rotor loads research is the development of rotor loads data bases. Research in rotor loads and a means of reducing rotor loads has been continuously guided by experimentation. Data obtained in flight tests or wind tunnel tests have been used to improve the capability to predict rotor loads and to find methods to reduce rotor loads. The effort and expense of obtaining a set of data may be justified by the immediate answers that are provided by the data, or in some cases, the major justification for the data is its long-term value in the form of a data base.

The government makes a major contribution to research in rotor loads either by funding or performing the experiments that lead to the development of data bases. The experimental data and data bases may be used in many ways and this use is sometimes published and sometimes kept proprietary. For this assessment, it is only possible to examine the published uses of data. Although the limitations of this approach are recognized, the approach is still considered useful.

The experimental data obtained over the period covered by this paper were examined, and if the data were provided either in tabulated form or on a formatted tape, then the data were considered to constitute a data base. Nine data bases were found and these are listed in Table 2 (refs. 169-175). Most of these data bases were used by the original investigators, at least to a limited extent, and this use is referred to as a "primary reference." If the data base was subsequently used by another investigator, then that use is referred to as a "secondary reference." Of the nine data bases, only one has been used regularly by subsequent investigators and that is the AH-1G OLS flight-test data base.

All of the data bases in Table 2 were funded by the government except for the SA 349-2 flight-test data base. The use of the AH-1G OLS flight test-data by subsequent users is clearly a success, but the lack of use of the other data bases is discouraging. It is recognized, as noted above, that the published use of a data base is not its only justification. Unpublished use of a data base to guide proprietary design or aircraft development may justify the expense of developing that data base. In addition, a well-documented data base may prove valuable for many years, and the lack of initial use does not mean that the data base may not become very useful. No better example of this facet of data base use can be seen than in Hooper's comparison of data bases many years after they were obtained (ref. 40). However, it is unclear whether the use of the government-developed data bases justifies the expense in creating them. Certainly the development of new data bases should not be undertaken without a substantial expectation of their future use.

Table 2 evaluates only the use of data bases developed during the time frame of this paper. A related question is what has been the use of all data bases during the past 13-14 years, not just the recently developed ones. This question is examined by looking only at a subset of available data bases, those that include both surface-pressure measurements and blade-moment measurements. The nine data bases that fall into this category are shown in Table 3 (refs. 176-180). First, all use

of these data bases in the time frame of the paper are categorized as "references." Secondly, when the data base was used by an organization other than the test aircraft manufacturers, then this is referred to as a "non-self reference." Of the nine major data bases, two have never been used. These are the CH-47A and AH-1G TAAT data bases for which tabulated data were never provided and the data on tape have been too difficult of access to encourage use. The UH-1 and XH-51A aircraft data bases have had only limited use in recent years. The NH-3A and CH-53A data bases have had fairly extensive use, but only by the aircraft manufacturer. Of the nine data bases, only three appear to be in widespread use--the CH-34 flight test, the CH-34 wind tunnel test, and the AH-1G OLS flight test. The development of a major rotor loads data base is clearly expensive, but the use that these data bases will be put to is never so clear.

An alternative approach of assessing the use of data bases is to compare the use of proprietary data bases with those that have been developed and supported by the government. Again, the basis for comparison is imperfect as only the published literature is used to judge comparative use. Sixty-five references to full-scale, flight-test data were noted in preparing this paper. Of these 60% referenced a government-developed data base, while the other 40% referenced company proprietary data bases. The use of proprietary data bases is, of course, much more significant for unpublished work. What governs the choice of a data base is not completely clear. However, it does appear that there are at least three primary factors: (1) ease of access to the data base, (2) test documentation, and (3) validation of the data. These factors are more easily accommodated in the development of a proprietary data base than a public one.

## CONCLUSIONS

The present paper has reviewed the research that has been performed in the area of rotor loads in the 13 to 14 year period since the 1973 AGARD Milan meeting and the 1974 hypothetical rotor comparison. The conclusions of this review are:

1. The detailed predictive capability of the present rotor loads analyses is barely satisfactory for the prediction of oscillatory loads. It is not satisfactory for the prediction of vibratory loads.

2. There is a pressing need for an improved rotor loads predictive capability within the government. At the present time, there is no clear evidence of what the major limitations are of the current rotor loads analyses for the prediction of vibratory loads. This information cannot be obtained without a systematic comparison of prediction and measurement using CAMRAD now, and 2GCHAS when it becomes available.

3. There is a significant need for quality data including blade-pressure measurements and extensive and complete structural measurements. Maximum efforts should be made to insure that the data are valid during both the experiment and the data-reduction process. In the case of aircraft flight test, there must be a commitment of open test time for subsequent tests. Development of data bases should proceed only if there is a firm, long-range program to use the data within the government.

4. The research in rotor loads reduction has demonstrated that there is a substantial potential for reduced vibratory loads in new rotor design. However, clear design guidelines have not been developed from research performed to date. Additional theoretical and experimental work is needed to understand the sources and mechanisms of vibration.

## RECOMMENDATIONS

As a result of this survey it is recommended that:

1. The government should continue the development of its own comprehensive rotor analyses, specifically CAMRAD, which is operational, and 2GCHAS, which is under development. It is important that this work be done by the government using their best analysts.
2. Systematic comparisons of theory and experiment for rotor loads should be expanded. These comparisons should specifically examine the behavior of the vibratory loads for harmonics three and higher.
3. A program of theoretical model testing should be started using CAMRAD. The objective of this testing should be to compare the relative merits of alternative theoretical models using experimental data where possible to discriminate between approaches.
4. The government should initiate a program of full-scale rotor testing with limited blade surface pressure instrumentation to support the development of rotor loads analyses and theoretical-model testing. This program should be considered complementary to the fully-instrumented rotor tests that are presently being planned.

## REFERENCES

1. Rabbott, J. P., Jr.; Lizak, A. A.; and Paglino, V. M.: A Presentation of Measured and Calculated Full-Scale Rotor Blade Aerodynamic and Structural Loads. USAAVLABS TR 66-31, 1966.
2. Ormiston, Robert A.: Comparison of Several Methods for Predicting Loads on a Hypothetical Helicopter Rotor. NASA SP-352, 1974.
3. Gabel, Richard: Current Loads Technology for Helicopter Rotors. AGARD Conf. Proc. No. 122, Mar. 1973.
4. Arcidiacono, Peter J.; and Carlson, Raymond G.: Helicopter Rotor Loads Prediction. AGARD Conf. Proc. No. 122, Mar. 1973.
5. Bennett, Richard L.: Rotor System Design and Evaluation Using a General Purpose Helicopter Flight Simulation Program. AGARD Conf. Proc. No. 122, Mar. 1973.
6. Piziali, R. A.: Rotor Aeroelastic Simulation--A Review. AGARD Conf. Proc. No. 122, Mar. 1973.
7. Loewy, Robert G.: Summary Analysis. AGARD Conf. Proc. No. 122, Mar. 1973.
8. Arcidiacono, Peter J.; and Sopher, Robert: Review of Rotor Loads Prediction Methods. AGARD Conf. Proc. No. 334, May 1982.
9. Johnson, Wayne: Recent Developments in the Dynamics of Advanced Rotor Systems. NASA TM 86669, 1985.
10. Friedmann, P. P.: Formulation and Solutions of Rotary-wing Aeroelastic Stability and Response Problems. Vertica, vol. 7, 1983, pp. 101-104.
11. Friedmann, P. P.: Recent Trends in Rotary-Wing Aeroelasticity. Paper No. 55, Twelfth Eur. Rotorcraft Forum, Sept. 1986.
12. Johnson, Wayne: Recent Developments in Rotary-Wing Aerodynamic Theory. AIAA Journal, vol. 24, Aug. 1986, pp. 1219-1244.
13. Yen, Jing G.; and Glass, Max: Helicopter Rotor Load Prediction. Preprint No. 6, Amer. Hel. Soc. Specialists Meeting on Helicopter Fatigue Methodology, Mar. 1980.
14. Dadone, L.: The Role of Analysis in the Aerodynamic Design of Advanced Rotors. AGARD Conf. Proc. No. 334, May 1982.

15. Landgrebe, A. J.: Overview of Helicopter Wake and Airloads Technology. Amer. Hel. Soc./Nanjing Aero. Inst. International Seminar--The Theoretical Basis of Helicopter Technology, Nov. 1985. Also: Paper No. 18, Twelfth Eur. Rotorcraft Forum, Sept. 1986.
16. McCroskey, W. J.; and Fisher, Richard K., Jr.: Detailed Aerodynamic Measurements on a Model Rotor in the Blade Stall Regime. J. Amer. Hel. Soc., vol. 17, no. 1, Jan. 1972, pp. 20-30.
17. Johnson, Wayne: Comparison of Three Methods for Calculation of Helicopter Rotor Blade Loading and Stresses Due to Stall. NASA TN D-7833, 1974.
18. Carta, F. O.; Casellini, L. M.; Arcidiacono, P. J.; and Elman, H. L.: Analytical Study of Helicopter Rotor Stall Flutter. Amer. Hel. Soc. 26th Annual National Forum, May 1970.
19. Arcidiacono, P. J.; Carta, F. O.; Casellini, L. M.; and Elman, H. L.: Investigation of Helicopter Control Loads Induced by Stall Flutter. USAAVLABS TR 70-2, 1970.
20. Johnson, Wayne: The Effect of Dynamic Stall on the Response and Airloading of Helicopter Rotor Blades. J. Amer. Hel. Soc., vol. 14, no. 2, Apr. 1969, pp. 68-79.
21. Johnson, Wayne: The Response and Airloading of Helicopter Rotor Blades Due to Dynamic Stall. Massachusetts Institute of Technology, ASRL TR 130-1, May 1970.
22. Gormont, Ronald E.: A Mathematical Model of Unsteady Aerodynamics and Radial Flow for Application to Helicopter Rotors. USAAMRDL TR 72-67, 1973.
23. Carlson, R. G.; Blackwell, R. H.; Commerford, G. L.; and Mirick, P. H.: Dynamic Stall Modeling and Correlation with Experimental Data on Airfoils and Rotors. NASA SP-352, 1974.
24. Blackwell, R. H.; and Commerford, G. L.: Investigation of the Effects of Blade Structural Design Parameters on Helicopter Stall Boundaries. USAAMRDL TR 74-25, 1974.
25. McCroskey, W. J.: Prediction of Unsteady Separated Flows on Oscillating Airfoils. AGARD Lecture Series No. 94, 1978.
26. McAllister, K. W.; Carr, L. W.; and McCroskey, W. J.: Dynamic Stall Experiments on the NACA 0012 Airfoil. NASA TP 1100, 1977.
27. Beddoes, T. S.: A Synthesis of Unsteady Aerodynamics Stall Effects, Including Hysteresis. Paper No. 17, First European Rotorcraft and Powered Lift Aircraft Forum, Sept. 1975.



28. Ericsson, L. E.; and Reding, J. P.: Dynamics Stall Analysis in the Light of Recent Numerical and Experimental Results. *J. Aircraft*, vol. 13, Apr. 1976, pp. 248-255.
29. Gangwani, Santu T.: Prediction of Dynamic Stall and Unsteady Airloads for Rotor Blades. *J. Amer. Hel. Soc.*, vol. 27, no. 4, Oct. 1982, pp. 57-64.
30. Gangwani, Santu T.: Synthesized Airfoil Data Method for Prediction of Dynamic Stall and Unsteady Airloads. NASA CR 3672, 1983.
31. Gangwani, Santu T.: Synthesized Airfoil Data Method for Prediction of Dynamic Stall and Unsteady Airloads. *Vertica*, vol. 8, 1984, pp. 93-118. Also: *Amer. Hel. Soc. 39th Annual Forum Proceedings*, May 1983, pp. 15-33.
32. Gangwani, Santu T.: Development of an Unsteady Aerodynamics Model to Improve Correlation of Computed Blade Stresses With Test Data. Paper No. 8, *Amer. Hel. Soc./NASA 2nd Decennial Specialists' Meeting on Rotorcraft Dynamics Proceedings*, Nov. 1984. Also: NASA CP 2400, 1985.
33. Sutton, L. R.; and Gangwani, S. T.: The Development and Application of an Analysis for the Determination Coupled Tail Rotor/Helicopter Air Resonance Behavior. USAAMRDL TR 75-35, 1975.
34. Shockey, Gerald A.; Cox, Charles R.; and Williamson, Joe W.: AH-1G Helicopter Aerodynamic and Structural Loads Survey. USAAMRDL TR 76-39, 1977.
35. Tran, C. T.; and Petot, D.: Semi-Empirical Model for the Dynamic Stall of Airfoils in View of the Application to the Calculation of Response of a Helicopter Blade in Forward Flight. Paper No. 48, *Sixth Eur. Rotorcraft and Powered Lift Aircraft Forum*, Sept. 1980.
36. Peters, David A.: Toward a Unified Aerodynamic Model for Use in Rotor Blade Stability Analyses. *Amer. Hel. Soc. 40th Annual Forum Proceedings*, May 1984, pp. 525-538.
37. Wilby, P. G.; Young, C.; and Grant, J.: An Investigation of the Influence of Fuselage Flow Field on Rotor Loads and the Effects of Vehicle Configuration. *Vertica*, vol. 3, 1979, pp. 79-94. Also: Paper No. 8, *Fourth European Rotorcraft and Powered Lift Aircraft Forum*, Sept. 1978.
38. Brotherhood, P.; and Riley, M. J.: Flight Experiments on Aerodynamic Features Affecting Helicopter Blade Design. *Vertica*, vol. 2, 1978, pp. 27-42.
39. Costes, J. J.: Unsteady Three-Dimensional Stall on a Rectangular Wing. Paper No. 30, *Twelfth Eur. Rotorcraft Forum*, Sept. 1986.

40. Hooper, W. E.: The Vibratory Airloading of Helicopter Rotors. Vertica, vol. 8, 1984, pp. 71-92. Also: Paper No. 46, Ninth Eur. Rotorcraft Forum, Sept. 1983.
41. Scheiman, James: A Tabulation of Helicopter Rotor-Blade Differential Pressures, Stresses, and Motions as Measured in Flight. NASA TM X-952, 1964.
42. Johnson, Wayne: Helicopter Theory. Princeton University Press, 1980.
43. Brotherhood, P.: An Appraisal of Rotor Blade-Tip Vortex Interaction and Wake Geometry from Flight Measurements. AGARD Conf. Proc. 134, May 1982.
44. Landgrebe, A. J.; and Bellinger, E. D.: An Investigation of the Quantitative Applicability of Model Helicopter Rotor Wake Patterns Obtained from a Water Tunnel. USAAMRDL TR 71-69, Dec. 1971.
45. Lehman, A. F.: Model Studies of Helicopter Rotor Flow Patterns. USAAVLABS TR 68-17, Apr. 1968.
46. Johnson, Wayne: Comparison of Calculated and Measured Model Rotor Loading and Wake Geometry. NASA TM 81189, 1980.
47. Biggers, James C.; Lee, Albert; Orloff, Kenneth L.; and Lemmer, Opal J.: Laser Velocimeter Measurements of Two-Bladed Helicopter Rotor Flow Fields. NASA TM 73238, 1977.
48. Egolf, T. A.; and Landgrebe, A. J.: Helicopter Rotor Wake Geometry and Its Influence in Forward Flight, Volume I - Generalized Wake Geometry and Wake Effect on Rotor Airloads and Performance. NASA CR 3726, 1983.
49. Egolf, T. A.; and Landgrebe, A. J.: Generalized Wake Geometry for a Helicopter Rotor in Forward Flight and Effect of Wake Deformation on Airloads. Amer. Hel. Soc. 40th Annual Forum Proc., May 1984, pp. 359-376.
50. Yamauchi, Gloria K.; Heffernan, Ruth M.; and Gaubert, Michel: Correlation of SA349/2 Helicopter Flight Test Data with a Comprehensive Rotorcraft Model. NASA TM 88351, 1987. Replaces Paper No. 74, Twelfth Eur. Rotorcraft Forum, Sept. 1986.
51. Rabbott, J. P., Jr.; Lizak, A. A.; and Paglino, V. M.: Tabulated CH-34 Blade Surface Pressures Measured at NASA/Ames Full Scale Wind Tunnel. SER-58399, Dec. 1965.
52. Miller, R. H.: Factors Influencing Rotor Aerodynamics in Hover and Forward Flight. Vertica, vol. 9, 1985, pp. 155-164. Also: Paper No. 11, Tenth Eur. Rotorcraft Forum, Aug. 1984.

53. Phelan, P. G.; and Tarzanin, F. J., Jr.: Restructuring the Rotor Analysis Program C-60. Paper No. 12, Amer. Hel. Soc./NASA 2nd Decennial Specialists' Meeting on Rotorcraft Dynamics Proceedings, Nov. 1984. Also: NASA CP 2400, 1985.
54. Heffernan, R.; and Gaubert, M.: Structural and Aerodynamic Loads and Performance Measurements of an SA349/2 Helicopter with an Advanced Geometry Rotor. NASA TM 88370, 1986.
55. Cowan, John; Dadone, Leo; and Gangwani, Santu: Wind Tunnel Test of a Pressure Instrumented Model Scale Advanced Rotor. Amer. Hel. Soc. 42nd Annual Forum Proceedings, June 1986, pp. 217-229.
56. Young, C.: Development of the Vortex Ring Wake Model and Its Influence on the Prediction of Rotor Loads. AGARD Conf. Proc. No. 334, May 1982.
57. Costes, J. J.: Calcul des Forces Aerodynamiques Instationnaires sur les Pales d'un Rotor d'Helicoptere. La Recherche Aerospatiale, No. 1972-2, 1972. Also: NASA TT F-15039, 1973.
58. Runyan, Harry L.; and Tai, Hsiang: Application of a Lifting Surface Theory for a Helicopter in Forward Flight. Paper No. 24, Eleventh Eur. Rotorcraft Forum, Sept. 1985.
59. Pierce, G. Alvin; and Vaidyanathan, Arnand R.: Helicopter Rotor Loads Using Discretized Matched Asymptotic Expansions. NASA CR 166092, May 1983.
60. Van Holten, Th.: On the Validity of Lifting Line Concepts in Rotor Analysis. Vertica, vol. 1, 1977, pp. 239-254.
61. Caradonna, F. X.; and Tung, C.: A Review of Current Finite Difference Rotor Flow Methods. Amer. Hel. Soc. 42nd Annual Forum Proceedings, June 1986, pp. 967-983.
62. Tung, Chee; Caradonna, Francis X.; and Johnson, Wayne R.: The Prediction of Transonic Flows on Advancing Rotors. J. Amer. Hel. Soc., vol. 31, no. 3, July 1986, pp. 4-9. Also: Amer. Hel. Soc. 40th Annual Forum Proceedings, May 1984, pp. 389-399.
63. Gabel, Richard: Rotor Mast Height. NASA CP 2400, 1985.
64. Freeman, Carl E.; and Wilson, John C.: Rotor-Body Interference (ROBIN) - Analysis and Test. Preprint No. 80-5, Amer. Hel. Soc. 36th Annual Forum, May 1980.
65. Huber, H.; and Polz, G.: Studies on Blade-to-Blade and Rotor-Fuselage-Tail Interferences. AGARD Conf. Proc. No. 334, May 1982.

66. Jepson, D.; Moffitt, R.; Hilzinger, K.; and Bissell, J.: Analysis and Correlation of Test Data From an Advanced Technology Rotor System. NASA CR 3714, 1983.
67. Johnson, Wayne: Performance and Loads Data on a Full-Scale Rotor with Four Tip Planforms. NASA TM 81229, 1980.
68. Johnson, Wayne; and Yamauchi, G. K.: Applications of an Analysis of Axisymmetric Body Effects on Rotor Performance and Loads. Paper No. 3, Tenth Eur. Rotorcraft Forum, Aug. 1984.
69. Yamauchi, Gloria; and Johnson, Wayne: Development and Application of an Analysis of Axisymmetric Body Effects on Helicopter Rotor Aerodynamics Using Modified Slender Body Theory. NASA TM 85934, 1984.
70. McKenzie, K. T.; and Howell, D. A. S.: The Prediction of Loading Actions on High Speed Semirigid Rotor Helicopters. AGARD Conf. Proc. No. 122, Mar. 1973.
71. Taylor, Robert B.; and Teare, Paul A.: Helicopter Vibration Reduction with Pendulum Absorbers. J. Amer. Hel. Soc., vol. 20, no. 3, July 1975, pp. 9-17.
72. Blackwell, R. H., Jr.: Blade Design for Reduced Helicopter Vibration. J. Amer. Hel. Soc., vol. 28, no. 3, July 1983, pp. 33-41. Also: Preprint No. 8, Amer. Hel. Soc. Specialists' Meeting on Helicopter Vibration, Nov. 1981.
73. Gaukroger, D. R.; and Hassal, C. J. W.: Measurement of Vibratory Displacements of a Rotating Blade. Vertica, vol. 2, 1978, pp. 111-120.
74. Gaukroger, D. R.; Payen, D. B.; and Walker, A. R.: Application of Strain Gauge Pattern Analysis. Paper No. 19, Sixth European Rotorcraft and Powered Lift Aircraft Forum, Sept. 1980.
75. Blackwell, R. H.; and Mirick, P. H.: Effect of Blade Design Parameters on Helicopter Stall Boundaries. Preprint No. 833, Amer. Hel. Soc. 30th Annual National Forum, May 1974.
76. Blackwell, R. H., Jr.; and Fredrickson, K. C.: Wind Tunnel Evaluation of Aeroelastically Conformable Rotors. USAAVRADCOM TR 80-D-32, 1981.
77. Blackwell, R. H.; Murrill, R. J.; Yeager, W. T., Jr.; and Mirick, P. H.: Wind Tunnel Evaluation of Aeroelastically Conformable Rotors. J. Amer. Hel. Soc., vol. 26, no. 2, Apr. 1981, pp. 31-39. Also: Preprint No. 80-23, Amer. Hel. Soc. 36th Annual Forum, May 1980.

78. Kottapalli, S. B. R.: Hub Loads Reduction by Modification of a Blade Torsional Response. Amer. Hel. Soc. 39th Annual Forum Proceedings, May 1983, pp. 173-179.
79. Taylor, Robert B.: Helicopter Vibration Reduction by Rotor Blade Modal Shaping. Amer. Hel. Soc. 38th Annual Forum Proceedings, May 1982, pp. 90-101.
80. Taylor, Robert B.: Helicopter Rotor Blade Design for Minimum Vibration. NASA CR 3825, 1984.
81. Esculier, Jacques; and Bousman, William G.: Calculated and Measured Blade Structural Response on a Full-Scale Rotor. Amer. Hel. Soc. 42nd Annual Forum Proceedings, June 1986, pp. 81-110.
82. Lee, B. L.: Experimental Measurements of the Rotating Frequencies and Mode Shapes for a Full Scale Helicopter Rotor in a Vacuum and Correlations with Calculated Results. Preprint No. 79-18, Amer. Hel. Soc. 35th Annual National Forum, May 1979.
83. Srinivasan, A. V.; Cutts, D. G.; and Shu, H. T.: An Experimental Investigation of the Structural Dynamics of a Torsionally Soft Rotor in Vacuum. NASA CR 177418, 1986.
84. Sharpe, David L.: An Experimental Investigation of the Flap-Lag-Torsion Aeroelastic Stability of a Small-Scale Hingeless Helicopter Rotor in Hover. NASA TP 2546, 1986.
85. Yen, Jing G.; and McLarty, Tyce T.: Analysis of Rotor-Fuselage Coupling and Its Effect on Rotorcraft Stability and Response. Vertica, vol. 3, 1979, pp. 205-219.
86. Lee, Charles D.; and White, James A.: Investigation of the Effect of Hub Support Parameters on Two-Bladed Rotor Oscillatory Loads. NASA CR-132435, 1974.
87. Sopher, Robert; and Kottapalli, S. B. R.: Correlation of Predicted Vibrations and Test Data for a Wind Tunnel Helicopter Model. Amer. Hel. Soc. 38th Annual Forum Proceedings, May 1982, pp. 102-113.
88. Sopher, Robert; Studwell, R. E.; Cassarino, S.; and Kottapalli, S. B. R.: Coupled Rotor/Airframe Vibration Analysis. NASA CR 3582, 1982.
89. Gabel, Richard; and Sankewitsch, Vladimir: Rotor-Fuselage Coupling by Impedance. Amer. Hel. Soc. 42nd Annual Forum Proceedings, June 1986, pp. 1-11.
90. Harvey, Keith W.: The Effect of Cyclic Feathering Motions on Dynamic Rotor Loads. NASA SP 352, 1974.

91. Hansford, Robert E.: Comparison of Predicted and Experimental Rotor Loads to Evaluate Flap-Lag Coupling with Blade Pitch. J. Amer. Hel. Soc., vol. 24, no. 5, Oct. 1979, pp. 3-11. Also: Preprint No. 78-19, Amer. Hel. Soc. 34th Annual National Forum, May 1978.
92. Bielawa, Richard L.: Blade Stress Calculations - Mode Deflection vs. Force Integration. J. Amer. Hel. Soc., vol. 24, no. 3, July 1978, pp. 10-16. Also: Amer. Hel. Soc. Symposium on Rotor Technology Proceedings, Aug. 1976.
93. Hansford, Robert E.: A Unified Formulation of Rotor Load Prediction Methods. J. Amer. Hel. Soc., vol. 31, no. 2, Apr. 1986, pp. 58-65. Also: Amer. Hel. Soc. 41st Annual Forum Proceedings, May 1985, pp. 73-83.
94. Tarzanin, F. J., Jr.; and Ranieri, J.: Investigation of Torsional Natural Frequency on Stall-Induced Dynamic Loading. USAAVLABS TR 73-94, 1974.
95. Tarzanin, F. J., Jr.; and Mirick, P. H.: Control Load Envelope Shaping by Live Twist. NASA SP-352, 1974.
96. Doman, Glidden S.; Tarzanin, Frank J.; and Shaw, John, Jr.: Investigation of Aeroelastically Adaptive Rotor Systems. Amer. Hel. Soc. Symposium on Rotor Technology Proceedings, Aug. 1976.
97. Blackwell, R. H.; and Merkley, D. J.: The Aeroelastically Conformable Rotor Concept. J. Amer. Hel. Soc., vol. 24, no. 4, July 1979, pp. 37-44. Also: Preprint No. 78-59, Amer. Hel. Soc. 34th Annual Forum, May 1978.
98. Weller, William H.: Experimental Investigation of Effects of Blade Tip Geometry on Loads and Performance for an Articulated Rotor System. NASA TP 1303, 1979.
99. Yeager, William T., Jr.; and Mantay, Wayne R.: Wind-Tunnel Investigation of the Effects of Blade Tip Geometry on the Interaction of Torsional Loads and Performance for an Articulated Helicopter Rotor. NASA TP 1926, 1981.
100. Yeager, William T., Jr.; and Mantay, Wayne R.: Loads and Performance Data from a Wind-Tunnel Test of Model Articulated Helicopter Rotors with Two Different Blade Torsional Stiffnesses. NASA TM 84573, 1983.
101. Sutton, Lawrence R.; White, Richard P., Jr.; and Marker, Robert L.: Wind-Tunnel Evaluation of an Aeroelastically Conformable Rotor. USAAVRADCOM TR 81-D-43, 1982.
102. Mantay, Wayne R.; and Yeager, William T., Jr.: Parametric Tips Effects for Aeroelastically Conformable Rotor Applications. NASA TM 85682, 1983. Also: Paper No. 53, Ninth Eur. Rotorcraft Forum, Sept. 1983.

103. Mantay, Wayne R.; and Yeager, William T., Jr.: Aeroelastic Considerations for Torsionally Soft Rotors. NASA TM 87687, 1986. Paper No. 9, Amer. Hel. Soc./NASA 2nd Decennial Specialists' Meeting on Rotorcraft Dynamics Proceedings, Nov. 1984, and NASA CP 2400, 1985, pp. 117-134.
104. Tarzanin, F. J., Jr.; and Vlaminck, R. R.: Investigation of the Effects of Blade Sweep on Rotor Vibratory Loads. NASA CR-166526, 1983.
105. Miura, H.: Overview: Applications of Numerical Optimization Methods to Helicopter Design Problems. NASA CP 2327, 1984.
106. Peters, David A.; Ko, Timothy; Korn, Alfred; and Rossow, Mark P.: Design of Helicopter Rotor Blades for Desired Placement of Natural Frequencies. Amer. Hel. Soc. 39th Annual Forum Proceedings, May 1983, pp. 674-689.
107. Pritchard, Jocelyn I.; Adelman, Howard M.; and Haftka, Raphael T.: Sensitivity Analysis and Optimization of Nodal Point Placement for Vibration Reduction. NASA TM 87763, 1986.
108. Friedmann, P. P.; and Shanthakumaran, P.: Optimum Design of Rotor Blades for Vibration Reduction in Forward Flight. J. Amer. Hel. Soc., vol. 29, no. 4, Oct. 1984, pp. 70-80.
109. Yen, Jing C.: Coupled Aeroelastic Hub Loads Reduction. Amer. Hel. Soc./Nanjing Aero. Inst. International Seminar - The Theoretical Basis of Helicopter Technology, Nov. 1985.
110. Hammond, C. E.: Wind Tunnel Results Showing Rotor Vibratory Loads Reduction Using Higher Harmonic Blade Pitch. J. Amer. Hel. Soc., vol. 28, no. 1, Jan. 1983, pp. 10-15. Also: Preprint No. 80-66, Amer. Hel. Soc. 36th Annual Forum, May 1980.
111. Wood, E. Roberts; Powers, Richard W.; Cline, John H.; and Hammond, C. Eugene: On Developing and Flight Testing a Higher Harmonic Control System. J. Amer. Hel. Soc., vol. 30, no. 1, Jan. 1985, pp. 3-20. Also: Amer. Hel. Soc. 39th Annual Forum Proceedings, May 1983, pp. 592-612.
112. McCloud, John L. III: An Analytical Study of a Multicyclic Controllable Twist Rotor. Preprint No. 932, Amer. Hel. Soc. 31st Annual National Forum, May 1975.
113. Hammond, C. Eugene; and Weller, William H.: Wind-Tunnel Testing of Aeroelastically Scaled Helicopter Rotor Models. U.S. Army Science Conference, June 1976.
114. Mantay, Wayne R.; and Rorke, James B.: The Evolution of the Variable Geometry Rotor, Amer. Hel. Soc. Symposium on Rotor Technology Proceedings, Aug. 1976.

115. Sadler, S. Gene: Development and Application of a Method for Predicting Rotor Free Wake Positions and Resulting Rotor Blade Air Loads. NASA CR 1911, 1971.
116. Landgrebe, A. J.; and Bellinger, E. D.: Experimental Investigation of Model Variable-Geometry and Ogee Tip Rotors. NASA CR 2275, 1974.
117. Gangwani, Santu T.: The Effect of Helicopter Main Rotor Blade Phasing and Spacing on Performance, Blade Loads, and Acoustics. NASA CR 2737, 1975.
118. Rorke, J. B.: Hover Performance Tests of Full-Scale Variable Geometry Rotors. NASA CR 2713, 1976.
119. Rabbott, John P., Jr.; and Niebanck, Charles F.: Experimental Effects of Tip Shape on Control Loads. Preprint No. 78-61, Amer. Hel. Soc. 34th Annual National Forum, 1978.
120. Stroub, Robert H.; Young, Larry A.; Keys, Charles N.; and Cawthorne, Matthew H.: Free-Tip Rotor Wind Tunnel Test Results. J. Amer. Hel. Soc., vol. 31, no. 3, July 1986, pp. 19-26. Also: Amer. Hel. Soc. 41st Annual Forum Proceedings, May 1985, pp. 387-411.
121. McCloud, John L.; and Kretz, Marcel: Multicyclic Jet-Flap Control for Alleviation of Helicopter Blade Stresses and Fuselage Vibration. NASA SP-352, 1974, pp. 233-238.
122. Harvey, K. W.; Blankenship, B. L.; and Drees, J. M.: Analytical Study of Helicopter Gust Response at High Forward Speeds. USAAVLABS TR 69-1, 1969.
123. Bergquist, Russell R.: Helicopter Gust Response Including Unsteady Aerodynamic Stall Effects. USAAMRDL TR 72-68, 1973.
124. Arcidiacono, Peter J.; Bergquist, Russell R.; and Alexander, W. T., Jr.: Helicopter Gust Response Characteristics Including Unsteady Aerodynamic Stall Effects. J. Amer. Hel. Soc., vol. 19, no. 4, Oct. 1974, pp. 34-43. Also: NASA SP-352, 1974, pp.
125. Gaonkar, G. H.: Gust Response of Rotor and Propeller Systems. J. Aircraft, vol. 18, May 1981, pp. 389-396.
126. Bir, Gunjit Singh; and Chopra, Inderjit: Gust Response of Hingeless Rotors. J. Amer. Hel. Soc., vol. 31, no. 2, Apr. 1986, pp. 33-46. Also: Amer. Hel. Soc. 41th Annual Forum Proceedings, May 1985, pp. 47-72.
127. Bir, Gunjit Singh; and Chopra, Inderjit: Prediction of Blade Stresses Due to Gust Loading. Paper No. 73, Eleventh Eur. Rotorcraft Forum, Sept. 1985.



128. Fuh, J. S.; Hong, C. Y. R.; Lin, Y. K.; and Prussing, J. E.: Coupled Flap-Torsional Response of a Rotor Blade in Forward Flight Due to Atmospheric Turbulence Excitations. J. Amer. Hel. Soc., vol. 28, no. 3, July 1983, pp. 3-12.
129. Prussing, J. E.; Lin, Y. K.; and Shiau, T. N.: Rotor Blade Flap-Lag Stability and Response in Forward Flight in Turbulent Flows. J. Amer. Hel. Soc., vol. 29, no. 4, Oct. 1984, pp. 81-87.
130. Dunham, R. Earl, Jr.; Holbrook, G. Thomas; Mantay, Wayne R.; Campbell, Richard L.; and Van Gunst, Roger W.: Flight-Test Experience of a Helicopter Encountering an Airplane Trailing Vortex. Preprint No. 1063, Amer. Hel. Soc. 32nd Annual National V/STOL Forum, May 1976.
131. Mantay, Wayne R.; Holbrook, G. Thomas; Campbell, Richard L.; and Tomaine, Robert L.: Helicopter Response of an Airplanes's Trailing Vortex. J. Aircraft, vol. 14, Apr. 1977, pp. 357-363.
132. Kim, Ki-Chung; Bir, Gunjit; and Chopra, Inderjit: Helicopter Response to an Airplane's Vortex Wake. Paper No. 43, Twelfth Eur. Rotorcraft Forum, Sept. 1986.
133. Tarzanin, Frank J., Jr.: Panel 1: Prediction of Rotor and Control System Loads. NASA SP-352, 1974.
134. McHugh, Frank J.: What Are the Lift and Propulsive Force Limits At High Speed for the Conventional Rotor? Amer. Hel. Soc. 34th Annual National Forum Proceedings, May 1978, pp. 1-12.
135. McHugh, Frank J.; Clark, Ross; and Solomon, Mary: Wind Tunnel Investigation of Rotor Lift and Propulsive Force at High Speed - Data Analysis. NASA CR 145217-1, 1977.
136. Van Gaasbeek, James R.: An Investigation of High-G Maneuvers of the AH-1G Helicopter. USAAMRDL TR 75-18, Apr. 1975.
137. Tarzanin, F. J., Jr.: Prediction of Control Loads Due to Blade Stall. J. Amer. Hel. Soc., vol. 17, no. 2, Apr. 1972, pp. 33-46. Also: Preprint 513, Amer. Hel. Soc. 27th Annual National Forum, May 1971.
138. Harris, Franklin D.; Tarzanin, Frank J. Jr.; and Fisher, Richard K., Jr.: Rotor High Speed Performance, Theory vs. Test. J. Amer. Hel. Soc., vol. 15, no. 3, July 1970, pp. 35-44.
139. Crimi, P.: Theoretical Prediction of the Flow in the Wake of a Helicopter Rotor. Cornell Aeronautical Laboratory Report No. BB-1994-S-1 and -2, Sept. 1965.

140. Ericsson, L. E.; and Reding, J. P.: Dynamic Stall of Helicopter Blades. J. Amer. Hel. Soc., vol. 17, no. 1, Jan. 1972.
141. Landgrebe, A. J.; and Egolf, T. A.: Rotorcraft Wake Analysis for the Prediction of Induced Velocities. USAAMRDL TR 75-45, 1976.
142. Scully, M. P.: Computation of Helicopter Rotor Wake Geometry and Its Influence on Rotor Harmonic Airloads. Massachusetts Institute of Technology, ASRL TR 178-1, Mar. 1975.
143. Davis, John M.: Rotorcraft Flight Simulation with Aeroelastic Rotor and Improved Aerodynamic Representation, Volume I - Engineer's Manual. USAAMRDL TR 74-10A, 1974.
144. Staley, James A.: Validation of Rotorcraft Flight Simulation Program Through Correlation with Flight Data for Soft-In-Plane Hingeless Rotors. USAAMRDL TR 75-50, 1976.
145. Briczinski, S. J.: Validation of the Rotorcraft Flight Simulation Program (C81) for Articulated Rotor Helicopters Through Correlation With Flight Data. USAAMRDL TR 76-4, 1976.
146. McLarty, Tyce T.: Rotorcraft Flight Simulation With Coupled Rotor Aeroelastic Stability Analysis, Volume I, Engineer's Manual. USAAMRDL TR 76-41A, 1977.
147. Van Gaasbeek, J. R.; McLarty, T. T.; and Sadler, S. G.: Rotorcraft Flight Simulation, Computer Program C81, Volume I - Engineer's Manual. USARTL TR 77-54A, 1979.
148. Van Gaasbeek, James R.: Rotorcraft Flight Simulation Computer Program C81 With DATAMAP Interface, Volume I - User's Manual. USAAVRADCOM TR 80-D-38A, 1981.
149. Shockey, G. A.; Williamson, J. W.; and Cox, C. R.: Helicopter Aerodynamics and Structural Loads Survey. Preprint 1060, Amer. Hel. Soc. 32nd Annual National Forum, May 1976.
150. Van Gaasbeek, James R.; and Austin, Edward E.: Digital Simulation of the Operational Loads Survey Flight Tests. Preprint No. 78-58, Amer. Hel. Soc. 34th Annual National Forum, May 1978.
151. Van Gaasbeek, James R.: Validation of the Rotorcraft Flight Simulation Program (C81) Using Operational Loads Survey Flight Test Data. USAAVRADCOM TR 80-D-4, 1980.
152. Merkley, Donald J.; and Ragosta, Arthur E.: DATAMAP and Its Impact on Prediction Programs. AGARD Conf. Proc. No. 334, May 1982.

153. Dompka, Robert V.; and Corrigan, John J.: AH-1G Flight Vibration Correlation Using NASTRAN and the C81 Rotor/Airframe Coupled Analysis. Amer. Hel. Soc. 42nd Annual Forum Proceedings, June 1986, pp. 45-61.
154. Yen, J. G.; and Weller, W. H.: Analysis and Application of Compliant Rotor Technology. Paper No. 11, Sixth Eur. Rotorcraft and Powered Lift Aircraft Forum, Sept. 1980.
155. Sheffler, Marc: Analysis and Correlation with Theory of Rotor Lift-Limit Test Data. NASA CR 159139, 1979.
156. Lemnios, A. Z.; and Smith, A. F.: An Analytical Evaluation of the Controllable Twist Rotor Performance and Dynamic Behavior. USAAMRDL TR 72-16, 1972.
157. Berman, Alex; Chen, Shyi-Yaung; Gustavson, Bruce; and Hurst, Patricia: Dynamic System Coupler Program (DYSCO 4.0), Volume I - Theoretical Manual. USAAVSCOM TR 85-D-24A, 1986.
158. Bielawa, Richard L.; Cheney, Marvin C., Jr.; and Novak, Richard C.: Investigation of a Bearingless Helicopter Rotor Concept Having A Composite Primary Structure. NASA CR 2637, 1976.
159. Bielawa, Richard L.: Aeroelastic Analysis for Helicopter Rotor Blades With Time-Variable, Nonlinear Structural Twist and Multiple Structural Redundancy - Mathematical Derivation and Program User's Manual. NASA CR 2638, 1976.
160. Bielawa, Richard L.: Aerolastic Analysis for Helicopter Rotors With Blade Appended Pendulum Vibration Absorbers - Mathematical Derivations and Program User's Manual. NASA CR 165896, 1982.
161. Sopher, Robert; and Hallock, Daniel W.: Development and Application of a Time-History Analysis for Rotorcraft Dynamics Based on a Component Approach. Paper No. 11, Amer. Hel. Soc./NASA 2nd Decennial Specialists' Meeting on Rotorcraft Dynamics Proceedings, Nov. 1984. Also: NASA CP 2400, 1985.
162. Johnson, Wayne: A Comprehensive Analytical Model of Rotorcraft Aerodynamics and Dynamics, NASA TM 81182, 1980.
163. Johnson, Wayne: Development of a Comprehensive Analysis for Rotorcraft - I. Rotor Model and Wake Analysis. Vertica, vol. 5, 1981, pp. 99-130.
164. Johnson, Wayne: Development of a Comprehensive Analysis for Rotorcraft - II. Aircraft Model, Solution Procedure and Applications. Vertica, vol. 5, 1981, pp. 185-216.

165. Fradenburgh, Evan A.: Aerodynamic Design of the Sikorsky S-76 SPIRIT Helicopter. J. Amer. Hel. Soc., vol. 24, no. 4, July 1979, pp. 11-19.
166. Gupta, B. P.: Blade Design Parameters Which Affect Helicopter Vibrations. Amer. Hel. Soc. 40th Annual Forum Proceedings, May 1984, pp. 207-217.
167. Yen, Jing C.; and Tanner, Hank: Design of UH-1 CMRB to Minimize Helicopter Vibration. Amer. Hel. Soc. 42nd Annual Forum Proceedings, June 1984, pp. 793-800.
168. Hansford, Robert E.: Rotor Load Correlation with the A. S. P. Blade. Amer. Hel. Soc. 42nd Annual Forum Proceedings, June 1986, pp. 13-26.
169. Charles F. Niebanck, "Model Rotor Test Data for Verification of Blade Response and Rotor Performance Calculations. USAAMRDL TR 74-29, 1974.
170. Morris, Charles E. K., Jr.; Tomaine, Robert L.; and Stevens, Dariene D.: A Flight Investigation of Performance and Loads for a Helicopter With NLR-1T Main-Rotor Blade Sections. NASA TM 80165, 1979.
171. Morris, Charles E. K., Jr.; Stevens, Dariene D.; and Tomaine, Robert L.: A Flight Investigation of Blade-Section Aerodynamics for a Helicopter Main Rotor Having NLR-1T Airfoil Sections. NASA TM 80166, 1980.
172. Morris, Charles E. K., Jr.; Tomaine, Robert L.; and Stevens, Dariene D.: A Flight Investigation of Performance and Loads for a Helicopter With 10-64C Main-Rotor Blade Sections. NASA TM 81871, 1980.
173. Morris, Charles E. K., Jr.: A Flight Investigation of Blade-Section Aerodynamics for a Helicopter Main Rotor Having 10-64C Airfoil Sections. NASA TM 83226, 1982.
174. Morris, Charles E. K., Jr.; Tomaine, Robert L.; and Stevens, Dariene D.: A Flight Investigation of Performance and Loads for a Helicopter With RC-SC2 Main-Rotor Blade Sections. NASA TM 81898, 1980.
175. Charles E. K. Morris, Jr., A Flight Investigation of Blade-Section Aerodynamics for a Helicopter Main Rotor Having RC-SC2 Airfoil Sections, NASA TM 83298, 1982.
176. Burpo, F.: Measurements of Dynamic Airloads on a Full-Scale Semi-Rigid Rotor TCREC TR 62-42, Dec. 1962.
177. Pruyn, R. R.: In-Flight Measurement of Rotor Blade Airloads, Bending Moments, and Motions, Together With Rotor Shaft Loads and Fuselage Vibration, On a Tandem Rotor Helicopter. USAAVLABS TR 67-9A, 1967.

178. Bartsch, E. A.: In-Flight Measurement and Correlation With Theory of Blade Airloads and Responses on the XH-51A Compound Helicopter Rotor, Volume I - Measurement and Data Reduction of Airloads and Structural Loads. USAAVLABS TR 68-22A, 1968.
179. Fenaughty, Ronald; and Beno, Edward: NH-3A Vibratory Airloads and Vibratory Rotor Loads. SER 611493, Jan. 1970.
180. Beno, Edward A.: CH-53A Main Rotor and Stabilizer Vibratory Airloads and Forces. SER 65593, June 1970.

TABLE 1.- CHARACTERISTICS OF ROTOR LOADS ANALYSES

Company	Code	Solution procedure	Structural dynamics			Aerodynamics <sup>a</sup>	
			Equations of motion	Modes included or finite elements	Structural and inertial coupling of modes or finite elements	Dynamic stall	Downwash
Bell Helicopter Textron	CB1	Numerical integration	Modal	12	Fully coupled normal modes; bending moments determined from modal moment distributions	BUNS option: Lift per Tarzanin, ref. 137 Moment per Carta et al., ref. 18 Drag per Harris et al., ref. 138 UNSAH option: Per Gormont, ref. 22	Modified momentum theory (default), prescribed/free wake by table input, ref. 139
Boeing Vertol	C-60	Harmonic response	Finite element	25 plus flex beam and cuff	Fully coupled	Lift/moment per Tarzanin, ref. 137 Drag per Harris et al., ref. 138	Deformed near wake, prescribed far wake
Kaman	6F	Integrating matrix operator	Modal	Rigid flapping Rigid lead-lag Rigid torsion 1 flap bending 1 torsion Rigid servoflap	Fully coupled. Bending moments determined from uncoupled equations at zero pitch	None	
McDonnell-Douglas Helicopter	DYSCO	Periodic shooting with Newton Raphson Method	Modal	5 flap 3 chord 3 torsion	Fully coupled	Lift per Tarzanin, ref. 137 Moment per Carta et al., ref. 18 Drag per Harris et al., ref. 138	Modified momentum theory
	DART	Numerical integration	Finite element	20	Fully coupled	Lift/moment per Ericsson and Reding, ref. 140. Steady drag	Free wake by table input
	RAVIB	Harmonic response	Finite element	20	Fully coupled	Gangwani, ref. 30	Free wake, ref. 115
	RACAP	Harmonic response	Finite element	30	Fully coupled	Option 1: Per Johnson, ref. 21 Option 2: Per Gangwani, ref. 30	Free wake, refs. 115 and 142
Sikorsky Aircraft	Y201	Numerical integration	Modal	Rigid flapping Rigid lead-lag 3 flap bending 2 chord bending 1 torsion	Uncoupled normal modes obtained for zero pitch and twist. Structural coupling terms included as forcing functions in modal equations	UTRC Method, ref. 18	Prescribed wake, ref. 141
NASA	GH00	Numerical integration	Modal	4 flap bending 3 chord bending 3 torsion	Fully coupled	Gangwani, ref. 30	Prescribed wake, ref. 141
	RDYNE	Numerical integration	Modal	30	Fully coupled	Quasi-steady	Influence coefficients ref. 141
	CAMRAD	Numerical integration	Modal	10 bending 5 torsion	Fully coupled	Option 1: Per Johnson, ref. 21 Option 2: Per Gormont, ref. 22	Free wake, ref. 142

<sup>a</sup>Yawed flow drag and  $C_{tmax}$ , ref. 138.

TABLE 2.- USE OF RECENT ROTOR LOADS DATA BASES.

Data base	Source	Type	Primary references	Secondary references
CH-34 model rotor wind tunnel test	Niebanck, 1974 (ref. 169)	Tape	1	1
AH-1G OLS flight test	Shockey <u>et al.</u> , 1977 (ref. 36)	Tape	2	8
AH-1G/NLR-1T flight test	Morris <u>et al.</u> , 1979 (refs. 170 and 171)	Tabulated	1	0
AH-1G/10-64C flight test	Morris <u>et al.</u> , 1980 (refs. 172 and 173)	Tabulated	1	0
AH-1G/RC-SC2 flight test	Morris <u>et al.</u> , 1980 (refs. 174 and 175)	Tabulated	1	0
S-76 rotor wind tunnel test	Johnson, 1980 (ref. 67)	Tabulated	2	2
ACR model rotor wind tunnel test	Yeager and Mantay, 1983 (ref. 100)	Tabulated	1	0
AH-1G/tip aeroacoustic test		Tape	0	0
SA 349-2 flight test	Heffernan and Gaubert, 1986 (ref. 54)	Tabulated/ tape	1	0

TABLE 3.- USE OF MAJOR ROTOR LOADS DATA BASES.

Data base	Source	Type	References	Non-self references
UH-1 flight test	Burpo, 1962 (ref. 176)	Tabulated	2	1
CH-34 flight test	Scheiman, 1964 (ref. 41)	Tabulated	10	8
CH-34 wind tunnel test	Rabbott <u>et al.</u> , 1966 (refs. 1 and 51)	Tabulated	7	5
CH-47A flight test	Pruyn, 1968 (ref. 177)	Tape	0	0
XH-51A flight test	Bartsch, 1968 (ref. 170)	Tabulated	2	1
NH-3A flight test	Fenaughty and Beno, 1970 (ref. 179)	Tabulated	4	1
CH-53A flight test	Beno, 1970 (ref. 180)	Tabulated	6	1
AH-1G/OLS flight test	Shockey <u>et al.</u> , 1977 (ref. 34)	Tape	10	5
AH-1G/TAAT flight test		Tape	0	0



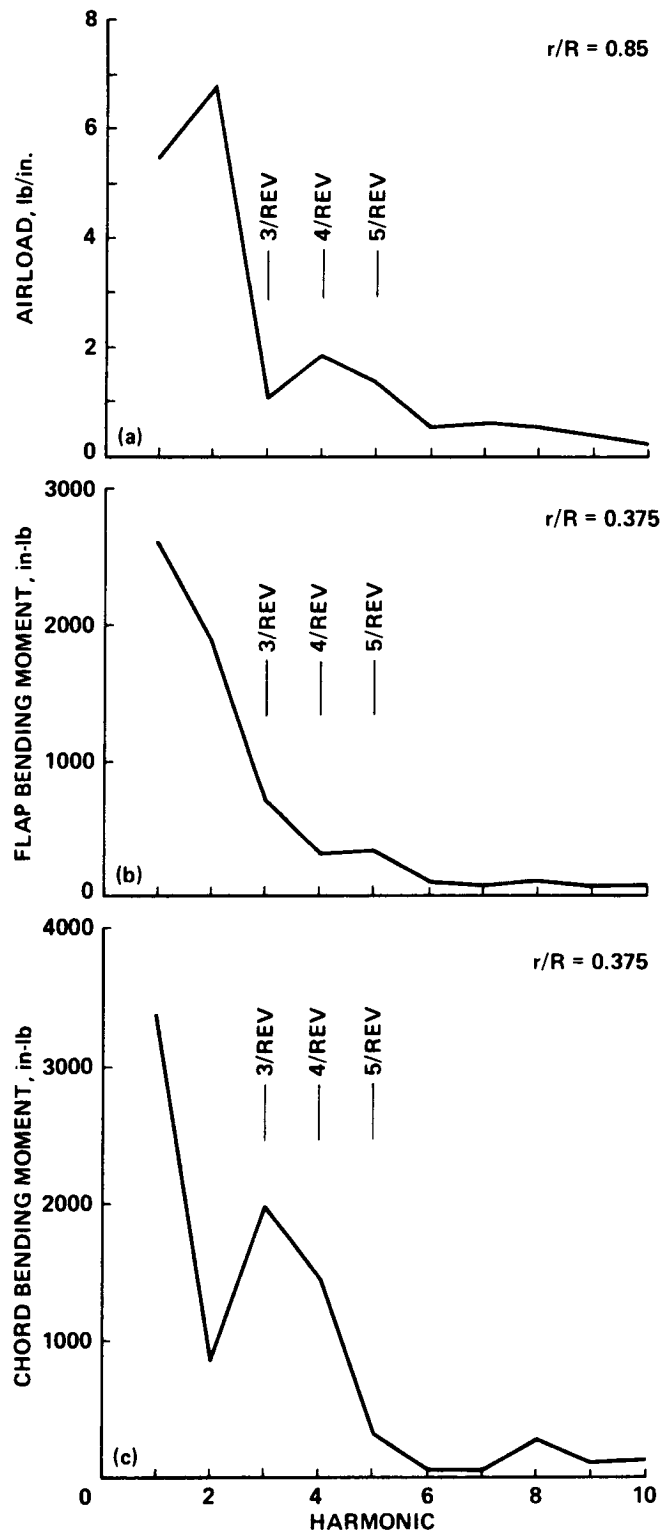


Figure 1.- Airloads and bending moments for CH-34 rotor in 40- by 80-Foot Wind Tunnel;  $\mu = 0.39$ ,  $\alpha_s = -5^\circ$  (ref. 1). (a) Airloads. (b) Flap bending moment. (c) Chord bending moment.

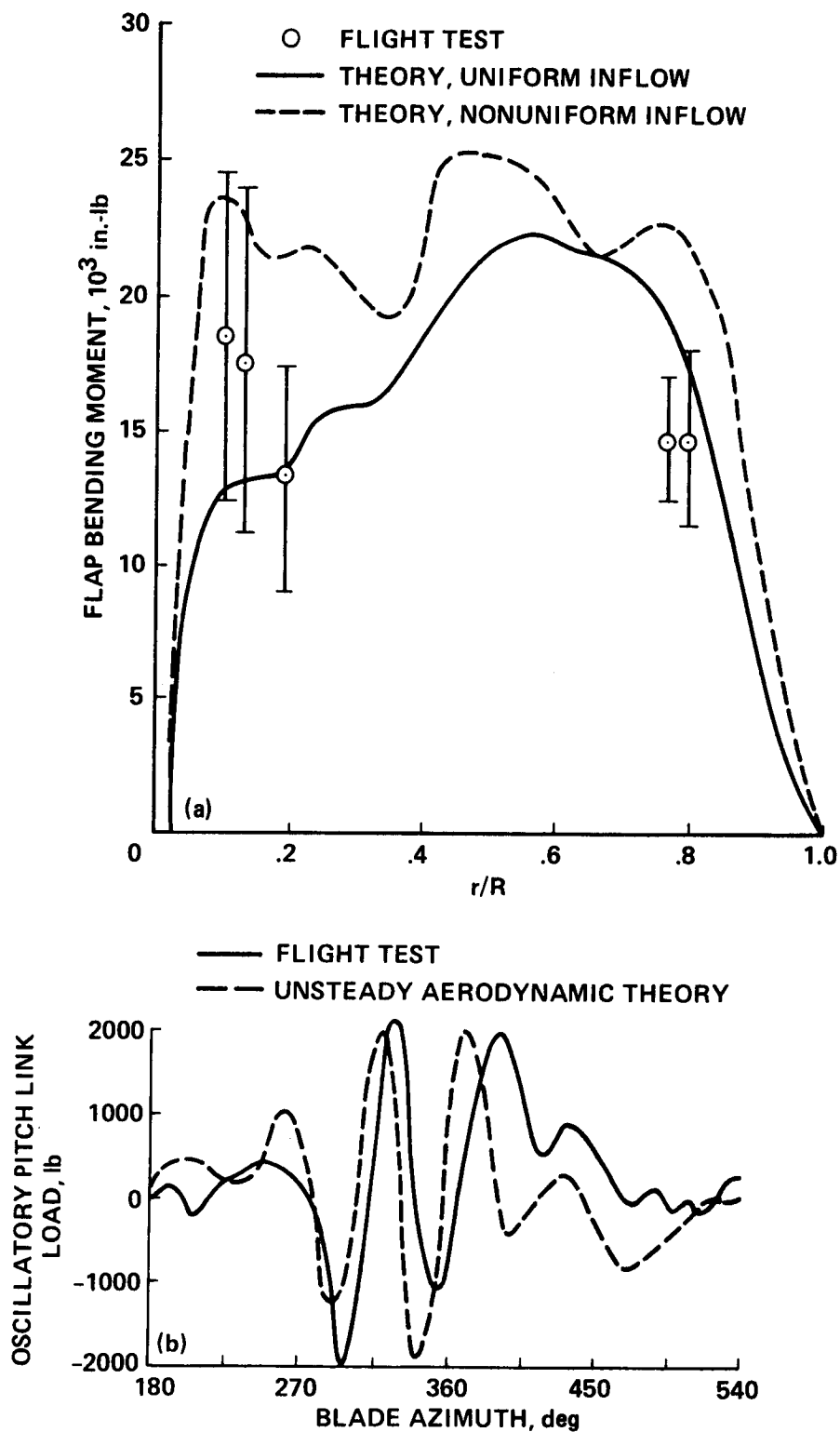


Figure 2.- Comparison of C-60 prediction with flight test data for CH-47C aft rotor;  $V = 123$  knots (ref. 3). (a) Oscillatory flap bending moment;  $C_T/\sigma = 0.114$ . (b) Oscillatory pitch link load;  $GW = 38,865$  lb.

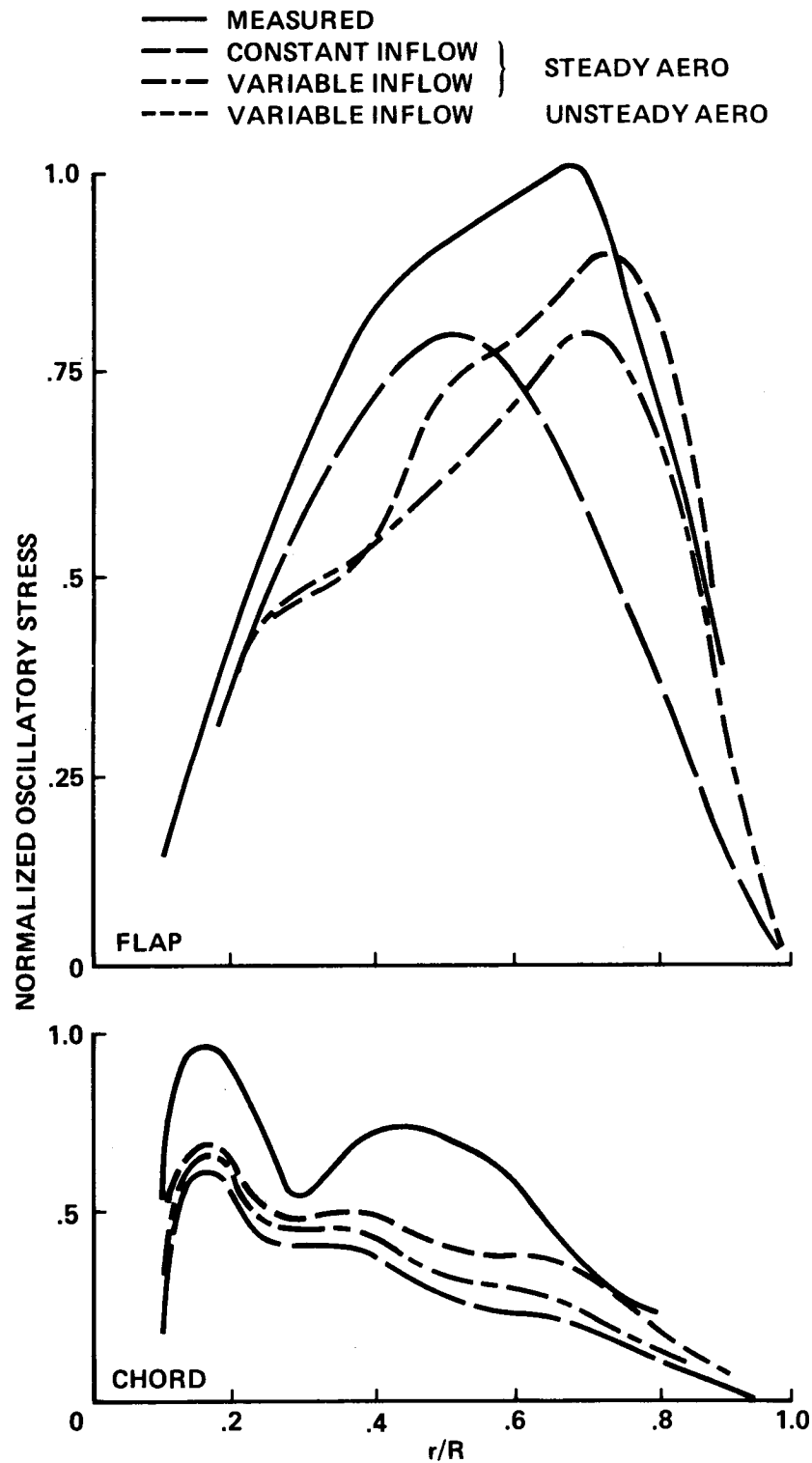


Figure 3.- Comparison of Y200 prediction with normalized oscillatory blade stress for an articulated rotor;  $\mu = 0.36$ ,  $C_L/\sigma = 0.0763$  (ref. 4).

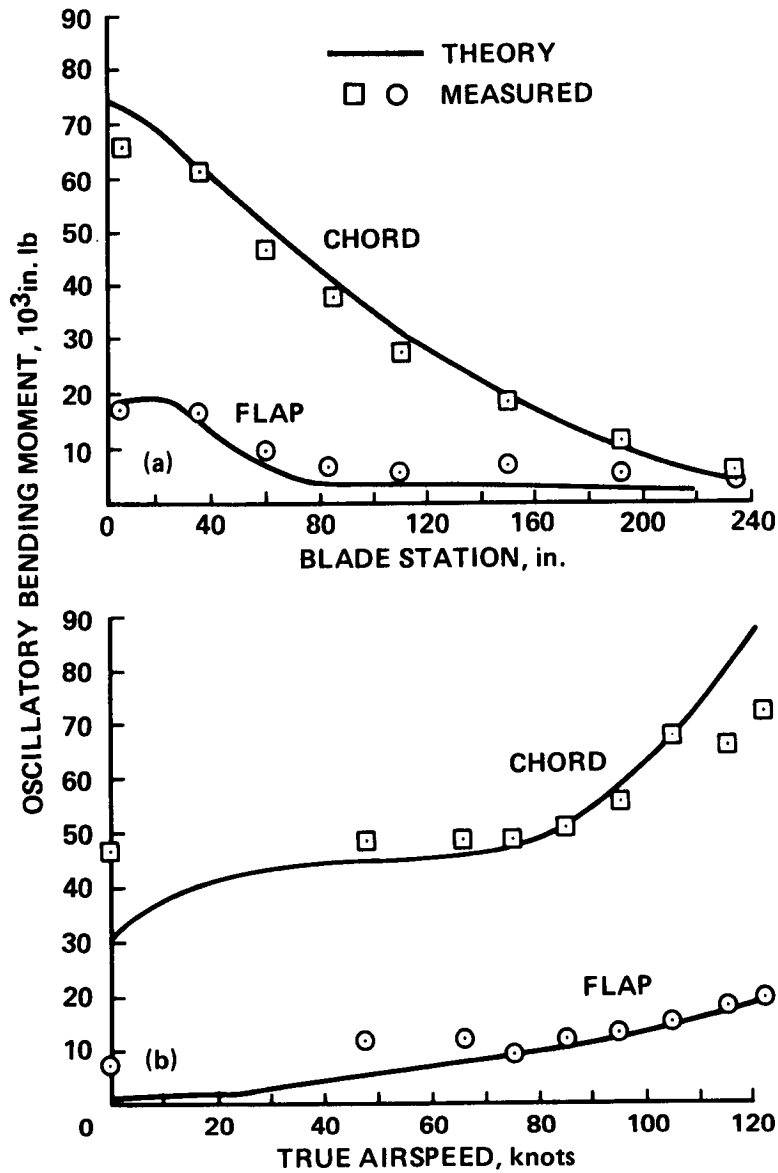


Figure 4.-Comparison of C81 prediction with flight test data for UH-1D; GW = 9,500 lb (ref. 5). (a) Oscillatory bending moment as a function of blade station; V = 115 knots. (b) Oscillatory bending moment as a function of airspeed; blade station 6.0 in.

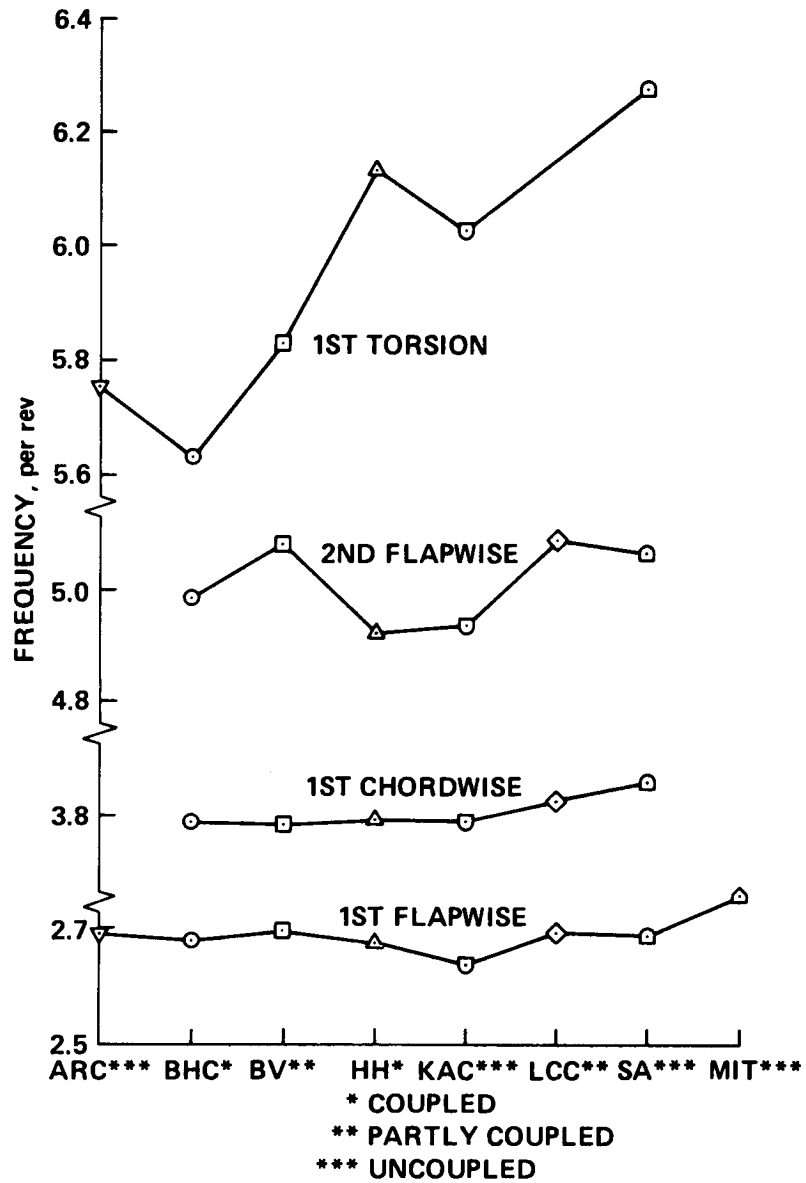


Figure 5.- Rotor blade rotating natural frequencies in vacuo;  $\theta_{0.75R} = 0^\circ$  (ref. 2).

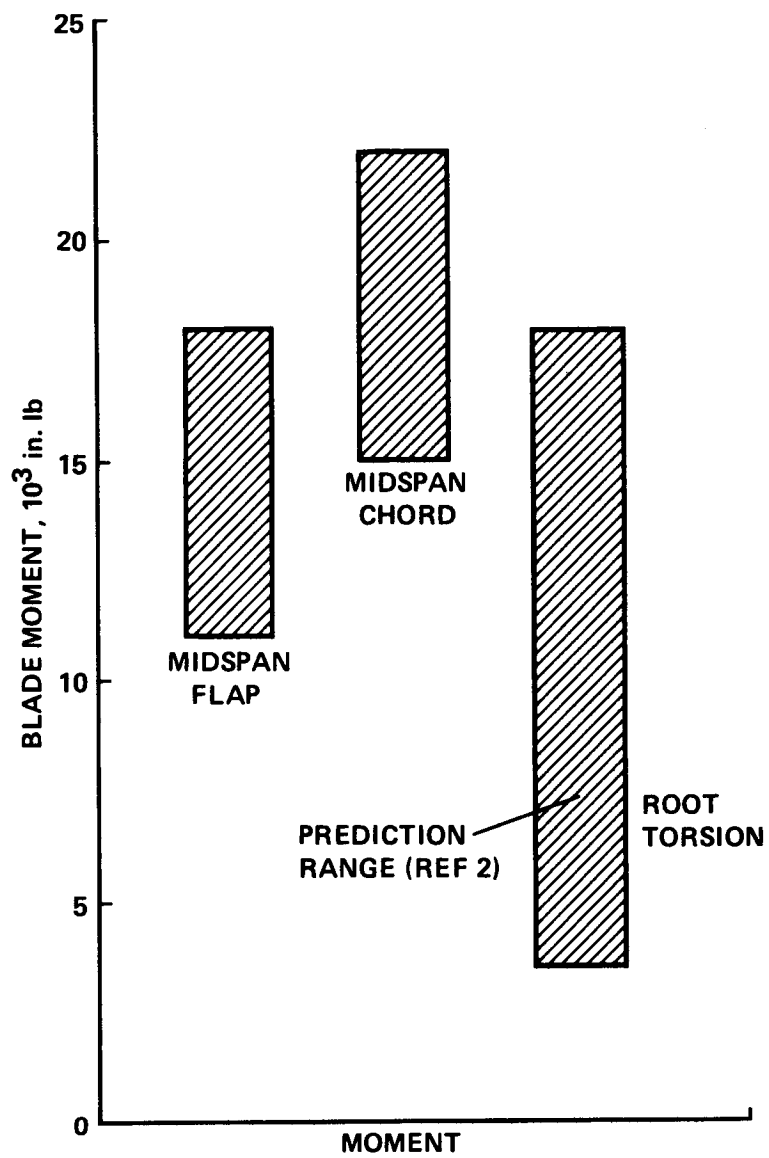


Figure 6.- Range of blade moment predictions for hypothetical rotor;  $\mu = 0.33$ , unsteady aerodynamics (ref. 8).

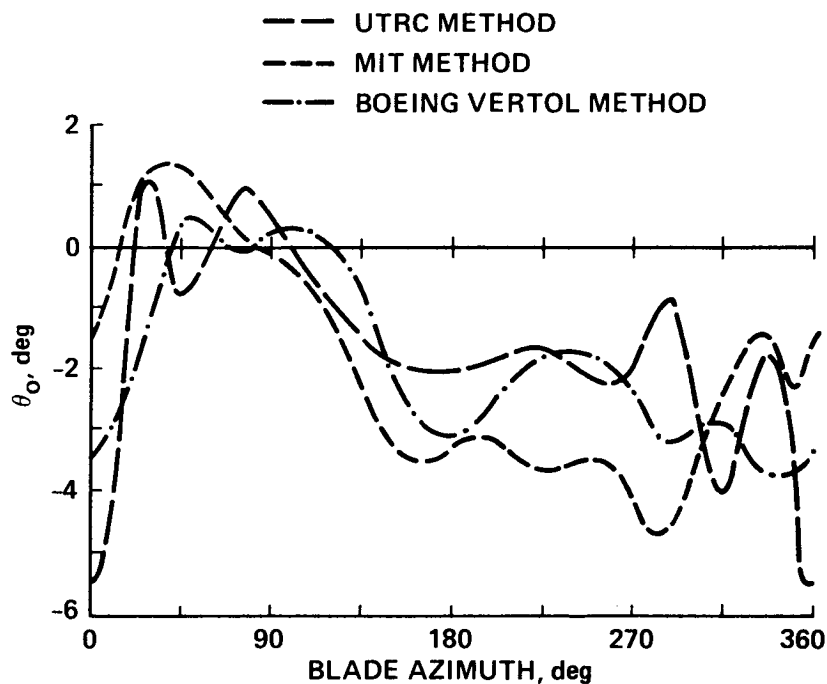


Figure 7.- Elastic torsion angle calculated for a hypothetical rotor using three dynamic stall models;  $\mu = 0.333$ ,  $C_T/\sigma = 0.09$  (ref. 17). UTRC Method: refs. 18 and 19; MIT Method: refs. 20 and 21; and Boeing Vertol Method: ref. 22.

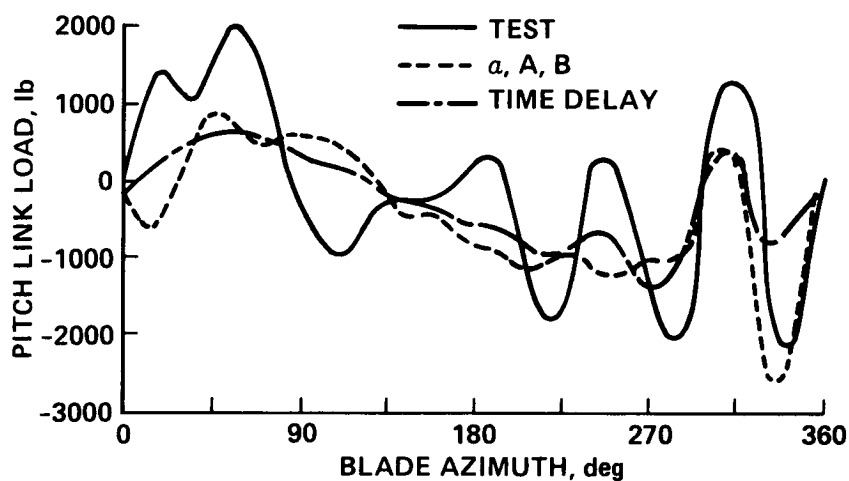


Figure 8.- Comparison of measured and predicted CH-53A pitch link loads using two dynamic stall models;  $GW = 42,000$  lb,  $V = 155$  knots (ref. 24).

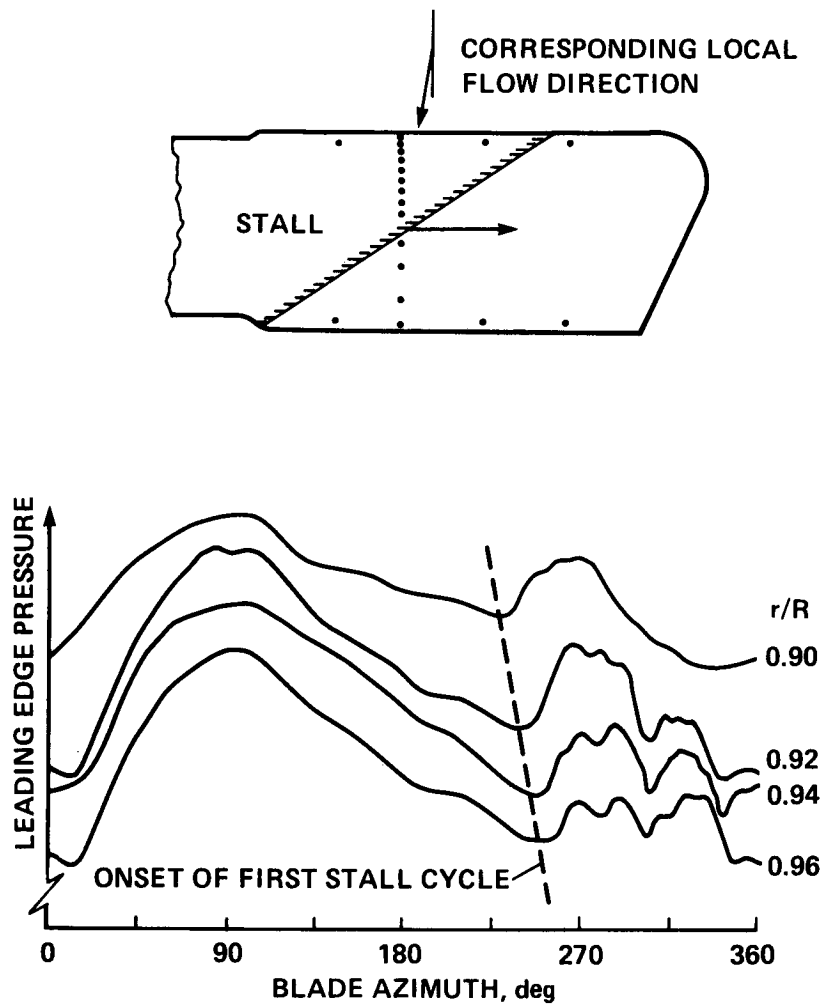


Figure 9.- Pressures measured at the leading edge of a modified blade tip on a Wessex helicopter (ref. 38).

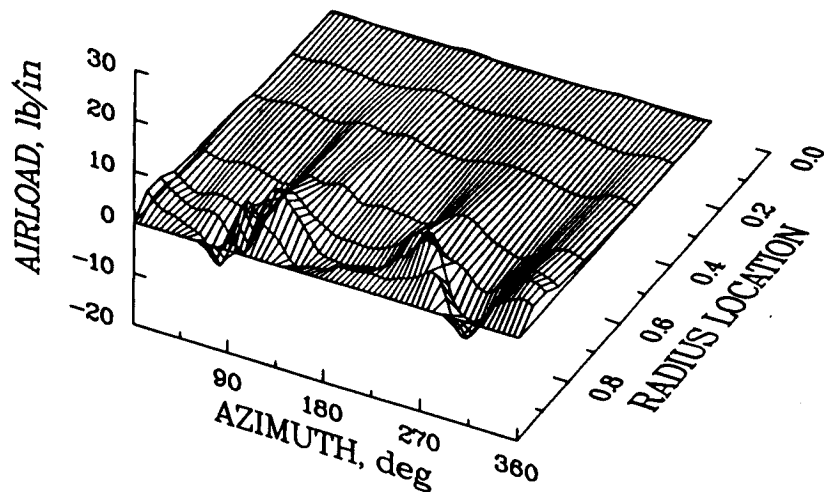


Figure 10.- Vibratory airloads (3-12 harmonics) measured on the CH-34 rotor in flight;  $\mu = 0.129$  (ref. 41).



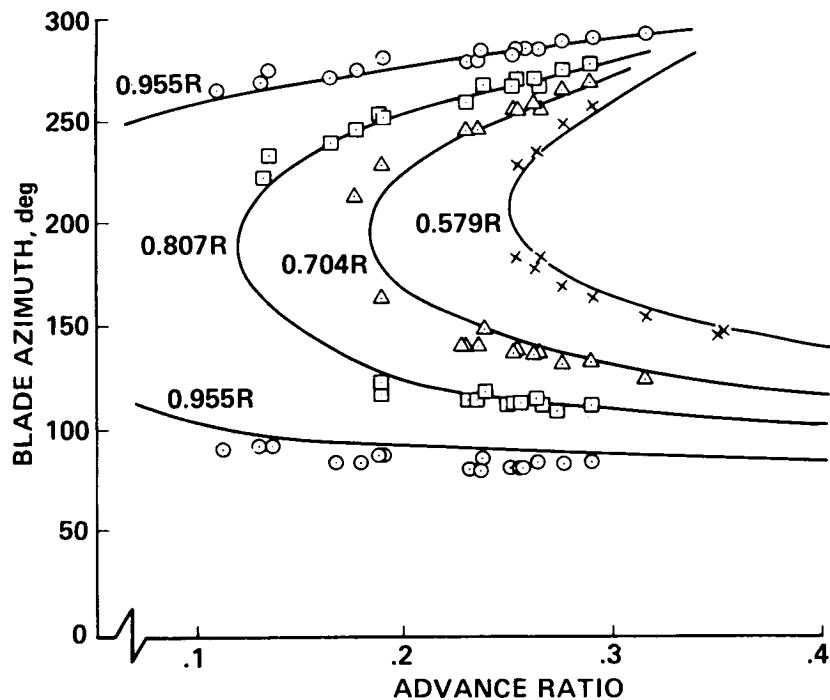


Figure 11.- Flight test measurements of blade-vortex intersections for four blade radial stations (ref. 43).

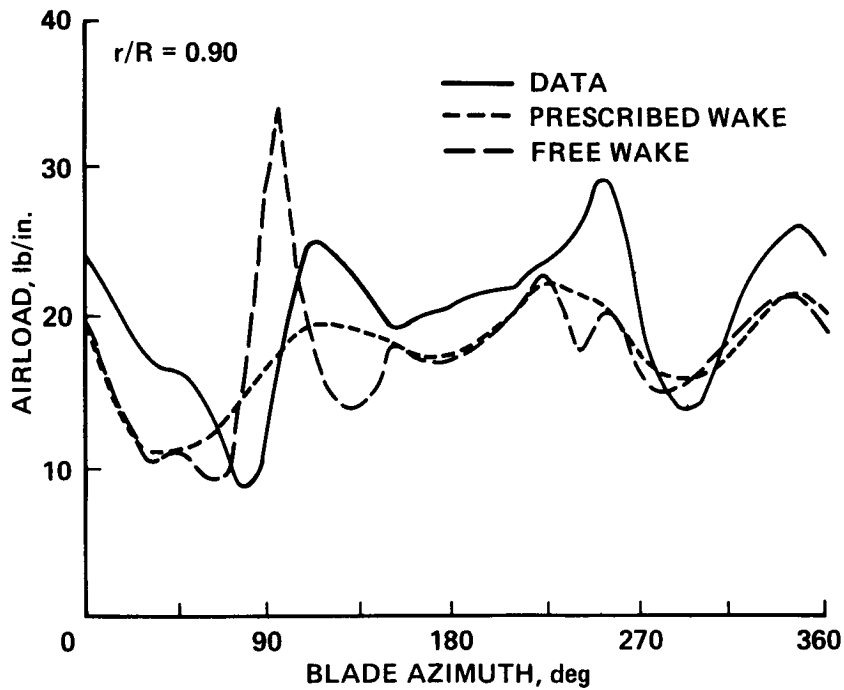


Figure 12.- Comparison of free and prescribed wake calculations with CH-34 flight test data;  $r/R = 0.90$ ,  $\mu = 0.129$  (ref. 48).

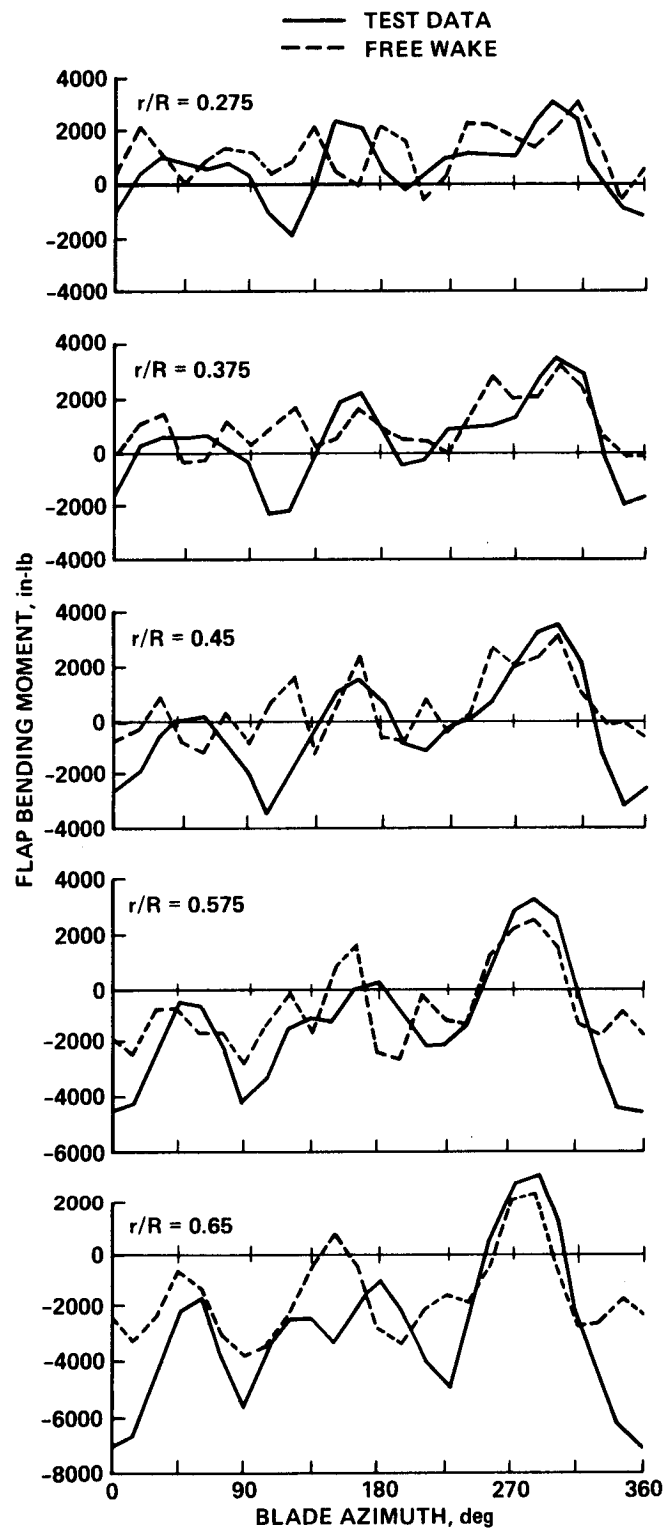


Figure 13.- Comparison of test data with free wake prediction for CH-34 flap bending moment data;  $\mu = 0.129$  (ref. 48).

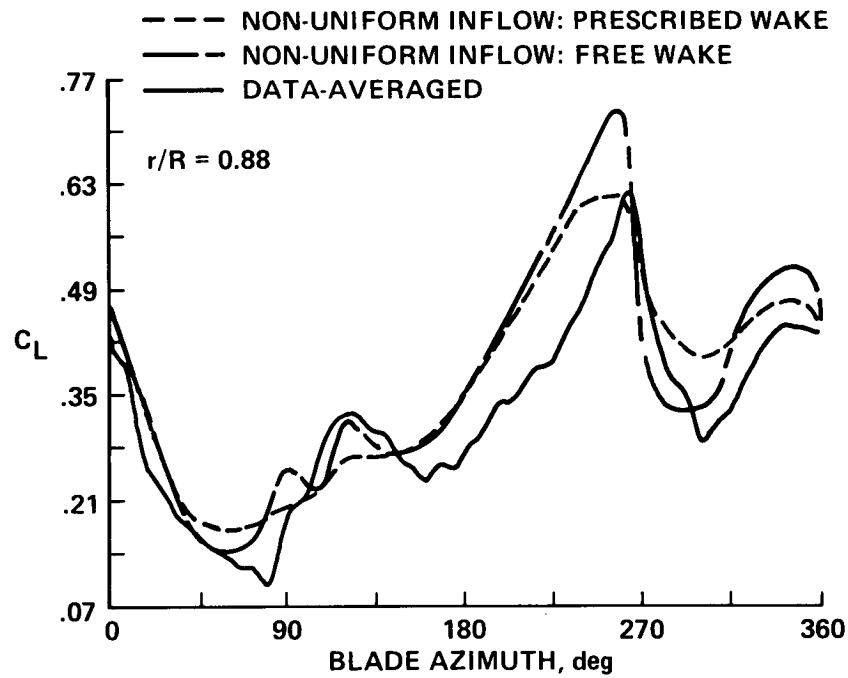


Figure 14.- Comparison of CAMRAD prediction of lift coefficient with SA 349-2 flight test data;  $\mu = 0.14$  (ref. 50).

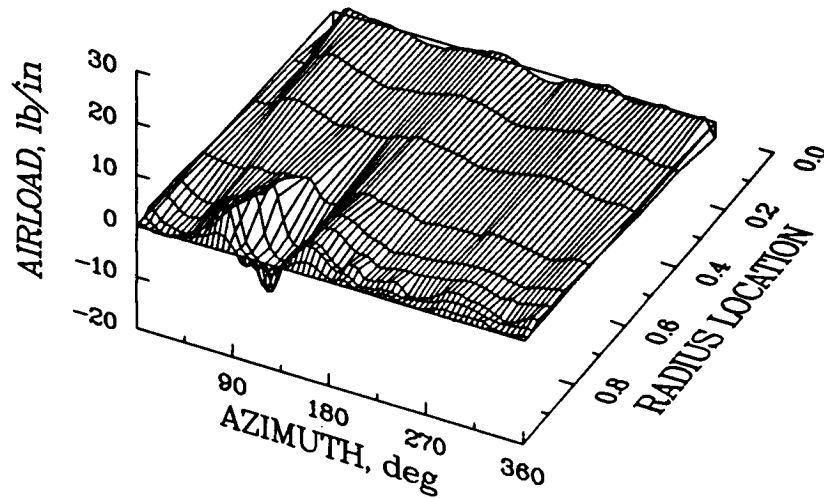


Figure 15.- Vibratory airloads (3-36 harmonics) measured on CH-34 rotor in wind tunnel;  $\mu = 0.39$  (refs. 1 and 51).

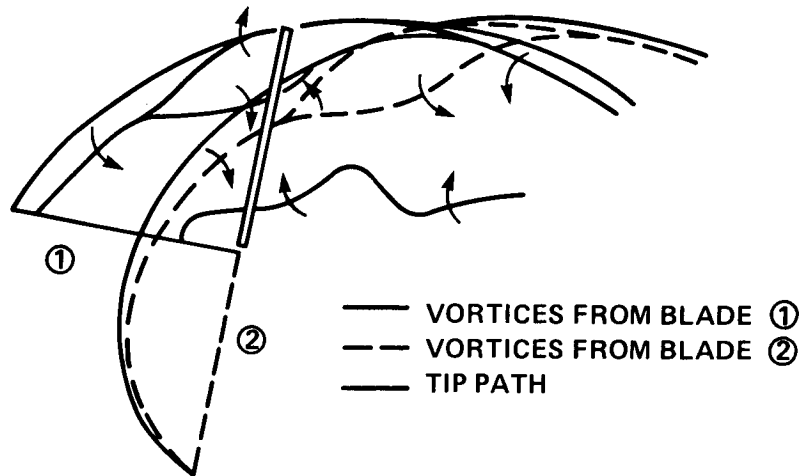


Figure 16.- Sketch of wake geometry for CH-34 high speed case (ref. 52).

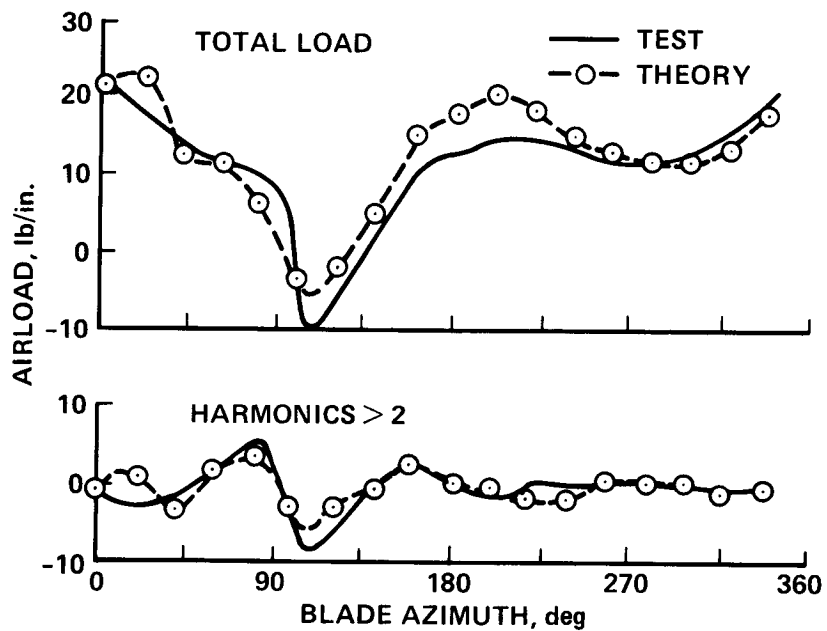


Figure 17.- Blade loading predicted at 0.90R compared to CH-34 wind tunnel measurements;  $\mu = 0.39$  (ref. 52).

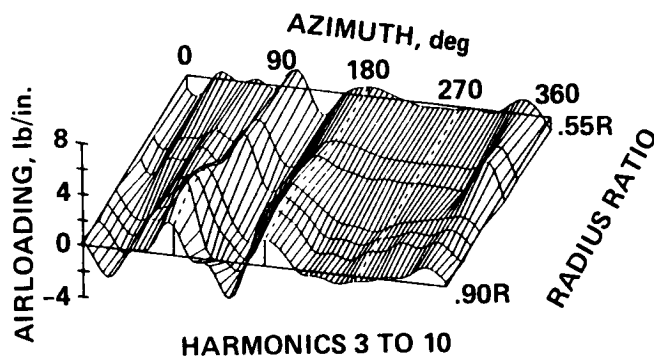


Figure 18.- Model-scale vibratory airloads (3-10 harmonics) for Model 360 rotor;  $\mu = 0.405$  (ref. 55).

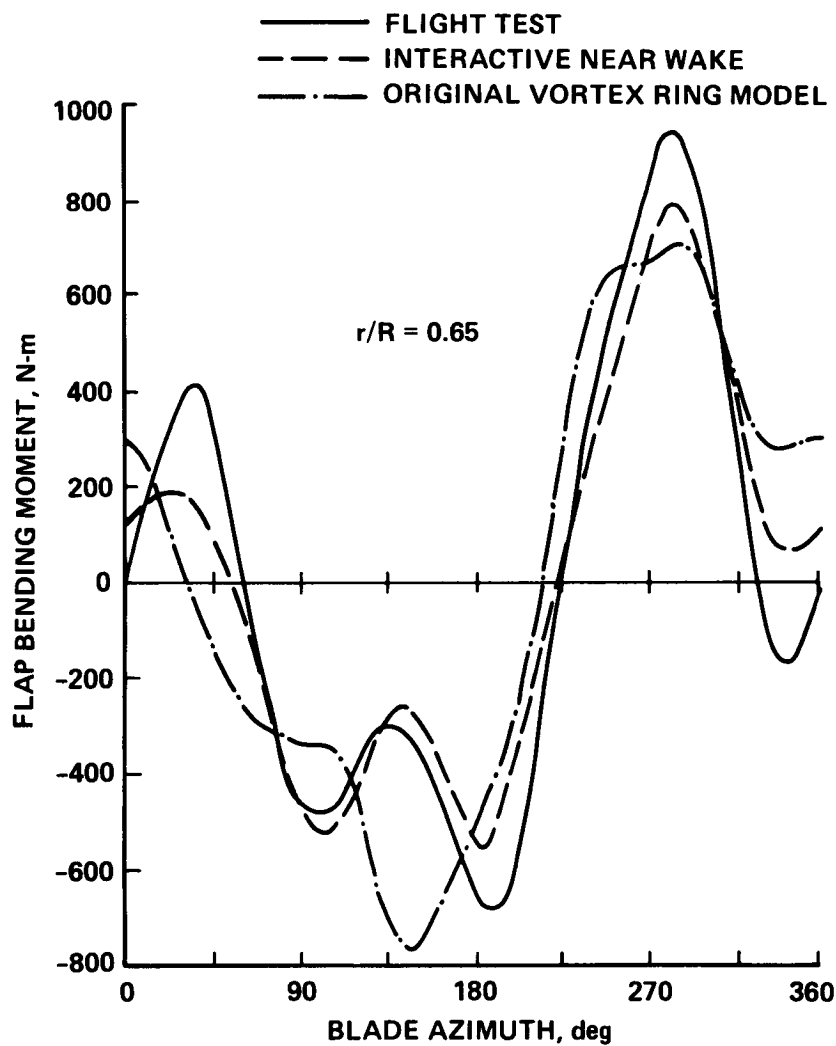


Figure 19.- Comparison of vortex ring wake model with flap bending moments on a Puma;  $\mu = 0.32$  (ref. 56).

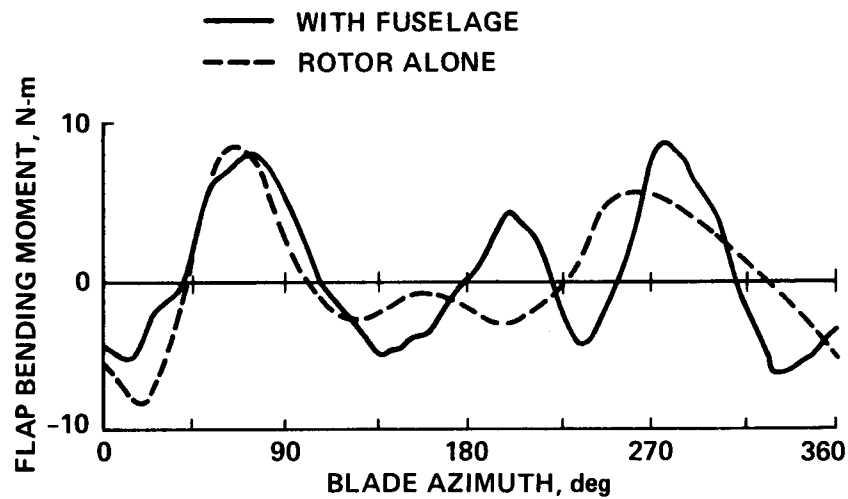


Figure 20.- Model rotor flap bending moments with and without a fuselage;  $\mu = 0.3$ ,  $\Omega = 600$  rpm (ref. 37).

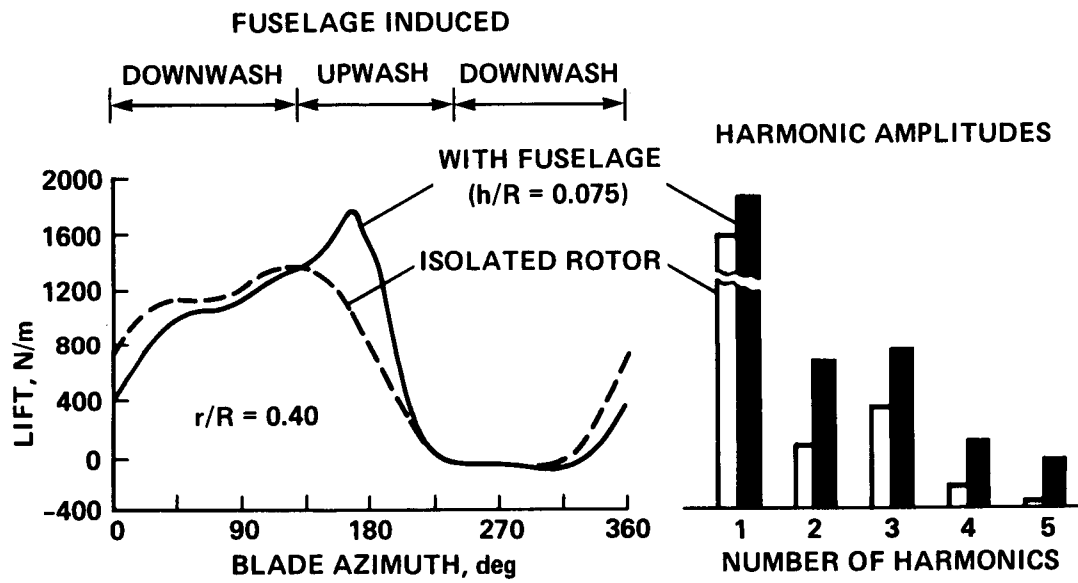


Figure 21.- Calculated effect of fuselage on blade lift and harmonic loads;  $V = 150$  knots,  $r/R = 0.40$  (ref. 65).

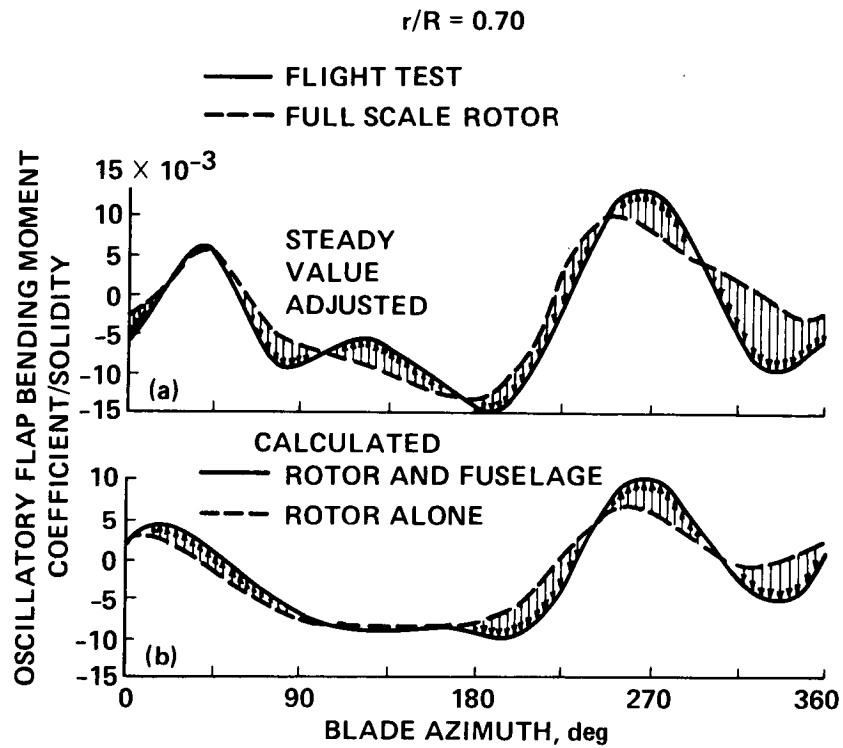


Figure 22.- Influence of fuselage on S-76 flap bending moments; GW = 10,300 lb,  $\mu = 0.375$  (ref. 66). (a) Comparison of flight test and wing tunnel test data. (b) Calculation for flight test case with and without fuselage.

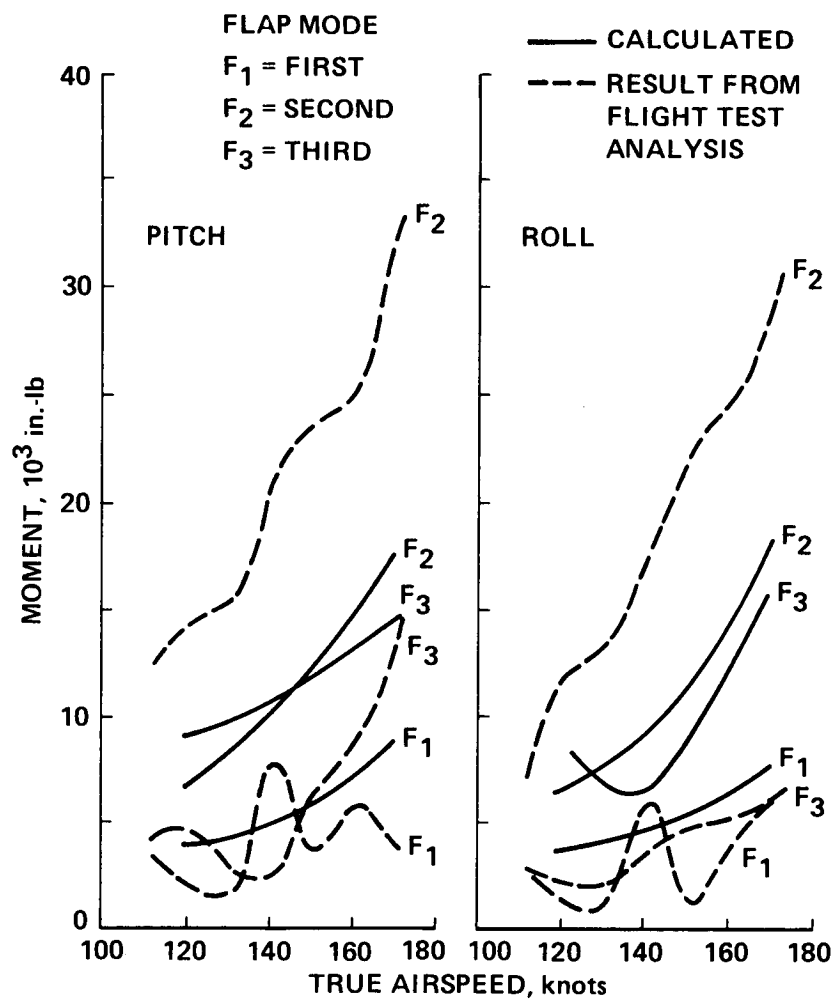


Figure 23.- Modal contributions to 4/rev hub pitch and roll moments for Lynx (ref. 70).

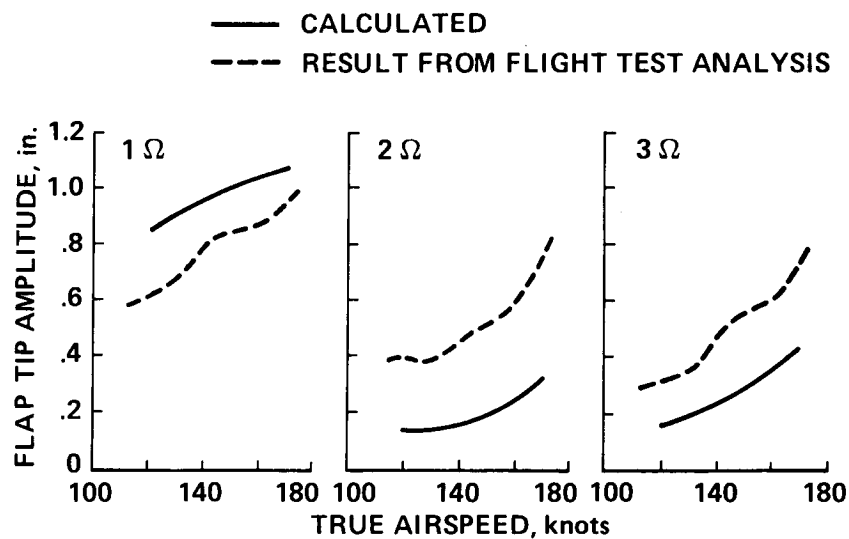


Figure 24.- Second flap mode harmonic amplitudes for Lynx (ref. 70).



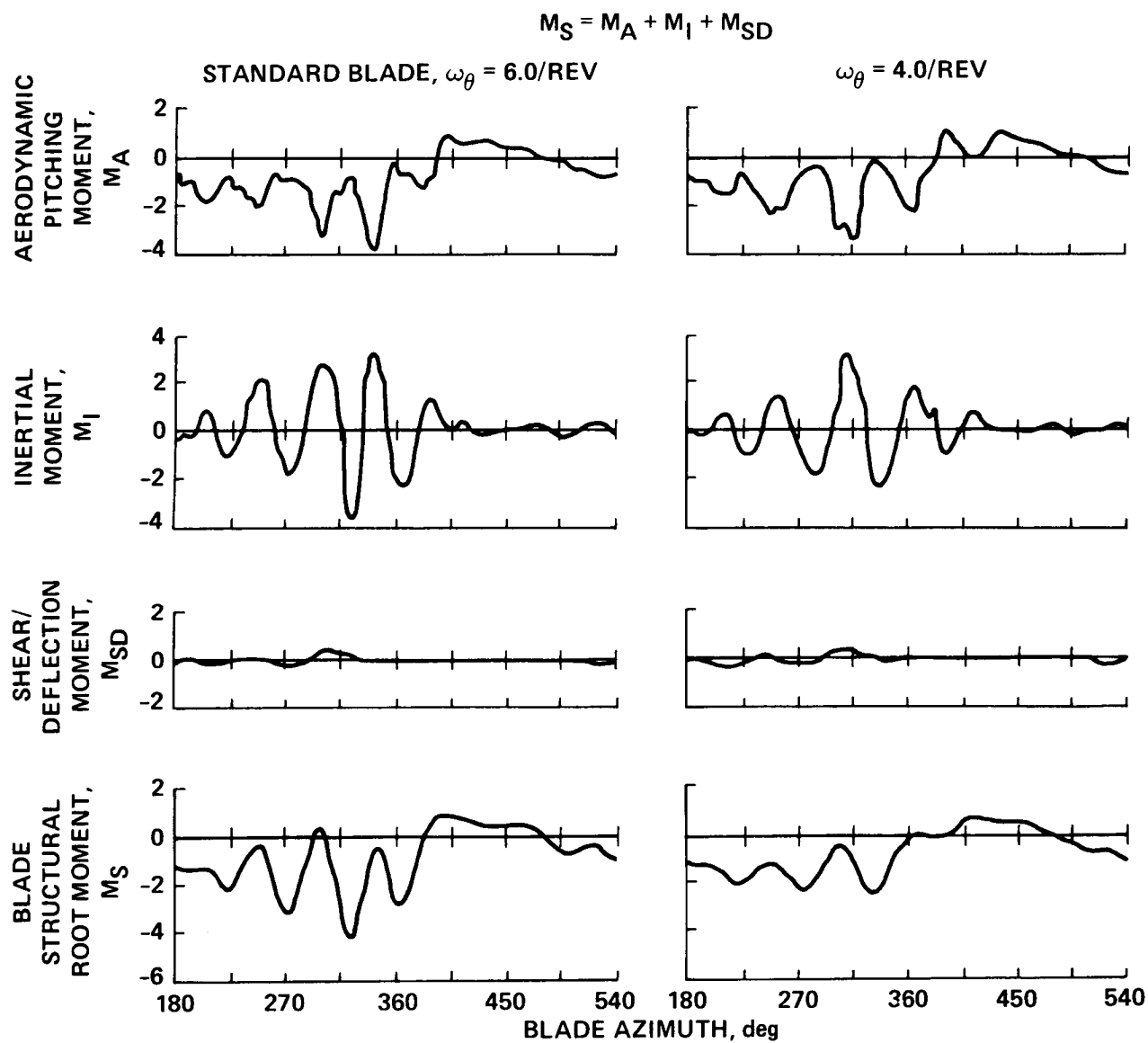


Figure 25.- Calculated effect of torsional frequency for CH-53A;  $V = 140$  knots,  $GW = 49,000$  lb (ref. 24).

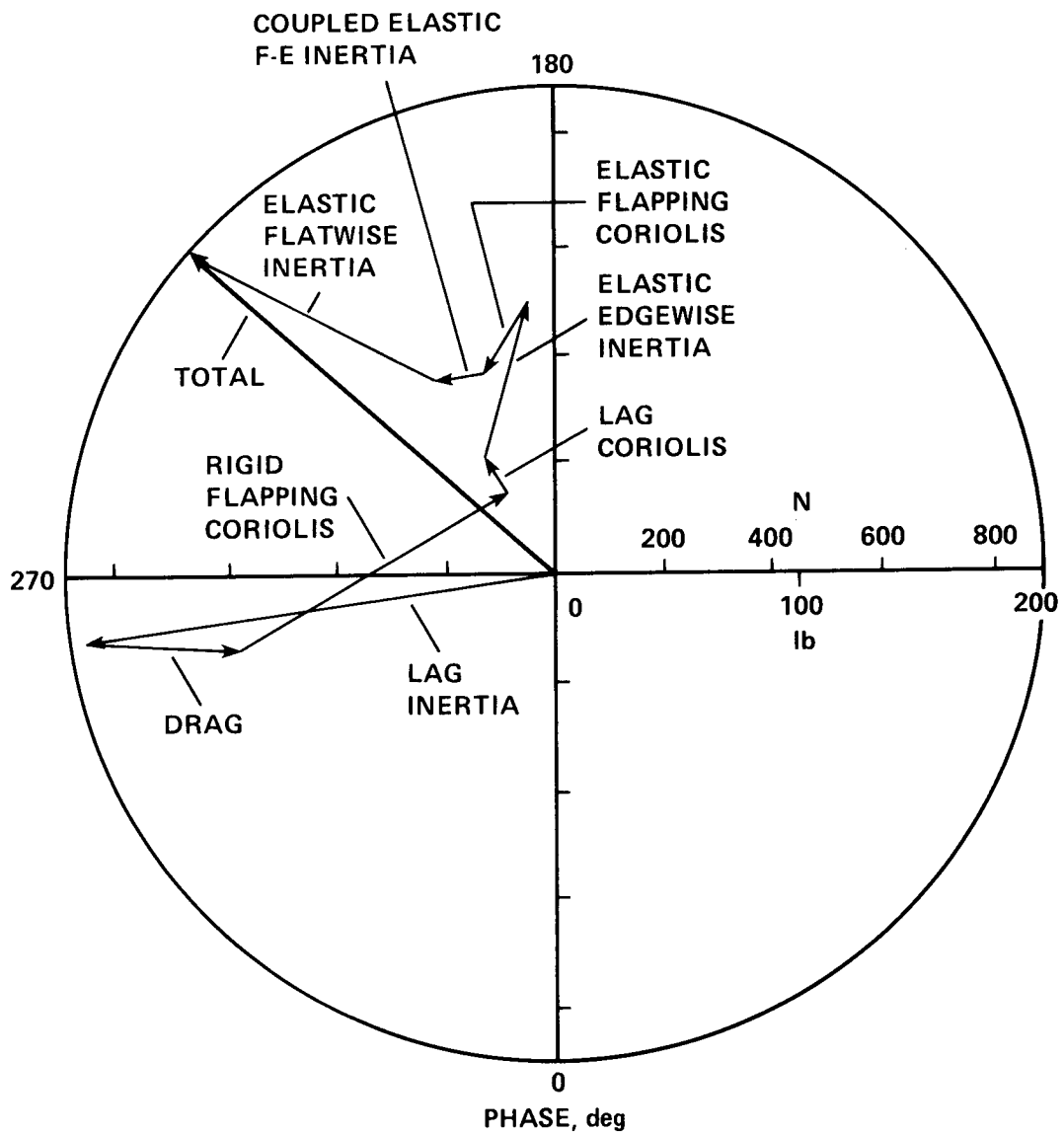


Figure 26.- Calculated 3/rev lateral shear for baseline blade;  $V = 160$  knots (ref. 80).

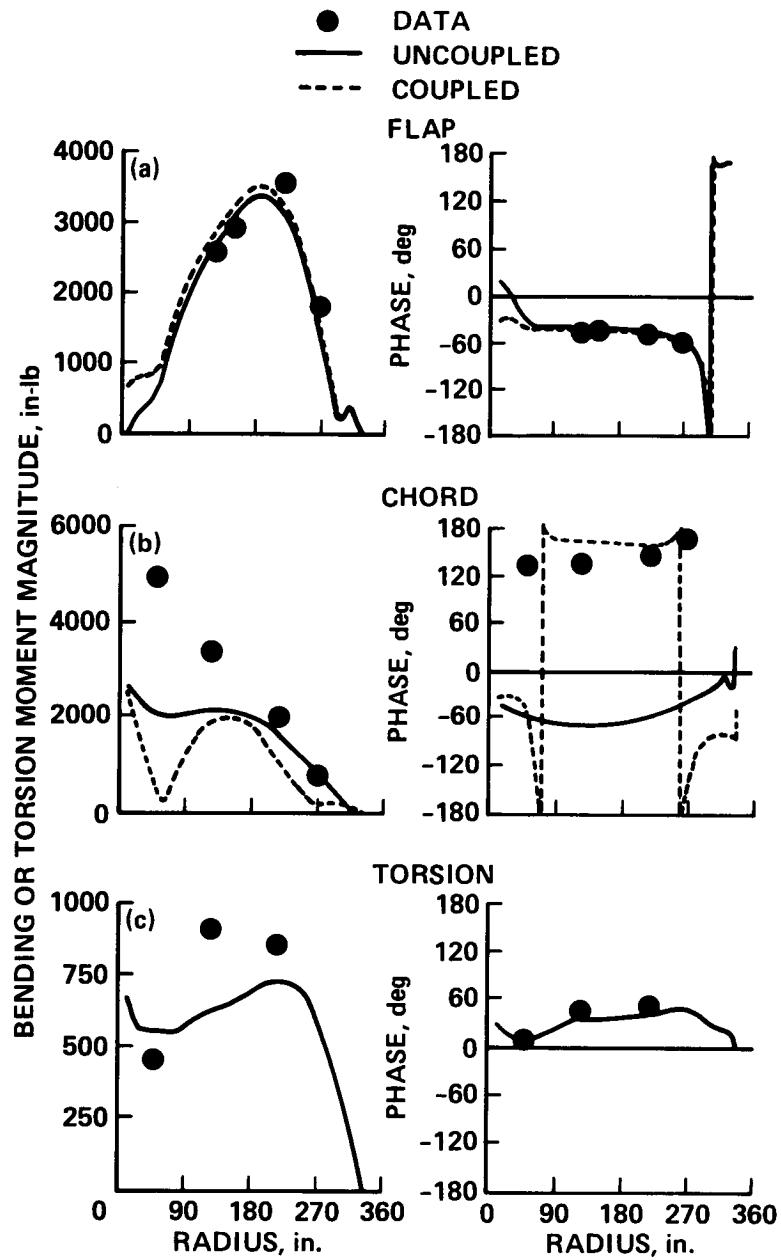


Figure 27.- First harmonic blade moments of CH-34 in wind tunnel obtained from measurement and calculations based on measured pressures;  $\mu = 0.39$ ,  $\alpha_s = -5^\circ$  (ref. 81). (a) Flap. (b) Chord. (c) Torsion.

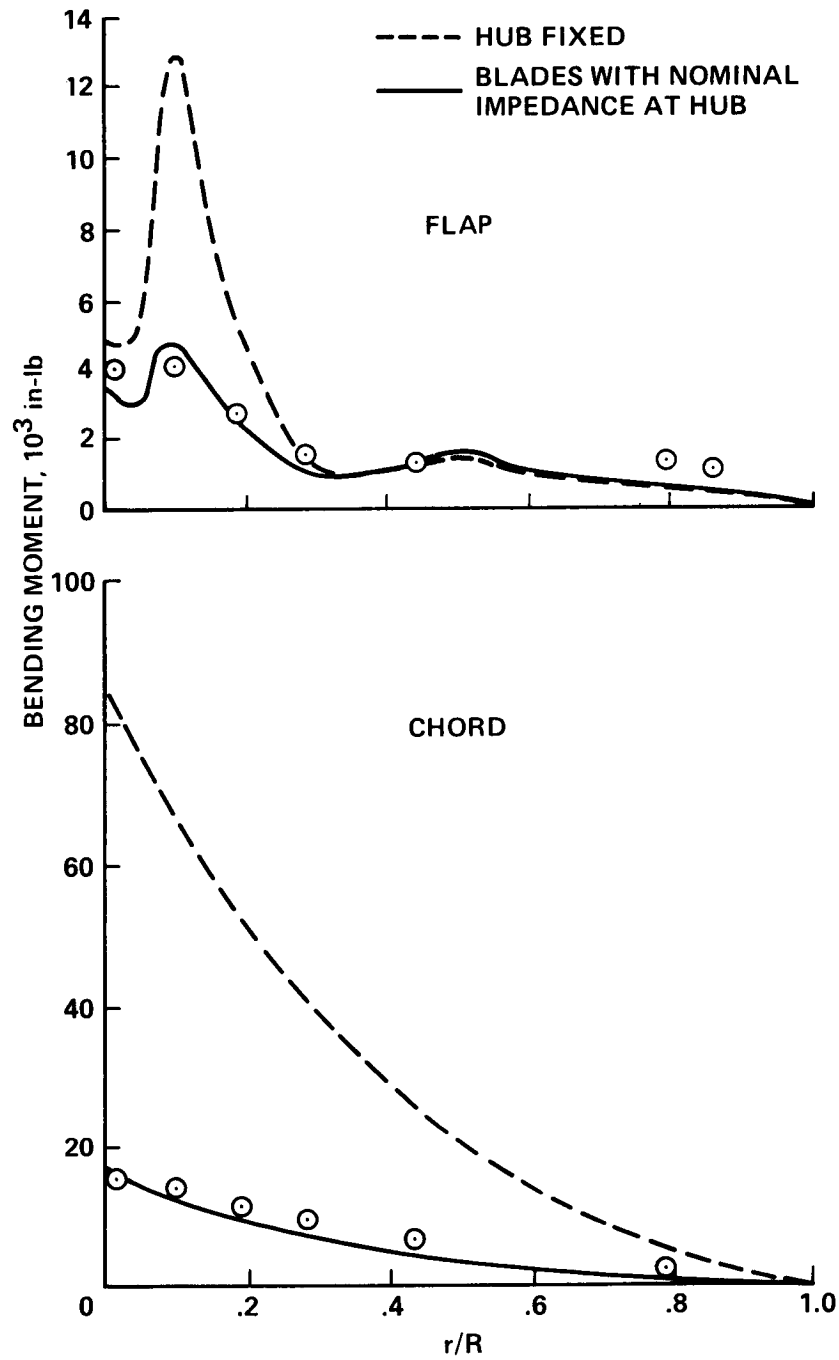


Figure 28.- Comparison of OH-58A blade bending moments with and without modeling of pylon impedance;  $V = 83$  knots (ref. 85).

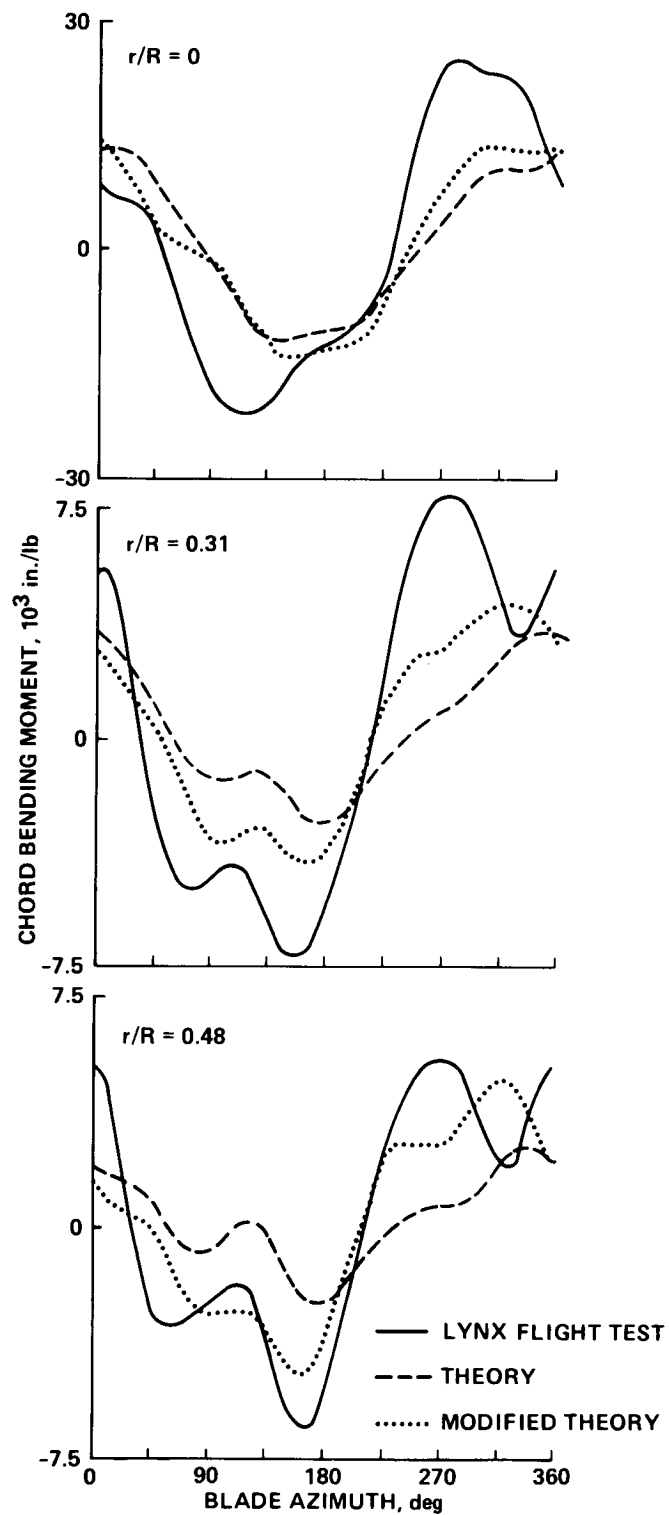


Figure 29.- Comparison of chord bending moments for the Lynx showing effect of modified theory;  $V = 122$  knots (ref. 91).

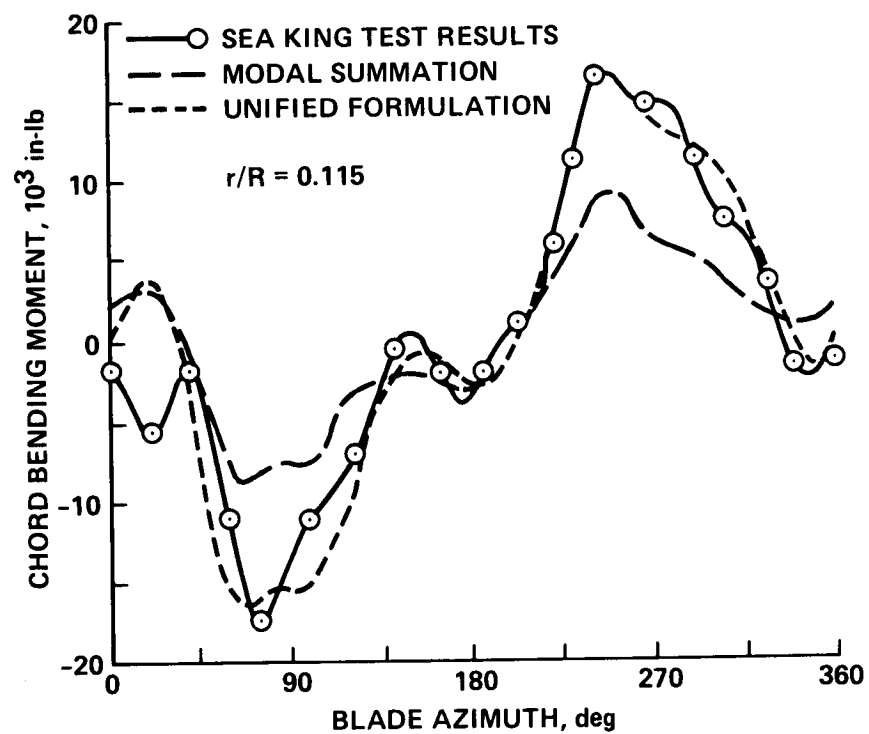


Figure 30.- Comparison of chord bending moment for Sea King with theory using modal summation and unified formulation;  $V = 120$  knots (ref. 90).

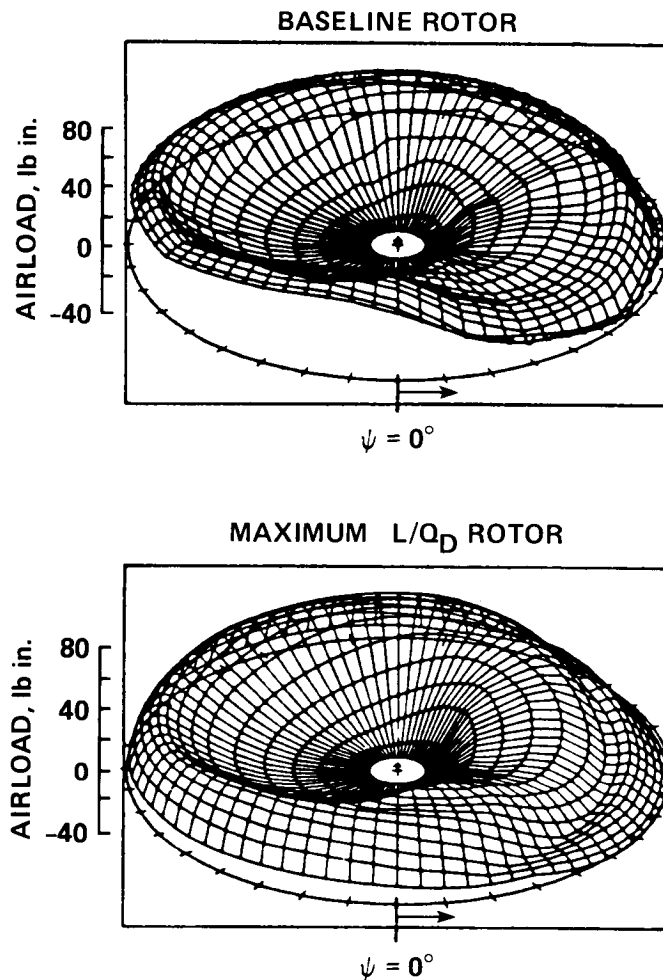


Figure 31.- Comparison of baseline and maximum  $L/Q_D$  rotor airload distribution using variable inflow;  $\mu = 0.3$ ,  $C_L/\sigma = 0.10$  (ref. 97).

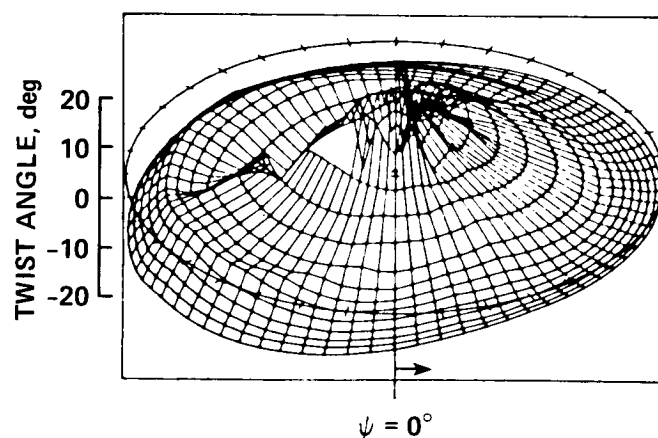


Figure 32.- Twist required to produce maximum  $L/Q_D$ ;  $\mu = 0.3$ ,  $C_L/\sigma = 0.10$  (ref. 97).

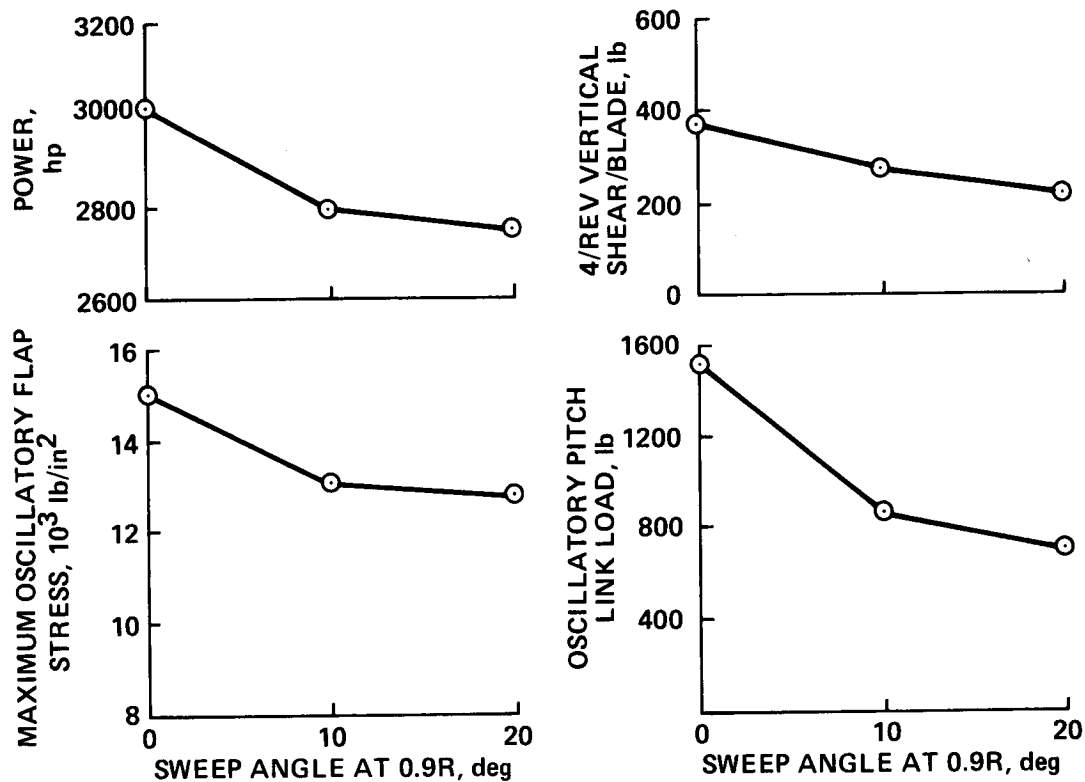
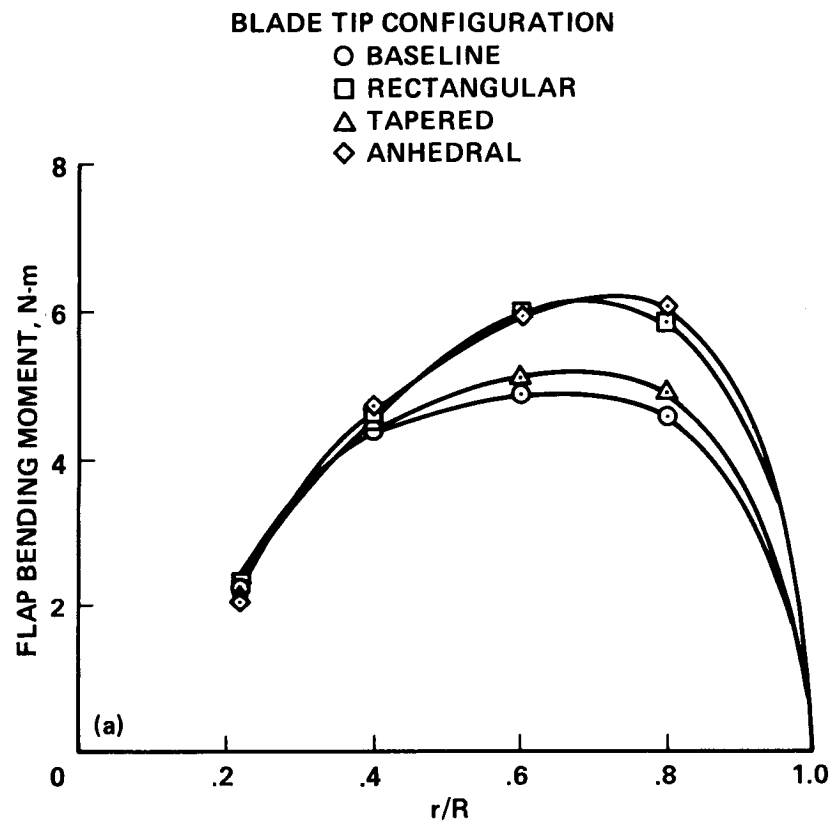


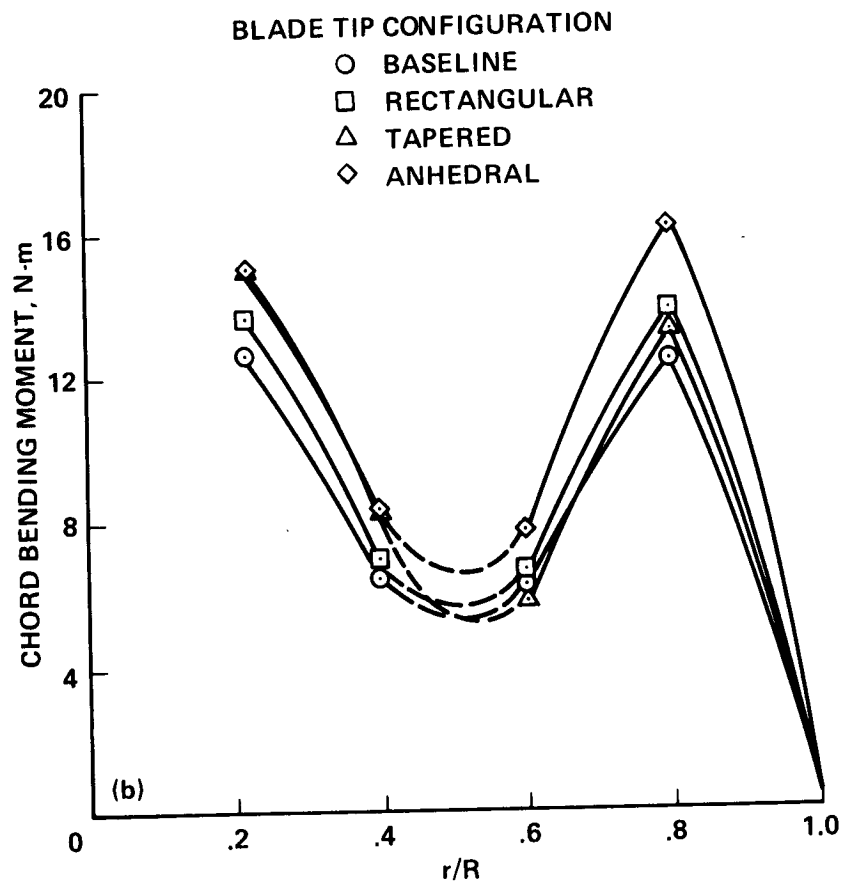
Figure 33.- Variation of power and rotor system loads with sweep angle for conformable rotor;  $\mu = 0.4$ ,  $C_L/\sigma = 0.085$  (ref. 97).





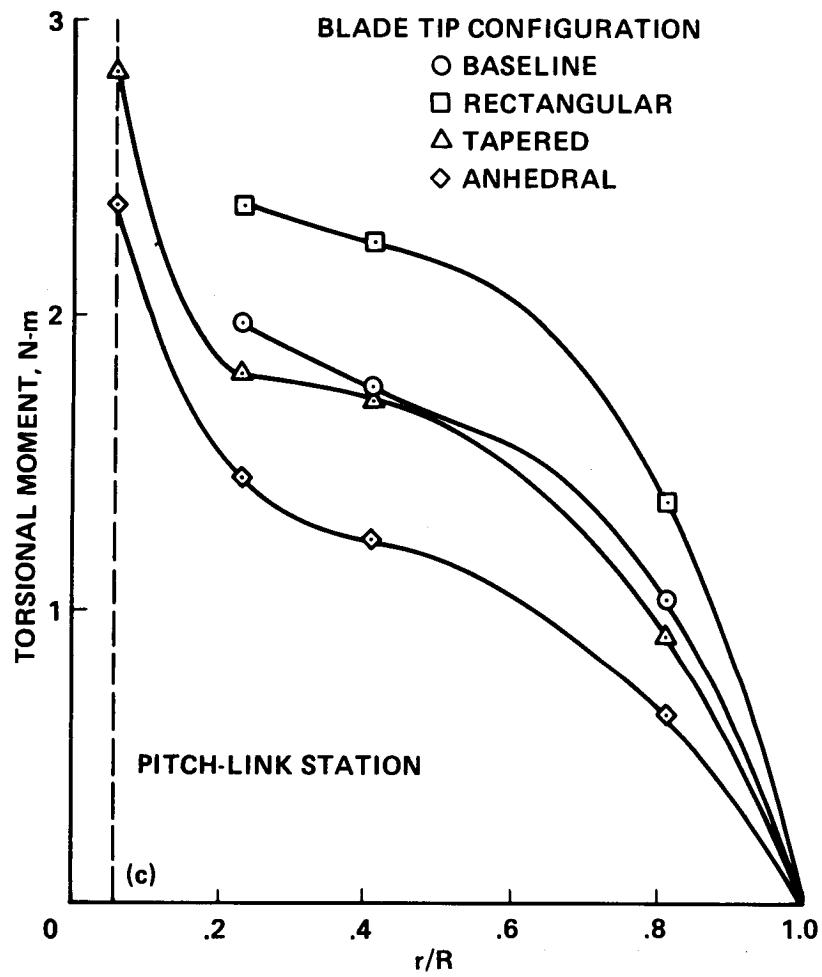
(a) Flap bending moment.

Figure 34.- Oscillatory blade moments for four tip configurations;  $\mu = 0.35$ ,  $C_L/\sigma = 0.09$  (ref. 98).



(b) Chord bending moment.

Figure 34.- Continued.



(c) Torsion moment.

Figure 34.- Concluded.

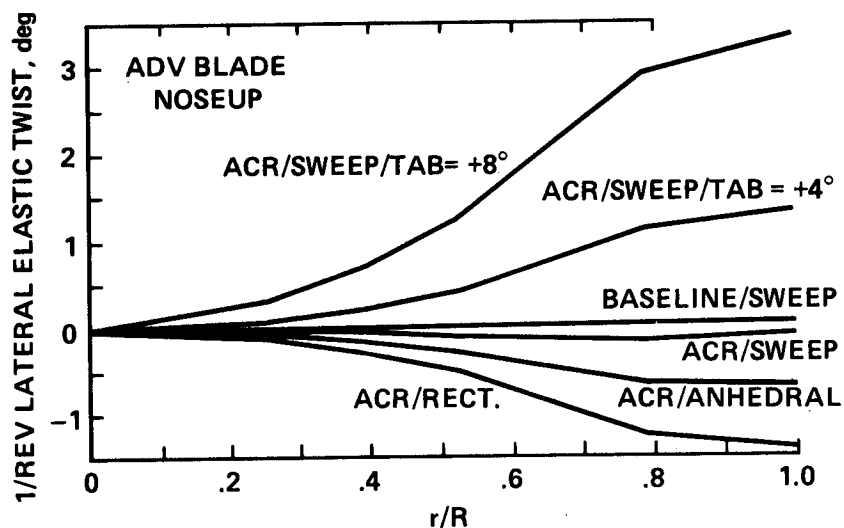


Figure 35.- 1/rev lateral twist of ACR configurations and baseline rotor;  $\mu = 0.3$ ,  $C_L/\sigma = 0.08$  (ref. 77).

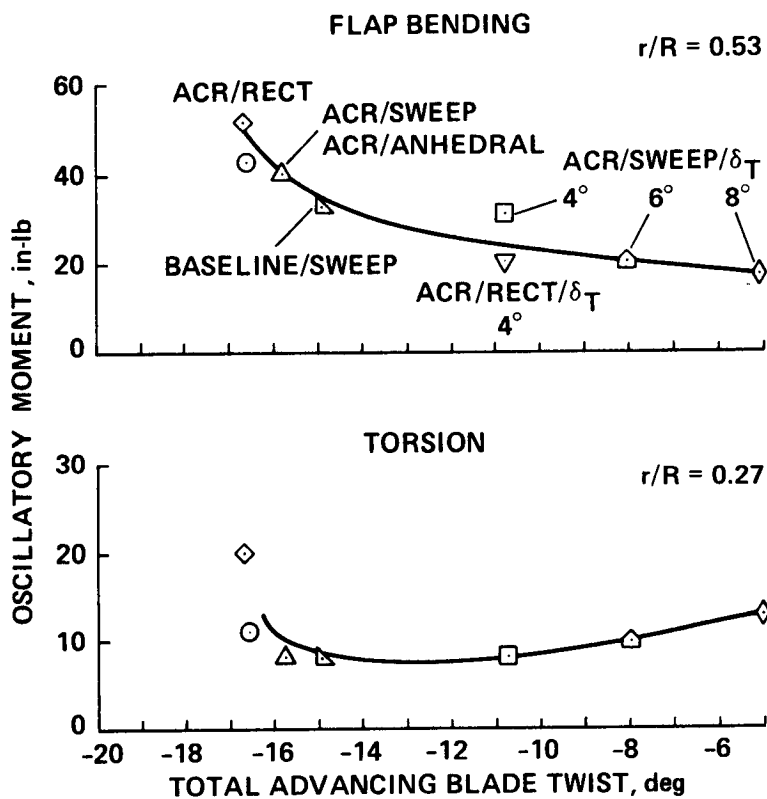


Figure 36.- Oscillatory moments as a function of total twist at  $\psi = 90^\circ$ ;  $\mu = 0.3$ ,  $C_L/\sigma = 0.08$  (ref. 77).

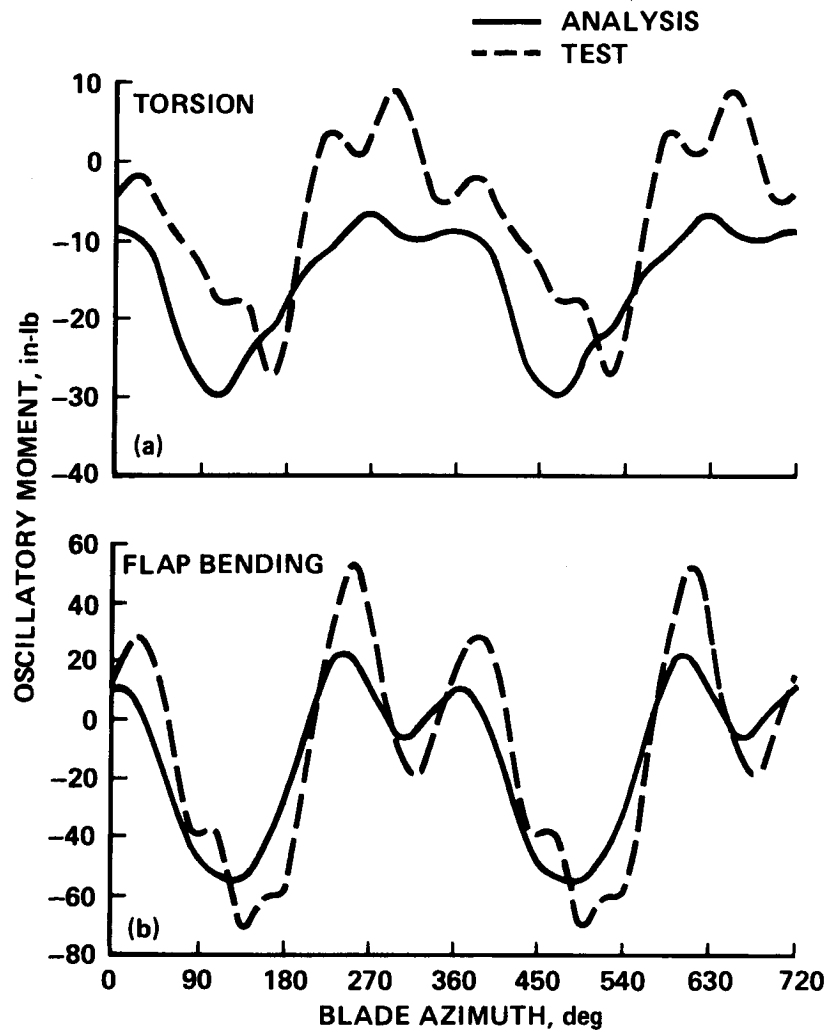


Figure 37.- Comparison of predicted and measured blade moment time histories;  $\mu = 0.3$ ,  $C_L/\sigma = 0.08$  (ref. 77). (a) Torsion moment. (b) Flap bending moment.

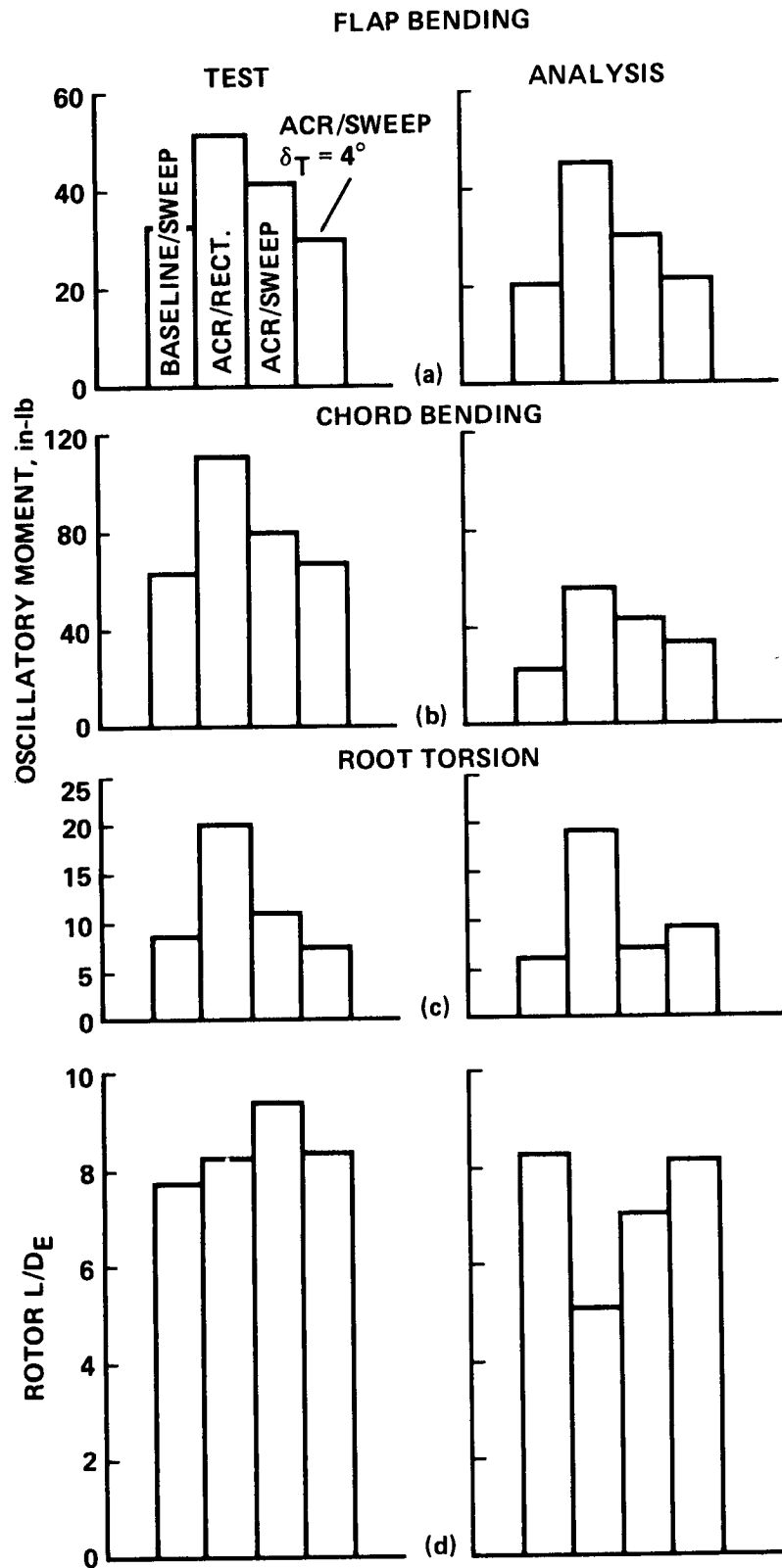


Figure 38.- Correlation of blade loads and rotor  $L/D_E$  for four model rotor configurations;  $\mu = 0.3$ ,  $C_L/\sigma = 0.08$  (ref. 77). (a) Oscillatory flap bending moment. (b) Oscillatory chord bending moment. (c) Oscillatory root torsion moment. (d) Rotor  $L/D_E$ .

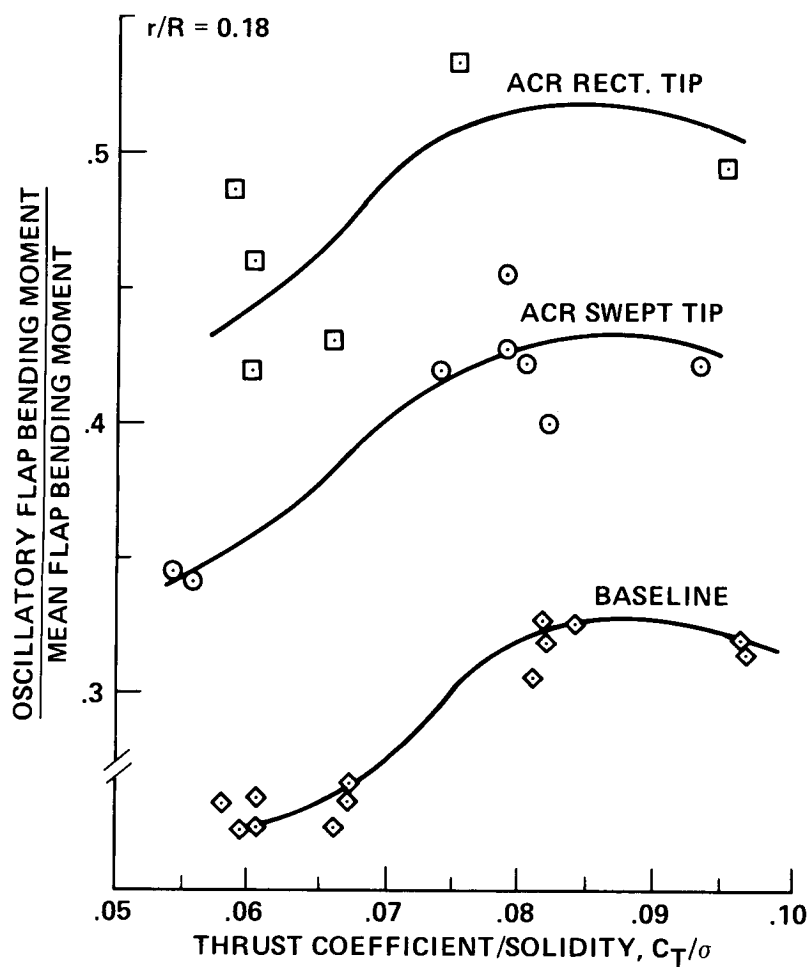


Figure 39.- Ratio of oscillatory flap bending moment to mean for three rotor configurations;  $\mu = 0.35$  (ref. 101).

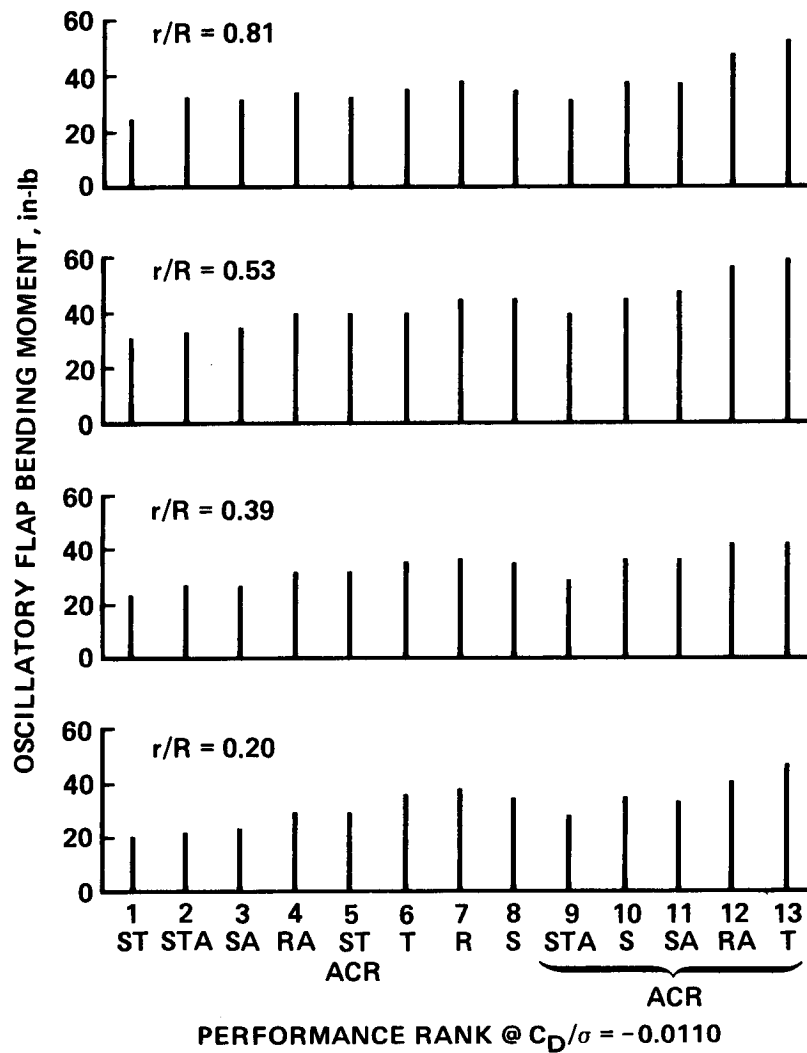


Figure 40.- Oscillatory flap bending moment relative to performance rank;  $\mu = 0.35$ ,  $C_L/\sigma = 0.0791$  (ref. 103).



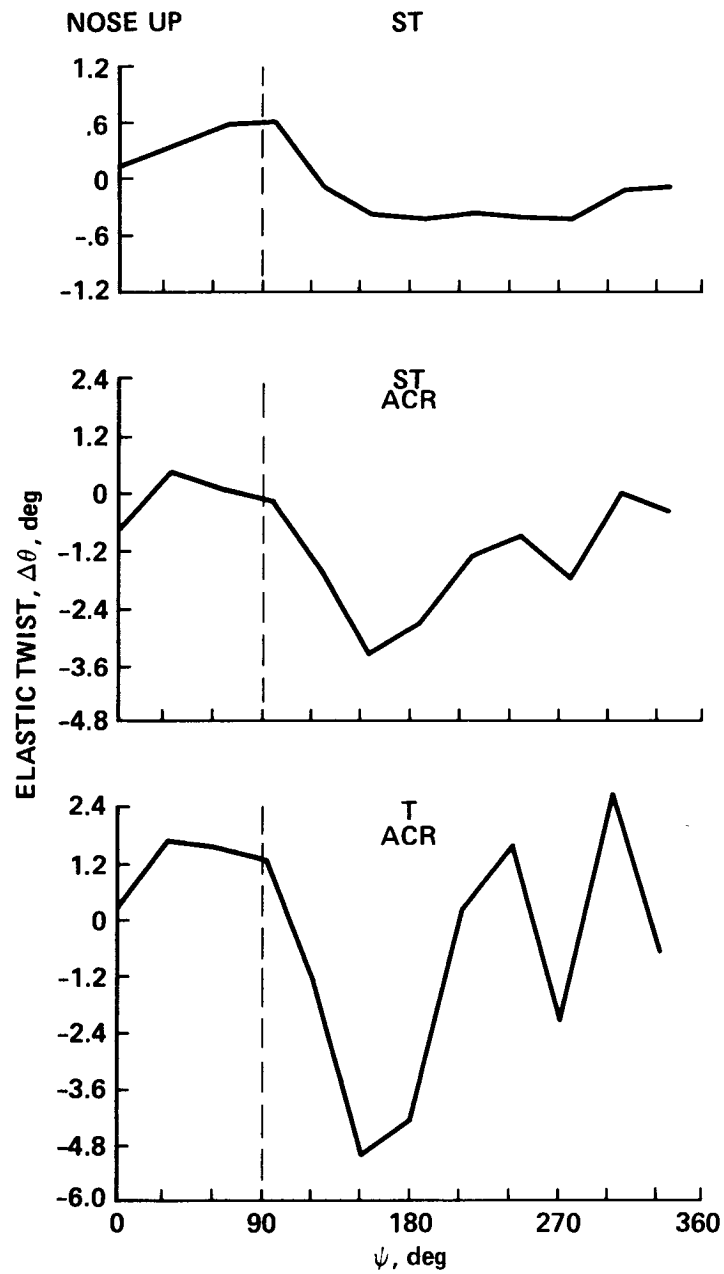


Figure 41.- Elastic twist as a function of azimuth for three rotor configurations;  
 $\mu = 0.35$ ,  $C_L/\sigma = 0.0791$  (ref. 103).

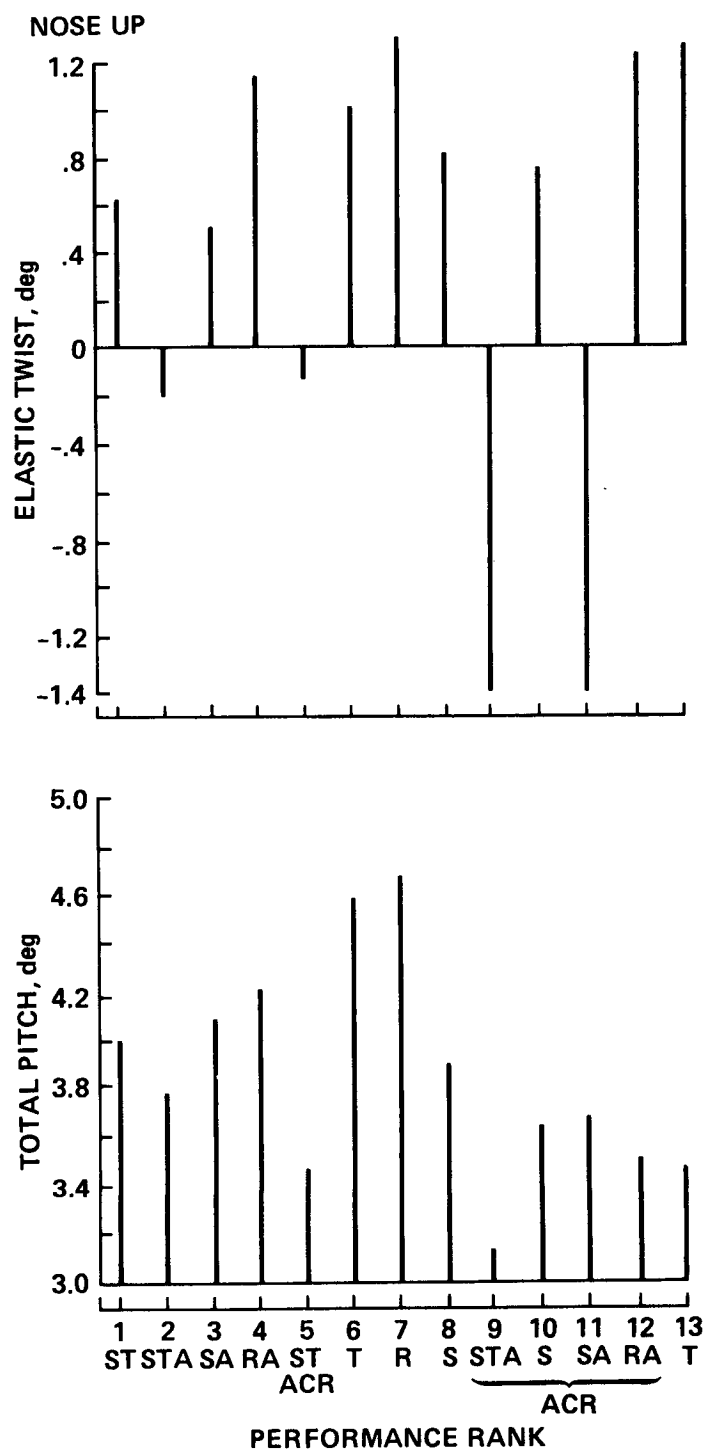


Figure 42.- Elastic twist at  $\psi = 90^\circ$  relative to performance rank;  $\mu = 0.35$ ,  $C_L/\sigma = 0.0791$  (ref. 103).

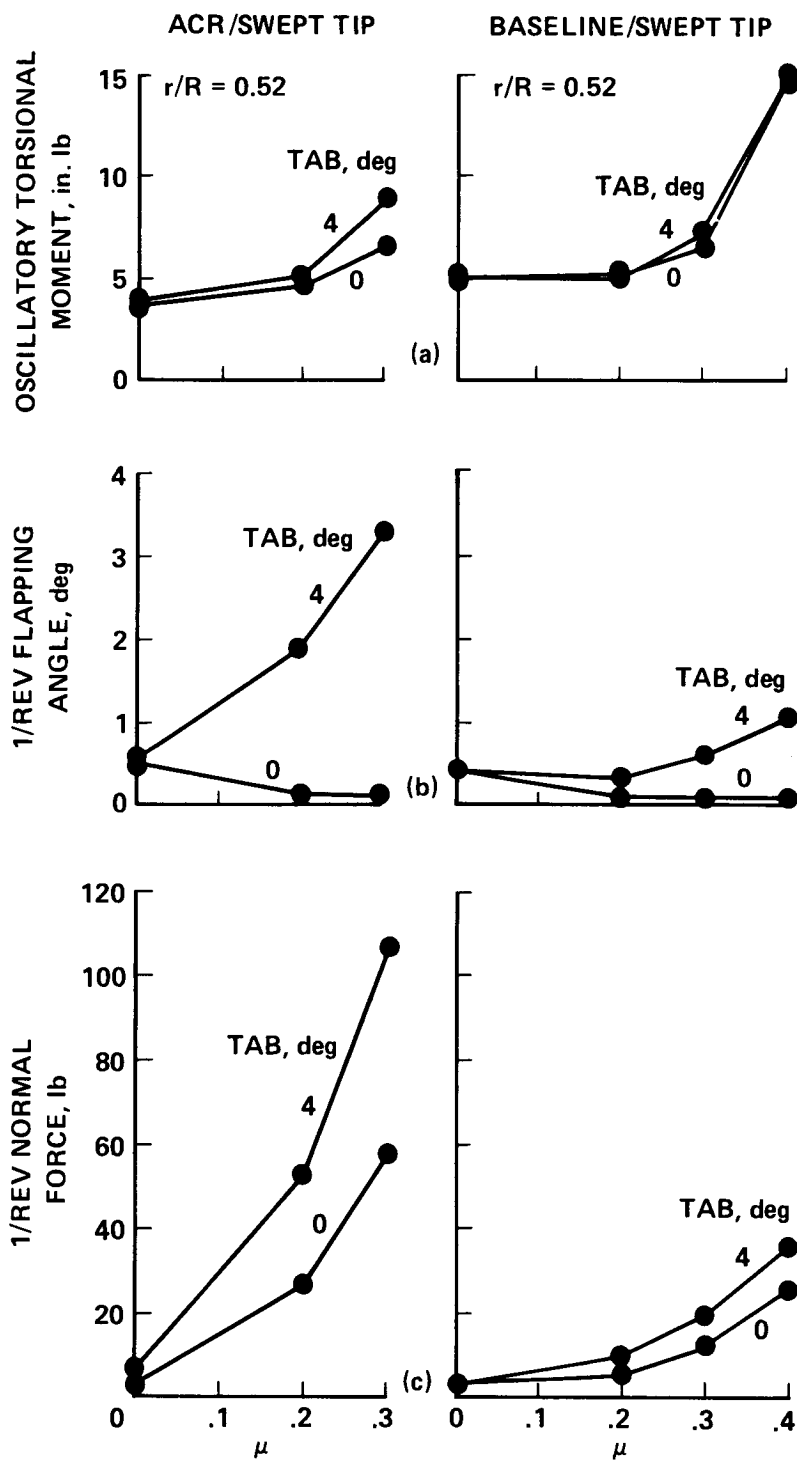
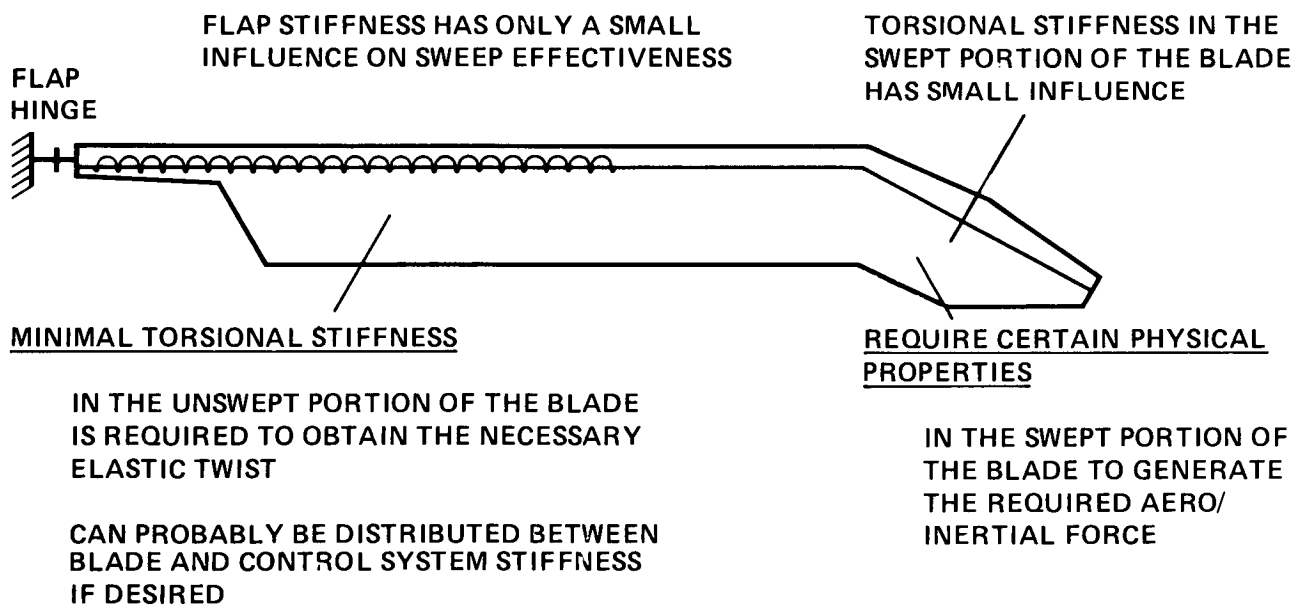


Figure 43.- Effect of tab deflection;  $C_L/\sigma = 0.0791$  (ref. 103). (a) Oscillatory torsion moment. (b) First harmonic flapping. (c) Fixed system normal loads.



#### MECHANISM:

AERO/INERTIAL FORCE OF THE SWEEP PORTION OF THE BLADE USED THE SWEEP ARM TO TWIST THE UNSWEPT PORTION OF THE BLADE .

IF THE PHASE AND AMPLITUDE OF THE SWEEP INDUCED ELASTIC TWIST REDUCES THE TIP DOWN TWIST ON THE ADVANCING BLADE AND REDUCES THE HIGHER HARMONIC TWIST FROM OTHER SOURCES, THE 4/REV VERTICAL HUB LOAD IS REDUCED.

Figure 44.- Understanding of hub loads reduction mechanisms (ref. 104).

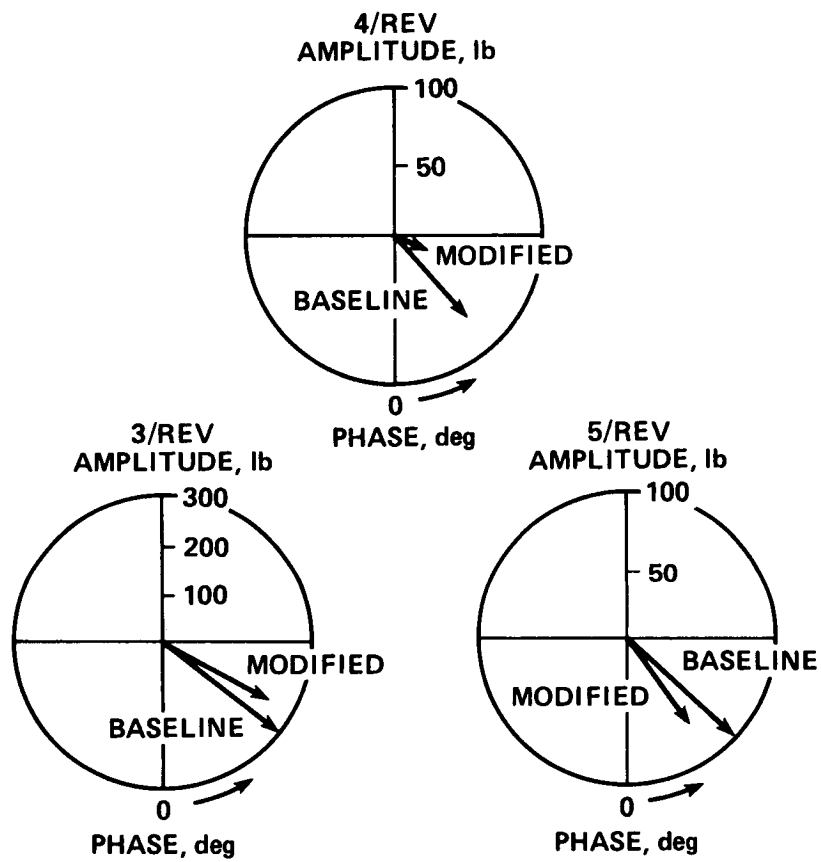


Figure 45.- Predicted reduction in blade root shears (ref. 79).

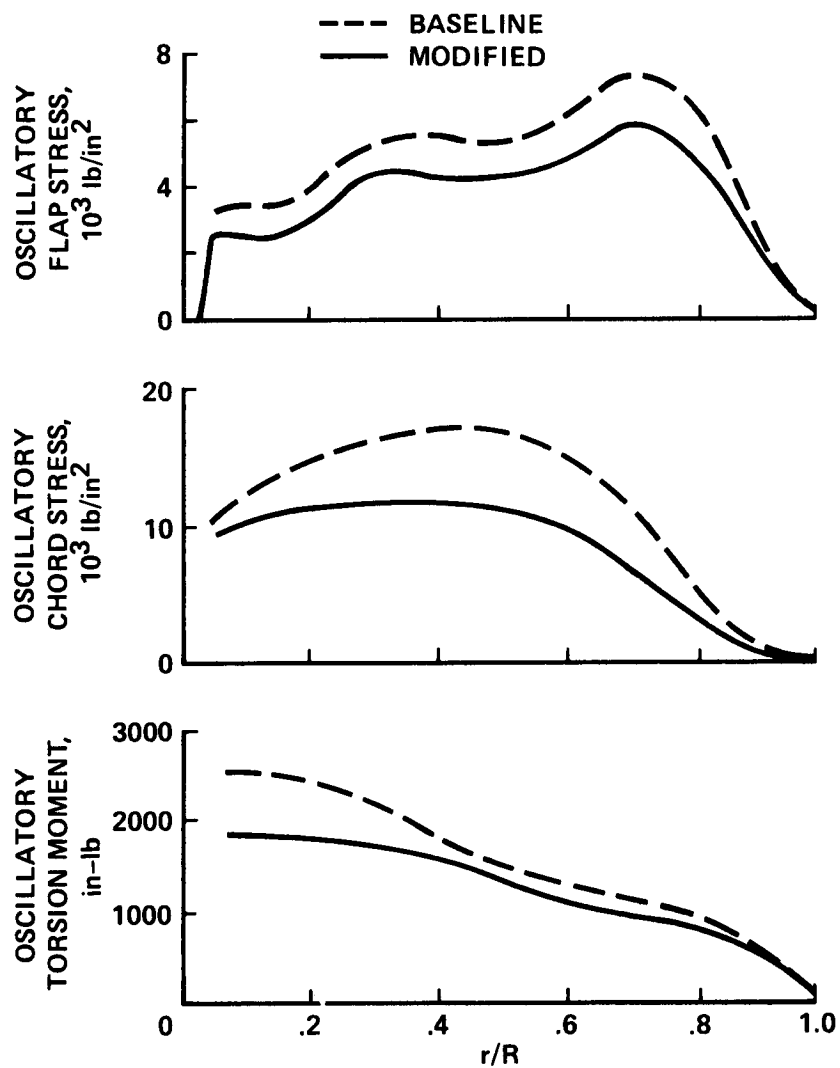


Figure 46.- Predicted reduction in blade stresses (ref. 79).

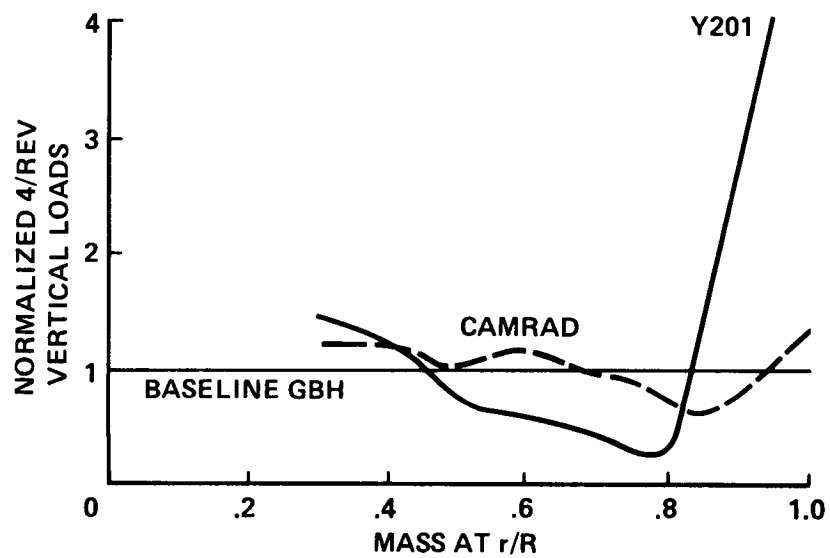


Figure 47.- Predicted 4/rev vertical loads for Growth Black Hawk as mass radial location is varied;  $\mu = 0.338$ ,  $C_L = 0.00608$ .

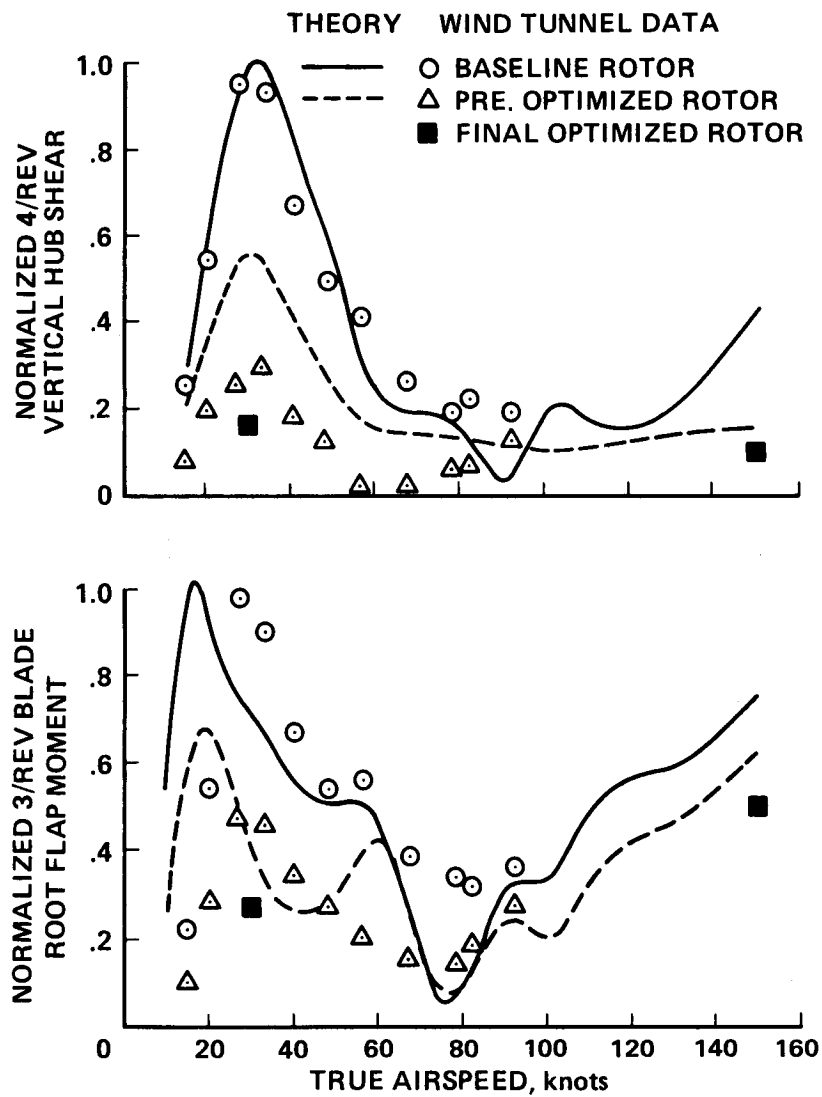


Figure 48.- Normalized 4/rev vertical hub shear and 3/rev blade root flap bending moment as a function of airspeed (ref. 109).



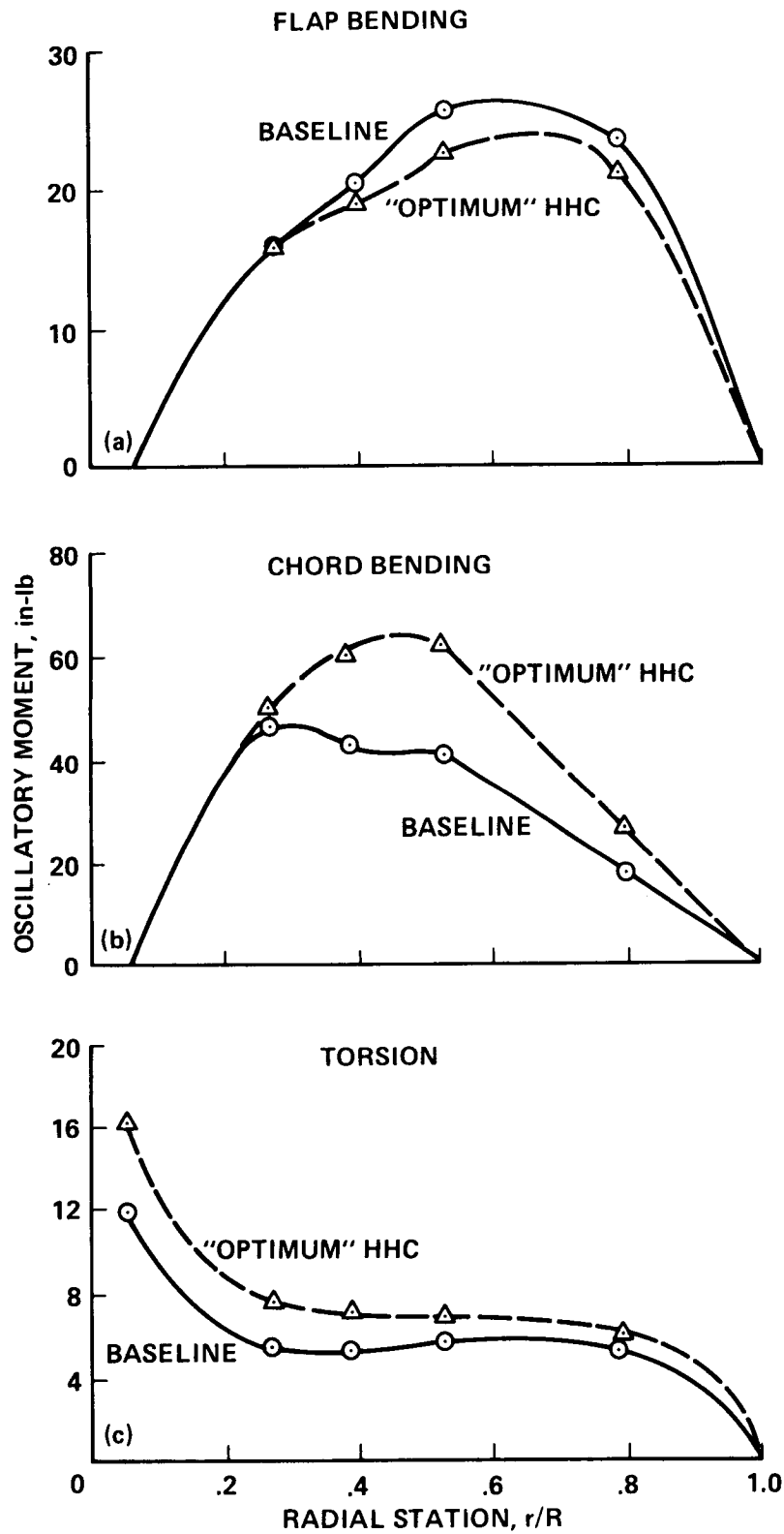


Figure 49.- Blade oscillatory loads with HHC;  $\mu = 0.3$  (ref. 110). (a) Flap bending moment. (b) Chord bending moment. (c) Torsion moment.

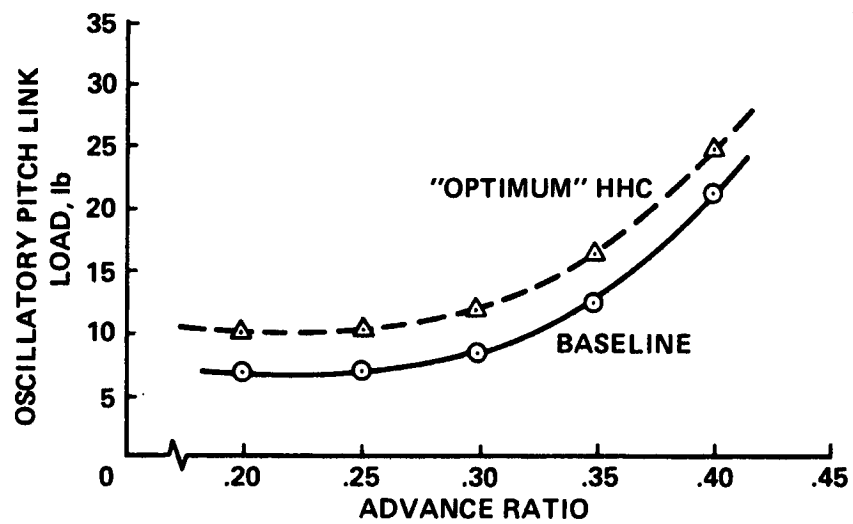
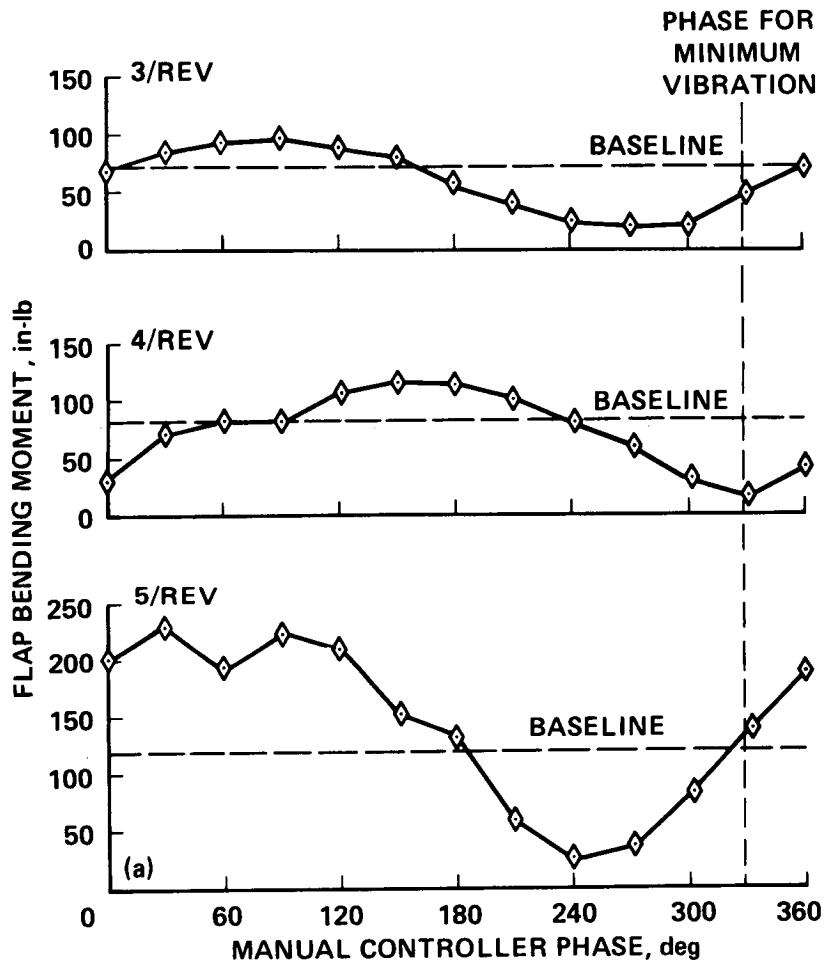
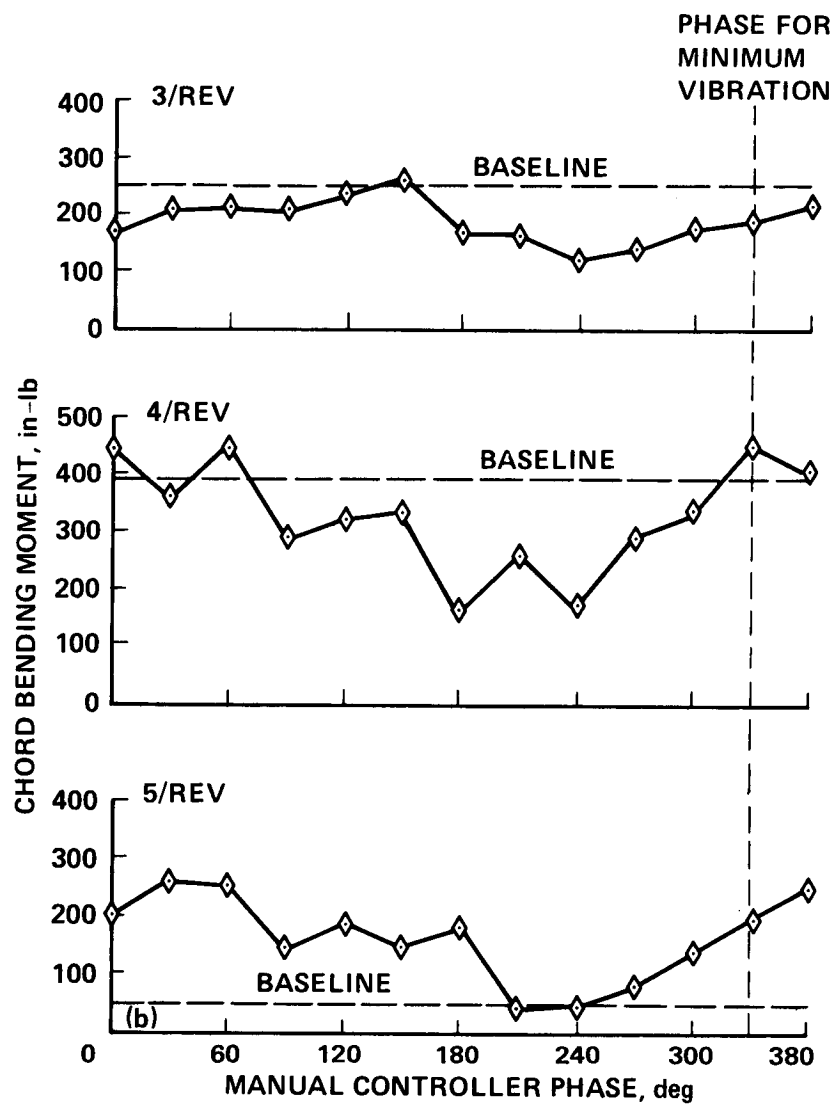


Figure 50.- Oscillatory pitch link loads with HHC (ref. 110).



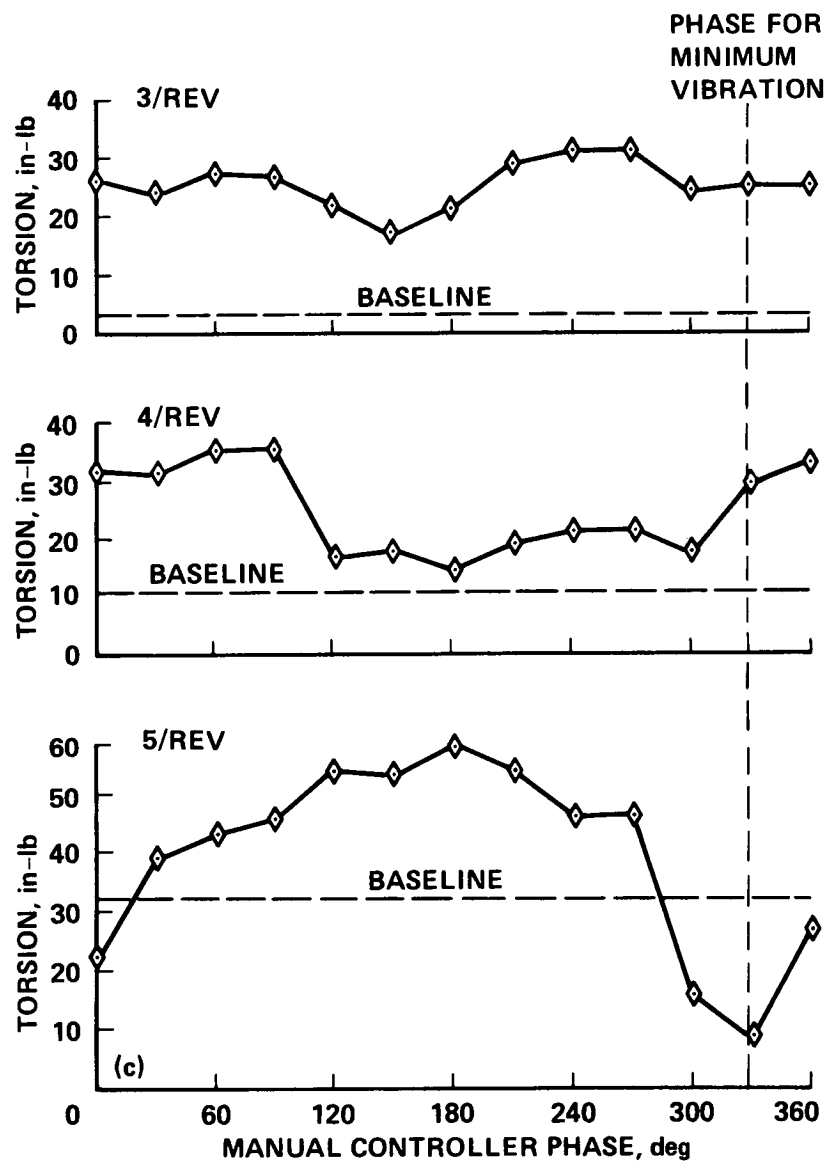
(a) Flap bending moment;  $r/R = 0.15$ .

Figure 51.- Effect of HHC on 3, 4, and 5/rev components of blade moments;  
 $V = 70$  knots (ref. 111).



(b) Chord bending moment;  $r/R = 0.17$ .

Figure 51.- Continued.



(c) Torsion moment;  $r/R = 0.17$ .

Figure 51.- Concluded.

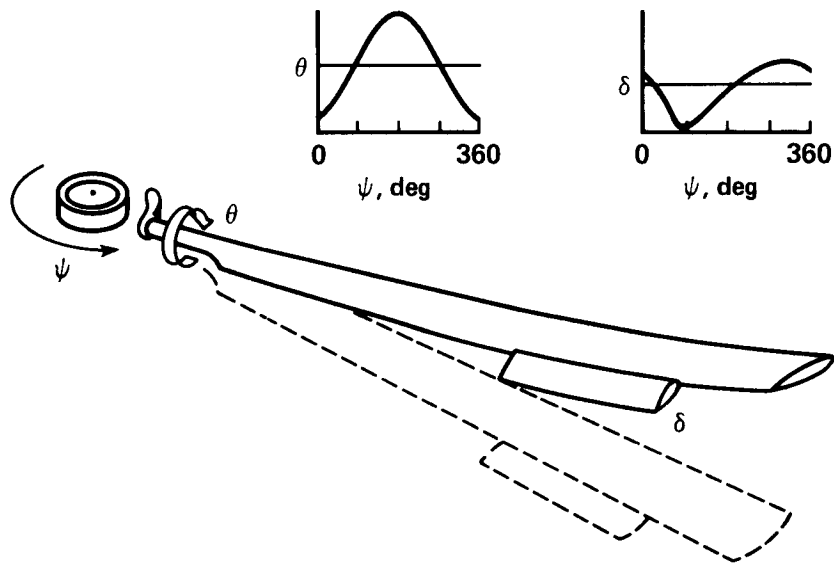


Figure 52.- Controllable twist rotor (CTR) schematic (ref. 112).

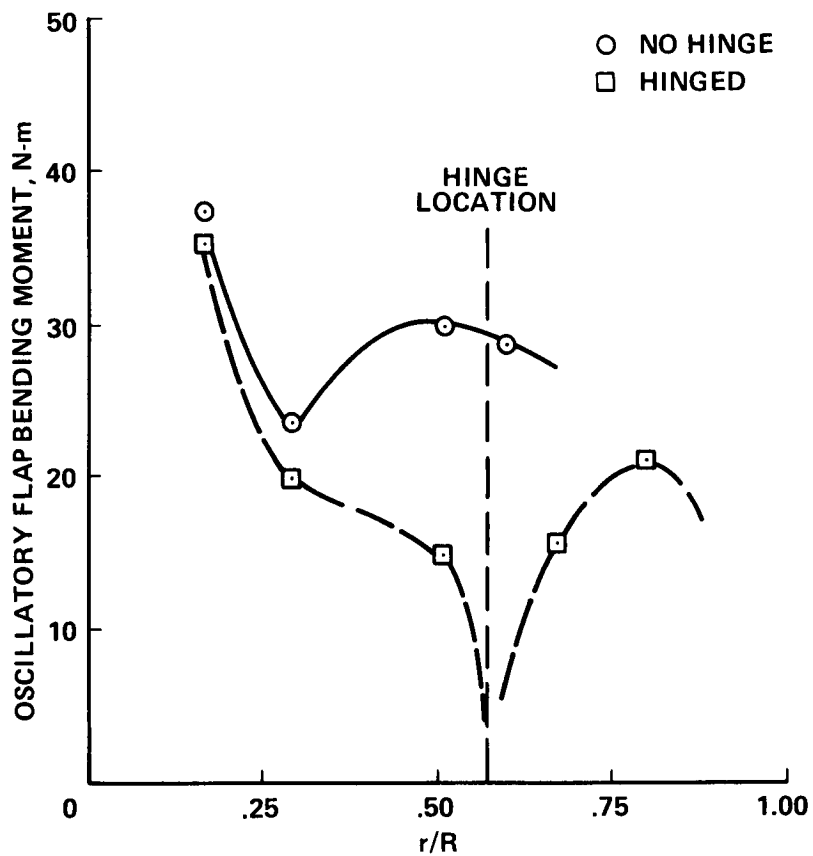


Figure 53.- Effect of mid-span hinge on teetering rotor blade oscillatory flap bending moment;  $\mu = 0.35$ ,  $C_L/\sigma = 0.025$  (ref. 113).

C-4

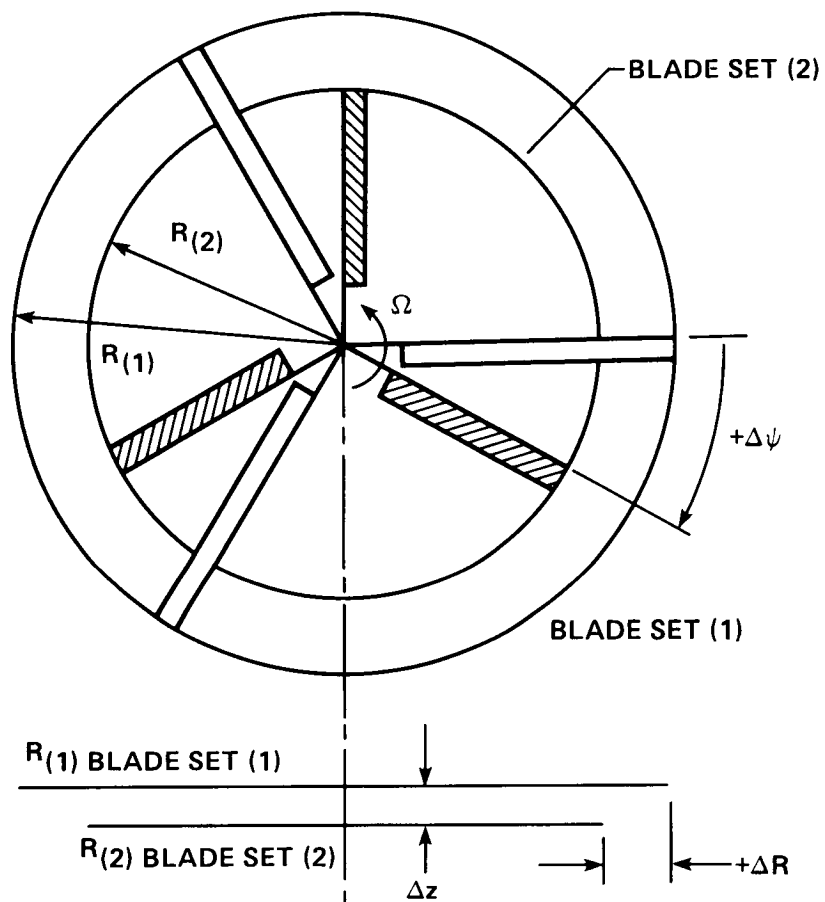


Figure 54.- Variable geometry rotor (VGR) parameters (ref. 114).

ORIGINAL PAGE IS  
OF POOR QUALITY

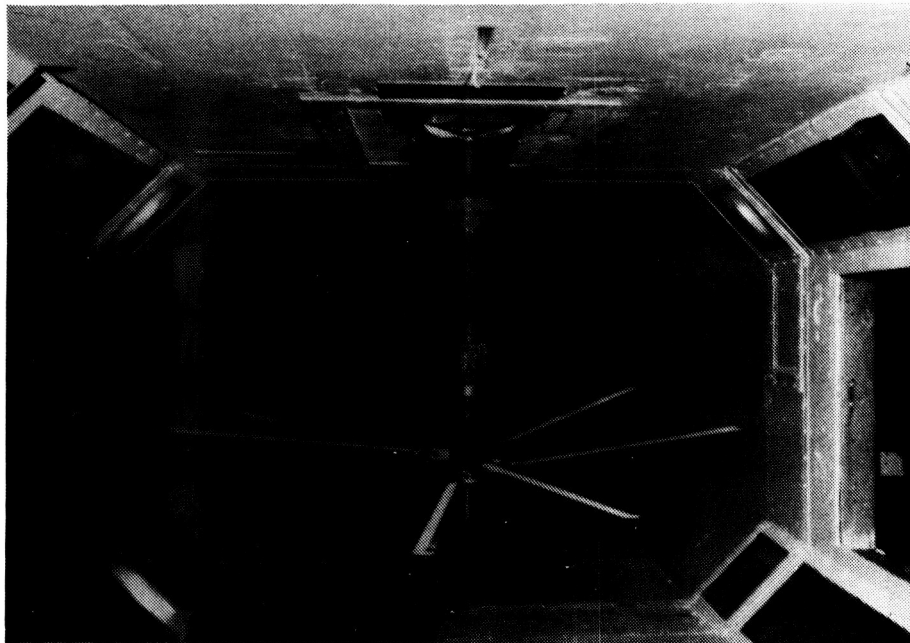


Figure 55.- Variable geometry rotor (VGR) in UTRC wind tunnel (ref. 116).

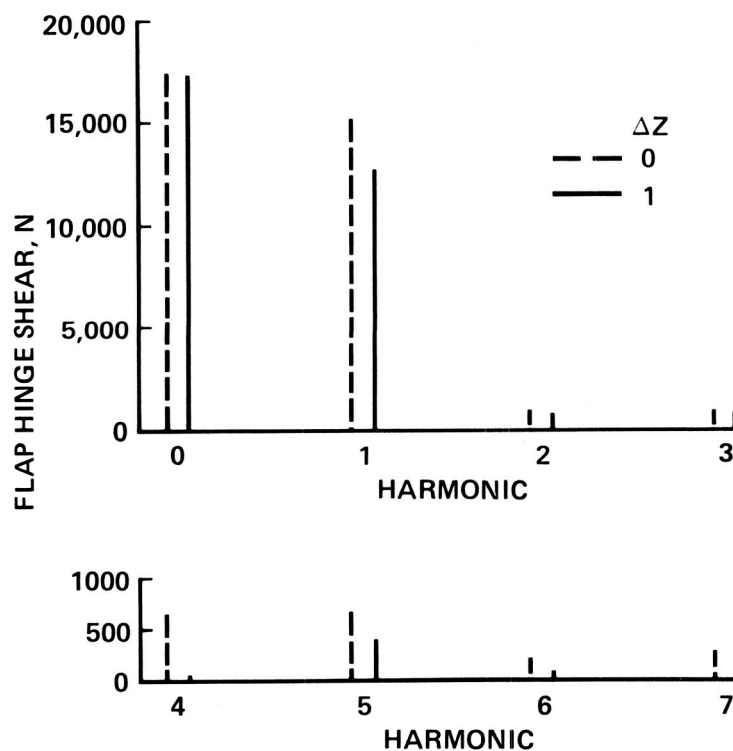
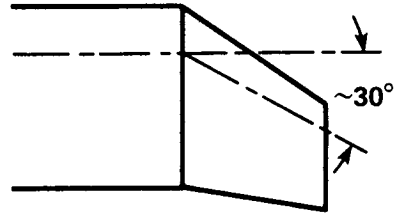


Figure 56.- Calculated upper rotor flap shears for VGR;  $\mu = 0.2$  (ref. 117).



**SWEPT/TAPERED**

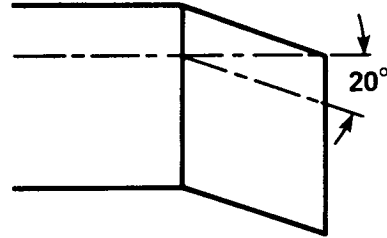


**TAPER RATIO = 0.6**

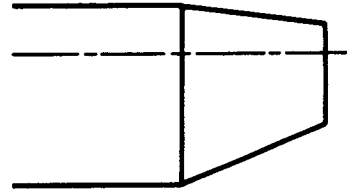
**TRAILING EDGE  
SWEEP = 10°**

**LEADING EDGE  
SWEEP = 35°**

**SWEPT**



**TAPERED**



**TAPER RATIO = 0.6**

**RECTANGULAR**

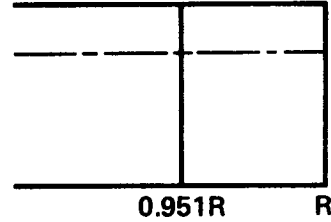
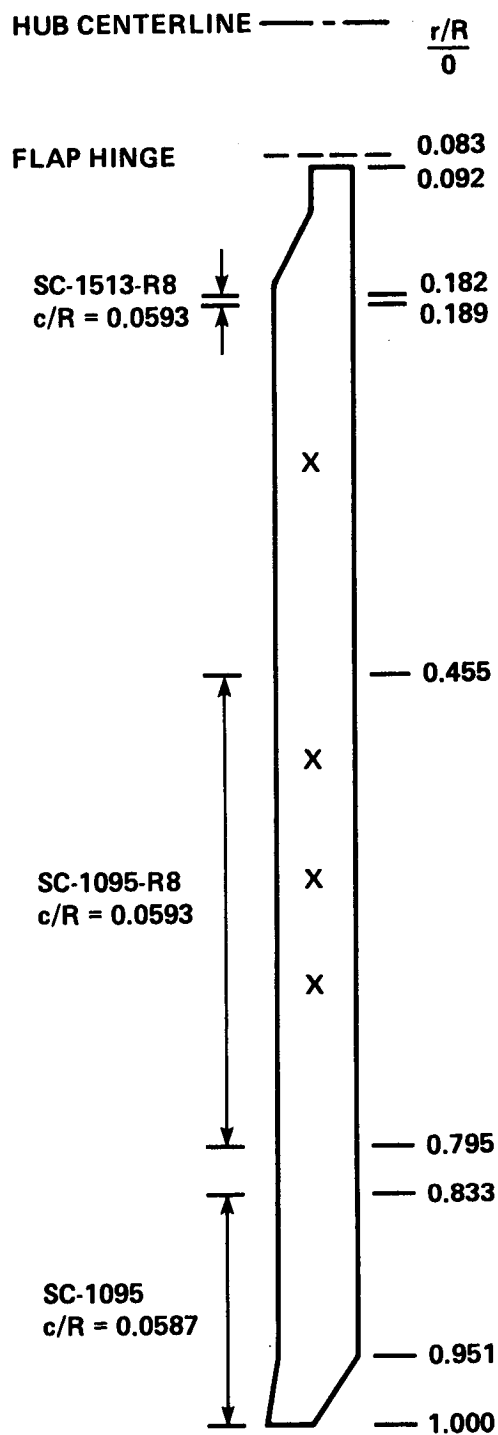
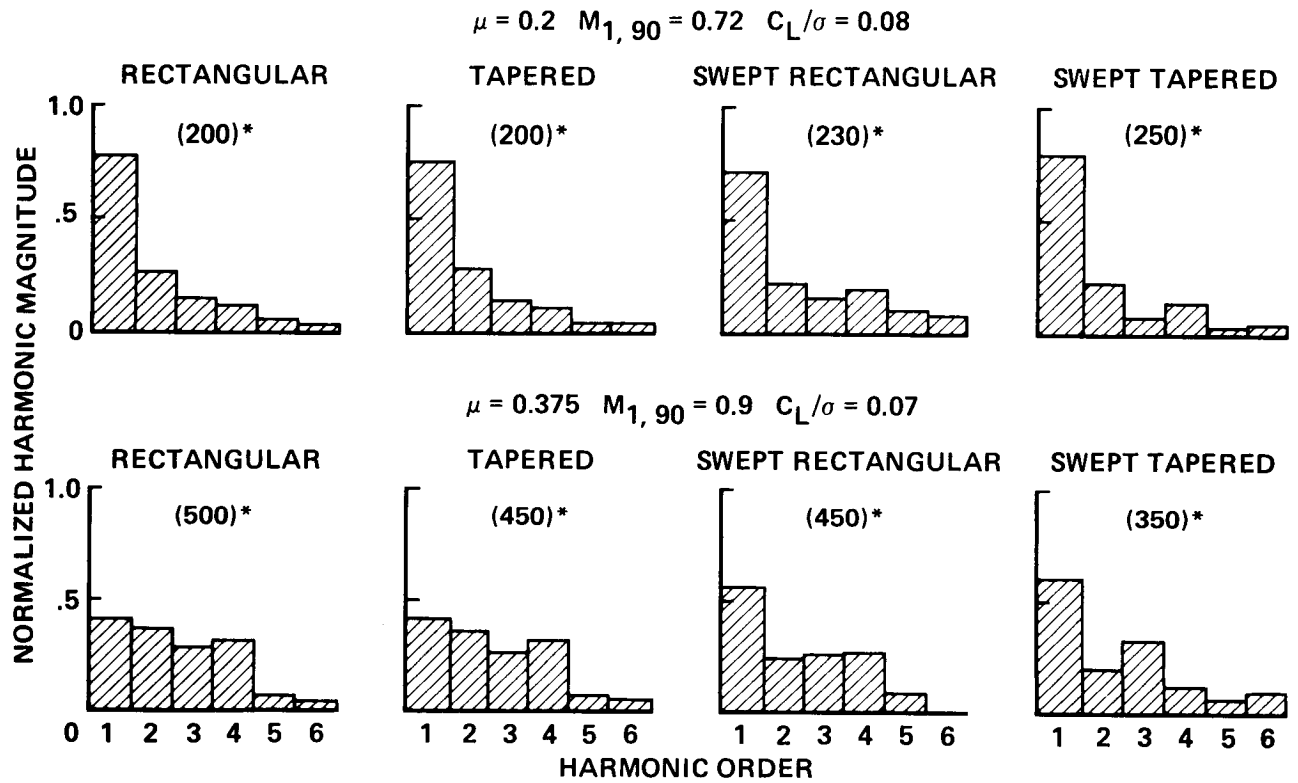


**Figure 57.- Tip planform geometry (ref. 67).**



X = BENDING GAGES

Figure 58.- Rotor blade geometry (ref. 67).



\*DENOTES HALF PEAK-TO-PEAK LOADING, lb

Figure 59.- Normalized measured control load harmonics for four blade tips (ref. 119).

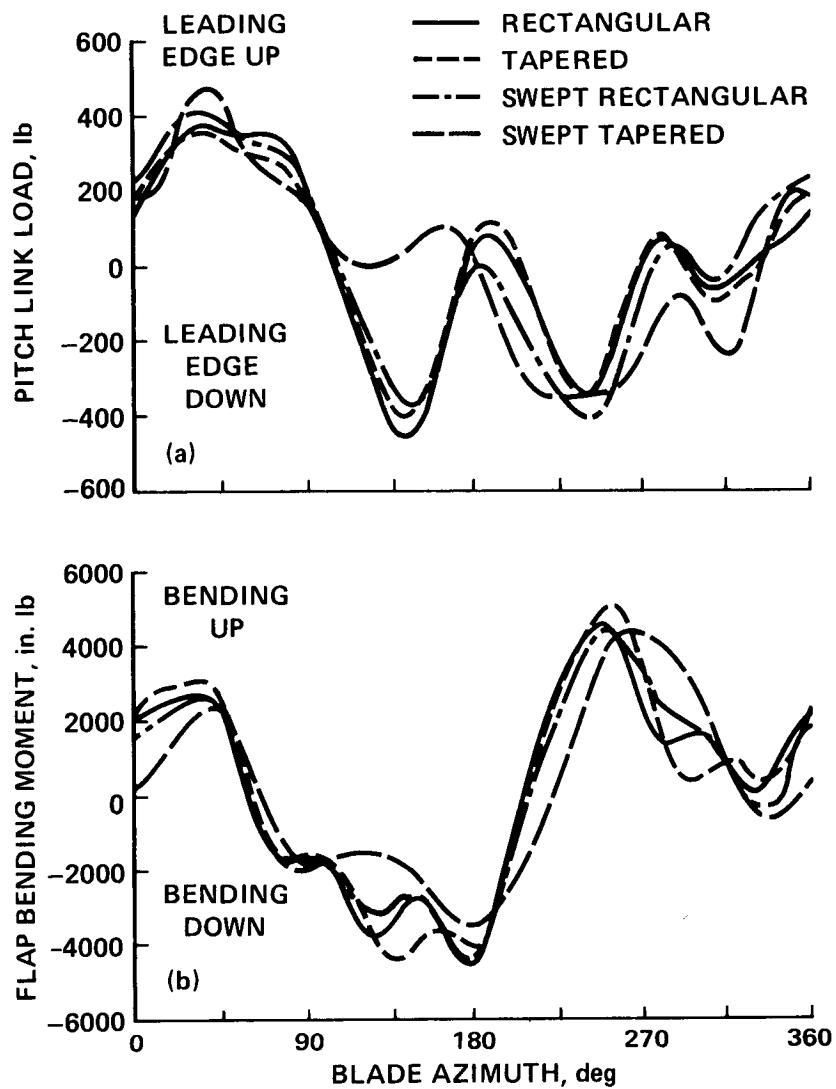
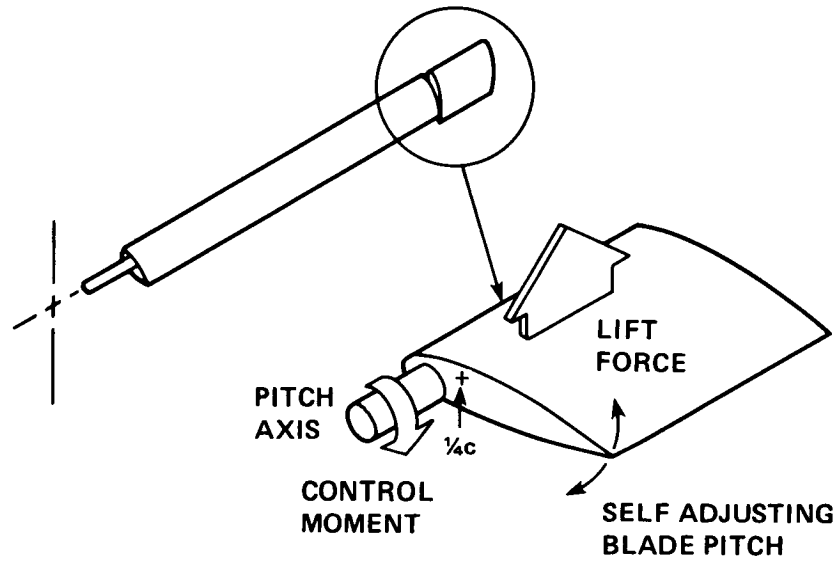


Figure 60.- Rotor loads as a function of blade azimuth for four blade tips;  $\mu = 0.38$ ,  $C_L/\sigma = 0.086$  (ref. 119). (a) Pitch link load. (b) Flap bending moment;  $r/R = 0.6$ .

### FREE-TIP CONCEPT



- IMPROVE PERFORMANCE
- REDUCE OSCILLATORY LOADS

Figure 61.- Free-tip rotor schematic (ref. 120).

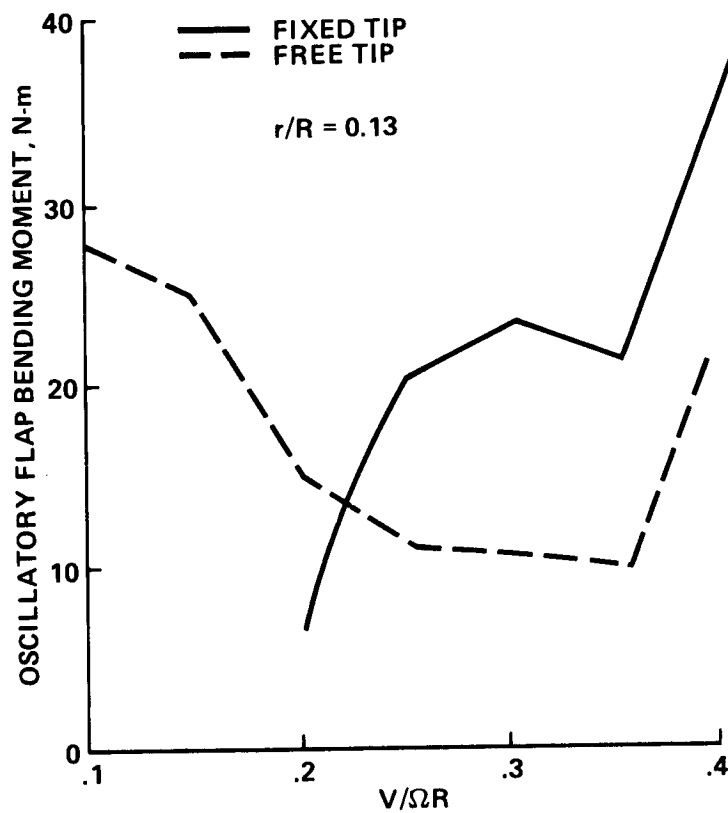


Figure 62.- Effect of free-tip on oscillatory flap bending moments;  $C_L/\sigma = 0.07$  (ref. 120).

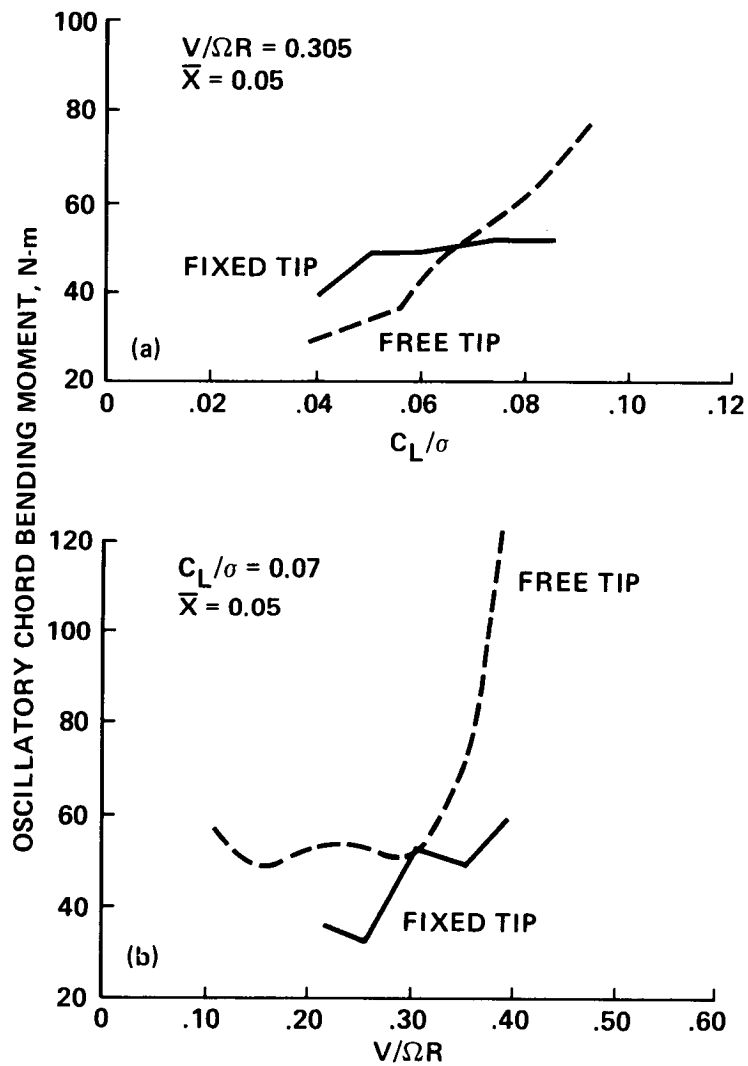


Figure 63.- Effect of free-tip on oscillatory chord bending moments (ref. 120).  
 (a) Chord bending as a function of rotor lift;  $\mu = 0.305$ . (b) Chord bending as a function of advance ratio;  $C_L/\sigma = 0.07$ .

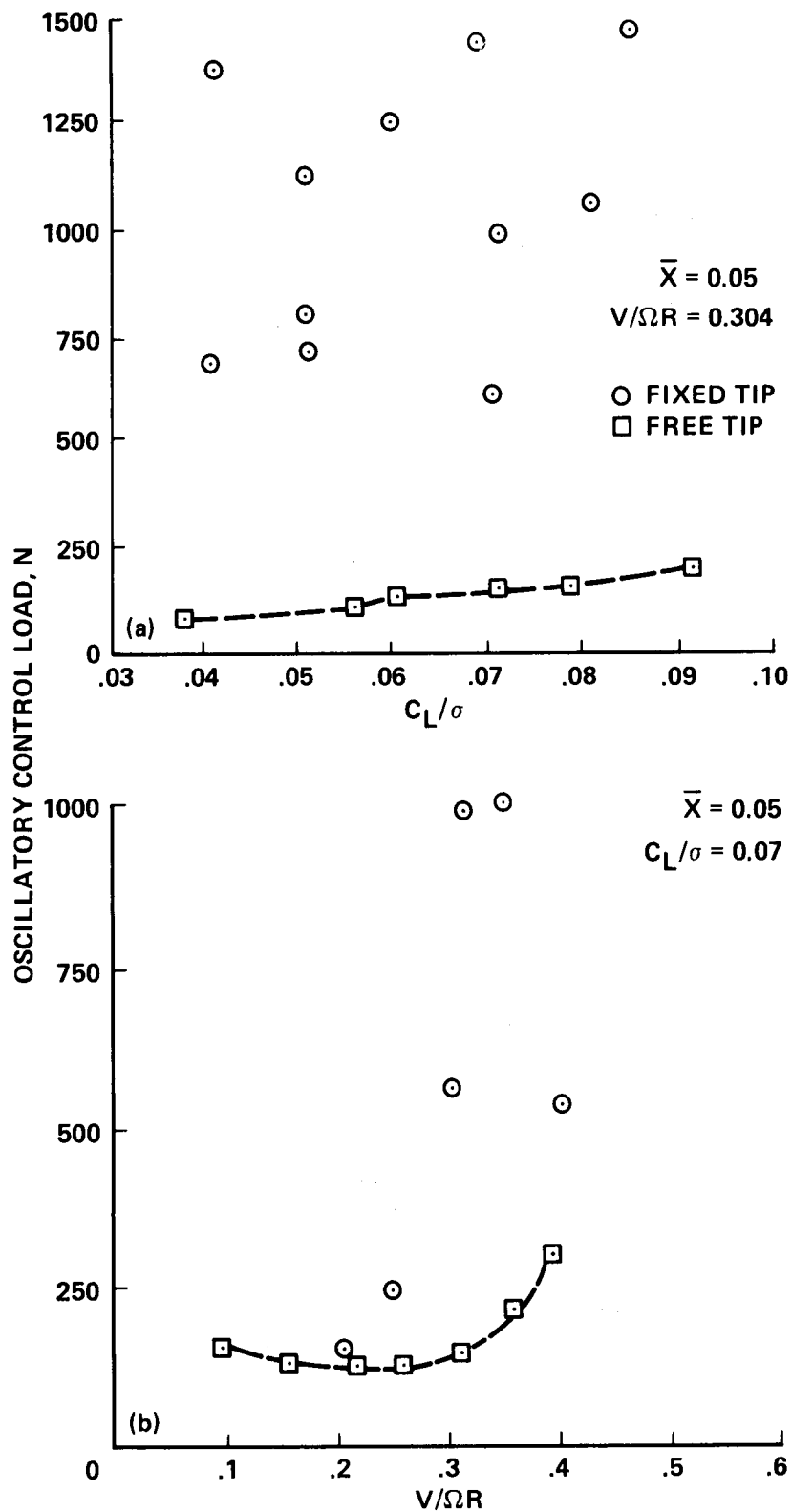


Figure 64.- Effect of free-tip on oscillatory pitch link loads (ref. 120).  
 (a) Oscillatory control load as a function of rotor lift coefficient;  
 $\mu = 0.304$ . (b) Oscillatory control load as a function of advance ratio;  
 $C_L/\sigma = 0.07$ .



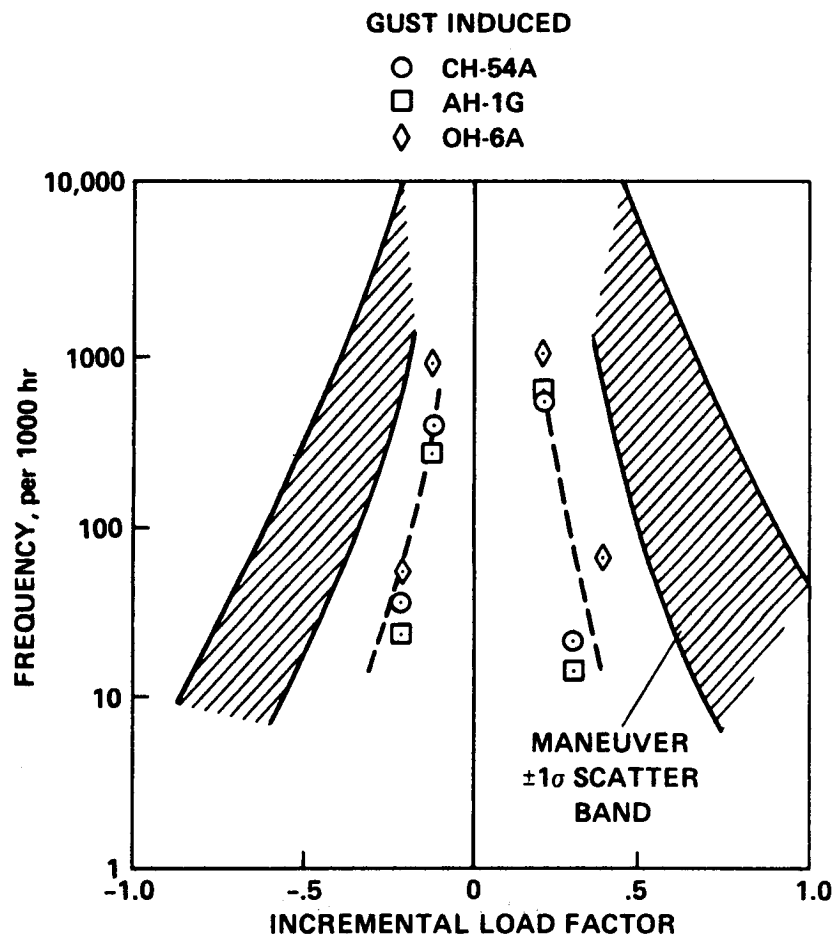


Figure 65.- Comparison of gust and maneuver induced loads (ref. 124).

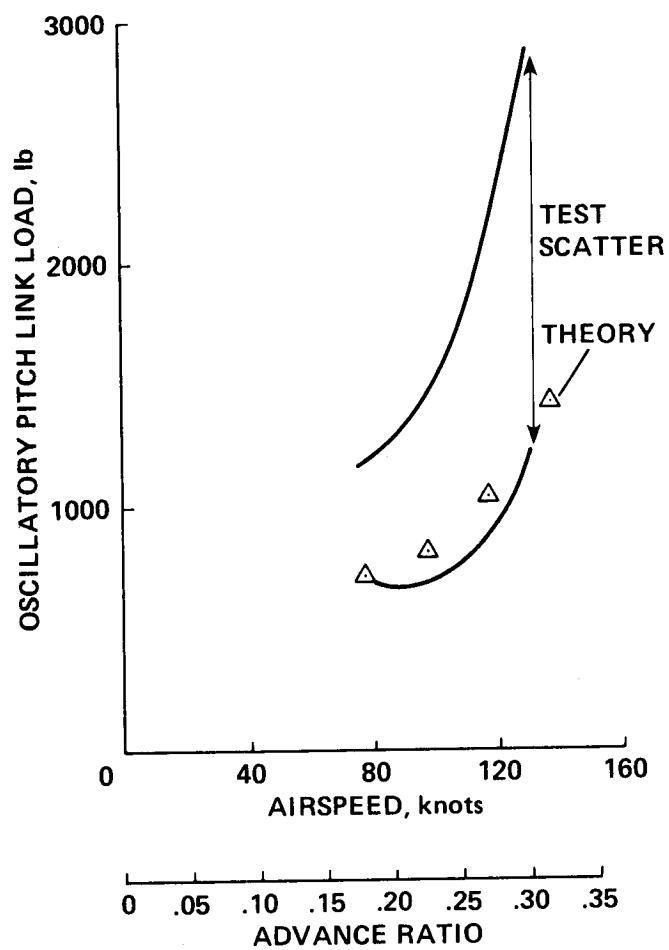


Figure 66.- Oscillatory pitch link load variation over five test flights for CH-47C;  $C_T/\sigma = 0.102$  (ref. 133).

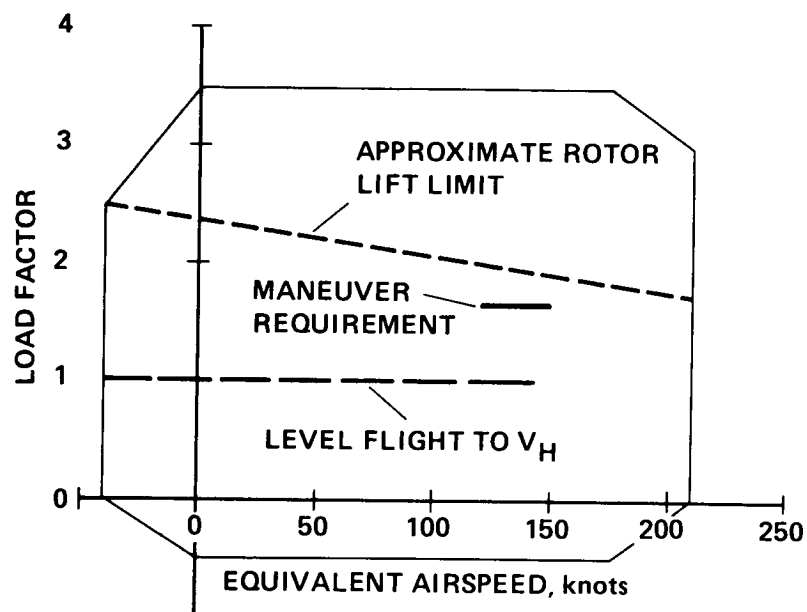


Figure 67.- V-n diagram for military helicopter. Approximate rotor lift limit from ref. 134.

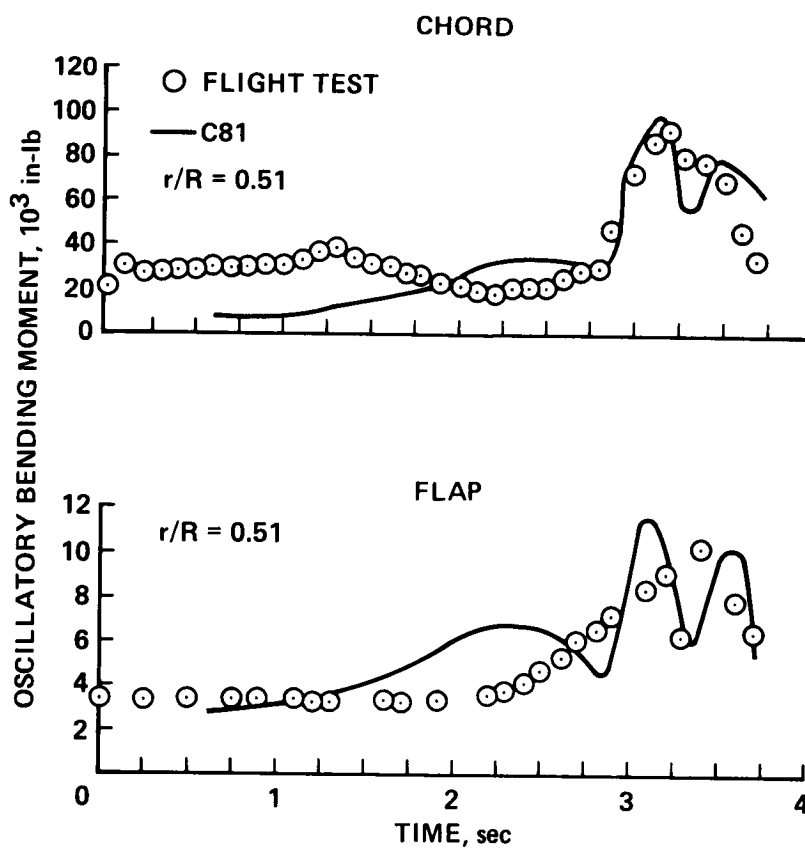


Figure 68.- Comparison of C81 predictions with measured oscillatory bending moments for AH-1G during a 2 g pull-up (ref. 136).

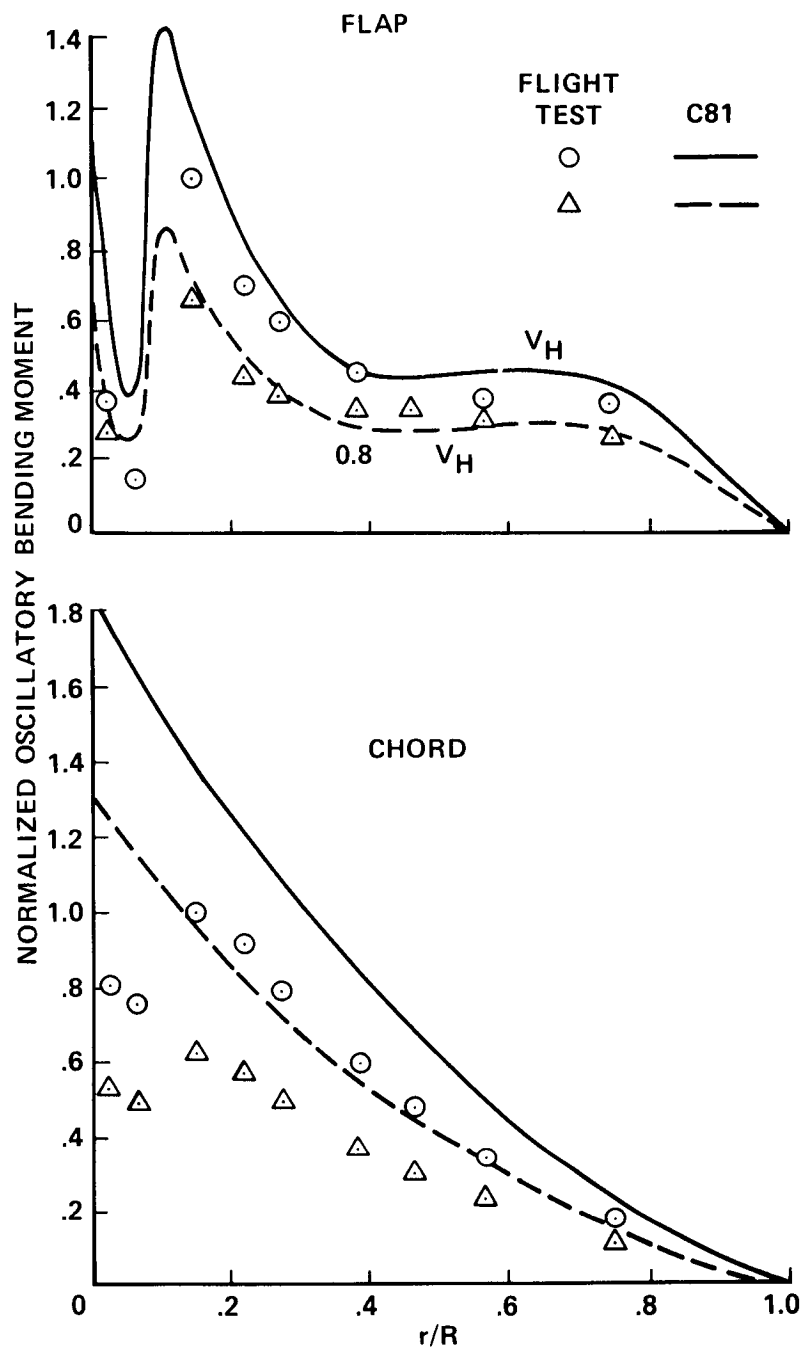


Figure 69.- Comparison of C81 and flight test oscillatory bending moments for a two-bladed teetering rotor. Bending moments normalized by oscillatory moment at  $r/R = 0.15$  and  $V_H$  (ref. 13).

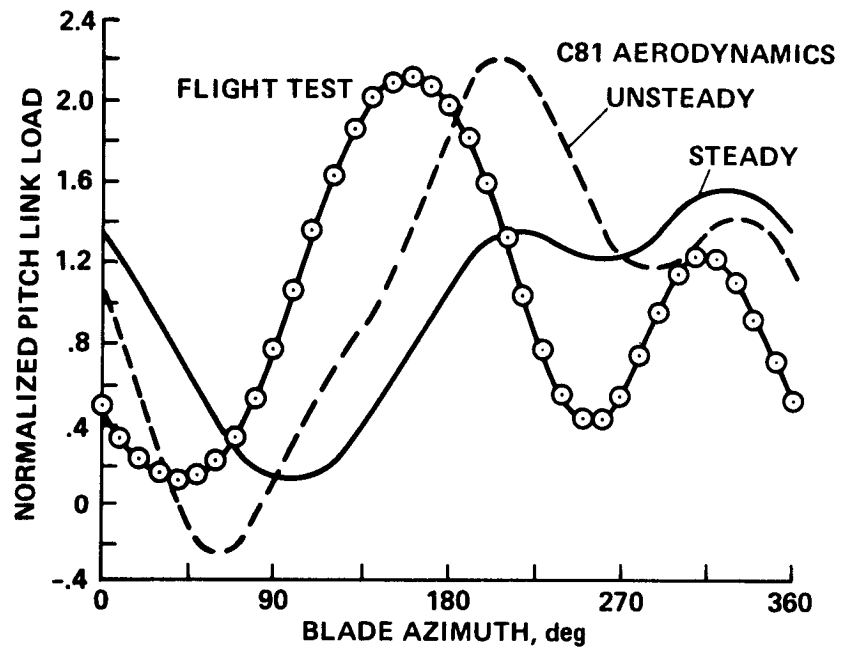


Figure 70.- Comparison of C81 and flight test measured pitch link load for two-bladed teetering rotor at  $V_H$ . Pitch link load normalized by measured mean load (ref. 13).

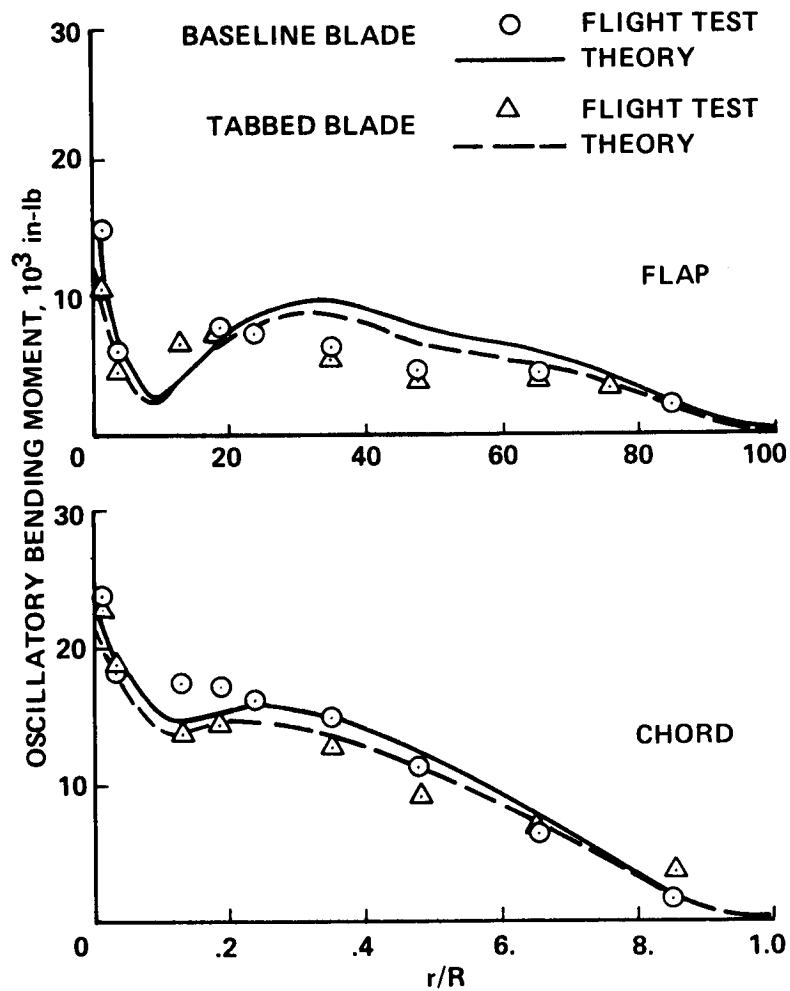


Figure 71.- Comparison of C81 with oscillatory bending moment distributions for a four-bladed rotor;  $\mu = 0.282$ ,  $t_c = 0.17$  (ref. 154).

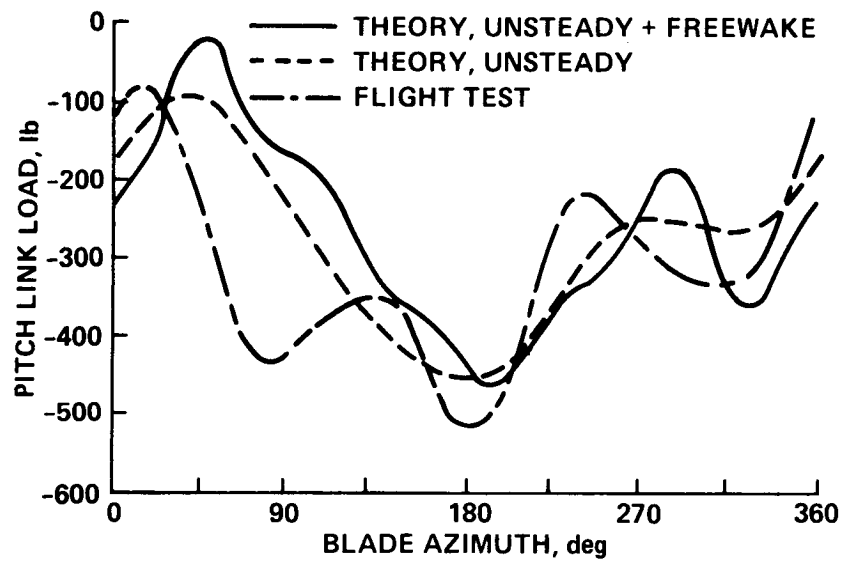


Figure 72.- Comparison of C81 with pitch link time history;  $\mu = 0.282$ ,  $t_c = 0.17$ ,  
tabbed blade (ref. 154).

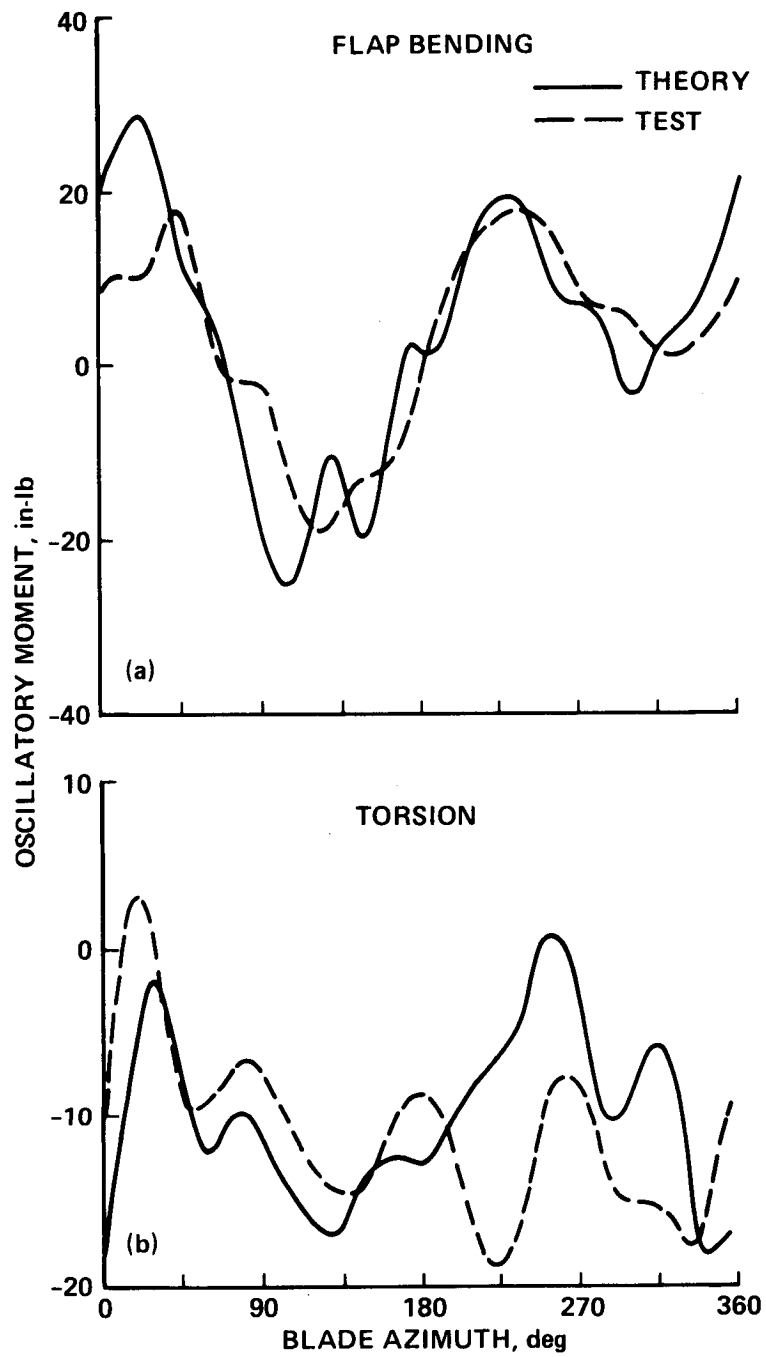


Figure 73.- Comparison of C-60 with midspan flap bending and torsion moments for an articulated model rotor;  $\mu = 0.40$ ,  $C_T/\sigma = 0.107$  (ref. 155).



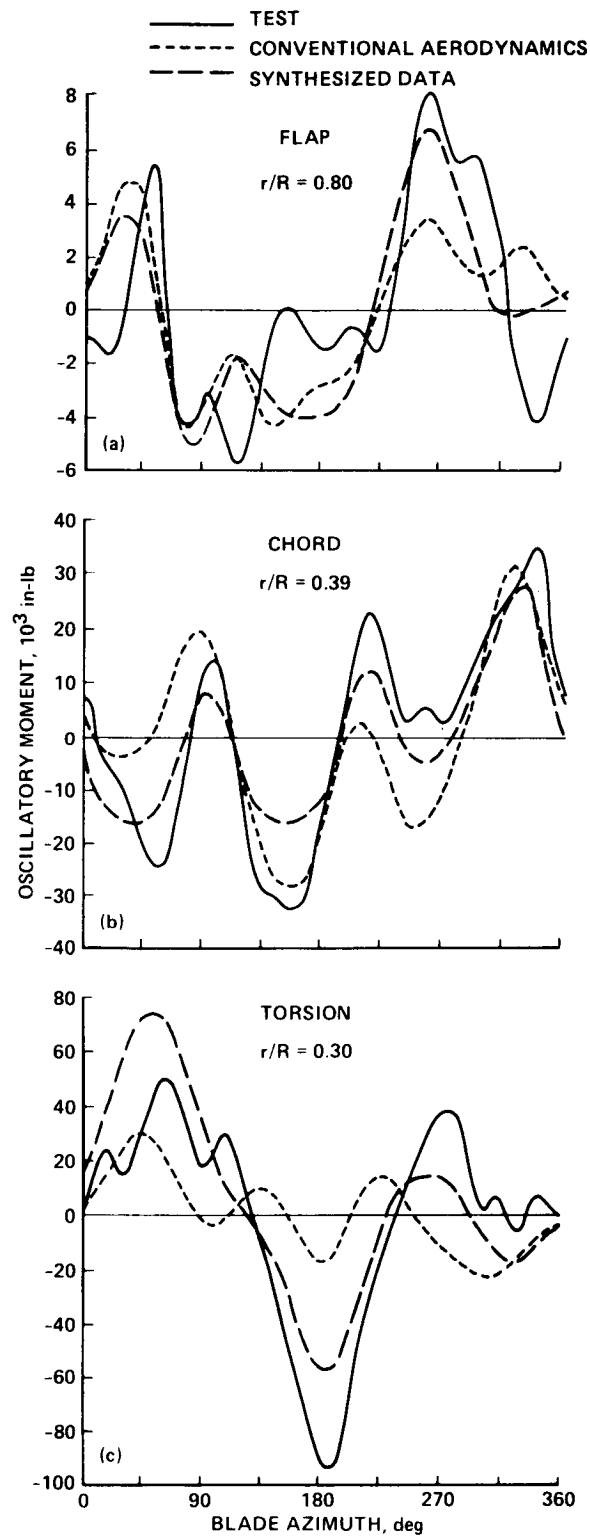


Figure 74.- Comparison of RAVIB with AH-1G OLS blade moment data;  $V = 142$  knots (ref. 32). (a) Flap bending moment;  $r/R = 0.80$ . (b) Chord bending moment;  $r/R = 0.39$ . (c) Torsion moment;  $r/R = 0.30$ .

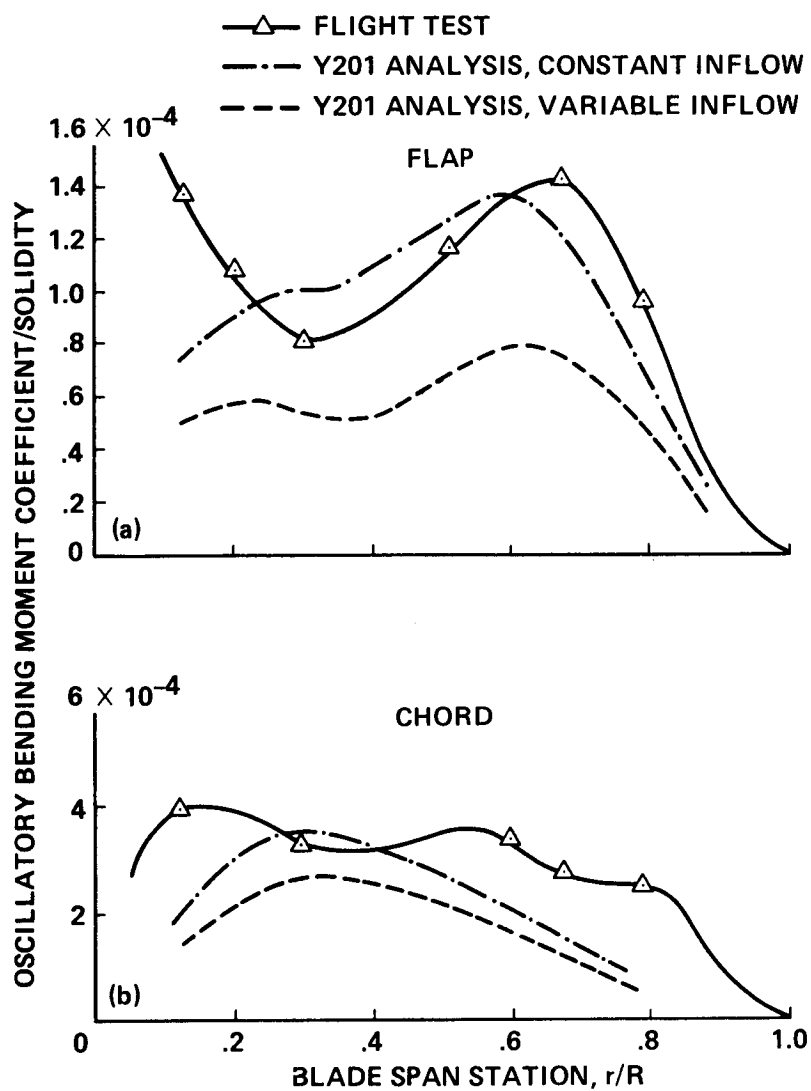


Figure 75.- Comparison of Y201 with radial distribution of flap and chord bending moments for S-76;  $\mu = 0.338$ , GW = 8,200 lb (ref. 66). (a) Flap bending moment. (b) Chord bending moment.

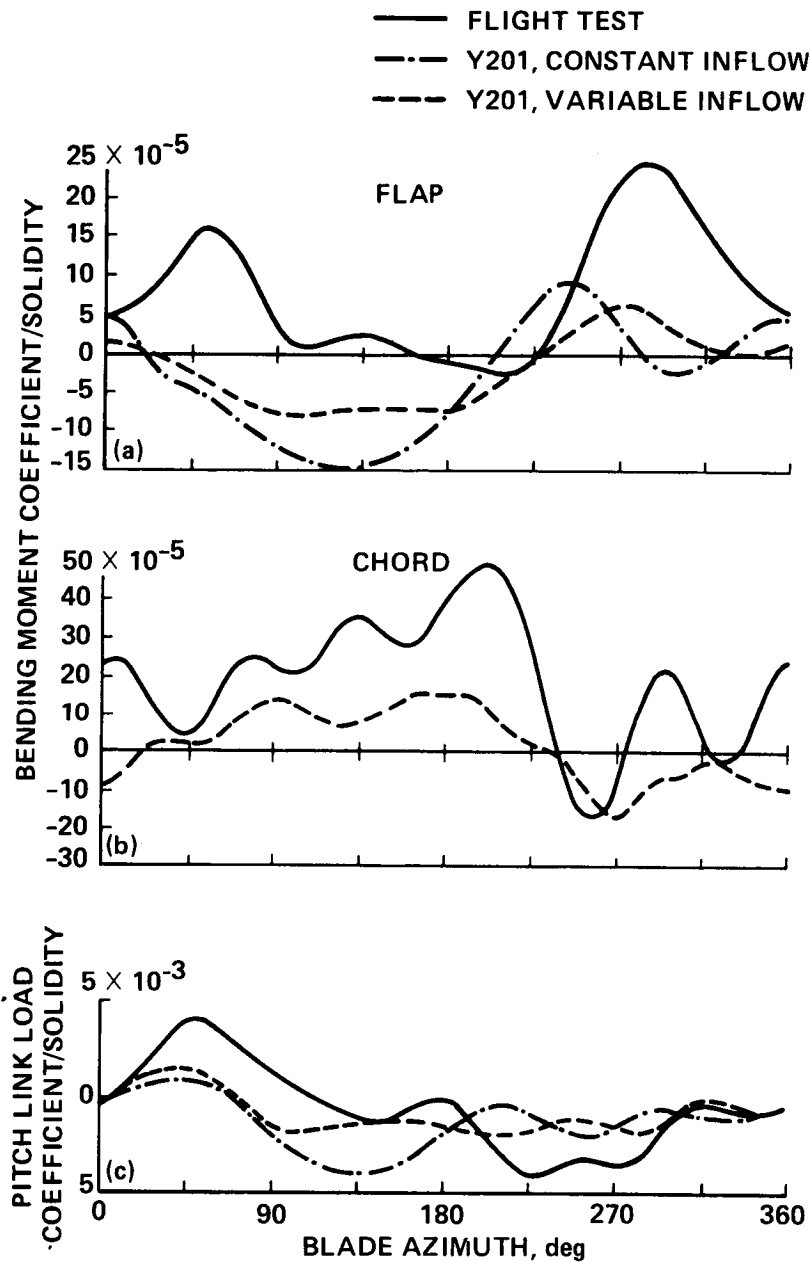


Figure 76.- Comparison of Y201 with flap and chord bending moment and pitch link load waveforms for S-76;  $\mu = 0.338$ , GW = 8,200 lb (ref. 66). (a) Flap bending moment. (b) Chord bending moment. (c) Pitch link load.

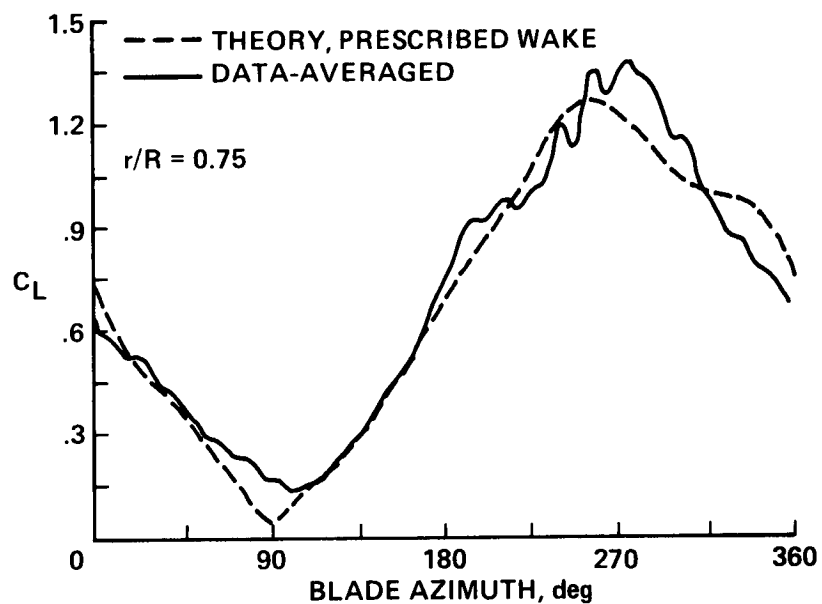


Figure 77.- Comparison of CAMRAD with SA 349-2 blade lift coefficient;  $\mu = 0.36$ ,  $C_T/\sigma = 0.071$  (ref. 50).

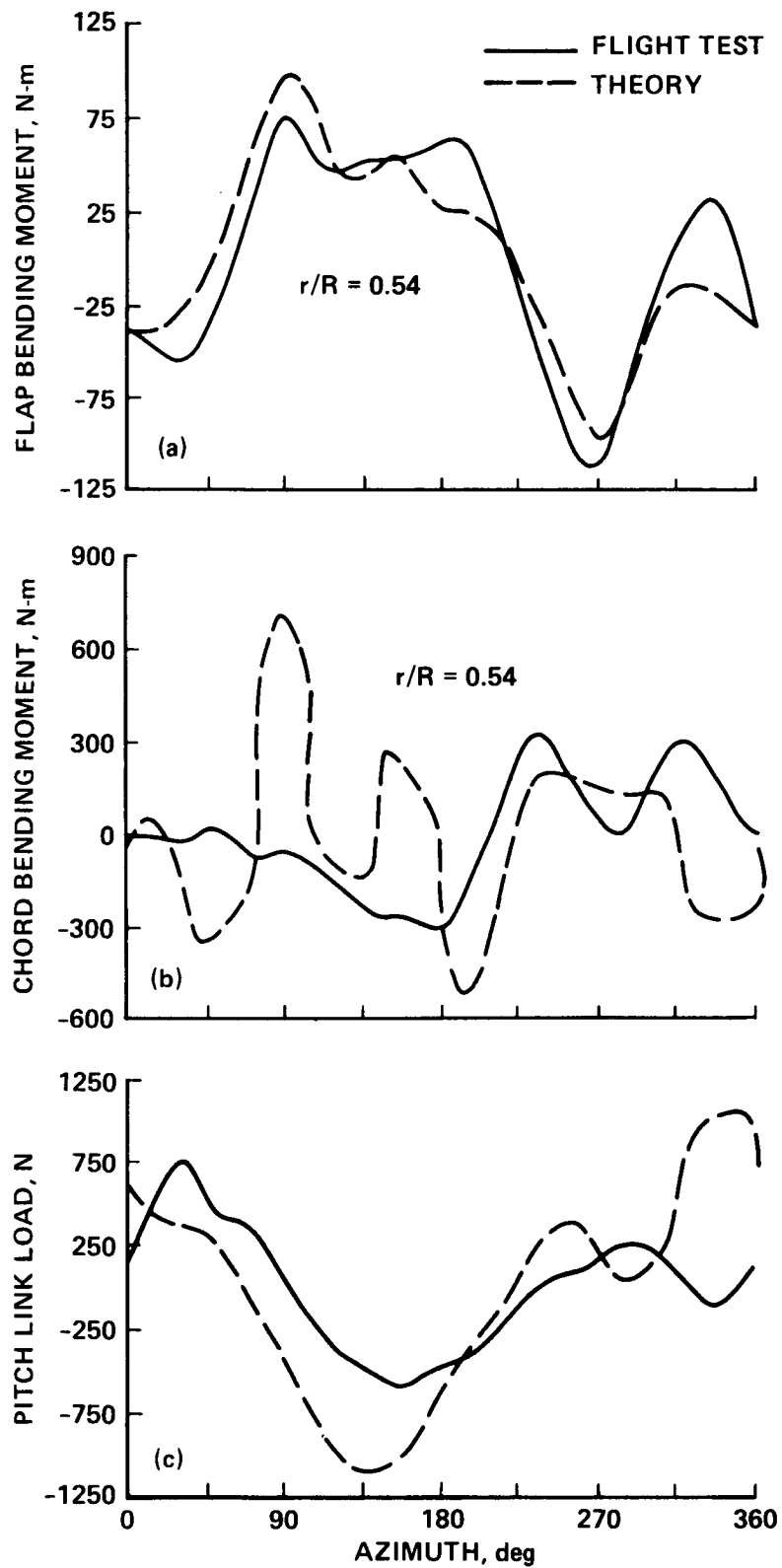


Figure 78.- Comparison of CAMRAD with SA 349-2 blade bending moments and pitch link load;  $\mu = 0.36$ ,  $C_T/\sigma = 0.071$  (ref. 50). (a) Flap bending moment;  $r/R = 0.54$ . (b) Chord bending moment;  $r/R = 0.54$ . (c) Pitch link load.

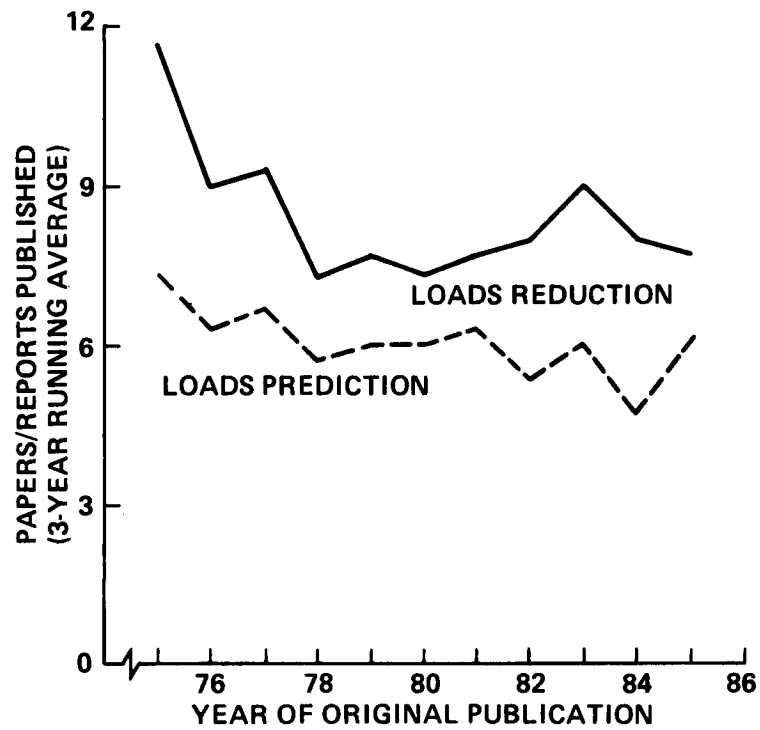


Figure 79.- Rotor loads research papers published per year.

## Comprehensive Rotorcraft Analysis Methods

Wendell B. Stephens  
2GCHAS Project Engineer  
Aeroflightdynamics Directorate  
U.S. Army Research and Technology Activity - AVSCOM  
Ames Research Center, Moffett Field, CA 94035-1099  
and  
Edward E. Austin  
Aerodynamics/Dynamics Team Leader  
Aviation Applied Technology Directorate  
U.S. Army Research and Technology Activity - AVSCOM  
Ft. Eustis, VA 23604-5577

March 23, 1987

### Abstract

The paper describes the development and application of comprehensive rotorcraft analysis methods in the field of rotorcraft technology. These large scale analyses and the resulting computer programs are intended to treat the complex aeromechanical phenomena that describe the behavior of rotorcraft. They may be used to predict rotor aerodynamics, acoustics, performance, stability and control, handling qualities, loads and vibrations, structures, dynamics, and aeroelastic stability characteristics for a variety of applications including research, preliminary and detail design, and evaluation and treatment of field problems. The principal comprehensive methods developed or under development in recent years and generally available to the rotorcraft community because of US Army Aviation Research and Technology Activity (ARTA) sponsorship of all or part of the software systems are the Rotorcraft Flight Simulation (C81), Dynamic System Coupler (DYSCO), Coupled Rotor/Airframe Vibration Analysis Program (SIMVIB), Comprehensive Analytical Model of Rotorcraft Aerodynamics and Dynamics (CAMRAD), General Rotorcraft Aeromechanical Stability Program (GRASP), and Second Generation Comprehensive Helicopter Analysis System (2GCHAS).

# 1 Introduction

For the past decade the Army Aviation Research and Technology Activity (ARTA) has sponsored programs directed toward the development of comprehensive rotorcraft analysis methods. The goals in sponsoring this development have been twofold. The first goal has been to provide a basis from which to advance the state-of-the-art in analysis methods. The second goal has been to provide the Government with analytical tools which could be used to evaluate present and proposed Army rotorcraft accurately, quickly and fairly. These analytical methods developed have also provided the rotorcraft manufacturers with tools which have been used in their own design efforts.

The rotorcraft industry matured and the vehicle proved to be vital to the Army's missions just as mainframe computers became available. Rotorcraft analysts made use of this new computational capability to solve numerically the complex sets of nonlinear differential equations that describe the aerodynamics and dynamics of rotorcraft. From specialized analyses formulated and programmed by one or two individuals there evolved more comprehensive analyses which merged two or more disciplines and which became important factors in unifying the design process (ref. [1]). However, Ormiston (ref. [2]) showed that the best industry analytical tools provided wide differences in the predicted loads for a hypothetical simple rotor system. The Army's UTTAS and AAH competitions exposed serious difficulties in modeling the elastic coupling in flexbeam rotor systems and in assessing the influence of main rotor wake on the fuselage and the tail. These problems were intimately related to inaccurate predictions in the technical disciplines of loads, vibrations, performance, stability and control, and aeroelastic stability. Schrage (ref. [3]) illustrated the problem that confronted the Army during the recent Advanced Helicopter Improvement Program (AHIP) Source Selection Evaluation Board (SSEB). The AHIP SSEB. The AHIP board used 27 different codes to accomplish this proposal evaluation. The analysis software had to be verified on similar data bases in advance of the board and available on computers to be used during the evaluation. The input and data bases for these programs were basically incompatible with one another and each program required a trained expert knowledgeable in its use. Thus, the inaccuracies and the incompatibilities of software available has spurred both Army and industry interest in improving the analysis methodology.

In order to address the need for better analytical tools for rotorcraft, the ARTA began focusing on near term and long range solutions to the multidiscipline analysis problems. In the near term, a current industry code was enhanced and encouraged for use as an industry standard. This was the C81 code (ref. [4]) developed by Bell Helicopter Textron. The primary funding for this enhancement came from the ARTA Aviation Applied Technology Directorate (AATD). Further, to establish an improved capability for analyzing designs for



low vibration rotorcraft and include the effects of rotor/airframe coupling, the development of the new SIMVIB code (refs. [5,6]) by Sikorsky Aircraft Corporation was supported by the ARTA Aerostructures Directorate (ASD). This particular code was to be used in support of an ongoing Army-NASA rotorcraft validation program effort.

To address the longer range problem of obtaining an advanced state-of-the-art code which would provide an industry-wide accepted standard for analysis, two other initiatives were undertaken. The AATD supported a set of three pre-designs for an interdisciplinary computer system that would address a broad range of technical disciplines. This interdisciplinary concept for the pre-design effort was referred to as the Second Generation Comprehensive Helicopter Analysis System (2GCHAS). The pre-designs were summarized in references [7,8,9]. The other initiative was an inhouse effort by NASA and the ARTA's Aeroflight-dynamics Directorate (AFDD) which resulted in the CAMRAD program (refs. [10,11,12]). This effort was referred to as a "generation and a-half" capability since it was more mathematically consistent and comprehensive than the available industry codes but still fell short of the ambitious 2GCHAS requirements.

The state of the rotorcraft analysis capability was thoroughly reviewed at the conclusion of the 2GCHAS pre-design activity at a workshop sponsored by the AFDD (ref. [13]). A review of the Army options at that time spawned three new efforts. First, the major long range goal of developing 2GCHAS was re-affirmed and the task for development of the code was assigned to the AFDD. Second, this effort was augmented by supporting a prototype code which addressed an approach to satisfying the dynamic coupling requirements for 2GCHAS using concepts introduced by Kaman Aerospace Corporation during the 2GCHAS pre-design (ref. [8]). The features addressed by the DYSCO code were basically related to structural dynamic modeling and little attention was given to aerodynamic modeling (ref. [14]). Third, an inhouse research effort to advance the state-of-the-art was initiated at the AFDD. This study was directed toward improvements in modeling elastic structures by developing a higher-order beam element capable of undergoing large elastic deformations, and implementing kinematic constraints capable of unrestricted rotations. The code developed from this research effort was referred to as GRASP (ref. [15]). Although the technical discipline capability in GRASP was limited to hover stability problems, the beam element and multi-body connectivity concepts were far in advance of what was being used in finite element codes and it was anticipated that these concepts would be included in future versions of 2GCHAS. Even though, strictly speaking, the GRASP code is not a multidisciplinary code, its influence on multidisciplinary code future development provides the justification for including it in the discussion of this paper.

The multidisciplinary codes developed by the ARTA sponsorship fall into three development categories. The industry-developed codes are C81, DYSCO,

and SIMVIB. The Government-developed codes are CAMRAD and GRASP. The 2GCHAS code occupies a unique category of joint industry-Government development. In the following sections the codes will be described briefly and compared with respect to function, math basis, and applications. Other codes have been surveyed in reference [16,17].

## 2 Program Descriptions

### 2.1 Rotorcraft Flight Simulation, C81

The Rotorcraft Flight Simulation code developed by Bell Helicopter Textron is best known by its program designation C81 (ref. [4]). It is nearly as old as the modern era in mainframe computers. It was originally programmed for the IBM Model 7070 computer as a rotor model to provide rotor inputs to an aircraft stability and control analysis. It has evolved through a combination of Government and Bell IR&D development funds and its use in SSEBs was an important factor as it became the most widely distributed first generation comprehensive analysis. C81 provides an interesting study in program evolution. As the original stability and control oriented program was given the capability for time varying maneuvers it was broken in to parts - a primary processing program and a post-processor to do plotting and analysis of time history data. When an aeroelastic rotor analysis was added, a rotor blade eigenanalysis was required to provide rotor blade natural frequencies and mode shapes, but it ran as a separate step. Recently, an aircraft design optimization feature has been wrapped around C81 and an executive has been added to control the various optional analyses in the system. It is this new program that will be discussed through the remainder of the paper.

The executive developed to accomplish this is designated the Rotorcraft Design Optimization Computer Program (RDOCP) and the suite of programs under its control include: (1) an input parsing and control program, (2) the system FORTRAN compiler, (3) the system linker; (4) the Myklestad Rotor Natural Frequency Program (rotor blade eigenanalysis), the C81 primary analysis and either of two commercially available nonlinear programming programs integrated into a single job step, (5) a Myklestad plotter, (6) the post-processor program for C81, (7) a C81 plotter, and (8) a DATAMAP interface program (ref. [18]). A schematic of the RDOCP executive is shown in figure 1. The input parse and control program sorts the input stream into files for each of these programs as required for the requested mode of operation and creates job control language for subsequent job steps. The inclusion of the system FORTRAN compiler and linker permit routine definition of nonstandard objective and constraint functions for the design optimization problem in FORTRAN as well as

temporary modification of the C81 code. The program has eight modes of operation: (1) Myklestad only, (2) C81 only, (3) Myklestad followed by C81, (4) Optimized Myklestad, (5) Optimized C81, (6) Myklestad followed by optimized C81, (7) Optimized Myklestad followed by C81, and (8) Optimized Myklestad and C81 together. While many operational enhancements have been made to C81 and program bugs have been eliminated, there have been no major technical discipline improvements to the primary C81 code in the last ten years.

In one of the more complex scenarios, the executive would enable the user to modify the C81 FORTRAN source code, create in FORTRAN his own objective and constraint functions for an optimization problem, relink the object modules, define the initial aircraft parameters using a previously defined database and NAMELIST changes, calculate rotor blade eigenvalues and eigenvectors, compute an aircraft trim condition using the complete set of governing nonlinear differential equations, and optimize the design as described by any of the continuous input variables. In a subsequent run the user could analyze the response of this design in a maneuver, interrupting the maneuver to determine stability derivatives at any moment using a perturbation technique, and plot any of several thousand available outputs on the line printer or a plotter. The user could save the output on a file and use the postprocessing code, DATAMAP, for additional analysis and graphical display.

The analysis is applicable to rotorcraft with up to two rotors in all common configurations. Rotor blade and pylon dynamics are represented using the modal method. Single load path teetering, gimballed, hingeless and articulated rotors may be modeled directly. Multiple load path rotors may be approximated in the Myklestad analysis by inputting hub mass and stiffness properties developed using NASTRAN, by using specially developed subroutines for specific bearingless configurations, or by adapting well-documented hub component subroutines to account for unique concepts. Pylon modes must also be calculated using an external analysis such as NASTRAN. The primary analysis capabilities are rotor and aircraft performance, flight path dynamics, airframe stability and control, and rotor loads in trimmed and maneuvering flight. Rotor aeroelastic stability may be inferred by simulation of an appropriate maneuver to excite the mode of interest and post-processing the response time history.

Rotor aerodynamic analysis options include 2-D airfoil coefficients from tables or curve fits; two methods to generate unsteady corrections, 3-D corrections, and modified Glauert inflow or harmonic coefficient inputs based on external data or analysis. Trim is obtained using a modified Newton-Raphson technique including either first harmonic elastic response or direct numerical integration of the system differential equations. In addition to the basic force/moment/one-per-rev flapping trim, other trim options include constant power climbs and descents, steady pullups and turns, rotor only and a number of others.

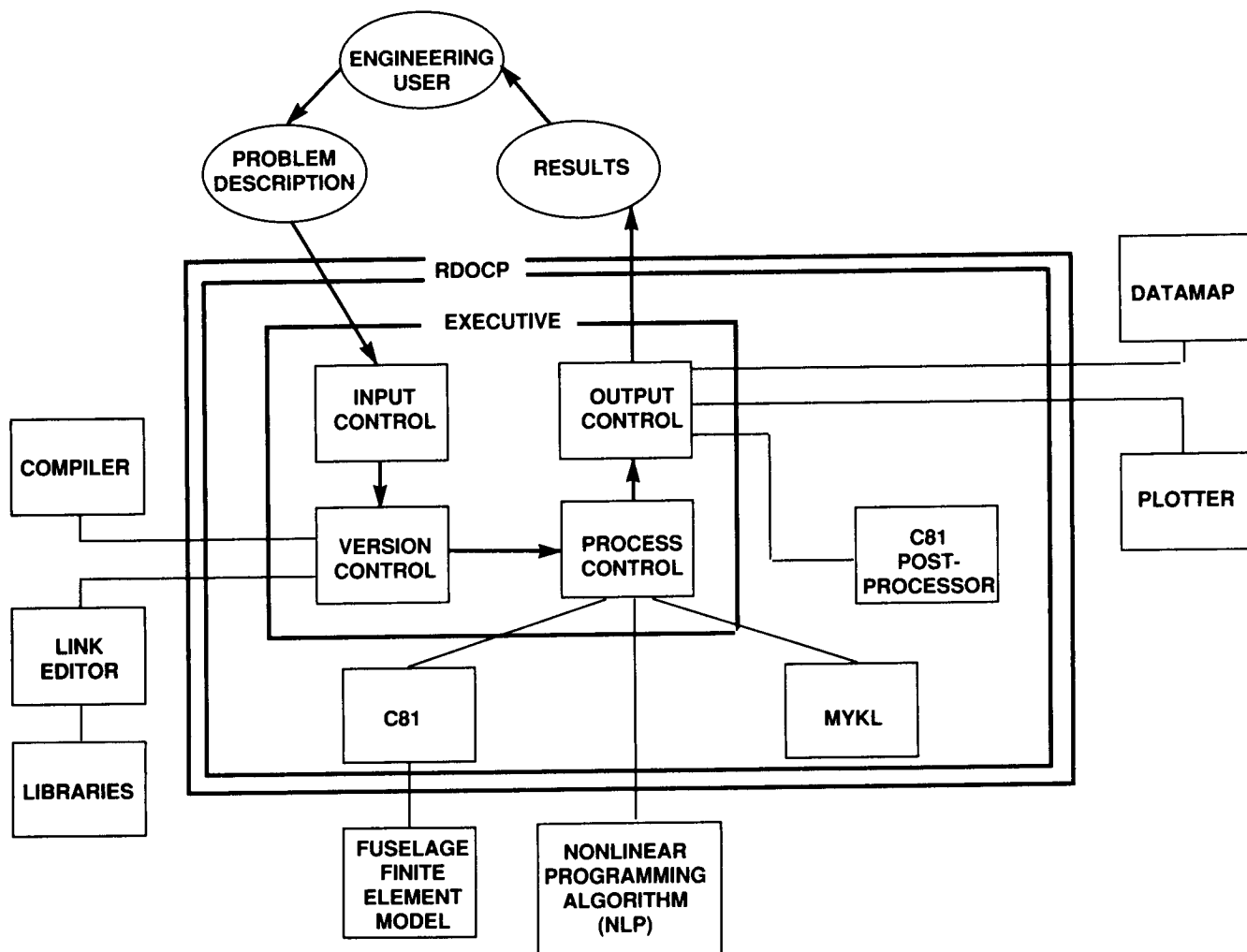


Figure 1: C81 modularity and command relationship.

Aircraft and analysis components are described using individual data groups which may be stored in a data base and include: airfoils as generalized curves or tables, rotors, rotor modes, pylon/fuselage modes, nonuniform induced velocity distribution, rotor induced velocities at lifting surfaces, fuselage, wing, stabilizing surfaces, jets, external stores, dive brakes, control rigging, bobweight, weapons and SCAS. Transient maneuvers which may be simulated include: control displacements from trim positions; rotor tilting; vertical, horizontal and vortex induced gusts; engine power changes; auxiliary thrust; weapon fire; changing RPM, rotor brake; SCAS failures; deployment of drag brakes and stores; and changing incidence angles of lifting surfaces. In addition there is a simplified pilot representation which attempts to maintain aircraft trim attitude upon experiencing these transient effects and a capability to follow a trajectory specified in terms of angular rates and normal load factor.

## 2.2 Dynamic System Coupler, DYSCO

In contrast to programs like C81 which grew as engineering analyses and subsequently had executive features added, DYSCO was initially developed as an executive concept demonstration which was almost totally devoid of useful technical analytical capabilities. The concept demonstrated by Kaman Aerospace Corporation (refs. [19,20]) was that transformation matrices similar to those proposed by Hurty, (reference [21]) could be used to assemble a set of rotorcraft system differential equations from a number of sets of subsystem differential equations by comparing the names the program user had assigned to the subsystems' degrees of freedom. In DYSCO, assigning the same arbitrary name to degrees of freedom in two subsystems couples the two systems together at those degrees of freedom, e.g., giving the name FRED to the lateral hub degree of freedom for a rotor and to the mast lateral degree of freedom for the fuselage equates those two components in the lateral direction (and the lateral direction only). Improved rotor modules and input facilities were added to the program after the initial demonstration was completed satisfactorily (ref. [22]). Experience with the resulting code indicated that DYSCO was well suited to the investigation of nonstandard airframe configurations such as those due to damage and that the addition of a rotor blade damage model would provide a comprehensive and easy-to-use damage assessment technology. Under an ongoing contract, the AATD is sponsoring development of the blade damage model, the incorporation of a global reference system and several other features. In addition, the Air Force sponsored the development of capabilities for applications not related to helicopters. Added capabilities are general modal representation of three-dimensional structures, a landing gear model, enhanced solution techniques, general forces, linear constraints and an improved eigenanalysis to include nonproportional damping terms. Demonstrations of these new capabil-

ities will be provided at the Air Force Wright Aeronautical Laboratories and the AATD in the spring of 1987.

The version of DYSCO discussed herein is DYSCO 4.0. The basic operational scenario for DYSCO is a three-step procedure which consists of defining the subsystems (or components), defining the system (or model), and executing a solution. The modularity of the DYSCO architecture is illustrated in figure 2. The components available in DYSCO include a modal, thin-beam fuselage, a rotor with rigid blades, a rotor with elastic blades, a rotor control system with elastic rods and swashplate, a general structural finite element, a nonlinear spring, and an arbitrary linear constraint. Force modules include a sinusoidal shaker, two-dimensional aerodynamics from empirical equations or tables, a more general rotor aerodynamics module, fuselage flat plate drag, and fuselage linear aerodynamics. The more complex rotor and fuselage aerodynamic modules are based primarily on the same technology as that contained in C81 and do not represent an improvement in the state-of-the-art.

As shown in figure 2, the solution module, "define solution" is separated functionally from the "form coupled system" math model formation. The solution modules available in DYSCO include eigenanalysis using the power method and the Householder method, a time history solution using Runge-Kutta, a Floquet stability analysis, a trim analysis using the technique of periodic shooting, and a frequency domain mobility calculation. The rotor, hub and airframe forces and responses are fully coupled and the system equations of motion are solved simultaneously.

The primary capability of DYSCO is to calculate dynamic response and loads, from which some overall performance predictions can be obtained. Until the global coordinate system is added, which will permit direct representation of gravitational effects, DYSCO will not be suitable for aircraft flight path dynamics predictions and there are no plans to extend the system to the areas of stability and control or to acoustics.

### **2.3 Coupled Rotor/Airframe Vibration Analysis Program, SIMVIB**

The concept for SIMVIB, as shown in figure 3 and described in reference [5], was to develop an interactive coupled rotor/airframe analysis package which could be used for preliminary design of new rotorcraft or for vibration treatments of existing aircraft with a emphasis on providing good interactive response. To do this, on-line computing requirements were kept low by doing the real number crunching computations off-line with a suite of programs provided with the base program. The effect of the fuselage on rotor aerodynamics, the rotor trim

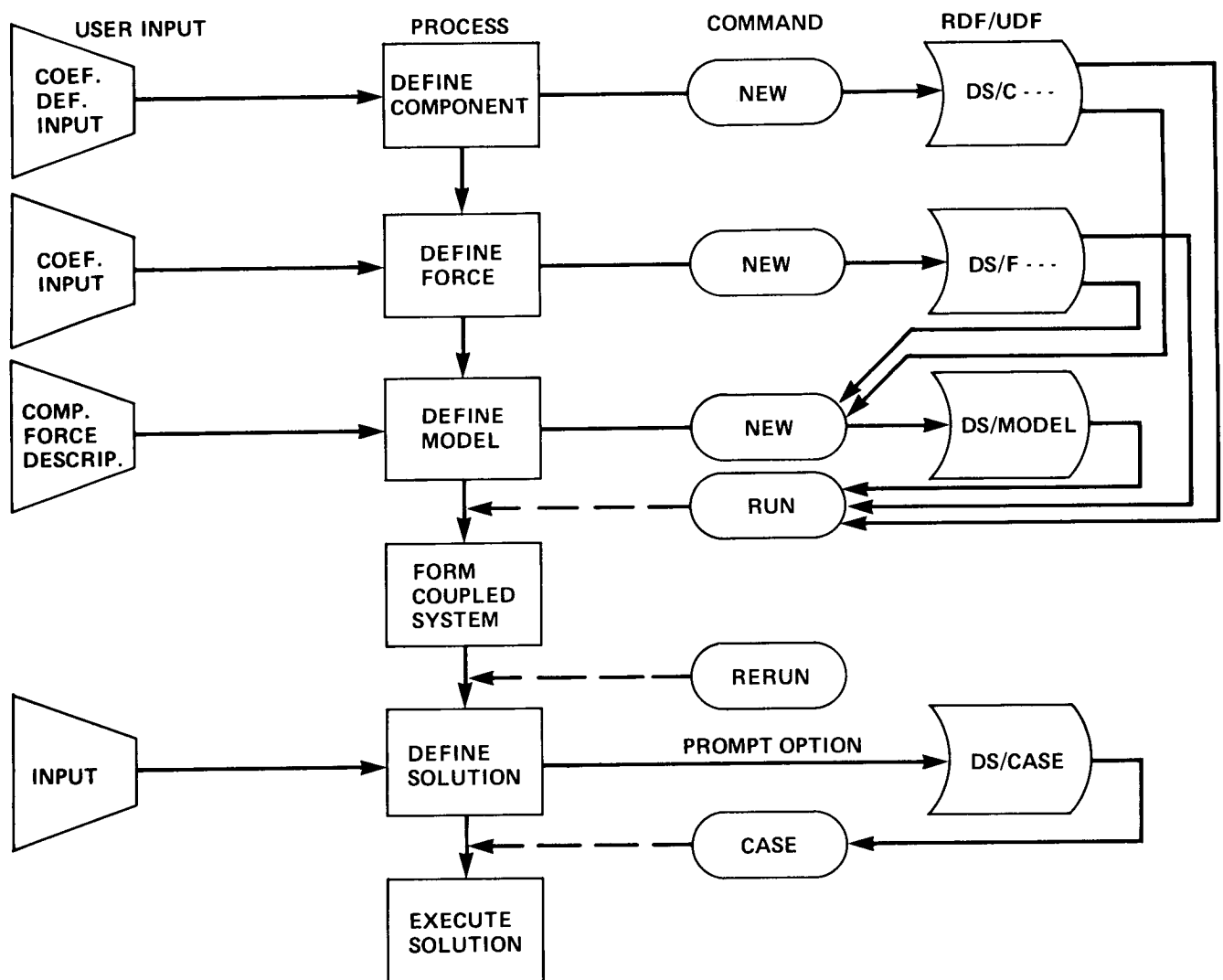


Figure 2: DYSCO modularity and command relationship.

state, rotor forces, rotor impedance, and fuselage vibratory forces as affected by the rotor are all calculated externally to the base program. The base program couples subcomponents using the Hurty method and provides steady forced response, time-varying response and eigenvalue solutions. Although a suite of programs was provided to perform the external calculations, any other analysis can be used if data formats are consistent with SIMVIB.

Figure 3 illustrates the data transfers between the base program and the suite of external programs. Iteration between programs is indicated by two separate arrows between the programs and the labels on the arrows characterize the data being transferred. The data transfers are accomplished by file transfers and the base program operates in a stand-alone mode to obtain solutions.

Substructures available in the base program include a vibration absorber, a generalized force, a uniform elastic beam, a connection constraint, an aeroelastic rotor model expressed in terms of mass, damping and stiffness matrices (for hover only), a modal representation of a dynamical structure, in-plane and out-of-plane bifilar absorbers, an anti-resonant isolator, and an impedance model of an aeroelastic rotor for hover or forward flight. Higher harmonic control is modeled by an externally derived transfer matrix relating hub forces and moments to swashplate inputs.

## **2.4 Comprehensive Analytical Model of Rotorcraft Aerodynamics and Dynamics, CAMRAD**

The CAMRAD program was developed in the late 1970's (refs. [10,11,12]). Its purpose was to provide a computationally reliable and efficient multidisciplinary dynamic and aerodynamic analysis for the design, testing and evaluation of rotors and rotorcraft. An excellent overview of the program and its applications is found in reference [23]. The analysis is applicable to general two-rotor aircraft configurations. The rotor systems allowed include articulated, hingeless, gimbaled, and teetering rotors with an arbitrary number of blades. The rotor configurations may be single main rotor, main rotor - tail rotor, side-by-side, tandem or tilting proprotor. The analysis capabilities extend to rotor performance, loads, and noise; helicopter vibration and gust response; flight dynamics and handling qualities; and system aeroelastic stability. The math model also includes a drive train set of equations which accounts for the engine, governor, shaft flexibility, and rotor rotational speed degrees of freedom.

The analysis capability is outlined in figure 4. The solution process begins with determining a trim state in which the rotor and airframe motion are periodic and the controls for a specified flight condition are calculated. The program allows the user to select various trim options based on the usual six



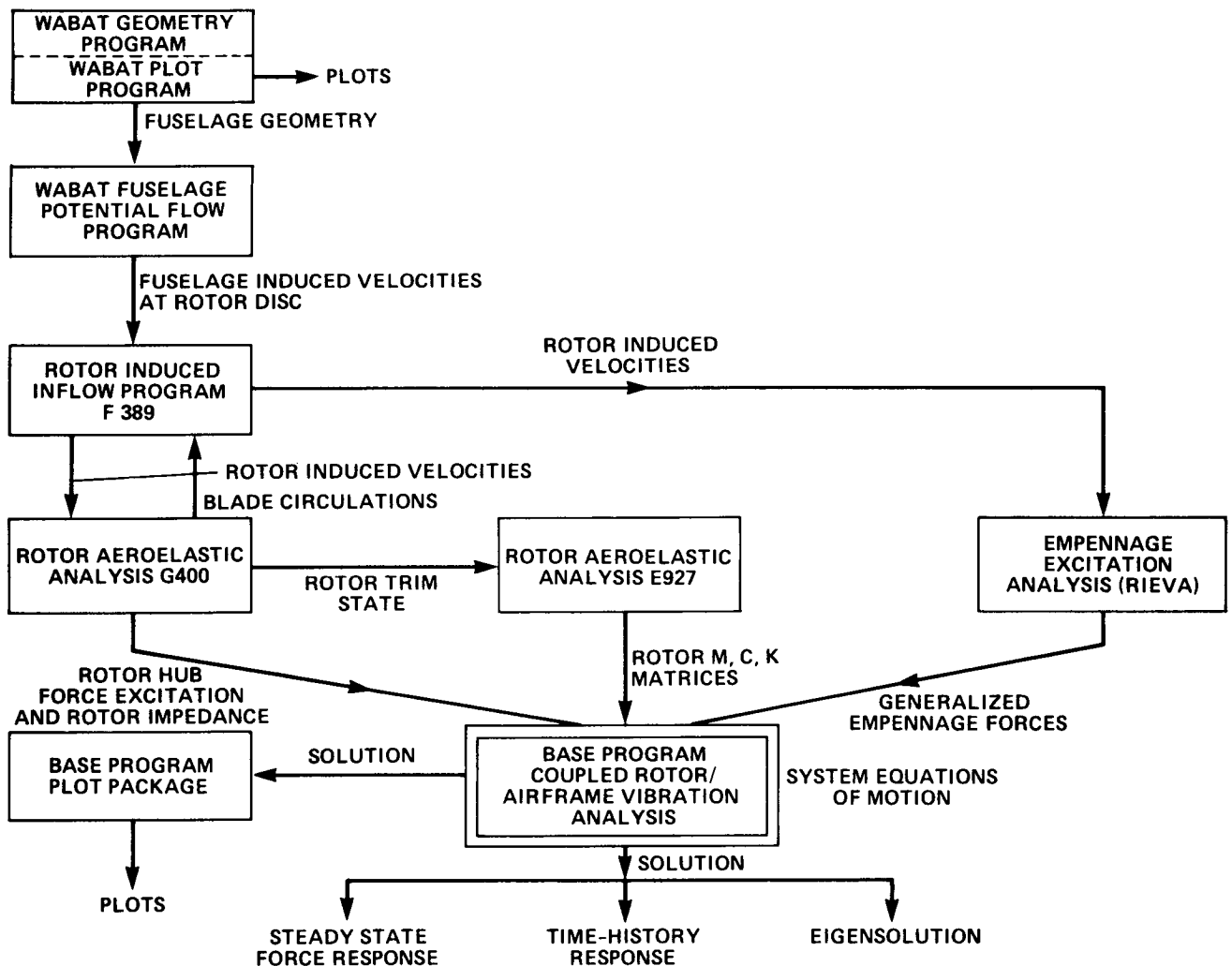


Figure 3: SIMVIB data flow diagram.

force and moment equations and an additional power available equation. There are 26 preset trim options in the code representing flight and wind tunnel trim conditions.

The transient and flight dynamics solutions are based on quasi-static rotor solutions. The trim, transient and flight dynamics solution procedures use a common rotor analysis. The solution of the equations is separated into two parts based on the assumption that the aircraft motion is quasi-static when compared with the rotor speed. This assumption allows the periodic rotor motion to be used for the transient motions of the helicopter as well as the trim motion. By taking advantage of the frequency separation of the rotor and aircraft motions, an economical solution procedure is obtained. One part, therefore, is the periodic, harmonic solution of the rotor and airframe vibration. The other part is the time domain solution airframe motion including the aircraft rigid body, rotor speed perturbations, and static elastic deflection of the airframe and drive train.

In the transient solution the rigid body equations of motion are numerically integrated for prescribed gusts or control inputs to calculate the nonequilibrium flight path. In the flight dynamics solution, perturbation of the body motion and controls are calculated yielding time invariant linear differential equations for the aircraft rigid body motions. The poles, zeros, and eigenvectors define the aircraft flying qualities.

Output from the trim, transient and flight dynamics solutions can be processed to obtain specific technical discipline output in performance, loads, vibration or noise prediction.

The flutter analysis constructs a linear set of differential equations for all variables of the aircraft and rotor(s) in order to define the system stability. The equations may be time invariant as for the axial flow flight conditions or time variant having periodic coefficients. In the latter case, a Floquet solution is obtained. Additional capabilities allows the periodic coefficients to be averaged and quasi-static reductions to be made if desired by the user.

The rotor aerodynamics is based on two-dimensional steady airfoil characteristics with corrections for three dimensional and unsteady flow effects, including dynamic stall. Three options of inflow calculation are allowed: uniform inflow, nonuniform inflow with prescribed-wake geometry and nonuniform inflow with free-wake geometry. The uniform inflow is based on an empirical model using momentum theory and includes a linear variation over the rotor disk. The rotor wake model is based on vortex lattice approximations of the wake and wake influence coefficients are calculated for incompressible flow. Rotor/rotor interference is accounted for as is interference velocities at the airframe. Wake rollup and distortion effects are included in the model.

STEADY STATE FLIGHT  
CONDITION

SOLVE FOR CONTROLS  
AND PERIODIC MOTION

NUMERICAL INTEGRATION  
OF TRANSIENT RESPONSE  
(QUASISTATIC ROTOR)

STABILITY DERIVATIVE  
CALCULATION (QUASI-  
STATIC ROTOR)

ANALYSIS OF TIME-  
INVARIANT LINEAR  
DIFFERENTIAL  
EQUATIONS

LINEAR DIFFERENTIAL  
EQUATIONS

ANALYSIS (TIME-  
INVARIANT OR PERIODIC)

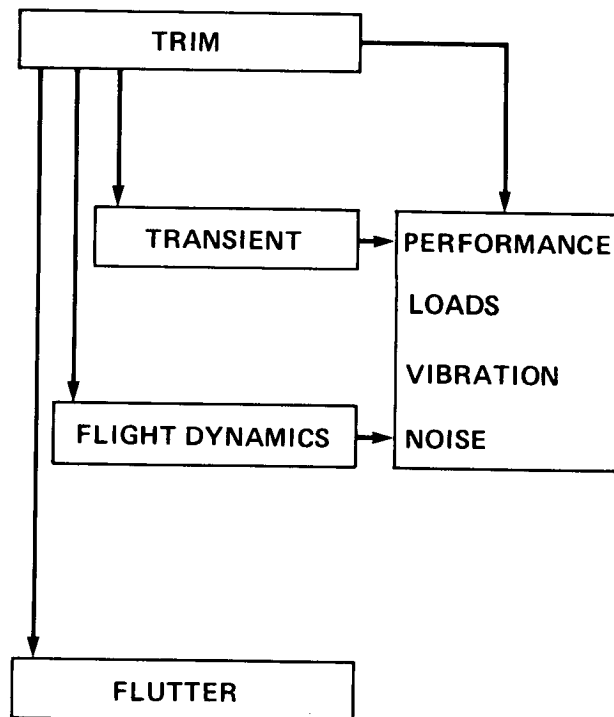


Figure 4: CAMRAD tasks and solutions.

## **2.5 General Rotorcraft Aeromechanical Stability Program, GRASP**

The GRASP program (ref. [15]) is an in-house code developed by the AAFD. It is an outgrowth of the FLAIR code (ref. [24]), and the problems associated with modeling a bearingless rotor system and elastic blades. The GRASP code was developed to apply advanced modeling and finite-element techniques to complex hub and blade behavior. In particular, blade/root kinematic modeling has been enhanced greatly by GRASP. The GRASP code is described as a hybrid between finite element codes and spacecraft-oriented multi-body programs. Using this combination, the coupling constraints at the blade root are general and can account for large rotations, time dependency, and nonlinearities. The substructuring in GRASP is extensive and allows the user to build up complex structures from a reasonably small library of elements and constraints. The main structural element in GRASP is the aeroelastic beam which is an elastic, kinematically-nonlinear, variable-order beam element subject to inertial, gravitational and aerodynamic loads. The equations of motion are not explicitly derived but are calculated inside the GRASP code. Although using small strain theory assumptions, the code development does not make any small angle approximations or use an ordering scheme to truncate terms. The analysis capabilities apply only to static nonlinear and linearized dynamic behavior. The program does not handle periodic terms and is therefore restricted to axial flight regimes. The stability problem is described as an asymmetric eigenproblem where the mass matrix is symmetric but the damping and stiffness matrices may be asymmetric. The mass matrix includes apparent mass from the air. A simple air mass model using induced inflow dynamics with uniform axial freestream velocity is used in GRASP.

In order to allow the modeling flexibility required, GRASP has an extensive executive capability referred to as an "information manager" to control the execution sequence and to manage the data structures. The information manager selects the dimension size required for each data structure during a run and efficiently manages the data.

## **2.6 Second Generation Comprehensive Helicopter Analysis System, 2GCHAS**

The 2GCHAS is a Government-sponsored project which had its origin in the mid-1970's. It was a response to a need by the Army for a more comprehensive analysis tool to be used by helicopter designers in the industry and aircraft evaluators in the Army. The basic concepts for the system were formulated in a series of competitive predesign studies (refs. [7,8,9]). The predesign studies

were initiated to define the requirements of the System from the both technology discipline and user-interface standpoints. These requirements were later summarized in reference [25]. The System is divided into two complexes; the Executive Complex and the Technology Complex. A contract was awarded to Computer Sciences Corporation to develop the Executive Complex prior to developing the Technology Complex. The Executive Complex precedes the Technology Complex by approximately two years in development. The completed 2GCHAS is expected to be available to the public in the third quarter of 1988 after System integration of the CPCI deliveries and as shown by the schedule chart in figure 5. The public release of the system is referred to as first level release (FLR). This release will only be for the VAX VMS operating system. It is the intent of ARTA to continue the code development and support over a period of time so that advanced technology modules can be added to the System and to allow the System to be converted to other operating systems.

The Executive Complex is that part of the System which controls the execution of the technology analyses, supports the run-time data management, provides a user interface for input and output, has available a database management system for I/O storage, and provides utilities for graphic and printed output of analysis runs. The development of the Executive Complex is accomplished in five builds, each of which is of approximately 6 months duration; the fourth build was delivered to the Project Office in February 1987 and the final build will be delivered in September 1987. The third build, which was delivered in September 1986, has been installed at the Technology Complex contractor sites for use in developing the technology software. The project office will upgrade the technology contractor deliveries after acceptance testing of the succeeding builds are complete. The schedule for the 2GCHAS development is shown in figure 5. The Executive Complex line in the figure depicts the time periods for the five builds.

The Technology Complex is that part of the System which provides the technical capability to perform particular interdisciplinary engineering analyses of rotorcraft such as performance, loads and vibration, aerodynamics, stability and controls, and aeroelasticity stability. This Complex has been divided into six contractual units called computer program configuration items (CPCIs). Four CPCIs were awarded in January of 1986 and two were awarded in January of 1987. All six contracts will be completed in the second quarter of 1988. The finite element library will be developed McDonnell Douglas Helicopter Company, the hierarchical assembly procedure and the maneuver and trim solution processes will be developed by Kaman Aerospace Corporation, the linear analysis and eigensolutions will be developed by Advanced Rotorcraft Technology, Incorporated, the aerodynamic capability will be developed by Boeing Vertol Company, the technology discipline output processing will be provided by Sikorsky Aircraft Corporation, and input processing and coordination capability will

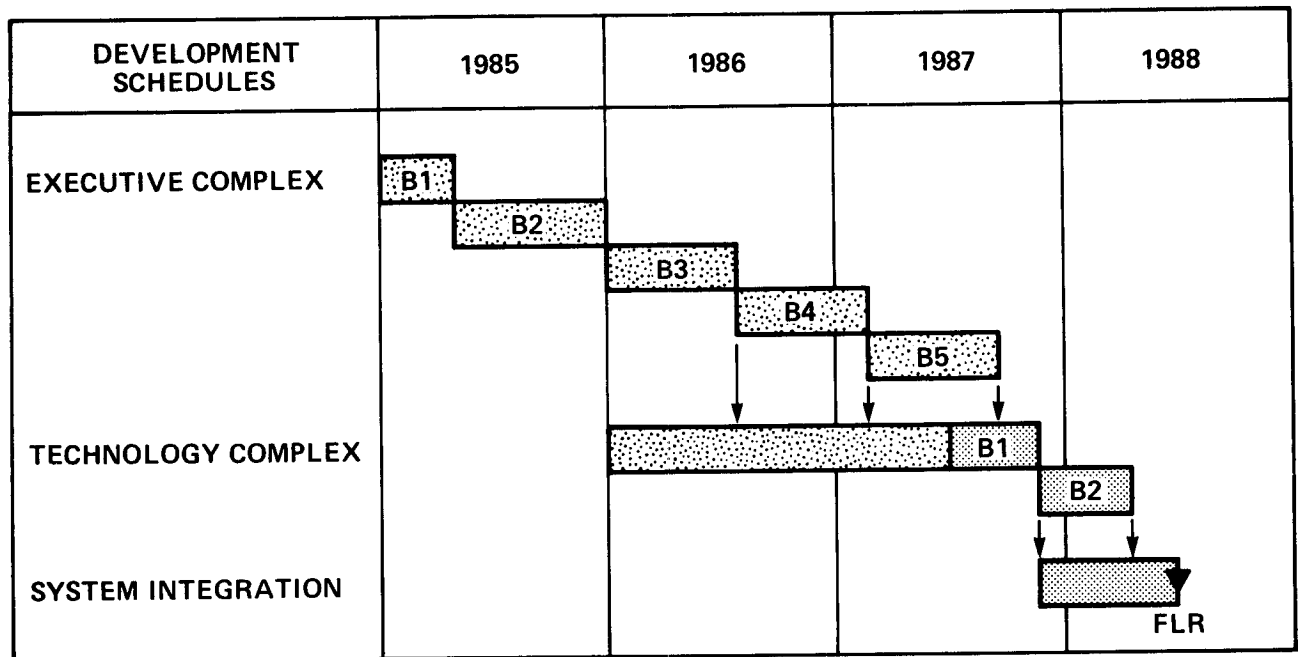


Figure 5: 2GCHAS schedule chart.

be provided by Sterling Software Incorporated. Most of the CPCIs' software delivery will be based on a two-build schedule as shown in figure 5.

The technology basis of the Technology Complex is a finite element, time domain assembly process with solution algorithms available for maneuver, periodic response, trim and eigenanalysis. The eigenanalysis extends to both constant and periodic coefficient equations. The assembly process is hierarchical with provision for modal synthesis, multipoint constraints, coordinate system transformations, singlepoint constraints, and multiblade coordinates. The aerodynamic computational capability includes the induced velocities and airload distributions. The induced velocities are calculated from momentum theory with vortex-element, prescribed-wake methods in both axial and forward flight regimes. The airloads are based on the lifting line strip theory approach. The solutions to maneuver, trim or eigenvalue equations of motion are postprocessed to provide the appropriate engineering discipline results in such areas as loads, performance, stability, etc.

The analysis flexibility of 2GCHAS is depicted in figure 6. The Technology Complex operations move from left to right beginning with the user model building activities. The fundamental calculation to be performed is the trim solution. Once the trim state has been established, the user may proceed to the transient (maneuver) calculation, perturb the equations of motion or go directly to the last column to obtain the desired engineering discipline data

from postprocessing the solution state. If the perturbed equations are used, the user may perform either an eigenanalysis or a transient analysis of the linearized equations. Again, after solving the equations, the user selects the appropriate engineering discipline output form for the data and displays the results on the screen, plotter, printer or external file. The Executive Complex assists the user in identifying the path through the various solution algorithms via a user language; allows the user to store, recall, restart or checkpoint data along the path; aids the input preparation processes; provides utilities for the graphic interface; manages the data and data structures during the runtime; and provides diagnostic and status information during the run. The figure depicts the executive compiling a user command in a sequential fashion.

### 3 Comparisons of Capabilities

For the most part, the programs discussed in this paper attempt to be "comprehensive" in function. This comprehensiveness can be interpreted in various ways, however. A program can be comprehensive by addressing each of the technical disciplines indicated in table 1. The program might also be deemed comprehensive if its modeling capability is general such as that found in finite element codes. Such a code would allow the math models to range from very simple to quite detailed thereby allowing the models generated to be applicable to preliminary design, detailed design and research studies. Comprehensive codes require executive services support which involve data base management, user language features, graphics interfaces, and efficient modular execution of program segments. The tables presented in this section attempt to address comprehensiveness from all of these standpoints.

In table 1 the codes are compared with respect to technical disciplines. The asterisk indicates the capability is presently in the code. The exception is the 2GCHAS code where the capabilities are not yet present but are under contract. Only the CAMRAD directly produces results in each discipline. Even the 2GCHAS code has deferred the acoustic predictive capability from the first set of its contracts. The C81 code has recently been enhanced to include an optimization capability. The SIMVIB base program is strictly a vibration reduction design tool. However, the other analyses in the package provide capabilities in the areas of loads, aeroelastic stability and performance. GRASP is restricted to stability applications and axial flight regimes. The DYSCO code has emphasized the solution to the governing sets of equations and has not been tailored to the specific engineering disciplines. The DYSCO code solves for both trim and transient response.

In table 2 the executive features of the codes are compared. The presence

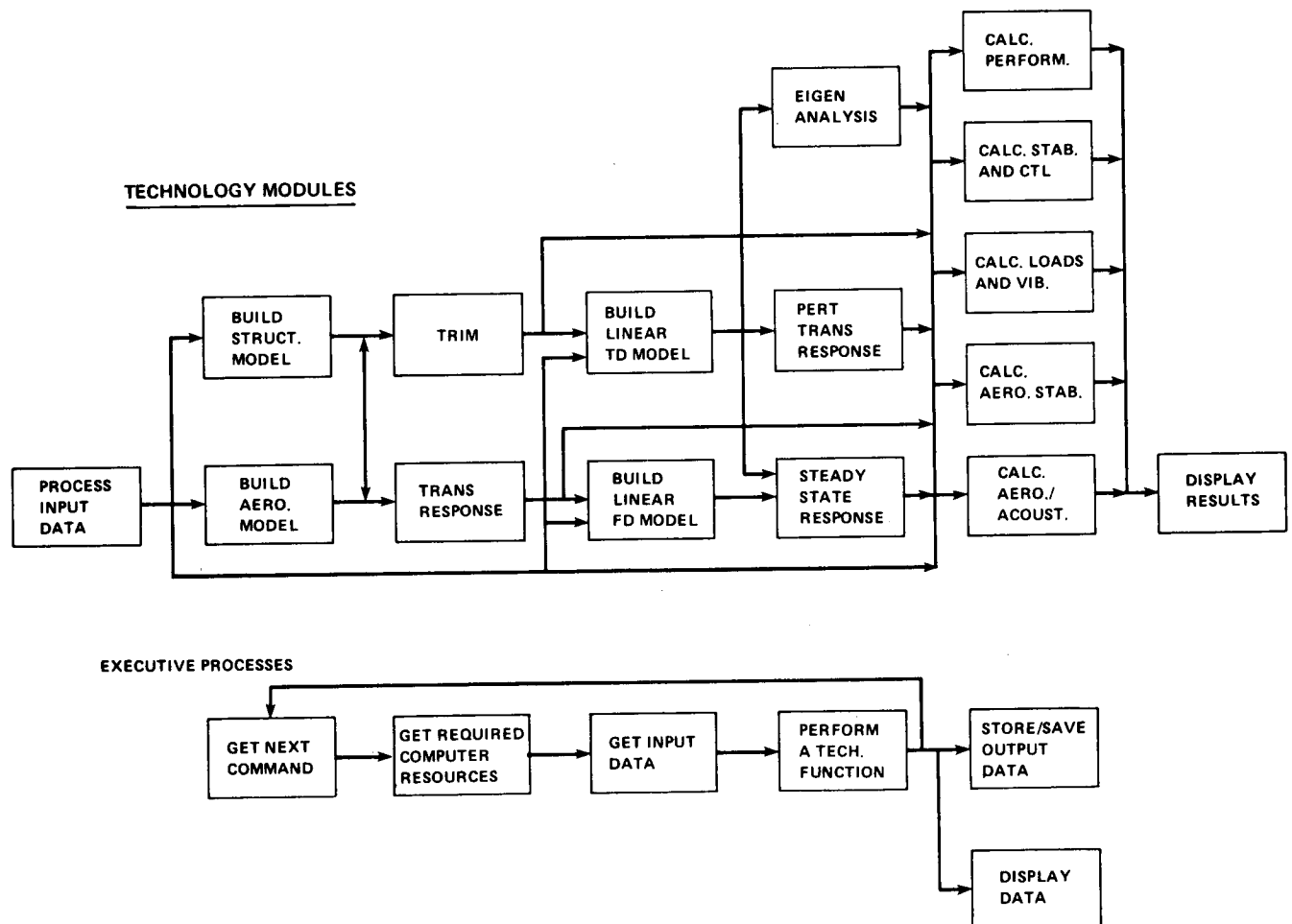


Figure 6: 2GCHAS Executive and Technology Complex functions.



Table 1: Comparison of Analysis Capabilities

Code	Per- form- ance	Loads and Vib.	Aero- elastic Stab.	Stab. and Control	Aero- dynam.	Other
C81	*	*	*	*	AF	Opt
CAMRAD	*	*	*	*	AF	Acst
DYSCO	*	*	*		AF	Dis
SIMVIB	*	*	*		AF	
GRASP		*	*		A	
2GCHAS	*	*	*	*	AF	

A = Axial flight, F = Forward flight, \* = capability present,  
Opt = optimization, Acst = acoustics prediction, Dis = dissimilar blades  
allowed

of the features is an indicator of ease of use and services available to user during an analysis run or set of runs. Two approaches have been used. Codes such as SIMVIB and C81 have attempted to make maximum use out of existing software to perform segments of the overall analysis. SIMVIB is described in figure 3 and couples the various wake geometry, inflow dynamics and modal blades codes together via external files. C81 relies on external codes to generate blade modes, provide graphic output and perform optimization tasks. The C81 code has automated the program coupling procedures by providing assistance to the user in recompilations and JCL declarations. The C81 graphics capability is provided by its own specialised plotting programs and by an interface with the DATAMAP package (ref. [18]). The remaining codes attempt to have all technical capabilities internal to their system. The CAMRAD program has an input preprocessor and has few other executive services. Its graphics capability is restricted to a line printer two dimensional printouts. The user must provide his own interface to an existing graphics programs. The DYSCO program provides an extensive input processor and an environment wherein elements, analyses, and output can be easily added to the system. A database exists to the extent that restarts and data modifications can be easily performed. A graphics capability is not currently a part of the system. The GRASP code has a sophisticated information manager built into the system which automates the dimension space needed from user inputs. It also provides services to the user in input preparation. It uses an internal program language to set procedures for analysis executions. Graphics are not included in the system. The 2GCHAS code has the most extensive executive. The executive provides a robust runtime database which can be saved, edited, and restarted. The executive traps all program crashes and provides an environment within 2GCHAS for input prepa-

Table 2: Comparison of Executive Features

Code	Executive	Data Base	Graphics	Coupled System
C81	Auto JCL	File I/O	Ext/Int	Programs
CAMRAD	Preprocessor	File I/O	Some	*
DYSCO	File R/W	File I/O		*
SIMVIB	File Sys	File I/O		Programs
GRASP	Info. Mgr.	Runtime	External	*
2GCHAS	User Lang/Procs	Runtime	Internal	*

\* = capability present

ration, graphics, and output control. The executive provides a user language to control the runtime execution. Alternatively, the user may write procedures in the user language or modules in FORTRAN which can be executed within the 2GCHAS environment. The graphics capability is linked directly to the DI-3000 commercial software package.

In table 3 the modeling capabilities of the programs are compared. All programs exhibit the ability to model a wide range of the current rotor types and at two least rotors within the model. The finite element-based codes (DYSCO, SIMVIB, GRASP, and 2GCHAS) have the potential for modeling an arbitrary number of rotors, even though the practical interest of one or two rotors is sufficient. In addition, the finite element codes are capable or have the potential, given an appropriate element library, of modeling a single blade as well as an arbitrary number of blades within the rotor system. The C81 and CAMRAD codes have a limit on the number blade modes which be used; the C81 code can include up to the 11 modes and the CAMRAD code can include 10 bending modes and 5 torsion modes. In all cases, the airframe component can be elastic although greater model detail is accounted for in the finite element model. Other aircraft components can be modeled as required by finite element codes and the CAMRAD codes provide the capability to model engine and transmission systems dynamics. Redundant load paths can be accounted for in the finite element codes provided the beam element properly accounts for axial extension. The fixed model programs (C81 and CAMRAD) provide the best aerodynamic modeling capabilities. In terms of wake geometry modeling and accounting for aerodynamic interferences these programs' capabilities are more mature and well matched to the analyses. The external program coupling of SIMVIB also provides a similar level of aerodynamic modeling. The 2GCHAS will be the first finite element code which attempts to emulate this level of aerodynamic modeling. Surprisingly, only CAMRAD and SIMVIB currently tie the nonlinear inflow calculation to a wake geometry and induced velocity calculation iteration.

Table 3: Comparison of Mathematical Model Features

Analysis	C81	CAMRAD	DYSCO	SIMVIB	GRASP	2GCHAS
Rotor Types	abghst	aghst	abghst	abghst	abghst	abghst
No of Rotors	2	2	4	*	*	*
No of blades	$\geq 2$	$\geq 2$	$\geq 1$	$\geq 1$	$\geq 3$	$\geq 1$
Blade Modes	11	10/5	5/5/3	FE	FE	FE
Elast Airfrm	Modal	Modal	FE/mod	FE	FE	FE
Components		Eng/Trns	FE/mod	FE	FE	FE
Redund Ld	approx		FE	FE	FE	FE
Inflow Dyn		*		*	*	*
Aero Inter	*	*				*
Free Wake		*				
Non inflow		*		*		*

a = articulated, b = bearingless, g = gimballed, h = hingeless, s = semiarticulated, t = teetering, FE = finite element, \* = capability present, mod = modal, 5/5/3 = flap/lag/torsion modes, 10/5 = bending/torsion modes

In table 4 the structural modeling building capabilities are summarized. The modal analysis capability is not internal to all codes. The C81 code uses a specially developed Myklestad code for developing its modes and only DYSCO requires the user to provide his own modes. A multiblade coordinate transformation is provided by those codes which perform an aeroelastic stability analysis in forward flight. Model building using a hierarchical tree is allowed to some degree in DYSCO and to a general level in GRASP and 2GCHAS. General kinematic constraints which couple the elements or components may be nonlinear in only the GRASP code. Limited nonlinear coupling is accounted for in the CAMRAD program. It will be necessary for the other finite element codes to adopt a Lagrange multiplier scheme which will allow nonlinear coupling. The GRASP provides a screw coupling capability that accounts for very large displacements or rotations similar to those which occur in robotics where multi-body mechanisms must be accounted for. Single point constraints or displacement boundary conditions are provided by all the programs.

## 4 Published Results

The purpose of this section is to provide some insight into how a particular code has performed when compared to experimental results. In most cases only one

Table 4: Comparison of Transformations Allowed

Transform	C81	CAMRAD	DYSCO	SIMVIB	GRASP	2GCHAS
Modal	see a	Int.	Ext.	G400	Int.	Int.
MBC	*	*			*	*
Tree Sub			Some	Some	*	*
Nonlinear		Some			*	
SPC	Some	*	*	*	*	*

\* = capability present, a = DYNAM06

result from the literature for each code is presented. An in-depth look at how the codes have performed in the area of predicting rotor loads has been provided in reference [26].

#### 4.1 C81 Correlation

The AATD sponsored three efforts to determine the validity of C81. The reference [27] effort was conducted by Bell Helicopter using AH-1G data and the 1976 version of the program. Since the present rotor analysis in C81 is nearly identical to the 1976 version, and since the Myklestad analysis at that time was valid for teetering rotors, the results shown in figure 7 are representative of the current program. The flight condition represented in the figure is for a forward velocity of 129 KTAS using data counter 615 of the 8319 pound AH-1G aircraft. The analysis results show that the steady moments do not compare well at the inboard stations with the flight data. The oscillatory or peak-to-peak loads, however, are in much better agreement. Both the measured and calculated results are dominated by the one-per-rev frequency content. For the one-per-rev case the outboard comparisons are poor. The agreement in the higher-per-rev distributions is much better.

References [28] and [29] document earlier correlation efforts conducted by contractors other than the program developer. Both efforts were performed using the 1974 version of the program which was the starting point for the 1976 improved program. Reference [28] describes serious shortcomings in the program and concludes that accuracy for predictions of H-53 and S-67 helicopter characteristics did not exceed that of other analyses which cost less to run. Reference [29] noted good correlation for trim and performance for the Messerschmitt-Boelkw-Blohm BO-105 helicopter, reasonable correlation of main rotor flap bending moments, and poor correlation of main rotor chord

and shaft bending moments. Difficulties were experienced in attempting correlation of the stability and control characteristics of the BO-105. Some of the difficulties reported in these references may be due to inexperience of the user, some on limitations of the Myklestad analysis, and some on the C81 program itself. AATD has recently sponsored an effort to improve the Myklestad analysis for hingeless and articulated rotors. Later versions of C81 have been used by the Bell Helicopter for in-house correlations with articulated and hingeless configurations with better results than those presented in these references.

## **4.2 DYSCO Correlation**

As discussed above, a current technology rotor analysis has only recently been added to DYSCO. The recent enhancement also included a correlation effort which was limited to rotorcraft performance characteristics. Some of the results are shown in figure 8. The only other published correlation was a comparison of ground resonance results using the Floquet stability analysis with the analytical results of Hammond (reference [30] for isotropic and nonisotropic hub characteristics. The results of the study (ref. [31]) showed exact agreement for all cases.

The results shown in figure 8 are taken from reference [22] where comparisons are made with operational loads survey test flight data (ref. [32]). Three DYSCO models are used in the comparison. The label, AH-1G, in figure 8 refers to the flight vehicle and the 36 refers to the data counter number in the flight test. The letter (S) in the label refers the DYSCO model with steady aerodynamics; the letter (U) refers to the DYSCO model with unsteady aerodynamics included; and the letters (B1S) refers to the DYSCO model with rigid out-of-plane mode and steady aerodynamics. The results for collective control, fuselage pitch and horsepower are generally good while the cyclic sine and cosine predictions are poor.

## **4.3 SIMVIB Correlation**

Published comparisons of SIMVIB predictions with test data are limited to references [5] and [33]. Reference [5] includes correlations with a one-sixth scale model rotor system tested in the NASA Langley Research Center Transonic Dynamics Tunnel with and without higher harmonic control inputs as shown in figures 9-(a), 9-(b), 9-(c). Agreement with fuselage accelerations, variation of blade moments with advance ratio, and radial distribution of bending moments is good. The prediction of bifilar mass motions shown in figure 9-(d) is excellent, but it should be noted that rotor forces were inferred from bifilar base

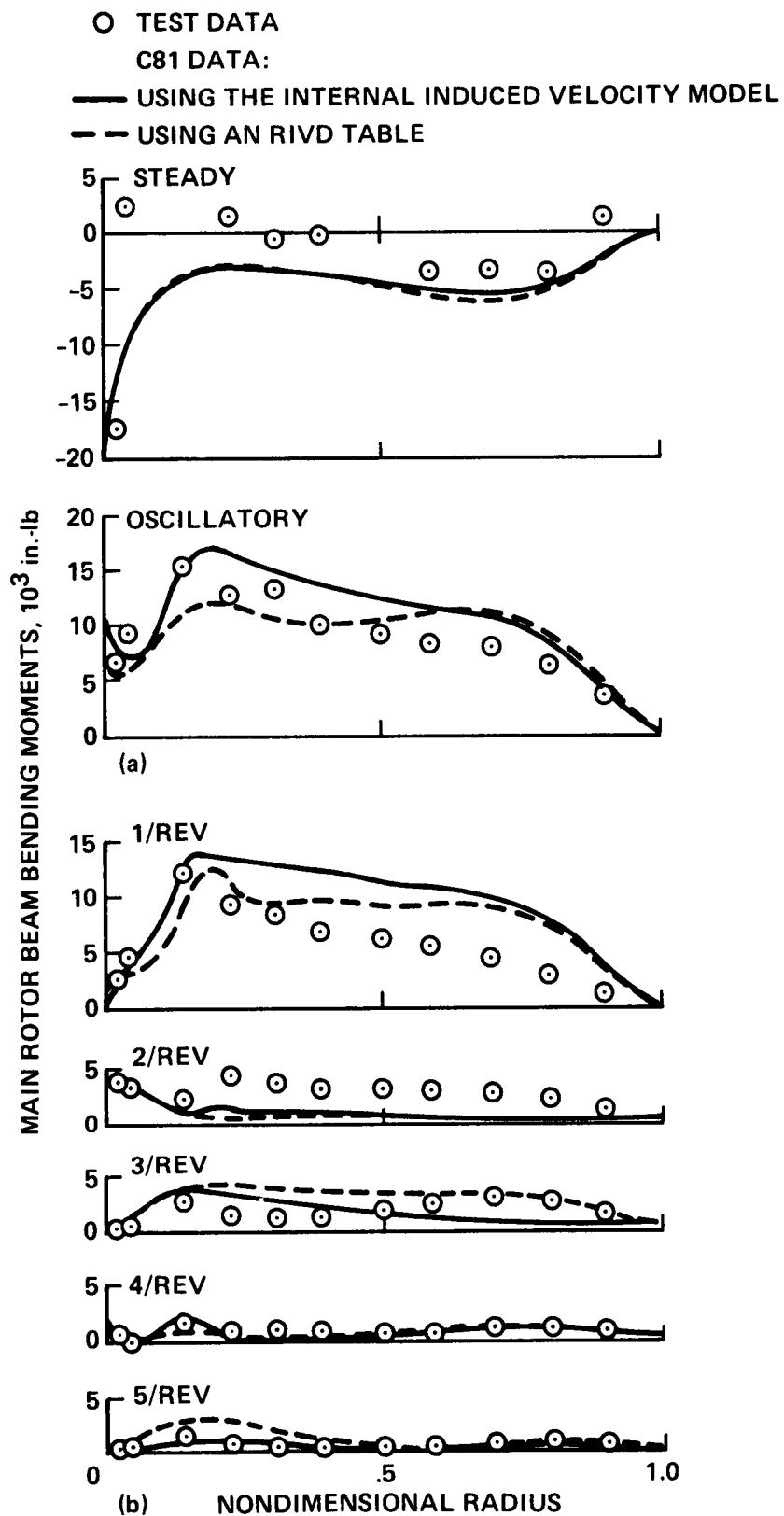


Figure 7: C81 results from reference 27.

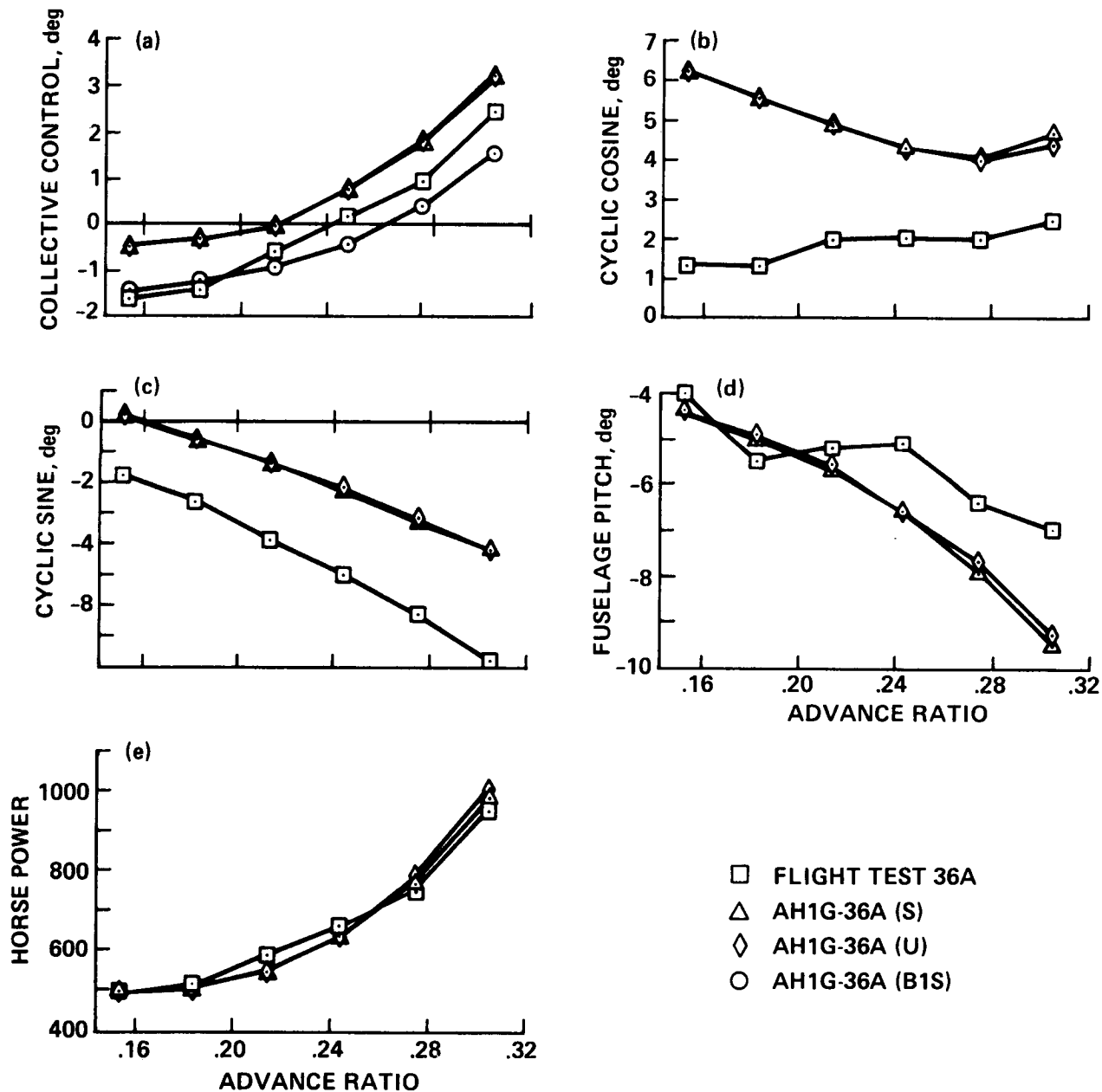


Figure 8: DYSCO results from reference 22.

accelerations, not from a rotor aerodynamic/dynamic analysis. A number of unvalidated applications are also provided in reference [5].

#### 4.4 CAMRAD Correlation

The CAMRAD code has been used extensively in the past few years as an analytical tool in many investigations. These investigations are summarised in the following applications: hover loading calculations using prescribed wake geometry (ref. [34]), lateral flapping calculations using nonuniform inflow and free wake geometry (ref. [35]), influence of unsteady aerodynamics on hingeless rotor ground resonance (ref. [36]), XV-15 tiltrotor performance, loads, and stability (ref. [37]), XH-59 ABC performance and loads (ref. [38]), fully consistent coupling with unsteady aerodynamics finite-difference calculations of advancing tip transonic flow (ref. [39]), body-induced flow effects on rotors (ref. [40]), hingeless rotor ground-resonance stability in forward flight (ref. [41]), hingeless rotor performance and stability in hover (ref. [42]), advanced technology LHX rotor performance (ref. [43]), V-22 tiltrotor model whirl flutter stability (ref. [44]), performance, loads and stability calculations for design of a high speed tiltrotor (ref. [45]), and correlation with flight test measurements of trim, blade loads, and blade airloading (ref. [46]).

The CAMRAD code has obtained wide acceptance due to its comprehensive analysis capability and consistent mathematical basis. The code development uses prudent compromises in modeling capability and solutions in order to compute performance, loads, trim states, transients, and stability characteristics efficiently. It has been used as a testbed for examining the improvement possible when the analysis is coupled via file transfer with another program which calculates the unsteady rotor flow from a three dimensional, full potential, finite difference code from computational flow dynamics formulations (ref. [39]).

Results from reference [46] are used to indicate the predictive ability of CAMRAD when compared with the SA 349/2 helicopter flight-test data. In the report, the capability to model the aerodynamic behavior is given primary attention. The results selected for presentation here will emphasize the dynamic behavior. Figure 10 shows the results for the flatwise and edgewise bending moments and torsion moment for a blade where the rotor is subject to a high speed - low thrust flight condition. The results presented in reference [46] ranged over several blade stations with the analysis and flight test data correlating better as radial station moves inboard. The results in figure 10 are for a blade station close to midspan. The figure illustrates that the analytical results are converged at six modes. The flatwise moment distribution around the rotor azimuth gives good correlation with the test data; the edgewise moments are not well predicted on the advancing side of the rotor disk. This error is attributed to the com-



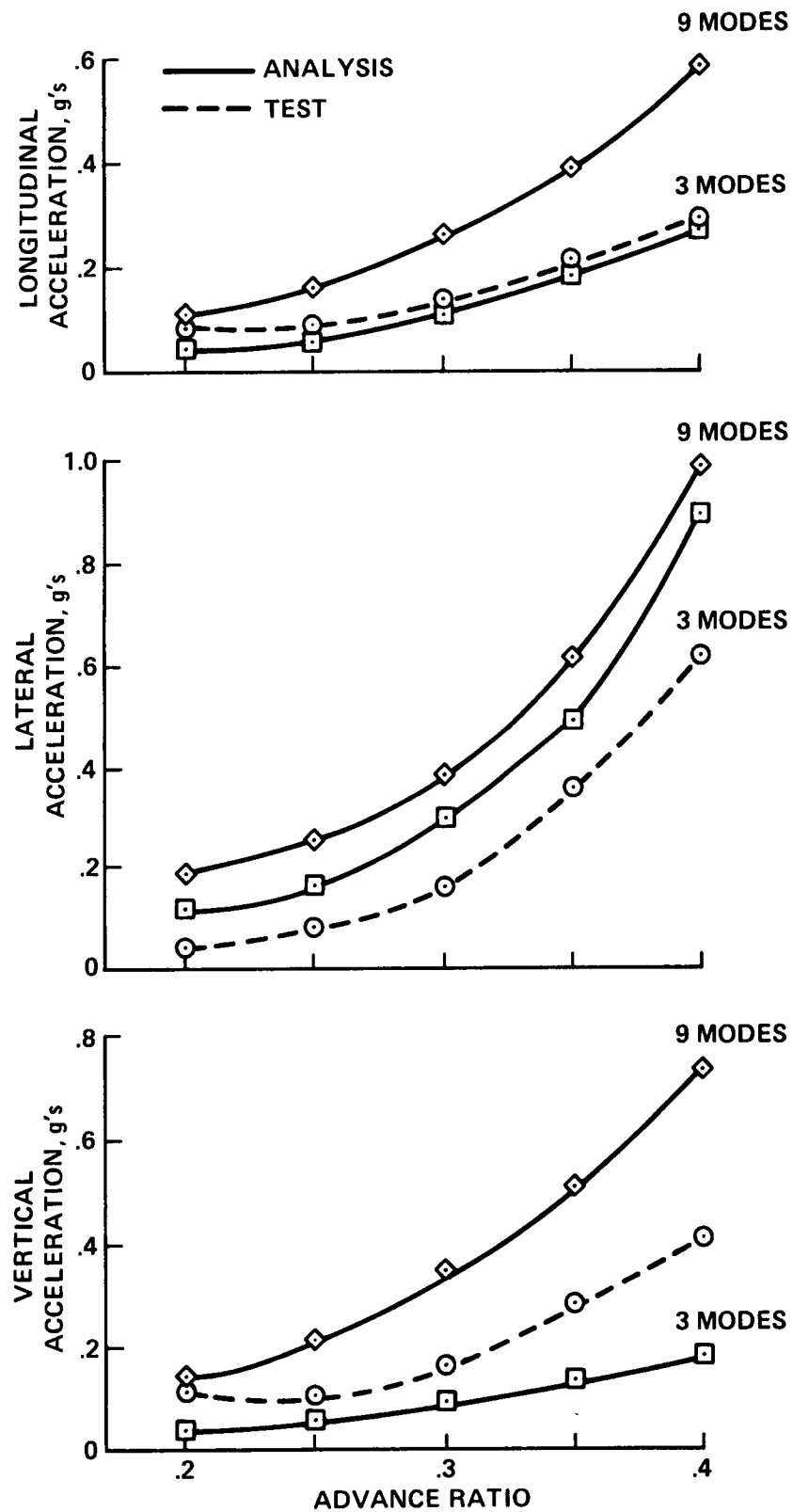


Figure 9: SIMVIB results from reference 5.

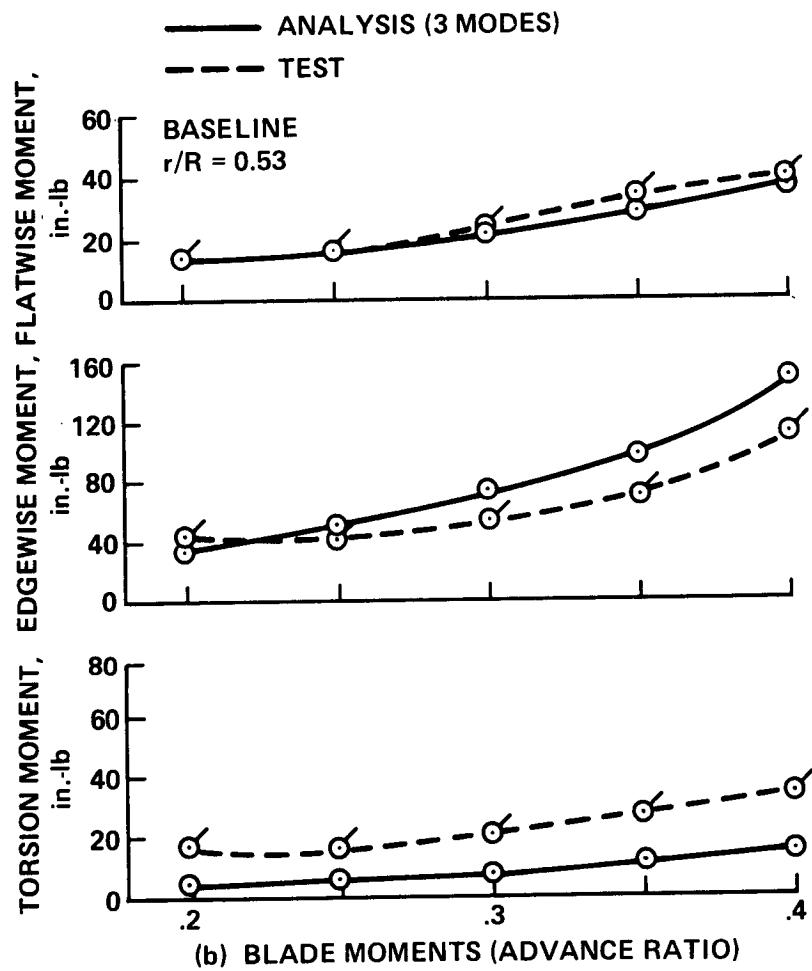
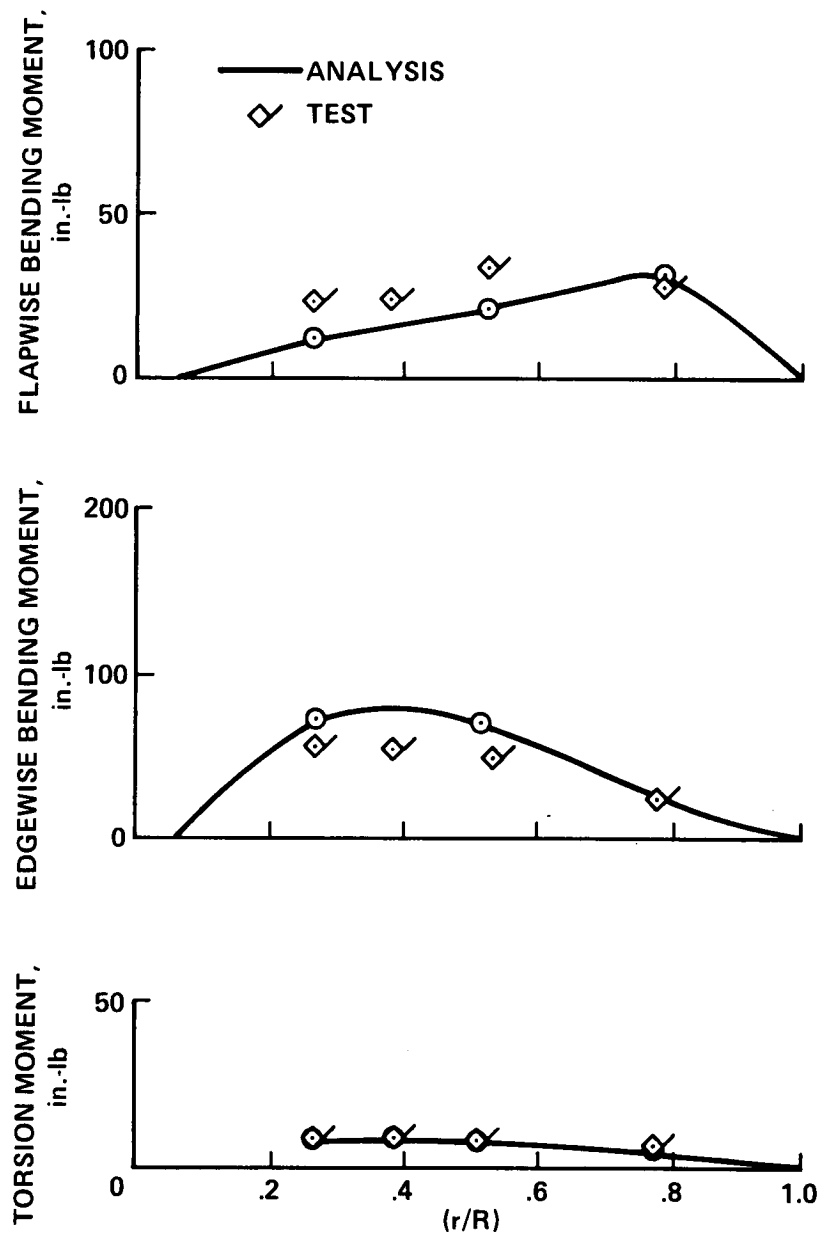


Figure 9: SIMVIB results - continued.



(c) BLADE MOMENTS (ADVANCE RATIO = 0.3)

Figure 9: SIMVIB results -- continued.

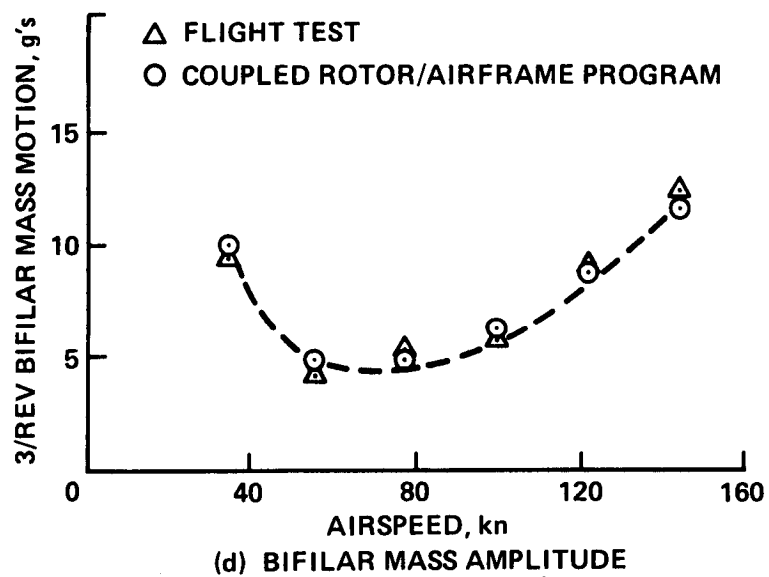


Figure 9: SIMVIB results – concluded.

compressibility effects not accounted for in the aerodynamic model. The torsional moment predictions are in reasonable agreement with test data. Convergence occurs with just two torsion modes required.

A low speed - low thrust flight condition case is also presented in reference [46]. Those results are duplicated here for variation of the coefficient of lift as a function of blade azimuth. At low speed the rotor wake stays in the vicinity of the blade and a strong blade-vortex interaction is obtained. A detailed wake geometry is needed to obtain good correlation for aerodynamic loads. As shown in figure 11, correlation to the wind tunnel data improves with each improvement to the wake geometry model for all blade stations. The uniform inflow analysis predicts the trends of lift variation around the rotor azimuth but not the details. The lift prediction is improved when the prescribed wake model is used. However, the free-wake model predicts the lift behavior very closely. It is in the area of aerodynamic modeling that CAMRAD excels. Even though lifting line theory is used, care has been taken to incorporate a free-wake geometry iteration with rollup and near and far wake effects included as well as corrections for blade tip, yawed flow, nonuniform inflow, dynamic stall, ground effect, and unsteady lift and moment.

#### 4.5 GRASP Correlation

The GRASP code has been recently completed and the validation efforts are underway. Extensive comparisons with the flap-lag-torsion aeroelastic stability experimental results presented in reference [47] are in progress and will be reported in reference [48]. Reference [49] compares the GRASP solutions with theoretical results of Ormiston [50] for the ground and air resonance stability of a coupled rotor-fuselage. Good agreement was obtained for these results. Also in reference [49] the GRASP code is compared with a basic experiment carried out at Princeton University (refs. [51,52,53]). Typical results of this latter comparison are shown in figure 12. The beam is a slender, nonrotating, cantilevered, uniform beam with a tip mass. The load angle  $\theta$  is varied from 0 to 90° at the beam root. These results show excellent agreement between the GRASP predictions and the experimental data for both the static deflection and the first flatwise and edgewise frequencies.

#### 4.6 2GCHAS Schedule

The 2GCHAS code is under development. The first public release of the code is scheduled for the third quarter of 1988 as shown in figure 5. At that time, validation efforts will be initiated to qualify the accuracy of the integrated System.

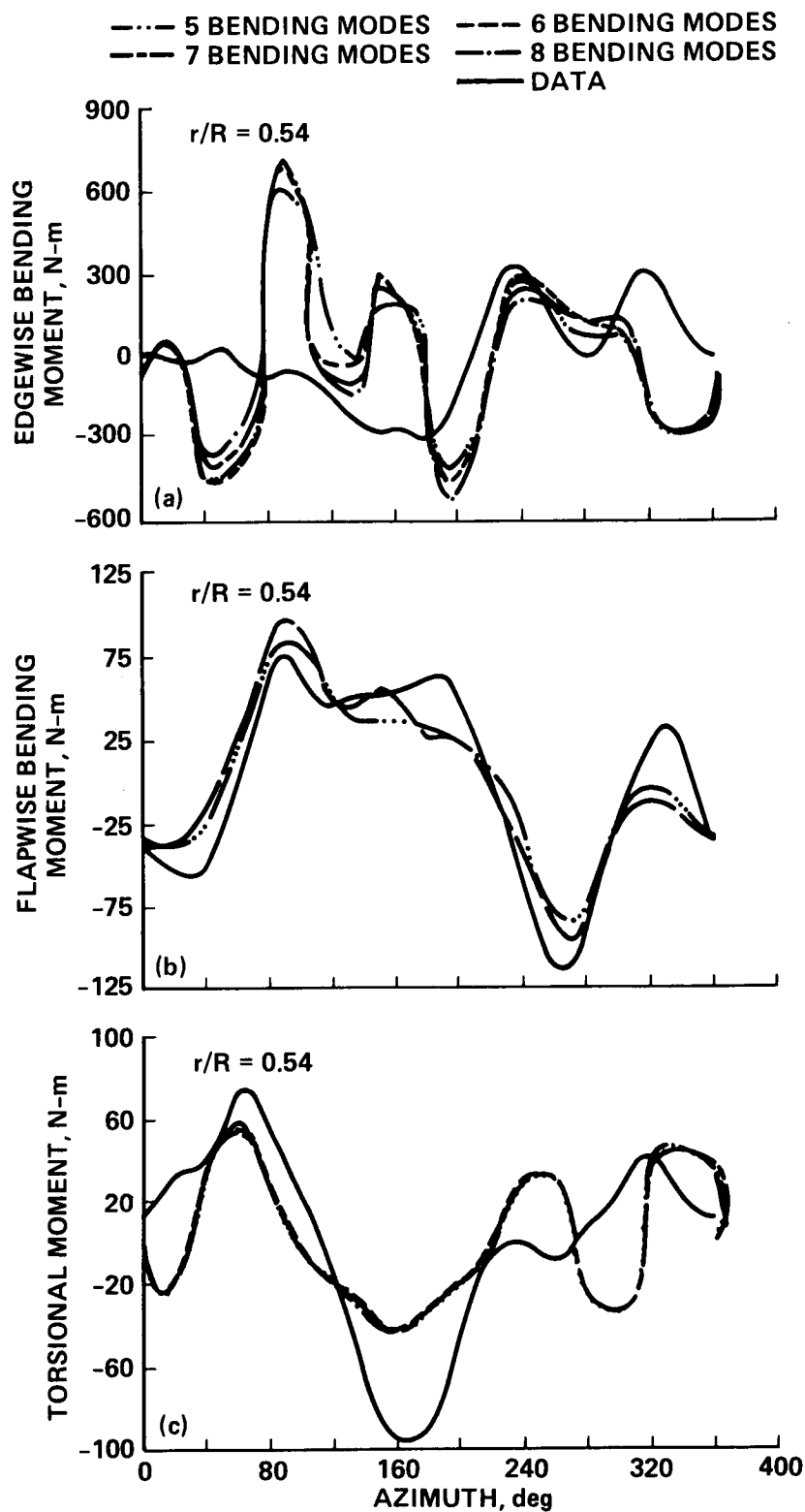


Figure 10: CAMRAD correlation from reference 46 for high speed ( $\mu = .36$ ) and low thrust ( $C_T/\sigma = 0.071$ ).

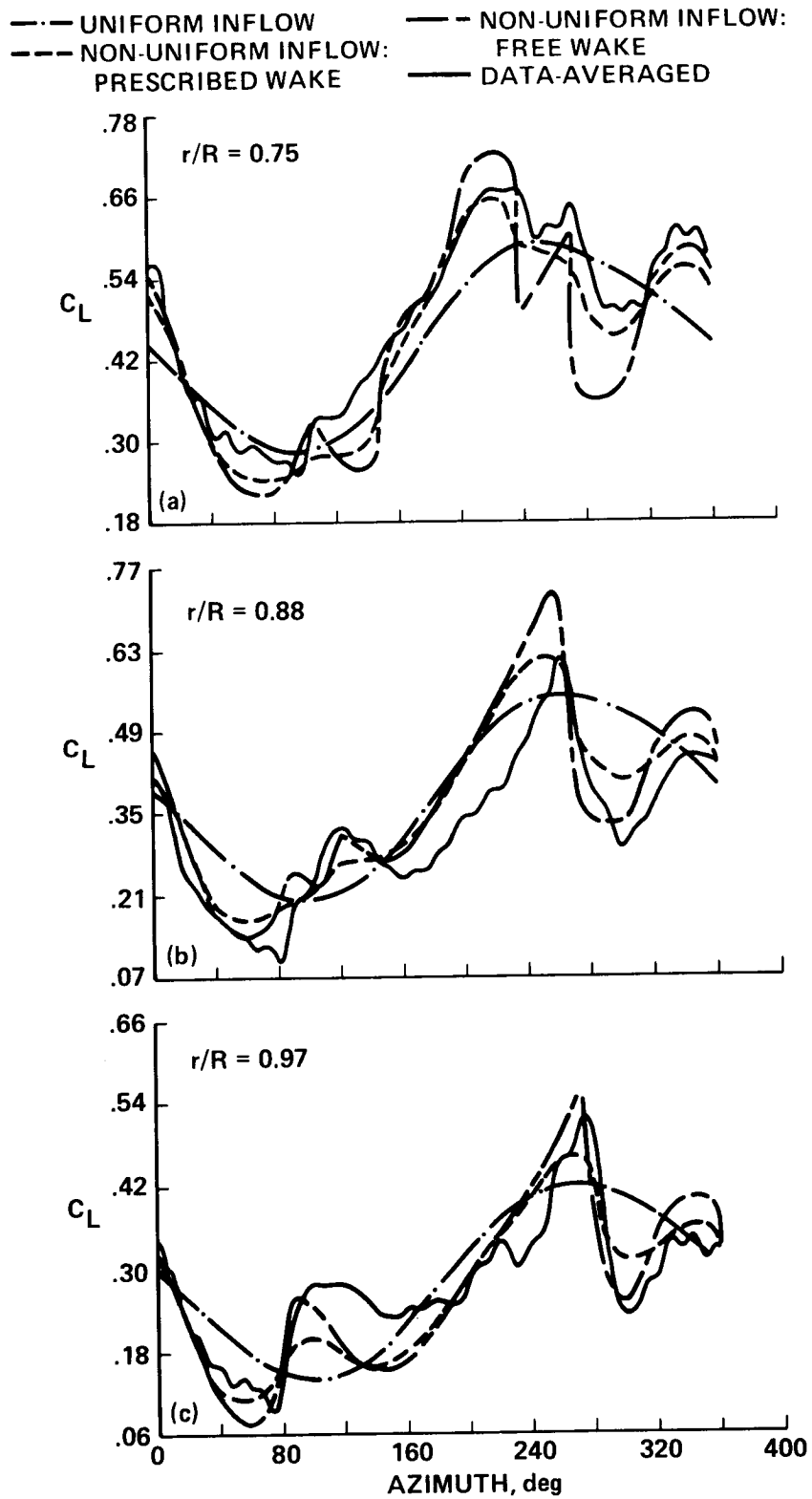


Figure 11: CAMRAD correlation from reference 46 for low speed ( $\mu = 0.14$ ) and low thrust ( $C_T/\sigma = 0.065$ ).

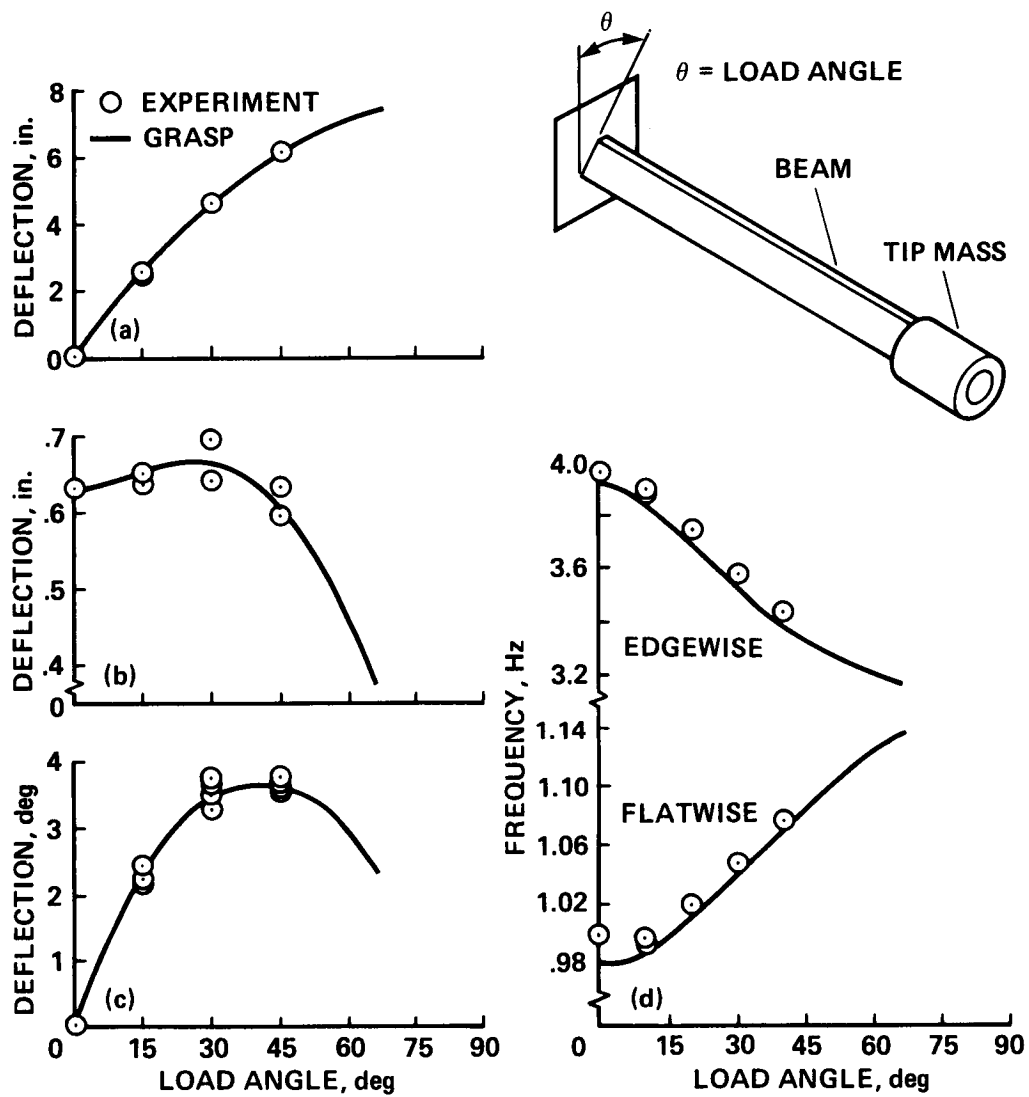


Figure 12: GRASP results from reference 49.



opment contractors will perform limited validation studies for their software contributions. The results of these initial validation studies will be available with the System document.

## 5 Concluding Remarks

The government's influence on interdisciplinary analysis software has been reviewed over the past decade. As a result of this involvement several significant advancements have been noted.

1. Both the government and the industry codes have become broader in scope and more consistent in the theoretical development. This is evident in the CAMRAD, GRASP and DYSCO codes presently and is anticipated for the 2GCHAS code.
2. New code development for interdisciplinary analysis requires an executive portion of the code to allow modular development and execution of the code subunits. 2GCHAS will have an extensive executive system. In addition, the other five codes discussed in this paper have addressed this feature to some extent. Even the oldest code surveyed, C81, recently underwent major modifications to allow a modular execution of its subsystems.
3. The trend in subunit development is to have all subprograms operate entirely in the executive environment. 2GCHAS, GRASP, DYSCO and CAMRAD are examples of this type of executive. C81 runs in an environment that appears to the user to be a single executive, but that executive actually runs up to eight separate job steps. The SIMVIB code uses a suite of independent programs which are coupled only by data files.
4. The structural modeling capability now exists to couple substructures. This capability is most easily incorporated in finite element based codes. The capability is best demonstrated in the GRASP code which combines finite element and multi-body coupling techniques. It is also demonstrated in the DYSCO and SIMVIB codes which include a linear Hurty coupling scheme for substructures. In these cases the subsystems being coupled do not have to be finite elements but must be consistent displacement-type math model formulations. The approach allows maximum flexibility in matching model details in the airframe and rotor system and computational efficiency when the finite element level of detail is not necessary. 2GCHAS will include the Hurty capability initially and then move to a more general approach including nonlinear coupling at a later date.

5. The inability to predict the rotorcraft aerodynamic environment and the time-varying aerodynamic loads on the rotors is perceived as the greatest impediment to good correlation between theory and test. Presently, aerodynamic modeling involves predicting the aerodynamic loads on a specific component with limited interference effects from other components accounted for. A general, interactional formulation is not available. There has been limited experience in interfacing advanced aerodynamics methodologies with comprehensive models. Comprehensive analysis methods with highly consistent dynamics components, reliable solution techniques and well documented interfaces to their aerodynamics analysis features should provide excellent test beds for advances in aerodynamics modeling. The mating of differencing schemes for unsteady aerodynamics of transonic tip flow to CAMRAD (ref. [39]) is an effort of this type. The 2GCHAS may provide additional impetus to generalizing aerodynamic approaches in software applications.
6. Validation of comprehensive codes is a massive, long term, and necessary undertaking. Comparisons with experimental data, other methods, closed form solutions and years of use in a production environment are necessary to build confidence in a design tool. The newer comprehensive codes will need continued government funding for validation studies to be performed to show both the areas acceptance and the areas where more rigorous development work must be done.
7. The modular component development and executive environment for multidiscipline analysis is in the infant stage and sufficient experience is not available to know how much of a boon this will be to research and to advancing the state of the art. However, it should at least be an asset to analysis and design problems and simplify and speed information and software transfer.
8. Wide distribution of government-sponsored software and theoretical developments should continue to be encouraged if the rotorcraft industry is to benefit fully from them. The importance of having widely accepted analysis tools available to industry and academia has been demonstrated by NASTRAN and other codes. Analyses and research have been conducted with these codes at manufacturing sites and universities. In addition to providing the immediate results for the research, the codes and their theoretical development have provided a basis for knowledgeable information exchanges. One form of the information exchange is to provide better prepared students from universities to the industry.
9. The government funding has been essential to the effort since the multidiscipline development requires broad areas of expertise and years of commitment.

## References

- [1] Kerr, Andrew W.; Potthast, A. J.; and Anderson, W. D.: An Interdisciplinary Approach to Integrated Rotor/Body Mathematical Modeling. AHS Symposium on the Status of Testing and Modeling for V/STOL Aircraft, Philadelphia, PA., October, 1972.
- [2] Ormiston, Robert A.: A comparison of Several Methods for Predicting Loads on a Hypothetical Helicopter Rotor. *Rotorcraft Dynamics*, Conference at Ames Research Center, Moffett Field, CA, February 13-15, 1974, NASA SP-352.
- [3] Schrage, Daniel A.: Use of Rotorcraft Computer Analysis for U. S. Government Design Assessment. *Computers & Mathematics with Applications*, Vol 12A, No. 1, 1986, pp. 1-9.
- [4] McLarty, T., et al: Rotorcraft Flight Simulation with Coupled Rotor Aeroelastic Stability Analysis, Vol. I. Engineer's Manual. USAAMRDL/TR-76-41A, May 1977.
- [5] Sopher, Robert; Studwell, R. E.; Cassarino, S.; and Kottapalli, S. B. R.: Coupled Rotor/Airframe Vibration Analysis. NASA CR-3582, November 1982.
- [6] Sopher, R.; Studwell, R. E.; Cassarino, S.; and Kottapalli, S. B. R.: Substructure Program for Analysis of Helicopter Vibrations. *Journal of the American Helicopter Society*, Vol. 28, No. 4, December 1983, pp. 14-21.
- [7] Predesign of the Second Generation Comprehensive Helicopter Analysis System. Computer Sciences Corporation, USARTL-TR-78-41, October 1978.
- [8] Predesign of the Second Generation Comprehensive Helicopter Analysis System. Control Data Corporation, USARTL-TR-78-43, October 1978.
- [9] Predesign of the Second Generation Comprehensive Helicopter Analysis System. Science Applications, Inc., USARTL-TR-78-42, October 1978.
- [10] Johnson, Wayne: A Comprehensive Analytical Model of Rotorcraft Aerodynamics and Dynamics, Part I: Analysis Development. NASA TM-81182, 1980.
- [11] Johnson, Wayne: A Comprehensive Analytical Model of Rotorcraft Aerodynamics and Dynamics, Part II: User's Manual. NASA TM-81183, 1980.
- [12] Johnson, Wayne: A Comprehensive Analytical Model of Rotorcraft Aerodynamics and Dynamics, Part III: Program Manual. NASA TM-81184, 1980.

- [50] Ormiston, R. A.: Rotor-Fuselage Dynamic Coupling Characteristics of Helicopter Air and Ground Resonance. Proceedings of the Theoretical Basis of Helicopter Technology, Nanjing Aeronautical Institute, Nanjing, China, Nov. 6-8, 1985.
- [51] Dowell, E. H.; and Traybar, J.: An Experimental Study of the Non-linear Stiffness of a Rotor Blade Undergoing Flap, Lag, and Twist Deformations. AMS Report No. 1194, Princeton University, Dec. 1975.
- [52] Dowell, E. H., and Traybar, J.: An Experimental Study of the Non-linear Stiffness of a Rotor Blade Undergoing Flap, Lag, and Twist Deformations. AMS Report No. 11257, Princeton University, Dec. 1975.
- [53] Dowell, E. H.; Traybar, J.; and Hodges, Dewey H.: An Experimental-Theoretical Study of the Non-linear Bending and Torsion Deformations of a Cantilever Beam. *Journal of Sound and Vibration*, 50, (4), 1977, pp. 533-544.

ROTORCRAFT AEROELASTIC STABILITY

Army-NASA Research 1967-1987

Robert A. Ormiston  
Chief, Rotorcraft Dynamics Division  
Aeroflightdynamics Directorate  
U.S. Army Aviation Research & Technology Activity

and

William G. Warmbrodt  
Chief, Rotary Wing Aeromechanics Branch  
NASA Ames Research Center

Moffett Field, California

and

Dewey H. Hodges  
Professor

and

David A. Peters  
Professor

Georgia Institute of Technology  
Atlanta, Georgia

SUMMARY

Theoretical and experimental developments in the aeroelastic and aeromechanical stability of helicopters and tilt-rotor aircraft are addressed. Included are the underlying nonlinear structural mechanics of slender rotating beams, necessary for accurate modeling of elastic cantilever rotor blades, and the development of dynamic inflow, an unsteady aerodynamic theory for low-frequency aeroelastic stability applications. Analytical treatment of isolated rotor stability in hover and forward flight, coupled rotor-fuselage stability in hover and forward flight, and analysis of tilt-rotor dynamic stability are considered. Results of parametric investigations of system behavior are presented, and correlations between theoretical results

---

Paper presented at the NASA/Army Rotorcraft Technology Conference, NASA Ames Research Center, March 17-19, 1987.

and experimental data from small- and large-scale wind-tunnel and flight testing are discussed.

## 1. INTRODUCTION

Aeroelastic stability, like other rotorcraft technologies, is a broad and complex subject. Extensive research has been conducted during the last 20 years prompted by the emergence of new technical challenges, as well as the establishment of Army research organizations and the NASA-Army agreement for cooperative research. Therefore, it is appropriate to survey the accomplishments during this period. The scope, depth, and technical sophistication of the work to be discussed have greatly increased. We now have an established and sound foundation and an active research program. The purpose of this survey is to present a comprehensive overview of Army-NASA research in rotorcraft aeroelastic stability accomplished over the past 20 years, to assess and summarize the major contributions of government research, and to identify needs and opportunities for future research and development.

It is of interest to define the state of the art in rotorcraft aeroelastic stability before 1970 as a background for this survey. Such a description should serve to highlight how far technology in this area has progressed. An outline of the key technology areas for this description is given in table 1. Before 1970, several research compound helicopters had extended rotorcraft flight-test experience to high-speed, high-advance ratio conditions. Examples of blade-stability problems were encountered at high advance ratios. However, as emphasis on high-speed rotorcraft shifted away from compound helicopters and toward the tilt rotor, these problems were not vigorously pursued. For conventional articulated- or teetering-rotor helicopters operating at moderate flight speeds, aeroelastic stability was not a significant concern. Although experience with the XV-3 tilt rotor had exposed significant potential for aeroelastic stability problems, only limited research was devoted to these problems.

The rotorcraft situation changed rather substantially as 1970 approached. Interest in the hingeless rotor intensified during the late 1960's, but vehicle development programs, including the AH-56A, began to expose the aeroelastic complexities of such systems. The hingeless-rotor YUH-61A UTTAS prototype did exhibit acceptable aeromechanical stability characteristics but was not selected for production. Even more advanced but structurally complex configurations such as the bearingless rotor were being explored. With the advent of the XV-15 program, the uncertainties about tilt-rotor aeroelastic stability took on much more urgency.

In terms of rotor-blade stability, the pre-1970 era dealt primarily with bending-torsion flutter, including wake-excited flutter. In the post-1970 era, these phenomena, together with the unique properties of hingeless- and bearingless-rotor configurations, opened up a new class of problems in aeroelastic instability. These problems were associated with the poorly understood structural dynamics

of cantilevered rotor blades. With the availability of Floquet theory, research in the post-1970 period also began to deal with the long standing problem of forward-flight aeroelastic stability.

For rotating-beam structural dynamics, the metal bladed-articulated rotors of the pre-1970 period could be quite adequately handled with the equations of linear beam theory and isotropic material properties. With the advent of hingeless and bearingless rotors and composite materials, rotor-blade structural dynamics became a complex nonlinear problem.

Unsteady aerodynamics theory for rotor-blade flutter in the pre-1970 period was relatively standard, based on two-dimensional Theodorsen and Loewy theories. In the post-1970 period, efforts were made to extend aerodynamic theory to include three-dimensional effects, dynamic inflow for simplified low-frequency aeroelastic stability, transonic tip aerodynamics, and dynamic stall effects.

In coupled rotor-body dynamics, the pre-1970 era dealt mainly with classical ground resonance of articulated rotors. The post-1970 period of hingeless rotors brought with it the complexity of aeromechanical instability, both on the ground and in flight, with greatly increased complexity owing to the importance of aerodynamics. In sum, the post-1970 era presented a very significant expansion of technical issues facing the aeroelastician.

The objectives of research and development on rotorcraft aeroelastic stability are to ultimately meet the needs of the rotorcraft user. For the user, either military or civilian, this means improving rotorcraft capability—for example, performance, speed, maneuverability, payload-range, and reliability—as well as reducing acquisition, operating, and maintenance costs. With respect to aeroelastic stability, this translates into reducing development cost and risk for improved rotorcraft and enabling the designer to exploit new technology with minimal risk of unforeseen aeroelastic instabilities. Without a firm technology base for aeroelastic stability, the designer may be forced to adopt a more conservative design of lower performance, or excessive testing may be required during development, thereby adversely affecting cost and schedule. Even more serious, an unexpected instability encountered during flight testing could seriously disrupt the schedule, cause major cost overruns, or even jeopardize the program.

The success of research and development to meet the objectives outlined above depends in part on the effectiveness of the approach employed. The success of the Army-NASA efforts in this field can be attributed in part to an approach that includes (1) developing a thorough understanding of the structural dynamics, aerodynamics, and aeroelastic stability characteristics of a wide variety of rotorcraft components and systems; (2) developing and validating improved theoretical analysis methods to predict stability; and (3) developing design approaches and concepts that eliminate or minimize the potential for aeroelastic instability.

Understanding dynamic phenomena can be achieved through parametric analytical studies or exploratory experimental investigations. Since understanding a dynamic system is often synonymous with being able to represent it mathematically, the derivation of analytical models, comparing them against measured data, and carefully studying and reconciling the results is a valuable part of the process. For complex physical systems, breaking the system down into a series of simpler problems is often essential to get to the core of the problem. Ultimately a thorough understanding of aeroelastic stability phenomena is essential to avoid problems in new designs and to minimize design compromises necessary to avoid instability.

Development of theoretical prediction methods is a key part of aeroelastic stability research. These methods permit the researcher to apply general knowledge in a precise way and ultimately equip the designer with concrete design tools. Developing analysis methods involves basic research in the subdisciplines of aeroelastic stability: materials, solid mechanics, numerical analysis, and further subspecialties. Validation of prediction methods is also essential. Developing analyses and computer programs in a rigorous way is a very exacting process, but success can never be determined nor is a program of much value unless it can be adequately validated. Done properly, validation can be as demanding as development of the theoretical analysis.

To be fully effective, experimental tests must be carefully planned to take into account the specific objectives of the validation. The experiment should be designed to eliminate phenomena not germane to the correlation; moreover, the physical properties of the model must be accurately determined. Careful planning will insure that proper interpretation of the correlation between theoretical and experimental results can be made.

Finally, satisfying research objectives also involves identifying means to forestall potential aeroelastic instability, whether through proper design practices, alternative design approaches to avoid problems, or generating concepts that may eliminate such instabilities.

This survey is intended to cover aeroelastic stability research in a broad sense, from the development of analysis methods to their effect on the development of flight vehicles. The material is organized in the following manner. Analysis methods are treated first in section 2, focusing on the development of equations for the prediction of rotorcraft aeroelastic stability. Included is a detailed discussion of underlying theory of kinematics and solid mechanics for rotating elastic beams, unsteady aerodynamics pertinent to rotorcraft aeroelastic stability (including dynamic inflow), and a limited treatment of solution methods used in aeroelastic stability analysis. The analysis methods section includes results of experimental investigations to validate basic theories for beam structural dynamics, unsteady aerodynamics, and solution methods. Experimental investigations or correlations of aeroelastic stability are not included.

In section 3, information about the aeroelastic stability characteristics and behavior of rotorcraft is surveyed. This includes results of parametric analytical investigations, experimental testing, and correlations to validate prediction



methods. The material is organized in order of increasing complexity of the physical system, beginning with stability of a single flapping blade up to fully coupled rotor-body dynamic systems. Section 4 surveys the experience gained in the design or development of specific rotorcraft systems from the point of view of how aeroelastic stability technology affected the development or yielded insights during design and testing of these systems. The organization of sections 2-4 necessarily leads to some overlap or duplication, for some research efforts naturally span two or even more of these sections. Finally, the results of the work surveyed are summarized, and the contributions of Army-NASA research in this field are assessed. Recommendations for future research are also provided.

A few comments are in order regarding this survey. It was intended that Army-NASA research contributions be emphasized in the material discussed herein. In order to provide perspective and technical continuity, selected non-government research and development efforts have been included where deemed appropriate. While it is hoped that all relevant government contributions have been accounted for, this survey is not complete for the field of aeroelastic stability as a whole. Furthermore, since the volume of work in the field is considerable, the treatment in the survey is necessarily limited in depth and the reader should refer to the references for more detail.

Mention is also in order regarding the distinctions between government and non-government research. For the purposes of this paper Army-NASA contributions include research and development conducted by the four directorates of the U.S. Army Aviation Research and Technology Activity (the Aeroflightdynamics Directorate (AFDD), the Propulsion Directorate, the Aerostructures Directorate, and the Aviation Applied Technology Directorate (AATD)); the NASA Ames, Langley and Lewis Research Centers; and academic or industry research supported by these government organizations. In the case of the Aeroflightdynamics Directorate this includes a number of investigations sponsored jointly with the Army Research Office. The material included herein but not derived from government or government sponsored efforts is denoted by an asterisk entry in the reference list.

## 2. ANALYSIS METHODS

This section deals with the development of analysis methods for calculating the aeroelastic and aeromechanical stability characteristics of rotorcraft including formulation of equations of motion to model aeroelastic stability behavior. This involves research in fundamental solid mechanics, structural dynamics, materials properties, rigid-body dynamics, and unsteady aerodynamics. This section also deals with the development of mathematical methods to solve the aeroelastic stability equations.

## STRUCTURAL DYNAMICS

Rotorcraft structural dynamics encompasses the mechanics of both rigid and flexible bodies generally used to model the structural, inertial, and mechanical characteristics of a rotorcraft or its components. The equations are useful for various rotorcraft applications, but here we focus on their use in aeroelastic stability analysis. This section will address the evolutionary development of rotorcraft equations, primarily the equations of motion for rotating elastic beams used in modeling the rotor blades and equations for coupled rotor-body systems including both helicopters and tilt-rotor aircraft.

It is a given among rotorcraft researchers that because of the complexity of the flow fields, an adequate description of rotary wing aerodynamics is well beyond the current state of the art. Because the mechanics of rotating structures is considerably less difficult than the aerodynamic problem, it is sometimes assumed that rotorcraft structural dynamics is an exact science. However this is not the case and the material presented below will describe the issues that researchers are dealing with.

### Rigid-Blade Equations

Early rotor-blade and rotorcraft analyses usually treated both hinged and cantilever elastic blades as hinged, rigid blades for the purposes of aeroelastic or aeromechanical stability. In the case of articulated rotor blades this is appropriate for many problems. For cantilever hingeless rotor blades, the hinged, rigid blade represents a greater degree of approximation. Nevertheless, when the blade bending flexibility is simulated with a rotational spring placed at the hinge, the resulting equations may be adequate for many applications. The equations are easier to derive, and the solutions can be computed much more economically. The approximate hinged-rigid-blade model has been widely used and served as a very effective means to initiate more refined analyses of elastic cantilever blades. The rigid-blade equations are also valuable when insight into dynamic behavior is sought.

In contrast to structural dynamics of elastic rotor blades, the equations of motion describing the mechanics of hinged-rigid blade models are well defined, even though the algebra can become very involved when many degrees of freedom are included. The principal issue in deriving approximate hinged-rigid-blade equations is the selection of the hinge geometry that will best simulate the elastic blade. The development of the hinged-rigid-blade models, their relative accuracy in representing elastic blades, and the results of aeroelastic stability investigations based on such approaches will be covered under Flap-Lag Stability in section 3.

### Development of Elastic-Blade Equations

The fundamental basis for rotor-blade equations of motion, and one of the key topics in rotorcraft aeroelastic analysis, is the structural dynamics of rotating

elastic beams. Over the last 20 years, extensive Army and NASA efforts have been devoted to the development of suitable equations to describe the elastic bending and torsion of rotating cantilever beams. Much of this effort has been directed toward the analysis of advanced hingeless and bearingless rotor blades. Although these mechanically simple configurations offer considerable benefit for rotorcraft, they also present a significant challenge for the structural dynamicist. The lack of hinges results in moderately large bending and torsional deformations of cantilever blades during rotorcraft operation. From a structural dynamics point of view these moderately large deformations give rise to geometrically nonlinear structural and inertial terms in beam equations, even when the material properties are linear and the strains are small.

In contrast to hingeless rotor blades, articulated rotor blades could usually be treated quite adequately with linear equations. Since the middle 1950's, the standard equations for this class of problems were the classic Houbolt and Brooks equations for combined flapwise bending, chordwise bending and torsion of twisted, nonuniform rotor blades (ref. 1). Although these equations are linear, they contain the geometrical stiffening, owing to centrifugal force, normally considered a nonlinear effect. These equations were the starting point for much of the subsequent development of nonlinear equations for elastic rotor blades.

The following sections will deal with nonlinear equations for elastic beams undergoing moderate deformations, the nonlinear kinematics of deformed beams, nonlinear torsion of pretwisted beams under axial tension, advanced theories for beams undergoing large rotation and small strains, bearingless rotor blades, finite-element formulations, and treatment of composite materials in rotor-blade equations.

Moderate deformation blade equations- As noted above, the accepted standard for elastic-blade equations was the work of Houbolt and Brooks (ref. 1). One of the first attempts at a complete derivation of equations suitable for aeroelastic analysis of both articulated and cantilever blades was the work of Arcidiacono, who developed nonlinear equations for combined flapwise bending, chordwise bending, and torsion motions of an elastic blade (ref. 2). The final modal equations were linearized for small motions and included a quasi-steady aerodynamic formulation as well.

The Aeroflightdynamics Directorate initiated research on development of nonlinear elastic-blade equations in order to treat aeroelastic stability of hingeless rotor blades. Early AFDD research considered the restricted problem of coupled flap and lead-lag elastic bending of torsionally rigid cantilever rotor blades. Ormiston and Hodges developed elastic-blade flap-lag equations to extend analysis capabilities beyond the rigid-blade equations (refs. 3,4). Their derivation was based on Hamilton's principle because of its suitability for complex problems, especially when the nonconservative aerodynamic forces are included. It also helps in correctly formulating the internal forces based on strain energy. The resulting flap-lag equations differed little from the Houbolt-Brooks equations except for a kinematical variable for axial displacement of the blade, based on nonlinear strain-displacement relations. The axial variable was eliminated from the equations by assuming the blades to be inextensible. This assumption neglects axial elastic

deformation of the blade and expresses axial displacement in terms of lateral displacements; this is the well-known kinematical foreshortening of the beam axis caused by bending. Points on the beam axis move radially as the blade bends, resulting in both steady-state and perturbation centrifugal forces and Coriolis forces. These effects are needed to capture essential nonlinear features of hingeless rotor flap-lag stability. Galerkin's method was used to reduce the partial differential equations to ordinary differential equations in terms of elastic bending modes.

Friedmann and Tong also developed equations for analysis of flapwise and chordwise bending of elastic cantilever rotor blades (ref. 5). Blade-pitch motion was treated as rigid-body rotation about the blade-root pitch axis and was restrained by a root spring that represented pitch-link flexibility. Aerodynamic and mass center chordwise offsets from the pitch axis were included. These equations accounted for axial foreshortening of the blade but did not include linear flap-lag structural coupling or distributed elastic torsion deformation along the length of the blade. Quasi-steady aerodynamic forces were included and these equations were used to study aeroelastic stability.

One of the most important features of an elastic cantilever beam is the nonlinear coupling between torsion and combined flapwise and chordwise bending. A schematic illustration of the nonlinear torsion produced by simultaneous flapwise and chordwise bending is given in figure 1. This coupling has a very powerful effect on hingeless rotor blade aeroelastic stability, the precise effects being very sensitive to the detailed structural and geometric properties of the blade. This problem has stimulated much research on beam theory and rotor-blade equations.

Hodges utilized Hamilton's principle to derive nonlinear equations for coupled bending and torsion of an elastic rotor blade (ref. 6). The nonlinear kinematical basis is an extended version of the formulation by Novozhilov (ref. 7). Hodges also introduced the idea of an ordering scheme to deal with the numerous higher-order terms that arise when geometric nonlinearities associated with moderate deformations are included in the equation formulation. The purpose of the ordering scheme was to simplify the equations by discarding higher-order terms in a reasonably consistent manner. There are minor inconsistencies in the kinematical equations of reference 6 associated with finite rotation and nonlinear beam kinematics that will be further addressed below. Hodges also developed a quasi-steady aerodynamic formulation and applied the equations to a modal analysis of aeroelastic stability of uniform cantilever rotor blades that clearly illustrated the significant influence of the nonlinear bending-torsion coupling terms.

One of the early AFDD objectives was to derive a system of nonlinear equations for cantilever rotor blades that would take the place of the Houbolt and Brooks equations. In a significant work, which has since become a standard in the field, and a starting point for many subsequent investigations, Hodges and Dowell derived the dynamic equations of motion governing coupled bending and torsion of twisted nonuniform rotor blades subject to arbitrarily applied loads (ref. 8). Hodges and Dowell used essentially the same ordering scheme as that of Hodges (ref. 6). Both Hamilton's principle and a Newtonian approach were used in the derivation of the

structural and inertial terms in the equations of motion. As discussed in reference 8, the Newtonian approach does not necessarily yield a symmetric structural operator and although the equations from the two methods are not identical, one set can be obtained from the other simply by taking linear combinations of the individual equations. The ordering scheme was carefully applied to insure self-adjoint structural and inertial operators. Both Hamilton's principle and the Newtonian method rely on a nonlinear strain-displacement relation that when used in conjunction with a linear constitutive law, permits the strain energy and force and moment resultants to be expressed in terms of blade-deformation variables.

The kinematical formulation of the Hodges-Dowell equations is based essentially on Green strain components, although Almansi strain components play an intermediate role in the formulation. The strain components were derived from a blade-displacement field that was in turn based on a deformed blade coordinate transformation developed by Peters (appendix, in ref. 8). This transformation, based on reference 9, allowed the inconsistencies in the equations of reference 6 to be rectified. In this formulation the torsional kinematical variable is defined as the integral of the torsional component of the curvature vector, a definition that has been used by only a few other investigators. The final results are given in the form of partial differential equations, accurate to second order, that include the effects of precone and cross-section chordwise offsets. These equations have been the basis for a number of refinements that will be discussed below, as well as for numerous investigations of hingeless rotor blade aeroelastic stability. Dowell applied these equations to derive modal equations for blades with radially varying properties in reference 10.

One of the principal contributions of the Hodges-Dowell elastic-blade equations was the nonlinear structural operator that properly represented the nonlinear bending-torsion coupling needed for cantilever blade aeroelasticity. To evaluate the accuracy of the theory, Dowell and Traybar conducted a series of laboratory experiments on static deformation and vibration of uniform elastic cantilever beams with large deflections (refs. 11,12). The Princeton beam data have since come to be regarded as a benchmark for evaluating nonlinear beam theories. In the experimental setup shown in figure 2, a 20-in. aluminum cantilever beam with unequal bending stiffnesses is loaded at the tip with a concentrated mass. As the load angle  $\theta$  of the beam is varied, the weight of the tip mass generates combined flatwise and edgewise loading that in turn produces a torsional deformation owing entirely to geometrically nonlinear effects. A comparison of the experimental data with the Hodges-Dowell theory presented in reference 13 and in figures 3 and 4 validates the nonlinear theory for moderate deformations. However, for load conditions in which the bending deformations exceeded the assumptions of the second-order theory, the correlation was poor. In figure 4, bending deformations as a function of the tip mass show how the Hodges-Dowell theory breaks down when the bending deflections become excessive; the flatwise deflection caused by a 5-lb load is 35% of the length of the 20-in. beam.

Nonlinear structural behavior also has a strong effect on beam-bending frequencies. The fundamental flatwise frequency of the beam when loaded in the edgewise

direction,  $\theta = 0^\circ$ , is compared with both linear and nonlinear theory in figure 5. The correlation with nonlinear theory is excellent in comparison with a linear theory since the static edgewise bending does not exceed moderate deformations. Closer examination of the correlation as the frequency approached zero prompted further study of the theory in connection with lateral buckling of slender beams. Hodges and Peters (ref. 14) found inconsistencies in classic theories of lateral buckling and developed an improved formula that matched the experimental data shown in figure 5. In a different comparison for bending frequencies shown in figure 6, moderate deformation theory is again shown to be inaccurate when large deformations are encountered.

Hodges and Ormiston modified the Hodges-Dowell equations to include variable flap-lag structural coupling and quasi-steady aerodynamics, and applied the equations to investigate hovering rotor-blade aeroelastic stability (ref. 15). The Hodges-Dowell equations were further extended by Hodges to include additional configuration parameters such as twist, droop, torque and hub offset, and a root pitch bearing with pitch-link elastic restraint (ref. 16). Galerkin's method was used to generate modal equations for radially uniform blades without chordwise offsets, including quasi-steady aerodynamic terms for the hover flight condition. The equations were very long and complicated partly because of the choice of variables and coordinate systems and partly because of the explicit appearance of the numerous configuration parameters. This complexity was one stimulus for later development of a finite-element approach so that all the parameters could be put into the analysis in generic form. The analysis was used by Hodges and Ormiston to study the stability of hingeless rotors with pitch-link flexibility (ref. 17).

The adequacy of the structural dynamics equations for rotating cantilever blades was examined by performing in-vacuum vibration experiments on a model rotor blade having uniform mass and stiffness properties (ref. 18). The equations derived by Hodges in reference 16 were checked by comparison with the experimentally measured vibration frequencies, as shown in figure 7.

The elastic-blade equations developed by Friedmann and Tong (ref. 5) were refined by Friedmann to treat moderately large deformations, and therefore, include nonlinear bending-torsion coupling in the structural operator as in the Hodges-Dowell equations (refs. 19,20). The resulting equations included distributed blade torsion in addition to rigid-body blade root pitch motion, linear flap-lag structural coupling, precone, and cross-section chordwise offsets. More refined equations including blade droop and aerodynamics for forward flight conditions were used for forward flight stability investigations by Friedmann and Reyna-Allende (ref. 21).

In a subsequent development, Rosen and Friedmann undertook an extensive re-derivation of the nonlinear equations for moderate deformation of elastic rotor blades based on the assumption of small strains and finite rotations (refs. 22,23). Only the structural operator was presented in the form of explicit partial differential equations; the inertial terms were left in general form. The equations were derived using both the Newtonian method and the principle of virtual work and improved on the previously developed equations in references 20 and 21.

The blade model was cantilevered at the rotor hub, with precone, pretwist, a symmetrical cross section, and chordwise offsets of the elastic axis, mass center, and tension axis. However, several aspects of the development were unusual, particularly in regard to the absence of warp in the formulation and the absence of certain well known terms in the torsion equation, as will be discussed below.

The Rosen-Friedmann equations were extended for application to rotor-blade aeroelastic stability analysis by including a more complete derivation of the inertial terms by Shamie and Friedmann (ref. 24). They also included a derivation of quasi-steady aerodynamic terms appropriate for the forward flight condition. The equations were transformed into modal equations by using Galerkin's method and linearized for use in studies of rotor aeroelastic stability in forward flight. The same equations were also used by Friedmann and Kottapalli for further applications studies (ref. 25).

Results obtained from an enhanced version of the Rosen-Friedmann equations were also compared with the Princeton beam data in reference 26 and typical results of that comparison are included in figures 3 and 4. The accuracy of the theory is confirmed by the data and is an improvement over that of the Hodges-Dowell equations. As pointed out by Hodges in reference 27, the two sets of equations for this problem are equivalent except that Rosen and Friedmann retained several third-order terms that become important for configurations in which the ratio of the edgewise to flatwise stiffness is large compared to unity.

Another derivation of the nonlinear elastic-blade equations was carried out by Kaza and Kvaternik who developed equations for elastic flap bending, lead-lag bending, and torsion in forward flight (ref. 28). Kvaternik et al. also developed flap-lag equations for arbitrarily large precone (ref. 29). The Kaza and Kvaternik equations in reference 28 are similar to the Hodges-Dowell equations (ref. 8), except for the following differences. Kaza and Kvaternik proposed two sets of equations, each with a distinct kinematical variable for torsional rotation. With the appropriate changes of kinematical variable, these two sets of equations and those of Hodges and Dowell can be shown to be essentially equivalent. Rather than use an ordering scheme as did Hodges and Dowell, Kaza and Kvaternik simply restricted the nonlinearities in the equations to second degree. Finally, Hodges and Dowell used the axial displacement as a kinematical variable whereas Kaza and Kvaternik used a kinematical variable defined as the integral of the axial strain (analogous to the torsional kinematical variable of Hodges and Dowell). These differences will be discussed below in connection with finite rotation.

Crespo da Silva derived hingeless-rotor-blade equations based on Hamilton's principle and solved them by the Galerkin method (ref. 30). An ordering scheme was used in which terms of one order higher in the ordering parameter are retained; thus the equations are valid to third order. The purpose of this work was to evaluate the influence of those higher-order terms in the equations. It is found that for stiff-inplane configurations having low torsional rigidity the influence of higher-order terms can be important. A typical example from Crespo da Silva et al. (refs. 31,32), is shown in figure 8, where the dashed lines show blade lead-lag

damping and frequency from second-order theory (e.g., ref. 15) and the solid lines give results with third-order terms retained.

Finite rotation- To adequately model helicopter blades in general and hingeless rotor blades in particular, the elastic deflections must be treated as moderately large and the resulting equations of motion will therefore be nonlinear. The previous section described the development of such equations. To derive these equations, it is necessary to first specify the geometry of the beam both in its undeformed state and in its deformed state at some particular instant in time. For typical beam theories, this involves expressing the position of a generic point on the elastic axis and the orientation of a coordinate frame attached at that point to adequately specify the location of every point in the beam. It is common practice in the helicopter rotor-blade literature to evaluate the transformation matrix between the deformed and undeformed states using a Euler-like sequence of three successive rotations. For linear mathematical models undergoing small rotations, the order of rotation does not affect the final form of the transformation matrix. However, in nonlinear analysis involving moderately large deformations, the final form of the transformation matrix, and subsequently the derived equations of motion, will depend on the rotation sequence. When rotations cannot be treated as small linear deformations they are termed finite rotations. The subject of nonlinear beam kinematics involving finite rotation is complex and sometimes controversial (e.g., Kaza and Kvaternik, ref. 33, regarding the correctness of various derivations of elastic-blade equations) and has attracted the attention of a number of researchers.

The kinematical basis of the Hodges-Dowell elastic blade equations (ref. 8) was derived from rigorous representation of nonlinear beam kinematics based in part on Peters' derivation of the deformed-blade transformation matrix (ref. 9). A similar set of kinematical relations was derived by Kvaternik and Kaza (ref. 34) and Kaza and Kvaternik (ref. 28), and led to the differences between the Kaza-Kvaternik equations and the Hodges-Dowell equations. These differences were addressed by Hodges et al. as part of a general treatment of nonlinear beam kinematics (ref. 35). One purpose of that work was to show that the sequence of rotational transformations used in defining the orientation of the cross section of a beam during deformation is immaterial. The kinematics of large-deformation geometry for a Euler-Bernoulli beam was developed, including the transformation matrix relating the local principal axes in the deformed state to space-fixed Cartesian axes, the components of angular velocity and virtual rotation vectors, the torsion, and the components of bending curvature. Nonlinear expressions were developed to relate the orientation of the deformed beam cross section, torsion, local components of bending curvature, angular velocity, and virtual rotation to deformation variables. These expressions were developed in an exact manner in terms of a quasi-coordinate in the space domain for the torsion variable. The entire formulation was shown to be independent of the sequence of the three rotations used to describe the orientation of the deformed-beam cross section. For more common cases in the literature in which one of the three rotation angles is used as the torsion variable, the resulting equations depend on the choice of the three angles. Differences in the equations, however, were demonstrated to be in form only since the torsion variables in such cases represent different rotations.



Following the general treatment of nonlinear beam kinematics of reference 35, additional work along the same line was carried out by Alkire (ref. 36). In this work the relationships between the twist variables associated with different rotation sequences, as well as corresponding forms of the transformation matrix, were studied, and the earlier work was extended to examine the role of blade built-in pretwist for sequences other than flap-lag-pitch and lag-flap-pitch. In addition to reiterating many of the conclusions of reference 35, Alkire developed a procedure for evaluating the transformation matrix that eliminated the Euler-like sequences altogether. The resulting form of the transformation matrix was unaffected by rotation sequence. This method, upon further analysis, turned out to be a variant of the Rodrigues formulation as shown by Hodges (ref. 37).

Another rather unusual approach was presented by Jonnalagadda and Pierce (ref. 38), and discussed by Hodges et al. (ref. 39). This approach, instead of using one of the orientation angles as the torsional variable, used the average of the two angles used by Kaza and Kvaternik (ref. 28). In the special case of moderate rotation, their method is equivalent to the Rodrigues formulation.

A survey of standard methods of representing finite rotation of rigid body kinematics in relation to nonlinear beam kinematics was presented by Hodges in reference 37. Orientation angles, Euler parameters, and Rodrigues parameters were reviewed and compared. These standard methods of representing finite rotations were applied to general kinematical relations for a large rotation beam theory. The resulting kinematical expressions were compared for both the standard methods and some additional methods found in the literature, such as quasi-coordinates and linear combinations of projection angles. The method of Rodrigues parameters is unique for both its simplicity and generality when applied to beam kinematics. Especially for large rotations, as might be encountered in the flexbeam portion of a bearingless rotor blade, the Rodrigues formulation was shown to be superior to all other methods.

Tension-torsion coupling- In the development of elastic-blade equations, the tension force and tension-torsion coupling have attracted considerable attention. This research expanded to encompass problems of constitutive laws and beam extensional vibrations.

Although the beam equations developed by Rosen and Friedmann (refs. 22,23) were similar to those previously developed, they omitted two well-known terms in the torsion equation that are present in work all the way back to that of Houbolt and Brooks (ref. 1). Previous analyses contain (1) a pretwist moment term owing to combined pretwist and tension and (2) a tension-torsion stiffness term that increases effective torsional stiffness owing to tension. Furthermore, these terms are present in the older analyses even for the limiting case of a beam with circular cross section, although the pretwist moment seems inconsistent since pretwist of a circular beam is arbitrary. Previous investigators had made use of a curvilinear coordinate system, which arises because of pretwist; unfortunately, a constitutive law appropriate for that type of coordinate system had not been used. The equations of Rosen and Friedmann were carefully derived based both on an orthogonal coordinate system and, in reference 22, on the same curvilinear coordinate system used by

previous investigators, except with an appropriate constitutive law. They concluded that the pretwist moment would not have been present, had previous investigators used an appropriate constitutive law, and that the tension-torsion stiffness term should be negligibly small for rotor blades. Although their derivation was carried out correctly, they assumed warping to be unimportant.

Hodges showed that when the analysis is done correctly and includes warping, both of these terms are present; but the form of the first term is different from that found in older works (ref. 40). In the limiting case of a beam with circular cross section, which does not warp, the pretwist moment vanishes, as expected. More significantly, however, for thin cross sections (like those of rotor blades) and with warping included, the pretwist moment reduces to a term very similar to that of Houbolt and Brooks and previous work as well. This problem was discussed further by Rosen (ref. 41) and Hodges (ref. 42). Later work by Rosen (ref. 43), based on an analysis essentially identical to that of Hodges (ref. 40), included warp and exhibited good agreement with experimental results for the pretwist moment of pretwisted strips.

The above discussion addressed the pretwist moment term. Friedmann and Rosen discarded the tension-torsion stiffness term, the one showing increased torsional rigidity owing to tension, based on an order-of-magnitude analysis. This term is present in Hodges's equations unaltered from the classic form. Petersen analyzed beam tension-torsion coupling and obtained a different form for this term, one in which the effective torsional stiffness increases because of tension for warping beams but does not increase for nonwarping beams (such as beams of circular cross section) (ref. 44). Why Petersen's analysis turned out this way was unknown at first. In an attempt to reconcile the analyses of Hodges and Petersen it was found that the main difference between their approaches was the constitutive law. Hodges had used the classic strain energy approach based on Green strain, whereas Petersen had used a strain energy based on Almansi strain. Hodges later showed that a rigorous small-strain analysis would qualitatively confirm Petersen's conclusion regarding the tension-torsion stiffness term (ref. 45).

The influence of the strain-energy function (or constitutive law) had been encountered before. Hodges found disagreements in the technical community concerning the extensional vibration of rotating beams (ref. 46). Depending on the strain-energy definition used (whether based on Green, Hencky, or Almansi strain), one could find significant differences in the trends of extensional frequency versus angular speed. Thus, it was concluded that without experiments or knowledge of second-order material constants, it would be impossible to determine the correct trend. The reason is that the different strain definitions contain terms of higher order in elongations. Use of Hooke's law implies linearity between some definition of stress and some definition of strain. The choice of stress and strain definitions is essentially arbitrary. The different choices imply different relationships between physical stress and strain, thus resulting in different predicted behavior. For Green strain the predicted extensional frequency will increase with rotor angular speed, whereas for the Hencky logarithmic strain, extensional frequency will

decrease with rotor angular speed. This is further discussed in Venkatesan and Nagaraj (refs. 47,48), Hodges (ref. 49), and Kvaternik and Kaza (ref. 34).

It was now clear that a similar situation existed for torsion in the presence of axial stress. The main reason for the differences between the equations of Petersen (ref. 44) and those of Hodges (ref. 40) is the form of the constitutive equation. In joint experimental and theoretical work, Degener et al. (ref. 50) have shown that the effective torsional stiffness of a circular-cross-section, nonwarping, rubber beam under large axial elongation actually decreases and is best predicted by the Hencky strain-energy function (fig. 9). A classical analysis based on Green strain energy is completely inadequate, and even the well-known neo-Hookean material strain energy function only performs fairly well. A strain-energy function closely associated with Petersen's formulation also performs well.

In other closely related work, Kaza and Kielb examined the effects of warping and pretwist on torsional vibrations of rotating beams (ref. 51). They found, based on an analysis similar to that of the older works (such as that of Houbolt and Brooks) that warping, pretwist, and tension increased the torsional stiffness of beams.

Advanced beam theories- Most of the effort in the development of elastic-blade equations, represented by the contributions of Hodges and Dowell (ref. 8), Kaza and Kvaternik (ref. 28), and Rosen and Friedmann (ref. 23), used a geometric nonlinear analysis based on the assumption that structural deformations were limited to moderate rotations. Although adequate for many applications in rotor-blade aeroelastic stability, this assumption has limitations. For example, bearingless-rotor flexbeams undergo combined bending and torsion deformations that produce large rotations, exceeding the moderate rotation of conventional analyses. Furthermore, the moderate rotation theories may be valid for a certain range of beam configuration parameters and then break down for other configurations. One example is the case of a thin beam for which the ratio of bending stiffnesses is small in some sense. Ideally, the magnitude of parameters in the equations for general-purpose analyses should not influence the structure of the equations themselves. Such an ideal is evidently not present in the ordering schemes of references 8 and 23 or in any arbitrary a priori restriction to second-degree nonlinearity, as in reference 28. Furthermore Stephens et al. showed that inconsistencies are virtually unavoidable in ordering schemes based on displacements and rotations when the magnitude of the torsion rigidity is small compared with the bending stiffnesses (ref. 52). Another shortcoming in the moderate rotation equations in references 8, 23, and 28 is that the effects of pretwist are not treated rigorously.

To address these problems, Hodges developed a more general system of nonlinear bending-torsion equations for pretwisted beams undergoing small strains and large rotations (ref. 53). Hodges abandoned the common assumption of moderate rotations. To avoid some of the limitations of previous analyses, Hodges modeled the kinematics of a slender beam without resorting to an ordering scheme for rotations or to arbitrary restrictions on degree of nonlinearity allowed in expressions involving displacement. The transformations used Tait-Bryan orientation angles although a parallel development based on Rodrigues parameters was included in an

appendix to reference 53. The kinematic relations that describe the orientation of the cross section during deformation were simplified by systematically ignoring the extensional strain compared with unity in those relationships. Open-cross-section effects such as warping rigidity and dynamics were ignored, but other influences of warp were retained. The beam cross section was not allowed to deform in its own plane and the stress-strain relation was assumed to be isotropic. Various means of implementation were discussed, including a finite-element formulation. This beam formulation was used as the basis for the GRASP finite-element, coupled rotor-body aeromechanical stability analysis that will be discussed below.

To evaluate the validity of this theory, particularly for the case of large deformations, Hodges (ref. 53) compared results for static deformations with the Princeton beam data from references 11 and 12. These comparisons are also included together with the earlier theories in figure 3 and show excellent agreement. Furthermore, the large-rotation theory also shows excellent agreement with the data in figure 6 for beam-bending natural frequencies.

Although Hodges's large-rotation equations in reference 53 represented a significant advance, they also contained limitations that stimulated further developments. First, these equations are restricted to beams to which the Euler-Bernoulli hypothesis applies. This restriction may be violated for composite rotor blades. Second, the treatment of tension-torsion coupling is somewhat weak. As in Hodges (ref. 40), the Green strain components were used and simplified based on heuristic geometrical arguments to a form valid for small strains and large rotations. In particular, the nonlinear term in the axial strain expression responsible for the tension-torsion coupling is difficult to identify based on geometrical arguments alone. Also, the derivations from Rosen and Friedmann (ref. 22) and Hodges (refs. 40,53) are very complex as a result of the curvilinear coordinate system. The derivation and simplification of the strain-displacement relations is so lengthy and tedious that the details are not included in reference 53.

To remedy these limitations, Hodges initiated development of a new definition of strain displacement relation for a beam based on the idea of engineering strain. The motivation was primarily that calculation of Green strain produces many superfluous terms that need to be removed by some process for small elongations and shears. The reason for this is that the Green strain principal values contain terms of the order of elongations squared. This gives rise to terms in the final strain expression which are of the order of "strain" squared in addition to the true strain. The Jaumann-Biot-Cauchy "engineering" strain tensor has principal values that are linear in elongation. Hodges (ref. 45) and Danielson and Hodges (ref. 54) present this new strain definition, starting with the engineering-strain definition and rigorously decomposing the finite rotation field. This work does not invoke the Euler-Bernoulli hypothesis in the kinematics and adds initial curvature to the description of the reference state of the beam. Most significantly, the algebra of dealing with the curvilinear coordinate system is greatly simplified with this formulation in comparison with previous ones.

These developments provide the basis for new advanced beam theories for small strains and finite rotations. The representation of finite rotation can be by any

method one desires. For large rotations Rodrigues parameters make the most sense. For moderate rotations a variant of the Rodrigues formulation, often called the finite-rotation vector, is preferred. This is the approach recommended for analytical schemes in which a polynomial expression is desirable for the strain components, such as a perturbation scheme.

A complete theory based on this kinematical formulation has yet to be developed. The initial curvature of the elastic axis and effects associated with open cross sections should also be incorporated. In order to be a practical tool for rotor-blade analysis, a modeling approach for anisotropic materials must somehow be included. This problem is not yet fully solved, but several investigators have begun to work, as discussed below, in connection with composite blade modeling.

Bearingless rotor analysis- This section will discuss Army-NASA research to develop analysis methods for bearingless-rotor systems, a specialized but important subclass of elastic blades. The bearingless rotor offers benefits for advanced rotorcraft development and simplifies rotor hubs by eliminating blade-pitch-change bearings, and thereby reducing weight, complexity, and maintenance, and increasing reliability and productivity. Although the physical structure is simplified, the bearingless rotor requires more sophisticated structural and aeroelastic analysis of the rotor hub and blades. The bearingless-rotor design is based on replacing blade-root hinges and bearings with a flexbeam sufficiently flexible in torsion to accommodate all blade-pitch-control motion provided by the pitch change bearing of articulated and hingeless rotors.

The bearingless rotor blade configuration is one of the most challenging problems for the rotorcraft structural dynamicist. Although the hingeless rotor blade is already complex, the bearingless rotor presents potentially more difficult problems because of the flexbeam and the blade-feathering mechanism. Basically, to accommodate blade motion and feathering, the flexbeam undergoes complex combined bending and torsion deformations that may be significantly larger than for a hingeless rotor blade. The elastic twist needed to accommodate blade feathering may be of the order of  $15^{\circ}$ - $20^{\circ}$ . At the same time, the flexbeam must carry the full centrifugal tension load of the blade. The pitch-control mechanism introduces a second load path for blade-root shears and moments and makes the system structurally redundant. Multiple flexbeams introduce additional structural complexities.

Combinations of flexbeam and pitch-control systems lead to a variety of bearingless-rotor types; the principal ones are depicted in figure 10. The most direct is a simple torque tube pinned at the hub and either pinned or cantilevered at the blade root. The cantilever pitch configuration is physically simple but structural interaction of the pitch arm, flexbeam, and elastic flexbeam generates complex aeroelastic coupling. The structural interaction may be reduced by a torque tube and snubber configuration. The snubber, located at the inboard end of a torque tube fixed to the blade root and enclosing the flexbeam, constrains translation of the torque tube. Given the unique structural characteristics, it is clear that conventional elastic-blade equations for hingeless rotor blades are not satisfactory for bearingless-rotor analysis. The purpose of this section is to describe the

development of analyses especially tailored to the unique requirements of bearingless rotors.

The first serious development of an aeroelastic analysis for bearingless rotors was due to Bielawa (ref. 55). The differential equations of motion were derived for the bending and torsional deformations of a nonlinearly twisted rotor blade operating in a steady flight condition including aeroelastic characteristics germane to composite bearingless rotors. The differential equations were formulated in terms of uncoupled vibratory modes with exact coupling effects owing to finite, time-variable blade pitch and with approximate second-order effects owing to twist. Also presented were derivations of the fully coupled inertia and aerodynamic load distributions, automatic pitch-change coupling effects, structural redundancy characteristics of the composite bearingless-rotor flexbeam-torque tube pitch-control system, and a description of the linearized equations appropriate for eigensolution analyses. These equations were used as the basis for the G400 code and aeroelastic investigations reported in reference 56.

Subsequently, Hodges developed a simplified analysis for coupled rotor-body stability of rotorcraft with bearingless-rotor blades. FLAIR (flexbeam air resonance) was intended for efficient application as a preliminary design tool and treated the blade as a rigid body, thereby avoiding the complexity of an elastic blade formulation (refs. 57,58). The objective was an analysis that possessed the simplicity of a rigid-blade model but included a relatively detailed treatment of the flexbeam and pitch-control system. The analysis was based on modeling the rotor blade as a rigid body attached to the hub by an elastic beam for the flexbeam portion of a bearingless-rotor blade. The flexbeam deflections were treated exactly for a Euler-Bernoulli beam segment, using the Kirchhoff-Love equations, which are valid for large rotations. An iterative structural analysis including geometric nonlinearities, solved by a shooting algorithm for two-point boundary-value problems, yielded the equilibrium deflected shape of the flexbeam. A numerical perturbation scheme was then used to obtain the stiffness matrix for the tip of the flexbeam. No ordering scheme was used. The flexbeam degrees of freedom were the three rotations and three translations of the outboard end of the flexbeam. The rigid-blade inertial, gravity, and quasi-steady aerodynamic equations were derived for arbitrarily large deflections and analytically linearized about equilibrium. The linear flexbeam and blade equations were developed as part of the coupled rotor-body analysis described later in this section under Helicopter Rotor-Body Equations. The treatment of the bearingless rotor in FLAIR was sufficiently flexible to permit analysis of all of the principal configurations in figure 10. The principal limitation of FLAIR was the lack of an elastic blade to capture the intermodal coupling characteristics typical of many bearingless-rotor blade instabilities.

Another bearingless-rotor analysis was developed by Sivaneri and Chopra, based on a finite-element approach for the isolated rotor blade including treatment of dual-flexbeam configurations (ref. 59).

The most recent development in bearingless rotor blade analysis is the GRASP code, a finite-element analysis developed by Hodges et al. to treat coupled rotor-body stability of a rotorcraft in hover (ref. 60). GRASP (General Rotorcraft

Aeromechanical Stability Program) is an advanced analysis system capable of modeling rotorcraft structures in a very general manner, including rotor-body coupling. In this sense it is not uniquely designed to handle bearingless-rotor blades; it simply has the capability to handle arbitrarily complex bearingless-rotor configurations along with numerous other rotor types as well. In fact, a general finite-element analysis provides the only realistic means to address the potential complexity of bearingless rotors. The elements and constraints in GRASP permit the modeling of large rotation elastic beams, rigid-body masses, and mechanical joints capable of translation and large rotation. The analysis includes quasi-steady aerodynamic formulation and dynamic inflow. A more complete description of the features of GRASP is given the following subsection and later in this section under Helicopter Rotor-Body Equations.

Finite element formulations- The previous sections described development of elastic-blade equations aimed at treating the fundamental nonlinear behavior of cantilever rotor blades. Applications to stability analysis typically use a modal approach to spatially discretize and solve the elastic-blade partial differential equations. A Galerkin approach is commonly used to generate ordinary differential equations in terms of a number of bending and torsion modes of the blade. There are a number of limitations to this approach and inevitably the use of finite-element methods is desirable. A considerable part of rotorcraft structural mechanics research effort has begun to focus in this direction.

Some of the limitations of the modal methods stem from complexities of deriving nonlinear equations for rotating beams. These equations can be extremely long and complicated. The problem is made worse by the explicit appearance of many structural and geometric configuration parameters that play an important role in the aeroelastic stability of hingeless rotor blades. For bearingless rotors, the redundant load paths present further difficulty. In addition to their complexity and lack of generality, the modal equations cannot accurately represent rotor blades having large or discontinuous radial variations in mass or in structural and geometric properties. With these difficulties as a stimulus, Army-NASA researchers began to investigate the application of finite-element methods to the problems of rotating slender beams undergoing nonlinear axial, bending, and torsional deformations.

In one of the first applications, Hohenemser and Yin studied a simple stability problem involving flap bending of rotor blades mounted on flexible supports (ref. 61). Strictly speaking, their approach utilized the transfer matrix technique, not a true finite element method, but one in common use in the rotorcraft field. Friedmann and Straub developed a weighted residual Galerkin-type finite-element method to study the aeroelastic stability of flap-lag motions of a hingeless rotor blade in the hovering flight condition (ref. 62). This method was also applied in references 63 and 64 to formulate the finite-element equations for flap-lag-torsion of hingeless rotor blades in forward flight and to investigate flap-lag stability characteristics in forward flight.

The method is based on the partial differential equations of equilibrium, which are discretized directly, using a local weighted residual Galerkin method. Each

element has eight nodal degrees of freedom representing flap and lag bending displacements and slopes at the ends of the element. The later analyses that treat torsion have three torsional degrees of freedom, one at each end of the element and one in the middle. Blade bending is discretized using conventional shape functions for beam bending based on cubic Hermite polynomials. Torsion is discretized using a quadratic function resulting in the additional internal nodal degree of freedom. The axial displacement has no degrees of freedom associated directly with it because the blade is assumed to be inextensional. The element matrices obtained in this procedure are dependent on the nonlinear equilibrium position. The element matrices are assembled using a conventional direct stiffness method. After assembly, a normal-mode transformation is used to reduce the number of nodal degrees of freedom.

In another investigation, Celi and Friedmann (ref. 65), treat the aeroelastic stability of swept-tip rotor blades using a Galerkin finite-element technique (ref. 62) including a special element for the structural, inertial, and aerodynamic terms of the swept tip. The element equations were based on the Shamie and Friedmann formulation (ref. 24).

Another approach to finite-element formulations for rotor blade aeroelasticity is based on a conventional local Rayleigh-Ritz finite-element method. Sivaneri and Chopra studied the problem of hingeless rotor blade flap-lag-torsion in hover and solved the nonlinear equilibrium equations using the finite-element analysis directly (ref. 66). A normal-mode method is used for the linearized flutter analysis. Chopra and Sivaneri (ref. 67) and Sivaneri and Chopra (ref. 59) extended this work with a more elaborate fifteen-degree-of-freedom beam finite element applied to analyze the hover stability of bearingless-rotor blades including multi-flexbeam configurations. There are two reasons for the additional degrees of freedom: (1) it is necessary to include the axial displacement explicitly in order to treat structures with multiple load paths such as bearingless rotor blades; and (2) it is necessary to have a more accurate interpolation of axial displacement so that inaccuracies in determining the effective bending stiffness, owing to a form of membrane locking, do not occur.

Early work at the Aeroflightdynamics Directorate was aimed at development of a finite-element analysis with ample modeling flexibility to deal with realistic bearingless-rotor-blade configurations. The work described above was based on discretization of the equations for a rotating blade having a specified orientation. That is, the finite-element equations were not sufficiently general to allow assembly of elements together at arbitrary angles to one another. An approach general enough to allow coupling of rotating blade elements together in such a manner still did not exist.

Furthermore, rotating beam finite elements are subject to a form of membrane locking that can generate serious errors, especially in portions of the structure where the geometric stiffness must be determined from the strain instead of from the integration of the loading, such as in a redundant load path (see ref. 59). One way to circumvent this problem is to introduce generalized coordinates associated with higher-order polynomials. Since redundant load paths are typical of bearingless-



rotor systems, early work at the Aeroflightdynamics Directorate was aimed at development of a variable-order finite element.

Hodges investigated the vibration and response of nonuniform rotating beams with discontinuities in mass and bending stiffness (ref. 68). The direct analytical method of Ritz was used by Hodges to generate finite elements with shape functions of arbitrary order (ref. 69). Free vibration and forced-response results were presented to establish the capabilities of the method. Results for planar bending of a rotating beam indicated excellent convergence to exact solutions, even at points of discontinuity and near boundaries. The development of this variable-order finite-element method continued to progress toward incorporation into conventional finite-element codes. Hodges and Rutkowski (ref. 70) and Hodges (ref. 71) provided details on development of shape functions and modified the work reported in reference 69 to a true finite-element form so that the generalized coordinates were actual displacements and slopes at ends of the element. In addition to the usual nodal displacements at the ends of the element, an arbitrary number of additional internal generalized coordinates were used.

Hodges extended the AFDD efforts in rotor-blade finite-element analysis to the implementation of a variable-order finite element based on the large rotation-beam theory (ref. 53). This element was the basis for the aeroelastic beam element developed for the GRASP analysis that will be discussed in more detail in this section under Helicopter Rotor-Body Equations.

The aeroelastic beam element developed for GRASP represents a slender-beam element without shear deformation that is subject to elastic, inertial, gravitational, and aerodynamic forces. The element is derived on the basis of small strains and large rotations (limited to  $90^\circ$  because of use of orientation angles to define finite rotation kinematics inside the element). The element degrees of freedom include a reference frame, structural nodes at the ends of the beam, an air node, and internal degrees of freedom for increased accuracy of beam-deformation calculations. The main element properties include mass, inertias, pretwist, axial, bending, and torsion stiffness, structural damping, and airfoil aerodynamic properties, including chordwise aerodynamic center offsets. The GRASP element is not intended to accommodate composite material properties.

One finding from Hodges et al. (ref. 35), which should be mentioned at this point for the benefit of ongoing finite-element development work, is that the torsional kinematical variable used by Hodges and Dowell (ref. 8), although suitable for integration and modal methods of solution, may not be suitable in a general-purpose finite-element context. This applies both to this variable, defined as the integral of the torsional component of the curvature vector, and to analogous axial displacement variables, defined as integrals of axial strain. The presence of integrals in the kinematical relations can introduce undesirable couplings into a finite-element analysis. The work by Hodges uses an angle, which is suitable for finite element work; use of Rodrigues parameters would also be suitable (ref. 53).

Composites- Most modern rotor blades are constructed from composite materials. The initial impetus for the use of composites was the very significant

improvement in fatigue life and damage tolerance of the blades and, later, the benefits afforded by the ability to incorporate more refined aerodynamics into planform and airfoil section geometries. For advanced rotor blades, composite materials provide opportunities for structural simplicity of hingeless and bearingless designs, and structural couplings to improve the aeroelastic stability of these configurations. Most structural models described above have been limited to isotropic material properties. Rotor blades and flexbeam structures are built up from composite materials, and cannot be regarded as isotropic. There may be coupling between extension, bending, and shear deformation; warping effects may be much more significant. These complexities generally invalidate the Euler-Bernoulli beam assumptions that plane beam cross sections remain plane and perpendicular to the elastic axis.

Work in this area can be classed in two distinct areas: (1) the development of modeling approaches so that the three-dimensional constitutive law for general anisotropic elasticity can be reduced to a simple one-dimensional form for the beam problem; and (2) the use of a specialized, simple model for the blade cross section in order to assess the stability of rotor blades for various values of ply orientation and other geometric parameters.

Work in the first category focuses on the determination of the shear center location and warp functions. Cross-section properties can then be evaluated for use in the one-dimensional beam theory, which has been developed with appropriate kinematics and material constants. Determination of the shear center location and warp functions can either be from use of a two-dimensional finite-element model of the blade cross section or analytically from simplified physical models for the cross section. Fundamental work by Rehfield and Murthy was aimed at representing nonclassical effects of composites on beam structural behavior (ref. 72). These effects are related to transverse shear, bending-related warping, and torsion-related warping. Bauchau developed an anisotropic beam theory in which out-of-plane cross-section warping is determined from a finite-element solution of a Laplace-type equation over the cross section (ref. 73). The solution is expressed in terms of an arbitrary number of so-called eigenwarpings. In practice, only a few eigenwarpings are needed.

More recently, Kosmatka developed a method for analyzing highly swept curved blades constructed of anisotropic composite materials (ref. 74). A finite-element model of the cross section yields both in-plane and out-of-plane warping functions and the shear center location. This method is applicable to rotor blades as well. Kim and Lee have developed a similar approach, although not as general (ref. 75). A considerably simpler approach was developed by Rehfield, in which a general cross section is approximated as a multi-celled box beam whose shear center location and warp function can be determined analytically (ref. 76). The Rehfield and Bauchau methods both yield results of comparable accuracy for box beams (ref. 77). None of these methods has yet been developed and validated to the degree necessary for general-purpose analysis of rotor-blade cross sections.

Work in the second category has been chiefly that of Chopra and his co-workers. Hong and Chopra developed a composite beam finite-element analysis for

flap-lag-torsion stability of a hingeless rotor blade in hover (ref. 78). The blade was treated as a single-cell-dominated shell beam composed of an arbitrary layup of composite plies. Stiffness coupling terms caused by bending-torsion and tension-torsion couplings were correlated with different composite ply layups. The results show that such couplings can have a significant effect on the stability.

### Coupled Rotorcraft Equations

Equations for isolated rotor blades have been discussed in previous sections; this section deals with coupled rotorcraft equations where the isolated blade equations are combined with equations of other blades or rotorcraft components such as fuselages, support systems, or nacelle-pylon-wing components. The most important coupling is that between the rotating and fixed system; this coupling is one of the central features of rotorcraft dynamics. Other important coupled systems involve rotor feedback control systems, certain rotor types such as teetering or gimbal rotors that structurally couple rotor blades, or even the dynamic inflow model. This section is divided into two principal areas, helicopter coupled rotor-body systems and tilt-rotor systems.

Helicopter rotor-body equations- Rotor-body coupling is important in aeroelastic stability because of the strongly destabilizing mechanical coupling that occurs for some rotorcraft configurations; for example, the classic ground resonance treated by Coleman and Feingold (ref. 79). When both aerodynamic and aeroelastic considerations are involved, this phenomenon is often termed aeromechanical stability. The principal issue in coupled rotor-body equations of motion is the fact that rotor-blade equations are written in a rotating frame of reference whereas fuselage equations are written in a nonrotating frame of reference. When arbitrarily large rigid-body motions of an elastically deforming fuselage are considered, this becomes a formidable problem in dynamics.

For most problems in aeroelastic stability, only small motions are involved and the problem is relatively straightforward. The use of a coordinate transformation from the blade-fixed rotating system to the body-fixed nonrotating coordinate system has long been used in deriving equations for rotorcraft analysis. Hohenemser and Yin developed a formal version of this technique known as multiblade coordinates that has since gained wide acceptance in the rotorcraft technical community (ref. 80). The multiblade transformation changes blade equations from a rotating frame of reference to a nonrotating frame of reference and also combines the equations for a given degree of freedom of  $k$  individual blades into a system of equations for the corresponding multiblade degrees of freedom for a rotor having  $k$  blades. It is particularly useful for formulating equations of coupled rotor-body systems, for simplifying the periodic-coefficient equations of motion of rotor blades in forward flight, and for providing rotor degrees of freedom that better lend themselves to physical interpretation of analysis results than individual blade degrees of freedom.

Within the scope of this survey, important work on coupled rotor-body aeromechanical stability of hingeless rotorcraft in hover was carried out by Cardinale

using a simplified modal representation for the blade together with coupled fuselage and control gyro equations (ref. 81). Hammond developed equations of motion, using the Coleman and Feingold physical model, to represent rotorcraft configurations having one of the blade dampers inoperative (ref. 82). In general, these equations have periodic coefficients, and Hammond used Floquet theory to solve them. Johnston and Cassarino developed a system of coupled rotor-body equations, based on a modal analysis of coupled flap-lag-torsion dynamics for an elastic blade (ref. 83). The equations were linearized for aeroelastic stability analysis in hover and forward flight. The latter equations were approximated by the constant-coefficient form of the multiblade coordinate equations. A more restricted example of coupled rotor-blade equations is the two-bladed teetering-rotor problem treated by Shamie and Friedmann (ref. 84). Hohenemser and Yin developed coupled equations for a rotor and elastic supports, using a finite-element formulation (ref. 61).

Johnson developed a very complete set of equations of motion for an analytical model of the aeroelastic behavior of a rotorcraft operating in a wind tunnel or in free flight (ref. 85). A unified development is presented for a wide class of rotors, helicopters, and operating conditions. The rotor model includes coupled flap-lag bending and blade torsion degrees of freedom, and is applicable to articulated, hingeless, gimbaled, and teetering rotors with an arbitrary number of blades. The aerodynamic model is valid for both high and low inflow, and for axial and forward flight. The rotor rotational speed dynamics, including engine inertia and damping, and the perturbation inflow dynamics are included. A normal-mode representation of the wind-tunnel test module, strut, and balance system is used. The aeroelastic analysis for the rotorcraft in flight is applicable to a general two-rotor aircraft, including single main-rotor and tandem helicopter configurations, and side-by-side or tilting proprotor aircraft configurations. The aircraft motion is represented by the six rigid-body degrees of freedom and the elastic free-vibration modes of the airframe. The aircraft model includes rotor-fuselage-tail aerodynamic interference, a transmission and engine dynamics model, and the pilot's controls. A constant-coefficient approximation for forward flight and a quasi-static approximation for the low-frequency dynamics are also described. The coupled rotorcraft or support dynamics are represented by a set of linear differential equations, from which the stability and aeroelastic response may be determined.

A simplified system of equations for air-ground resonance of hingeless rotors in hover was developed by Ormiston for application to parametric investigations reported in reference 86. The equations of motion treat a simplified model of a hingeless-rotor helicopter having spring-restrained, hinged-rigid blades with flap-lag motion (ref. 87). Kinematic aeroelastic couplings were included to represent the effects of blade torsion and typical couplings of hingeless blades.

Hodges developed a coupled rotor-body analysis for aeromechanical stability of bearingless-rotor helicopters in hover, axial flight, and ground contact. A detailed derivation of the equations of motion for FLAIR (flexbeam air resonance) is given in references 57 and 58. Treatment of the bearingless blade was described earlier in this section. The fuselage is treated as a rigid body and the landing gear as simple spring elements. The equations are limited to hover and axial flight

and include four rigid-body degrees of freedom for the fuselage pitch and roll angular motion, and longitudinal and lateral translations.

The analysis was based on the set of generalized forces owing to inertia, gravity, body springs and dampers (for the aircraft in ground contact), quasi-steady aerodynamics, and the flexbeam structure. All of these generalized forces (except those caused by flexbeam structural loads) were written exactly, for arbitrarily large deflections, and analytically linearized about equilibrium. The linearized perturbation forces and moments associated with the flexbeam structure, the pitch-control links, body springs and dampers, and inertial, gravitational, and aerodynamic loadings, when combined, yielded a system of constant-coefficient, linear, homogeneous, ordinary differential equations in the nonrotating reference system. Only the cyclic multiblade rotor modes were retained. Solutions were obtained by standard eigenanalysis. Results of stability investigations will be discussed below. The FLAIR analysis was used to support the design development of the Boeing Vertol Bearingless Main Rotor (refs. 88-90), and it has been extended and used in support of the ITR/FRR bearingless rotor preliminary design as reported by Hooper (ref. 91).

Warmbrodt and Friedmann also developed equations of motion for coupling rotor-fuselage and rotor-support systems (refs. 92,93). An aerodynamic formulation is included for hover and forward flight. The equations are written in partial differential equation form and are applicable to the aeroelastic stability problem. The importance of an ordering scheme for deriving a consistent set of nonlinear coupled rotor-body equations is emphasized.

Following earlier work (ref. 85), Johnson extended the general rotorcraft analysis to a more comprehensive analysis known as CAMRAD (refs. 94-96). Intended for application to both rotorcraft dynamic response and stability, this comprehensive analysis is intended for calculating performance, loads, noise, vibration, gust response, flight dynamics, handling qualities, and aeroelastic stability. The equations applicable for aeroelastic stability are similar to those developed in reference 85.

A coupled rotor-fuselage analysis for application to multi-rotor hybrid heavy-lift vehicles was developed by Venkatesan and Friedmann (refs. 97,98). These equations represent the blades as spring-restrained, flap-lag hinged-rigid blades and the fixed system as rigid bodies attached to a flexible supporting structure. The aerodynamic formulation is derived for hover and forward flight.

The GRASP analysis developed by Hodges et al. (ref. 60) is a major development for coupled rotorcraft systems. GRASP (General Rotorcraft Aeromechanical Stability Program) is a hybrid of a finite-element program and a spacecraft-oriented multibody program. GRASP differs from standard finite-element programs by incorporating multiple levels of substructures which can translate or rotate relative to other substructures without small-angle approximations. This capability facilitates the modeling of rotorcraft structures, including the rotating-nonrotating interface and details of the blade-root kinematics for various rotor types. GRASP treats aeroelastic effects, including dynamic inflow (treated later in this section) and non-

linear aerodynamic coefficients. The aeroelastic beam element of GRASP was described in more detail earlier in this section under Finite-Element Formulation. The analysis includes the equations of equilibrium for the hover flight condition and calculates linearized perturbation equations for stability analyses. To illustrate how a problem is defined using the hierarchical substructuring of the GRASP system, a simple coupled rotor-body problem was chosen for modeling. This example is illustrated in figure 11 (from ref. 60). Three blades are combined to form a rotor subsystem which is in turn combined with the air mass and fuselage rigid-body elements to form the complete coupled rotor-body system.

Tilt rotor analysis methods- Analysis of tilting proprotor dynamics has historically drawn from rotorcraft technology. Tilt-rotor aeroelastic stability analysis is fundamentally similar to coupled rotor-body helicopter dynamics; the differences in analysis are mainly a matter of detail, primarily the complexity of the physical system and the many degrees of freedom needed to insure a reasonably complete dynamic analysis. In general, tilt-rotor analysis must include coupled wing bending and torsion, pylon pitch and yaw, rotor-blade flap bending, lead-lag bending and torsion, as well as rotor speed and rigid-body airframe degrees of freedom. Although the rotors operate in axial flow conditions when in the hover and airplane modes, forward flight operation in the helicopter mode and the intermediate nacelle tilt conversion mode introduce the same periodic coefficient effects into the equations of motion as experienced by the helicopter. Some of the differences between helicopter and tilt-rotor analysis include larger rotor speed variations, larger collective pitch range and blade twist, high inflow aerodynamics, and different rotor-airframe wake interference effects.

Before the period addressed in this survey, government researchers contributed to the development and understanding of theories of propeller-nacelle whirl flutter, using simplified methods to understand the mechanisms and predict the relevant phenomena. Typical analyses were developed by Reed and Bland, Houbolt and Reed, and Reed; this work will be discussed in section 3 under Tilt-Rotor Aircraft Stability. These methods treated the propeller blades as rigidly attached to a hub mounted on a nacelle free to pivot in pitch and yaw. Aerodynamic forces for the axial flow condition typically were derived from simple quasi-steady strip theory. Such an approach, although generally sufficient for classical propeller whirl flutter, is not adequate for tilt-rotor aircraft configurations. Additional requirements for such analyses were addressed independently in the works of Kvaternik and Johnson.

Kvaternik developed a proprotor aeroelastic stability analysis including wing, nacelle, and rotor-blade degrees of freedom (ref. 99). All elements were modeled as rigid bodies with spring-restrained hinges where appropriate. The nacelle included pitch and yaw degrees of freedom and the rotor blades were hinged for flap motions. The effectiveness of this analysis in predicting proprotor whirl flutter was verified by extensive comparisons with model test data described by Kvaternik and Kohn (ref. 100). This analysis was the basis for later extensions that included provisions for a gimbaled hub with offset coning hinges, blade lead-lag motion, a modal representation of the airframe structure, full span free-free or semispan

cantilevered configurations, and rigid-body aircraft degrees of freedom. Nonthrusting-, windmilling-, and cruise-mode flight conditions were included. This analysis was named PASTA (Proporotor Aeroelastic Stability Analysis) and was later used in support of V-22 aeroelastic model testing in the NASA Langley Transonic Dynamics Tunnel.

Johnson developed a series of tilt-rotor aeroelastic stability analyses later incorporated in the comprehensive CAMRAD analysis for rotorcraft performance, loads, stability and control, aeroelastic stability, and acoustics. CAMRAD contains the capability to predict the linear stability characteristics of tilt-rotor configurations in various flight conditions (ref. 94). The initial development of the tilt-rotor equations, reported in reference 101, treated a semispan configuration consisting of a cantilever wing, nacelle, and proprotor and modeled uncoupled flap and lead-lag bending of elastic rotor blades, and elastic beam and chord bending and torsion of the wing. Quasi-steady aerodynamic forces were included and equations for rotors having two or more blades were developed. For the two-bladed configurations the equations included periodic coefficients; for rotors having three or more blades, the use of the multiblade transformation yielded equations with constant coefficients. The equations in reference 101 were used by Johnson to correlate with full-scale experimental test data of two semispan wing-nacelle-proprotor models.

Johnson extended his analysis in reference 102 by refining the rotor modeling to include coupled elastic flap and lead-lag bending modes, rigid pitch motion of the blades to reflect pitch control system flexibility, blade elastic torsion, gimbal tilt, and rotor speed perturbations. The aerodynamic model treated high and low inflow, axial and nonaxial flight. The effects of compressibility and static stall on the airfoil coefficients were included. The rotor model included gimbal undersling, torque offset, precon, droop, sweep, and feather axis offset. Blade section center of gravity, aerodynamic center, and tension axis offsets from the elastic axis were included. In reference 103, Johnson added an engine-transmission-governor model including an interconnect shaft between the two rotors, refined the method for treating kinematic pitch-bending coupling of the blade, and extended the rotor aerodynamics model to include reverse flow. In reference 85, Johnson continued development of rotorcraft aeroelastic analysis, generalizing a system of coupled rotor-body equations to treat multirotor helicopters (single main rotor and tail rotor, twin rotor tandem) and symmetric tilt-rotor vehicles in both free flight or in wind tunnel or ground contact conditions. For tilt rotors, this analysis was advanced over previous work because it included complete rigid-body aircraft degrees of freedom and two complete proprotors. Linearized small-perturbation equations were developed for aeroelastic stability analysis.

Finally, this analytical model was used as the basis for the CAMRAD comprehensive rotorcraft analysis for use in predicting performance loads, stability and control, and acoustics characteristics in addition to aeroelastic stability (ref. 94). Johnson used these analyses for a number of research investigations of tilt-rotor aeroelastic stability that will be discussed below. Johnson used XV-15 wind-tunnel and flight-test data for comparison with the CAMRAD analysis to assess its adequacy to predict tilt-rotor aircraft performance, loads, and stability

(ref. 104). Generally the aeroelastic stability prediction capability was judged to be good; however, additional capabilities were considered desirable for future configurations such as bearingless rotors.

In summary, the development of aeroelastic stability analysis capability described herein has had and will continue to have a significant effect on the successful development of the revolutionary tilt-rotor aircraft concept.

## UNSTEADY AERODYNAMICS

This section will treat developments in rotor unsteady aerodynamics applicable to rotorcraft aeroelastic stability.

Unsteady aerodynamics of rotor blades is considerably more complex than that of fixed wings for which flutter analysis for three-dimensional, unsteady, compressible flow is reasonably well developed. For the rotor blade, many aeroelastic stability problems may be successfully treated with two-dimensional quasi-steady aerodynamics; however, there is also a need to treat unsteady, compressible flow, dynamic stall, and varying free-stream velocity, as well as three-dimensional effects of returning wake sheets and variable sweep angle. In view of these complications, progress in advanced unsteady aerodynamics for rotary wing applications has been slow, and researchers and designers alike have had to rely on approximate simplified methods.

Most rotary-wing aerodynamics research has been directed toward rotor performance, loads, vibrations, and stability and control. For these applications, rotor aerodynamics generally is divided into two parts: rotor-blade airfoil section airloads and rotor-wake-induced inflow. The rotor-blade section airloads are calculated using approximate or empirical methods such as linear steady or unsteady thin-airfoil theory, or from airfoil aerodynamic coefficients tabulated as a function of angle of attack and Mach number. Empirical corrections are applied to account for blade sweep, compressibility, static and dynamic stall, and blade-vortex interaction effects. The wake-induced velocity is needed to define the local blade-section angle of attack from which blade-section airloads are calculated. Various momentum and discrete vortex-wake theories have been developed for the rotor-induced inflow. The formulations for airfoil airloads and wake-induced velocity are solved together with the blade dynamic response equations either by numerical integration in the time domain, or by iteratively calculating the response coefficients in the frequency domain.

In general, this approach provides the rotor transient or steady-state periodic airloads that can be used to calculate rotor performance, loads, vibrations, and vehicle stability and control. However, these methods do not yield direct information on rotor aeroelastic stability characteristics. It is sometimes possible to use direct numerical integration of the rotor loads equations to determine stability, but it is more desirable to solve linear differential equations by means of eigenanalysis to obtain stability characteristics directly.



In general, rotor-blade flutter analysis employing unsteady aerodynamic theory is carried out using methods adopted from fixed-wing flutter analysis. Fixed-wing unsteady aerodynamic theory, in contrast to the typical rotorcraft approach described above, generally relates the airfoil airloads directly to the motion of the airfoil—combining airfoil-section airloads and wake-induced inflow in a single analytical model. The unsteady aerodynamic theory is generally formulated in the frequency domain—harmonic airloads expressed in terms of harmonic airfoil motions. Aeroelastic stability equations therefore assume airfoil motion to be harmonic and solutions that satisfy this assumption therefore determine the neutral stability condition.

If a time-domain aerodynamic theory is available, it is preferable to use a standard eigenanalysis solution yielding both damping and frequency for conditions of arbitrary stability. The latter approach is typically used for quasi-steady theory but is more difficult for sophisticated unsteady aerodynamics.

The scope of this section will cover a variety of unsteady aerodynamic developments, including two-dimensional linear and nonlinear unsteady aerodynamic theory; finite state models; three-dimensional unsteady aerodynamic theory; and dynamic inflow, a simplified three-dimensional unsteady actuator disc rotor wake model.

### Two-Dimensional Unsteady Aerodynamics

As noted above, rotary-wing aeroelastic stability has borrowed from methods developed for fixed-wing flutter analysis. Classical Theodorsen unsteady aerodynamic theory is applicable for rotor-blade bending-torsion flutter and is commonly applied in quasi-steady form (ref. 105). Loewy's theory, which extends Theodorsen theory to the hovering rotor problem, approximately represents the effects of wake vorticity of previous blade passages (ref. 106). Greenberg's theory is commonly applied to account for the effects of varying free-stream velocity of rotor-blade airfoil sections caused by forward flight or inplane motion of the blade (ref. 107). These theories formed a basis for government research activities addressed in this survey.

One area addressed by government researchers is the application of these two-dimensional, unsteady aerodynamic theories to rotor-blade problems. The elastic motion of a fixed-wing configuration is clearly defined, but a rotor blade undergoing moderately large deformations in elastic bending and torsion and pitch rotations is kinematically more complex and requires special attention. Relating the rotor-blade motion variables to the airfoil-motion variables of two-dimensional unsteady aerodynamic theory was addressed by Johnson (ref. 108), Kaza and Kvaternik (ref. 109), Friedmann and Yuan (ref. 110), and Peters (ref. 111). These works indicate that a failure to properly include the aerodynamic theory in the aeroelastic analysis can lead to erroneous stability predictions.

Recent efforts have also been made to transform rotor unsteady aerodynamic theories from the frequency domain to the time-domain. Frequency-domain formulations are not convenient to use for aeroelastic stability analysis and,

except for neutral stability conditions, provide only an approximation to unsteady aerodynamics for transient motion. Dinyavari and Friedmann developed approximate time-domain models for Loewy and Greenberg unsteady aerodynamic theories (ref. 112). The finite-state models were obtained by using Padé approximants of the appropriate lift deficiency functions contained in the Loewy and Greenberg theories. The approximation did not, however, capture the oscillatory behavior of the Loewy lift-deficiency function that represents the effects of wake vorticity shed by previous revolutions of the rotor blades.

The Greenberg finite-state model was applied to predict aeroelastic stability of a rotor blade in hover and forward flight (ref. 113). Friedmann and Venkatesan also formulated another technique for approximating the Loewy lift-deficiency function (refs. 114-116). This method, derived from linear control system theory and termed the Bode plot method, involves curve fitting an approximate function for the Bode plot of the lift-deficiency function. This model may be incorporated in rotor aeroelastic equations and solved by eigenanalysis techniques to yield frequency and damping characteristics. Although these methods are not yet in common use by rotorcraft analysts, they are an important step in beginning to take advantage of analysis capabilities that are in use in the fixed-wing field.

Two-dimensional linear unsteady aerodynamic theory, even without nonlinear stall behavior, is a valuable and powerful tool for predicting rotor aeroelastic stability in the hover flight condition, but there are serious theoretical limitations for forward flight applications. As advance ratio increases, reverse flow and localized high-lift conditions produce time-varying nonlinear stall effects. Recent research aimed at aeroelastic stability analysis applications has begun to focus on nonlinear aerodynamics problems.

Ormiston and Bousman used quasi-steady stall analysis for application to flap-lag stability in hover (ref. 117). It was shown that the static nonlinearities in the airfoil lift and drag coefficients versus angle of attack, when included in a linearized aeroelastic analysis, were sufficient to adequately account for differences observed between measured blade-lead-lag damping and predictions based on unstalled airfoil theory.

Rogers has recently made progress in adapting nonlinear dynamic stall models to aeroelastic stability analysis in forward flight (ref. 118). Dynamic stall models have been developed for use in rotor airloads analysis, that is, in predicting rotor blade dynamic response and the associated unsteady blade airloads in forward flight, primarily in steady-state, trimmed flight conditions. These are usually empirical models in either the time domain or frequency domain and they rely on experimental data obtained from oscillating airfoil testing. Tran and Petot developed a time domain model consisting of differential equations relating the unsteady aerodynamic coefficients to airfoil motion variables (ref. 119). The parameters in these equations are functions of mean angle of attack of the airfoil and are derived from airfoil test data. However the formulation is valid for arbitrary motion rather than just simple harmonic motion. Rogers and Peters used the Tran-Petot nonlinear stall model to analyze the flapping stability of a rotor blade in forward flight

c-5

(ref. 118). The model was used to numerically calculate a nonlinear periodic equilibrium solution for rotor-blade response in forward flight.

Thereafter the nonlinear equations were analytically linearized for small-perturbation motions about the periodic equilibrium solution. The resulting periodic coefficient, linear differential equations were solved by Floquet theory to yield frequency and damping of the blade flapping motion.

Peters extended the Tran-Petot dynamic stall model with the objective of developing a unified model for unsteady aerodynamic lift of a two-dimensional airfoil section for use in rotor-blade aeroelastic stability analysis (ref. 111). The model is unified in the sense that it explicitly distinguishes between airfoil pitch and plunge motion and includes unsteady velocity, reverse flow, and large angles of attack. The model also reduces to Greenberg theory at small angles of attack and further reduces to Theodorsen theory for steady velocity.

### Three-Dimensional Unsteady Aerodynamics

There is much to be done for three-dimensional unsteady aerodynamics applicable to rotor-blade aeroelastic stability. An important early work in the field by Miller developed an analytical formulation for unsteady airloading (ref. 120). Substantial contributions have been made at ONERA by Dat (ref. 121), and more recently by Runyan and Tai (ref. 122). The problem, even in linear form, is a difficult one that has not attracted sufficient attention by rotorcraft researchers. Nevertheless, a rational, three-dimensional linear unsteady aerodynamic theory applicable to forward flight would be very useful for basic aeroelastic stability analyses in forward flight.

Much of the problem of three-dimensional unsteady aerodynamics of rotors lies in the complexity of the rotor configuration. In the case of fixed-wing unsteady aerodynamics, the extension from the two-dimensional airfoil problem to the three-dimensional problem involves the spanwise variations in airloads distribution and (implicitly) the associated shed and trailed vorticity convected from the wing by the free-stream velocity in an undeformed planar sheet.

Linear potential-flow theory has been used to develop rigorous unsteady lifting-surface aerodynamic theories (e.g., vortex doublet lattice). For the three-dimensional rotor blade, there are also the effects of the helical wake configuration, the effects of unsteady variations in free-stream velocity and direction, and the effects of other blades on the rotor. For the purposes of aeroelastic stability, the wake geometry may be assumed undeformed, and the perturbation unsteady aerodynamics may be obtained from linear theory.

Dat has developed linear three-dimensional unsteady lifting-line and lifting-surface theories for rotor blades, using an integral equation formulation based on the acceleration potential including linear compressibility effects. The theory has been applied to aeroelastic stability analysis of proprotor blades in axial flight as reported by Dat (ref. 123).

A similar theory has been developed by Runyan and Tai (refs. 122,124). They developed a lifting-surface theory for a helicopter rotor blade in forward flight utilizing the concept of the linearized acceleration potential and a doublet lattice procedure. The method was applied to rotor blade forced-response airload calculations. Results are also calculated for the rotor-blade airload response to an oscillatory blade-pitch excitation. Although the theory was not applied to an aeroelastic stability analysis, it would be suitable for such investigations.

### Dynamic Inflow

Background- Dynamic inflow is a simplified model for the unsteady induced inflow of a rotor. It treats the inflow but not the airloads part of unsteady aerodynamic theory. When used with quasi-steady airfoil theory, it provides a convenient, inexpensive, unsteady aerodynamic model that is useful for a number of rotor and coupled rotor-body low-frequency aeroelastic stability problems. In some respects, it may be thought of as a low-frequency approximation for a linear, three-dimensional, unsteady aerodynamic theory for a rotor blade. Dynamic inflow represents the rotor as an actuator disk, in effect ignoring the higher frequency influence of the airfoil shed wake while including the effect of the trailing wake. In contrast with the relatively limited unsteady aerodynamic research efforts discussed above, dynamic inflow theory has been the focus of considerable study. This section will review the significant accomplishments in this area, and also indicate the effect of this work on rotorcraft aeroelastic stability analysis.

By 1971, it had already been established, although it was not widely recognized, that the induced inflow of a rotor responds in a dynamic fashion to changes in rotor lift. Amer recognized that the roll damping of a helicopter was significantly affected by the induced-flow gradients from the asymmetric lift associated with the rolling motion (ref. 125). Sissingh was able to quantify this phenomenon through a set of equations that related the induced-flow gradient to the lift gradient (ref. 126). Curtiss and Shupe showed that the Sissingh theory could be placed in the form of a lift-deficiency function, involving an equivalent Lock number (ref. 127).

Although these theories are only quasi-steady representations which assume that inflow responds instantly to changes in thrust, it is important to recognize that the induced inflow response to rotor loads can involve significant time delays. In fact, Carpenter and Fridovich had performed experiments on the thrust and inflow response of a helicopter rotor to step inputs in collective pitch and had found time constants of the order of the apparent mass of an impermeable disk (ref. 128). Furthermore, Loewy's theory, a two-dimensional approximation to unsteady rotor aerodynamics, had been shown to yield a lift deficiency that exactly matches the Sissingh result at zero frequency, but that approached unity as frequency increases (ref. 106). Yet, despite this rather extensive knowledge based on the low-frequency behavior of the unsteady aerodynamics of rotors, no general theory existed that could model these aerodynamics in hover, in axial flight, and in forward flight. Furthermore, there was no comprehensive set of data to compare with prospective

theories. Government-sponsored research changed this situation beginning in the early 1970's.

Initial interest in rotor inflow resulted from an Aeroflightdynamics Directorate experimental investigation of the response characteristics of hingeless rotors at high advance ratios. This work was carried out on a 7.5-ft-diam rotor model in the AFDD 7- by 10-Foot Wind Tunnel (fig. 12) under a contract with Lockheed California Company. The objective was to obtain a comprehensive set of data to define the static and dynamic response characteristics of typical hingeless rotors to support applications, including vehicle feedback control systems for stability augmentation, gust alleviation, and vibration reduction. The tests involved a simplified four-bladed rotor having untwisted blades of very high lead-lag bending and torsional stiffness to emphasize the basic flapping response dynamics. The model was operated at sufficiently low lift and tip speeds that stall and compressibility effects were largely avoided. This series of tests is described by Kuczynski and Sissingh (refs. 129,130), Kuczynski (ref. 131), and London et al. (ref. 132).

Very low thrust testing in hover and forward flight up to advance ratios of 1.75 for high flap stiffness ( $p = 1.33 - 2.33$ ) is described in reference 129. Rotor thrust, roll, and pitch moments were measured in response to steady-state collective, cyclic, and shaft-angle inputs. In reference 130, harmonic excitation of the cyclic control was introduced to determine the rotor thrust, pitch, and roll moment frequency response functions in hover and forward flight, up to  $\mu = 1.44$ . Steady-state testing was carried out for lower flap stiffness ( $p = 1.17$ ) and advance ratios from  $\mu = 0.07$  to 0.44. In reference 131, the blade-root bending stiffness was reduced to achieve blade-flap frequencies ( $p = 1.125$  to 1.28) more representative of typical hingeless rotors. For these tests both the cyclic controls and rotor shaft were harmonically excited for the frequency-response tests. The last series of tests (ref. 132), was intended to gather data for moderate and high rotor thrust levels at low to moderate advance ratios. Advance ratios included  $\mu = 0$  to 0.5 and collective pitch ranged from  $0^\circ$  to  $20^\circ$ . Again, static and harmonic cyclic and shaft motion excitations were applied.

Static inflow model- One objective of these 7.5-ft model investigations was to verify a rotor-response analysis based on linear quasi-steady aerodynamics to predict the flapping response of a rotor blade in high-advance-ratio forward flight for low-lift conditions without stall or compressibility. Measured data from static control response derivatives (thrust and hub moment coefficients,  $C_T$ ,  $C_L$ ,  $C_M$ , with respect to collective and cyclic pitch,  $\theta_0$ ,  $\theta_s$ ,  $\theta_c$ ) were compared to a rotor-blade flapping response analysis including several elastic flap bending modes, linear quasi-steady aerodynamics with reversed-flow effects, and a harmonic balance solution procedure retaining an arbitrary number of harmonics (ref. 133). Comparisons of data and theory revealed very substantial quantitative and qualitative differences, especially at low advance ratios. Those differences could not be explained in terms of any known modeling errors and led to consideration of the effects of induced inflow.

The results of these investigations were reported by Ormiston and Peters (ref. 134). First, the steady-state momentum theory inflow models of Sissingh, Curtiss, and Shupe were formulated in terms of matrix equations to relate perturbations in the inflow gradients to perturbations in the thrust, roll moment, and pitch moment of the rotor. These perturbation inflow gradients characterized in a relatively simple way the complex nonuniform induced-velocity field of a lifting rotor. They represent a time- and space-averaged measure of the mean, lateral, and longitudinal gradients of the rotor-induced inflow distribution. This inflow model takes the form of a diagonal matrix of coupling coefficients, the L matrix, that was easily combined with the rotor-blade response analysis of reference 133. In hover

$$\begin{Bmatrix} d\lambda_o \\ d\lambda_s \\ d\lambda_c \end{Bmatrix} = \frac{1}{2v} [L] \begin{Bmatrix} dC_T \\ -dC_L \\ -dC_M \end{Bmatrix} \quad \text{where} \quad [L] = \begin{bmatrix} 1/2 & 0 & 0 \\ 0 & -2 & 0 \\ 0 & 0 & -2 \end{bmatrix} \quad (1)$$

aero

and where  $v$  is the mean induced inflow of the rotor.

This model was then incorporated in the flapping response analysis described in reference 134. As shown in figure 13, it brought the theoretical predictions and experimental data into excellent agreement for the hover condition. The effect of the inflow on the rotor moment response derivatives is simply a result of the fact that a perturbation thrust is accompanied by a like perturbation in inflow. For example, increased blade pitch increases rotor thrust which increases inflow, reducing the angle of attack, and thereby reducing a part of the original thrust increase. This effect reduces the rotor thrust derivative. The same effect occurs for rotor pitch and roll moments. Since the sensitivity of inflow perturbations is inversely proportional to the mean rotor inflow, the effect illustrated in figure 13 is much more pronounced at low rotor thrust than at high rotor thrust. The momentum theory concept works well in hover where the distribution of inflow perturbations corresponds closely to the distribution of rotor-blade lift perturbations. This situation does not hold in forward flight and the simple diagonal L-matrix was not nearly as successful in correlating with the experimental data. This led to the search for a more general L-matrix that would include off-diagonal coupling between inflow and loads.

Simple vortex models postulated in reference 134 were more successful than momentum theory but the best result was a numerical empirical model for the L-matrix generated by a parameter identification process to provide the best fit for the measured rotor derivatives. Figure 14 shows the measured rotor control derivatives in forward flight compared with the two different inflow models: momentum theory and the empirical model. As noted above, momentum theory is not satisfactory for forward flight, whereas the empirical model gives good results, confirming the utility of the general L-matrix form of the inflow model. It may be seen that the

effects of inflow are most pronounced at low advance ratios. Again it is noted that these results are for the nonlifting rotor condition.

To illustrate the effect of thrust and advance ratio on the sensitivity of rotor derivatives to the steady-state perturbation inflow model, figure 15 shows a typical hub-moment derivative calculation with and without the inflow. The mean inflow  $v$  is a measure of the rotor thrust. In hover, the hub-moment derivative vanishes for zero thrust ( $v = 0$ ). In forward flight the effect of inflow decreases with advance ratio.

Dynamic inflow model- Although an understanding of the effects of induced inflow on rotor response was not one of the original objectives of the Lockheed experimental program, the results were significant for hingeless rotors with large control derivatives and their important role in vehicle response and handling qualities. The effect of induced inflow on articulated rotor control characteristics received little attention because articulated rotor hub moments are small to begin with. Beyond the effects on stability and control, the effects of inflow were the subject of considerable speculation regarding air and ground resonance stability. It was theorized that air and ground resonance stability of hingeless rotors benefited substantially from the high rotor flap-damping characteristic of hingeless-rotor blades. It was further speculated that loss of rotor damping at low rotor lift (analogous to reductions of hub-moment derivatives) might therefore degrade the ground resonance stability of hingeless-rotor helicopters. Because ground resonance is a dynamic phenomenon, it was also postulated that such a reduction in rotor flap damping at low rotor thrust might not occur for unsteady motions at the ground-resonance frequencies. Therefore, it was of interest to determine the transient response characteristics of the perturbation inflow mode.

At this point Peters developed a formulation to model the transient response of the static inflow model (ref. 135). He assumed that the inflow perturbations would respond with a first-order time lag to perturbations in the rotor airloads. This is equivalent to postulating an apparent mass for the air, where the inertia of the air mass prevents the static perturbation inflow from establishing itself instantaneously in response to rotor airload perturbations. Combining the static inflow model with the apparent mass terms, Peters set forth the inflow model now known as dynamic inflow theory.

$$\begin{bmatrix} K_m & 0 & 0 \\ 0 & -K_I & 0 \\ 0 & 0 & -K_I \end{bmatrix} \begin{Bmatrix} d\dot{\lambda}_o \\ d\dot{\lambda}_s \\ d\dot{\lambda}_c \end{Bmatrix} + v [L]^{-1} \begin{Bmatrix} d\lambda_o \\ d\lambda_s \\ d\lambda_o \end{Bmatrix} = \begin{Bmatrix} dC_T \\ -dC_L \\ -dC_m \end{Bmatrix}_{\text{aero}} \quad (2)$$

The apparent mass  $K_m$  and apparent inertia  $K_I$  were taken from potential flow solutions for impermeable disks. This formulation for the apparent inertia terms

was a generalization of the approach used by Carpenter and Fridovich (ref. 128) to model the unsteady uniform inflow for a rotor with unsteady thrust response. In equation (2), a mass-flow parameter,  $V$ , allows the L-matrix to be applied for combinations of thrust ( $v$ ), climb ( $\lambda$ ), and forward flight ( $\mu$ )

$$V = \frac{\mu^2 + (\lambda + v)(\lambda + 2v)}{\sqrt{\mu^2 + (\lambda + v)^2}} \quad (3)$$

Peters also developed a complex lift-deficiency function (for roll and pitch) that included the time-delay effects. That function involves a reduced frequency based on the steady inflow velocity. This established the strong relationship between dynamic inflow theory and other theories of unsteady aerodynamics.

The Peters dynamic inflow model was first correlated with experimental data obtained by Hohenemser and Crews. Here the blade pitch of a small two-bladed hovering rotor model was harmonically excited in the rotating system. The resulting blade flapping was measured over a wide range of frequencies. Crews et al. (ref. 136) compared the results calculated using the dynamic inflow theory with measured data as shown in figure 16 and confirmed the excellent representation provided by the very simple dynamic inflow formulation although they used time-constants chosen to give a best fit with the data instead of the  $K_M$  and  $K_I$  values of Peters.

More extensive correlations were carried out by Peters, with the 7.5-ft-diam Lockheed model-rotor data further confirming the success of the dynamic inflow theory in representing the perturbation wake effects over a wide frequency range in hover and forward flight (ref. 135). Typical hover results presented in figure 17, are based on the measured data from references 130 and 131; they show that the contribution of static inflow alone is adequate at low frequencies but actually worsens the correlation at higher frequencies. At higher frequencies, predictions without any perturbation inflow are better than including static inflow alone. Adding the apparent mass effects to static inflow corrects the prediction at higher frequencies without appreciably influencing the results at low frequencies. The full dynamic inflow model thus provides a very satisfactory result over the full range of frequencies. Similar results are observed in forward flight as shown in figure 18; here the static inflow is based on the empirical inflow model.

In addition to the investigations based on the 7.5-ft model-rotor data, Hohenemser and his associates carried out extensive experimental studies of dynamic inflow under AFDD support. Although the original intent was to study rotor-blade flapping response to stochastic excitation, it was evident that the results of basic frequency response tests did not agree with theory, as noted previously. Hohenemser and Crews presented results in both hover and forward flight for the flapping response to harmonic blade pitch excitation of a 16-in.-diam torsionally rigid, two-bladed model rotor (ref. 137). Progressing and regressing cyclic pitch excitation was accomplished by a unique variable-frequency pitch-control mechanism in the rotating system that avoided free-play problems of conventional swashplate, actuators, and pitch-link mechanisms in the nonrotating system. This mechanism also



permitted excitation of progressing and regressing blade flapping over a wide frequency range. Test data were obtained in hover and advance ratios up to 0.8, for low to moderate values of collective pitch. A description of the two-bladed model and initial test results were also reported by Hohenemser and Crews (ref. 138).

As discussed above, these data were compared with dynamic inflow theory in reference 136. Hohenemser and Crews obtained additional data for a four-bladed rotor model in hover and forward flight, including hot-wire measurements of the unsteady downwash in the hover condition (ref. 139). Since the solidity of the four-bladed rotor was larger than that of the two-bladed rotor, the effects of dynamic inflow were also larger. Further measurements of unsteady downwash were obtained in reference 140.

Hohenemser and his associates also introduced the use of formal parameter identification theory to determine the inflow gains and time-constants associated with the dynamic inflow mode (refs. 141-147). These techniques were based on measurements of transient response obtained from the small-scale rotor model following modifications to the cyclic pitch excitation system. The identified coefficients for the inflow model were in very close agreement with momentum theory in hover. Identification of forward flight inflow parameters was not as successful as in hover, a result of the inability to excite collective modes.

Refined theory- The next significant refinement of dynamic inflow was the development of a rigorous aerodynamic formulation for the steady-state forward flight perturbation inflow model, the L-matrix. Although the empirical model was accurate and quite satisfactory for the rotor in edgewise flow and low rotor lift, it did not extend to very low advance ratios and, therefore, could not transition continuously to hover. Furthermore, it lacked a rigorous theoretical basis and suffered numerical singularities at certain advance ratios.

For these reasons researchers began to pursue more satisfactory alternatives. For a simplified aerodynamic formulation, such as dynamic inflow, an actuator disk theory was considered an appropriate basis on which to develop a more rigorous formulation. Following early NASA research (e.g., ref. 148) on actuator disk vortex theory models, Ormiston represented the rotor loading as a series of azimuthal and radial distributions of bound circulation (ref. 149). The Biot-Savart law was used to determine induced inflow influence coefficients associated with each circulation function. With a sufficient number of circulation functions, the L-matrix could be determined. This approach was not carried to completion and the solution to the problem awaited the efforts of other investigators. Mangler had previously calculated the induced flow for an actuator disk representation of a rotor (ref. 150). He used the potential-flow solution discovered by Kinner, who represented the aerodynamic loading of a circular disk by a complete series of radial and azimuthal pressure functions. Joglekar and Loewy, extended the Mangler work and evaluated the induced inflow for additional pressure functions. (ref. 151).

Using Joglekar and Loewy's work as a basis, Pitt and Peters successfully developed a rigorous, elegant, and practical L-matrix for dynamic inflow theory (refs. 152-154). They found that the Kinner potential functions would yield the

matrix coefficients analytically in closed form as a function of advance ratio and disk angle of attack. These coefficients were applicable for any advance ratio and at any disk angle of attack. Furthermore they extended the Kinner theory to the unsteady case and showed that under the assumption that velocities are mutually in phase, the exact potential-flow theory takes on a form identical to the dynamic-inflow theory of equation (2). The apparent-mass terms depend on the spanwise lift distribution but agree with those for an impermeable disk for the simplest distributions. The L-matrix is the closed-form static inflow result and is insensitive to the details of lift distribution. The Pitt-Peters dynamic inflow theory is given by

$$\begin{bmatrix} \frac{128}{75\pi} & 0 & 0 \\ 0 & \frac{-16}{45\pi} & 0 \\ 0 & 0 & \frac{-16}{45\pi} \end{bmatrix} \begin{Bmatrix} \dot{\lambda}_o \\ \dot{\lambda}_s \\ \dot{\lambda}_c \end{Bmatrix} + V \begin{bmatrix} 1/2 & 0 & \frac{15\pi}{64} \sqrt{\frac{1 - \sin\alpha}{1 + \sin\alpha}} \\ 0 & -\frac{4}{1 + \sin\alpha} & 0 \\ \frac{15\pi}{64} \sqrt{\frac{1 - \sin\alpha}{1 + \sin\alpha}} & 0 & -\frac{4}{1 + \sin\alpha} \end{bmatrix} \begin{Bmatrix} d\lambda_o \\ d\lambda_s \\ d\lambda_c \end{Bmatrix} = \begin{Bmatrix} dC_T \\ -dC_L \\ -dC_M \end{Bmatrix}_{\text{aero}}$$

where  $V$  is given by equation (3) and  $\alpha$  is the wake angle of attack at the rotor disk. In hover ( $\alpha = 90^\circ$ ), the theory reduces identically to momentum theory and in edgewise flow ( $\alpha = 0^\circ$ ) it takes on a structure very similar to that of the empirical model. At intermediate disk angles, the L-matrix of equation (4) agrees with results extracted from a prescribed-wake discrete vortex element analysis.

The Pitt-Peters dynamic inflow model was extensively compared with experimental data by Gaonkar and Peters (ref. 155) using the original data of references 129-131, including data not used in the previous correlations. Figure 19 shows typical comparisons for static derivatives and although the Pitt-Peters does not agree quite as well as the empirical model, it represents the major physical effects very well. Figure 20 gives a typical correlation of unsteady data for rotor response in forward flight.

Effects of dynamic inflow on rotorcraft stability- As described above, dynamic inflow is a relatively simple model of the unsteady aerodynamics of the rotor wake that is suprisingly effective and accurate in representing the static and low-frequency dynamic inflow response phenomena. Since the theory is expressed in a time-domain differential-equation form it is a simple matter to incorporate it into rotorcraft stability analyses. A number of these investigations have provided further understanding of the nature of dynamic inflow in addition to demonstrating improvements in prediction accuracy available by including dynamic inflow effects. It may be noted that using such an approach constitutes an approximation for the more rigorous finite-blade (as opposed to an actuator disk), three-dimensional unsteady aerodynamic theories discussed in previous sections. In effect, dynamic inflow theory in conjunction with quasi-steady aerodynamics for the rotor blade airloads represents a low-frequency approximation to Loewy theory.

As noted, dynamic inflow theory is easily incorporated in rotorcraft dynamic analysis. Ormiston studied the effect on rotor flap dynamics; flap damping was greatly affected at low rotor thrust and the effect varied significantly between the regressing, collective, and progressing modes (ref. 156). The dynamic inflow model introduces additional degrees of freedom, leading to inflow modes similar to augmented states found in other finite-state unsteady aerodynamic theories. Peters and Gaonkar found similar results for rotor flap-lag stability in forward flight (ref. 157). Although dynamic inflow mainly influences the rotor-blade flap modes, coupling between blade flap and lead-lag motions results in a secondary effect of dynamic inflow on lead-lag damping. It was found as a result that the rotor regressing lead-lag mode was significantly influenced by dynamic inflow.

In another investigation, Bousman encountered significant discrepancies between theory and small-scale model experimental data for damping of coupled rotor-body roll and pitch-mode damping at low rotor thrust conditions (ref. 158). It was postulated that these low measured damping levels were attributable to the effects of dynamic inflow for reasons similar to rotor-response results shown above. Gaonkar et al. performed coupled rotor-body stability analyses including dynamic inflow and confirmed the hypothesis (ref. 159). In addition, the effects of dynamic inflow also accounted for anomalies in regressing lead-lag damping of ground- and air-resonance modes noted in Bousman's results. Subsequently, Johnson (refs. 160,161) presented predictions of coupled rotor-body frequencies with and without dynamic inflow and compared them with Bousman's data as shown in figures 21(a) and 21(b).

For rotor speeds above 400 rpm, predictions of regressing inplane mode frequency ( $\zeta_R$ ) without dynamic inflow correlate well with data in figure 21(a). Correlation of predicted body-roll-mode frequency ( $\phi$ ) is fair but predictions of body pitch ( $\theta$ ) and flap regressing ( $\beta_R$ ) modes are poor. However, when dynamic inflow is included (fig. 21(b)), all of the calculated frequencies agree with the experimental data. Of particular interest is the branch labeled  $\lambda$ . The analysis identified this as a coupled inflow and flap regressing mode dominated by the inflow degrees of freedom. These important results show that in effect, the inflow model completely changes the character of the coupled rotor-body dynamics for this configuration. Thus, one would not expect to be able to predict rotor-body dynamics without dynamic inflow.

Several additional works on dynamic inflow might be noted. Gaonkar et al. (ref. 162) and Nagabhushanam and Gaonkar (ref. 163) investigated the properties of extended dynamic inflow models, including a  $5 \times 5$  L-matrix in place of the  $3 \times 3$  L-matrix described above. The  $5 \times 5$  L-matrix model included second-harmonic cyclic inflow degrees of freedom and associated second-harmonic components of the rotor airload distribution. It was found that if the number of inflow degrees of freedom exceeded the number of blades in the rotor, inconsistent results for rotor dynamic characteristics would be obtained. Later work indicated that the inconsistency was due to an incorrect assumption regarding the radial distribution of lift for the second-harmonic airload.

More recent developments include the extension of dynamic inflow theory into a higher frequency range. The original work of Pitt and Peters allowed for an arbitrary number of harmonics of induced flow, although only two were used. As shown by Gaonkar and Peters in reference 164, it now appears that by including additional harmonics, the theory of dynamic inflow will automatically include a three-dimensional version of Loewy theory (for hover and forward flight) which implicitly includes a near-wake approximation to the Theodorsen function. Correlations with data showed that the new theory is superior to former unsteady theories for all cases considered.

Significant progress has been made in development, validation, and application of rotor dynamic inflow theory. It offers an efficient and effective tool for expanding capabilities in analyzing rotorcraft aeroelastic stability.

## SOLUTION METHODS

This section addresses Army-NASA contributions to the development of methods for solving rotorcraft aeroelastic stability equations. The following material deals with automated equation derivation, solution of the dynamic equilibrium equations, and stability solutions using both Floquet theory and perturbation methods.

### Automated Symbolic Manipulation

A relatively recent development in rotorcraft aeroelastic stability is the application of symbolic manipulation programs to derive rotorcraft equations of motion. Because of the complexity of the equations of motion for even a moderately sophisticated rotorcraft model, derivation of the equations by hand is a tedious, time-consuming, and error-prone process. With this stimulus some very promising work has been carried out to automate the derivation of rotorcraft equations of motion. Nagabhushanam et al. described a self-contained FORTRAN IV symbolic processor, HESL (Helicopter Equations for Stability and Loads) that is capable of both deriving and solving rotorcraft stability equations (ref. 165). In contrast to general-purpose manipulations such as FORMAC or MACSYMA, HESL is specifically designed for rotorcraft applications. This processor derives state equations for a given ordering scheme, including energy expressions, generalized aerodynamic forces, the Lagrangian formulation, linear perturbation equations, and the multiblade coordinate transformation. It also carries out the subsequent numerical computations to determine system stability. A flowchart for these processes is shown in figure 22. This processor was used by Reddy (ref. 166), Reddy and Warmbrodt (ref. 167), and Reddy (ref. 168) to treat the flap-lag-torsion stability of an elastic blade, including dynamic inflow, in hover and forward flight. The numerical results, compared with previously published results, indicated the powerful capability represented by this approach. Typical results shown in figure 23 (from ref. 166,293) for flap-lag-torsion stability of an elastic hingeless rotor blade in hover are compared with results obtained using the Hodges-Dowell equations

(ref. 8). The lead-lag damping versus collective pitch shows small differences that Reddy (ref. 166), was able to relate to terms in the structural and aerodynamic operators of references 8 and 28.

A similar approach using MACSYMA was described by Crespo da Silva and Hodges, who investigated computerized symbolic manipulation to develop the equations of rotor-blade stability in forward flight and solved them using a multiple time-scales perturbation analysis (ref. 169). The derivation and the solution were both part of a single operation involving MACSYMA. Also, the equations used by Crespo da Silva and Hodges were derived by symbolic manipulation, and portions of the computer program used to solve the equations were output from MACSYMA (ref. 31).

### Solution for Dynamic Equilibrium

In general, many rotorcraft aeroelastic stability problems are governed by nonlinear equations. However, for many important cases, it is desirable to determine the stability characteristics from linear perturbation equations of motion about a steady-state equilibrium solution of the nonlinear equations. In the hover condition, the nonlinear equilibrium solution is generally constant and the linear perturbation equations are constant-coefficient, ordinary differential equations. In the forward flight condition, the nonlinear equilibrium solution is generally periodic in time (dynamic equilibrium) and the linear perturbation equations have periodic coefficients. In either case, standard eigenanalysis or Floquet analysis techniques are available to determine stability characteristics. The solution for the steady-state dynamic equilibrium solution is not as straightforward.

There are actually two tasks involved in the determination of the dynamic equilibrium solution. First, even if the rotor collective and cyclic pitch controls are known, there is the problem of finding the periodic solution to a set of nonlinear differential equations with periodic coefficients. This is complicated by the fact that the periodic solution may not be stable. The second problem is that the blade controls are generally not known a priori. Instead, the analyst is supplied with a set of trim constraint equations (e.g., six components of force and moment equilibrium) that must be satisfied. Therefore, the second response problem is to find the unknown controls (an inverse problem), as well as the periodic response associated with the unknown controls such that the vehicle satisfies the trim constraints. Over the past 10 years, considerable government-funded work has been directed at these important issues. This work has resulted in a number of solution strategies for both the periodic solution (response) and the trim-control solution.

The periodic response problem is reviewed first. For the hover case, this is a static response which can be solved by Newton-Raphson or other nonlinear equation solvers; for example, as in references 6 and 15. In forward flight, however, the problem is dynamic response. The most fundamental solution strategy is that of simple time-marching. Gaonkar et al. showed that Hamming's modified predictor-corrector is among the most cost-effective marching algorithms (ref. 170). However, recent work by Panda and Chopra has also shown that finite elements in time can also be competitive, provided they are correctly formulated in a bilinear-operator

notation (ref. 171). The problem with time-marching of any kind, however, is that it becomes cumbersome as damping decreases; and it is not feasible at all for unstable systems. This is because time-marching will not converge to an unstable equilibrium. Therefore, other methods have been developed for the periodic-response problem that can generally be divided into two categories.

The first category is that of transition-matrix methods. These rely on the transition matrix, or an approximation to it, over one period of motion in order to iterate on the periodic equilibrium. For linear problems, convergence is assured provided there are no neutrally stable eigenvalues with integer-multiple frequencies. For nonlinear problems, the system is assumed linear in each iteration. Such methods have proven very robust in terms of finding the solution. The method of Schrage and Peters finds the eigenvalues and periodic eigenvectors of the approximate transition matrix and uses modal expansion to determine the response (ref. 172). The methods of Friedmann and Shamie (ref. 173), Friedmann and Kottapalli (ref. 174), and Panda and Chopra (ref. 171) use the transition matrix in a convolution integral to generate the linearized response in each iteration. A similar method, called periodic shooting, used by O'Malley et al. in reference 175, gives numerically identical results but without the need for convolution or expensive eigenanalysis. A good review of transition-matrix methods is given by Friedmann (ref. 176).

The second category of methods for the periodic-response problem is that of harmonic balance techniques. These place the equations in the frequency domain before solving and, as with transition-matrix methods, they assume a linear solution within each iteration (ref. 177). The robustness of these methods depends critically on the extent to which nonlinearities are linearized and placed on the left-hand side of the equations. Strategies that include only inertial terms on the left-hand side often fail; and strategies that linearize all terms are very robust.

Methods of trim solution will now be addressed. Trim strategies can generally be divided into three categories. The first category is that of algebraic trim equations which must be solved along with the response. In some cases, these are from simplified equations and can be solved in closed form (ref. 178). In other cases, these equations come naturally from a full harmonic balance and must be solved iteratively. A second category of solution strategies is Newton-Raphson iteration. Here, no explicit equations are developed, but controls are adjusted based on numerically determined improvements in the constraint conditions. This has been the most widely used method for large, production analysis codes: O'Malley et al. (ref. 175) and Johnson (ref. 94). However, the method is not robust and often fails to converge. To combat this, analysis codes often apply the iteration only to a simplified set of rotor equations. Thus, the system is often not truly trimmed. The third category of strategies is that of auto-pilot equations (ref. 179). Here, a controller is designed to continuously monitor equilibrium conditions and update the pilot controls accordingly. Gains and time-constants are critical; and sometimes an adaptive controller is needed.

The government-sponsored research referenced above has not only developed the techniques listed, but it has also applied them to a large class of rotor

problems. These applications have led to the conclusions listed above and have identified natural matches between methods. For example, the automatic pilot is ideally suited to time-marching techniques (ref. 179), and the Newton-Raphson technique for controls is ideally suited for combination with periodic shooting (ref. 180). Furthermore, each of these two combinations has a set of problems (depending on damping and order) for which it is optimal. Algebraic equilibrium equations are naturally amenable to the harmonic-balance method, and these are useful in problems of rotor-body coupling or when the aerodynamics are in the frequency domain. Thus, the government-sponsored research in response and trim has developed to the point that the new methods can be applied to practical problems.

### Stability Analysis

In the hover condition for constant-coefficient equations of motion, stability is normally determined from the characteristic roots obtained from standard eigenanalysis techniques. Hodges presents a simplified algorithm for determining stability when it is not necessary to evaluate all of the eigenvalues of a system of linear equations (ref. 181). This method is computationally advantageous for cases in which stability must be determined for a large number of system parameter values as might be the case in constructing stability boundaries.

In the forward flight condition, and in hover with unsymmetric or two-bladed rotors, the linear stability equations have periodic coefficients. Many investigators have pursued solutions for this important problem in rotorcraft dynamics. Although supported in part by the results of previous investigators, Peters and Hohenemser carried out the first extensive application of multivariable Floquet theory to problems of rotorcraft aeroelastic stability, primarily the flapping stability of a single rigid blade in forward flight (ref. 182). Peters generated the Floquet transition matrix by numerical integration of the equations of motion for one period, and then determined the corresponding eigenvalues and eigenvectors. Following publication of this work, many investigators began to apply Floquet theory to rotorcraft aerelastic stability problems. Some of the subsequent work was intended to reduce the computational cost of generating the Floquet transition matrix. Friedmann and Silverthorn applied an approximate method developed by Hsu, a generalization of the rectangular ripple method, to substantially reduce the computational time for Floquet analysis (ref. 183). Hammond developed a refined version of the numerical integration technique of Peters that required only a single-pass integration of the equations for one period, rather than  $n$  integrations for an  $n$ -order system (ref. 82). Both these methods are also described by Friedmann et al. (ref. 184). Further discussion of this subject is contained in Gaonkar et al. (ref. 170) and Friedmann (ref. 176).

### Perturbation Methods

Perturbation methods have been applied to a number of problems in rotorcraft dynamics and are the object of continuing research. Use of perturbation methods has

typically fallen into two categories. First there is the use of perturbation methods in the space domain to approximate vibration frequencies, mode shapes, and buckling behavior of rotating beams. The significance of this work is mainly in the results. Peters was able to derive approximate, closed-form solutions to the free-vibration frequencies and mode shapes for uncoupled flap, lag, and torsion of rotating, elastic cantilever blades (ref. 185). Hodges later extended this work to include blades clamped off the axis of rotation (ref. 186). This work was also extended by Peters and Hodges to obtain simple, closed-form expressions for the inplane buckling of rotating beams (ref. 187).

The second category is the use of perturbation methods in the time-domain to obtain information about the response and stability. Tong (ref. 188) and Friedmann and Tong (ref. 189) used perturbation methods to study nonlinear flap-lag dynamics of rigid and elastic blades in hover and forward flight. Johnson used perturbation methods to study the flapping stability of rigid blades in forward flight (refs. 190-193). Crespo da Silva and Hodges also investigated the application of perturbation techniques to rotor-blade stability in forward flight (ref. 169). The significance of this latter work is that it has the potential to bypass Floquet theory, making use instead of analytical techniques such as the method of multiple time-scales. Such methods tend to become intractable by traditional manual approaches. However, when coupled with powerful, general-purpose symbolic manipulation programs such as MACSYMA it becomes a practical tool. This method is yet to be fully developed for general rotor-blade analysis, however.

### 3. INVESTIGATIONS OF AEROELASTIC STABILITY CHARACTERISTICS

The previous section described the development of methods to analyze and predict the aeroelastic stability of a variety of rotorcraft configurations in various operating conditions. Although methods in themselves tell little about rotorcraft behavior and stability characteristics, they may be used to generate such information. In this section, the results of Army-NASA investigations to study and identify such behavior and stability characteristics will be described. Such investigations may involve parametric analyses using the prediction methods described in the previous section, experimental testing to explore rotorcraft stability characteristics, or correlations of theoretical predictions and experimental data to check underlying assumptions and validate the theory. All of this is important because advancing rotorcraft technology is a difficult process, and it requires a thorough understanding of the fundamental physical behavior of rotorcraft aeroelastic stability, whether obtained through analysis or experiment, and it requires a high level of confidence in theoretical prediction capability that can only be achieved by careful checking of theory against experimental measurements.

In this section the material is divided into somewhat arbitrary categories, isolated blade-flapping stability, isolated blade flap-lag stability, isolated blade flap-lag-torsion stability, coupled rotor-body stability, bearingless-rotor stability, tilt-rotor aircraft stability, and an analysis correlation effort undertaken in



connection with the ITR/FRR Project. In the section on flap-lag stability, material on the development of analysis methods for rigid-hinged blades has been included here instead of in section 2. In addition, the material on coupled rotor-body, bearingless rotor, and tilt-rotor aircraft stability is arranged differently from that in section 2.

## FLAPPING STABILITY

The flapping stability of a rotor blade in forward flight is a basic problem of rotorcraft dynamics because it is one of the simplest systems on which to represent the effects of periodically varying aerodynamic damping and stiffness. Many investigators have addressed this problem, both to study methods of solving periodic-coefficient differential equations and to understand the stability characteristics of rotor blades described by such equations. Peters and Hohenemser significantly advanced this work both in their introduction of Floquet theory to solve periodic-coefficient equations and in clearly describing the complex forward flight behavior of a rigid blade with a flapping hinge (ref. 182). These results illustrated the existence of parameter regions (such as Lock number and advance ratio) where the characteristic roots exhibit natural frequencies of half or integer multiples of rotor speed, 0.5 or 1 per rev, that remain constant for an extended range of parameter values. This only occurs for constant-coefficient systems when the frequency is zero. Peters and Hohenemser presented numerous plots of damping contours in the Lock number-advance ratio plane illustrating the effects of pitch-flap coupling, flap hinge spring stiffness, and hub-moment feedback. A typical result shows regions of an 0.5 and 1 per rev natural frequency and the high advance ratio stability boundary (fig. 24).

Yin and Hohenemser studied the same stability problem after transforming the equations into multiblade coordinate form (ref. 194,195). They found that neglecting the periodic terms in these equations, a constant-coefficient approximation yielded results of acceptable accuracy for the low-frequency modes up to advance ratios of about 0.8. Hohenemser and Yin extended this work to include the effects of blade torsion and flap-bending flexibility on stability in forward flight (ref. 196). The effect of blade flexibility, in comparison with a rigid hinged-blade model, was shown to reduce flap-mode damping in forward flight, especially at higher advance ratios.

Johnson applied the perturbation method of multiple time-scales to the rigid flapping-blade problem in forward flight (refs. 190-193), confirming and clarifying some details of the results of Peters and Hohenemser. He developed approximate analytical expressions for the eigenvalues quite accurate for advance ratios up to about 0.5. Johnson also gave a comprehensive and detailed review of the many earlier studies of this problem before the work of Peters and Hohenemser (ref. 193). He also presented a thorough discussion of the dynamic behavior of the flapping blade in forward flight.

Biggers also investigated the accuracy of constant-coefficient approximations for this problem (ref. 197). Beginning with the forward-flight, blade-flapping equations in multiblade coordinate form, he showed that constant-coefficient approximation of these equations was reasonably accurate for moderate advance ratios up to about 0.5. This was considerably better than would be obtained for a constant-coefficient approximation of the isolated blade-flapping equations written in the rotating reference frame. Typical results of Biggers compare the variation of the flap-mode frequency with advance ratio for a constant-coefficient approximation of the multiblade flapping equations with exact Floquet analysis results (fig. 25).

Rogers studied blade-flapping stability in forward flight to examine dynamic stall effects; this work was discussed earlier in section 2. Finally, Crespo da Silva and Hodges used a computerized symbolic processor to perform a perturbation analysis of rigid, hinged, flapping-blade stability (ref. 169).

## FLAP-LAG STABILITY

Analysis of rotor blade flap-lag degrees of freedom enables the researcher to investigate the most basic characteristics of cantilever rotor blades, including both hingeless and bearingless configurations. For articulated rotor blades, flap-lag dynamics are generally not important unless aeroelastic couplings are introduced in the blade-pitch control system. Although flap-lag analyses of hingeless rotor blades omit the important torsion effects and are, therefore, not generally of practical use, they do permit the underlying structural, inertial, and aerodynamic coupling of flap and lead-lag motions to be investigated with more clarity. Some of the earliest work in this field was carried out by Young who drew attention to nonlinear flap-lag coupling, generating some controversy in the process (ref. 198). Hohenemser and Heaton then studied the same problem and concluded that the effects of the nonlinearities could be adequately accounted for by linearizing the flap-lag equations for small-perturbation motions (ref. 199). At this point government researchers began to investigate these problems.

### Hover Analytical Investigations

For investigations of flap-lag stability in the hover conditions, results of rigid-blade analyses are treated separately from results of elastic-blade analyses.

Rigid blade analyses- In keeping with increased interest in hingeless rotors, and a lack of information about such systems, Ormiston and Hodges initiated a study of flap-lag stability to gain a general understanding of their basic aeroelastic stability characteristics (ref. 3). They used the rigid-hinged-blade analysis of Hohenemser and Heaton (ref. 199) as a starting point. The flap-lag equations are fundamentally nonlinear, and a proper formulation for stability analysis requires linearization to derive small-perturbation equations of motion. Standard eigen-analysis then yields the characteristic roots that define stability of the small-

perturbation motions. Hohenemser and Heaton applied such a procedure, thereby improving on Young's original flap-lag analysis. In reference 3, Ormiston and Hodges refined the analysis of Hohenemser and Heaton, correcting an error in the linearization procedure of reference 199, and investigated the stability characteristics of hingeless rotor blades for a wide range of parameters. These investigations used the simplified, rigid blade with discrete spring-restrained hinges to represent the bending flexibility of a cantilever elastic blade as originally proposed by Young (ref. 200). This approach simplified the equations of motion and clarified the mechanisms that determined flap-lag stability.

Ormiston and Hodges extended this concept to provide a more complete representation of hingeless rotor blades, by introducing a double spring system to distinguish between the flexibility contained in the hub inboard of the pitch bearing and the flexibility contained in the blade outboard of the pitch bearing (fig. 26(a)). Thus the rigid-hinged blade model shown in figure 26(b) included two sets of flap and lead hinge springs, one set fixed inboard of the pitch bearing and a second set outboard of the pitch bearing and rotating with the blade as pitch angle changes. The parameter  $R$ , generally varying between 0 and 1, defined the hub-to-blade distribution of flexibility. When all of the bending flexibility is located in the hub and none in the blade, there is no structural flap-lag coupling and  $R = 0$ . When the flexibility is in the blade and not in the hub,  $R = 1$ , and the structural flap-lag coupling is roughly proportional to blade pitch angle. Combinations of hub and blade flexibility are represented by intermediate values of  $R$  according to a simple formula. Curtiss has also proposed additional versions of this hub and blade hinge spring model (ref. 201).

It should also be noted that for the rigid-blade model, the sequence of rotations of the rigid blade is defined by the chosen arrangement of physical hinges; in reference 3, a lag-flap sequence was chosen. This means that the flap hinge is radially outboard of the lead-lag hinge and moves with the blade during lead-lag motion. The kinematics of the flap-lag hinge sequence are slightly different and lead to small differences in the aeroelastic stability characteristics compared with the lag-flap hinge sequence, as will be addressed below. The effect of hinge sequence is much more pronounced when a discrete hinge is also included to represent torsion of an elastic blade.

The basic flap-lag stability characteristics of the rigid blade in hover were investigated in reference 3 and are illustrated in figure 27. For rotor blades having a flap hinge spring ( $p > 1.0$ ), a flap-lag instability can occur when the lead-lag natural frequency is close to the flap frequency and when the flap frequency is near  $(4/3)^{1/2}$ . The nonlinear inertial and aerodynamic moments produce flap-lag coupling terms in the linearized perturbation equations that vary in proportion to blade-pitch angle. Thus the regions of instability in figure 27 expand as blade pitch increases. The simplified flap-lag equations were used by Ormiston and Hodges to develop several closed-form expressions to describe flap-lag stability characteristics and stability boundaries.

The results of Ormiston and Hodges showed the strong influence of flap-lag elastic coupling; for example, as the structural coupling parameter  $R$  increases,

the region of flap-lag stability in figure 27 shifts to higher lead-lag frequencies until it ceases to exist for practical configurations. Other results delineated the differences between stiff- and soft-inplane blade configurations (fig. 28). Soft-inplane configurations are generally stable, independent of structural flap-lag coupling, whereas stiff-inplane configurations typically exhibit flap-lag instability at some intermediate level of flap-lag structural coupling.

Flap-lag instabilities described are typically relatively weak; a small amount of structural damping is often sufficient to stabilize the blade. Blade-pitch couplings, however, may cause very large changes in flap-lag stability. Ormiston and Hodges included the effects of kinematic pitch-lag coupling with results shown in figure 29. For soft-inplane configurations, positive pitch-lag coupling (pitch up with lead) is destabilizing for all values of flap-lag structural coupling. The behavior of the stiff-inplane configuration is considerably more complex; depending on the flap-lag structural coupling, both positive and negative pitch-lag coupling may be destabilizing. Reference 3 also included blade precone, and it was found that although precone could be either stabilizing or destabilizing, its effect was not large for torsionally rigid blades. Ormiston attempted to identify aeroelastic couplings that would augment lead-lag damping to help control coupled rotor-body instabilities such as air and ground resonance (ref. 202). A combination pitch-lag and flap-lag elastic coupling was most effective in increasing the damping of the isolated blade at zero pitch.

Peters used the flap-lag equations of Ormiston and Hodges to derive approximate but useful closed-form analytical expressions for the lead-lag damping as a function of the various configuration parameters (ref. 203). He was also able to show that minimum stability occurs when the blade-tip motion moves along a straight line bisecting the blade chord and the direction of mean airflow velocity, the axis of minimum damping.

The rigid-blade flap-lag results of Ormiston and Hodges served to identify many of the basic characteristics of hingeless-rotor-blade aeroelastic stability, the nature of destabilizing aerodynamic and inertial flap-lag coupling, the important role of flap-lag structural coupling, the essential differences between soft- and stiff-inplane configurations, and how the important effects of pitch-lag coupling depend on flap-lag structural coupling and lead-lag natural frequency. Much of this behavior has been reflected in numerous subsequent works that have included blade elastic bending, torsion, forward flight aerodynamics, and rotor-body coupling.

As noted above, when a continuous elastic blade is modeled in an approximate way by using a spring-hinged rigid blade, the order of rotations about the discrete flap and lead-lag hinges will influence the geometric orientation of the blade in space. The influence of the flap and lead-lag hinge sequence on the stability of the system was investigated by Kaza and Kvaternik who compared the results obtained for the flap-lag sequence with results (fig. 27) obtained with the lag-flap sequence (ref. 204). The change in hinge sequence introduces a small effective pitch-lag coupling that alters the stability boundaries for low flap stiffness configurations as shown in figure 30.

As originally formulated by Young the rotor-blade flap-lag equations are nonlinear (ref. 198). However, it has been shown that the nonlinear aerodynamic and inertial terms are relatively weak and that the linearized solutions discussed above are usually satisfactory. Tong studied nonlinear flap-lag stability of the hinged rigid blade in references 188 and 205 and determined the regions of linear instability that would produce stable or unstable limit cycles, as shown in figure 31. He was also able to estimate limit cycle amplitudes of stable limit cycles using perturbation methods.

Elastic blade analyses- In addition to studying the flap-lag stability of the simplified rigid, spring-hinged representation of the elastic cantilever blade, Ormiston and Hodges also treated a uniform elastic blade, using a modal analysis method, and showed that with proper treatment of nonlinear aerodynamic and inertial coupling in the elastic blade equations, the two representations exhibit very similar behavior (ref. 3). Additional results were reported in reference 4.

Other investigators also studied the flap-lag stability of elastic blades in hover. In reference 5, Friedmann developed and solved the elastic-blade flap-lag equations, achieving results similar to those in reference 4, although flap-lag structural coupling was not included. In references 206 and 207, Friedmann examined the effects of mode shape on flap-lag stability and showed that the rigid blade with appropriate hinge offset would agree closely with elastic blade stability boundaries, as shown in figure 32. In references 206 and 208 Friedmann found that the effects of precone had a strong effect on flap-lag stability, although this was later found to be due to an extraneous term in the equations (ref. 209). Friedmann and Tong (ref. 189) also studied the nonlinear flap-lag stability of an elastic blade, using perturbation methods, again identifying regions where linear instabilities result in stable limit cycles; White also studied flap-lag stability of elastic blades in hover, using a collocation method of solution (ref. 210). His results, including the effects of flap-lag structural coupling, correspond to those in reference 4.

Further investigations of elastic blade flap-lag stability were carried out by Straub and Friedmann, using the finite-element method (refs. 62,64). Typical results in figure 33 show a comparison of flap-lag stability boundaries for the finite-element method, and a conventional modal method for a uniform elastic blade in hover. These results show the basic effect that flap-lag structural coupling shifts the region of flap-lag instability to increasingly stiff-inplane configurations as  $R$  increases from 0 to 1. Reddy compared elastic and rigid-blade models for flap-lag stability and also included the effects of dynamic inflow (ref. 166,168).

Effects of unsteady aerodynamics- Only limited investigation of the effects of unsteady aerodynamics on flap-lag stability have been carried out. Since flap-lag instability occurs at a low frequency, unsteady aerodynamics has not been considered important. Kunz (ref. 211) used Theodorsen and Loewy unsteady aerodynamic theories to calculate flap-lag stability of the rigid, spring-restrained hinged-blade model of a four-bladed rotor and showed moderately large effects, especially with Loewy theory, at larger blade-pitch angles, as shown in figure 34. More recently,

Dinyavari and Friedmann used a finite-state representation of Greenberg's unsteady aerodynamic theory to calculate flap-lag stability of the rigid-hinged blade model (ref. 113). Results shown in figure 35 indicate a moderate effect, roughly consistent with results of Kunz using Theodorsen unsteady aerodynamics.

### Forward Flight Analytical Investigations

Early work on flap-lag stability of hingeless rotor blades in forward flight included the original work of Young (ref. 198). Tong and Friedmann also studied nonlinear flap-lag stability in hover and forward flight using perturbation techniques (refs. 188,189,207,208). In reference 189 they concluded that for moderate advance ratios the periodic coefficients in forward flight would not have a large effect on flap-lag stability unless the lead-lag frequency is near 0.5 or 1.0 per rev.

The analysis of flap-lag stability in forward flight only received serious attention after the utility of Floquet theory had been widely recognized. This afforded a practical means of dealing with linear periodic-coefficient equations of motion. However, the nonlinear properties of the flap-lag equations with reverse flow introduced some additional problems such as determining a periodic steady-state solution, satisfying the trim condition of the rotor, and obtaining linearized equations. Early investigations of flap-lag stability in forward flight were conducted by Friedmann and Silverthorn, using an elastic-blade model and a modal solution method (refs. 212-214). An approximate method was used to treat the reversed-flow region and a simplified trim procedure was used, based on the hover trim solution. Nevertheless, stability results were sensitive to several system parameters, including reversed flow, mode shapes, and flap-lag structural coupling. Typical results shown in figure 36 illustrate the effect of reverse flow on lead-lag damping.

An extensive investigation of hingeless rotor blade flap-lag stability in forward flight was conducted by Peters in (ref. 215). This study was based on the hinged, rigid-blade model having reverse flow and including contributions to the periodic coefficients arising from the steady-state blade response and cyclic pitch associated with specific forward flight trim conditions. Figure 37 illustrates the importance of different trim conditions on the variation of lead-lag damping with advance ratio. Figure 38 illustrates one of the unusual properties of periodic-coefficient systems. For configurations with lead-lag natural frequencies close to 1 or 0.5 per rev, instabilities may occur that exhibit the integer or half-integer frequencies characteristic of periodic-coefficient systems. For the flap-lag problem, these regions of parametric instability are quite restricted. Other configurations exhibit "conventional" instabilities; that is, the frequencies may take on any value.

Figure 39 summarizes the effects of flap-lag structural coupling on forward flight flap-lag stability and, as discussed previously, the stiff-inplane configuration is more sensitive to these effects than the soft-inplane configuration. These results illustrate the basic flap-lag stability behavior of soft- and stiff-inplane

rotor blades in forward flight. Peters also presented results showing the effects of pitch-flap and pitch-lag kinematic couplings on stability.

Kaza and Kvaternik (ref. 204) studied flap-lag stability of the rigid-hinged blade in forward flight, including approximating the periodic-coefficient equations with the constant-coefficient set obtained by transforming the blade equations in the rotating system to multiblade coordinate equations in the fixed system, and dropping periodic-coefficient terms, as Biggers did in reference 197 and as is shown in figure 25. The results, shown in figure 40 for the same case considered by Peters (fig. 39), illustrate that the collective and regressing lead-lag modes from the constant-coefficient equations are quite adequate up to relatively high advance ratios. A similar study was carried out by Gaonkar and Peters (ref. 216). Gaonkar and Peters investigated the effects of dynamic inflow on hinged-rigid blade flap-lag stability in forward flight (ref. 157). Lead-lag damping of stiff- and soft-inplane configurations is illustrated in figure 41; depending on the particular configuration parameters and the advance ratio, this unsteady aerodynamic effect may significantly alter the stability.

In reference 173, Friedmann and Shamie revisited the elastic-blade flap-lag stability problem in forward flight by considering more representative trim conditions and including the periodic equilibrium solution in the linearized stability equations. Their results, an example of which is shown in figure 42, confirmed the findings of Peters about the sensitivity of stability to the details of the trim solution. In a related work, Shamie and Friedmann studied the problem of flap-lag stability of a two-bladed teetering rotor in forward flight and compared the results with those of a single isolated blade (ref. 217).

Finite-element techniques have also been applied to the elastic-blade flap-lag problem in forward flight; typical results of Straub and Friedmann (refs. 63,64) are shown in figure 43. Here, both the first and second lead-lag mode damping are presented for a trimmed flight condition. Finally, Reddy and Warmbrodt calculated flap-lag stability of an elastic blade in forward flight, using modal equations and retaining two bending modes for each bending direction (ref. 218). The results, shown in figure 44 for soft- and stiff-inplane blades with and without flap-lag structural coupling, are for trimmed flight conditions and may be compared with rigid-blade results in figure 39. These results were developed using a symbolic processor to generate and solve the equations.

#### Flap-Lag Experiments in Hover and Forward Flight

A series of experiments using small-scale model rotors was conducted at the Aeroflightdynamics Directorate specifically to verify the results of analytical investigations of the flap-lag stability of simplified rigid-hinged-blade models in hover and forward flight. The flap-lag system does not represent a practical configuration since typical rotor systems generally exhibit varying degrees of pitch control and blade torsional flexibility. However, from a research point of view, the restricted flap-lag experiment greatly simplifies the process of correlating and interpreting analytical and experimental results. These experiments were designed

to minimize as many sources of error and uncertainty as possible in order to provide a clear test of the essential features of the flap-lag stability analysis. To this end the blades were designed to be as rigid as possible in bending and torsion. Flexures placed at the blade root to represent spring-restrained hinges were used to eliminate, as much as possible, the nonlinear damping of hinges and bearings. The hub-support system was designed to be sufficiently stiff to maintain a fixed hub, isolated-blade condition.

The experimental technique consisted of initiating transient lead-lag motions and measuring the decay rate to determine damping of the lead-lag mode. Figure 45 illustrates the hover test stand experimental apparatus and figure 46 the layout of the hub flexures used to simulate flap and lead-lag hinges. The straight flexures represented simple flap and lead-lag hinge springs; the skewed flexures provided, in addition, kinematic pitch-flap and pitch-lag aeroelastic couplings. Both the straight and skewed flexures could provide flap-lag structural coupling if they are rotated in pitch with the blade. Hover tests were performed using a two-bladed 5.5-ft-diam rotor.

The typical results in figure 47 are from Ormiston and Bousman (refs. 117,219, 220); they show the variation of lead-lag damping with blade-pitch angle for two different blade and hub configurations. The experimental results in figure 47(a) confirm the destabilizing effects of flap-lag aerodynamic and inertial coupling predicted by linear analysis. In addition, however, at high pitch angles the linear analysis fails to predict the abrupt onset of instability. This was subsequently determined to be due to airfoil stall that with suitable modification to the analysis, could be reasonably well predicted. The results in figure 47(b) illustrate a stiff-inplane configuration where the effects of stall were stabilizing. Another experimental investigation was aimed at confirming the effectiveness of aeroelastic couplings postulated by Ormiston (ref. 202) to enhance lead-lag damping of hingeless rotor blades. Results of Bousman et al. (ref. 221) shown in figure 48 illustrate how combined flap-lag structural coupling and pitch-lag coupling significantly increase the rotor-blade lead-lag damping.

Another flap-lag stability experiment to investigate intermediate values of flap-lag structural coupling ( $R \approx 0.5$ ), using blades with distributed bending flexibility, was conducted by Curtiss and Putman at Princeton University (ref. 222), using the apparatus and rotor hub described above. Test results agreed well with analysis, even though the rigid-hinged-blade analysis was used to model the elastic blade.

Although a considerable amount of analytical research has been conducted on forward flight flap-lag stability, relatively little experimental research has been carried out. An extensive experimental study of flap-lag stability in forward flight was conducted at the Aeroflightdynamics Directorate and reported by Gaonkar et al. (ref. 223). A 5.5-ft-diam three-bladed model rotor (fig. 49) similar to that used for hover experiments described above, was tested up to a moderately high (0.55) advance ratio. In order to simplify operation and minimize nonlinear lead-lag damping of pitch bearings, the model did not have a swashplate. Collective pitch was changed manually and the rotor was trimmed to minimize steady-state blade



flapping by varying the angle of attack of the rotor shaft. The results in figure 50 show the variation in lead-lag damping with advance ratio for several shaft angles at 0° and 3° collective pitch. Agreement between data and theory is very good except for the high shaft angle condition at 3° collective pitch. The inclusion of airfoil stall improved the correlation for this case but degraded correlation for the other cases. The detailed mechanisms of the stall influence are not yet clear since the rotor is operating at moderate lift levels; however, large angles of attack do exist for some regions of the rotor disc.

These experiments have done much to help our understanding of the dynamic behavior of hingeless rotor blades and have provided a large body of high-quality rotor-stability data that is useful for confirming theoretical predictions.

### FLAP-LAG-TORSION STABILITY

Flap-lag-torsion stability of cantilever rotor blades represents one of the important problems in rotorcraft aeroelastic stability. The effects of torsion generally tend to overpower the effects of coupled flap-lag structural dynamics. When blade torsion is coupled with flap and lead-lag bending, practical problems in aeroelastic stability of hingeless and bearingless rotor blades may be addressed. Articulated rotor blades are not strongly influenced by the structural bending-torsion coupling so important for cantilever rotor blades. Articulated rotor blades generally experience flap bending-torsion flutter, a result of unsteady aerodynamics and chordwise offsets of the airfoil mass, elastic, and aerodynamic centers (cf. ref. 224). Much of the research on cantilever blade flap-lag-torsion stability has focused on the effects of nonlinear bending-torsion structural coupling, as will be illustrated below. However, the chordwise aerodynamic offset couplings are also important for cantilever rotor blades and they, too, will be addressed.

### Hover Analytical Investigations

Before aeroelastic analysis of cantilever rotor blades that are fully elastic in bending and torsion, a simpler problem was addressed by Friedmann and Tong (ref. 5). They studied the stability of cantilever blades flexible in flap and lead-lag bending and with rigid body root pitch motion restrained by pitch-link flexibility. Results also presented in references 207 and 208 by Friedmann show the strong effect of root pitch motion stability as shown in figure 51.

With the development by Hodges and Dowell (ref. 6,8) of the general nonlinear equations applicable to combined bending and torsion of elastic cantilever rotor blades as described above, means were available to investigate the dynamic stability characteristics of hingeless rotor blades. Many studies were devoted to analysis of simple blades having radially uniform properties to help facilitate understanding of the essential dynamic phenomena. Several early studies of this kind were carried out by Hodges (ref. 6) and by Hodges and Ormiston (refs. 15,17,225). Typical basic

results are shown in figure 52 (from ref. 225) where stability boundaries are plotted as a function of the torsion natural frequency, a measure of torsional rigidity.

These results illustrate how the introduction of blade-torsion flexibility progressively alters the stability of the simpler flap-lag bending problem. It may be seen that the effects of torsion are significant for some configurations even at quite high torsion frequencies. Also presented are results of calculations that include the bending-torsion structural coupling but omit torsion dynamics. In this case the bending-torsion coupling generates effective pitch-lag and pitch-flap aeroelastic couplings that control stability in a manner consistent with the results of the simple rigid-hinged blade flap-lag analyses discussed above. Only for very flexible blades does torsion dynamics significantly alter flap-lag-torsion stability, because most of the effect of torsion flexibility is due to structural coupling.

Because the torsion structural coupling is so powerful, small amounts of blade precone or droop, usually introduced to reduce steady blade stresses, can have a large effect on stability. Figure 53 illustrates the influence of precone for configurations with ( $R = 1.0$ ) and without ( $R = 0$ ) structural flap-lag coupling (ref. 15). At low rotor thrust, the steady blade bending counteracting the built-in precone produces a destabilizing pitch-lag coupling effect that causes a "precone instability." As thrust increases and the blade equilibrium deflection coincides with the precone orientation, the destabilizing coupling is removed, and stability returns. At higher rotor thrust, other instabilities may occur, especially for stiff-inplane configurations without flap-lag structural coupling. The effects of droop can be similar to precone. Droop is a built-in flap rotation of the blade outboard of the pitch bearing, whereas for precone the pitch bearing axis has the same built-in flap rotation as the blade and hence remains in alignment with it. The similarity between the effects of precone and droop is determined by the ratio of pitch-link stiffness to blade-torsional rigidity,  $f$ . Results in figure 54 (from ref. 17) compare the effects of precone and droop on flap-lag-torsion stability boundaries and show that depending on the value of  $f$ , precone and droop have identical or very different effects on the flap-lag-torsion stability boundaries.

In reference 226, Johnson presented results of a flap-lag-torsion stability analysis for comparison with the results of reference 15 in order to validate the analysis of reference 85. Good qualitative agreement was found.

Friedmann extended earlier results by investigating flap-lag-torsion stability of blades with elastic torsion, using improved equations (ref. 19). These equations retained root pitch motion and added flap-lag structural coupling and airfoil chordwise offsets. Results in figure 55 (from ref. 20) show the effect of aerodynamic center offsets on stability and divergence boundaries. Friedmann also showed that structural damping is moderately effective in eliminating the precone instability.

Reddy investigated flap-lag-torsion stability of elastic blades in hover, including the effects of dynamic inflow (refs. 166,168). His results were obtained using computerized symbolic manipulation to derive and solve modal equations for

elastic blades. This permitted an easy means of examining the influence of small terms in the equations of motion. Figure 56 illustrates the effects of dynamic inflow on lead-lag damping at a moderate collective pitch angle.

To deal with practical rotor-blade configurations, especially bearingless-rotor blades, more advanced structural analysis methods are needed and researchers have begun to address this area. Chopra and Sivaneri (ref. 66,67) applied finite-element methods to the elastic-blade flap-lag-torsion problem (fig. 57) and demonstrated close agreement with earlier modal-analysis results from reference 15. More advanced work by Hong and Chopra treated hingeless rotor blades constructed of composite materials (ref. 78). Using a finite-element method, they showed how aeroelastic tailoring of the spar ply layup configuration could stabilize or destabilize the lead-lag mode damping. A root locus plot shown in figure 58 illustrates these results.

There have been other applications of flap-lag-torsion aeroelastic stability analysis, including circulation control rotors by Chopra and Johnson (ref. 227) and constant-lift and free-tip rotors by Chopra (ref. 228).

### Effects of Unsteady Aerodynamics

The effect of unsteady aerodynamics on flap-lag-torsion stability in hover has also been investigated. Pierce and White examined the effect of compressibility on flap-pitch flutter owing to Theodorsen and Loewy aerodynamics (ref. 229). Friedmann and Yuan (ref. 110) studied the influence of different unsteady aerodynamic theories on flap-lag-torsion stability, as shown in figure 59. These theories included classical incompressible unsteady aerodynamic theory such as Theodorsen and Loewy, compressible theories such as Possio, Jones, and Rao, in comparison with conventional quasi-steady theory. In some cases the influence of unsteady aerodynamics is small; in other cases it may be significant.

### Flap-Lag-Torsion Hover Experiments

A number of experiments on flap-lag-torsion stability of hingeless rotors in the hub fixed condition have been conducted in order to validate analysis of cantilever rotor-blade stability. Sharpe (ref. 230) tested a 5.5-ft-diam two-bladed model rotor intended specifically to validate the theoretical analyses of references 16 and 17. The cantilever blades were designed to be uniform in mass and stiffness and with no chordwise offsets of aerodynamic or mass centers. Blade-root-to-hub attachments were designed to provide variations in precone, droop, and pitch restraint stiffness. An illustration of the model is given in figure 60. Typical lead-lag damping measurements are shown together with theoretical predictions in figure 61. The comparisons with theory reveal that the analysis is quite accurate at low pitch angles, whereas there are significant differences at higher blade pitch angles. These differences are attributed in part to airfoil stall effects magnified by the low test Reynolds number. Figure 62 demonstrates that the variations of

damping with precone and droop are accurately predicted for  $\theta_0 = 2^\circ$  where airfoil stall effects are not present.

Another experimental investigation of flap-lag-torsion stability was conducted in the NASA Ames 40- by 80-Foot Wind Tunnel with a full-scale, four-bladed BO-105 soft-inplane hingeless rotor. Because of the size of the rotor test apparatus, the rotor-blade stability results were considered representative of a fixed hub condition. Warmbrodt and Peterson compared measured regressing lead-lag damping against the CAMRAD theory for varying numbers of elastic blade modes with and without dynamic inflow (refs. 59,231-233). The results shown in figure 63 illustrate that correlation is improved with the addition of additional modes and dynamic inflow.

### Forward Flight Flap-Lag-Torsion Analysis

In the late 1960's, before development of strong interest in aeroelastic stability characteristics of hingeless rotor blades, an investigation of articulated-rotor instability at high speeds was sponsored by the Aviation Applied Technology Directorate. This study involved prediction and correlation with experimental data of articulated-rotor bending-torsion flutter (ref. 234); stall flutter (ref. 235); torsional divergence (ref. 236); and flapping and flap-lag stability (ref. 237). The predictions were obtained from stability analyses based on the equations derived by Arcidiacono in reference 2 which were also included as a part of the AATD-sponsored investigation. The bending-torsion flutter analysis used a classic fixed-wing approach; for the rotor in forward flight, a fixed azimuth approximation was used, holding aerodynamic properties constant corresponding to the particular azimuth being analyzed. The torsional divergence analysis was based on a similar assumption. Results emphasized the importance of airfoil aerodynamic center chordwise offset from the cross-section center of mass. Subsequent experimental investigations of Niebanck and Bain confirmed that the fixed azimuth assumption is very conservative (ref. 238). The flap-lag analysis of articulated-rotor blades, based on forced and transient response calculations, did not produce any unstable behavior in forward flight.

For the experimental investigation of reference 238, a 9-ft-diam, dynamically scaled, articulated-rotor model with several unbalanced chordwise center of mass positions was tested at speeds up to 300 knots and at advance ratios up to 1.0. A variety of unstable blade responses were encountered, including stall flutter, advancing-blade flutter, retreating-blade divergence, and flapping instability. The experimental results were compared with the analyses described above.

With the availability of Floquet theory and the increasing experience obtained from fully coupled flap-lag-torsion stability analysis in hover, government-sponsored researchers began to turn attention to the forward flight analysis of cantilever rotor blades. These studies were marked by progressive refinements in the analyses as the equations were improved and restrictive assumptions removed. Nevertheless it must be noted that this is a problem of considerable complexity. It involves determining the nonlinear trim state of a system of many degrees of freedom (if multiple modes for blade bending or torsion deflection are retained) in response

to unsteady excitation, obtaining linearized system equations, and performing a Floquet analysis. Some early results of Friedmann and Reyna-Allende (ref. 21) are shown in figure 64 for flap, lead-lag, and torsion-mode damping versus advance ratio. More refined results of Shamie and Friedmann (ref. 24) were based on equations derived from reference 22; the results are shown in figure 65. Differences in the results shown in figures 64 and 65 were attributed to the differences in the equations used in the two analyses. In general, the results of these two studies showed similar trends. Further investigation using multiple modes for bending and torsion deflections and improved solution procedures was carried out by Friedmann and Kottapalli in (ref. 174). Typical results for soft- and stiff-inplane configurations for both propulsive and moment trim conditions are shown in figure 66. These results again confirmed the general findings that stiff-inplane configurations are less stable than soft-inplane blades.

Reddy and Warmbrodt (ref. 168,218) also studied the flap-lag-torsion problem in forward flight and identified the effects of dynamic inflow and elastic coupling for soft- and stiff-inplane cantilever rotor blades as shown in figures 67(a) and 67(b). These results are in good agreement with those in figure 66, even though the blade parameters are not identical. The results of this investigation are unique in that they provide a clear and relatively complete picture of the aeroelastic stability behavior of hingeless rotor blades in forward flight. Furthermore, these results have been compared with work of earlier investigators, allowing some judgments to be made about the validity of the results when, as in the case of flap-lag-torsion stability of hingeless rotor blades in forward flight, appropriate experimental data are not available for correlation purposes.

#### COUPLED ROTOR-BODY STABILITY

An important class of rotorcraft stability problems arises from mechanical coupling between the rotor-system degrees of freedom and motions of the fuselage. This coupling gives rise to the classic ground resonance of articulated-rotor systems studied extensively by Coleman and Feingold (ref. 79) and others beginning in the early 1940's. With the emerging interest in hingeless rotors in the 1960's, mechanical instability began to receive renewed attention for configurations having lead-lag natural frequencies below rotor speed (soft-inplane). In the case of hingeless rotors, the strong rotor-body coupling generated by the cantilever blades significantly increased the complexity of the mechanical instability and created the potential for air resonance, as well as ground resonance. The work of Cardinale and his co-workers on the XH-51A Matched Stiffness Rotor helicopter (ref. 81), and of Lytwyn and Miao on the BO-105 (ref. 239) illustrate early efforts in aeromechanical stability. For stiff-inplane configurations, mechanical instability is not of practical concern; however the effects of rotor-body coupling may aggravate aeroelastic instabilities arising from blade or control-system characteristics. During the last 20 years, a significant amount of government-sponsored research on coupled rotor-body stability has been carried out, including analytical investigations and large- and small-scale experiments. This section will address coupled rotor-body

stability problems of conventional articulated and hingeless rotor helicopters. Rotor-body stability bearingless rotor and tilt rotor systems is discussed later in separate sections.

### Analytical Investigations in Hover and Forward Flight

Under AFDD sponsorship, Hohenemser and Yin investigated the stability and response of coupled rotor-body systems with feedback controls in order to understand fundamental rotor-stability characteristics and identify means to reduce gust response in high-speed forward flight. Hohenemser and Yin studied the whirl dynamics of a flapping rotor coupled to a body with pitch and roll angular freedom and found that whirl instability could occur for some configurations at high advance ratio (ref. 196). In reference 240 they studied feedback control systems designed to improve response characteristics and gust response of hingeless rotors operating at high advance ratios without inducing aeroelastic instabilities. Further studies of this type were conducted in references 241 and 242. Finally, Hohenemser and Yin investigated the stability of a flapping rotor on flexible supports using a finite-element formulation (ref. 61). Results showed how higher flap-bending modes could couple with support dynamics and influence stability of the coupled rotor-body system.

One important problem in the area of classic mechanical instability is the case of a rotor with one lag-damper inoperative. This asymmetric rotor problem gives rise to periodic coefficients in the equations of motion, even in the hover condition. Hammond treated this problem using both Floquet theory eigenanalysis and direct numerical integration (ref. 82). Typical results are shown in figure 68; they illustrate how the modal dynamic behavior increases in complexity and how the system can be destabilized as a result of losing one damper.

As noted above, hingeless rotorcraft mechanical instability is more complex than classical ground resonance. Early analyses of hingeless-rotor air and ground resonance were carried out in support of full-scale rotorcraft development programs; for example, the BO-105, XH-51, WG-13, and YUH-61A. However, there did not exist a clear understanding of the role of hingeless-rotor configuration parameters in determining aeromechanical stability. Aerodynamic damping acting through the hingeless-rotor flapwise hub moments was thought to counter air and ground resonance. The unsteady wake effects were not understood. Very little work had been done to study blade aeroelastic couplings; consequently, designers had little information to help make important design decisions.

In order to address these issues, government-sponsored analytical and experimental research was undertaken by the Army and NASA to develop a better understanding of this topic and thus help to design rotorcraft free of such instabilities. Ormiston carried out an extensive parametric investigation of hingeless-rotorcraft air and ground resonance using a simplified model consisting of a rigid-body fuselage and rigid-spring-restrained blades with flap-lag degrees of freedom (refs. 86, 87, 243). Initial results were presented in reference 243. Typical results are shown in figures 69 and 70 (from ref. 86); they show the effects of rotor

aerodynamics and collective pitch on ground- and air-resonance stability boundaries for a wide range of configurations. The results indicate that hingeless-rotor aerodynamic damping is stabilizing for air resonance but that as flap stiffness increases, stability decreases (contrary to what might be expected).

The effectiveness of aeroelastic couplings to alleviate air-resonance instability was also investigated, as shown in figure 71. Although blade aeroelastic coupling can be very effective in many cases, it is difficult to alleviate mechanical instability over a wide range of operating conditions for a fixed set of configuration parameters. The results of this study revealed that aeromechanical instability of soft-inplane hingeless-rotor helicopters is indeed a very complex subject, even for the simplified physical model employed in the analysis. In another study, Ormiston explored in depth the detailed properties of the coupled rotor-body dynamic modes and how they influenced air resonance behavior (ref. 87).

Other investigators have studied the effects of dynamic inflow on hingeless-rotor air resonance. Since the aerodynamic damping resulting from cantilever blade-flap stiffness exerts a powerful influence on hingeless rotor dynamics, it would be expected that dynamic inflow might have a potentially significant effect on air resonance stability. Gaonkar et al. (ref. 159) extended the aeromechanical stability investigation of Ormiston to include dynamic inflow; a typical result is shown in figure 72. In this example air resonance was stabilized; in other results the opposite was shown to occur. Nagabhushanam and Gaonkar extended the rotor-body hover analysis to forward flight and studied the effects on stability of dynamic inflow models and trim methods, for soft- and stiff-inplane configurations (ref. 163). A typical result in figure 73 shows how strongly the trim condition influences coupled rotor-body stability in forward flight. In reference 244, Johnson also analyzed the aeromechanical stability of a soft-inplane helicopter in forward flight, using the equations developed in reference 85. Another approach receiving renewed attention is the use of feedback control to stabilize air resonance instability. Straub and Warmbrodt showed promising results using a relatively basic approach, with cyclic lag and body angular rate feedback to control cyclic pitch (ref. 245).

Venkatesan and Friedmann also studied coupled rotor-body stability of a multi-rotor hybrid airship (ref. 98,246).

#### Rotor-Body Experiments in Hover and Forward Flight

One of the first experimental investigations of rotor-body aeromechanical stability was conducted by Burkham and Miao at Boeing Vertol, using a 1/14th-scale, Froude-scaled model of the BO-105 helicopter (ref. 247). An important series of experiments was conducted at the Aeroflightdynamics Directorate by Bousman (refs. 158,248,249) to confirm analytical results obtained in reference 86 for hingeless-rotor aeromechanical stability. The resulting data, obtained for the hover condition using a 5.5-ft-diam model, are noteworthy for both quantity and quality and have been used in numerous aeroelastic correlations. Several rotor and body configurations were tested over a range of rotor speed and collective pitch for

different fuselage restraints and blade aeroelastic couplings. Frequency and damping were obtained for all measurable fuselage and blade modes. As in previous AFDD experiments, rigid-hinged blades with flap and lead-lag flexures were used. In addition a simulated in-vacuum condition was tested, using non-airfoil shaped stub blades.

Figure 74 shows the in-vacuum rotor configuration mounted on a motor-transmission gimbal frame structure that represented a fuselage with pitch and roll degrees of freedom. Frequency and damping results versus rotor speed for this model are shown in figure 75 (from ref. 249). Comparison with Hodges' FLAIR analysis (ref. 57) shows excellent correlation for the frequencies of four rotor and body modes and excellent correlation for lead-lag damping of the regressing lead-lag mode. This would be expected for a clean mechanical model without aerodynamic effects. These results confirmed that the physical model, configuration definition, test, and data analysis procedures were sufficiently refined to produce very high quality data.

The airfoil-blade rotor configuration, mounted on an improved fuselage frame having flex pivots in place of ball-type gimbal bearings, is shown in figure 76. In figure 77, a sampling of regressing lead-lag mode damping results from reference 158 exhibits very low data scatter and agrees well with predictions of the FLAIR theory. These results clearly confirmed trends predicted by earlier analyses for the basic effects of rotor speed that reduce damping at body pitch and roll frequency coalescences, the destabilizing effect of collective pitch, and the influence of aeroelastic couplings where damping is dependent on configuration. Systematic discrepancies between theory and measured results for some configurations indicate that not all phenomena are accurately accounted for; likely candidates were postulated to be unsteady aerodynamics, and possibly, blade flexibility.

Bousman's experimental results also led to new insights about the role of unsteady aerodynamics in low-frequency coupled rotor-body dynamics. The effects of dynamic inflow on coupled rotor-body modal frequencies were discussed above in section 2. The measured damping data also provided confirmation of suspected sources of discrepancies in body-pitch and roll-mode damping, as shown in figure 78 by calculations by Johnson with and without dynamic inflow (refs. 160,161). The effects of dynamic inflow on lead-lag regressing mode damping are shown in figure 79, where dynamic inflow marginally improves the agreement between analysis and data. Interestingly, Johnson's predicted lead-lag regressing-mode damping with dynamic inflow does not agree with the data as well as Bousman's prediction without dynamic inflow in reference 158, using Hodges's FLAIR analysis. This indicates that the prediction of aeromechanical stability may be rather sensitive to small details of the analysis. Friedmann and Venkatesan also correlated analyses with Bousman's data (refs. 250,251). They also confirmed the favorable effects of dynamic inflow on the correlation, and furthermore, in reference 250, their predictions of regressing lead-lag damping correlated well with data at high rotor-blade collective pitch angles where correlation was rather poor for the FLAIR analyses.

Other coupled rotor-body experiments have been carried out; Yeager et al. tested a hingeless-rotor research model in the Langley Transonics Dynamics Tunnel



for hover and forward flight conditions (refs. 252,253). Good correlation was achieved with predictions by the CAMRAD analysis.

## BEARINGLESS-ROTOR STABILITY

The bearingless-rotor configuration, a refinement of the basic hingeless rotor, has been the subject of much development activity by the helicopter technical community and the focus of a significant amount of government research. The isolated bearingless-rotor blade encompasses all of the basic flap-lag-torsion aeroelastic stability characteristics of hingeless blades described above, as well as additional complications of the flexbeam and pitch control mechanisms. Because of the wide variations in different bearingless rotor configurations and the more pronounced effects of higher blade-bending modes, bearingless-rotor stability characteristics can be more difficult to understand or to generalize than those for hingeless rotor blades.

Since most of the applications have been soft-inplane configurations, many bearingless-rotor investigations have also treated air and ground resonance and thus included coupled rotor-body dynamics. It is, therefore, appropriate to survey both isolated rotor blade as well as coupled rotor-body studies, as a single topic in this section.

### Bearingless-Rotor Stability Analysis

Bielawa carried out one of the first analytical investigations of bearingless-rotor aeroelastic stability using the G400 analysis described above to evaluate the stability of candidate full-scale bearingless rotors for application to the RSRA aircraft. Hover stability results were presented in reference 56 for soft- and stiff-inplane isolated (fixed hub) rotor-blade configurations having snubbed torque tubes. Instabilities were evident at high collective pitch angles, and these were aggravated by airfoil stall effects. The first three flap-bending modes, the first two edgewise-bending modes, and the torsion mode were highly coupled and led to very complex behavior.

Development of FLAIR by Hodges (described earlier in section under Helicopter Equation) was initiated to support the full-scale Bearingless Main Rotor (BMR) developed and flight tested on a BO-105 helicopter by Boeing Vertol under Army AATD sponsorship. The BMR development program is described in more detail in a later section. The simplified FLAIR analysis considered the blades to be rigid in bending and torsion, attached to a uniform stiffness flexbeam modeled by exact nonlinear bending-torsion equations for a continuous flexible beam. The rotor was attached to a rigid-body fuselage having pitch and roll degrees of freedom. Quasi-steady aerodynamic theory was used for the hover condition only. The FLAIR analysis was used by Hodges in reference 186 to identify the configuration parameters that would maximize the air and ground resonance stability of the BMR configuration

(ref. 58). The Boeing Vertol BMR configuration corresponds to Case II in figure 10. Parameters such as flexbeam and blade precone, droop, sweep, and flexbeam pre-pitch were studied. Air resonance was easily stabilized over a reasonable rotor speed range; however, ground resonance was more difficult. The FLAIR analysis was also checked by Hodges (ref. 88) against model-scale BMR experimental measurements of air and ground resonance stability reported in reference 254. Typical results are shown in figure 80 for two different BMR configurations; there is generally good agreement between FLAIR and the measured data.

Sivaneri and Chopra developed a finite-element, bearingless-rotor blade analysis capable of modeling a twin flexbeam configuration (refs. 59,67). They compared the accuracy of a simplified approach using a single flexbeam to represent a dual flexbeam configuration, an approach that they found to be inaccurate in some cases.

### Bearingless-Rotor Experimental Investigations

Considerable experience in testing bearingless rotors has been gained through government research and development activities, including development of prototype systems. Only a part of this has been focused to meet specific research objectives; therefore, there is a need for continuous experimental investigations in this area.

A moderate amount of experimental testing data has been accumulated through development testing of prototype rotorcraft systems. These developments are discussed in section 4. The Boeing Vertol Bearingless Main Rotor (BMR) program was particularly noteworthy for the amount of test data obtained (refs. 89,90). Extensive test data for the 1/5.86-Froude-scaled BMR model was reported by Chen et al. (ref. 254). An interesting correlation of model data, full-scale flight-test data, the FLAIR analysis, and the Boeing Vertol C-45 rigid-blade analysis for a hover air resonance condition of the BO-105/BMR is shown in figure 81. Following the BMR flight-test program, extensive experimental testing of the full-scale BMR rotor was conducted in the 40- by 80-Foot Wind Tunnel as described in section 4. Typical experimental results from reference 255 are shown in figure 82 together with predictions from a Boeing Vertol code. The rotor apparatus used for the wind-tunnel testing provided a nearly hub-fixed condition for the rotor, therefore, the results represent isolated rotor-blade stability.

A series of experimental investigations using a small-scale bearingless-rotor model was carried out at AFDD by Dawson with the specific intent of verifying the FLAIR analysis and of investigating bearingless-rotor stability characteristics in general (ref. 256). This model was designed to accommodate variations of a wide variety of flexbeam and control-system geometric parameters to permit testing a wide variety of bearingless-rotor types. These features are illustrated in the exploded view of the hub, flexbeam, pitch control torque tube, and pitch links (fig. 83). The model was tested in both two- and three-bladed versions. Typical results from reference 256 for lead-lag damping versus blade-pitch angle are shown in figure 84 at two different rotor speeds and for two different pitch-control configurations. The correlation with the FLAIR analysis is reasonably good; however, instances of flutter involving unsteady aerodynamics not treated by FLAIR were also

encountered. Further experimental investigation by Bousman and Dawson of the flutter results identified several distinct types of flutter that may be experienced by bearingless rotors (ref. 257).

Finally, a considerable amount of small-scale experimental data has been obtained by Weller and Peterson for the air resonance characteristics of an advanced bearingless rotor in hover and forward flight (refs. 258-260). These results are more fully described in section 4. In addition, small-scale experimental studies in connection with the ITR/FRR Project were conducted in hover and forward flight, as noted in section 4. The Boeing Vertol ITR bearingless-rotor model testing was reported by Mychalowycz (ref. 261).

### TILT-ROTOR AIRCRAFT STABILITY

In the early 1960's, considerable attention was given to the problem of rotor-pylon stability of tilt-rotor aircraft. Before the emergence of the tilt-rotor, research had been performed in efforts to understand the problem of classical propeller whirl-flutter instability where nacelle pitch and yaw motions are coupled through gyroscopic effects of a spinning rigid propeller. Reed and Bland (ref. 262) and Houbolt and Reed (ref. 263) investigated both classical propeller whirl flutter and static divergence, using rigid-rotor models. A comprehensive review of propeller whirl flutter by Reed can be found in reference 264.

Actual tilting proprotor stability analyses were subsequently found to be considerably more complicated than classical propeller whirl flutter. The importance of rotor flapping for tilting proprotor configurations was first investigated by Young and Lytwyn (ref. 265). Using a representation including yaw and pitch motion of a rigid nacelle and with rigid flapping for each blade, it was shown that a forward whirl instability was possible but would be self-limiting because of nonlinear aerodynamics. Most importantly, it was found that increased blade flexibility reduced the pitch and yaw stiffness requirements for proprotor whirl flutter, thereby allowing weight reductions for the pylon mounting in tilt-rotor aircraft.

During development and testing of the Army Bell XV-3 tilt-rotor aircraft, further investigations of proprotor whirl flutter were carried out by Hall (ref. 266) and Edenborough (ref. 267); they provided additional understanding of rotor-pylon dynamics. Two potentially unstable modes were identified for an XV-3-type tilt-rotor aircraft: a pylon mode at a frequency near the natural frequency of the pylon, with little rotor flapping, requiring little damping for stabilization; and a rotor mode at much lower frequency, with large rotor flapping, requiring substantial damping for stabilization.

### Coupled Rotor, Pylon, and Rigid-Body Dynamics

In the early 1970's, following initiation of the XV-15 program, the government increased efforts to improve analysis capabilities and understanding of tilt-

proprotor aircraft stability. Up to this time, no dynamic analysis of a full rotor-pylon-wing-airframe system had not been undertaken. Kvaternik developed the analysis of reference 99 to better understand wing-rotor dynamics using a linear analysis of an idealized proprotor in cruise-mode flight with rigid, spring-restrained flapping blades. This analysis was used to predict the aeroelastic stability of a small-scale model of the Bell Model 266 tested in the Langley Transonic Dynamics Tunnel. Figure 85 shows a comparison of experimental and analytical results for two configurations of the model, with and without aerodynamics. The analysis of reference 99, together with an extensive small-scale-model test program conducted in the Langley Transonic Dynamics Tunnel with Grumman (ref. 100), was used by Kvaternik and Kohn to investigate the applicability of a simple mathematical model to predict whirl flutter for both backward and forward whirl modes. The model is shown in figure 86. The study showed the ability to predict dynamic stability from such a simple mathematical model using linear aerodynamics for both types of rotor-pylon instabilities. Additional descriptions of these investigations are reported in references 268 and 269.

In support of the development testing of the XV-15 tilt-rotor aircraft, Johnson used a sophisticated analysis for predicting tilt-rotor aeroelastic stability behavior. The initial analysis (ref. 101) treated rotor-blade flap and lag elastic bending and wing beam bending, chord bending, and torsion, and was used to study the sensitivity of analytical predictions to various elements of the theoretical model. This analysis was also used for comparisons with results of two full-scale semispan prop-rotor-wing models tested in the NASA Ames 40- by 80-Foot Wind Tunnel. The Boeing Vertol soft-inplane proprotor configuration tested in the wind tunnel is shown in figure 87; measured results for damping of the wing vertical bending mode for a Boeing Vertol soft-inplane configuration are compared with analytical predictions in figure 88. Johnson also discussed these results in reference 270.

Johnson further investigated the sensitivity of tilt-proprotor stability to details of the analytical model (ref. 271). That investigation used an extended version of the equations of reference 101, including coupling of rotor-blade flap-lag bending deflections, blade torsion, additional blade-bending modes, rotor rotational speed perturbations, and wing aerodynamic forces. Typical results (fig. 89) indicate the importance of blade-pitch and blade-lag motion on wing bending-mode damping. In reference 103 Johnson investigated the influence of the rotor shaft (rotational) degree of freedom. When rotor shaft angular rotation is unlocked from the wing tip rotation (which accompanies wing tip vertical deflections), rotor aerodynamic damping no longer damps wing vertical bending motion, resulting in a pronounced destabilizing effect. He also showed that interconnect shaft dynamics were important in coupled rotor-wing antisymmetric modes, as shown by the typical results in figure 90. Johnson also investigated the importance of pitch-lag coupling on proprotor stability (ref. 272). Proprotors have built-in blade precone for relieving high steady blade-flap bending moments in hover. However, in the cruise mode, with reduced rpm and significantly reduced thrust, the elastic bending decreases the blade coning. The resulting negative pitch-lag coupling then becomes destabilizing. This coupling can be reduced using increased control-system

stiffness or by introducing blade droop. This work also investigated the effects of lift divergence at high speed where compressibility effects reduce aeroelastic stability, as shown in figure 91.

In preliminary studies for the XV-15 aircraft, a soft-inplane proprotor was investigated analytically and experimentally by Alexander et al. (ref. 273). Unlike a stiff-inplane rotor system, a soft-inplane system can experience air resonance at low speed when the regressing lead-lag motion coalesces with the wing vertical bending mode. Once again, the rotor rotation degree of freedom is very important; otherwise the wing mode is incorrectly predicted to be highly damped. The results of this study showed excellent damping predictions compared with full-scale 40- by 80-Foot Wind Tunnel data for the full-scale semispan Boeing Vertol rotor-nacelle-wing model.

Subsequent to the XV-15 wind-tunnel and flight-test program, Johnson (ref. 104) assessed the capability to predict performance, loads, and stability of the XV-15 aircraft, using the CAMRAD comprehensive analysis of reference 94. The conclusions from that study for tilting proprotor dynamics recognize the established confidence in predicting whirl flutter for the configurations that have been built and tested. However, new configurations with expanded flight capabilities will require new treatment and analyses to overcome current shortcomings.

A good indication of the capabilities for predicting proprotor whirl stability is provided in figure 92, which shows test results obtained for a V-22 Osprey model tested in the NASA Langley Transonic Dynamics Tunnel (refs. 274-276). Measured damping data for several test configurations are compared with predictions by CAMRAD, PASTA, and a Bell analysis DYN4. Although some preliminary adjustment in the input parameters of the analyses is usually necessary, the agreement between test and analysis is reasonably good.

#### Methodology Assessment

It is a given that theoretical prediction methods for rotorcraft aeroelastic stability require validation of some sort to be accepted as trustworthy. There are many ways of doing this. Three typical approaches are to check the predictions with (1) a known closed-form analytical solution to a theoretical problem, (2) results from other validated programs, and (3) experimental data.

A useful way to validate individual computer programs and at the same time assess the analytical state of the art in a given technical field is to analyze the same problem with several programs and compare the results. This has value for hypothetical problems (comparing only computer results), but it is obviously more desirable to analyze a problem for which experimental data are also available. Such an exercise is particularly useful in the rotorcraft dynamics technical community, especially given the many independent computer programs used within the industry. Validation for these codes is often minimal or limited to a narrow range of vehicle or rotor configurations. Taken collectively, the comparisons serve to calibrate the prediction methods for specific applications and identify areas where additional

research effort might have a high payoff. The results often provide the clues or information useful in upgrading individual codes.

A methodology assessment of this type was conducted by the Aeroflightdynamics Directorate in connection with the ITR/FRR Project in June 1983 (ref. 277). Aeroelastic stability predictions were compared with a variety of carefully selected experimental data encompassing simple and complex rotor blades; isolated rotor and coupled rotor-body configurations; and small- and large-scale rotors operating in hover, wind-tunnel, and flight-test conditions. A total of eight different prediction codes from industry, universities, and government laboratories were included in the comparisons. The results were very useful, and a few are included herein to illustrate some of what was learned.

The first case is for the elastic hingeless-rotor-blade model discussed in section 3. Data for lead-lag damping in the hover condition (ref. 230) are used to compare with predictions for two cases, one without built-in blade droop and the other with  $-5^\circ$  droop. Predicted results without droop (fig. 93(a)) are relatively good for most of the analyses except at higher pitch angles where airfoil stall occurs. The situation changes completely for the droop configuration, shown in figure 93(b). Now the correlation is poor and there is a wide spread among the predictions. The only difference in the two cases was a "small change" in rotor geometry. Since the bending-torsion behavior of cantilever elastic blades is very sensitive to the precone and droop, it may be concluded that the basic structural dynamics was not adequately modeled. One benefit of such comparisons is the insight and stimulus to correct such discrepancies by identifying the sources of error in the program. Although such a problem had not been previously suspected, the G400 analysis was revised to correct the undiscovered problems in the analytical treatment of the blade structural deformations. The revised G400 results included in figure 93 were a substantial improvement over the original calculations.

Another example is regressing lead-lag mode damping of the coupled rotor-body dynamic system of Bousman described previously. Figure 94 shows experimental data at  $\theta = 9^\circ$  (ref. 158) compared with the predicted results of various analyses. Again, there is a considerable scatter in the predictions, even though the general trends are reasonably well represented. Given that only quasi-steady aerodynamic theory and hinged-rigid blade dynamics are included, it would be expected that the predictions would be in much closer agreement.

In order to determine the sources of differences between the various predictions it is necessary to compare the equations directly at some level or to compare predictions for a simplified problem in stages until the differences are accounted for.

#### 4. EFFECT OF AEROELASTIC STABILITY CHARACTERISTICS ON ROTORCRAFT SYSTEMS

Previous sections have addressed the development of analysis methods for aeroelastic stability and investigations of the different types of aeroelastic stability

phenomena exhibited by rotor blades and coupled rotor-body systems. This section will describe the effect of aeroelastic stability considerations on the design of specific rotorcraft systems. Insights provided by development and testing experience will also be addressed. The purpose is to identify the government research that contributed to the development of these systems, such as helping to insure freedom from instability, resolving unexpected occurrences of aeroelastic instability, or supporting research on a particular class of rotor systems to overcome inherent aeroelastic stability limitations.

## HINGELESS ROTORS

During the 1960's considerable interest arose in the hingeless rotor as a natural step in the evolution of a simpler, lighter, and more reliable helicopter rotor. Much of the early interest was sparked by the Lockheed CL-475 and XH-51A gyro-controlled, rigid-rotor vehicles, the MBB BO-105, and the Westland WG-13 Lynx. Hingeless rotors offer a number of advantages such as elimination of heavy, bulky, and unreliable hinges and bearings of articulated rotors and the potential to eliminate lead-lag dampers used to prevent ground resonance. The many possible configurations and associated design variables complicate the subject of hingeless-rotor aeroelastic stability, and the potential for instability makes it central to the design of a successful system.

### AH-56A Cheyenne

The U.S. Army Lockheed AH-56A Cheyenne was a high-speed compound helicopter designed as an advanced aerial fire support system. The gyro-controlled stiff-inplane hingeless rotor was derived from the highly successful Lockheed XH-51 demonstrator aircraft that was flown as both a pure and compound helicopter. The hingeless rotor, combined with a mechanical gyro feedback control system, provided high maneuverability and low gust response. The stiff-inplane rotor precluded the need for lag dampers to suppress ground or air resonance instability. However, during flight testing the AH-56A revealed several aeroelastic instabilities not encountered with the XH-51, a result of differences in design details of the scaled-up AH-56A configuration. Furthermore, the hingeless rotor was a significant departure from conventional articulated rotor configurations, and the complex behavior of stiff-inplane hingeless rotors was not adequately understood at the time. As a result, this experience stimulated a wide range of basic research into the aeroelastic stability of hingeless-rotor systems and indeed much of AFDD research grew out of AH-56A development experiences. Following the conclusion of the AH-56A program, the U.S. Army Aviation Systems Command and the Aeroflightdynamics Directorate sponsored a Lockheed effort to document the experience obtained regarding dynamics phenomena of this aircraft. This information is contained in reports by Donham and Cardinale (ref. 278) and Johnston and Connor (ref. 279). Additional sources for this and other information are Johnston and Cook (ref. 280), Anderson (ref. 281), and Anderson and Johnston (ref. 282).

During early development of the AH-56A, two problems received most attention. The 1P-2P phenomenon (ref. 278) occurred at low rotor speed in the presence of high rotor hub moments as might occur in ground contact, where nonlinear blade-feathering moments resulting from combined flap and lead-lag bending were fed back into the control gyro in such a way as to produce a coupled rotor-gyro instability. The second problem, termed 1/2 P-Hop (refs. 279,282), involved coupling of the lead-lag regressing mode, vehicle roll mode, collective rotor flapping, and vehicle vertical translation near the regressing inplane frequency of about 0.5 per rev. This phenomenon occurred in high-speed flight and led to loss of an aircraft.

Because of the high advance ratio and proximity to a half-integer frequency, the 1/2 P-Hop stimulated interest in the use of Floquet theory to treat periodic-coefficient systems. To further study the problem, the AH-56A was installed in the 40- by 80-Foot Wind Tunnel at Ames for further testing under controlled conditions (fig. 95). Early in the test, while at a moderate-speed, high-thrust condition a rotor pitch-up divergence occurred that destroyed the test vehicle. This instability was attributed to aerodynamic stall-feathering moments overpowering and destabilizing the normal gyro feedback generated by rotor flapping. Following this incident, the Advanced Mechanical Control System (AMCS) was developed, using direct flap feedback from the blades instead of indirect feathering moments. This eliminated the source of both the 1P-2P and moment stall instabilities. A final problem of the reactionless mode instability was encountered during a low-speed, high-gross-weight condition (refs. 279,281). This was essentially an isolated-blade flap-lag-torsion instability of the type discussed previously.

During the AH-56A Cheyenne development, government researchers worked closely with Lockheed engineers to attempt to understand the new phenomena being encountered and to devise means to eliminate the problems. This program was instrumental in revealing the complexity of stiff-inplane hingeless-rotor aeroelastic stability and the necessity of a firm technology base on which to launch a major development program. Government research subsequently confirmed the complexity of hingeless-rotor aeroelastic stability characteristics and provided key information to guide further rotor system developments.

### Bell Flexhinge Rotor

The two-bladed teetering rotor has long been synonymous with Bell Helicopter Textron but in recent years the company has developed several production hingeless-rotor helicopters and has flight tested a prototype bearingless rotor. These accomplishments were preceded by an active research and development effort, much of it in cooperation with or sponsored by the government. While much of this research addressed flying qualities, rotor loads, and vibration characteristics, aeroelastic stability played a prominent role in the later stages of development. Early Bell hingeless rotors from the first Model 47 flown in 1957 to the Model 609 flexbeam rotor tested on the UH-1 under Army sponsorship in 1972 (ref. 283) were stiff-inplane configurations. The chief drawbacks of these rotors were excessive chord-wise blade stresses in high-speed and maneuvering flight.



To resolve these problems, Bell evolved a soft-inplane version of the Model 609 rotor, using elastomeric lag hinges and dampers, and demonstrated greatly reduced chordwise bending moments in flight tests. The dampers insured air and ground resonance stability. Bell initiated further investigations of the aeromechanical stability of soft-inplane rotors using a small-scale research and development rotor, the Model 652, having capabilities to vary the aeroelastic coupling parameters. In cooperation with the U.S. Army Aerostructures Directorate and NASA Langley, the Model 652 rotor was extensively tested for aeromechanical stability in the Transonic Dynamics Tunnel, as reported by White and Weller (ref. 284). They investigated effects of elastomeric damping, kinematic pitch-lag coupling, pitch-flap coupling, flap-lag coupling, and hub stiffness. They also analytically investigated ground resonance using combinations of rotor blade pitch-lag and flap-lag coupling that Ormiston found effective for increasing lead-lag damping of a fixed-hub rotor (ref. 202). However, for coupled rotor-body configurations including pylon flexibility, they were unable to stabilize both the pylon and ground-resonance mode with a single combination of couplings.

Bell completed development of a refined version of a soft-inplane hingeless rotor, the Model 654, using elastomeric dampers to insure ground and air resonance stability, and conducted successful flight testing of a Model 206L aircraft (ref. 285). Bell used a similar approach to insure stability of the Flexhinge Rotor, subject of a predesign study for candidate rotor systems for the Rotor Systems Research Aircraft (ref. 286).

## BEARINGLESS ROTORS

The hingeless-rotor concept is based on simplifying the rotor hub by eliminating blade flap and lead-lag hinges and carefully designing the structure to permit necessary blade-motion response without incurring excessive bending stresses. The bearingless rotor simply extends this idea and eliminates the blade-pitch-change bearing as well, substituting a flexbeam of sufficient torsional flexibility to accommodate the required pitch-change motion of the blade. Elimination of the rotor-hub bearings significantly reduces weight, complexity, and maintenance, thereby increasing helicopter productivity and reliability. However, aeroelastic complexity of the bearingless rotor introduces new unknowns in the development of advanced rotorcraft.

### XH-51A Matched-Stiffness Rotors

The XH-51A Matched Stiffness Rotor program was conducted by Lockheed California Company under sponsorship of the Aviation Applied Technology Directorate to improve the gyro-controlled rigid-rotor design proved by the basic XH-51A aircraft. The basic gyro control system was designed to sense rotor-flapping motion caused by external disturbances and to feed back appropriate cyclic pitch to counter the flapping response. The mechanical system for sensing blade-flapping moments also

sensed blade-pitch moments that could potentially contaminate the feedback signal. Hence any reduction of blade-torsion moments was desirable. The nonlinear torsion moments, which result from combined flap and lead-lag bending, vanish for rotor blades with equal flap and lead-lag bending stiffnesses; therefore, the so-called matched-stiffness blade promised to eliminate a principal source of gyro-control contamination and permit a reduction in the size of the gyro. When the lead-lag stiffness was reduced to match the flap stiffness, the rotor also became soft-inplane, and therefore susceptible to ground and air resonance. The study of these phenomena became the principal focus of the program.

While the design for a matched stiffness configuration was being formulated, it was also decided to incorporate another feature: replacement of the feather bearings with a flexbeam, thus converting the hingeless rotor to a bearingless rotor. No auxiliary damping was used in the design of the rotor. As reported by Cardinale (ref. 81) and Donham et al. (ref. 287) the XH-51A Matched Stiffness Rotor system did not exhibit a sufficiently wide stable range of rotor speed to operate safely throughout the flight envelope. Nevertheless, the ground and air resonance boundaries were extensively documented for ground-contact conditions and for hover and low-speed flight, and a number of configuration changes were evaluated and correlated with theoretical analyses. The program provided valuable experience that aided later bearingless-rotor development programs such as that of the Boeing Vertol Bearingless Main Rotor.

### Composite Bearingless-Rotor Design Studies

Increasing interest in bearingless rotors, together with the development of the Army-NASA Rotor Systems Research Aircraft (RSRA) for flight testing advanced rotor systems, resulted in government sponsorship of several preliminary design studies of candidate rotor systems. These studies emphasized the application of composite materials to the bearingless-rotor concept and gave special consideration to the requirements for adequate levels of aeroelastic stability. These studies were discussed by Swindlehurst in reference 288.

One of the first studies of the bearingless rotor for eliminating all hinges and bearings through the use of composite materials was initiated at UTRC in 1968. In the Composite Bearingless Rotor (CBR) concept, two flexbeam members crossed at the center of the rotor form the spars of a four-bladed rotor. The early UTRC work led to Army and NASA support for analytical and design studies including composite materials investigations, small-scale model testing, development and correlation of stability analysis with test data, and preliminary design layouts of a full-scale rotor. Results of this work were reported by Bielawa et al. (ref. 56). Both two- and four-bladed stiff-inplane configurations with pinned-pinned torque tube and cantilever torque tube pitch-control systems were wind-tunnel tested in the fixed hub condition. The G400 program developed by Bielawa (ref. 55) was used for this investigation. Principal aeroelastic test results and correlations with analysis involved blade-bending moment response and stresses. The results also verified the analysis, in that all experimental cases observed to be stable were also predicted

to be stable. Experimental results did indicate a tendency for the cantilever torque tube configuration to exhibit adverse pitch coupling resulting from torque-tube flapwise motion under some operating conditions.

The full-scale Composite Bearingless Rotor design used a four-bladed 62-ft-diam rotor sized for an S-61 class aircraft. Two torque tube configurations were designed, a cantilever torque tube and a snubbed torque tube to eliminate the potential for adverse couplings owing to flapwise motion of the torque tube observed in the model tests. An aeroelastic stability analysis of the full-scale snubbed torque tube configuration was carried out using the G400 analysis for both stiff- and soft-inplane versions of the design and showed both configurations to be stable for the conditions analyzed.

Another government-funded design study was undertaken by Boeing Vertol to evaluate the feasibility of a four-bladed Composite Structures Rotor (CSR) for installation and testing on the NASA-Army RSRA (ref. 289). The CSR design was roughly similar to the BMR configuration, having twin flexbeams, a torque shaft between the flexbeams, and no auxiliary elastomeric damping. Design of 53-ft-diam and 60-ft-diam rotors were studied and air and ground resonance analyses performed using the equivalent-hinged, rigid-blade C-45 analysis. This exercise revealed the difficulty of analyzing a complex elastic system, such as the bearingless rotor, with a discrete, equivalent-hinged analysis.

Although the flexbeam designs for the 53-ft and 60-ft rotors were the same, the different blade lengths led to different locations for the equivalent flap and lead-lag hinge, such that the C-45 flap and lead-lag hinge sequences for the two designs were different. For the 53-ft-diam rotor, the sequence was flap-lag-pitch; for the 60-ft-diam rotor, the sequence was lag-flap-pitch. This difference was sufficient to cause moderately large differences in the stability of the two rotors. For the 60-ft rotor, it was necessary to reduce the chordwise frequency to insure aeromechanical stability.

### Boeing Vertol Bearingless Main Rotor

The Applied Technology Directorate sponsored a very successful Boeing Vertol program to develop and flight test the Bearingless Main Rotor (BMR) on the BO-105 aircraft; the purpose was to demonstrate concept feasibility with emphasis on aeroelastic stability. The principal objectives of the project were to demonstrate that acceptable aeroelastic stability, structural loads, and flying qualities could be achieved with such a rotor. The rotor design concept was an outgrowth of Boeing's YUH-61A stiff-inplane bearingless tail rotor. The four-bladed BMR was designed to replace the BO-105 hingeless rotor; the existing hub and inboard portions of the blade were removed and replaced with a bearingless hub, dual fiberglass flexbeams and a torque tube cantilevered to the blade and pinned at the hub (fig. 96). The basic dynamic properties of the BO-105 rotor were retained, with moderate flapwise stiffness, soft-inplane chordwise stiffness, and no auxiliary lead-lag dampers. The results of the design effort were reported by Harris et al. (ref. 290).

Marginal air and ground resonance characteristics of the XH-51A Matched Stiffness Rotor and a desire to avoid the use of lag dampers served to focus considerable attention on aeroelastic stability in the early phases of the BMR program. Extensive small-scale-model testing was conducted to check theoretical stability predictions. Test results (refs. 254,290) confirmed a reasonably wide rotor speed range of stable operation, generally in agreement with the predicted characteristics. The Boeing Vertol predictions were obtained from the C-45 analysis of a simplified spring-restrained hinged-rigid blade. With careful exercise of engineering judgment in the selection of effective hinge configuration parameters for the bearingless rotor, reasonably accurate predictions of stability could be made. The need for a more rigorous approach to better support the BMR design was recognized, however, and led to the development of the FLAIR analysis by Hodges, as described in section 2. In an effort to determine the most effective aeroelastic couplings to prevent air and ground resonance instability, parametric studies were conducted using the C-45 and FLAIR analyses; FLAIR results are published in reference 58. Both analysis and model test results indicated that a combination of flap-lag structural coupling from blade negative-droop outboard of the flexbeam were most effective for aeroelastic stability. Aeroelastic stability characteristics determined during flight testing of the BMR on the BO-105 aircraft were reported by Dixon (ref. 90), Staley and Reed (ref. 291), and Staley et al. (ref. 89).

Extensive ground and air resonance tests were conducted in a variety of ground contact and flight conditions. Initial ground testing revealed lower than expected stability, and led to minor modifications of the skid landing gear to raise the body frequency slightly. Air resonance damping was similar to theoretical and model test data. The BMR was slightly less stable than the baseline BO-105 hingeless rotor, and this was attributed in part to lower inherent structural damping of the BMR flexbeam-blade structure. Nevertheless, the BMR demonstrated a major advance in rotor-system technology and remains the only damperless, bearingless rotor successfully tested throughout the vehicle flight envelope.

Following flight testing, the BMR was installed in the 40- by 80-Foot Wind Tunnel at Ames to gather additional data on rotor stability characteristics as well as performance, loads, and flight-control characteristics outside the BO-105 aircraft flight envelope. The wind-tunnel testing also included modifications to vary the pitch-link stiffness and addition of elastomeric damper strips to increase flexbeam structural damping. The results of the wind-tunnel test, reported by Sheffler et al. (ref. 292) and Warmbrodt and McCloud (ref. 293), indicated that the relatively simple modification of adding elastomeric damping strips was very effective in increasing the lead-lag damping in all cases tested. Sheffler et al. subsequently reported on model testing of an advanced BMR II flat-strap configuration that was also stabilized with the use of elastomeric damping strips (ref. 294).

#### Bell Advanced Bearingless Rotor

Following the successful development of the Model 654 soft-inplane hingeless rotor and application of that technology to several production aircraft, Bell

initiated a program to design and test an advanced bearingless rotor. This effort produced the very successful Model 680 rotor system, which was flown on a Model 222 aircraft. As a part of that program, Bell sought to improve in-house analysis capabilities for predicting the aeroelastic stability of bearingless-rotor configurations.

In support of this work, NASA Ames sponsored a model-scale experimental program to obtain data for determining the adequacy of these prediction methods. The small-scale model was similar to the Model 680 configuration—a four-bladed, soft-inplane bearingless rotor with a single element flexbeam and a torque tube with a snubber and elastomeric damper. Blade coning, sweep, pitch flap and pitch lag couplings, and fuselage inertial properties could be changed to conduct parametric studies. The model was tested in hover and forward flight for both fixed hub and coupled rotor-body configurations. The testing and results were reported by Weller (refs. 258,259) and by Weller and Peterson (ref. 260). In general the Bell analytical predictions were in good agreement with the measured test data. It was also concluded that for this rotor configuration the effects of rotor geometric and structural design parameters on stability were not large, and that an auxiliary elastomeric damper was the best means of insuring acceptable mechanical stability.

#### Integrated Technology Rotor/Flight Research Rotor

The Integrated Technology Rotor/Flight Research Rotor (ITR/FRR) Project was undertaken by the Aeroflightdynamics and Aviation Applied Technology Directorates of the U.S. Army Aviation Research and Technology Activity, and NASA Ames, to advance rotor-system technology by combining advances in the structures, dynamics, materials, aerodynamics, and acoustics technical disciplines to design and demonstrate, through actual full-scale flight test, the benefits of an optimized rotor system. Although the project was not funded as far as the full-scale flight test phase, sufficient research and development was completed that it significantly influenced related and follow-on programs. The project consisted of several phases and efforts, undertaken primarily through industry contracts. A methodology assessment exercise was conducted to evaluate the adequacy of industry aeroelastic stability prediction capabilities, as described in section 3. Concept definition studies were undertaken by five helicopter industry contractors to examine the feasibility of various hub concepts for further consideration during preliminary design. Many of these hub concepts were bearingless-rotor configurations, and design features to generate aeroelastic couplings and to enhance aeroelastic stability were examined. Bousman et al. presented an overview of these studies in reference 295. An example of one damperless, bearingless-hub design examined by Bell Helicopter Textron is illustrated in figure 97.

Three contracts were awarded to conduct preliminary design of ITR/FRR rotors. A significant part of these studies included testing small-scale models to confirm the aeroelastic stability of the candidate designs. The Boeing Vertol design reported by Mychalowycz was a single-flexbeam bearingless rotor with a torque-tube pitch control system having an offset shear pin at the hub to introduce pitch-lag

aeroelastic coupling (ref. 261). Hooper used the FLAIR analysis to conduct parametric studies of the ITR hub coupling parameters to optimize the aeroelastic stability characteristics (ref. 91). Negative droop and an offset of the torque-tube shear pivot to introduce pitch-lag coupling were effective in inhibiting air and ground resonance instability. No auxiliary elastomeric damping was included. Bell Helicopter Textron designed a refinement of the Model 680 bearingless-rotor configuration and included a torque tube with snubber and elastomeric damper. The Sikorsky design was based on the elastic gimbal rotor design originally studied by Carlson and Miao (ref. 296).

The results of the ITR/FRR Project served to identify the technical readiness of several advanced rotor technologies. Regarding aeroelastic stability of bearingless rotors, a consensus on the feasibility of a damperless configuration was not reached. The definition of blade and flexbeam frequencies, and the identification of aeroelastic couplings to insure aeromechanical stability over a sufficient range of rotor speed and vehicle operating conditions, is a difficult design task; at the present time, most designers will opt for a lower-risk approach that incorporates auxiliary elastomeric lead-lag damping.

Related structural issues of flexbeam strength and flexibility are better understood, but more progress is needed. It is worth noting that the government-sponsored preliminary design studies prompted a parallel MDHC-funded program that culminated in successful flight testing of the HARP bearingless rotor on the Model 500 helicopter. In addition NASA will sponsor fabrication and testing of a large-scale version of the Boeing Vertol ITR in the NASA Ames 40- by 80-Foot Wind Tunnel.

#### TILT-ROTOR AIRCRAFT

The U.S. Army Bell XV-3 Convertiplane was designed in the early 1960's. It used a two-bladed, teetering-rotor system to partially decouple the gyroscopic rotor moments from the pylon, and the blades were designed with conventional negative pitch-flap coupling to reduce rotor flapping during low-speed maneuvers. Development of the XV-3 aircraft identified many of the dynamic problems of tilt-rotor aircraft, including proprotor whirl flutter, which occurred during full-scale wind-tunnel testing in the NASA Ames 40- by 80-Foot Wind Tunnel.

With the conclusion of the XV-3 program and the initiation of the Advanced Composite Aircraft Program leading to the development of the XV-15, considerable work was done to better understand the shortcomings of the XV-3 design and the importance of rotor elastic motions, rotor couplings, control system flexibility, drive train effects, and wing dynamics. Gaffey made an important contribution by investigating the use of positive pitch-flap coupling for improving flap-lag stability of stiff-inplane rotors in high inflow axial flight (ref. 297). Although the XV-3 used negative pitch-flap coupling to minimize flapping during maneuvers in the high-speed airplane mode, Gaffey showed that a possible coalescence of the flap and lead-lag frequencies of the rotor blade could lead to flap-lag instability. The use

of positive pitch-flap coupling prevents such a coalescence, thereby stabilizing flap-lag motion; Gaffey also showed that positive coupling was equally effective in controlling flapping motion.

### XV-15 Tilt Rotor Research Aircraft

The XV-15 Tilt Rotor Research Aircraft was developed as a joint NASA-Army effort to demonstrate the solution of the key technical problems of this configuration (fig. 98). Substantial government efforts were devoted to developing the technology base needed to deal with aeroelastic stability issues of the tilt rotor. This work has been discussed in detail in sections 2 and 3. At the appropriate point, the government initiated a full-scale proof-of-concept aircraft program to complete the technology development process. Following a competitive preliminary design phase, Bell was selected to design and manufacture two XV-15 aircraft. Extensive government participation in this program contributed to its ultimate success. The following will describe some of the aeroelastic stability considerations relevant to the program.

The XV-15 proprotor design was the result of 15 years of technology development. The three-bladed proprotors use a gimbaled hub to minimize gyroscopic coupling between the rotor and the pylon. The blades are stiff inplane to avoid air and ground resonance, and are similar to hingeless helicopter rotor blades in many respects. Positive pitch-flap coupling of the blades was used to stabilize flap-lag motion and to minimize rotor flapping during maneuvers, based on Gaffey's findings described above. The blade flap frequency was chosen, in part, to minimize pylon stiffness requirements for proprotor whirl-flutter stability. Gaffey et al. (ref. 298) and Johnson (refs. 270,272,299) summarize much of the dynamics-related technology development during aircraft design.

The results of the dynamics testing of the XV-15 aircraft are reported by Marr et al. (ref. 300) and by Bilger et al. (ref. 301). The aeroelastic stability of the aircraft has been cleared to speeds up to 300 knots at altitude. At very high speeds (and at high altitude with the reduction in the speed of sound), lift divergence over a significant portion of the rotor is stabilizing for proprotor dynamics. XV-15 whirl-flutter stability was not a problem.

The successful development of the XV-15 aircraft was the culmination of efforts to demonstrate the ability to effectively control potential aeroelastic instability that hindered acceptance of the revolutionary tilt rotor concept. The NASA and Army contributions in research and the development of the basic technology, as well as management of the XV-15 aircraft program, were major accomplishments.

### V-22 Osprey Aircraft

The V-22 Osprey tilt rotor being developed by the U.S. Marine Corps is tangible proof of the potential brought to fruition with the XV-3 and XV-15 research aircraft. The development of the V-22 is benefiting from significant support from NASA

and Army researchers and experimental facilities. Activities in the area of aeroelastic stability will be discussed below.

A detailed summary of the dynamic stability analysis and testing of the proposed V-22 tilting proprotor system is presented by Popelka et al. (ref. 302). An initial rotor design by the Bell-Boeing team used XV-15 technology with a three-bladed, stiff-inplane, gimballed hub rotor system. However, after initial testing in the Langley Transonics Dynamics Tunnel, aeroelastic stability characteristics were found to be poor. Because of the improved rotor blade airfoils with a higher lift-curve slope, rotor aerodynamics effects reduced the proprotor whirl-flutter stability boundary. Since the rotor precone angle was chosen for hover, destabilizing negative pitch-lag coupling was generated in the airplane mode. To reduce this coupling, lower the effective pitch flap coupling angle, and reduce the resultant aerodynamic moment transmitted to the rotor hub as well, a coning hinge was added to each blade. The result of this design modification was to markedly improve the whirl-flutter stability well beyond the operational envelope of the V-22 aircraft. This gimballed-coning hub required the modification of the Bell Helicopter dynamics prediction code and the codes of Kvaternik (ref. 99) and Johnson (ref. 94). This new hub configuration was also used in predicting the dynamic performance of a high-speed tilt-rotor design (ref. 303) using the modified analysis of reference 94.

Although a great deal has been learned about tilting proprotor dynamics, future designs will likely use more advanced hub configurations (benefiting from the use of composite materials and redundant load path designs) requiring new analyses. Higher airspeeds will require better understanding of the influence of compressible aerodynamics on proprotor stability. True optimization of the design process for rotor-  
pylon-wing aeroelastic stability has yet to be attempted. Also, the use of active controls has yet to be fully investigated for the potential of improving tilting proprotor stability characteristics.

#### OTHER ROTOR SYSTEMS

In addition to the rotor systems described in the previous sections, government research and development efforts have also addressed the aeroelastic stability of a number of other rotor configurations. These will be briefly described below.

The search for high-speed aircraft having vertical takeoff and landing capability has led to consideration of a number of configuration concepts. The compound helicopter has received much attention, and slowing, stopping, or stowing the rotor has been studied as a way of minimizing or eliminating the aerodynamic problems of operating rotors at high forward speeds. All of these concepts involve high advance ratio conditions. Watts et al. report results of 40- by 80-Foot Wind Tunnel tests of a Lockheed gyro-stabilized slowed-stopped hingeless rotor (ref. 304). Aeroelastic analysis and comparisons with test data were undertaken to determine the ability to predict coupled rotor-gyro stability under extreme operating conditions of low



rotor speed and very high advance ratios. Results showed that relatively simple aerodynamic theory was reasonably accurate for these conditions.

In the course of development of advanced bearingless-rotor systems, valuable experience has been gained from earlier development of bearingless helicopter tail rotors constructed from composite materials. The government has supported research and development on several such systems where aeroelastic stability required careful considerations in design. Maloney described the elastic pitch beam rotor developed by Kaman, a two-bladed teetering rotor using a fiberglass flexbeam for blade-pitch change motion, coning deflections, and chordwise bending (ref. 305). The rotor was designed for application to full-scale aircraft and was tested and demonstrated to have acceptable stability characteristics.

Boeing Vertol also gained bearingless rotor experience with a tail rotor application. In the course of development of the YUH-61A UTTAS aircraft prototype, a mechanically simple but structurally advanced four-bladed stiff-inplane fiberglass tail-rotor was introduced. This rotor used a cantilever torque tube configuration that permitted significant aeroelastic coupling of bending and torsion motions. During development testing a number of instabilities were encountered including stall flutter and high-amplitude lead-lag limit cycle motions. A stable configuration evolved through extensive trial and error testing and modifications. Because of the complex behavior of the bearingless rotor, analytical methods were of limited use in predicting or identifying solutions to observed instabilities. The extensive aeroelastic stability data obtained in this program were sufficiently valuable, however, that it was documented (under government sponsorship) by Edwards and Miao (ref. 306).

The Sikorsky ABC compound helicopter was developed under sponsorship of the U.S. Army. The two three-bladed coaxial, high-flap stiffness rotors form a unique stiff-inplane hingeless-rotor system. To confirm the general adequacy of the design, including aeroelastic stability, the flight rotors were tested in the 40- by 80-Foot Wind Tunnel (ref. 307); flight-test results were reported in reference 308. Without auxiliary dampers, the lead-lag damping of the blades was very low, but adequate stability was maintained throughout the flight envelope.

The constant-lift rotor (CLR) and free-tip rotor (FTR) designs use airfoil sections that are free to pivot on the spar of the rotor blade in order to maintain nearly uniform lift during forward flight and thereby minimize the vibratory response of helicopter rotor blades in forward flight. However, the additional degrees of freedom provide more opportunities for aeroelastic stability, and investigations of the flap-lag-torsion stability of these design were carried out by Chopra for the hover flight condition (refs. 309,310). With suitable selection of aeroelastic design parameters, it was possible to identify stable configurations.

## 5. CONCLUSION

The material presented herein shows the extensive involvement of the Army and NASA in rotorcraft aeroelastic stability research. In most of the areas addressed, significant technology advances have occurred as a result of this research. Some of these areas were essentially nonexistent 20 years ago. As a result, the technical community is in a much stronger position to deal with the risks of aeroelastic instability of new rotor systems. In this section, the key contributions of Army-NASA research will be summarized, followed by recommendations for future efforts.

### SUMMARY OF ARMY-NASA RESEARCH CONTRIBUTIONS

1. A substantial capability for predicting helicopter and tilt-rotor aeroelastic stability now exists, capable of treating rotorcraft structural dynamics and aerodynamics in considerable detail. Hover flight conditions are relatively straightforward, and very substantial progress has been made in forward flight prediction capabilities. In addition to conventional articulated-rotor systems, hingeless-rotor stability analysis is now nearly routine, and bearingless rotors can be satisfactorily treated in many respects. Prediction capability resides in a number of different analyses, many of which have been extensively validated with experimental data.

2. A comprehensive understanding of the aeroelastic stability characteristics of hingeless rotorcraft now exists. This includes nonlinear bending-torsion coupling, structural flap-lag coupling, the influence of kinematic aeroelastic coupling, the effects of aerodynamics and rotor body coupling on aeromechanical stability, and the effects of dynamic inflow and dynamic stall on aeroelastic stability. The differences between soft- and stiff-inplane hingeless rotors have been identified, and this has contributed to shift emphasis away from stiff-inplane and toward soft-inplane configurations for new rotorcraft.

3. The technology base for tilt-rotor aeroelastic stability has expanded substantially. Validated prediction codes now exist to treat fully coupled systems, including rotor, pylon, wing, and fuselage dynamics. Parametric studies have contributed to a good general understanding of tilt-rotor systems including the effects of rotor-blade in-plane, pitch, and torsion motions, drive train coupling effects, and compressible airfoil aerodynamics.

4. An extensive experimental data base has been generated, for small-scale models and full-scale aircraft, for both helicopter and tilt-rotor configurations. The data are of high quality, much of them obtained from experiments specifically designed to acquire data for correlation with prediction methods.

5. A solid theoretical basis for the structural dynamics of nonlinear beams has been established. The subject has been investigated by numerous researchers, and the theory has been validated experimentally. The moderate deformation theory,

valid for small strain, has been extended from moderate rotation to large rotation deformations. Advanced nonlinear finite-element methods are being developed and characteristics of composite materials can now be treated for some simple cases.

6. Dynamic inflow theory is a substantial development that has found wide acceptance by rotorcraft aeroelasticians. It has been placed on a rigorous theoretical foundation and has been extensively validated with experimental data. Because of its accuracy, simplicity, and computational efficiency, it has been found useful in other disciplines such as rotorcraft flight dynamics. It is also amenable to refinement for application to higher-frequency aeroelastic phenomena.

7. Mathematical methods for solving rotorcraft aeroelastic stability equations have also advanced significantly. Floquet theory for periodic coefficient linear systems is now in common use and the rotating-to-fixed system transformation has been formalized as multiblade coordinates. Recent work has also demonstrated significant potential for the use of symbolic processors for automatic generation of the complex multi-degree-of-freedom rotorcraft equations of motion.

8. In addition to generic rotorcraft aeroelastic stability research, invaluable knowledge and progress have resulted from full-scale systems design, testing, and development of advanced rotorcraft and rotorcraft components. These efforts are the final proof of the contributions of aeroelastic stability research development. Full-scale development and flight test of aircraft such as the Bell XV-15 and the Boeing Vertol BMR have been particularly effective in demonstrating mastery of aeroelastic stability technology for critical dynamic phenomena.

## RECOMMENDATIONS

Although the last 20 years have witnessed great progress in the technology of rotorcraft aeroelastic stability, not all of the problems have been solved. A great many pressing needs and attractive opportunities remain, and these should be vigorously pursued. As new rotorcraft systems evolve, continual emphasis will be required to address these new problems. The following general recommendations are offered for consideration.

1. It is usually taken for granted that aeroelasticians can apply Newton's second law without error and when the results of analysis are unsatisfactory the aerodynamic theory is often faulted. There is evidence that structural dynamics analysis is not yet adequately understood and that prediction of rotating-beam dynamics is not yet solved. More experimental data are needed. The most complex of all rotorcraft structures are rotor hubs, blades, and blade-to-hub attachments; they deserve more attention under the influence of pure inertial loading.

2. Vibration testing of rotating blades in vacuum should continue and be expanded to include more structurally complex blade and hub configurations, including nonuniform properties, typical bearingless configurations, and blade structures composed of composite materials. Careful experiments, correlated with analysis, may

reveal analysis deficiencies in solid mechanics, material properties, and structural damping effects.

3. The structural mechanics basis is now available for a large-rotation small-strain beam theory. Such development should be continued, and a modeling approach should be included for anisotropic materials. This will provide a capability to analyze fully the most complex structural rotor-blade flexbeam configurations now envisioned.

4. As the primary structural material for rotor blades, fiber-reinforced composites deserve the full attention of the aeroelastician. Capability of modeling and analyzing composite materials for rotorcraft applications needs to be substantially improved.

5. Finite-element methods are necessary for effective aeroelastic analysis of future rotorcraft. These methods need to be made more effective for dealing with rotating blades and for coupling rotating and nonrotating structures.

6. Computational efficiency of rotorcraft aeroelastic analysis needs to be improved. As the number of degrees of freedom increases, the solutions for nonlinear systems in forward flight have become more difficult. The trim and dynamic equilibrium solutions need to be improved and made more robust. Without practical solution methods, the benefits of improvements in structural and aerodynamic theory may not be realized.

7. Many of the analytical prediction methods developed have emphasized narrow research investigations. Prediction capability for a broad range of applications is needed. Prediction capability of research codes should be incorporated into comprehensive analyses (e.g., 2GCHAS) to make the technology more readily available to the designer.

8. More attention should be devoted to linear, three-dimensional unsteady aerodynamics theory for rotor-blade flutter analysis. In the age of computational fluid dynamics, numerically efficient methods are needed for rapid flutter analysis of rotor blades when stall and shocks are not present. New blade- and tip-shape configurations will depart from the traditional design practice of chordwise coincident elastic, aerodynamic, and mass centers, and thus will require more attention to deal with classical flutter.

9. At the same time, the most advanced unsteady aerodynamic research capabilities, focused on formulations for aeroelastic stability, should be directed at nonlinear problems of transonic flow and airfoil stall. In addition, a better understanding of the role of dynamic stall on rotor-blade flutter in forward flight is needed.

10. An excellent experimental data base has been obtained for small-scale, low-tip-speed hingeless and bearingless rotors and rotor-body systems. This data base should be expanded to include representative full-scale tip speeds and higher Reynolds numbers. Structural configurations should include examples of both simple

and complex blades. Emphasis should be on forward flight, but these models need to be fully tested in hover as well. Isolated rotors are best; the effects of rotor-body coupling are much more tractable analytically.

11. Rotor-blade flutter experiments should be conducted for configurations having significant chordwise offsets of aerodynamic, mass, and elastic centers to test new unsteady aerodynamic theories and gain experience with more advanced blade design concepts.

12. Full-scale rotor testing should be maintained to provide periodic exposure to the real world environment of aeroelastic stability.

13. Directed analysis assessment correlation exercises should be continued. These provide unique opportunities to address and correct unwarranted assumptions, derivation errors, coding errors, and other anomalies of individual analysis methods. To achieve maximum return, the causes of discrepant results need to be traced back to their source.

14. The tilt rotor is a key vehicle of the future. The technology base has grown enormously in the past 15 years, and it must continue to advance. Analyses tailored to the unique structural and aerodynamic features of the tilt rotor need to be pursued. Modeling compressible aerodynamics needs to be better understood and potential applications of active controls to improve stability characteristics should be pursued.

15. Research on the fundamental aeroelastic stability characteristics of bearingless rotors should continue. Notwithstanding the extensive results obtained to date, a sure formula for a damperless bearingless rotor has eluded the technical community. Research should continue in order to find a solution for this problem.

## REFERENCES

1. Houbolt, John C.; and Brooks, George W.: Differential Equations of Motion for Combined Flapwise Bending, Chordwise Bending, and Torsion of Twisted Nonuniform Rotor Blades. NACA Report 1346, 1958.
2. Arcidiacono, P. J.: Steady Flight Differential Equations of Motion for a Flexible Helicopter Blade with Chordwise Mass Unbalance. USAAVLABS TR 68-18A, vol. 1, Feb. 1969.
3. Ormiston, R. A.; and Hodges, D. H.: Linear Flap-Lag Dynamics of Hingeless Helicopter Rotor Blades in Hover. J. Am. Helicopter Soc., vol. 17, no. 2, Apr. 1972, pp. 2-14.
4. Hodges, Dewey H.; and Ormiston, Robert A.: Nonlinear Equations for Bending of Rotating Beams with Applications to Linear Flap-Lag Stability of Hingeless Rotors. NASA TM X-2770, 1973.
5. Friedmann, P.; and Tong, P.: Dynamic Nonlinear Elastic Stability of Helicopter Rotor Blades in Hover and in Forward Flight. NASA CR-114485. (Also TR 166-3, Massachusetts Institute of Technology, ASRL, Cambridge, Mass., May 1972.)
6. Hodges, Dewey Harper: Nonlinear Bending and Torsion of Rotating Beams with Application to Linear Stability of Hingeless Helicopter Rotors. Ph.D. thesis, Stanford University, Palo Alto, Calif., Dec. 1972.
7. Novozhilov, V. V.: Foundations of the Nonlinear Theory of Aeroelasticity. Translated ed., Graylock Press, Rochester, N.Y., 1953.\*
8. Hodges, D. H.; and Dowell, E. H.: Nonlinear Equations of Motion for the Elastic Bending and Torsion of Twisted Nonuniform Rotor Blades. NASA TN D-7818, 1974.
9. Peters, David A.; and Ormiston, Robert A.: The Effects of Second Order Blade Bending on the Angle of Attack of Hingeless Rotor Blades. J. Am. Helicopter Soc., vol. 18, no. 4, Oct. 1973, pp. 45-48.
10. Dowell, E. H.: A Variational-Rayleigh-Ritz Modal Approach for Non-Uniform Twisted Rotor Blades Undergoing Large Bending and Torsional Motion. AMS Report No. 1193, Princeton University, Princeton, N.J., Nov. 1974.

---

\*Research not derived from government or government-sponsored efforts.

11. Dowell, E. H.; and Traybar, J.: An Experimental Study of the Nonlinear Stiffness of a Rotor Blade Undergoing Flap, Lag, and Twist Deformations. AMS Report No. 1194, Princeton University, Princeton, N.J., 1975. (Also NASA CR-137968, 1975.)
12. Dowell, E. H.; and Traybar, J.: An Experimental Study of the Nonlinear Stiffness of a Rotor Blade Undergoing Flap, Lag, and Twist Deformations. AMS Report No. 1257, Princeton University, Princeton, N.J., 1975. (Also NASA CR-137969, 1975.)
13. Dowell, E. H.; Traybar, J.; and Hodges, D. H.: An Experimental Theoretical Correlation Study of Non-Linear Bending and Torsion Deformations of a Cantilever Beam. J. Sound and Vibration, vol. 50, no. 4, Feb. 22, 1977, pp. 533-544.
14. Hodges, Dewey H.; and Peters, David A.: On the Lateral Buckling of Uniform Slender Cantilever Beams. Int. J. Solids/Structures, vol. 11, no. 12, Dec. 1975, pp. 1269-1280.
15. Hodges, D. H.; and Ormiston, R. A.: Stability of Elastic Bending and Torsion of Uniform Cantilever Rotor Blades in Hover with Variable Structural Coupling. NASA TN D-8192, 1976.
16. Hodges, D. H.: Nonlinear Equations of Motion for Cantilever Rotor Blades in Hover with Pitch Link Flexibility, Twist, Precone, Droop, Sweep, Torque Offset, and Blade Root Offset. NASA TM X-73,112, 1976.
17. Hodges, Dewey H.; and Ormiston, Robert A.: Stability of Hingeless Rotor Blades in Hover with Pitch Link Flexibility. AIAA J., vol. 15, no. 4, Apr. 1977, pp. 475-482.
18. Srinivasan, A. V.; Cutts, D. G.; and Shu, H. T.: An Experimental Investigation of the Structural Dynamics of a Torsionally Soft Rotor in a Vacuum. NASA CR-177418, 1986.
19. Friedmann, Peretz: Influence of Structural Damping, Preconing, Offsets, and Large Deflections on the Flap-Lag-Torsional Stability of a Cantilevered Rotor Blade. AIAA Paper 75-780, Denver, Colo., 1975.
20. Friedmann, P.: Influence of Modeling and Blade Parameters on the Aeroelastic Stability of a Cantilevered Rotor. AIAA J., vol. 15, no. 2, Feb. 1977, pp. 149-158.
21. Friedmann, Peretz; and Reyna-Allende, M.: Aeroelastic Stability of Coupled Flap-Lag-Torsional Motion of Helicopter Rotor Blades in Forward Flight. AIAA Paper 77-455, San Diego, Calif., 1977.

22. Rosen, A.; and Friedmann, P.: Nonlinear Equations of Equilibrium for Elastic Helicopter or Wind Turbine Blades Undergoing Moderate Deformation. Report UCLA-ENG7718, U. California at Los Angeles, rev. June 1977. (Also NASA CR-159478, 1978.)
23. Rosen, Aviv; and Friedmann, Peretz P.: Nonlinear Equations of Equilibrium for Elastic Helicopter or Wind Turbine Blades Undergoing Moderate Deformation. NASA CR-159478, 1978.
24. Shamie, J.; and Friedmann, P.: Effect of Moderate Deflections on the Aeroelastic Stability of a Rotor Blade in Forward Flight. Paper No. 24, Proceedings of the 3rd European Rotorcraft and Powered Lift Aircraft Forum, Aix-en-Provence, France, Sept. 1977, pp. 24.1-24.37.
25. Friedmann, P. P.; and Kottapalli, S. B. R.: Rotor Blade Aeroelastic Stability and Response in Forward Flight. Paper No. 14, Proceedings of the 6th European Rotorcraft and Powered Lift Aircraft Forum, Sept. 1980, pp. 14.1-14.34.
26. Rosen, A.; and Friedmann, P.: The Nonlinear Behavior of Elastic Slender Straight Beams Undergoing Small Strains and Moderate Rotations. J. Appl. Mech., vol. 46, no. 1, Mar. 1979, pp. 161-168.
27. Hodges, Dewey H.: Discussion of The Nonlinear Behavior of Elastic Slender Straight Beams Undergoing Small Strains and Moderate Rotations. A. Rosen and P. Friedmann, eds. J. Appl. Mech., vol. 47, no. 3, Sept. 1980, p. 688.
28. Kaza, K. R.; and Kvaternik, R. G.: Nonlinear Aeroelastic Equations for Combined Flapwise Bending, Chordwise Bending, Torsion, and Extension of Twisted Nonuniform Rotor Blades in Forward Flight. NASA TM-74059, 1977.
29. Kvaternik, R. G.; White, W. F.; and Kaza, K. R.: Nonlinear Flap-Lag-Axial Equations of a Rotating Beam with Arbitrary Precone Angle. Proceedings of the AIAA SDM Conference, Bethesda, Md., Apr. 1978, pp. 214-227.
30. Crespo da Silva, M. R. M.: Flap-Lag Torsional Dynamic Modeling of Rotor Blades in Hover and in Forward Flight, Including the Effect of Cubic Nonlinearities. NASA CR-166194, 1981.
31. Crespo da Silva, Marcelo R. M.; and Hodges, Dewey H.: Nonlinear Flexure and Torsion of Rotating Beams with Application to Helicopter Rotor Blades. I. Formulation. Vertica, vol. 10, no. 2, 1986.
32. Crespo da Silva, Marcelo R. M.; and Hodges, Dewey H.: Nonlinear Flexure and Torsion of Rotating Beams with Application to Helicopter Rotor Blades. II. Results for Hover. Vertica, vol. 10, no. 2, 1986.



33. Kaza, K. R. V.; and Kvaternik, R. G.: A Critical Examination of the Flap-Lag Dynamics of Helicopter Rotor Blades in Hover and in Forward Flight. Paper No. 1034, 32nd Annual National V/STOL Forum of the American Helicopter Society, Washington, D.C., 1976.
34. Kvaternik, Raymond G.; and Kaza, Krishna R. V.: Nonlinear Curvature Expressions for Combined Flapwise Bending, Chordwise Bending, Torsion and Extension of Twisted Rotor Blades. NASA TM X-73997, 1976.
35. Hodges, D. H.; Ormiston, R. A.; and Peters, D. A.: On the Nonlinear Deformation Geometry of Euler-Bernoulli Beams. NASA TP-1566, 1980.
36. Alkire, K.: An Analysis of Rotor Blade Twist Variables Associated with Different Euler Sequences and Pretwist Treatments. NASA TM-84394, 1984.
37. Hodges, Dewey H.: Finite Rotation and Nonlinear Beam Kinematics. Vertica, vol. 11, no. 1/2, 1987, pp. 297-308.
38. Jonnalagadda, V. R. P.; and Pierce, G. Alvin: Nonlinear Deformation of Rotating Beams--An Alternative Method of Formulation. J. Am. Helicopter Soc., vol. 30, no. 2, Apr. 1985, pp. 68-70.\*
39. Hodges, Dewey H.; Peters, David A.; Pierce, G. Alvin; and Jonnalagadda, V. R. P.: Comment on "Nonlinear Deformation of Rotating Beams--An Alternate Method of Formulation." Technical Note, J. Am. Helicopter Soc., July 1986.
40. Hodges, D. H.: Torsion of Pretwisted Beams Due to Axial Loading. J. Appl. Mech., vol. 47, no. 2, June 1980, pp. 393-397.
41. Rosen, Aviv: Discussion of "Torsion of Pretwisted Beams Due to Axial Loading." J. Appl. Mech., vol. 48, no. 3, Sept. 1981, pp. 697-780.\*
42. Hodges, Dewey H.: Author's Closure to A. Rosen's Discussion of "Torsion of Pretwisted Beams Due to Axial Loading." J. Appl. Mech., vol. 48, no. 3, Sept. 1981, pp. 680-681.
43. Rosen, A.: Theoretical and Experimental Investigation of the Nonlinear Torsion and Extension of Initially Twisted Bars. J. Appl. Mech., vol. 50, no. 2, pp. 321-326, 1983.\*
44. Petersen, D.: Interaction of Torsion and Tension in Beam Theory. Vertica, vol. 6, no. 4, 1982, pp. 311-325.\*
45. Hodges, Dewey H.: Nonlinear Beam Kinematics for Small Strains and Finite Rotations. Vertica, vol. 11, no. 3, 1987, pp. 573-589.
46. Hodges, Dewey H.: On the Extensional Vibrations of Rotating Bars. Int. J. Non-Linear Mech., vol. 12, no. 5, 1977, pp. 293-296.

47. Venkatesan, C.; and Nagaraj, V.T.: On the Axial Vibrations of Rotating Bars. J. Sound and Vibration, vol. 74, 1981, pp. 143-147.\*
48. Venkatesan, C.; and Nagaraj, V.T.: Authors' Reply to Comments on "On the Axial Vibration of Rotating Bars" by D. H. Hodges. J. Sound and Vibration, vol. 87, no. 3, 1983, pp. 516-518.\*
49. Hodges, Dewey H.: Comments on "On the Axial Vibration of Rotating Bars." J. Sound and Vib., vol. 87, no. 3, Apr. 8, 1983, pp. 513-515.
50. Degener, Manfred; Hodges, Dewey H; and Petersen, Dieter: Analytical and Experimental Study of Beam Torsional Stiffness with Large Elongation. To be published in J. Appl. Mech., 1987.
51. Kaza, K. R. V.; and Kielb, R. E.: Effects of Warping and Pretwist on Torsional Vibration of Rotating Beams. J. Appl. Mech., vol. 51, Dec. 1984, pp. 913-920.\*
52. Stephens, Wendell B.; Hodges, Dewey H.; Avila, John H.; and Kung, Ru-Mei: Stability of Nonuniform Rotor Blades in Hover Using a Mixed Formulation. NASA TM-81226, 1980. (Also, AVRADCOM TR 80-A-10, Aug. 1980.)
53. Hodges, D. H.: Nonlinear Equations for Dynamics of Pretwisted Beams Undergoing Small Strains and Large Rotations. NASA TP-2470, 1985. (Also, AVSCOM TR 84-A-5, May 1985.)
54. Danielson, Donald A.; and Hodges, Dewey H.: Nonlinear Beam Kinematics by Decomposition of the Rotation Tensor. J. Appl. Mech., vol. 54, June 1987, pp. 258-262.
55. Bielawa, R. L.: Aeroelastic Analysis for Helicopter Rotor Blades with Time Variable, Nonlinear Structural Twist and Multiple Structural Redundancy--Mathematical Derivation and Program User's Manual. NASA CR-2638, 1976.
56. Bielawa, R. L.; Cheney, Jr.; M. C. and Novak, R. C.: Investigation of a Bearingless Helicopter Rotor Concept Having a Composite Primary Structure. NASA CR-2637, 1976.
57. Hodges, D. H.: Aeromechanical Stability of Helicopters with a Bearingless Main Rotor. Pt I: Equations of Motion. NASA TM-78459, 1978; Pt II: Computer Program. NASA TM-78460, 1978.
58. Hodges, D. H.: A Theoretical Technique for Analyzing Aeroelastic Stability of Bearingless Rotors. AIAA J., vol. 17, no. 4, Apr. 1979, pp. 400-407.
59. Sivaneri, N. T.; and Chopra, I.: Finite Element Analysis for Bearingless Rotor Blade Aeroelasticity. J. Am. Helicopter Soc., vol. 29, no. 2, Apr. 1984.

60. Hodges, Dewey H.; Hopkins, A. Stewart; Kunz, Donald L.; and Hinnant, Howard E.: Introduction to GRASP--General Rotorcraft Aeromechanical Stability Program--A Modern Approach to Rotorcraft Modeling. Proceedings of the 42nd Annual National Forum of the American Helicopter Society, Washington, D.C., 1986, pp. 739-756.
61. Hohenemser, K. H.; and Yin, S. K.: Finite Element Stability Analysis for Coupled Rotor and Support Systems. NASA CR-152024, 1977.
62. Friedmann, P. P.; and Straub, F.: Application of the Finite Element Method to Rotary-Wing Aeroelasticity. J. Am. Helicopter Soc., vol. 25, no. 1, Jan. 1980, pp. 36-44.
63. Straub, F. K.; and Friedmann, P. P.: A Galerkin Type Finite Element Method for Rotary-Wing Aeroelasticity in Hover and Forward Flight. Vertica, vol. 5, no. 1, 1981, pp. 75-98.
64. Straub, F. K.; and Friedmann, P. P.: Application of the Finite Element Method to Rotary Wing Aeroelasticity. NASA CR-165854, 1982.
65. Celi, R.; and Friedmann, P. P.: Aeroelastic Modeling of Swept Tip Rotor Blades Using Finite Elements. Proceedings of the 43rd Annual National Forum of the American Helicopter Society, St. Louis, Mo., 1987, pp. 257-269.
66. Sivaneri, N. T.; and Chopra, I.: Dynamic Stability of a Rotor Blade Using Finite Element Analysis. AIAA J., vol. 20, no. 5, May 1982, pp. 716-723.
67. Chopra, Interjit; and Sivaneri, Nithiam Ti: Aeroelastic Stability of Rotor Blades Using Finite Element Analysis. NASA CR-166389, 1982.
68. Hodges, Dewey H.: Vibration and Response of Nonuniform Rotating Beams with Discontinuities. J. Am. Helicopter Soc., vol. 24, no. 5, Oct. 1979, pp. 43-50.
69. Hodges, Dewey H.: Direct Solutions for Sturm-Liouville Systems with Discontinuous Coefficients. AIAA J., vol. 17, no. 8, Aug. 1979, pp. 924-926.
70. Hodges, Dewey H.; and Rutkowski, Michael J.: Free-Vibration Analysis of Rotating Beams by a Variable-Order Finite-Element Method. AIAA J., vol. 19, no. 11, Nov. 1981, pp. 1459-1466.
71. Hodges, Dewey H.: Orthogonal Polynomials as Variable-Order Finite Element Shape Functions. AIAA J., vol. 21, no. 5, May 1983, pp. 796-797.
72. Rehfield, L. W.; and Murthy, P. L. N.: Toward a New Engineering Theory of Bending: Fundamentals. AIAA J., vol. 20, no. 5, May 1982, pp. 693-699.\*

73. Bauchau, O. A.: A Beam Theory for Anisotropic Materials. J. Appl. Mech., vol. 52, June 1985, pp. 416-422.\*
74. Kosmatka, J.: Structural Dynamic Modeling of Nonisotropic Blades by the Finite Element Method. Ph.D. Dissertation, Mechanical, Aerospace, and Nuclear Engineering Department, University of California at Los Angeles, Los Angeles, Calif., Oct. 1986.\*
75. Kim, Y. H.; and Lee, S. W.: A New Approach to Finite Element Modeling of Composite Helicopter Rotor Blades. Presented at the U.S. Army Research Office Workshop on Dynamics and Aeroelastic Stability Modeling of Rotor Systems, Georgia Institute of Technology, Atlanta, Ga., Dec. 1985.\*
76. Rehfield, Lawrence W.: Design Analysis Methodology for Composite Rotor Blades. Seventh DOD/NASA Conference on Fibrous Composites in Structural Design, Denver, Colo., June 1985.\*
77. Bauchau, O. A.: Composite Box Beam Analysis: Theory and Experiments. J. Reinforced Plastics and Composites, vol. 6, Jan. 1987, pp. 25-35.\*
78. Hong, C.-H.; and Chopra, I.: Aeroelastic Stability Analysis of a Composite Rotor Blade. J. Am. Helicopter Soc., vol. 30, Apr. 1985, pp. 57-67.\*
79. Coleman, Robert P.; and Feingold, Arnold M.: Theory of Self-Excited Mechanical Oscillation of Helicopter Rotors with Hinged Blades. NACA TR-1351, 1956.
80. Hohenemser, K. H.; and Yin, S. K.: Some Applications of the Method of Multi-blade Coordinates. J. Am. Helicopter Soc., vol. 17, no. 3, July 1972, pp. 1-12.\*
81. Cardinale, Salvatore V.: Soft In-Plane Matched-Stiffness/Flexure-Root-Blade Rotor System Summary Report. USAAVLABS TR 68-72, Aug. 1969.
82. Hammond, C. E.: An Application of Floquet Theory to the Prediction of Mechanical Instability. J. Am. Helicopter Soc., vol. 19, no. 4, Oct. 1974, pp. 14-23.
83. Johnston, R. A.; and Cassarino, S. J.: Aeroelastic Rotor Stability Analysis. USAAMRDL-TR-75-40, 1976.
84. Shamie, J.; and Friedmann, P.: Aeroelastic Stability of Complete Rotors with Application to a Teetering Rotor in Forward Flight. Paper No. 1031, 32nd Annual National V/STOL Forum of the American Helicopter Society, Washington, D.C., May 1976. (Also, J. Am. Helicopter Soc., Oct. 1977.)\*
85. Johnson, Wayne: Aeroelastic Analysis for Rotorcraft in Flight or in a Wind Tunnel. NASA TN D-8515, 1977.

86. Ormiston, Robert A.: Aeromechanical Stability of Soft Inplane Hingeless Rotor Helicopters. Paper No. 25, 3rd European Rotorcraft and Powered Lift Aircraft Forum, Aix-en-Provence, France, Sept. 1977.
87. Ormiston, R. A.: Rotor-Fuselage Dynamic Coupling Characteristics of Helicopter Air and Ground Resonance. Proceedings of the AHS/NAI Conference, The Theoretical Basis of Helicopter Technology, Nanjing Aeronautical Institute, Nanjing, China, Nov. 1985.
88. Hodges, D. H.: An Aeromechanical Stability Analysis for Bearingless Rotor Helicopters. J. Am. Helicopter Soc., vol. 24, no. 1, Jan. 1979, pp. 2-9.
89. Staley, J. A.; Gabel, R.; and McDonald, H. I.: Full Scale Ground and Air Resonance Testing of the Army-Boeing Vertol Bearingless Main Rotor. Paper No. 79-23, Proceedings of the 35th Annual National Forum of the American Helicopter Society, May 1979.\*
90. Dixon, P. C. G.: Design, Development, and Flight Demonstration of the Loads and Stability Characteristics of a Bearingless Main Rotor. USA AVRADCOM-TR-80-D-3, June 1980.
91. Hooper, W. Euan: Parametric Study of the Aeroelastic Stability of a Bearingless Rotor. NASA CP-2400, 1984.\*
92. Warmbrodt, William; and Friedmann, Peretz: Formulation of the Aeroelastic Stability and Response ASD Problem of Coupled Rotor/Support Systems. AIAA Paper 79-0732, AIAA/ASME/ASCE/AHS 20th SDM Conference, St. Louis, Mo., 1979.
93. Warmbrodt, W.; and Friedmann, P.: Formulation of Coupled Rotor/Fuselage Equations of Motion. Vertica, vol. 3, no. 3, 1979, pp. 254-271.
94. Johnson, W.: A Comprehensive Analytical Model of Rotorcraft Aerodynamics and Dynamics. Pt I. Analysis Development. NASA TM-81182, 1980.
95. Johnson, Wayne: Development of a Comprehensive Analysis for Rotorcraft. I. Rotor Model and Wake Analysis. Vertica, vol. 5, no. 2, 1981, pp. 99-129.
96. Johnson, Wayne: Development of a Comprehensive Analysis for Rotorcraft. Pt II. Aircraft Model, Solution Procedure, and Applications. Vertica, vol. 5, no. 3, 1981, pp. 185-216.
97. Venkatesan, C.; and Friedmann, P. P.: Aeroelastic Effects in Multirotor Vehicles with Application to a Hybrid Heavy Lift System. Pt I. Formulation of Equations of Motion. NASA CR-3822, 1984.

98. Venkatesan, V.; and Friedmann, P. P.: Aeroelastic Effects in Multirotor Vehicles. Pt II. Methods of Solution and Results Illustrating Coupled Rotor/Body Aeromechanical Stability. NASA CR-4009, 1987.
99. Kvaternik, R. G.: Studies in Tilt Rotor VTOL Aircraft Aeroelasticity. NASA TM X-69496 and TM X-69497, 1973.
100. Kvaternik, R. G.; and Kohn, J. S.: An Experimental and Analytical Investigation of Proprotor Whirl Flutter. NASA TP 1047, 1977.
101. Johnson, W.: Dynamics of Tilting Proprotor Aircraft in Cruise Flight. NASA TN D-7677, 1974.
102. Johnson, W.: Analytical Model for Tilting Proprotor Aircraft Dynamics, Including Blade Torsion and Coupled Bending Modes, and Conversion Mode Operation. NASA TM X-62369, 1974.
103. Johnson, W.: The Influence of Engine/Transmission/Governor on Tilting Proprotor Aircraft Dynamics. NASA TM X-62455, 1975.
104. Johnson, W.: An Assessment of the Capability to Calculate Tilting Prop-Rotor Aircraft Performance, Loads, and Stability. NASA TP-2291, 1984.
105. Theodorsen, T.: General Theory of Aerodynamic Instability and the Mechanism of Flutter. NACA Report 496, 1949.
106. Loewy, R. G.: A Two Dimensional Approach to the Unsteady Aerodynamics of Rotary Wings. J. Aeronaut. Sci., vol. 24, no. 2, Feb. 1957, pp. 82-98.\*
107. Greenberg, J. M.: Airfoil in Sinusoidal Motion in a Pulsating Stream. NACA TN-1326, 1947.
108. Johnson, W.: Application of Unsteady Airfoil Theory to Rotary Wings. J. Aircraft, vol. 17, no. 4, Apr. 1980, pp. 285-286.
109. Kaza, K. R. V.; and Kvaternik, R. G.: Application of Unsteady Airfoil Theory to Rotary Wings. J. Aircraft, vol. 18, no. 7, July 1981, pp. 604-605.
110. Friedmann, P.; and Yuan, C.: Effects of Modified Aerodynamic Strip Theories on Rotor Blade Aeroelastic Stability. AIAA J., vol. 15, no. 7, July 1977, pp. 932-940.
111. Peters, D. A.: Toward a Unified Model for Use in Rotor Blade Stability Analyses. J. Am. Helicopter Soc., vol. 30, July 1985, pp. 32-42.

112. Dinyavari, M. A. H.; and Friedmann, P. P.: Unsteady Aerodynamics in Time and Frequency Domains for Finite Time Arbitrary Motion of Rotary Wings in Hover and Forward Flight. AIAA Paper 84-0988, Proceedings AIAA/ASME/ASCE/AHS 25th SDM Conference, Palm Springs, Calif., May 1984, pp. 266-282.
113. Dinyavari, M. A. H.; and Friedmann, P. P.: Application of the Finite State Arbitrary Motion Aerodynamics to Rotor Blade Aeroelastic Response and Stability in Hover and Forward Flight. AIAA Paper 85-0763, Proceedings of AIAA/ASME/ASCE/AHS 26th SDM Conference, Orlando, Fla., Apr. 1985, pp. 522-535.
114. Friedmann, P. P.; and Venkatesan, C.: Finite State Modeling of Unsteady Aerodynamics and Its Application to a Rotor Dynamic Problem. Paper No. 72, Proceedings of the 11th European Rotorcraft Forum, London, Sept. 1985.
115. Venkatesan, C.; and Friedmann, P. P.: A New Approach to Finite State Modeling of Unsteady Aerodynamics. AIAA Paper 86-0865CP, Proceedings of AIAA/ASME/ASCE/AHS 27th SDM Conference, San Antonio, Tex., May 1986, pp. 178-191.
116. Friedmann, P. P.: Arbitrary Motion Unsteady Aerodynamics and Its Application to Rotary-wing Aeroelasticity. Proceedings of the 42nd Annual National Forum of the American Helicopter Society, Washington, D.C., June 1986, pp. 757-776.
117. Ormiston, R. A.; and Bousman, W. G.: A Study of Stall Induced Flap-Lag Instability of Hingeless Rotors. J. Am. Helicopter Soc., vol. 20, no. 1, Jan. 1975, pp. 20-30.
118. Rogers, J. P.: Application of an Analytic Stall Model to Time-History and Eigenvalue Analysis of Rotor Blades. J. Am. Helicopter Soc., vol. 29, Jan. 1984, pp. 25-33.\*
119. Tran, C. T.; and Petot, D.: Semi-Empirical Model for the Dynamic Stall of Airfoils in View of the Application to the Calculation of Responses of a Helicopter Blade in Forward Flight. Vertica, vol. 5, no. 1, 1981, pp. 35-53.\*
120. Miller, R. H.: Rotor Blade Harmonic Airloading. AIAA J., vol. 2, no. 7, July 1964, p. 1260.\*
121. Dat, R.: La theorie de la surface portant appliquee a l'aile fixe et a l'helice. Rech. Aerospatiale No. 1973-4, Traduction ESRO-TT-90, 1974.\*
122. Runyan, Harry L.; and Tai, Hsiang: Application of a Lifting Surface Theory for a Helicopter in Forward Flight. Vertica, vol. 10, no. 3/4, 1986, pp. 269-280.

123. Dat, R.: Development of Basic Methods Needed to Predict Helicopter Aeroelastic Behaviour. *Vertica*, vol. 8, no. 3, 1984, pp. 209-228.\*
124. Tai, H.; and Runyan, Harry L.: Lifting Surface Theory for a Helicopter Rotor in Forward Flight. Second Decennial Specialists' Meeting on Rotorcraft Dynamics, AHS/NASA-Ames Research Center, Moffett Field, Calif., Nov. 1984.
125. Amer, K. B.: Theory of Helicopter Damping in Pitch or Roll and Comparison with Flight Measurements. NACA TN-2136, 1948.
126. Sissingh, G. J.: The Effect of Induced Velocity Variation on Helicopter Rotor Damping in Pitch or Roll. Aeronautical Research Council (Great Britain), Paper No. 101, Technical Note No. Aero. 2132, Nov. 1952.\*
127. Curtiss, H. C., Jr.; and Shupe, N. K.: A Stability and Control Theory for Hingeless Rotors. 27th Annual National Forum of the American Helicopter Society, Washington, D.C., May 1971.\*
128. Carpenter, P. J.; and Fridovich, B.: Effect of a Rapid Blade Pitch Increase on the Thrust and Induced Velocity Response of a Full Scale Helicopter Rotor. NASA TN-3044, 1953.
129. Kuczynski, W. A.; and Sissingh, G. J.: Research Program to Determine Rotor Response Characteristics at High Advance Ratios. NASA CR-114290, 1971.
130. Kuczynski, W. A.; and Sissingh, G. J.: Characteristics of Hingeless Rotors with Hub Moment Feedback Controls Including Experimental Rotor Frequency Response. NASA CR-114427 (Vol. I) and NASA CR-114428 (Vol. II), 1972.
131. Kuczynski, W. A.: Experimental Hingeless Rotor Characteristics at Full Scale First Flap Mode Frequencies. NASA CR-114519, 1972.
132. London, R. J.; Watts, G. A.; and Sissingh, G. J.: Experimental Hingeless Rotor Characteristics at Low Advance Ratio with Thrust. NASA CR-114684, 1973.
133. Peters, David A.; and Ormiston, Robert A.: Flapping Response Characteristics of Hingeless Rotor Blades by a Generalized Harmonic Balance Method. NASA TN D-7856, 1975.
134. Ormiston, Robert A.; and Peters, David A.: Hingeless Helicopter Rotor Response with Nonuniform Inflow and Elastic Blade Bending. *J. Aircraft*, vol. 9, no. 10, Oct. 1972, pp. 730-736.
135. Peters, David A.: Hingeless Rotor Frequency Response with Unsteady Inflow. Proceedings of the AHS/NASA Ames Specialists' Meeting on Rotorcraft Dynamics, NASA SP-352, 1974.



136. Crews, S. T.; Hohenemser, K. H.; and Ormiston, R. A.: An Unsteady Wake Model for a Hingless Rotor. J. Aircraft, vol. 10, no. 12, Dec. 1973, pp. 758-760.
137. Hohenemser, Kurt H.; and Crews, S. T.: Further Experiments with Progressing/Regressing Rotor Flapping Modes. NASA CR-114711, 1973.
138. Hohenemser, Kurt H.; and Crews, S. T.: Model Tests on Unsteady Rotor Wake Effects. J. Aircraft, vol. 10, no. 1, Jan. 1973, pp. 58-60.
139. Hohenemser, K. H.; and Crews, S. T.: Experiments with a Four-Bladed Cyclic Pitch Stirring Model Rotor. NASA CR-137572, 1974.
140. Hohenemser, K. H.; and Crews, S. T.: Additional Experiments with a Four-Bladed Cyclic Pitch Stirring Model Rotor. NASA CR-137966, 1975.
141. Hohenemser, K. H.; Banerjee, D.; and Yin, S. K.: Methods Studies on System Identification from Transient Rotor Tests. NASA CR-137965, 1975.
142. Hohenemser, K. H.; Banerjee, D.; and Yin, S. K.: Rotor Dynamic State and Parameter Identification from Simulated Forward Flight Transients. NASA CR-137963, 1976.
143. Hohenemser, K. H.; Banerjee, D.; and Yin, S. K.: Rotor Dynamic State and Parameter Identification from Simulated Forward Flight Transients. NASA CR-137963, 1976.
144. Hohenemser, K. H.; and Crews, Sam T.: Unsteady Hovering Wake Parameters Identified from Dynamic Model Tests. NASA CR-152022, 1977.
145. Hohenemser, K. H.; and Banerjee, D.: Application of System Identification to Analytical Rotor Modeling from Simulated and Wind Tunnel Dynamic Test Data. NASA CR-152023, 1977.
146. Banerjee, D.; Crews, S. T.; Hohenemser, K. H.; and Yin, S. K.: Identification of State Variables and Dynamic Inflow from Rotor Model Dynamic Tests. J. Am. Helicopter Soc., vol. 22, no. 2, Apr. 1977, pp. 28-36.
147. Banerjee, D.; Crews, S. T.; and Hohenemser, K. H.: Parameter Identification Applied to Analytic Hingeless Rotor Modeling. J. Am. Helicopter Soc., vol. 24, no. 1, Jan. 1979, pp. 26-32.
148. Heyson, H. H.; and Katzoff, S.: Induced Velocities Near a Lifting Rotor with Non-Uniform Disk Loading. NASA TR-1319, 1957.
149. Ormiston, R. A.: An Actuator Disk Theory for Rotor Wake Induced Velocities. AGARD Specialists' Meeting on the Aerodynamics of Rotary Wings, Marseilles, France, AGARD CP-111, Sept. 1972, pp. 2-1 to 2-19.

150. Mangler, K. W.: Calculation of the Induced Velocity Field of a Rotor. Royal Aircraft Establishment Report No. 2247, London, Feb. 1948.\*
151. Joglekar, M.; and Loewy, R.: An Actuator-Disk Analysis of Helicopter Wake Geometry and the Corresponding Blade Responses. USAAVLABS TR 69066, 1970.
152. Pitt, D. M.: Rotor Dynamic Inflow Derivatives and Time Constants from Various Inflow Models. Dissertation, Washington University, St. Louis, Mo., USATSARCOM TR 81-2, Dec. 1980.\*
153. Pitt, D. M.; and Peters, D. A.: Theoretical Prediction of Dynamic Inflow Derivatives. Vertica, vol. 5, no. 1, Mar. 1981, pp. 21-34.\*
154. Pitt, D. M.; and Peters, D. A.: Rotor Dynamic Inflow Derivatives and Time Constants from Various Inflow Models. Paper No. 55, 9th European Rotorcraft Forum, Stresa, Italy, Sept. 1983.\*
155. Gaonkar, G.; and Peters, D.: Effectiveness of Current Dynamic-Inflow Models in Hover and in Forward Flight. J. Am. Helicopter Soc., vol. 31, Apr. 1986, pp. 47-57.\*
156. Ormiston, R. A.: Application of Simplified Inflow Models to Rotorcraft Dynamic Analysis. J. Am. Helicopter Soc., vol. 21, no. 3, July 1976, pp. 34-39.
157. Peters, D. A.; and Gaonkar, G. H.: Theoretical Flap-Lag Damping with Various Dynamic Inflow Models. J. Am. Helicopter Soc., vol. 25, no. 3, July 1980, pp. 29-36.
158. Bousman, W. G.: An Experimental Investigation of the Effects of Aeroelastic Couplings on Aeromechanical Stability of a Hingeless Rotor Helicopter. J. Am. Helicopter Soc., vol. 26, no. 1, Jan. 1981, pp. 46-54.
159. Gaonkar, G. H.; Mitra, A. K.; Reddy, T. S. R.; and Peters, D. A.: Sensitivity of Helicopter Aeromechanical Stability to Dynamic Inflow. Vertica, vol. 6, no. 1, 1982, pp. 59-75.\*
160. Johnson, Wayne: The Influence of Unsteady Aerodynamics on Hingeless Rotor Ground Resonance. NASA TM-81302, 1981. (Also USAAVRADCOM TR 81-B-16, July 1981.)\*
161. Johnson, W.: Influence of Unsteady Aerodynamics on Hingeless Rotor Ground Resonance. J. Aircraft, vol. 29, no. 8, Aug. 1982, pp. 668-673.
162. Gaonkar, G. H.; Sastry, V. V. S. S.; and Reddy, T. S. R.: On the Adequacy of Modeling Dynamic Inflow for Helicopter Flap-Lag Stability. Paper No. 3.11, 8th European Rotorcraft Forum, Aix-en-Provence, France, 1982.\*

163. Nagabhushanam, J.; and Gaonkar, G. H.: Rotorcraft Air Resonance in Forward Flight with Various Dynamic Inflow Models and Aeroelastic Couplings. *Vertica*, vol. 8, no. 4, 1984, pp. 373-394.\*
164. Gaonkar, G. H.; and Peters, D. A.: Review of Dynamic Inflow Modeling for Rotorcraft Flight Dynamics, AIAA Paper 86-0845-CP, Proceedings of the AIAA/ASME/ASCE/AHS 27th SDM Conference, San Antonio, Tex., 1986.\*
165. Nagabhushanam, J.; Gaonkar, G. H.; and Reddy, T. S. R.: Automatic Generation of Equations for Rotor-Body Systems with Dynamic Inflow for A Priori Ordering Schemes. Paper No. 37, Proceedings of the 7th European Rotorcraft Forum, Garmisch-Partenkirchen, Sept. 1981.\*
166. Reddy, T. S. R.: Flap-Lag Damping of an Elastic Rotor Blade with Torsion and Dynamic Inflow in Hover from Symbolically Generated Equations. AIAA Paper 84-0989-CP, Palm Springs, Calif., 1984.
167. Reddy, T. S. R.; and Warmbrodt, W.: The Influence of Dynamic Inflow and Torsional Flexibility on Rotor Damping in Forward Flight from Symbolically Generated Equations. NASA CP-2400, 1984.
168. Reddy, T. S. R.: Symbolic Generation of Elastic Rotor Blade Equations Using a FORTRAN Processor and Numerical Study of Dynamic Inflow Effects on the Stability of Helicopter Rotors. NASA TM-86750, 1986.
169. Crespo da Silva, M. R. M.; and Hodges, D. H.: The Role of Computerized Symbolic Manipulation in Rotorcraft Dynamic Analysis. *Computers and Mathematics with Applications*, vol. 12A, no. 1, 1986, pp. 161-172.
170. Gaonkar, G. H.; Simha Prasad, D. S.; and Sastry, D.: On Computing Floquet Transition Matrices for Rotorcraft. *J. Am. Helicopter Soc.*, vol. 26, no. 3, July 1981, pp. 56-61.\*
171. Panda, B.; and Chopra, I.: Flap-Lag-Torsion Stability in Forward Flight. *J. Am. Helicopter Soc.*, vol. 30, Oct. 1985, pp. 30-39.\*
172. Schrage, Daniel P.; and Peters, David A.: Effect of Structural Coupling Parameters on the Flap-Lag Forced Response of a Rotor Blade in Forward Flight Using Floquet Theory. *Vertica*, vol. 3, no. 2, 1979, pp. 177-185.\*
173. Friedmann, P.; and Shamie, J.: Aeroelastic Stability of Trimmed Helicopter Blades in Forward Flight. *Vertica*, vol. 1, no. 3, 1977, pp. 189-211.
174. Friedmann, P. P.; and Kottapalli, S. B. R.: Coupled Flap-Lag-Torsional Dynamics of Hingeless Rotors in Forward Flight. *J. Am. Helicopter Soc.*, vol. 27, no. 4, Oct. 1982, pp. 28-36.

175. O'Malley, James A, III; Izadpanah, Amir P.; and Peters, D. A.: Comparisons of Three Numerical Trim Methods for Rotor Air Loads. Paper No. 58, Ninth European Rotorcraft Forum, Stresa, Italy, Sept. 1983.\*
176. Friedmann, P. P.: Numerical Methods for Determining the Stability and Response of Periodic Systems with Application to Helicopter Rotor Dynamics and Aeroelasticity. Computers and Mathematics with Applications, vol. 12A, no. 1, 1986, pp. 131-148.\*
177. Eipe, Abraham: Effect of Some Structural Parameters on Elastic Rotor Loads by an Iterative Harmonic Balance. Ph.D. Dissertation, Washington University, St. Louis, Mo., Dec. 1979.\*
178. Wei, F.-S.; and Peters, D. A.: Lag Damping in Autorotation by a Perturbation Method. Paper No. 78-25, 34th Annual National Forum of the American Helicopter Society, Washington, D.C., 1978.\*
179. Peters, D. A.; Kim, B. S.; and Chen, H. S.: Calculation of Trim Settings for a Helicopter Rotor by an Optimized Automatic Controller. J. Guidance, Control & Dynamics, vol. 7, no. 1, Jan.-Feb. 1984, pp. 85-91.\*
180. Peters, David A.; and Izadpanah, Amir P.: Helicopter Trim by Periodic Shooting with Newton-Raphson Iteration. Proceedings of the 37th Annual National Forum of the American Helicopter Society, New Orleans, La., 1981, pp. 217-226.\*
181. Hodges, Dewey H.: A Simplified Algorithm for Determining the Stability of Linear Systems. AIAA J., vol. 15, no. 3, Mar. 1977, pp. 424-425.
182. Peters, David A.; and Hohenemser, Kurt H.: Application of the Floquet Transition Matrix to Problems of Lifting Rotor Stability. J. Am. Helicopter Soc., vol. 16, no. 2, Apr. 1971, pp. 25-33.\*
183. Friedmann, P.; and Silverthorn, L. J.: Aeroelastic Stability of Periodic Systems with Application to Rotor Blade Flutter. AIAA J., vol. 12, no. 11, Nov. 1974, pp. 1559-1565.
184. Friedmann, P.; Hammond, C. E.; and Woo, T.: Efficient Numerical Treatment of Periodic Systems with Application to Stability Problems. Int. J. Numerical Methods in Engineering, vol. 11, July 1977, pp. 1117-1136.
185. Peters, David A.: An Approximate Solution for the Free Vibrations of Rotating Uniform Cantilever Beams. NASA TM X-62,299, Sept. 1973.
186. Hodges, Dewey H.: An Approximate Formula for the Fundamental Frequency of Uniform Rotating Beams Clamped Off the Axis of Rotation. J. Sound and Vibration, vol. 77, no. 1, July 8, 1981, pp. 11-18.

187. Peters, D. A.; and Hodges, D. H.: In-Plane Vibration and Buckling of a Rotating Beam Clamped Off the Axis of Rotation. J. Appl. Mech., vol. 47, no. 2, June 1980, pp. 398-402.
188. Tong, Pin: The Nonlinear Instability in Flap-Lag of EE, PM Rotor Blades in Forward Flight. NASA CR-114524, 1971.
189. Friedmann, P.; and Tong, P.: Nonlinear Flap Lag Dynamics of Hingeless Helicopter Blades in Hover and in Forward Flight. J. Sound and Vibration, vol. 30, no. 1, 1973, pp. 9-31.
190. Johnson, Wayne: A Perturbation Solution of Helicopter Rotor Flapping Stability. NASA TM X-62,165, 1972.
191. Johnson, Wayne, A Perturbation Solution of Rotor Flapping Stability. Paper No. 72-955, AIAA 2nd Atmospheric Flight Mechanics Conference, Palo Alto, Calif., Sept. 1972.
192. Johnson, Wayne: A Perturbation Solution of Helicopter Rotor Flapping Stability. J. Aircraft, vol. 10, no. 5, May 1973, pp. 257-258.
193. Johnson, Wayne: Perturbation Solutions for the Influence of Forward Flight on Helicopter Rotor Flapping Stability. NASA TM X-62,361, 1974.
194. Yin, Sheng-Kuang; and Hohenemser, Kurt H.: The Method of Multiblade Coordinates in the Linear Analysis of Lifting Rotor Dynamic Stability and Gust Response at High Advanced Ratio. Paper No. 512, 27th Annual National V/STOL Forum of the American Helicopter Society, Washington, D.C., May 1971.
195. Hohenemser, K. H.; and Yin, S. K.: Analysis of Gust Alleviation Methods and Rotor Dynamics Stability. NASA CR-114387, 1971.
196. Hohenemser, Kurt H.; and Yin, S. K.: Effects of Blade Torsion, of Blade Flap Bending Flexibility and of Rotor Support Flexibility on Rotor Stability and Random Response. NASA CR-114480, 1972.
197. Biggers, J. C.: Some Approximations to the Flapping Stability of Helicopter Rotors. J. Am. Helicopter Soc., vol. 14, no. 4, Oct. 1974, pp. 24-33.
198. Young, M. I.: A Theory of Rotor Blade Motion Stability in Powered Flight. J. Am. Helicopter Soc., vol. 9, no. 3, July 1964.\*
199. Hohenemser, K. H.; and Heaton, P. W.: Aeroelastic Instability of Torsionally Rigid Helicopter Blades. J. Am. Helicopter Soc., vol. 12, no. 2, Apr. 1967, pp. 1-13.\*

200. Young, Maurice I., Dr.: A Simplified Theory of Hingeless Rotors with Application to Tandem Helicopters. Proceedings of the 18th Annual National Forum of the American Helicopter Society, Washington, D.C., May 1962.\*
201. Curtiss, H. C., Jr.: Sensitivity of Hingeless Rotor Blade Flap-Lag Stability in Hover to Analytical Modeling Assumptions. AMS Report No. 1236, Princeton University, Princeton, N.J., 1975. (Also, NASA CR-137967, 1975.)
202. Ormiston, R. A.: Techniques for Improving the Stability of Soft-Inplane Hingeless Rotors. NASA TM X-62390, 1974.
203. Peters, David A.: An Approximate Closed-Form Solution for Lead-Lag Damping of Rotor Blades in Hover. NASA TM X-62,425, 1975.
204. Kaza, K. R. V.; and Kvaternik, R. G.: Examination of the Flap-Lag Stability of Rigid Articulated Rotor Blades. J. Aircraft, vol. 16, no. 12, Dec. 1979.
205. Tong, Pin: Nonlinear Instability of a Helicopter Blade. Paper No. 72-956, AIAA 2nd Atmospheric Flight Mechanics Conference, Palo Alto, Calif., Sept. 1972.
206. Friedmann, Peretz: Investigation of Some Parameters Affecting the Stability of a Hingeless Helicopter Blade in Hover. NASA CR-114525, 1972.
207. Friedmann, P.: Aeroelastic Instabilities of Hingeless Helicopter Blades. J. Aircraft, vol. 10, no. 10, Oct. 1973, pp. 623-631.
208. Friedmann, P.: Some Conclusions Regarding the Aeroelastic Stability of Hingeless Helicopter Blades in Hover and in Forward Flight. J. Am. Helicopter Soc., vol. 18, no. 4, Oct. 1973, pp. 13-23.
209. Ormiston, Robert A.; and Hodges, Dewey H.: Discussion of Some Conclusions Regarding the Aeroelastic Stability of Hingeless Helicopter Blades in Hover and Forward Flight. J. Am. Helicopter Soc., vol. 20, no. 3, July 1975, pp. 46-47.
210. White, William F., Jr.: Importance of Helicopter Dynamics to the Mathematical Model of the Helicopter. AGARD Flight Mechanics Panel, Specialists' Meeting, LARC, Nov. 1974.
211. Kunz, Donald L.: Effects of Unsteady Aerodynamics on Rotor Aeroelastic Stability. NASA TM-78,434, 1977.
212. Friedmann, P.; and Silverthorn, L. J.: Aeroelastic Stability of Coupled Flap-Lag Motion of Hingeless Helicopter Blades at Arbitrary Advance Ratios. NASA CR-132,431, 1974.

213. Friedmann, P.; and Silverthorn, L. J.: Flap-Lag Dynamics of Hingeless Helicopter Blades at Moderate and High Advance Ratios. Presented at AHS/NASA Ames Specialists' Meeting on Rotorcraft Dynamics, Feb. 13-15, 1974.
214. Friedmann, P.; and Silverthorn, L. J.: Aeroelastic Stability of Coupled Flap-Lag Motion of Hingeless Helicopter Blades at Arbitrary Advance Ratios. J. Sound and Vibration, vol. 39, no. 4, 1975, pp. 409-428.
215. Peters, D. A.: Flap-Lag Stability of Helicopter Rotor Blades in Forward Flight. J. Am. Helicopter Soc., vol. 20, no. 4, Oct. 1975, pp. 2-13.
216. Gaonkar, G. H.; and Peters, D. A.: Use of Multiblade SIU Coordinates for Helicopter Flap-Lag Stability with Dynamic Inflow. J. Aircraft, vol. 17, no. 2, Feb. 1980, pp. 112-118.\*
217. Shamie, J.; and Friedmann, P.: Aeroelastic Stability of Complete Rotors with Application to a Teetering Rotor in Forward Flight. J. Sound and Vibration, vol. 53, no. 4, Aug. 1977, pp. 559-584.
218. Reddy, T. S. R.; and Warmbrodt, William: Forward Flight Aeroelastic Stability from Symbolically Generated Equations. J. Am. Helicopter Soc., vol. 31, no. 3, July 1986, pp. 35-54.
219. Ormiston, Robert A.; and Bousman, William G.: A Theoretical and Experimental Investigation of Flap-Lag Stability of Hingeless Helicopter Rotor Blades. Presented at the 8th Army Science Conference, West Point, N.Y., June 1972.
220. Ormiston, Robert A.; and Bousman, William G.: A Theoretical and Experimental Investigation of Flap-Lag Stability of Hingeless Helicopter Rotor Blades. NASA TM X-62,179, 1972.
221. Bousman, W. G.; Sharpe, D. L.; and Ormiston, R. A.: An Experimental Study of Techniques for Increasing the Lead-Lag Damping of Soft Inplane Hingeless Rotors. Paper No. 1035, 32nd Annual National V/STOL Forum of the American Helicopter Society, Washington, D.C., May 1976.
222. Curtiss, H. C., Jr.; and Putman, W. F.: An Experimental Investigation of the Flap-Lag Stability of a Hingeless Rotor with Comparable Levels of Hub and Blade Stiffness in Hovering Flight. NASA CR-151924, 1976.
223. Gaonkar, G. H.; McNulty, M. J.; and Nagabhushanam, J.: An Experimental and Analytical Investigation of Isolated Rotor Flap-Lag Stability in Forward Flight. Paper No. 66, 11th European Rotorcraft Forum, London, England, Sept. 1985.
224. Miller, R. H.; and Ellis, C. W.: Helicopter Blade Vibration and Flutter. J. Am. Helicopter Soc., vol. 1, no. 3, July 1956, pp. 19-38.\*

225. Hodges, D. H.; and Ormiston, R. A.: Stability of Elastic Bending and Torsion of Uniform Cantilevered Rotor Blades in Hover. AIAA Paper 73-405, Proceedings of 14th AIAA/ASME/ASCE/AHS SDM Conference, Williamsburg, Va., Mar. 20-22, 1973.
226. Johnson, Wayne: Flap/Lag/Torsion Dynamics of a Uniform, Cantilever Rotor Blade in Hover. NASA TM 73,248, 1977.
227. Chopra, I.; and Johnson, W.: Flap-Lag-Torsion Aeroelastic Stability of Circulation-Controlled Rotors in Hover. J. Am. Helicopter Soc., vol. 24, no. 2, Apr. 1979.
228. Chopra, I.: Dynamic Analysis of Constant-Lift and Free Tip Rotor. J. Am. Helicopter Soc., vol. 28, Jan. 1983, pp. 24-33.
229. Pierce, G. Alvin; and White, William F., Jr.: Unsteady Rotor Aerodynamics at Low Inflow and Its Effects on Flutter. AIAA Paper 72-959, Palo Alto, Calif., 1972.
230. Sharpe, David L.: An Experimental Investigation of the Flap-Lag-Torsion Aeroelastic Stability of a Small-Scale Hingeless Helicopter Rotor in Hover. NASA TP-2546, 1986. (Also, AVSCOM TR 850A-9, Jan. 1986.)
231. Peterson, Randall L.; and Warmbrodt, William: Hover Test of a Full-Scale Hingeless Helicopter Rotor: Aeroelastic Stability, Performance, and Loads Data. NASA TM-85892, 1984.
232. Warmbrodt, W.; and Peterson, R. L.: Hover Test of a Full-Scale Hingeless Rotor. NASA TM-85990, 1984.
233. Warmbrodt, William; and Peterson, Randall L.: Hover Test of a Full-Scale Hingeless Rotor. Paper No. 68, Tenth European Rotorcraft Forum, The Hague, Netherlands, Aug. 1984.
234. Astill, Clifford J.; and Niebanck, Charles F.: Prediction of Rotor Instability at High Forward Speeds. Vol. II Classical Flutter. USAAVLABS TR-68-18B, Feb. 1969.
235. Carta, Franklin O.; and Niebanck, Charles F.: Prediction of Rotor Instability at High Forward Speeds. Vol. III. Stall Flutter. USAAVLABS TR-68-18C, Feb. 1969.
236. Niebanck, Charles F.; and Elman, H. L.: Prediction of Rotor Instability at High Forward Speeds. Vol. IV. Torsional Divergence. USAAVLABS TR-68-18D, Feb. 1969.



237. Elman, H. L.; Niebanck, Charles F.; and Bain, Lawrence J.: Prediction of Rotor Instability at High Forward Speeds. Vol. V. Flapping and Flap-Lag Instability. USAAVLABS TR-68-18E, Feb. 1969.
238. Niebanck, Charles F.; and Bain, Lawrence J.: Rotor Aeroelastic Instability and Transient Characteristics. USAAVLABS TR-69-88, Feb. 1970.
239. Lytwyn, R. T.; and Miao, W.: Airborne and Ground Resonance of Hingeless Rotors. Paper No. 414, 26th Annual National Forum of the American Helicopter Society, Washington, D. C., 1970.\*
240. Hohenemser, Kurt H.; and Yin, S. K.: The Effects of Some Rotor Feedback Systems on Rotor-Body Dynamics. NASA CR-114709, 1973.
241. Hohenemser, K. H.; and Yin, S. K.: On the Use of First Order Rotor Dynamics in Multiblade Coordinates. Paper No. 831, 30th Annual National Forum of the American Helicopter Society, Washington, D.C., 1974.
242. Hohenemser, K. H.; and Yin, S. K.: Methods Studies Toward Simplified Rotor-Body Dynamics. NASA CR-137570, 1974.
243. Ormiston, Robert A.: Concepts for Improving Hingeless Rotor Stability. Presented at the AHS Mideast Region Symposium on Rotor Technology, Essington, Pa., Aug. 1976.
244. Johnson, Wayne: Calculated Dynamic Characteristics of a Soft-Inplane Hingeless Rotor Helicopter. NASA TM-73,262, 1977.
245. Straub, F. K.; and Warmbrodt, W.: The Use of Active Controls to Augment Rotor/Fuselage Stability. J. Am. Helicopter Soc., vol. 30, July 1985, pp. 13-22.
246. Venkatesan, C.; and Friedmann, P.: Aeromechanical Stability Analysis of a Hybrid Heavy Lift Multirotor Vehicle in Hover. J. Aircraft, vol. 22, Nov. 1985, pp. 965-972.
247. Burkam, John E.; and Miao, Wen-Liu: Exploration of Aeroelastic Stability Boundaries with a Soft-in-Plane Hingeless-Rotor Model. Paper No. 610, 28th Annual National Forum of the American Helicopter Society, Washington, D.C., May 1972.\*
248. Bousman, William G.: An Experimental Investigation of Hingeless Helicopter Rotor-Body Stability in Hover. NASA TM-78489, 1978. (Also, AVRADCOM TR 78-17 (AM), June 1978.)
249. Bousman, W. G.; and Hodges, D. H.: An Experimental Study of Coupled Rotor-Body Aeromechanical Instability of Hingeless Rotors in Hover. Vertica, vol. 3, no. 3/4, 1979, pp. 221-244.

250. Friedmann, P. P.; and Venkatesan, C.: Coupled Rotor/Body Aeromechanical Stability Comparison of Theoretical and Experimental Results. J. Aircraft, vol. 22, Feb. 1985, pp. 148-155.
251. Friedmann, P. P.; and Venkatesan, C.: Influence of Unsteady Aerodynamic Models on Aeromechanical Stability in Ground Resonance. J. Am. Helicopter Soc., vol. 31, Jan. 1986, pp. 65-74.
252. Yeager, W. T.; Hamouda, M. H.; and Mantay, W. R.: Aeromechanical Stability of a Hingeless Rotor in Hover and Forward Flight: Analysis and Wind Tunnel Tests. NASA TM-85653, 1983. (Also, AVRADCOM TR 83-B-5, Aug. 1983.)
253. Yeager, W. T. Jr.; Hamouda, M. H.; and Mantay, W. R.: Aeromechanical Stability of a Hingeless Rotor in Hover and Forward Flight: Analysis and Wind Tunnel Tests. Paper No. 54, Proceedings of the 9th European Rotorcraft Forum, Stresa, Italy, Sept. 1983.
254. Chen, C.; Staley, J. A.; Miao, W.; and Harris, F. D.: Aeroelastic Stability Test Results for a 1/5.86 Scale Model of a Bearingless Main Rotor System on the BO-105 Helicopter. Boeing Vertol Company Report D210-11245-1, July 1977.
255. Warmbrodt, W.; McCloud, J. L. III; Sheffler, M.; and Staley, J.: Full-Scale Wind-Tunnel Test of the Aeroelastic Stability of a Bearingless Main Rotor. Vertica, vol. 6, no. 3, 1982, pp. 165-180.
256. Dawson, S.: An Experimental Investigation of the Stability of a Bearingless Model Rotor in Hover. J. Am. Helicopter Soc., vol. 28, no. 4, Oct. 1983, pp. 29-34.
257. Bousman, W. G.; and Dawson, S.: Experimentally Determined Flutter from Two- and Three-Bladed Model Bearingless Rotors in Hover. J. Am. Helicopter Soc., vol. 31, July 1986, pp. 45-53.
258. Weller, William W.: Correlating Measured and Predicted Inplane Stability Characteristics for an Advanced Bearingless Rotor. NASA CR-166280, 1982.
259. Weller, W. H.: Correlation and Evaluation of Inplane Stability Characteristics for an Advanced Bearingless Main Rotor Model. NASA CR-166448, 1983.
260. Weller, W. H.; and Peterson, R. L.: Inplane Stability Characteristics for an Advanced Bearingless Main Rotor Model. J. Am. Helicopter Soc., vol. 29, no. 3, July 1984, pp. 45-53.
261. Mychalowycz, Evhen M.: Integrated Technology Rotor/Flight Research Rotor Preliminary Design. AVSCOM TR-86-D-8, Mar. 1987.

262. Reed, W. H., III; and Bland, S. R.: An Analytical Treatment of Aircraft Propeller Precession Instability. NASA TN D-659, 1961.
263. Houbolt, J. C.; and Reed, W. H., III: Propeller-Nacelle Whirl Flutter. J. Aeronaut. Sci., vol. 29, no. 3, Mar. 1962.
264. Reed, W. H., III: Review of Propeller-Rotor Whirl Flutter. NASA TR R-264, 1967.
265. Young, M. I.; and Lytwyn, R. T.: The Influence of Blade Flapping Restraint of the Dynamic Stability of Low Disk Loading Propeller-Rotors. J. Am. Helicopter Soc., vol. 12, no. 4, Oct. 1967.\*
266. Hall, W. E., Jr.: Prop-Rotor Stability at High Advance Ratios. J. Am. Helicopter Soc., vol. 11, no. 2, Apr. 1966.\*
267. Edenborough, H. K: Investigation of Tilt Rotor VTOL Aircraft Rotor-Pylon Stability. J. Aircraft, vol. 5, no. 6, Mar. 1968.\*
268. Kvaternik, Raymond G.: Experimental and Analytical Studies in Tilt-Rotor Aeroelasticity. Presented at AHS/NASA Ames Research Center Specialists' Meeting on Rotorcraft Dynamics, Moffett Field, Calif., Feb. 1974.
269. Kvaternik, Raymond G.: A Review of Some Tilt-Rotor Aeroelastic Research at NASA-Langley. J. Aircraft, vol. 18, no. 5, May 1976, pp. 357-363.
270. Johnson, W.: Theory and Comparison with Tests of Two Full-Scale Prop-Rotors. NASA SP-352, 1974.
271. Johnson, W.: Analytical Modeling Requirements for Tilting Proprotor Aircraft Dynamics. NASA TN D-8013, 1975.
272. Johnson, W.: The Influence of Pitch-Lag Coupling on the Predicted Aeroelastic Stability of the XV-15 Tilting Proprotor Aircraft. NASA TM X-73213, Feb. 1977.
273. Alexander, H. R.; Hengen, L. M.; and Weiberg, J. A.: Aeroelastic Stability Characteristics of a V/STOL Tilt-Rotor Aircraft with Hingeless Blades: Correlation of Analysis and Test. J. Am. Helicopter Soc., vol. 20, no. 2, Apr. 1975.
274. Johnson, W.: Assessment of Aerodynamic and Dynamic Models in a Comprehensive Analysis for Rotorcraft. Computers and Mathematics, May 1985.
275. Research and Technology, 1985 Annual Report of the Langley Research Center. NASA TM-87623, 1985.

- 276. Popelka, D.; Sheffler, M.; and Bilger, J.: Correlation of Stability Test Results and Analysis for the 1/5-Scale V-22 Aeroelastic Model. J. Am. Helicopter Soc., vol. 32, no. 2, Apr. 1987.\*
- 277. ITR Methodology Assessment Workshop. Proceedings of the U.S. Army Research & Technology Laboratory (AVRADCOM) and NASA Ames Research Center Conference, Moffett Field, Calif., June 1983 (to be published).
- 278. Donham, R. E.; and Cardinale, S. V.: Flight Test and Analytical Data for Dynamics and Loads in a Hingeless Rotor. U.S. Army Contract DAAJ01-73-C-0286, Lockheed Report LR 26215, Dec. 1973.
- 279. Johnston, J. F.; and Conner, F.: The Reactionless In-Plane Mode of Stiff-In-Plane Hingeless Rotors. LR 26214, Lockheed-California Company, Dec. 1973.
- 280. Johnston, J. F.; and Cook, J. R.: AH-56A Vehicle Development. Paper No. 574, 27th Annual National Forum of the American Helicopter Society, Washington, D.C., May 1971.\*
- 281. Anderson, W. D.: Investigation of Reactionless Mode Stability Characteristics of a Stiff In-Plane Hingeless Rotor System. AHS Preprint No. 734, 29th Annual National Forum of the American Helicopter Society, Washington, D.C., 1973.\*
- 282. Anderson, W. D.; and Johnston, J. F.: Comparison of Flight Data and Analysis for Hingeless Rotor Regressive Inplane Mode Stability. NASA SP-352, 1974.\*
- 283. Hughes, Charles W.; and Wernicke, Rodney K.: Flight Test of a Hingeless Flexbeam Rotor System, USAAMRDL-TR-74-38, June 1974.
- 284. White, Bill; and Weller, William: The Flexhinge Rotor. American Helicopter Society Mideast Region Symposium on Rotor Technology, Essington, Pa., Aug. 1976.
- 285. Cresap, Wesley L.; Myers, Alan W.; and Viswanathan, Sathy P.: Design and Development Tests of a Four-Bladed Light Helicopter Rotor System. Paper No. 78-7, 34th Annual National Forum of the American Helicopter Society, Washington, D.C., May 1978.\*
- 286. White, B. P.: Predesign Study of the Flexhinge Rotor for the Rotor Systems Research Aircraft. NASA CR-145162, July 1977.
- 287. Donham, R. E.; Cardinale, S. V.; and Sachs, I. B.: Ground and Air Resonance Characteristics of a Soft In-Plane Rigid Rotor System. J. Am. Helicopter Soc., vol. 14, no. 4, Oct. 1969.

288. Swindlehurst, Carl E., Jr.: Development of the Composite Bearingless Main Rotor System. Paper presented at the American Helicopter Society Mideast Regional Symposium on Rotor Technology, Essington, Pa., Aug. 1976.
289. Advanced System Design Study of a Composite Structures Rotor. NASA CR-145092, 1977.
290. Harris, Franklin D.; Cancro, Patrick A.; and Dixon, Peter G. C.: The Bearingless Main Rotor. Paper No. 4, 3rd European Rotorcraft and Powered-Lift Aircraft Forum, Aix-en-Provence, France, Sept. 1977.
291. Staley, James A.; and Reed, Donald A.: Aeroelastic Stability and Vibration Characteristics of a Bearingless Main Rotor. Boeing Vertol Document D210-11498-1, Vols. I,II, June 1979.
292. Sheffler, Marc; Staley, James; Hoover, James; Sovjak, Cheryl; and White, Fred: Full Scale Wind Tunnel Investigation of a Bearingless Main Helicopter Rotor Final Report. NASA CR-152373, 1980.
293. Warmbrodt, William; and McCloud, John L. III: A Full-Scale Wind Tunnel Investigation of a Helicopter Bearingless Main Rotor. NASA TM-81321, 1981.
294. Sheffler, M.; Warmbrodt, W.; and Staley, J.: Evaluation of the Effect of Elastomeric Damping Material on the Stability of a Bearingless Main Rotor System. American Helicopter Society Mideast Region Meeting on Rotor System Design, Philadelphia, Pa., Oct. 1980.
295. Bousman, William G.; Ormiston, Robert A.; and Mirick, Paul H.: Design Considerations for Bearingless Rotor Hubs. Paper No. A-83-39-62-1000, presented at the 39th Annual National Forum of the American Helicopter Society, St. Louis, Mo., 1983.
296. Carlson, Raymond G.; and Miao, Wen-Liu: Aeroelastic Analysis of the Elastic Gimbal Rotor. NASA CR-166287, 1981. (Also, USAAVRADCOM TR 82-A-3, May 1981.)
297. Gaffey, T. M.: The Effect of Positive Pitch-Flap Coupling (Negative  $w_3$ ) on Rotor Blade Motion Stability and Flapping. J. Am. Helicopter Soc., vol. 14, no. 2, Apr. 1969.\*
298. Gaffey, T. M.; Yen, J. G.; and Kvaternik, R. G.: Analysis and Model Tests of the Proprotor Dynamics of a Tilt-Proprotor VTOL Aircraft. Air Force V/STOL Technology and Planning Conference, Las Vegas, Nev., Sept. 1969.
299. Johnson, W.: Predicted Dynamic Characteristics of the XV-15 Tilting Proprotor Aircraft in Flight and in the 40- by 80-Foot Wind Tunnel. NASA TM X-73158, 1976.

300. Marr, R. L.; Blackman, S.; Weiberg, J. A.; and Schroers, L. G.: Wind Tunnel and Flight Test of the XV-15 Tilt Rotor Research Aircraft. Paper No. 79-54, 35th Annual National Forum of the American Helicopter Society, Washington, D.C., 1979.
301. Bilger, J. M.; Marr, R. L.; and Zahedi, A.: Results of Structural Dynamic Testing of the XV-15 Tilt Rotor Research Aircraft. J. Am. Helicopter Soc., vol. 27, no. 2, Apr. 1982.\*
302. Popelka, David; Sheffler, Marc; and Bilger, Jim: Correlation of Stability Test Results and Analysis for the 1/5 Scale V-22 Aeroelastic Model. Paper presented at the 41st Annual National Forum of the American Helicopter Society, Fort Worth, Tex., 1985.\*
303. Johnson, W.; Lau, B. H.; and Bowles, J. V.: Calculated Performance, Stability, and Maneuverability of High-Speed Tilting Prop-Rotor Aircraft. NASA TM-88349, 1986.
304. Watts, G. A.; London, R. J.; and Snoddy, R. J.: Trim, Control, and Stability of a Gyro-Stabilized Hingeless Rotor at High Advance Ratio and Low Rotor Speed. NASA CR-114362, 1971.
305. Maloney, P. F.; and Porterfield, J. D.: Elastic Pitch Beam Tail Rotor. TR 76-35, U.S. Army Air Mobility R&D Lab, 1976.
306. Edwards, W. T.; and Miao, W.: Bearingless Tail Rotor Loads and Stability. Boeing Vertol Co. Report No. D210-11025-1 (USAAMRDL TR-76-16), 1976.
307. Full-Scale Wind Tunnel Investigation of the Advancing Blade Concept Rotor System. USAAVLABS Technical Report 7-25, U.S. Army Aviation Material Laboratories, Fort Eustis, Va., Aug. 1971.
308. Advancing Blade Concept (ABC) Technology Demonstrator. Applied Technology Laboratory, U.S. Army Research and Technology Laboratories (AVRADCOM), Fort Eustis, VA., Apr. 1977.
309. Chopra, Inderjit: Flap-Lag-Torsion Flutter Analysis of a Constant Lift Rotor. NASA CR-152244, Jan. 1979.
310. Chopra, I.: Dynamic Analysis of a Free-Tip Rotor. 1) Paper No. 81-0618-CP, presented at AIAA/ASME/ASCE/AHS 22nd SDM Conference, Atlanta, Ga., Apr. 6-10, 1981.

**TABLE 1.- TECHNOLOGY BACKGROUND FOR ROTORCRAFT AEROELASTIC  
STABILITY: PRE-1970 PERIOD COMPARED WITH POST-1970**

TECHNOLOGY \ APPLICATIONS	PRE 1970	POST 1970
	ARTICULATED/ TEETERING MODERATE SPEED	HINGELESS/BEARINGLESS TILT ROTOR
BLADE STABILITY	BENDING-TORSION FLUTTER  WAKE FLUTTER	BENDING-TORSION FLUTTER WAKE FLUTTER FLAP-LAG TORSION FLOQUET THEORY
BEAM EQUATIONS	LINEAR ISOTROPIC MATERIALS	NONLINEAR MULTIPLE LOAD PATH STRUCTURES COMPOSITE MATERIALS
UNSTEADY AERODYNAMICS	2-D AERODYNAMICS THEODORSEN/LOEWY	2-D/3-D AERO THEODORSEN/LOEWY DYNAMIC INFLOW DYNAMIC STALL TRANSONIC AERO
GROUND RESONANCE AIR RESONANCE	CLASSICAL GROUND RESONANCE	COMPLEX/AEROMECHANICAL GROUND RESONANCE AIR RESONANCE HOVER, FORWARD FLIGHT

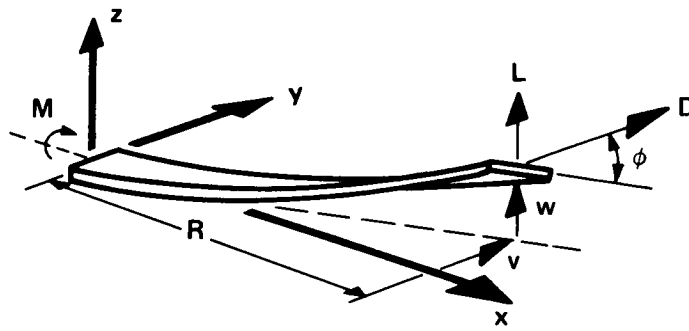


Figure 1.- Nonlinear torsion of an elastic cantilever beam resulting from simultaneous flapwise and chordwise bending.

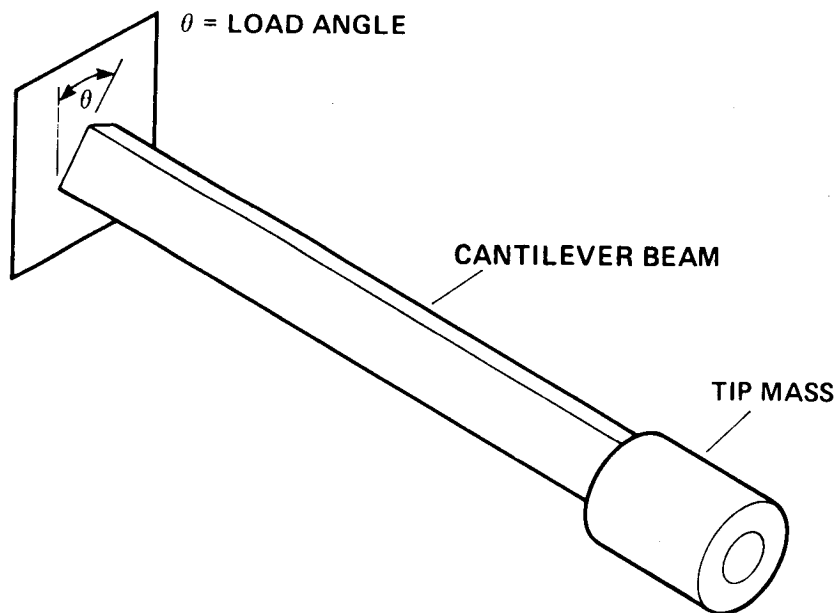


Figure 2.- Experimental arrangement for inducing nonlinear torsion by subjecting an elastic cantilever beam to combined flatwise and edgewise bending by varying load angle of tip-mass gravity force.



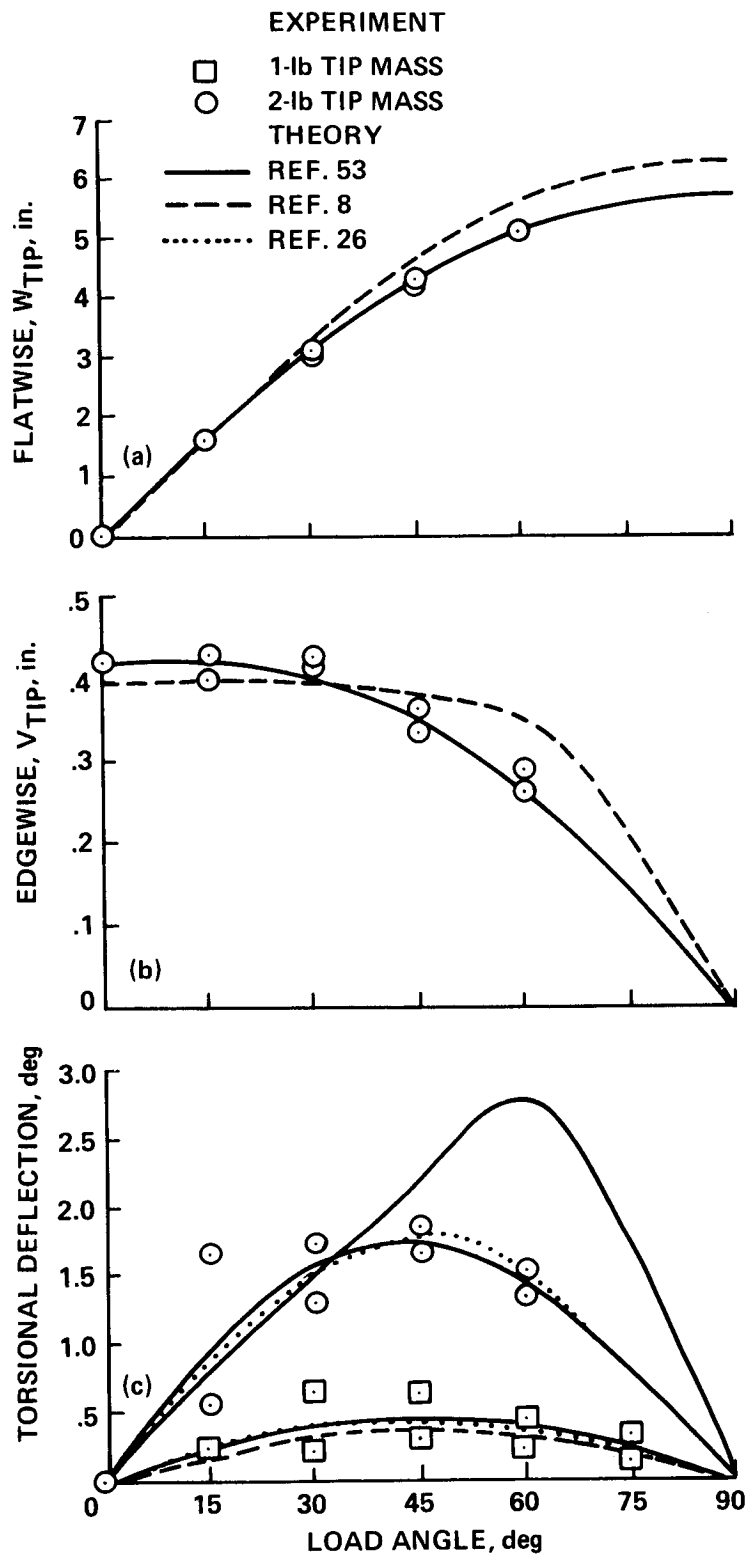


Figure 3.- Static deflections of Princeton beam compared with theoretical predictions. (a) Flatwise deflection. (b) Edgewise deflection. (c) Torsion deflection.

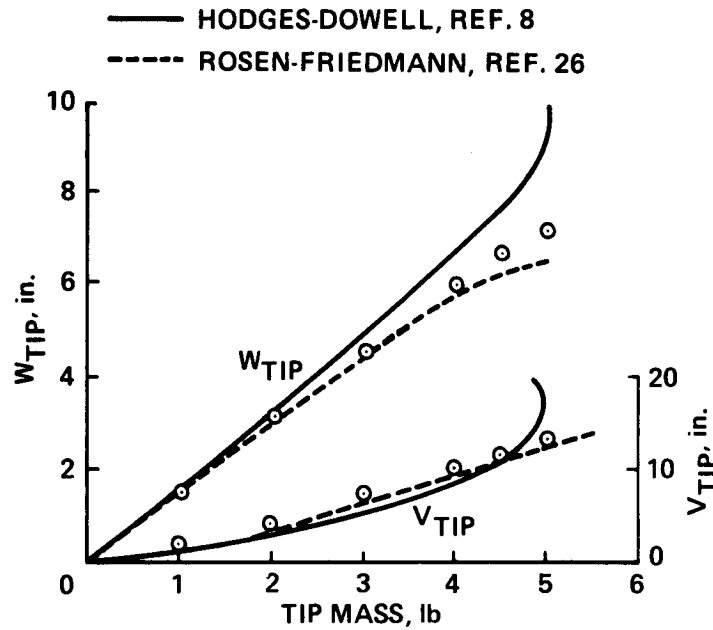


Figure 4.- Static flatwise and edgewise deflections of Princeton beam compared with theoretical predictions for 30° load angle.

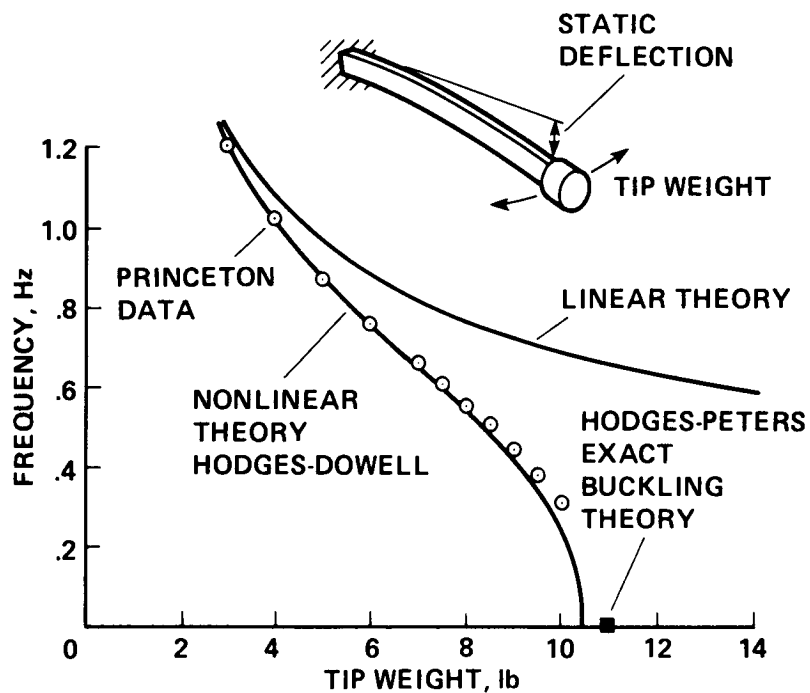


Figure 5.- Flatwise bending frequency of Princeton beam as a function of static edgewise loading together with nonlinear buckling.

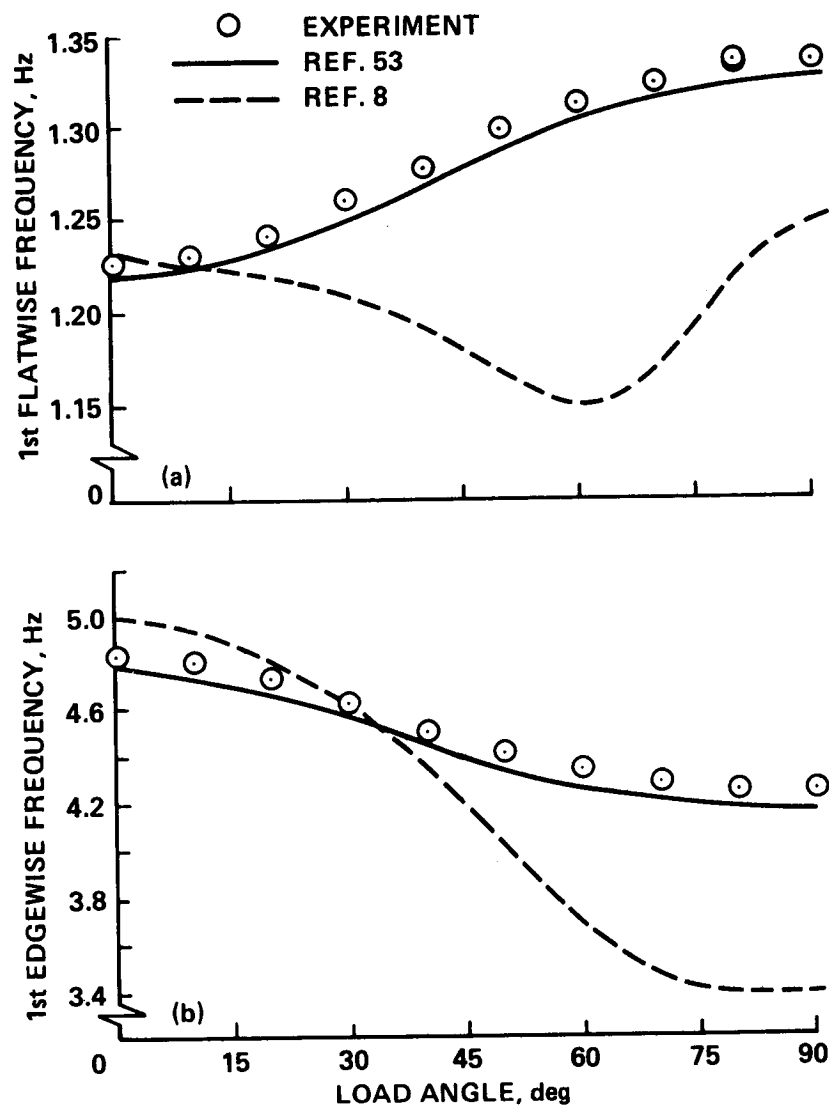


Figure 6.- Bending frequencies of Princeton beam as a function of load angle compared with theoretical predictions; 2-lb tip mass. (a) Flatwise frequency. (b) Edgewise frequency.

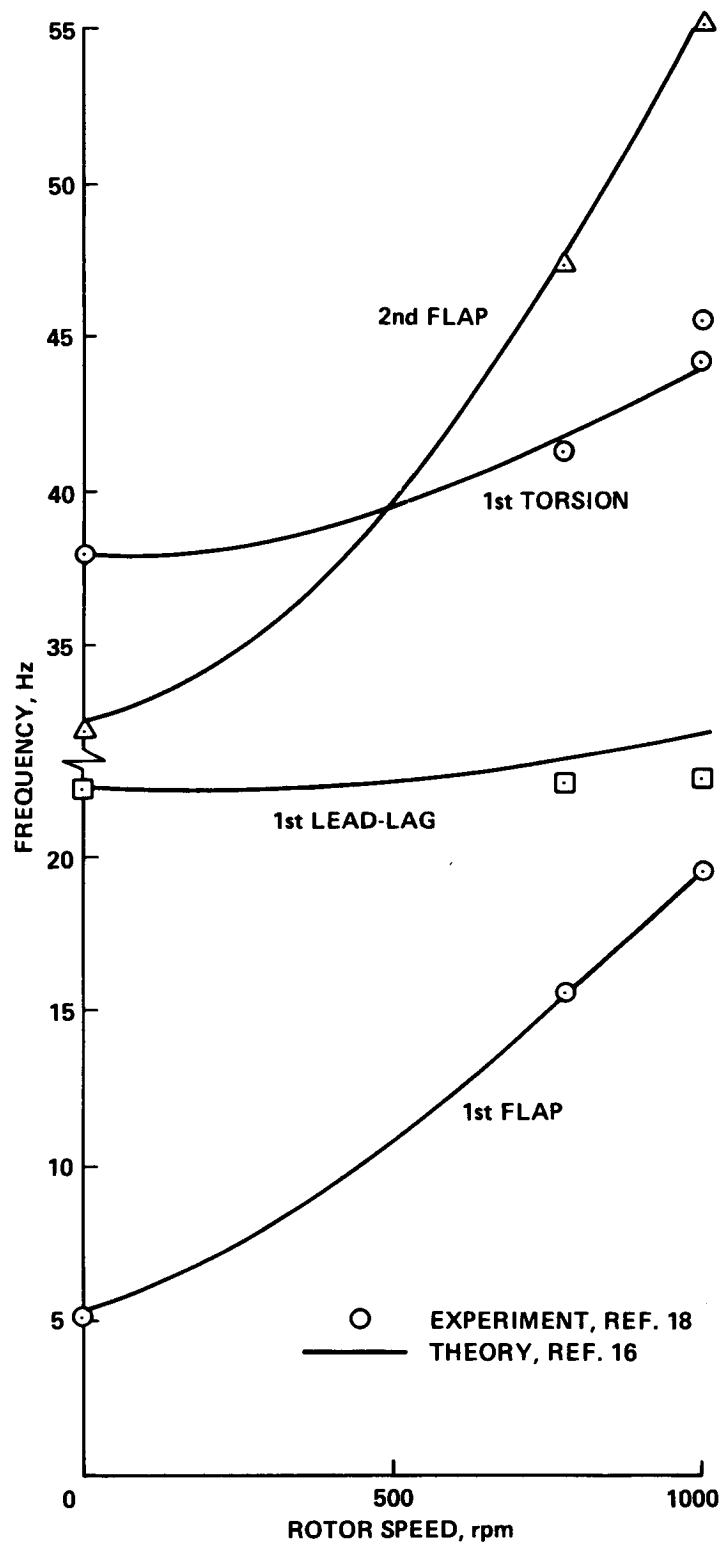


Figure 7.- Comparison of experimental and theoretical natural frequencies of a uniform cantilever elastic blade rotating in vacuum.

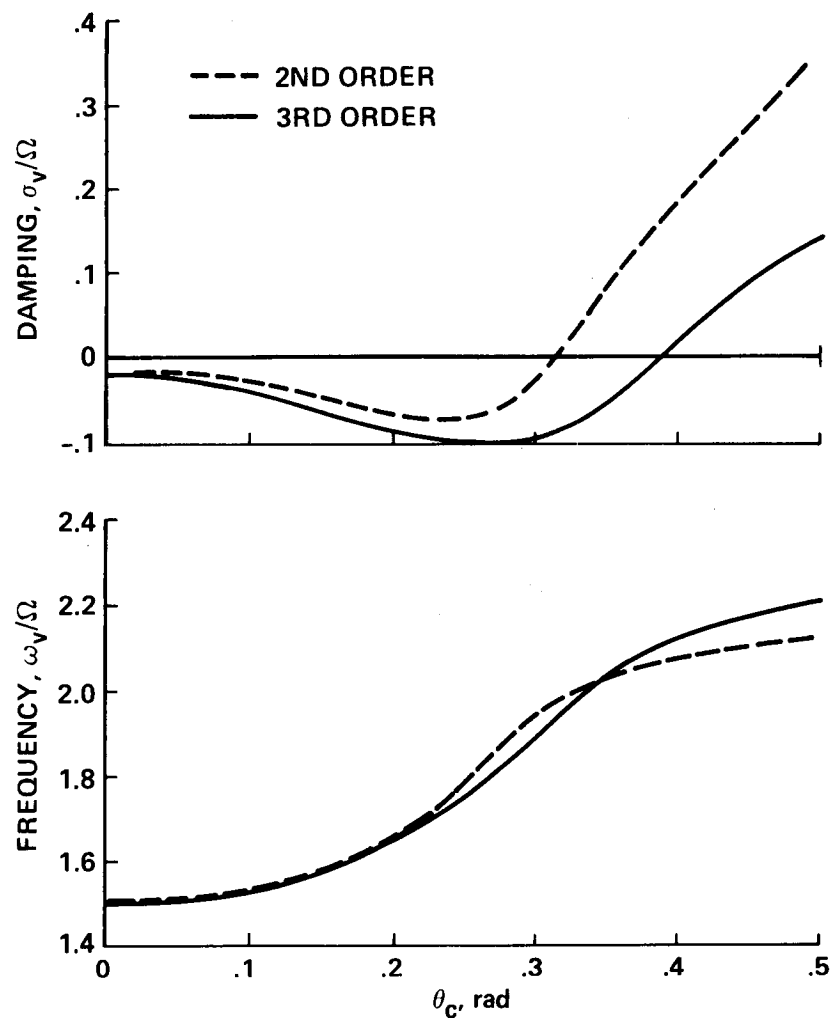


Figure 8.- Effect of third-order terms in elastic beam bending-torsion equations on predicted stiff-inplane rotor-blade lead-lag mode damping and frequency versus blade collective pitch;  $\bar{\omega}_w = 1.15$ ,  $\bar{\omega}_v = 1.5$ ,  $\bar{\omega}_\phi = 2.5$ .

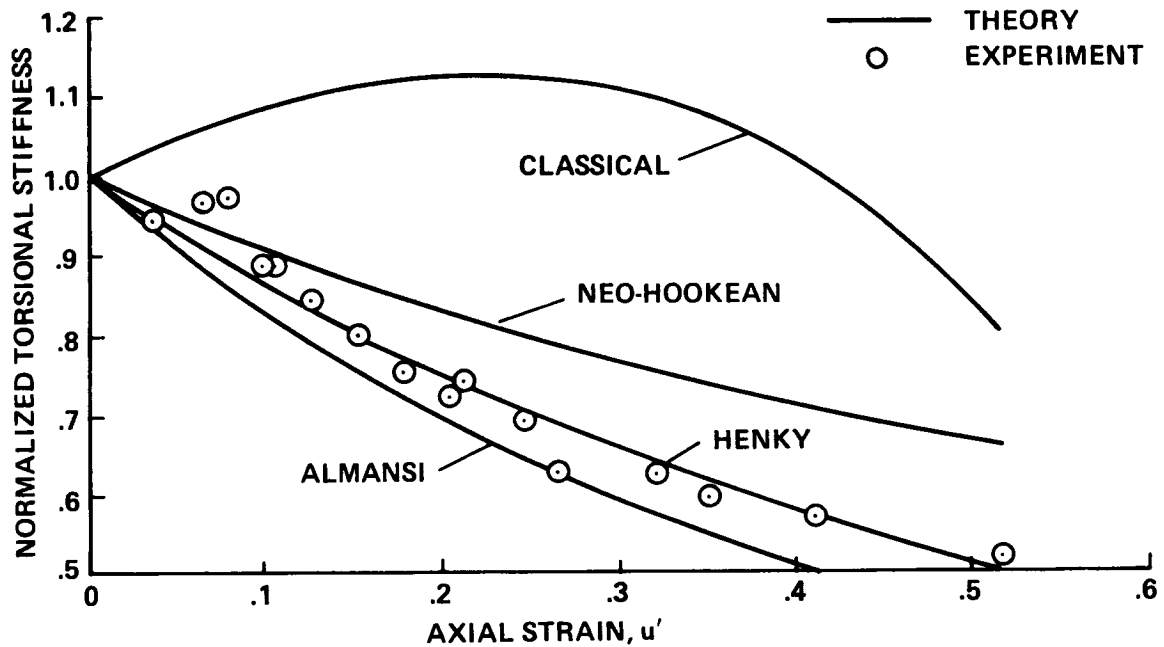


Figure 9.- The effect of axial strain on torsional stiffness for a beam of circular cross section.

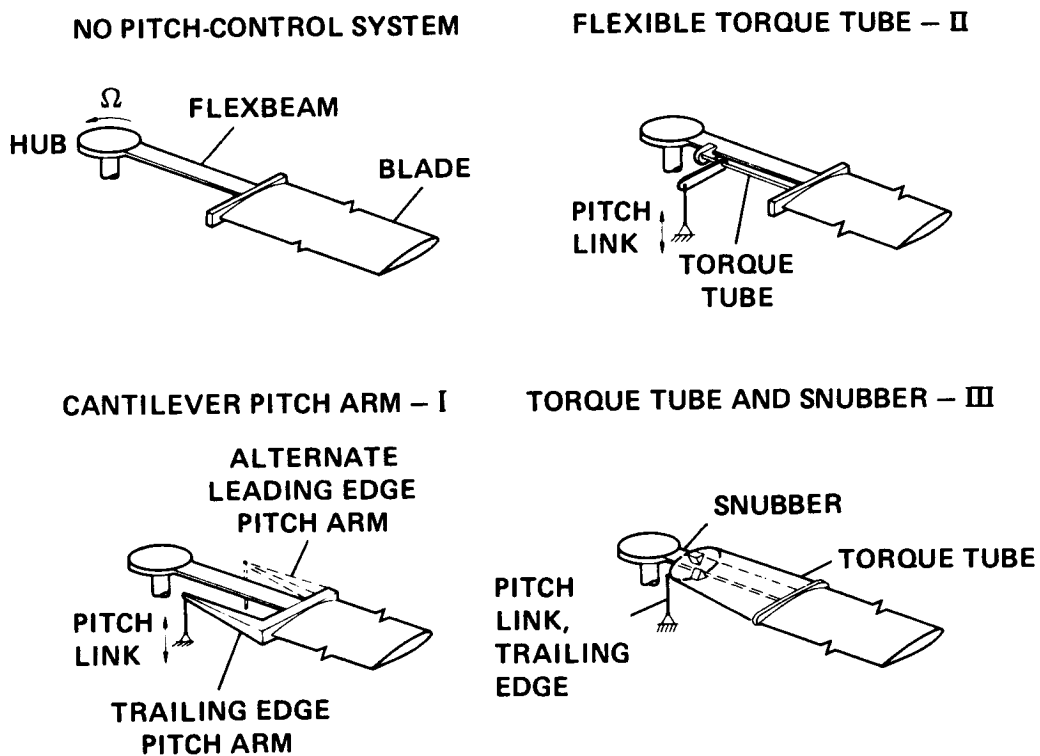


Figure 10.- Principal configurations for bearingless rotor blade pitch-control systems.

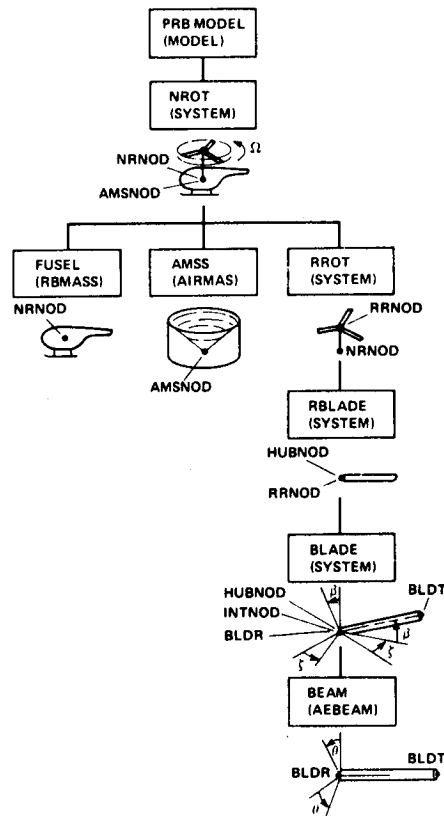


Figure 11.- Modeling a rotorcraft system with the elements and subsystems of GRASP.

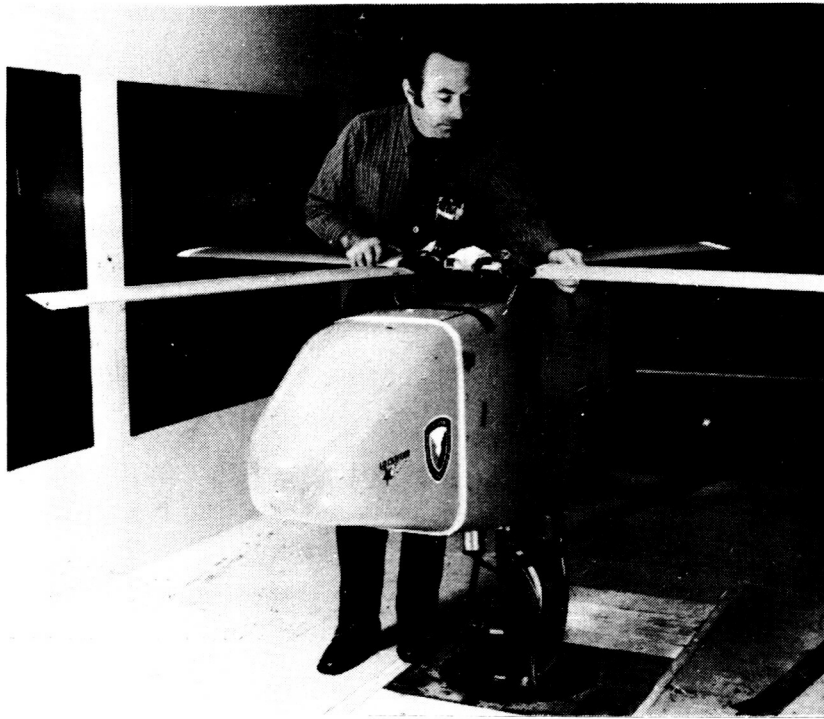


Figure 12.- Lockheed 7.5-ft-diam hingeless rotor model installed in Aeroflight-dynamics Directorate 7- by 10-ft wind tunnel.

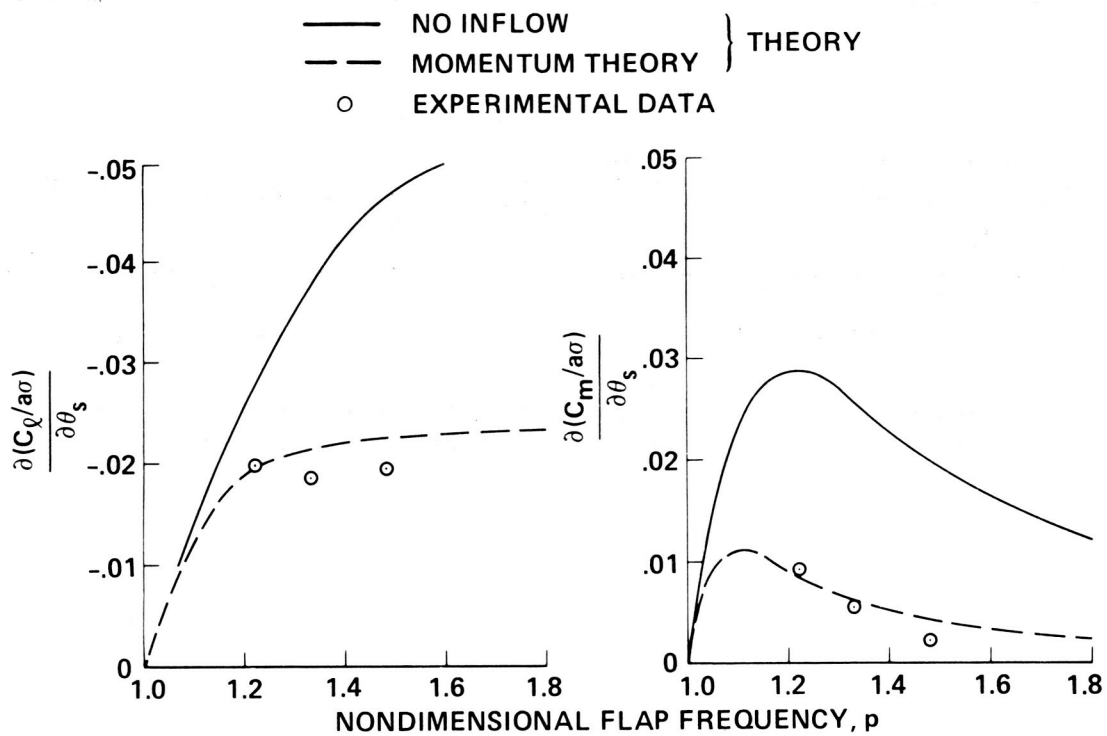


Figure 13.- Effect of dynamic inflow on static hub moment response derivatives of a hingeless rotor in hover at 4° collective pitch.

ORIGINAL PAGE IS  
OF POOR QUALITY



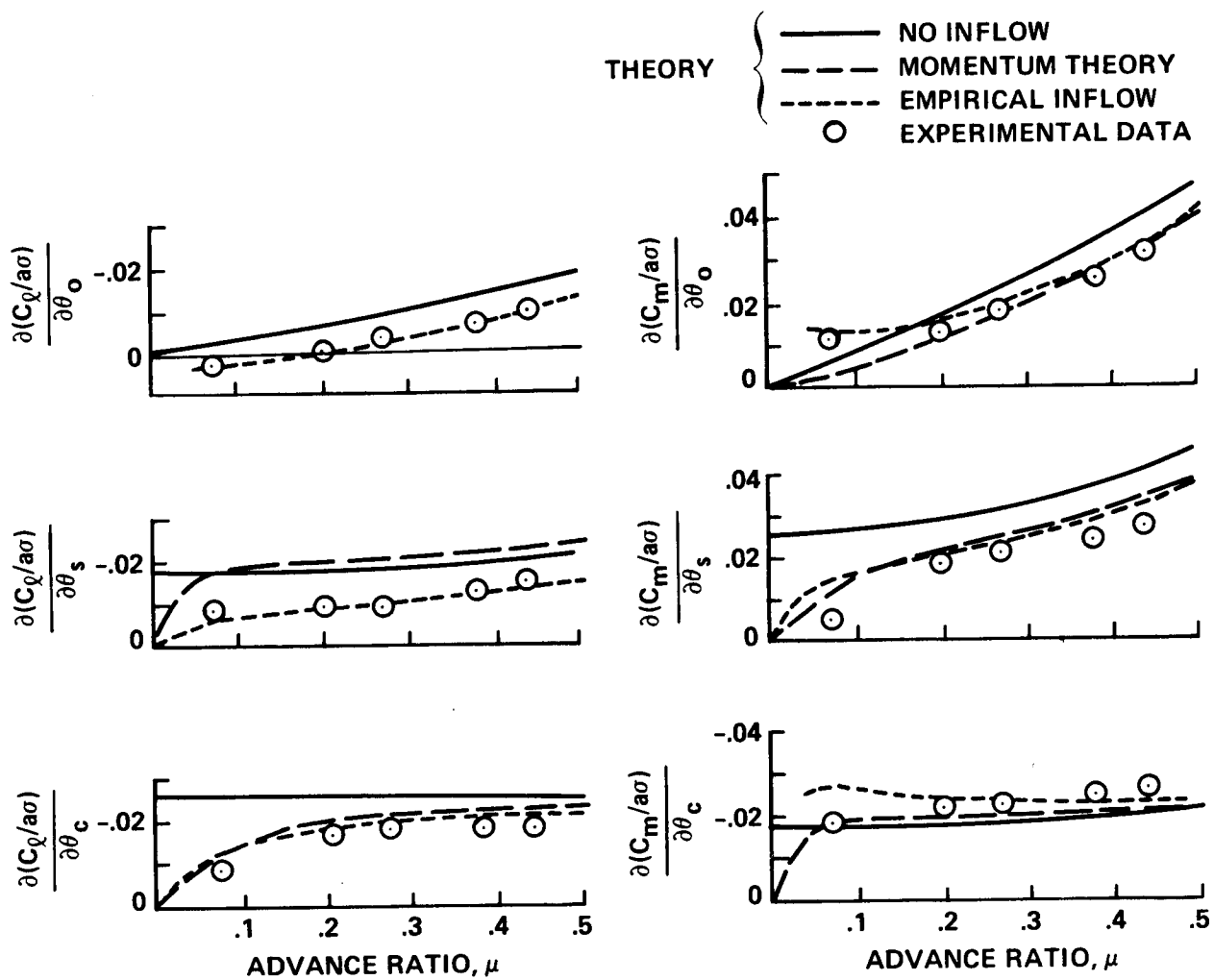


Figure 14.- Effect of dynamic inflow on static hub moment response derivatives of a hingeless rotor in forward flight at 0° collective pitch.

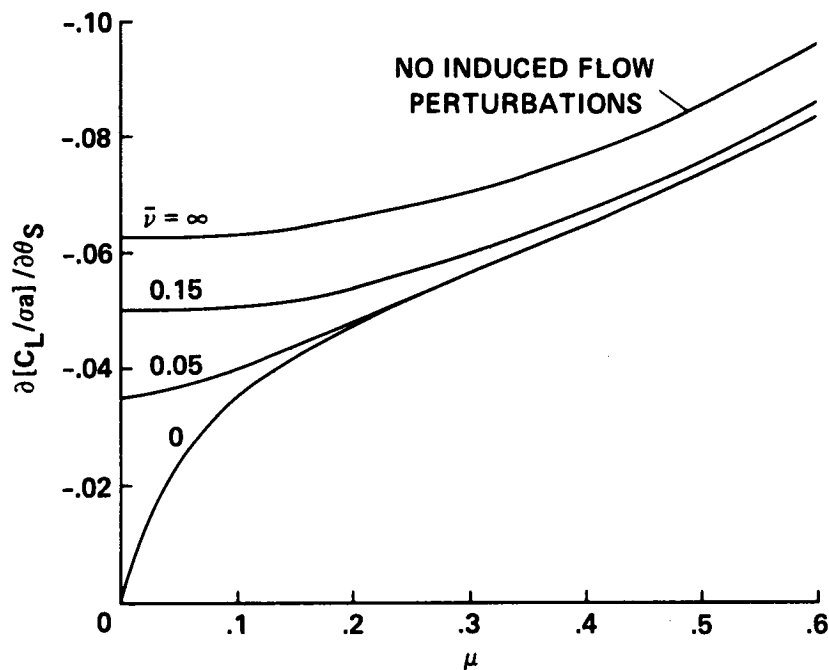


Figure 15.- Effect of mean inflow and advance ratio (contained within static inflow model) on a typical rotor hub moment response derivative.

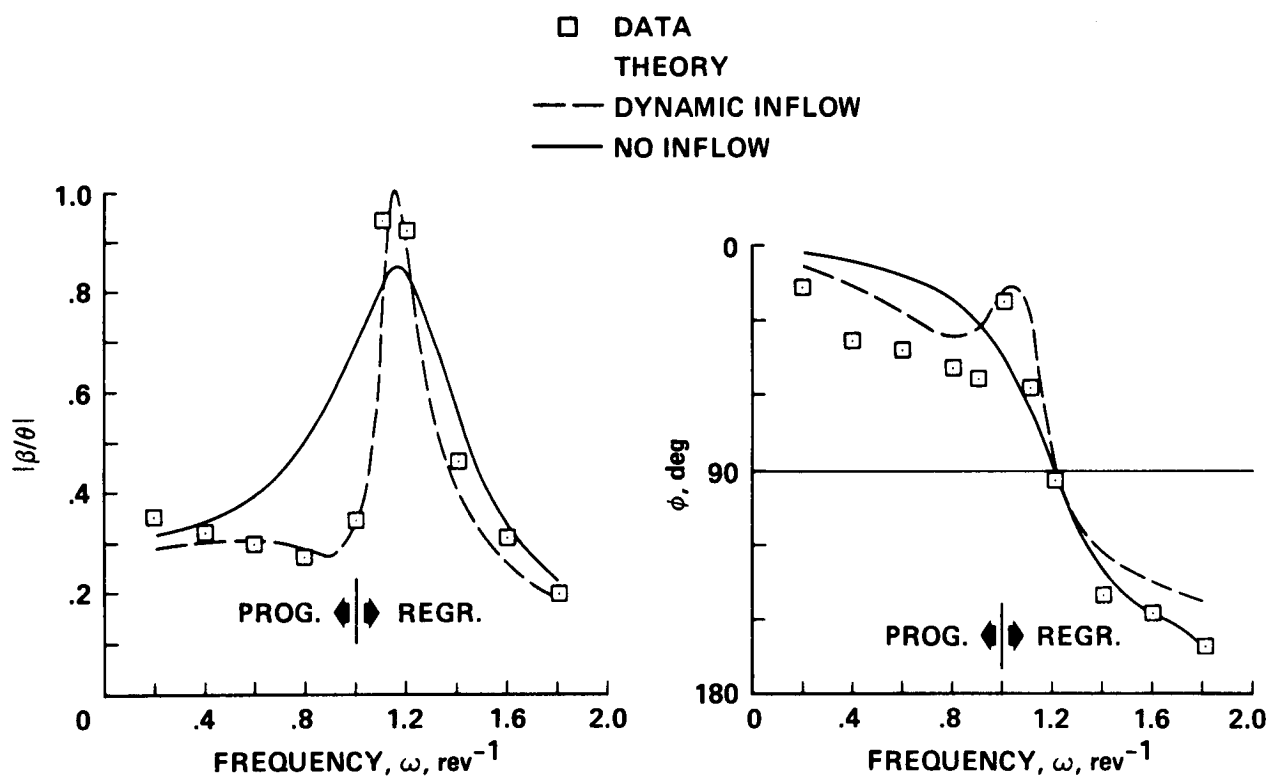


Figure 16.- Effect of dynamic inflow on frequency response of blade flapping to blade pitch excitation of a hovering rotor at 2° collective pitch.

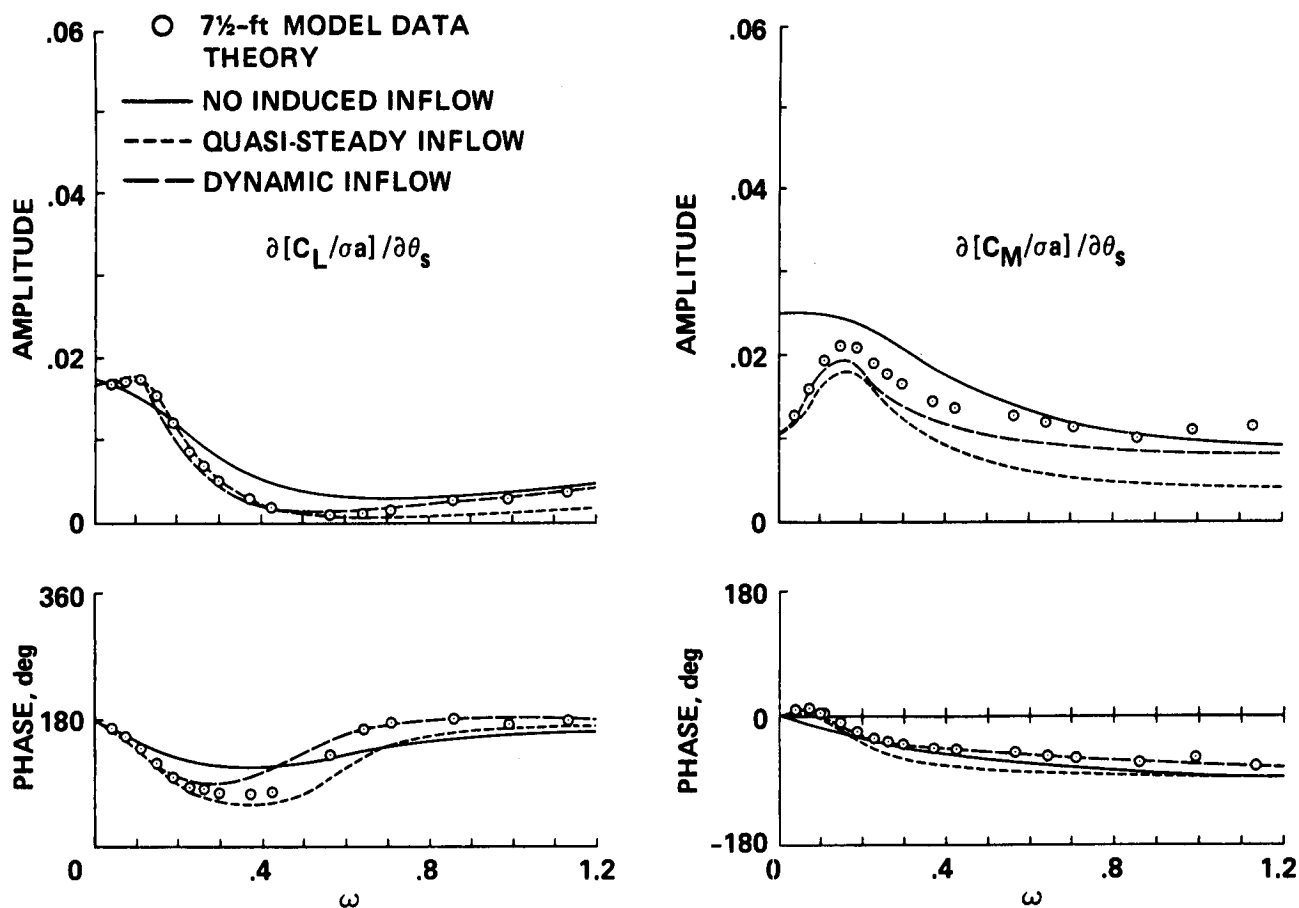


Figure 17.- Effect of momentum theory dynamic inflow on rotor-hub moment frequency response to cyclic pitch excitation for a hingeless rotor model in hover at  $4^\circ$  collective pitch.

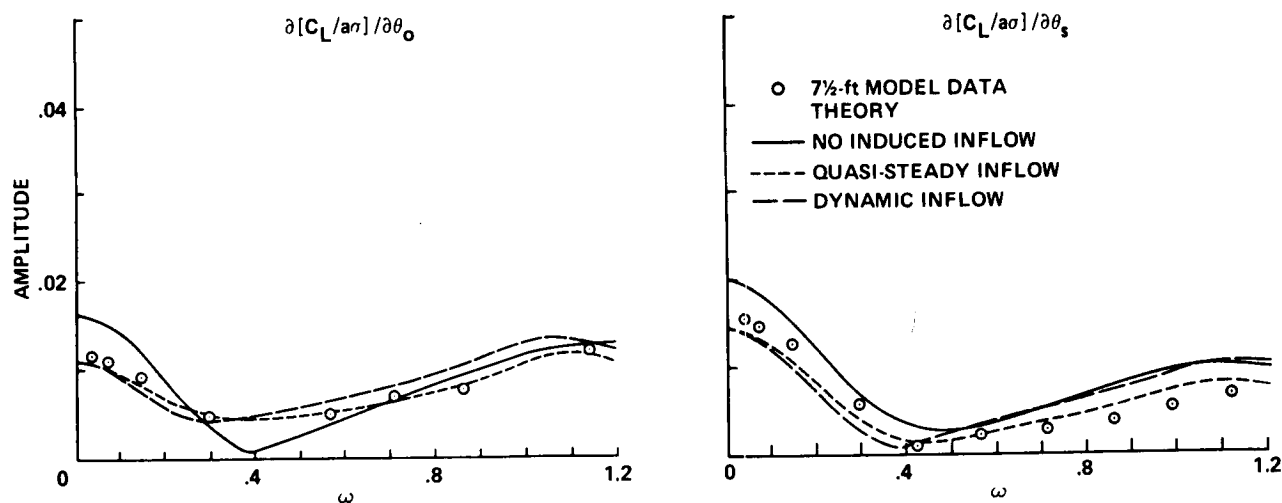


Figure 18.- Effect of empirical dynamic inflow model on rotor-hub moment frequency response to collective and cyclic pitch excitation for a hingeless rotor model in forward flight at 0.51 advance ratio and  $0^\circ$  collective pitch.

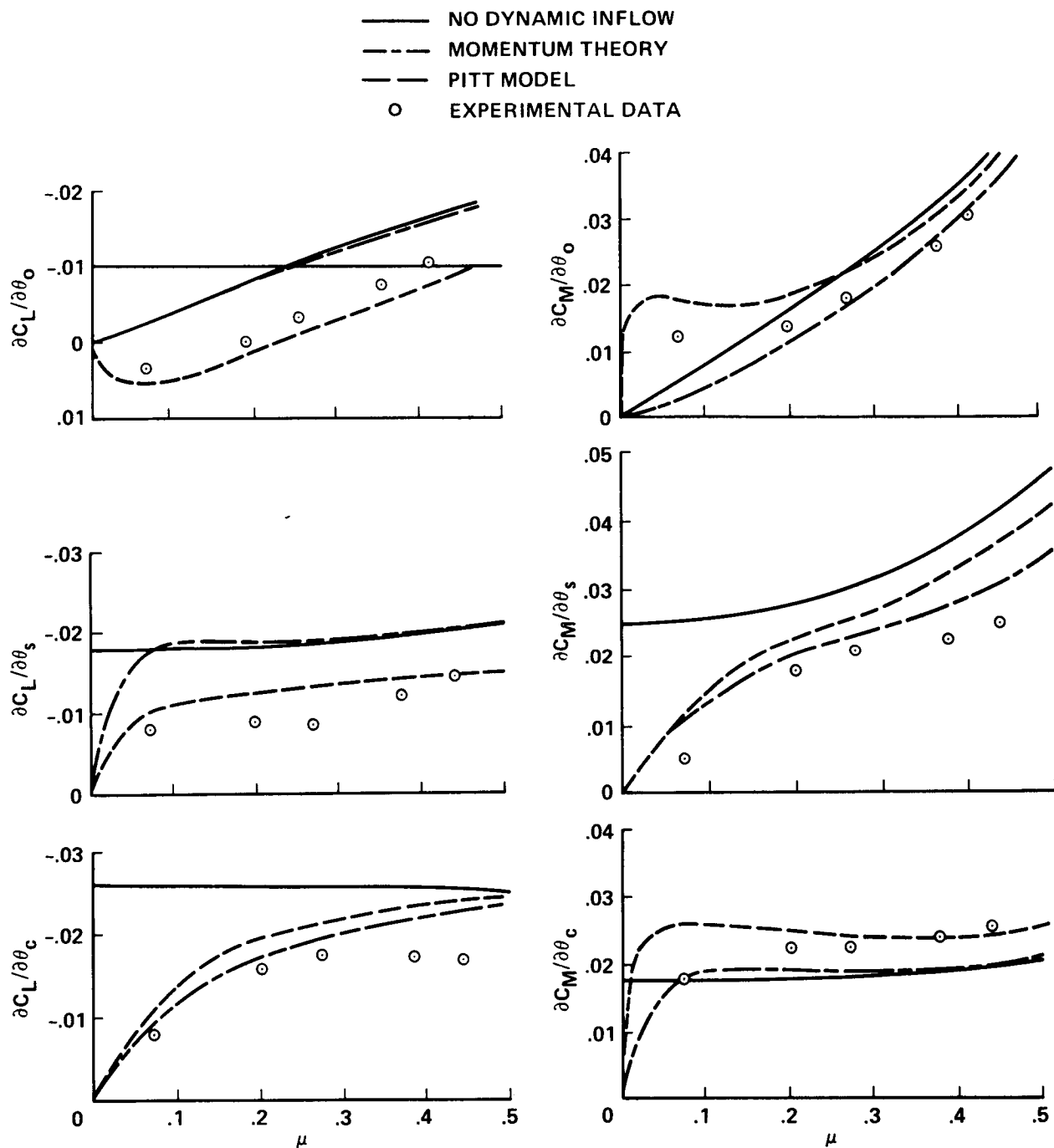


Figure 19.- Correlation of Pitt-Peters dynamic inflow theory with experimental data for static rotor-hub moment response derivatives in forward flight at 0° collective pitch.

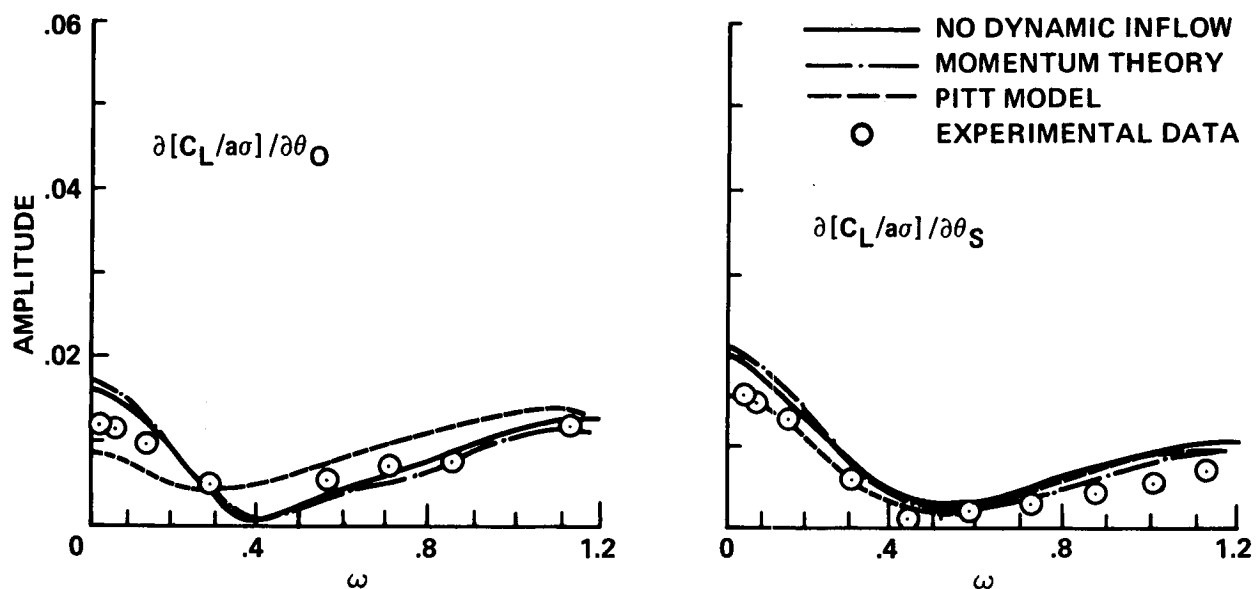


Figure 20.- Correlation of Pitt-Peters dynamic inflow theory with experimental data for rotor frequency response for a hingeless rotor in forward flight at 0.51 advance ratio at 0° collective pitch.

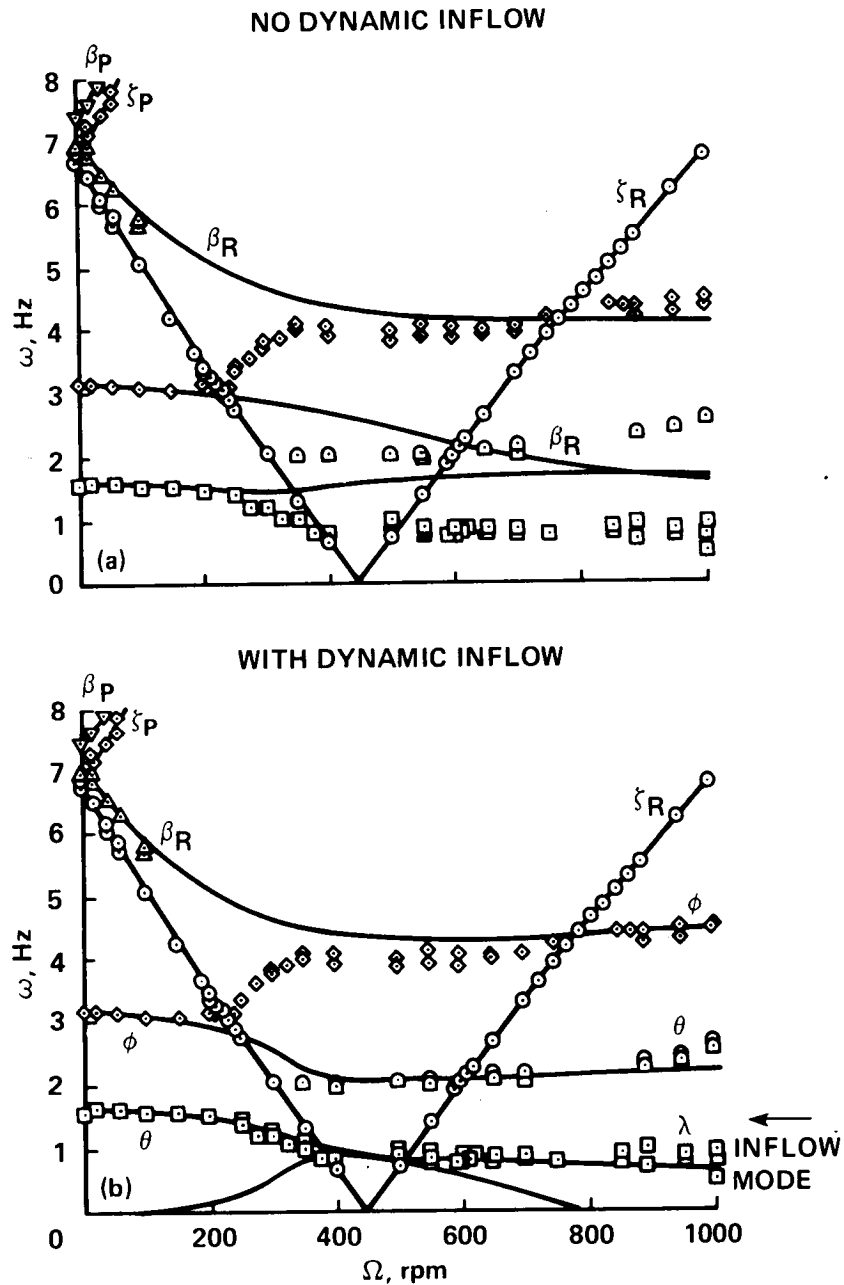


Figure 21.- Effects of dynamic inflow on the coupled rotor-body frequencies of a helicopter model in hover at  $0^\circ$  collective pitch. (a) Without dynamic inflow. (b) With dynamic inflow.

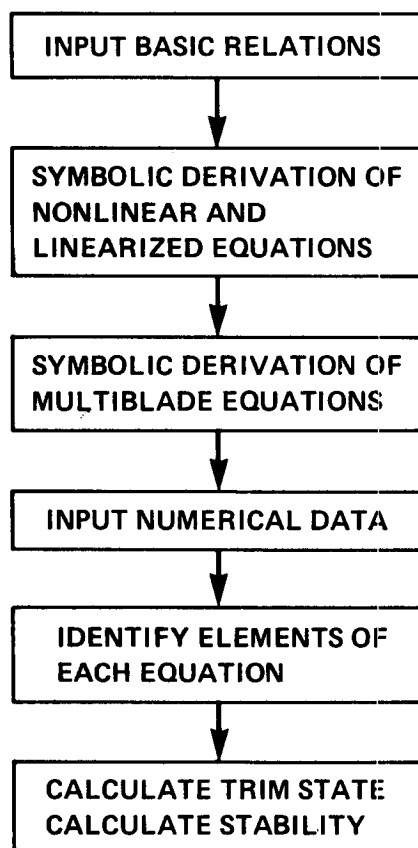


Figure 22.- Flowchart for derivation and solution of aeroelastic stability equations with an automatic symbolic manipulation program.

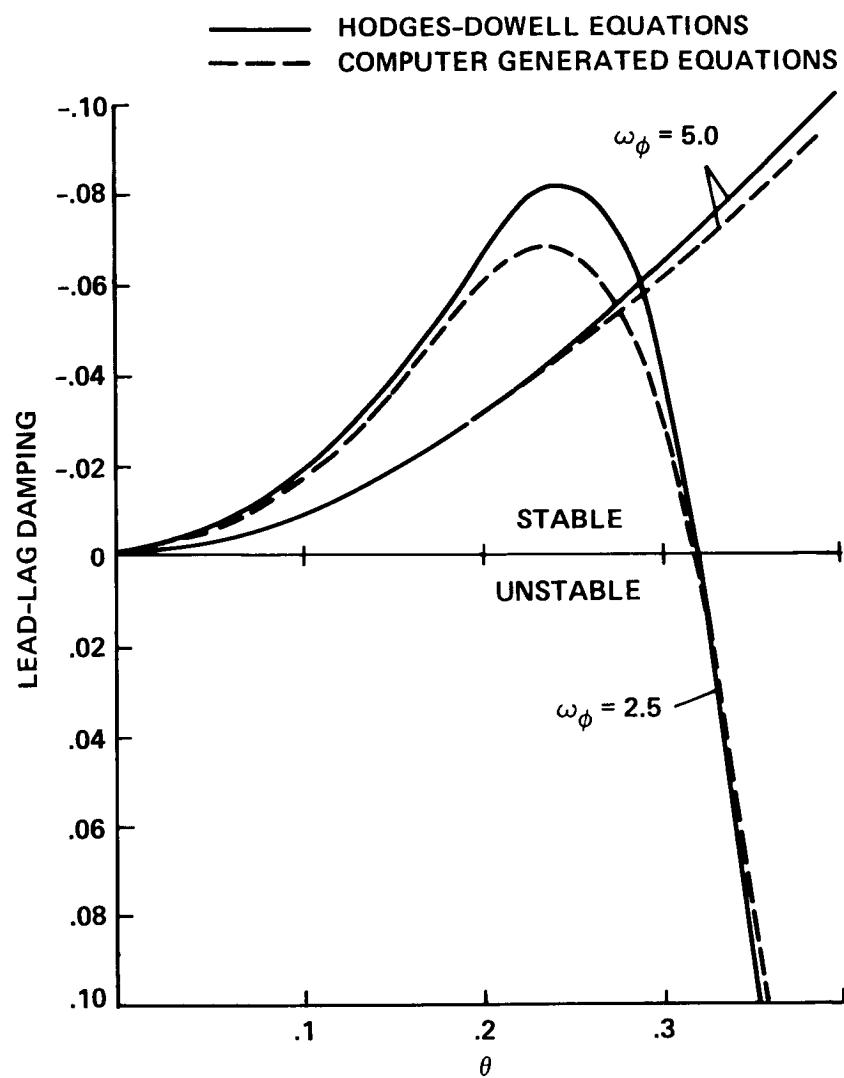


Figure 23.- Comparison of aeroelastic stability results obtained with conventional and computer-generated equations.



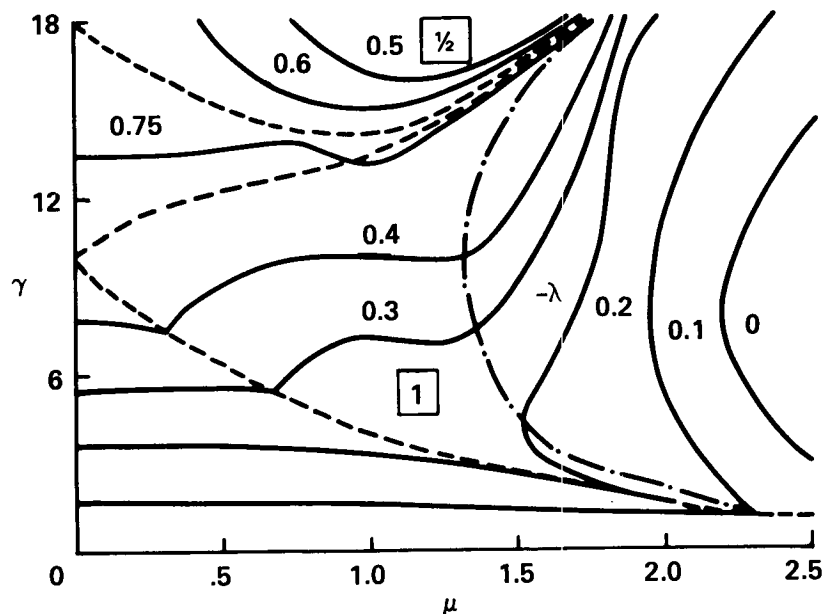


Figure 24.- Floquet theory results for contours of constant damping for spring restrained hinged-rigid blade in forward flight:  $p = 1.15$ .

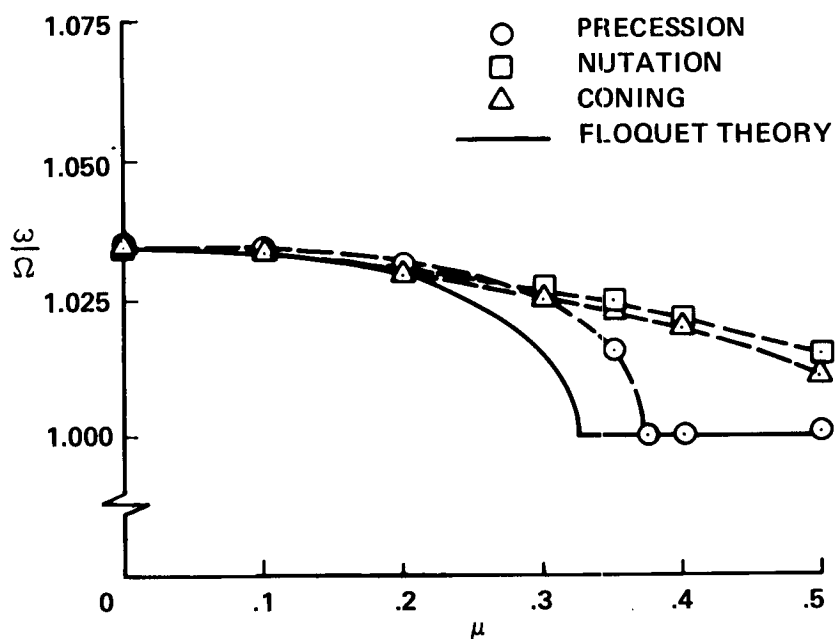


Figure 25.- Comparison of approximate constant coefficient multiblade equations and exact Floquet theory for frequency of hinged-rigid blade in forward flight:  $p = 1.1$ ,  $\gamma = 6$ .

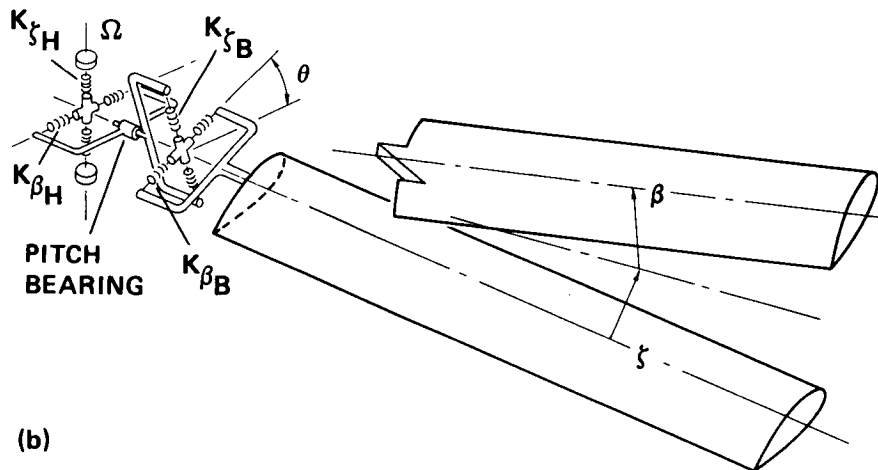
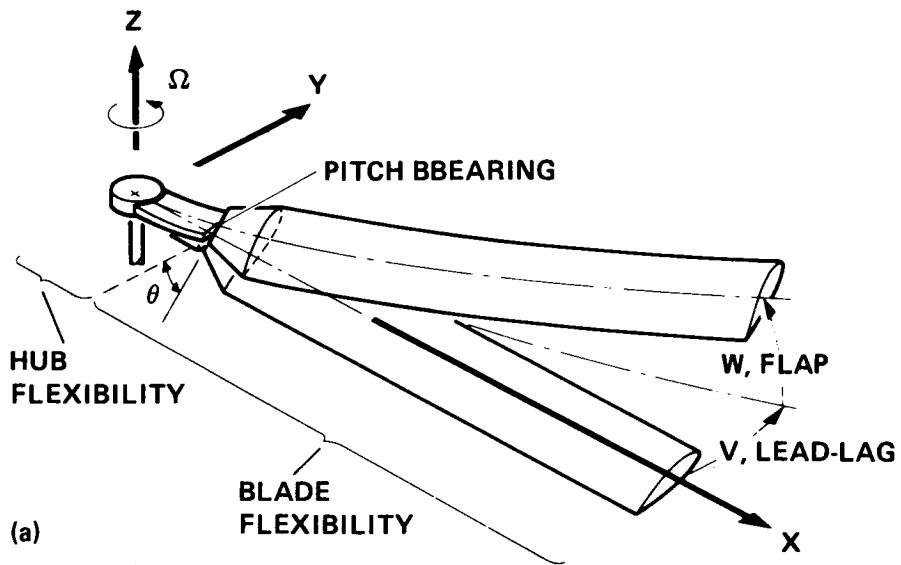


Figure 26.- Modeling of hingeless rotor blade for flap-lag stability analysis. (a) Hub and blade segments of elastic rotor blade. (b) Hinged-rigid blade representation with hub and blade flap-lag spring systems.

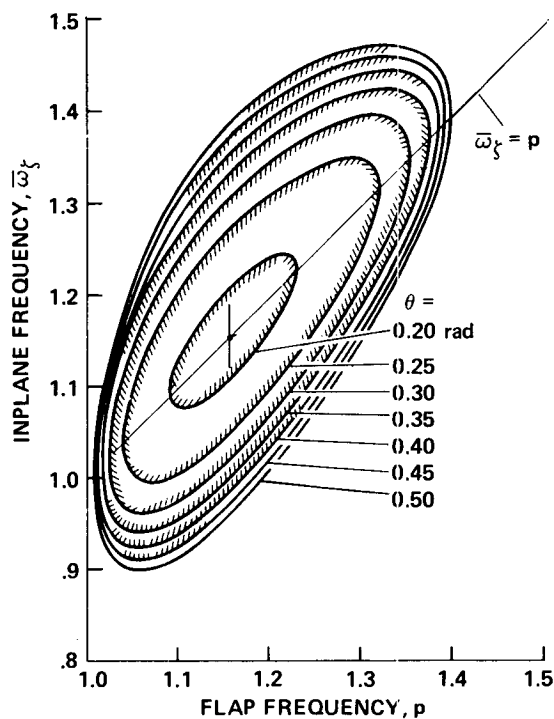


Figure 27.- Basic flap-lag stability boundaries for hinged-rigid blade in hover:  
 $R = 0$ ,  $\gamma = 5.0$ ,  $\sigma = 0.5$ .

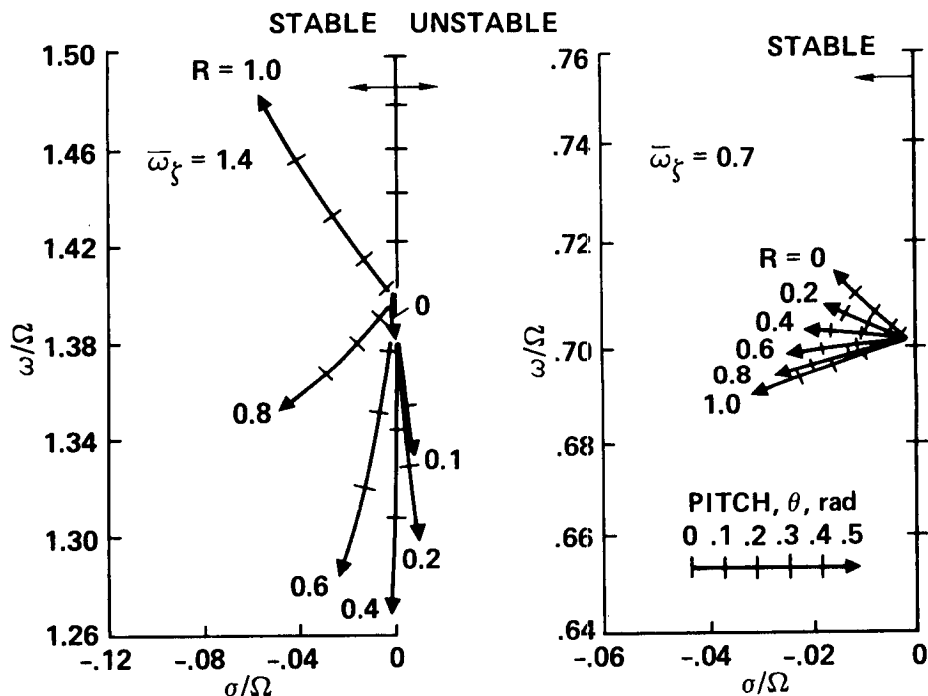


Figure 28.- Locus of lead-lag mode roots of hinged-rigid blade flap-lag system in hover for stiff- and soft-inplane configurations having variable flap-lag structural coupling:  $p = \sqrt{4/3}$ ,  $\gamma = 5$ ,  $\sigma = 0.05$ .

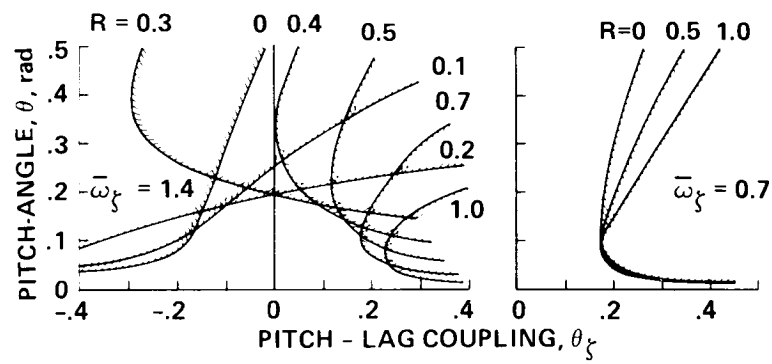


Figure 29.- Effect of pitch-lag coupling on flap-lag stability boundaries in hover of soft- and stiff-inplane hinged-rigid blades:  $p = \sqrt{4/3}$ ,  $\gamma = 5$ ,  $\sigma = 0.05$ .

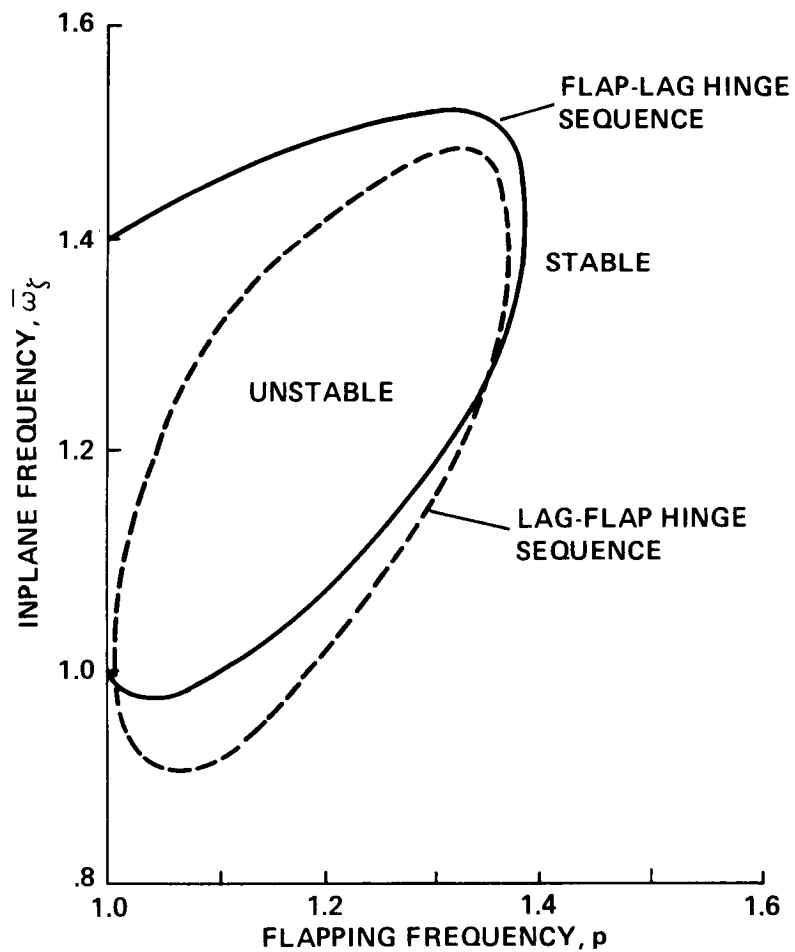


Figure 30.- Effect of hinge sequence on flap-lag stability of hinged-rigid blade in hover:  $\theta = 0.4$  rad,  $\gamma = 5$ ,  $\sigma = 0.05$ ,  $R = 0$ .

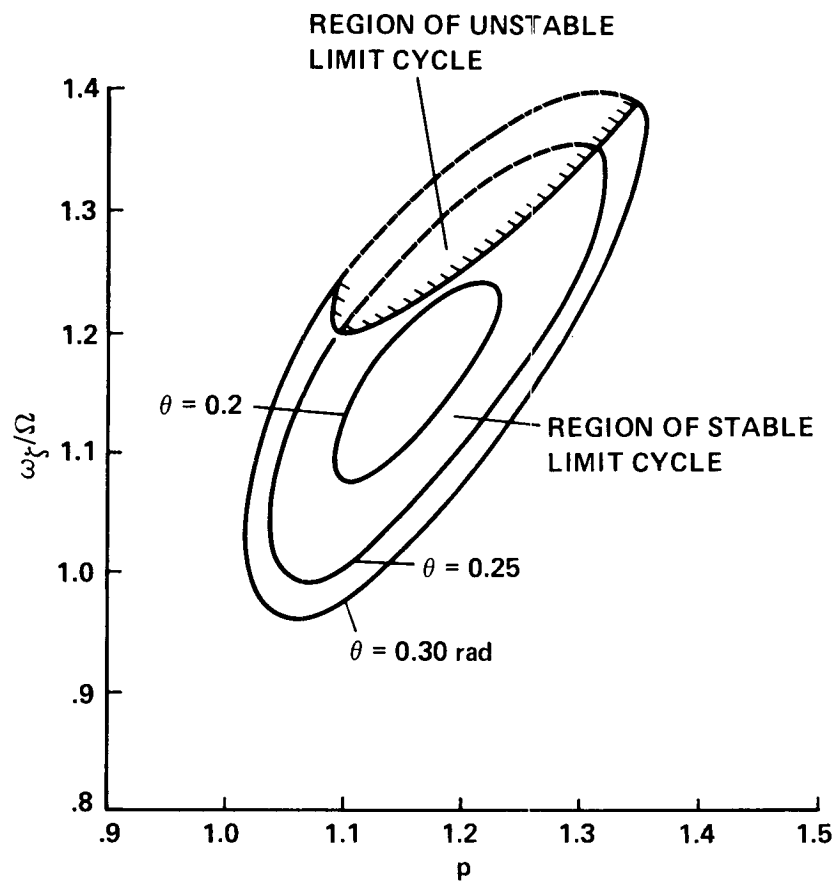


Figure 31.- Nonlinear flap-lag stability for hinged-rigid blade in hover:  $\gamma = 5$ ,  
 $\sigma = 0.05$ .

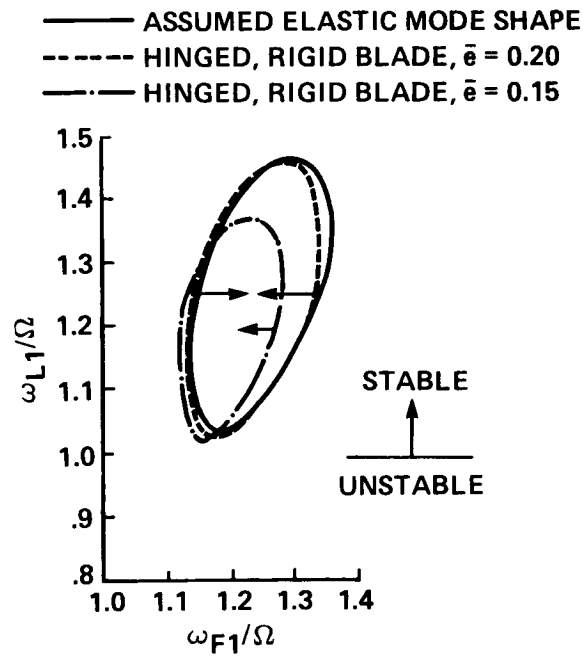


Figure 32.- Comparison of flap-lag instability for offset-hinged-rigid blade with elastic blade in hover:  $\theta = 0.2$  rad,  $\gamma = 10$ ,  $\sigma = 0.05$ .

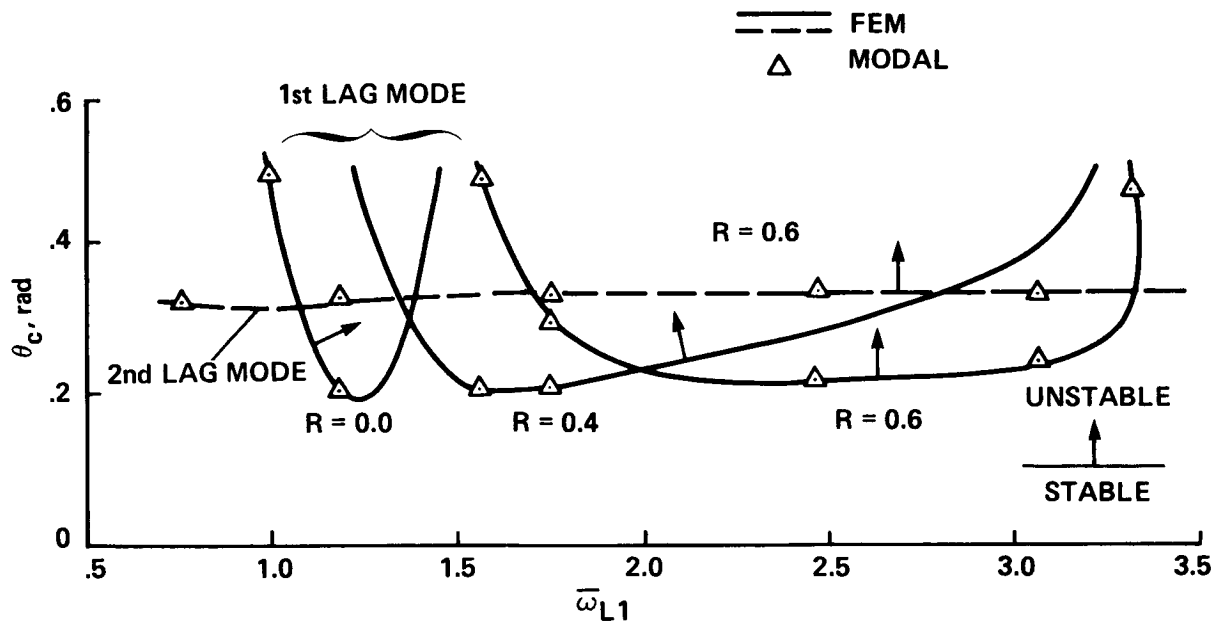


Figure 33.- Comparison of flap-lag stability boundaries of elastic blade in hover calculated with modal and finite-element methods:  $\bar{\omega}_{F1} = 1.15$ ,  $\gamma = 5$ ,  $\sigma = 0.1$ .

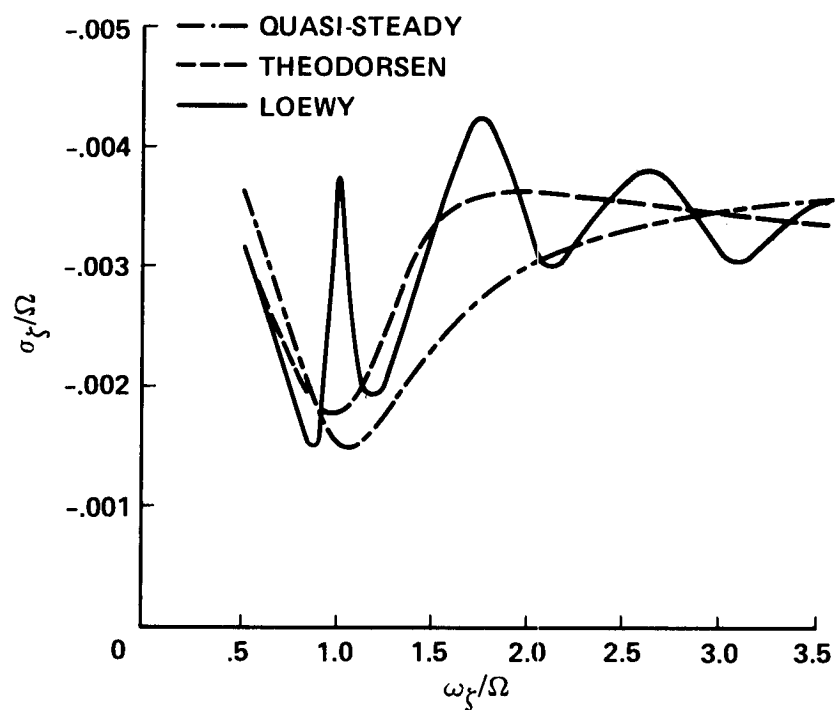


Figure 34.- Effects of unsteady aerodynamics on flap-lag stability of a hinged-rigid rotor blade in hover:  $p = 1.1$ ,  $\theta_0 = 0.1$  rad,  $\gamma = 8$ ,  $\sigma = 0.05$ ,  $R = 0$ ,  $b = 1$ .

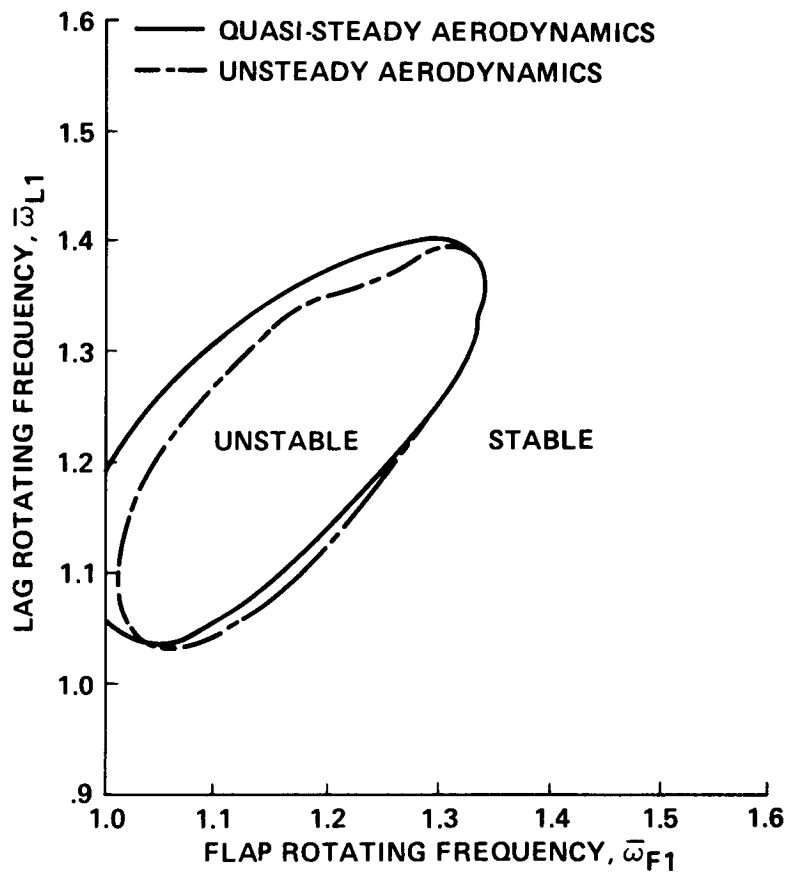


Figure 35.- Effects of finite-state model of Greenberg unsteady aerodynamic theory on flap-lag stability of hinged-rigid blade in hover:  $\theta = 0.25$  rad,  $\gamma = 5$ ,  $\sigma = 0.05$ ,  $R = 0$ ,  $b = 4$ .



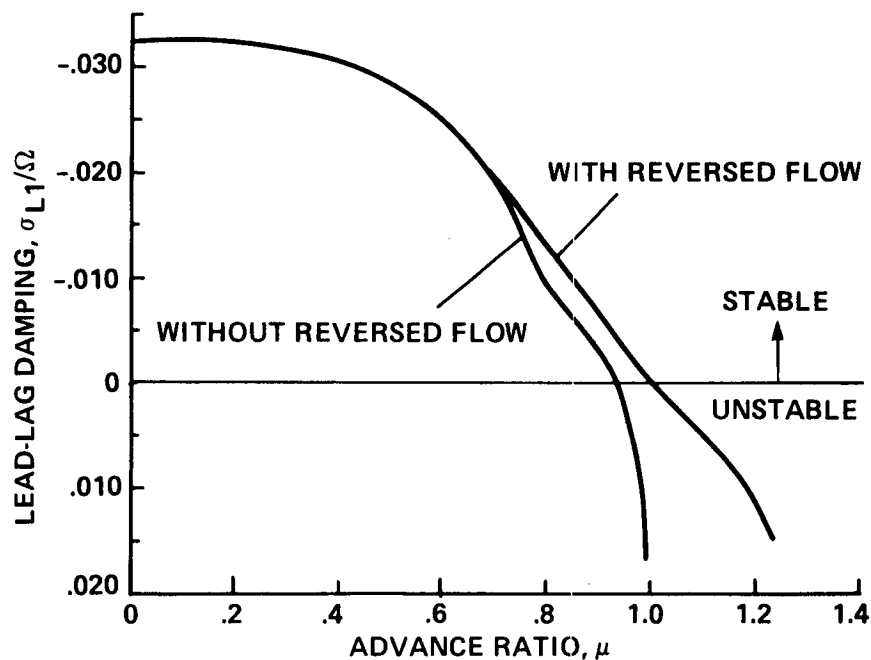


Figure 36.- Effects of reverse flow on lead-lag damping of elastic blade flap-lag analysis in forward flight:  $\theta_0 = 0.15$  rad,  $\bar{\omega}_{F1} = 1.175$ ,  $\bar{\omega}_{L1} = 1.283$ ,  $\gamma = 10$ ,  $\sigma = 0.05$ .

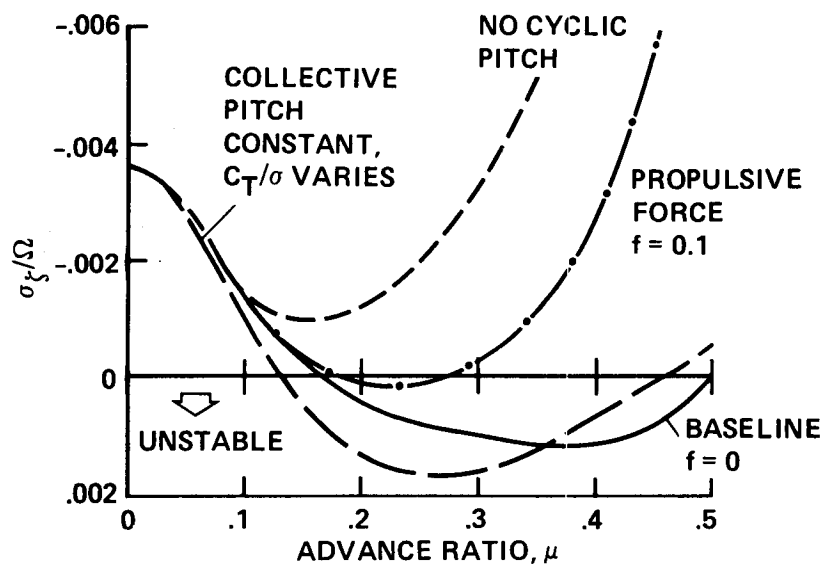


Figure 37.- Effects of trim condition on lead-lag damping of hinged-rigid blade flap-lag analysis in forward flight:  $p = 1.15$ ,  $\bar{\omega}_{\xi} = 1.4$ ,  $\gamma = 5$ ,  $\sigma = 0.05$ ,  $R = 0$ .

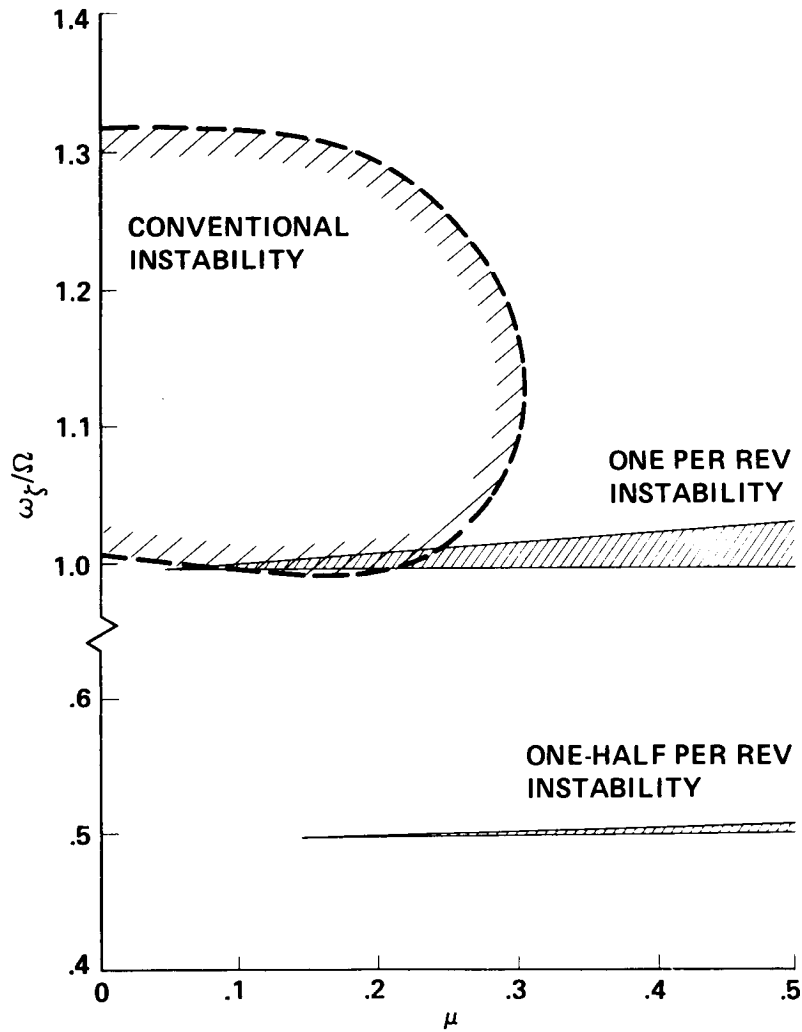


Figure 38.- Flap-lag stability boundaries in forward flight for hinged-rigid blade analysis illustrating conventional and parametric instability regions:  
 $C_T/\sigma = 0.2$ ,  $\gamma = 5$ ,  $\sigma = 0.05$ ,  $R = 0$ .

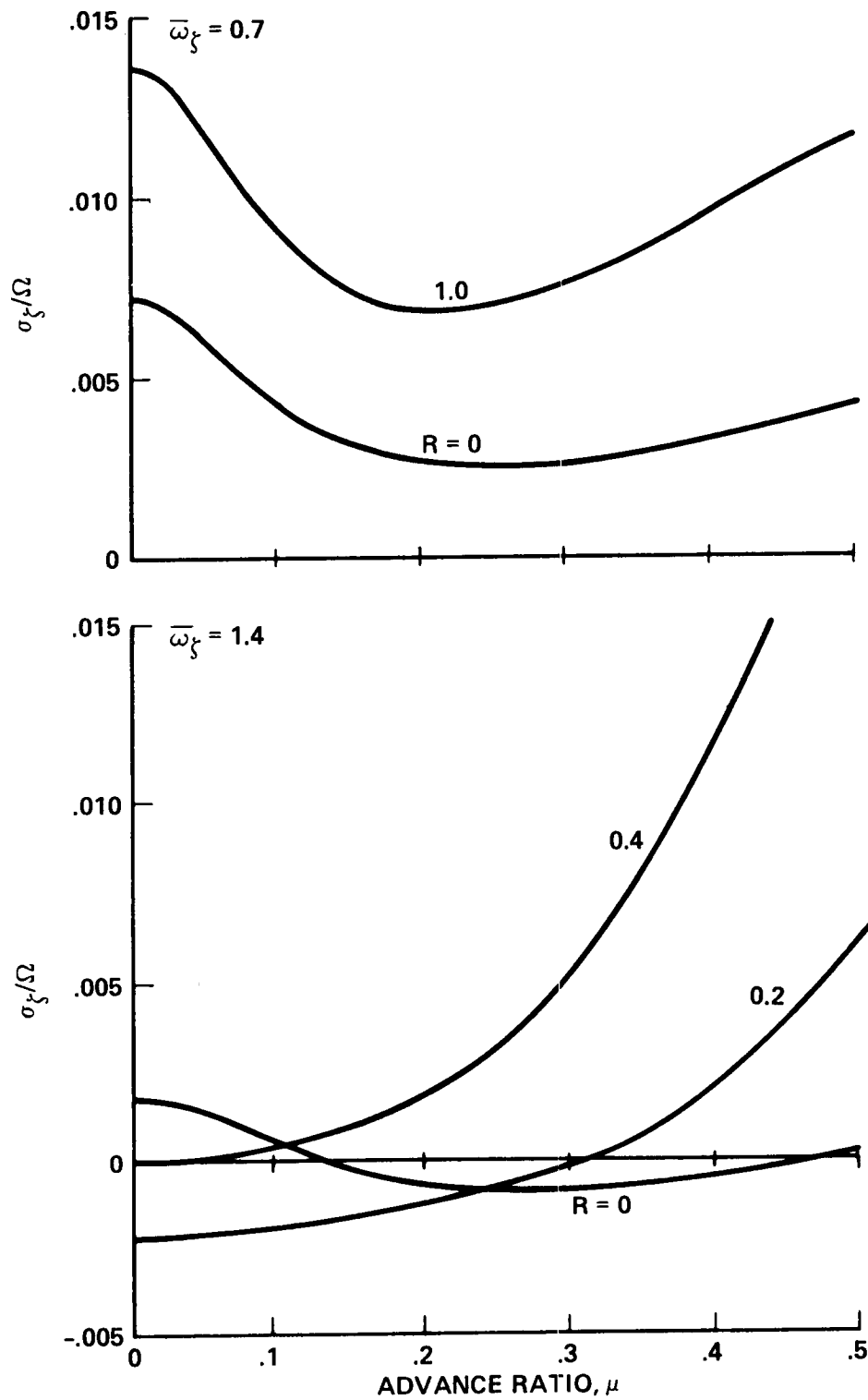


Figure 39.- Effects of flap-lag structural coupling on lead-lag damping of soft- and stiff-in-plane hinged-rigid blades in forward flight:  $p = 1.15$ ,  $C_T/\sigma = 0.2$ ,  $\bar{f} = 0$ ,  $\gamma = 5$ .

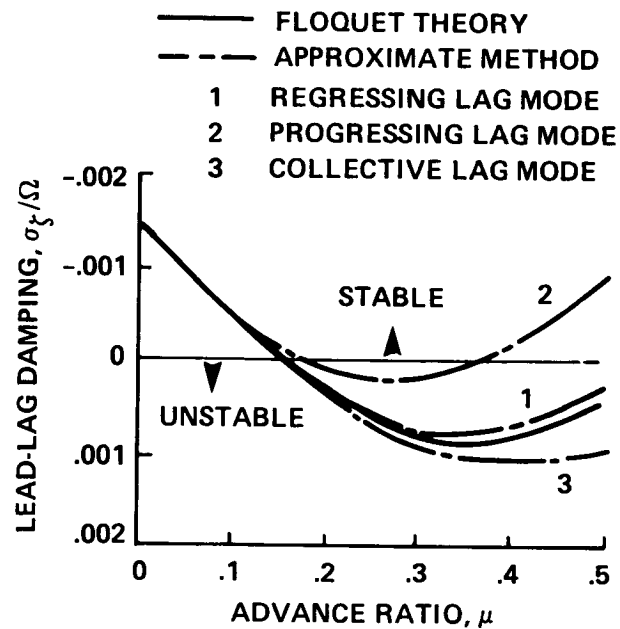


Figure 40.- Comparison of approximate constant coefficient multiblade equations with exact Floquet theory result for lead-lag damping of hinged-rigid blade flap-lag analysis in forward flight:  $p = 1.15$ ,  $\omega_z = 1.4$ ,  $C_T/\sigma = 0.2$ ,  $\bar{f} = 0$ ,  $\gamma = 5$ ,  $R = 0$ .

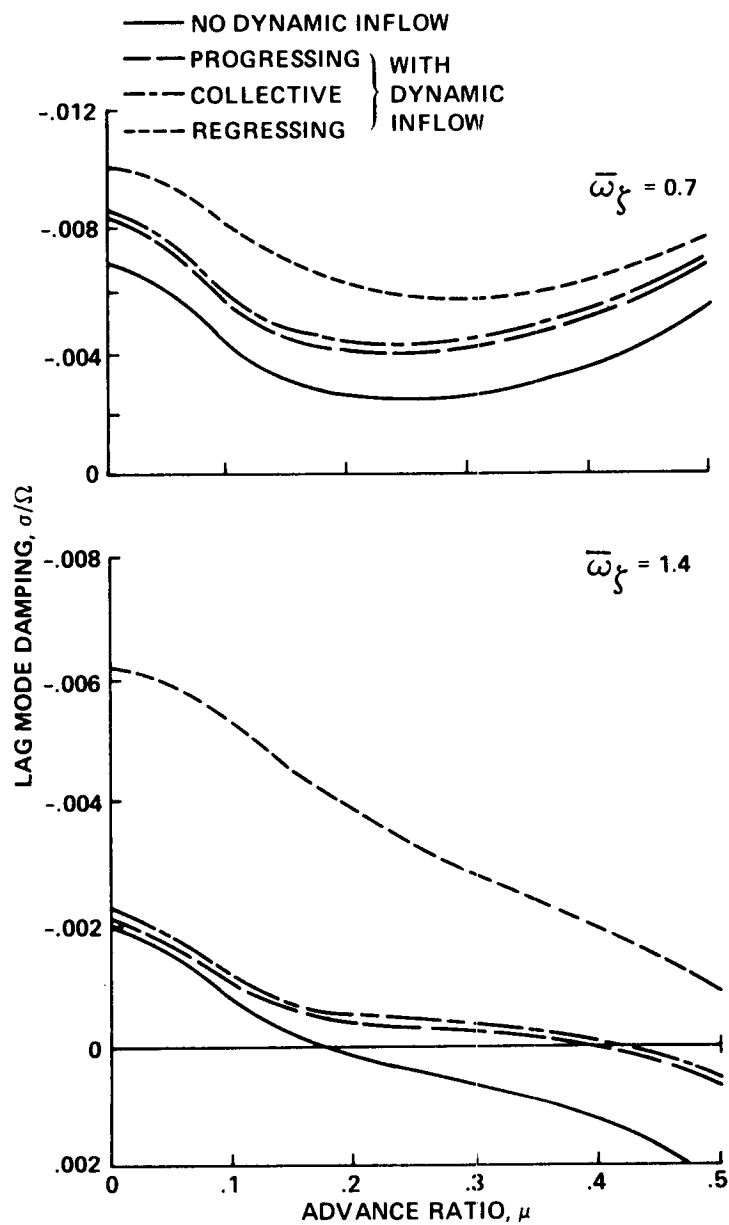


Figure 41.- Effects of dynamic inflow on lead-lag damping in forward flight for soft- and stiff-in-plane hinged-rigid blade flap-lag analysis:  $p = 1.15$ ,  $\gamma = 5$ ,  $\sigma = 0.05$ .

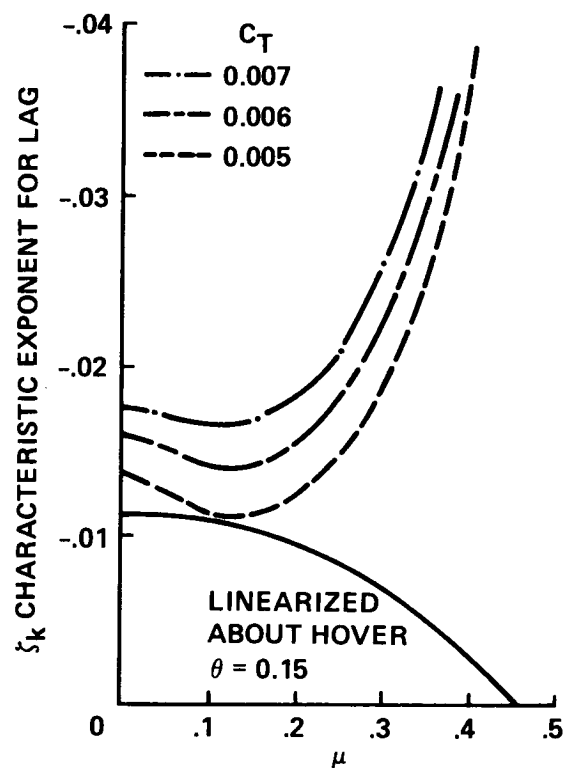


Figure 42.- Effects of trim condition on lead-lag damping of elastic blade flap-lag analysis in forward flight:  $\theta_0 = 0.15$  rad,  $p = 1.175$ ,  $\bar{\omega}_\zeta = 1.28$ ,  $\gamma = 10$ ,  $\sigma = 0.05$ .

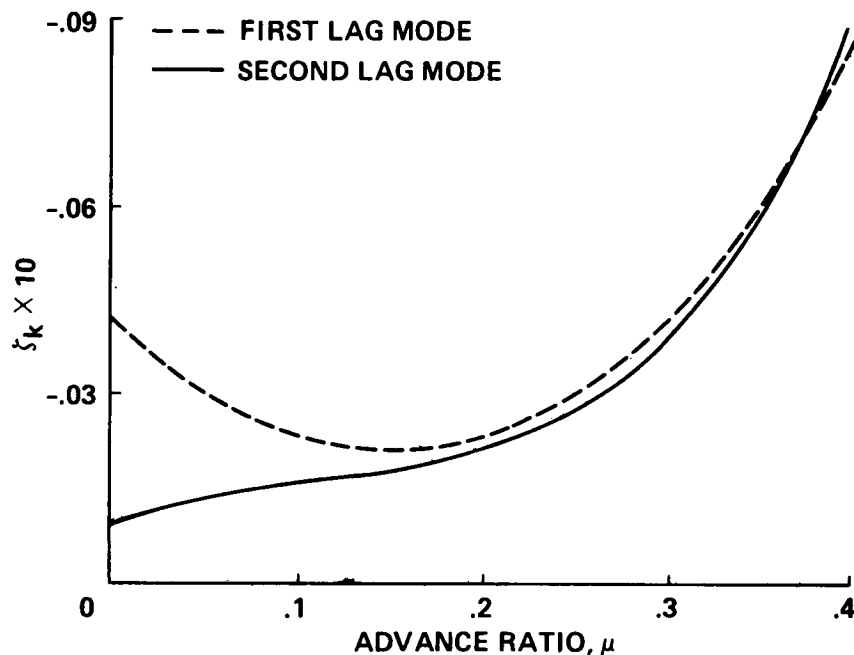


Figure 43.- Finite element calculation of lead-lag damping in forward flight for elastic blade flap-lag analysis:  $p = 1.125$ ,  $\bar{\omega}_\zeta = 0.732$ ,  $C_W = 0.005$ ,  $\gamma = 5.5$ ,  $\sigma = 0.07$ ,  $R = 0.6$ .

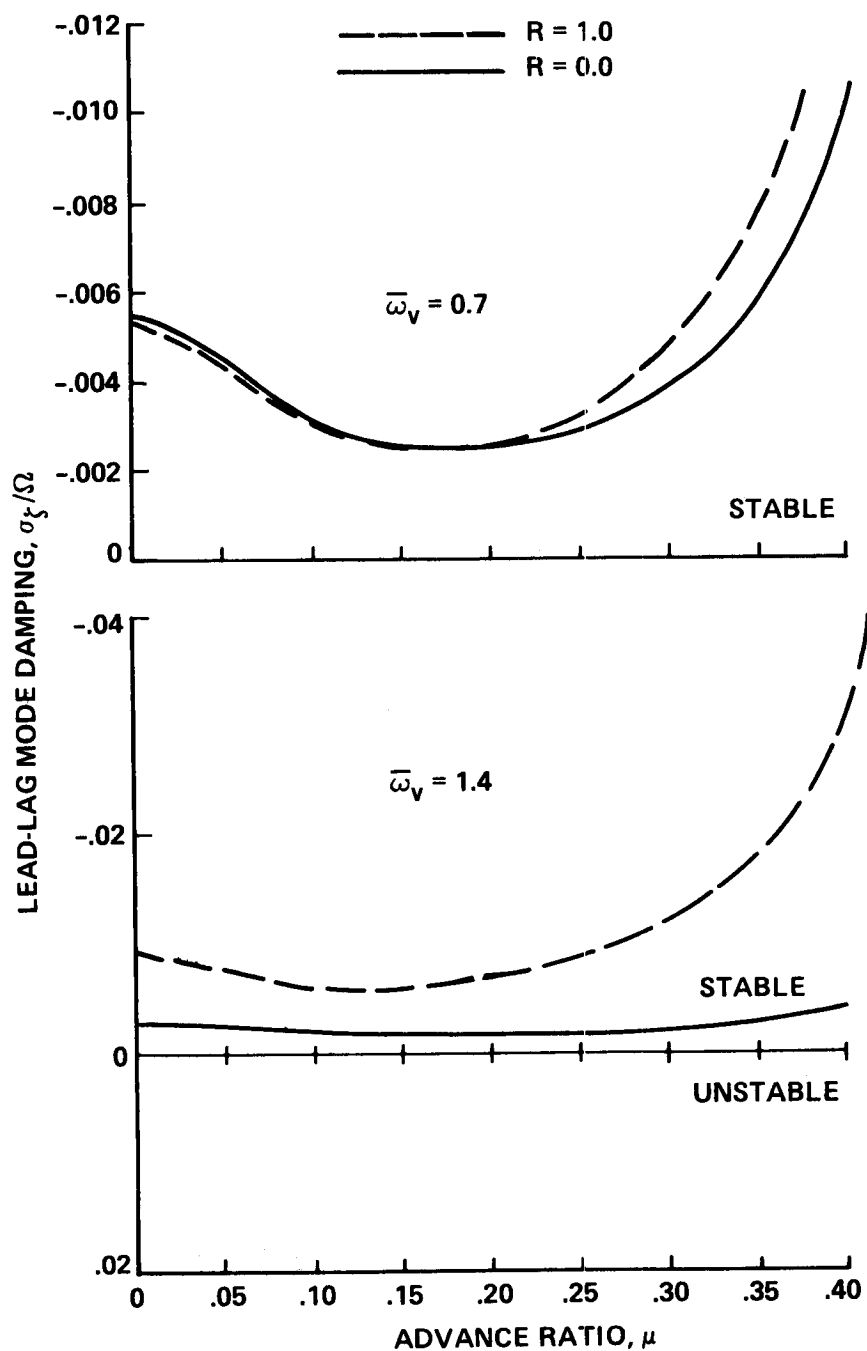


Figure 44.- Effects of flap-lag structural coupling on lead-lag damping of soft- and stiff-inplane elastic blade flap-lag analysis in forward flight:  $p = 1.15$ ,  $C_T/\sigma = 0.7$ ,  $\bar{f} = 0.012$ ,  $\gamma = 5$ ,  $\sigma = 0.10$ .

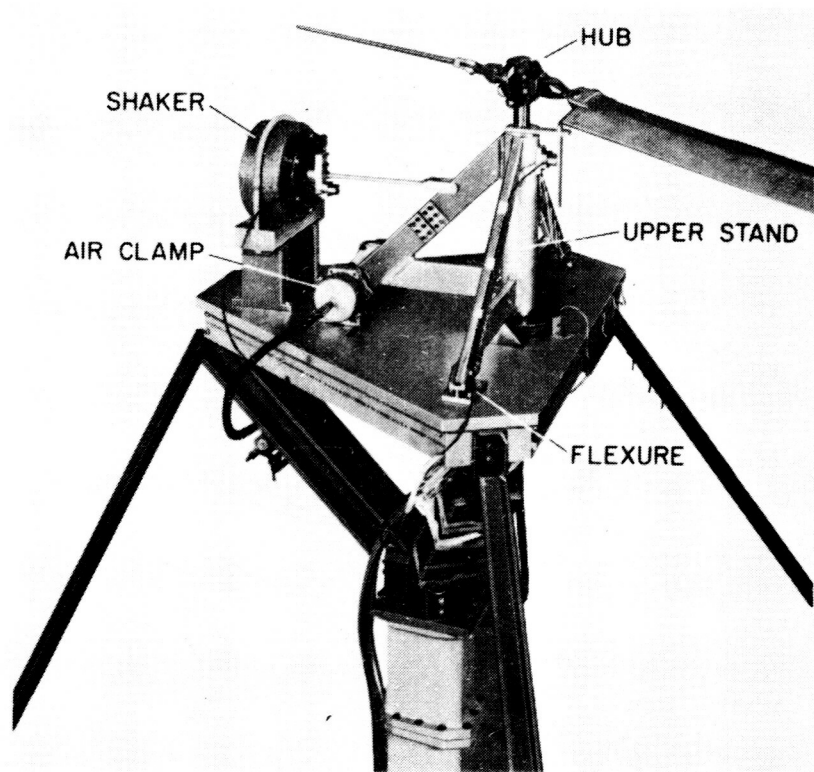


Figure 45.- Two-bladed 5.5-ft-diam flap-lag model rotor for hover experiments.

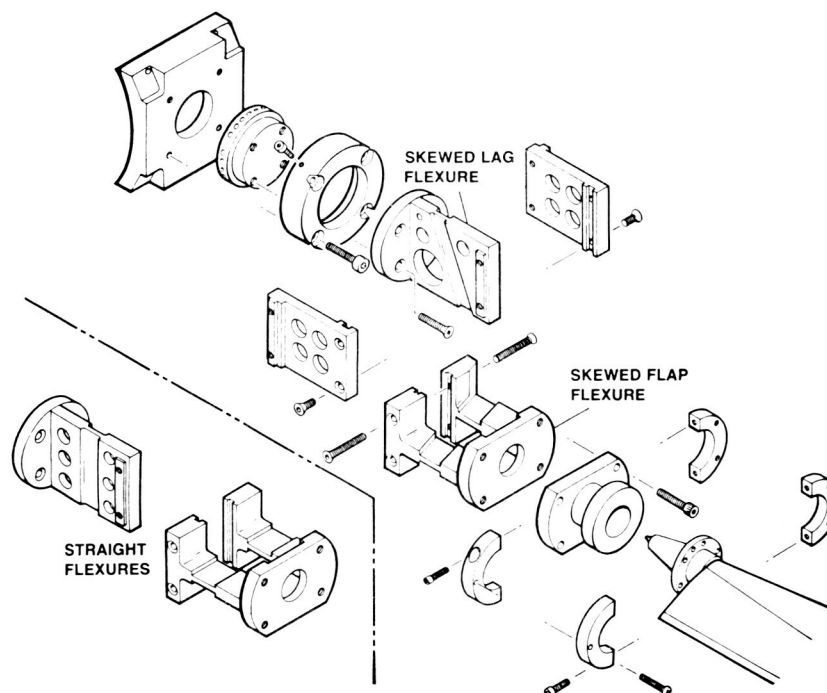


Figure 46.- Hub flexures to simulate spring restrained hinges for rigid blade flap-lag model rotor.



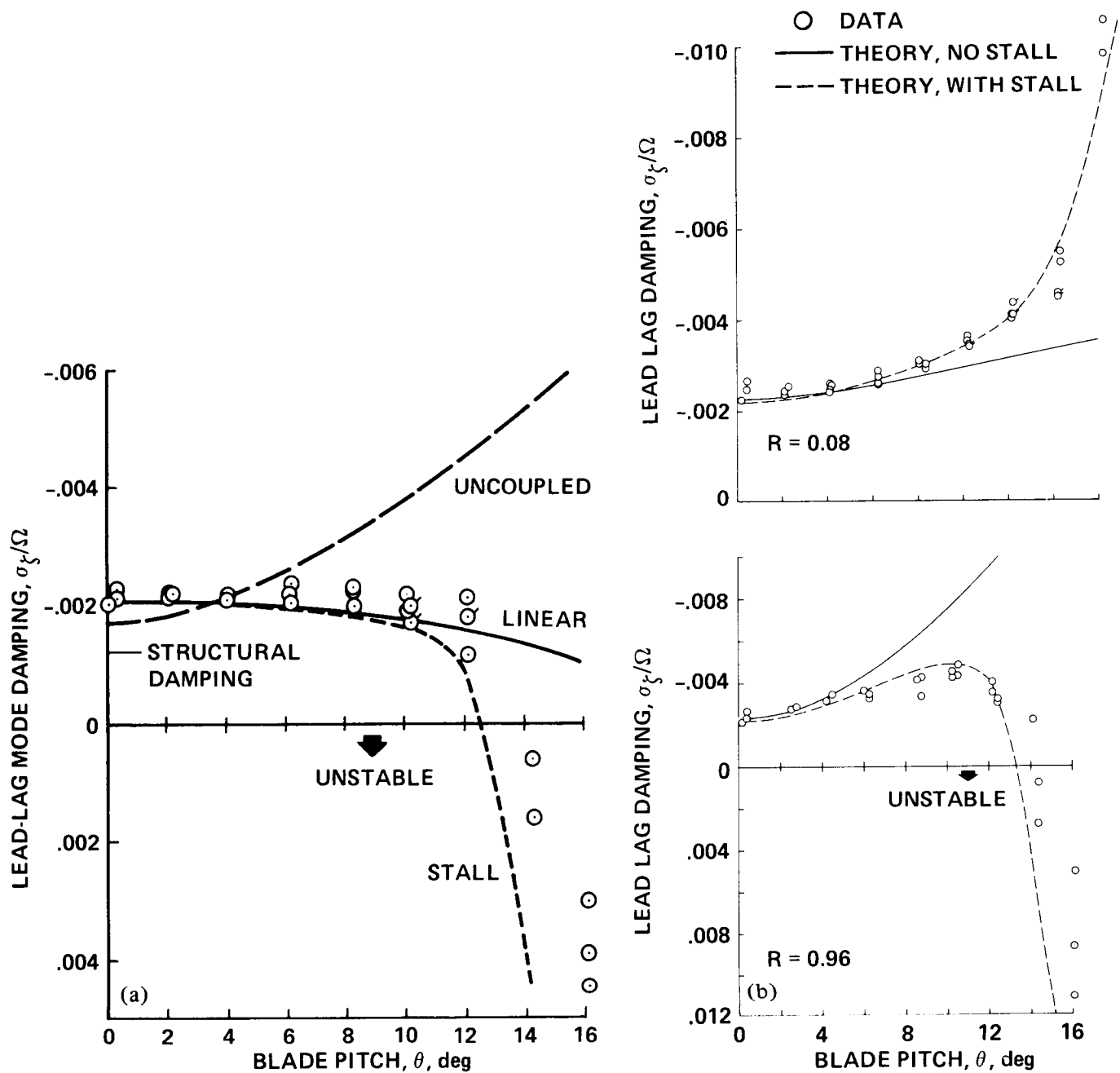


Figure 47.- Experimental lead-lag damping of flap-lag model in hover compared with theory with and without airfoil stall effects:  $\gamma = 2.84$ ,  $\sigma = 0.0601$ ,  $R = 0.08$ .  
 (a)  $p = 1.17$ ,  $\bar{\omega}_{\zeta} = 1.21$ . (b)  $p = 1.28$ ,  $\bar{\omega}_{\zeta} = 1.62$ .

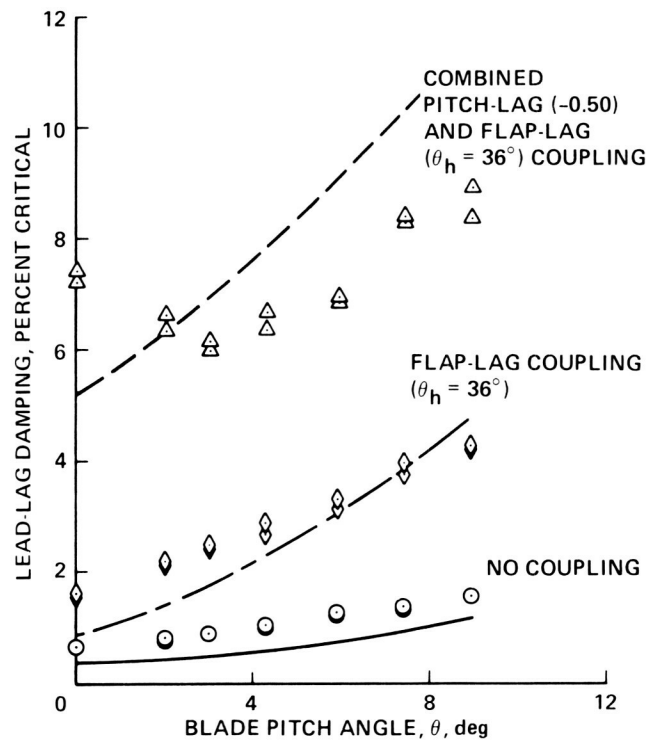


Figure 48.- Effects of aeroelastic couplings on experimental and theoretical lead-lag damping of flap-lag model in hover:  $\bar{\omega}_\zeta = 0.7$ ,  $\gamma = 7.99$ ,  $\sigma = 0.033$ .

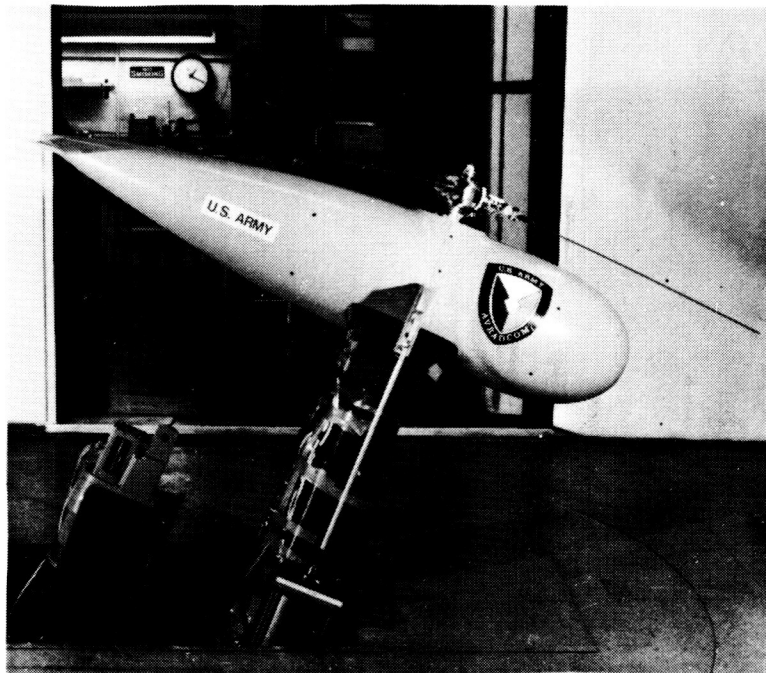


Figure 49.- Three-bladed flap-lag model rotor in 7- by 10-Foot Wind Tunnel.

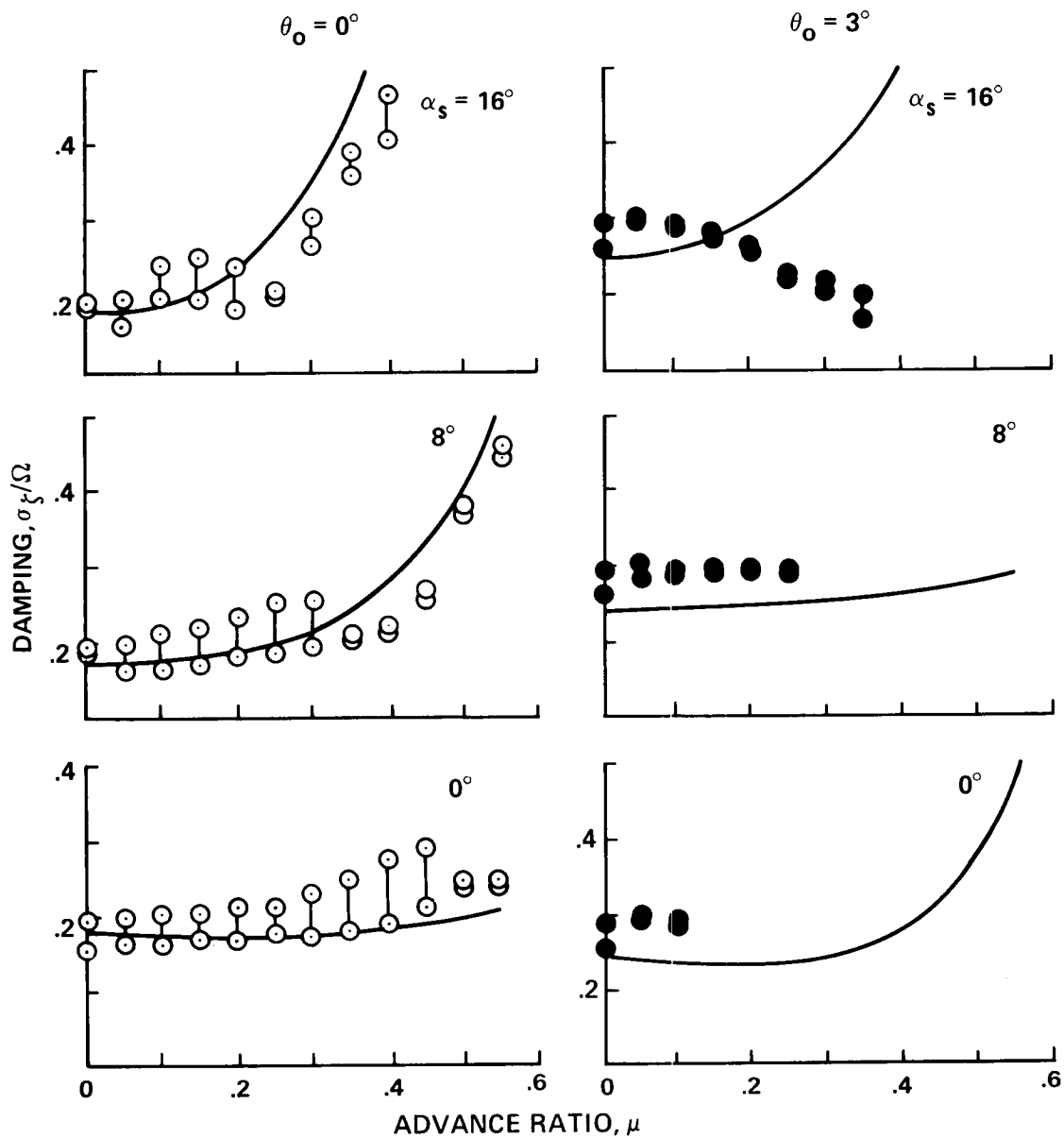


Figure 50.- Experimental lead-lag regressing mode damping of flap-lag model in forward flight compared with theory:  $\Omega = 1000$  rpm,  $\gamma = 7.54$ ,  $\sigma = 0.0494$ ,  $R = 0$ .

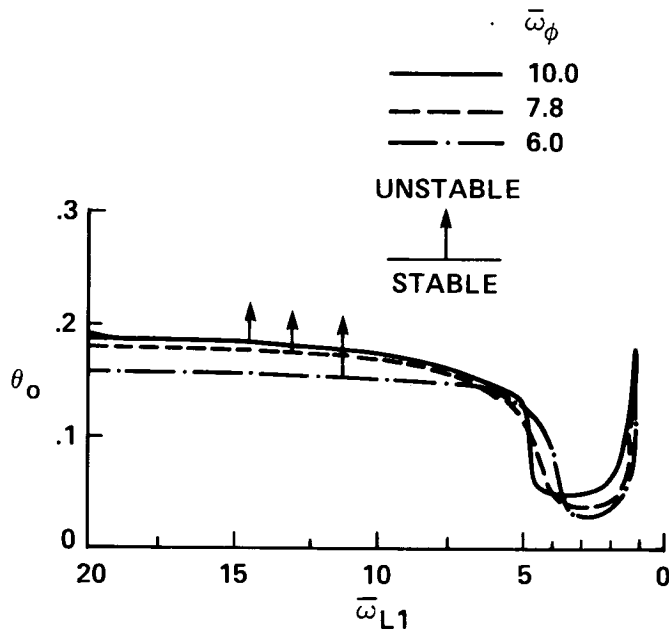


Figure 51.- Stability boundaries for rotor-blade elastic flap-lag bending and rigid-body root pitch in hover:  $\bar{\omega}_{F1} = 1.2$ ,  $\gamma = 8$ ,  $\sigma = 0.08$ .

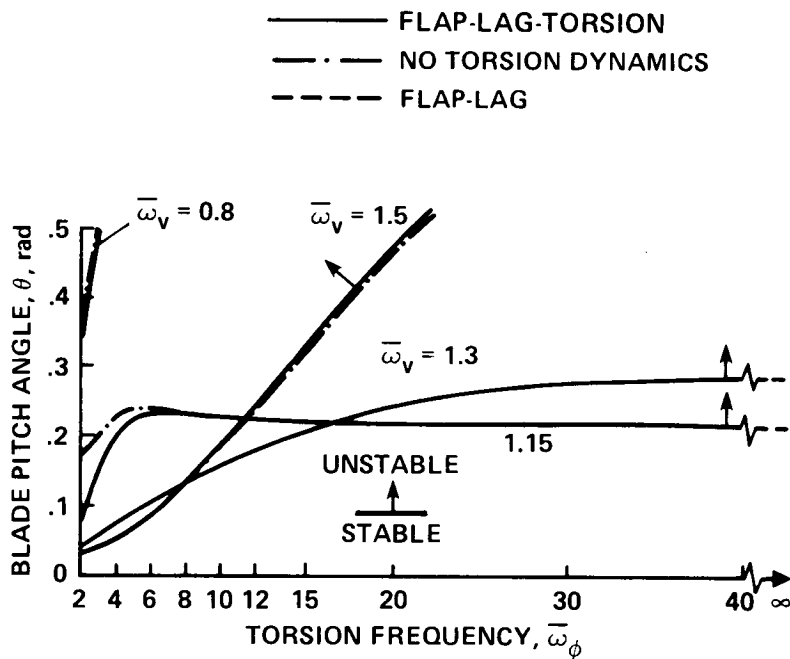


Figure 52.- Comparison of flap-lag-torsion stability boundaries for elastic blade in hover for different treatment of torsion motion:  $\bar{\omega}_w = 1.15$ ,  $\gamma = 5$ ,  $\sigma = 0.1$ ,  $R = 0$ .

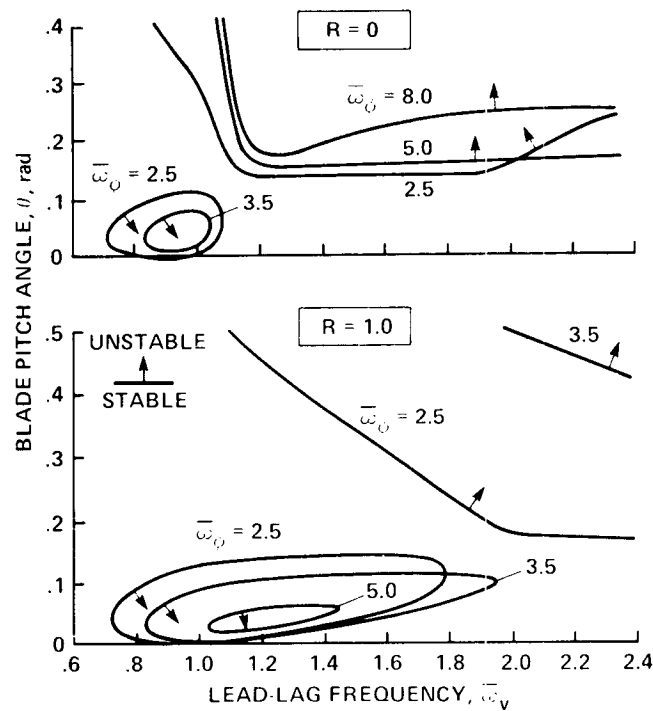


Figure 53.- Effects of flap-lag structural coupling and precone on elastic blade flap-lag-torsion stability boundaries in hover:  $\bar{\omega}_w = 1.15$ ,  $\gamma = 5$ ,  $\sigma = 0.1$ ,  $\beta_{pc} = 0.05$  rad.

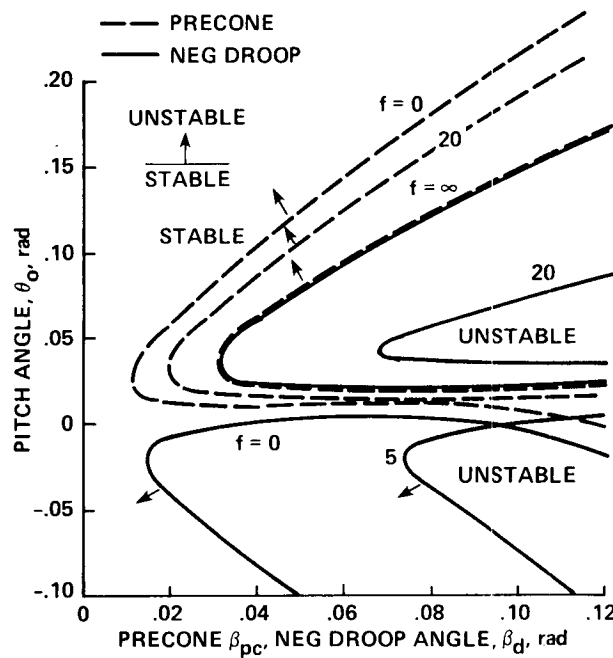


Figure 54.- Effects of precone, droop, and blade torsion-to-pitch link flexibility ratio on elastic blade flap-lag-torsion stability boundaries in hover:  $\bar{\omega}_w = 1.15$ ,  $\bar{\omega}_v = 1.3$ ,  $\bar{\omega}_\phi = 4.0$ ,  $\gamma = 5$ ,  $\sigma = 0.1$ ,  $R = 1$ .

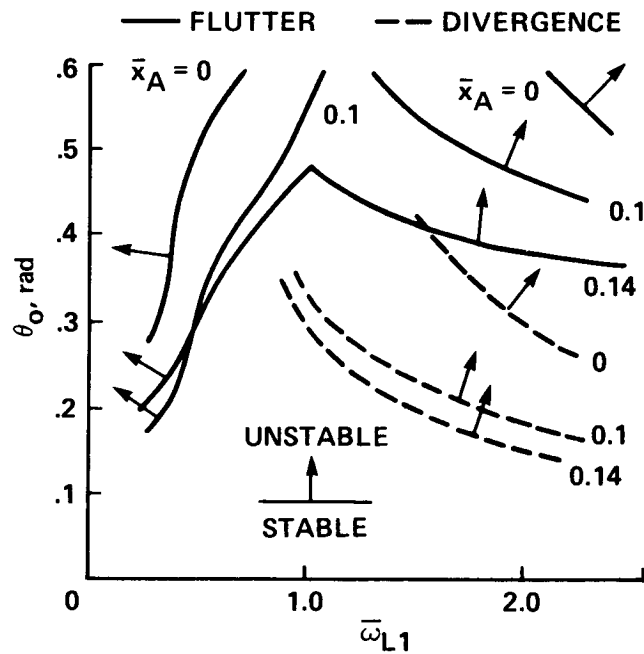


Figure 55.- Effects of chordwise aerodynamic center offsets on elastic blade flap-lag-torsion stability boundaries in hover:  $\bar{\omega}_{F1} = 1.14$ ,  $\bar{\omega}_{\phi} = 4.5$ ,  $\gamma = 8$ ,  $\sigma = 0.08$ .

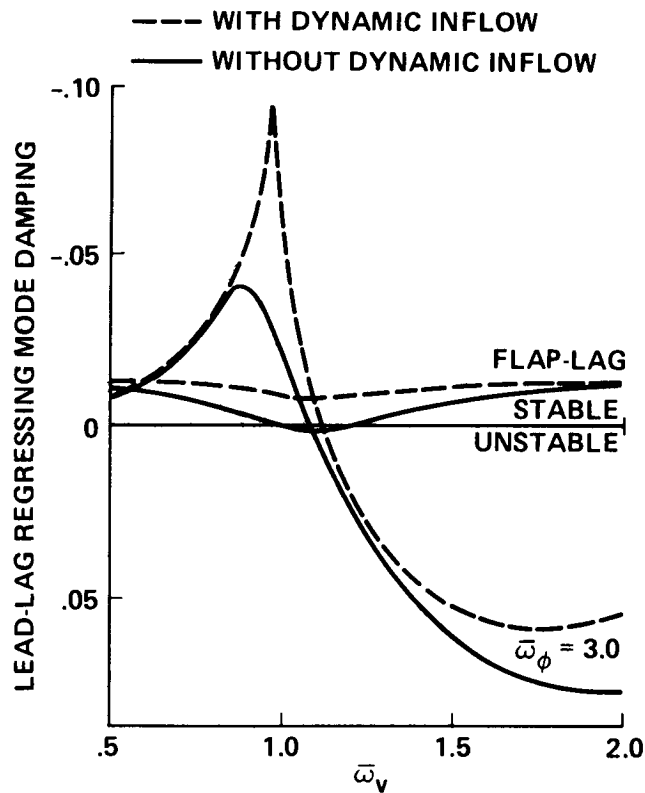


Figure 56.- Effects of dynamic inflow on regressing lead-lag mode damping of elastic blade flap-lag-torsion analysis in hover:  $\theta = 0.3$  rad,  $\bar{\omega}_w = 1.15$ ,  $\bar{\omega}_{\phi} = 5$ ,  $\gamma = 5$ ,  $\sigma = 0.1$ ,  $R = 0$ .

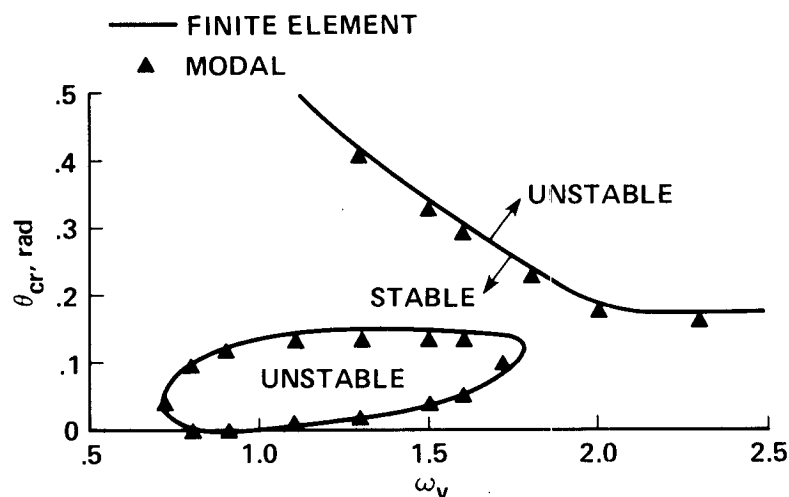


Figure 57.- Comparison of finite element and modal analysis results for flap-lag-torsion of elastic blade in hover:  $\bar{\omega}_w = 1.15$ ,  $\bar{\omega}_\phi = 2.5$ ,  $\gamma = 5$ ,  $\sigma = 0.1$ ,  $R = 1$ ,  $\beta_{pc} = 0.05$  rad.

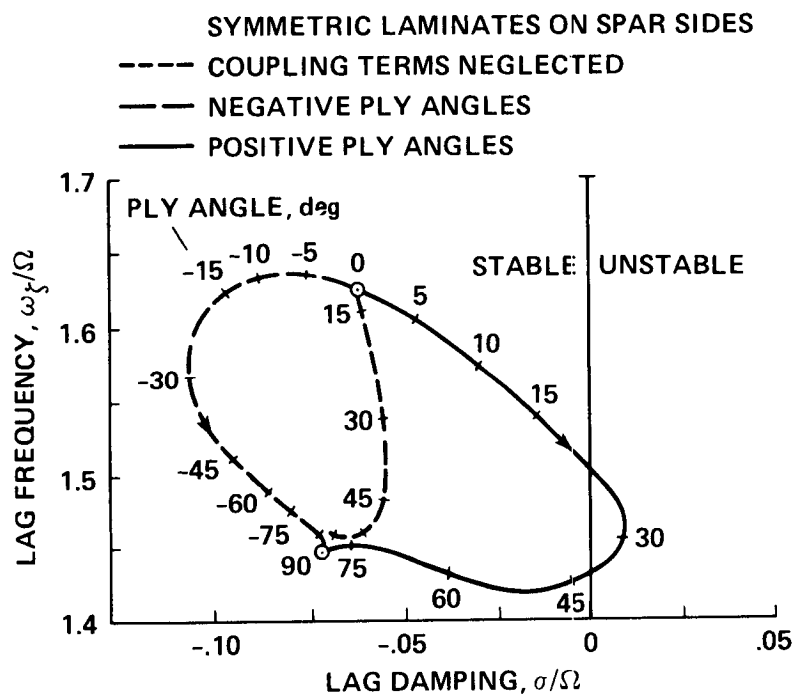


Figure 58.- Effects of composite material ply layup configuration on lead-lag frequency and damping of elastic blade flap-lag-torsion analysis in hover:  $C_T/\sigma = 0.1$ ,  $\gamma = 5$ ,  $\sigma = 0.1$ .

ORIGINAL PAGE IS  
OF POOR QUALITY

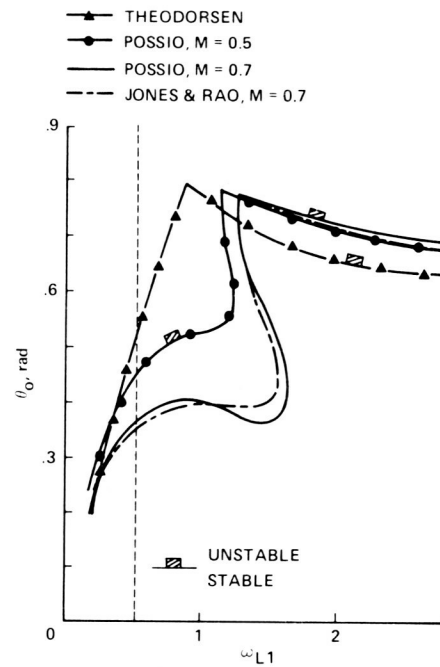


Figure 59.- Effects of unsteady aerodynamics and compressibility on elastic blade flap-lag-torsion stability boundaries in hover:  $\bar{\omega}_{F1} = 1.142$ ,  $\bar{\omega}_{T1} = 6.17$ ,  $\gamma = 8$ ,  $\sigma = 0.08$ ,  $\bar{x}_A = 0.2$ .

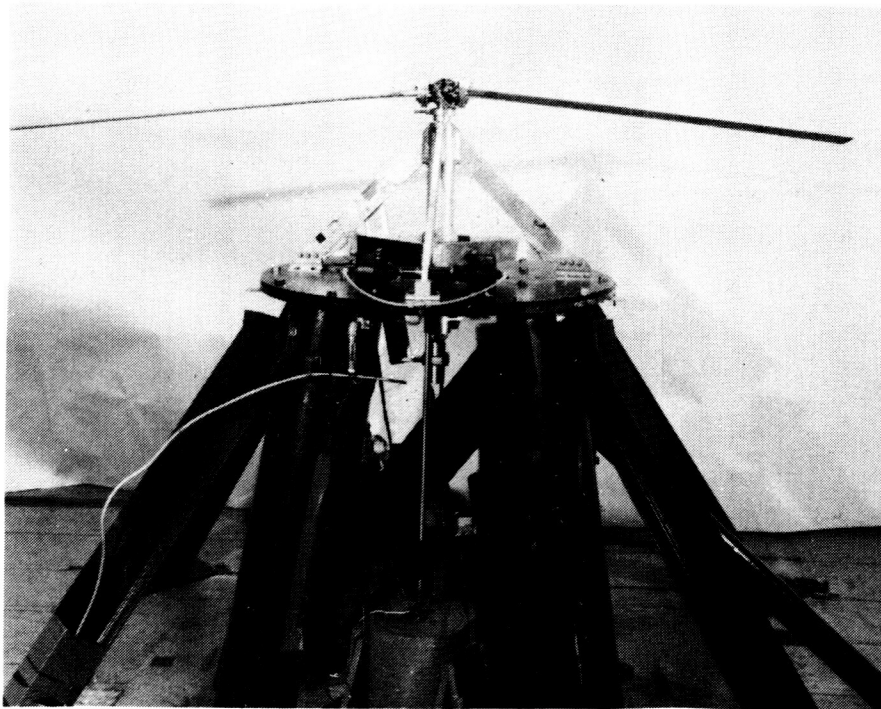


Figure 60.- Small scale 5.5-ft-diam elastic blade-rotor model for flap-lag torsion experiments in hover.



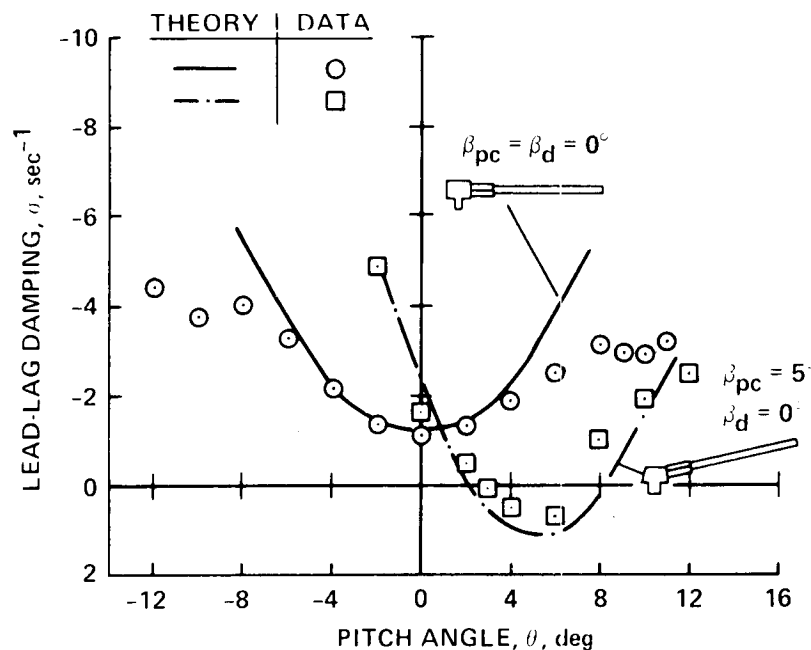


Figure 61.- Comparison of experimental and theoretical results for lead-lag mode damping of small-scale flap-lag-torsion model in hover with and without precone:  $\bar{\omega}_w \approx 1.13$ ,  $\bar{\omega}_v \approx 1.4$ ,  $\bar{\omega}_\phi \approx 2.6$ .

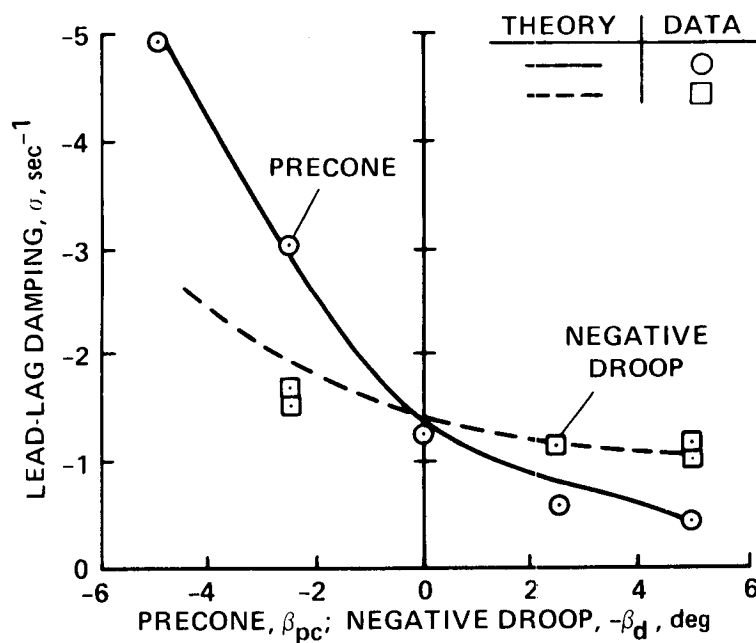


Figure 62.- Comparison of experimental and theoretical results for lead-lag mode damping of small-scale flap-lag-torsion model in hover as a function of precone and droop:  $\theta_0 = 2^\circ$ .

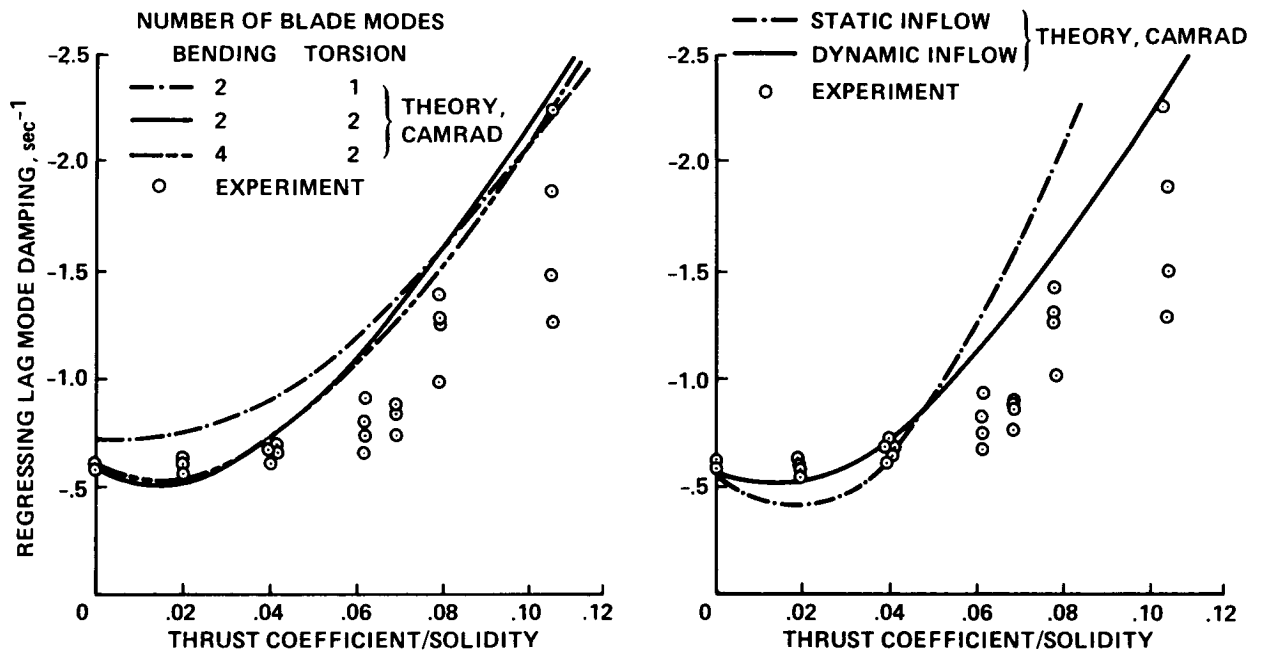


Figure 63.- Comparison with theory of experimental lead-lag mode damping of full-scale BO-105 rotor tested in 40- by 80-Foot Wind Tunnel.

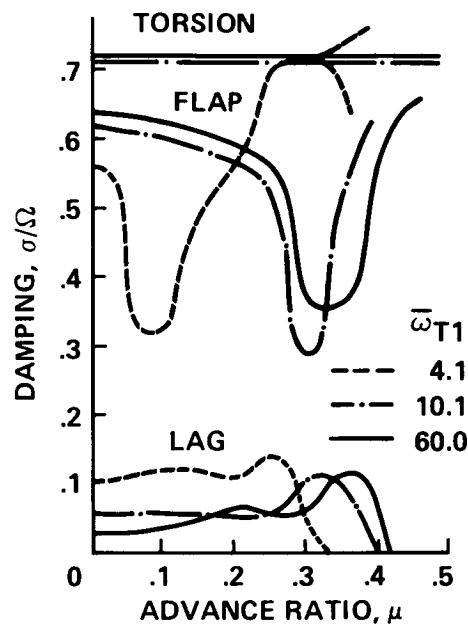


Figure 64.- Modal damping for elastic blade flap-lag-torsion analysis in forward flight:  $\bar{\omega}_{F1} = 1.1$ ,  $\bar{\omega}_{L1} = 0.902$ ,  $\gamma = 10$ ,  $\sigma = 0.05$ ,  $C_W = 0.01$ .

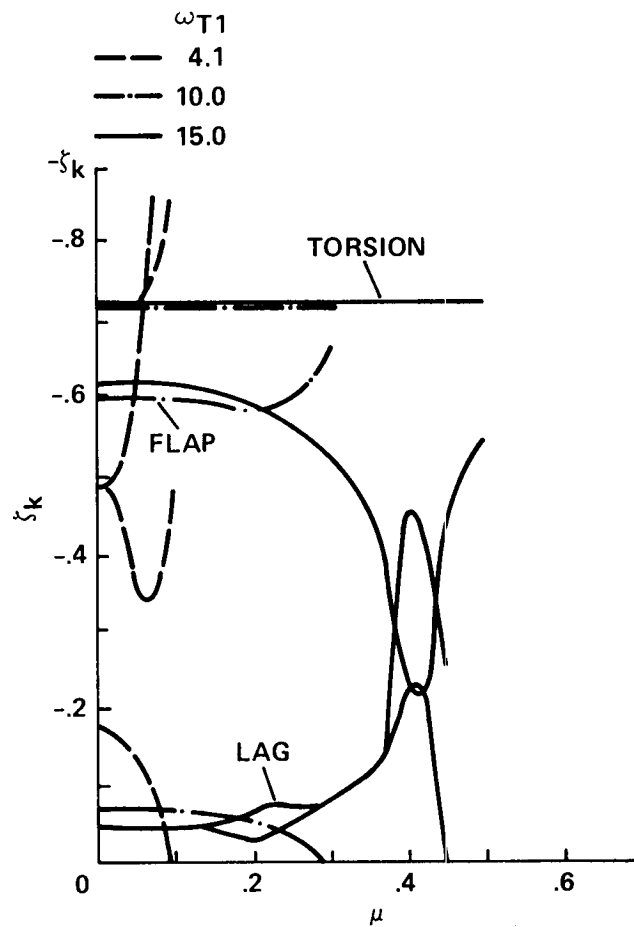


Figure 65.- Modal damping for elastic blade flap-lag-torsion analysis in forward flight with improved equations:  $\bar{\omega}_{F1} = 1.1$ ,  $\bar{\omega}_{L1} = 0.902$ ,  $\gamma = 10$ ,  $\sigma = 0.05$ ,  $C_W = 0.01$ .

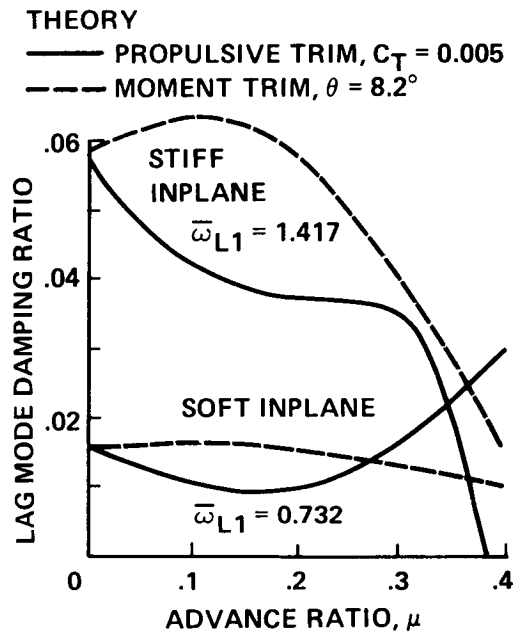


Figure 66.- Lead-lag mode damping for elastic blade flap-lag-torsion analysis in forward flight for two trim conditions:  $\bar{\omega}_{F1} = 1.125$ ,  $\bar{\omega}_{T1} = 3.176$ ,  $\gamma = 5.5$ ,  $\sigma = 0.07$ ,  $R = 1$ .

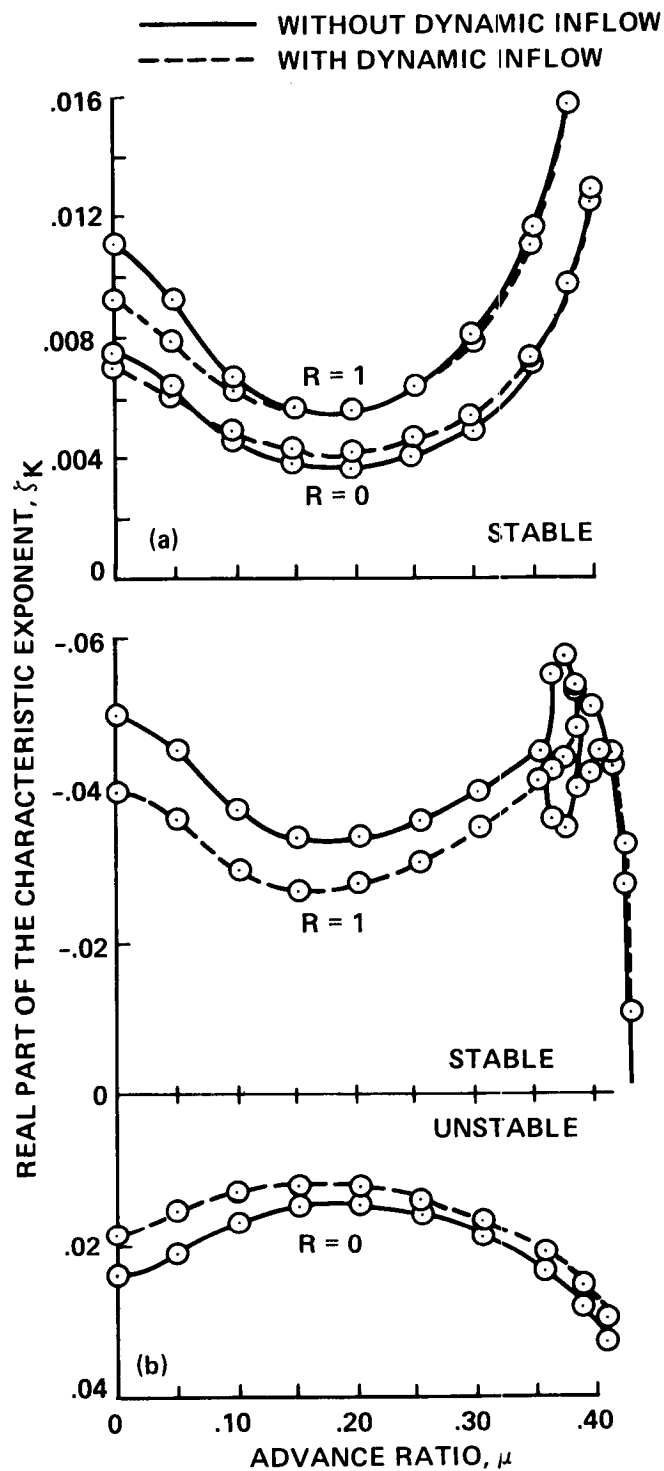


Figure 67.- Effects of dynamic inflow and flap-lag structural coupling on lead-lag regressing mode damping for elastic blade flap-lag-torsion analysis in forward flight:  $\bar{\omega} = 1.15$ ,  $\gamma = 5$ ,  $\sigma = 0.1$ . (a) Soft inplane:  $\bar{\omega}_V = 0.7$ . (b) Stiff inplane:  $\bar{\omega}_V = 1.4$ .

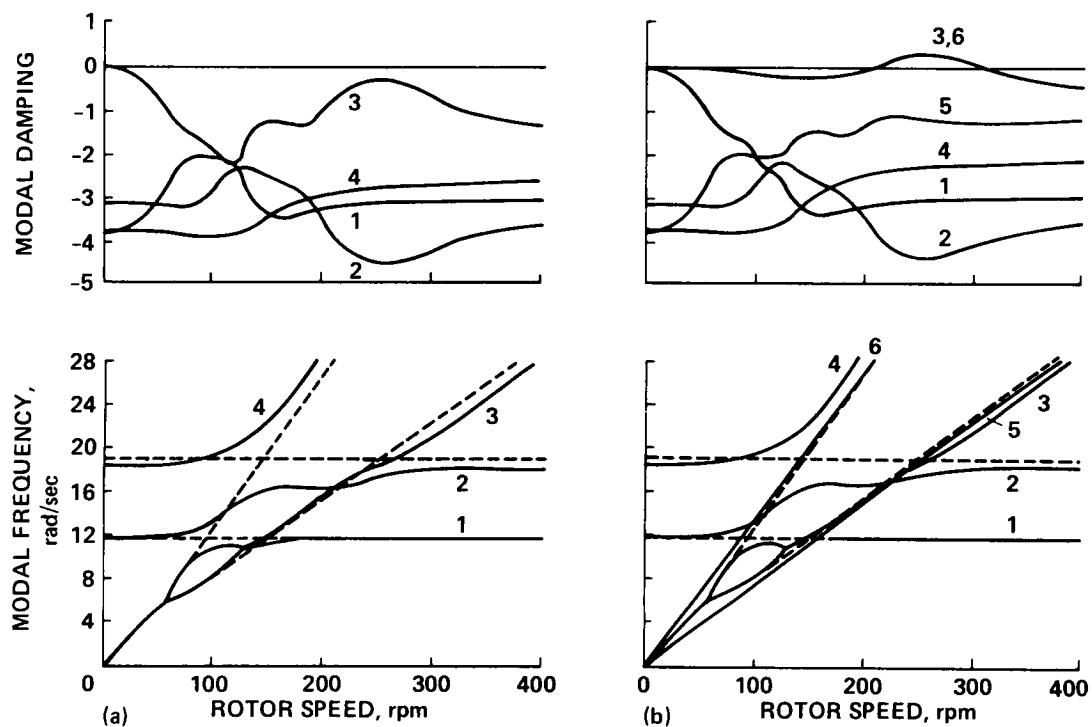


Figure 68.- Effects of blade dissimilarity on ground-resonance stability analysis of articulated rotor system. (a) All blade lead-lag dampers operative. (b) One damper inoperative.

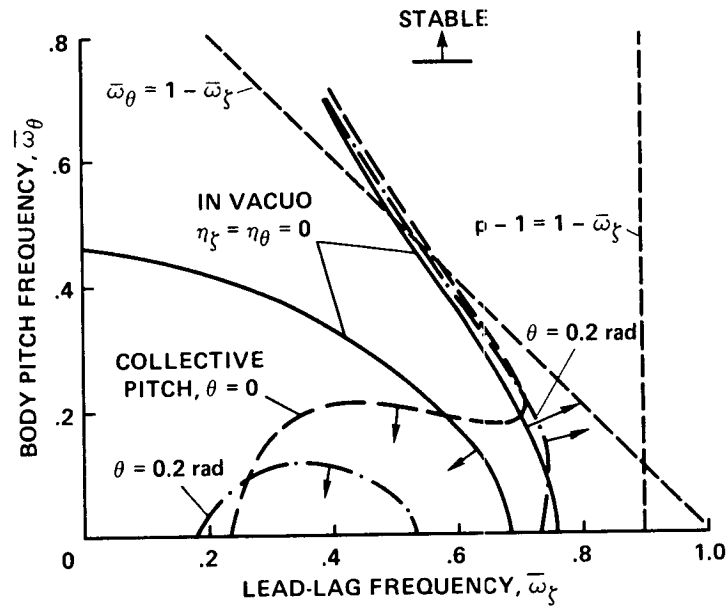


Figure 69.- Hingeless rotor ground-resonance stability boundaries with hinged-rigid blade flap, lead-lag, and body pitch degrees of freedom:  $p = 1.1$ ,  $\gamma = 5$ ,  $\sigma = 0.05$ ,  $R = 0$ .

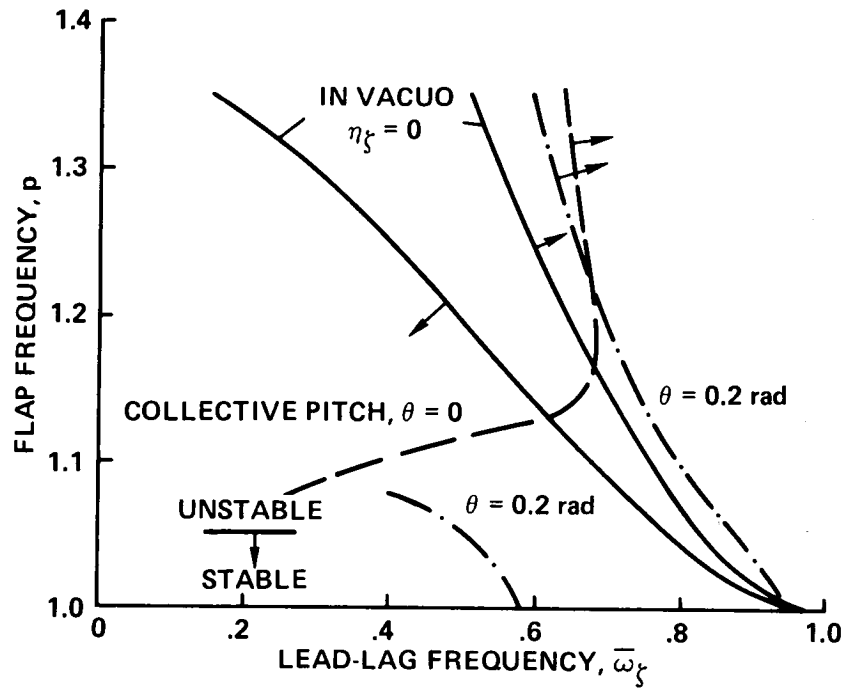


Figure 70.- Hingeless-rotor air-resonance stability boundaries with hinged-rigid blade flap, lead-lag, and body pitch degrees of freedom in hover:  $\gamma = 5$ ,  $\sigma = 0.05$ .

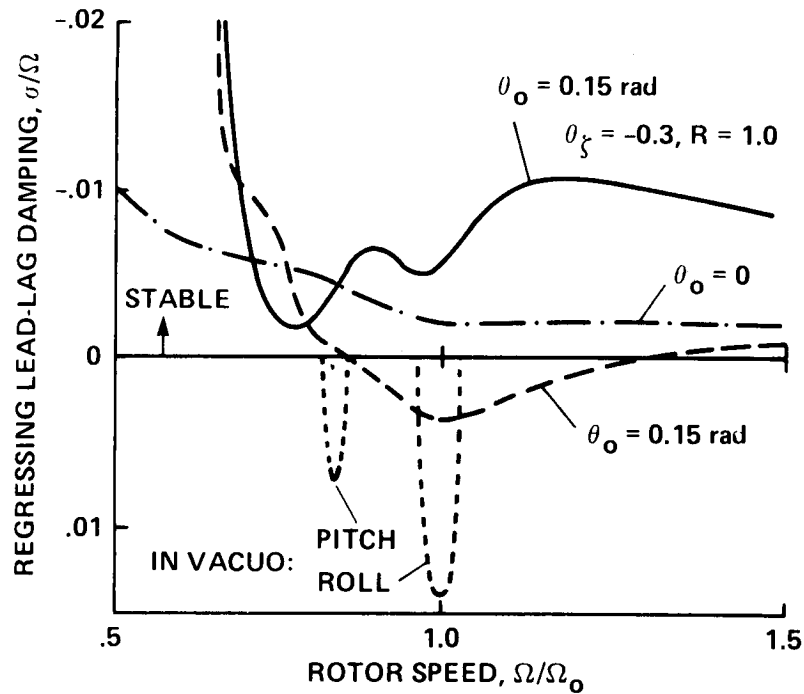


Figure 71.- The effects of aerodynamics, thrust, and aeroelastic couplings on hingeless-rotor air resonance in hover as a function of rotor speed:  $p_0 = 1.1$ ,  $\bar{\omega}_{\tau_0} = 0.7$ ,  $\gamma = 5$ ,  $\sigma = 0.05$ .



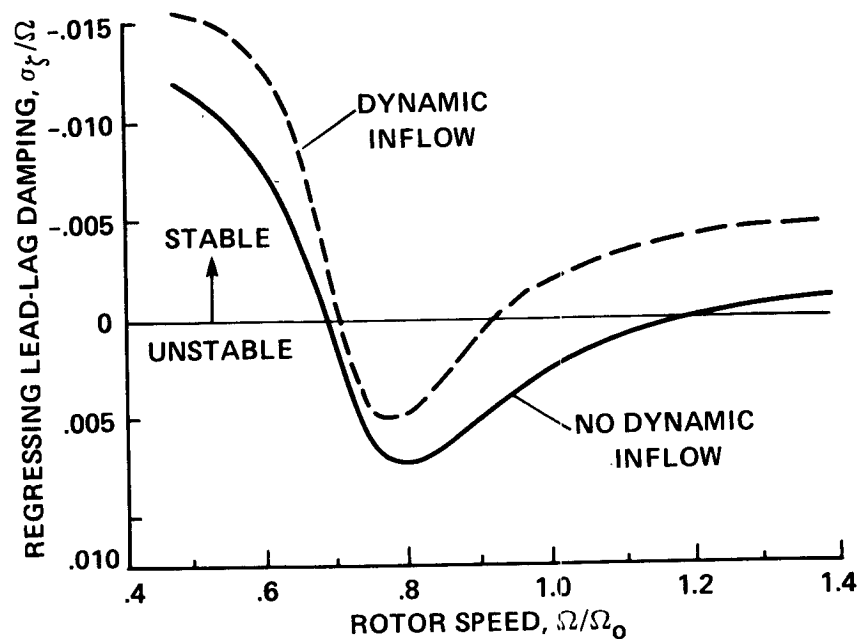


Figure 72.- Effect of dynamic inflow on hingeless-rotor air resonance for a matched stiffness configuration:  $\theta_0 = 0.3$  rad,  $p_0 = 1.1$ ,  $\bar{\omega}_{\zeta_0} = 0.458$ .

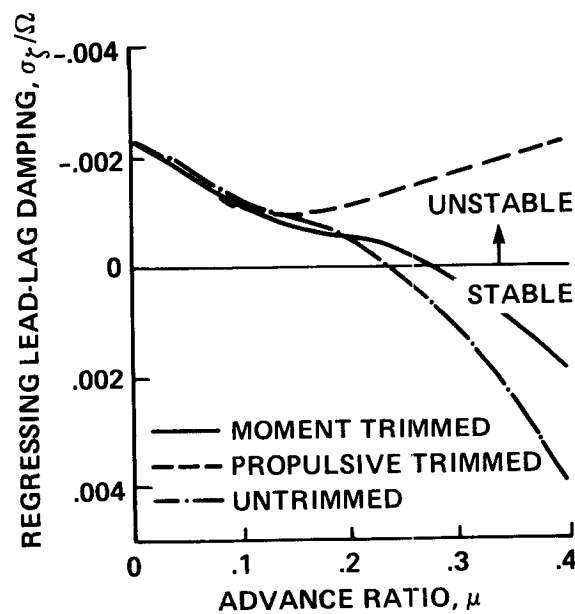


Figure 73.- Coupled rotor-body lead-lag regressing mode damping in forward flight for various trim conditions:  $p = 1.15$ ,  $\bar{\omega}_{\zeta} = 0.7$ ,  $C_T/\sigma = 0.2$ .

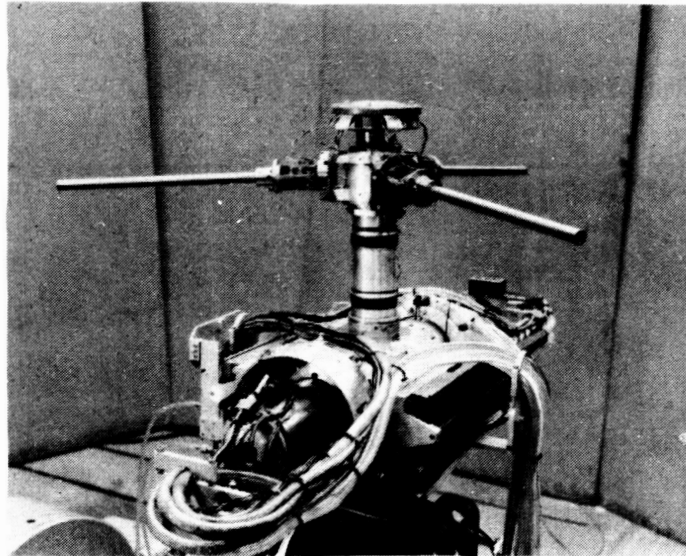


Figure 74.- Small-scale rotor model for coupled rotor-body stability experiments with non-airfoil blades to simulate in vacuum conditions.

ORIGINAL PAGE IS  
OF POOR QUALITY

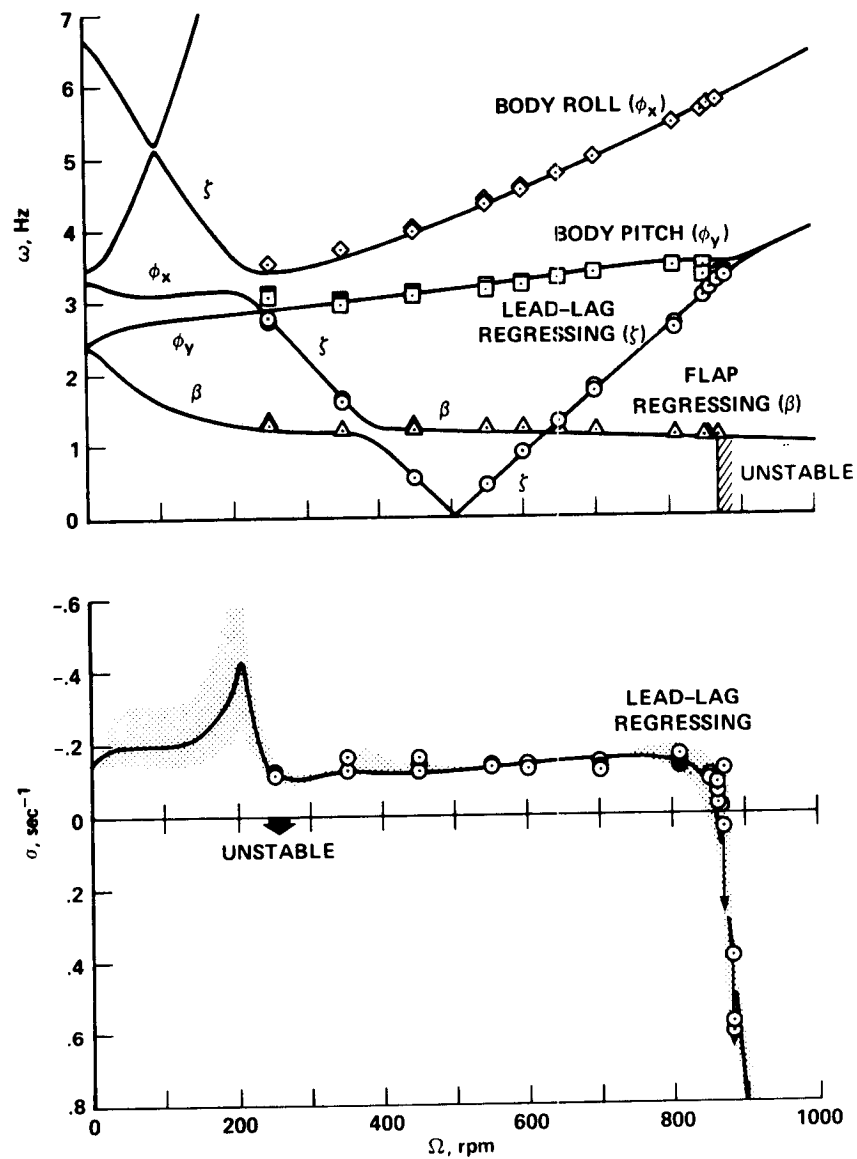


Figure 75.- Comparison of experimental and theoretical frequency and damping as a function of rotor speed for coupled rotor-body model with simulated in vacuum blades.

ORIGINAL PAGE IS  
OF POOR QUALITY

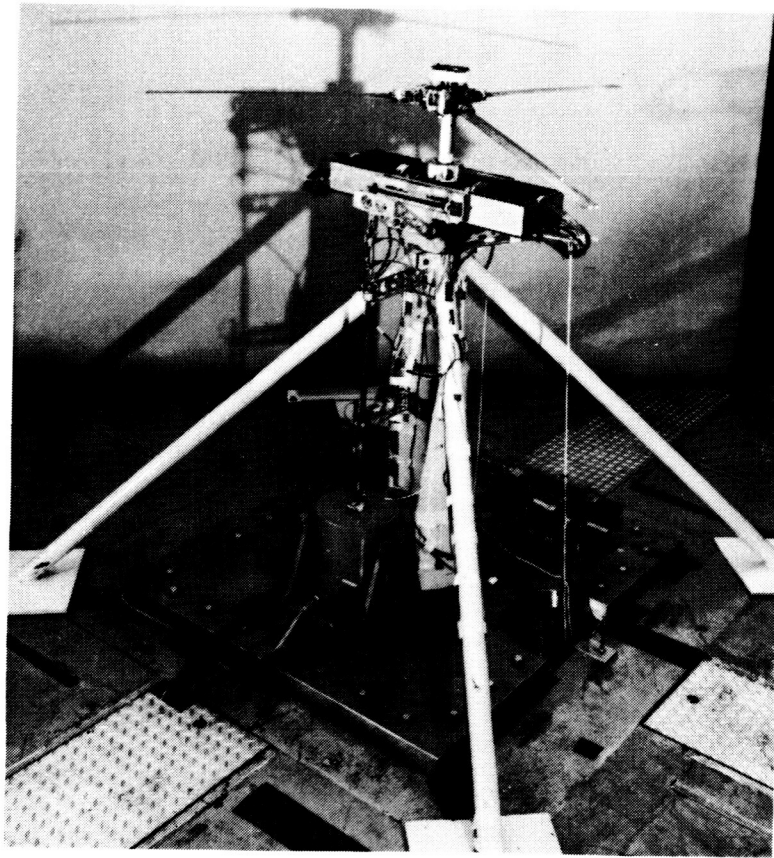


Figure 76.- Small-scale rotor model for coupled rotor-body hover stability experiments with 5.5-ft-diam three-bladed rotor.

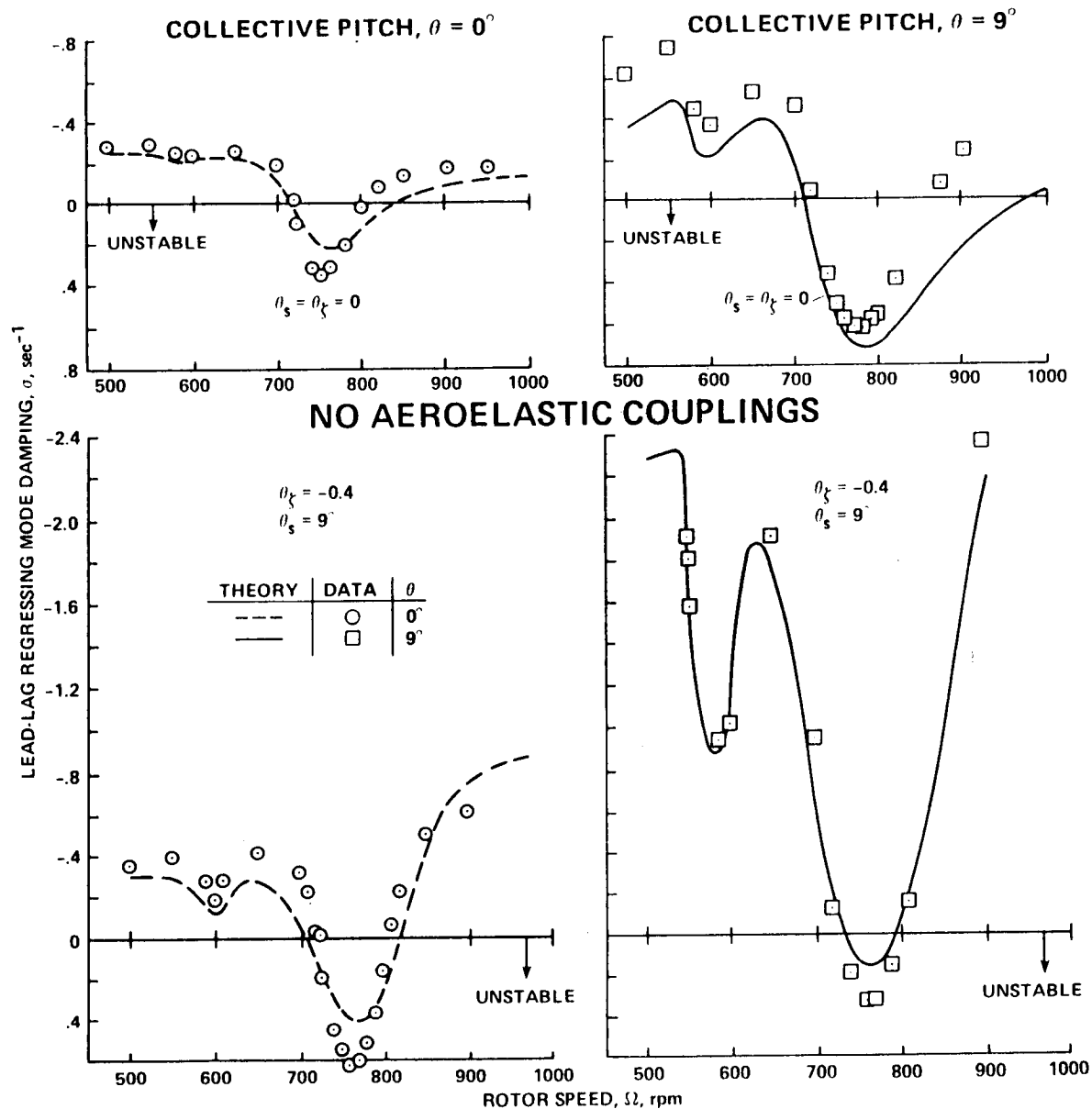
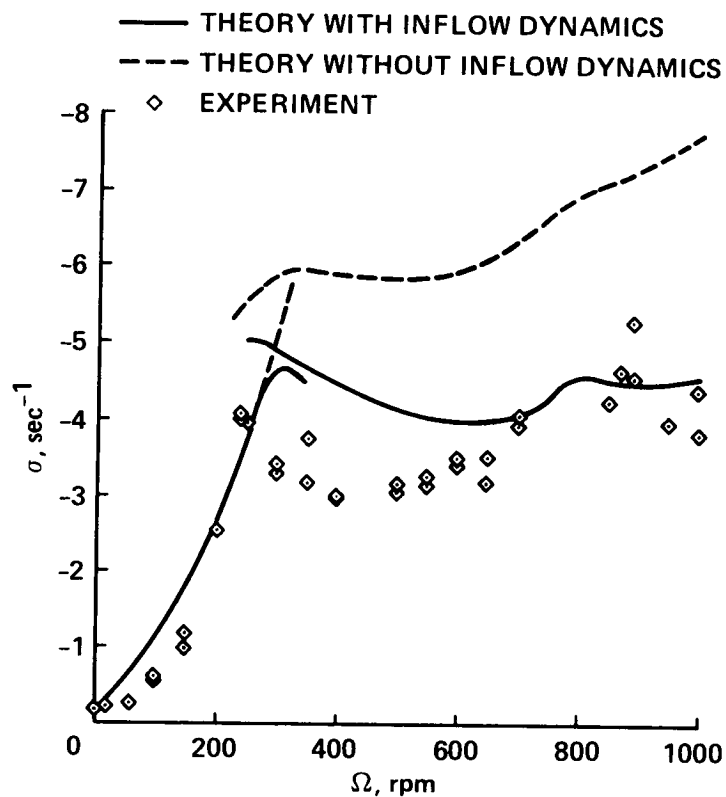


Figure 77.- Comparison of experimental and theoretical regressing lead-lag mode damping for coupled rotor-body model in hover including effects of aeroelastic coupling.



JOHNSON, 1982 (AFDD)

Figure 78.- Comparison of experimental and theoretical roll-mode damping for coupled rotor-body model in hover including effects of dynamic inflow.

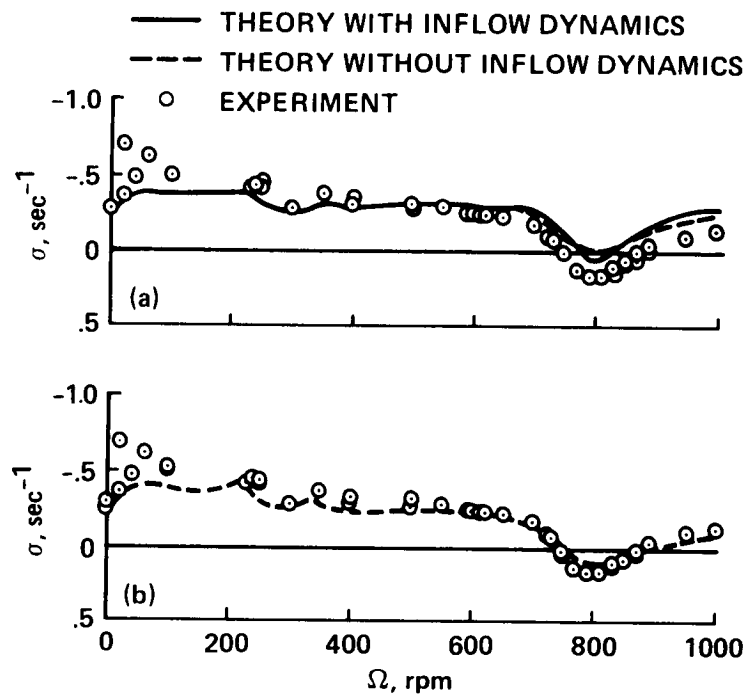


Figure 79.- Comparison of experimental and theoretical regressing lead-lag mode damping for coupled rotor-body model in hover. (a) Johnson's results including dynamic inflow. (b) Bousman's result without dynamic inflow.

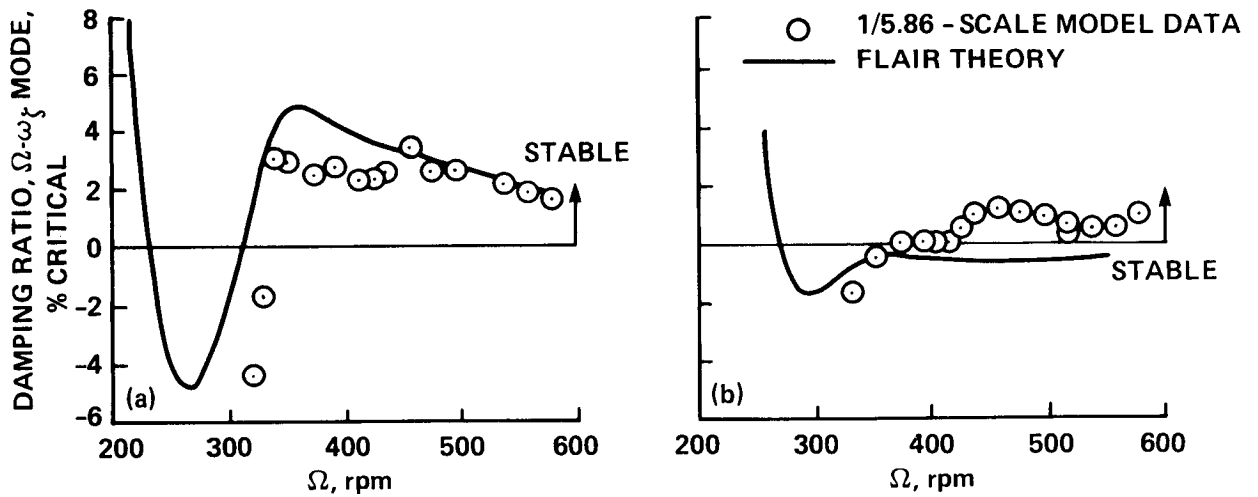


Figure 80.- Comparison of small-scale bearingless-rotor model experimental results for lead-lag regressing mode damping with FLAIR analysis,  $\gamma = 3.64$ ,  $\sigma = 0.07$ .  
 (a)  $\theta_f = 6^\circ$ ,  $\theta_b = 2.5^\circ$ ,  $\theta_b = 1.95^\circ$ . (b)  $\theta_f = 0^\circ$ ,  $\theta_b = 2.5^\circ$ ,  $\theta_b = 7.95^\circ$ .

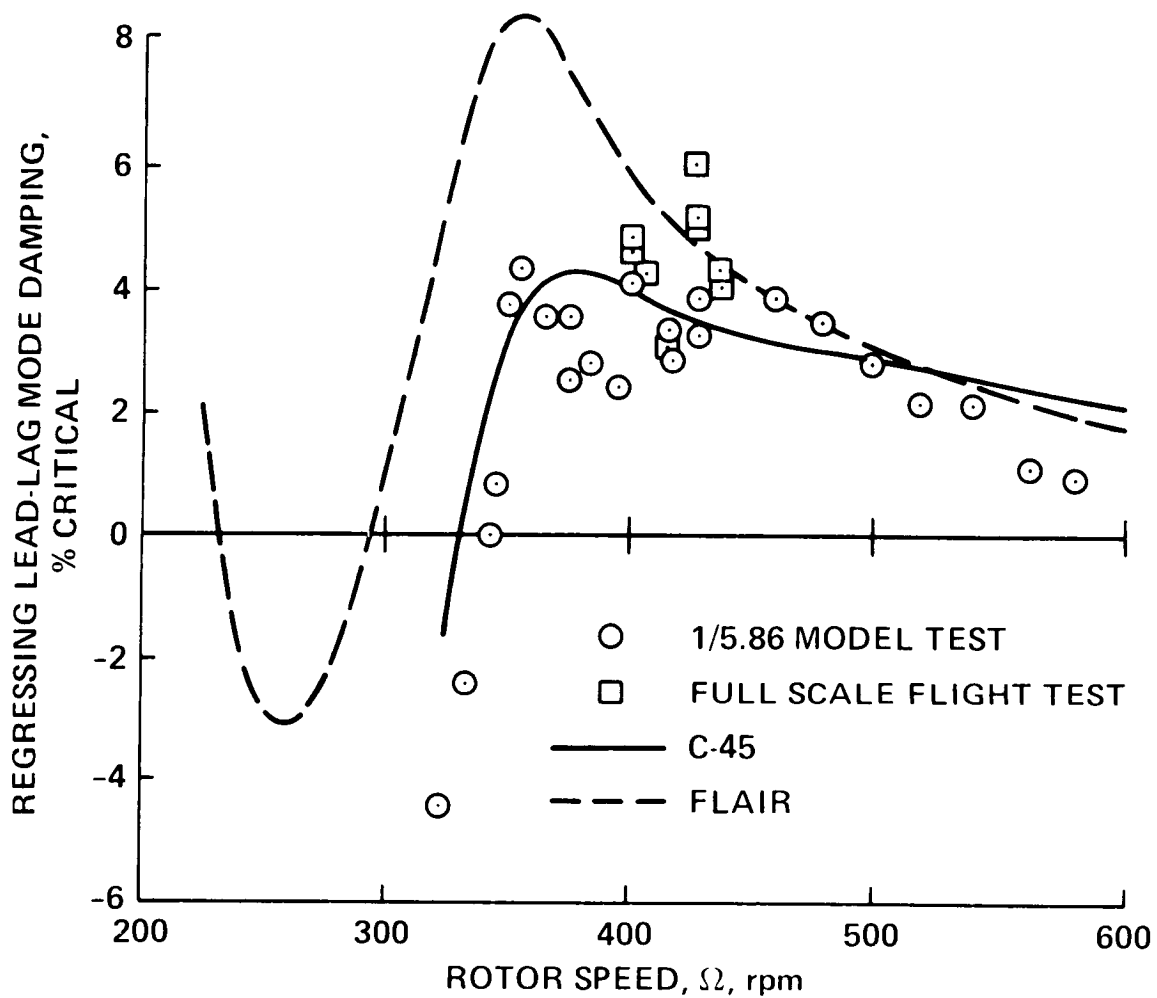


Figure 81.- Comparison of several experimental and theoretical results for hover air-resonance stability of Boeing Vertol BO-105 bearingless main rotor (BMR).



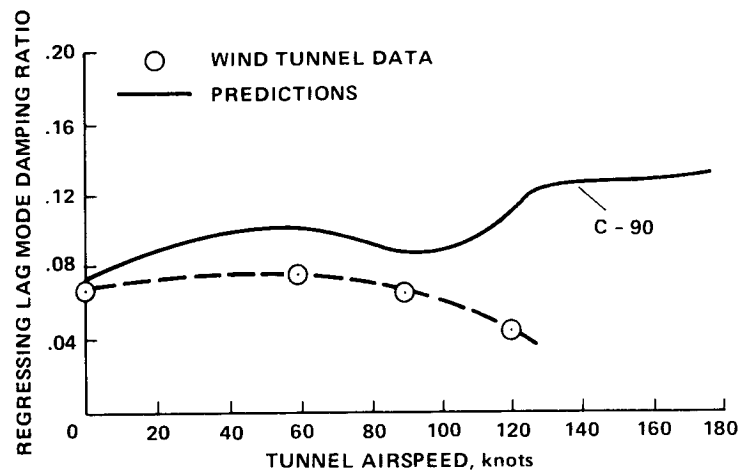


Figure 82.- Comparison of Boeing Vertol BMR 40- by 80-Foot Wind-Tunnel data with analysis for forward flight.

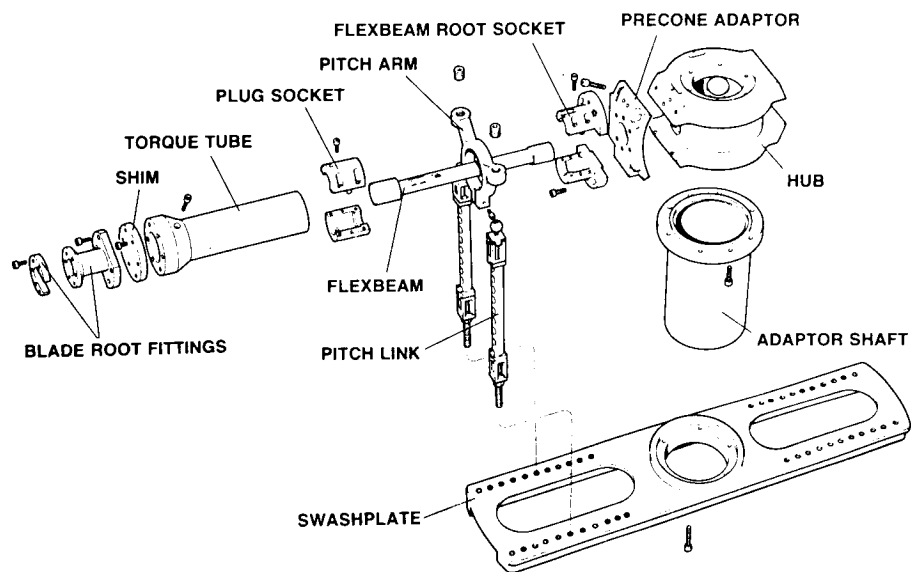


Figure 83.- Hub flexbeam and pitch-control system components of small-scale experimental bearingless rotor model.

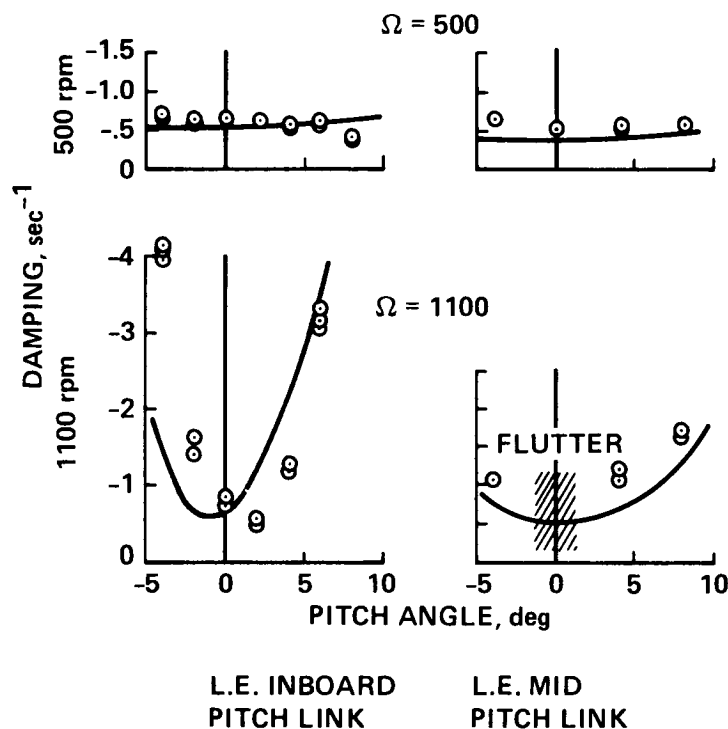


Figure 84.- Comparison of FLAIR theory with experimental measurements of lead-lag damping for small-scale, 2-blade bearingless-rotor model.

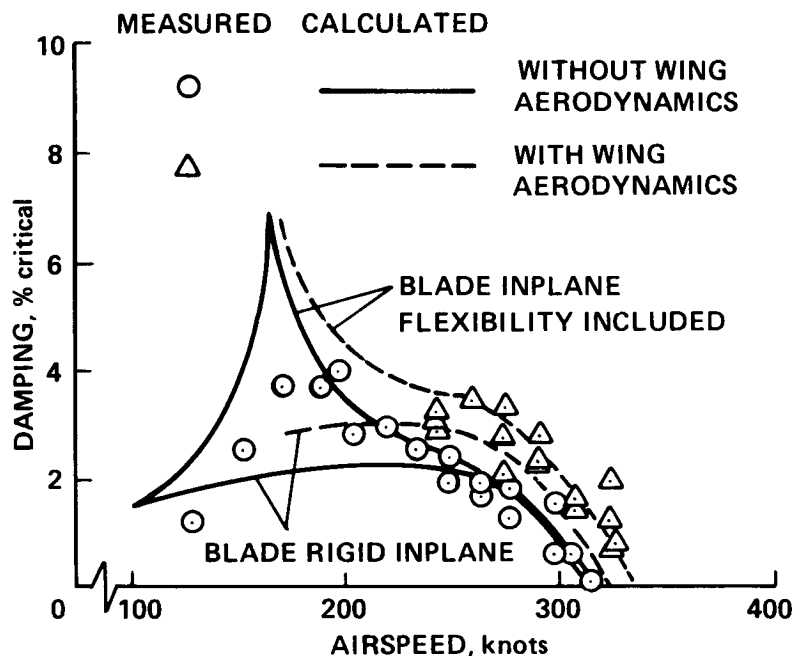


Figure 85.- Comparison of measured small-scale model wing beam mode damping with theory for Bell Model 266 tilt-rotor configuration.

ORIGINAL PAGE IS  
OF POOR QUALITY

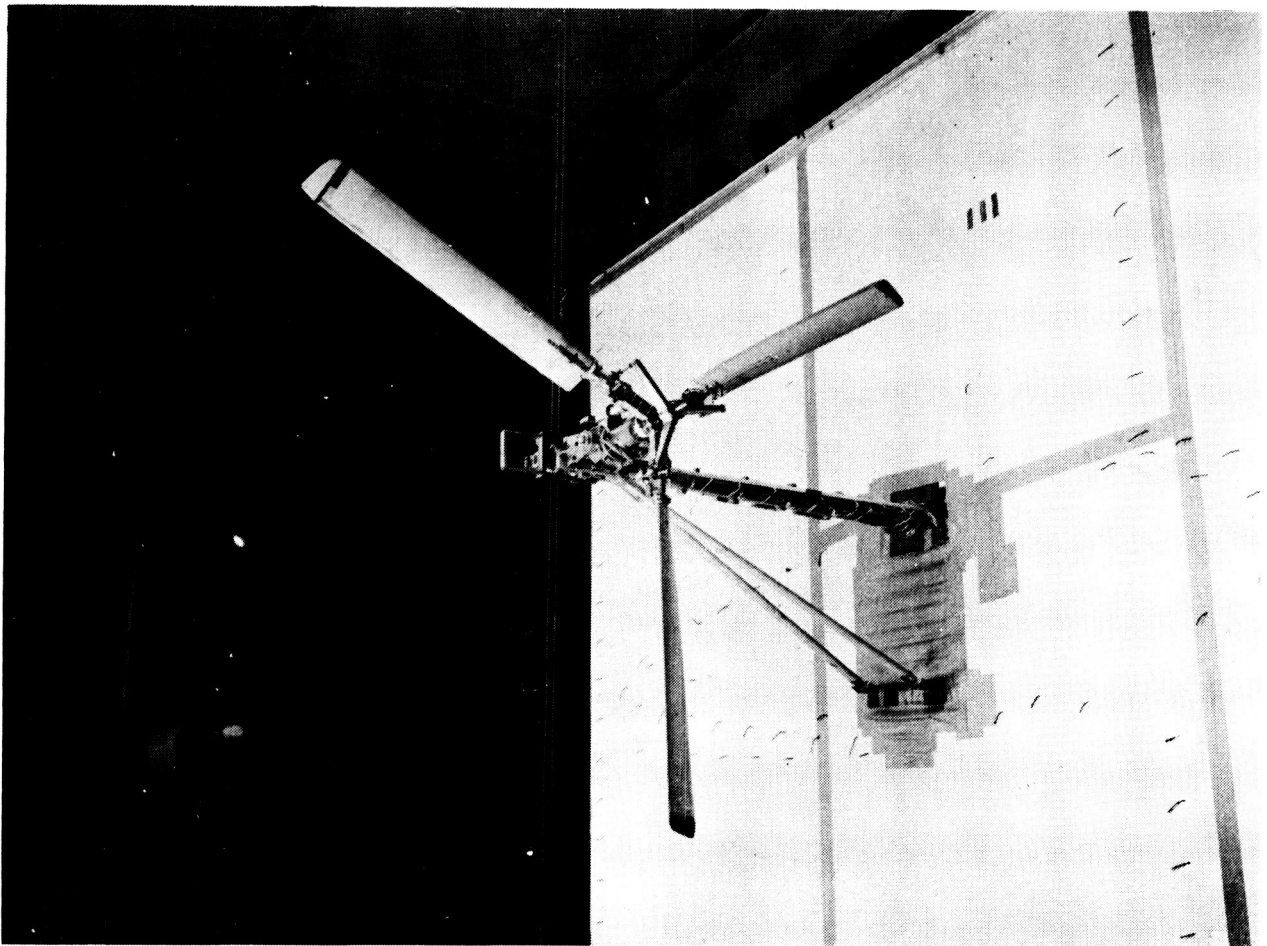


Figure 86.- Small-scale rotor, pylon, wing tilt-rotor research model installed in Langley Transonic Dynamics Tunnel.

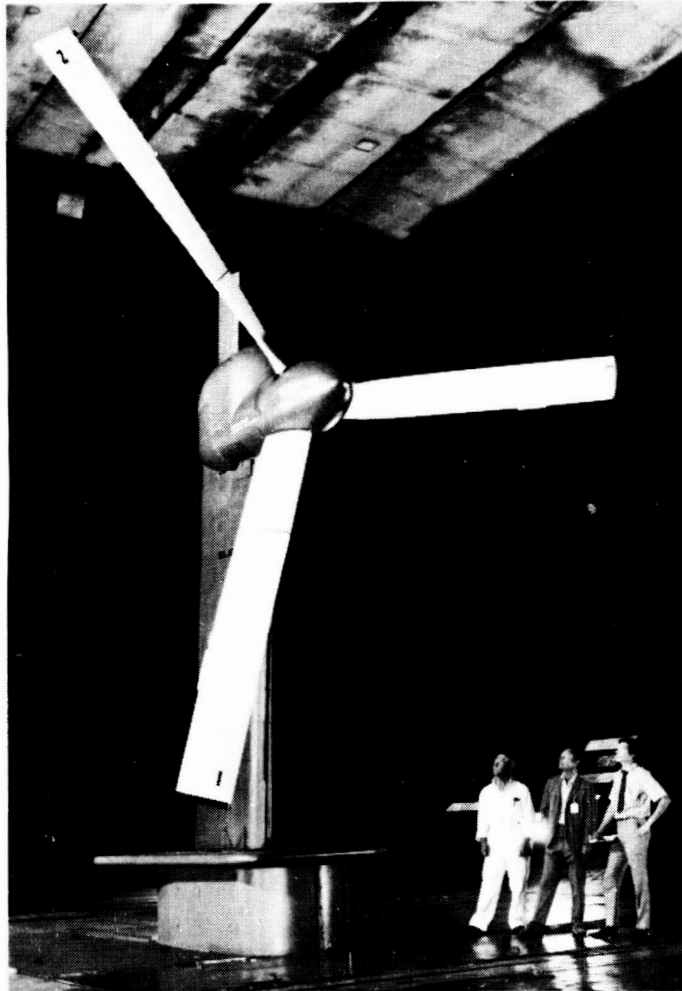


Figure 87.- Full-scale semispan rotor-pylon-wing model installed in Ames 40-by 80-Foot Wind Tunnel.

ORIGINAL PAGE IS  
OF POOR QUALITY

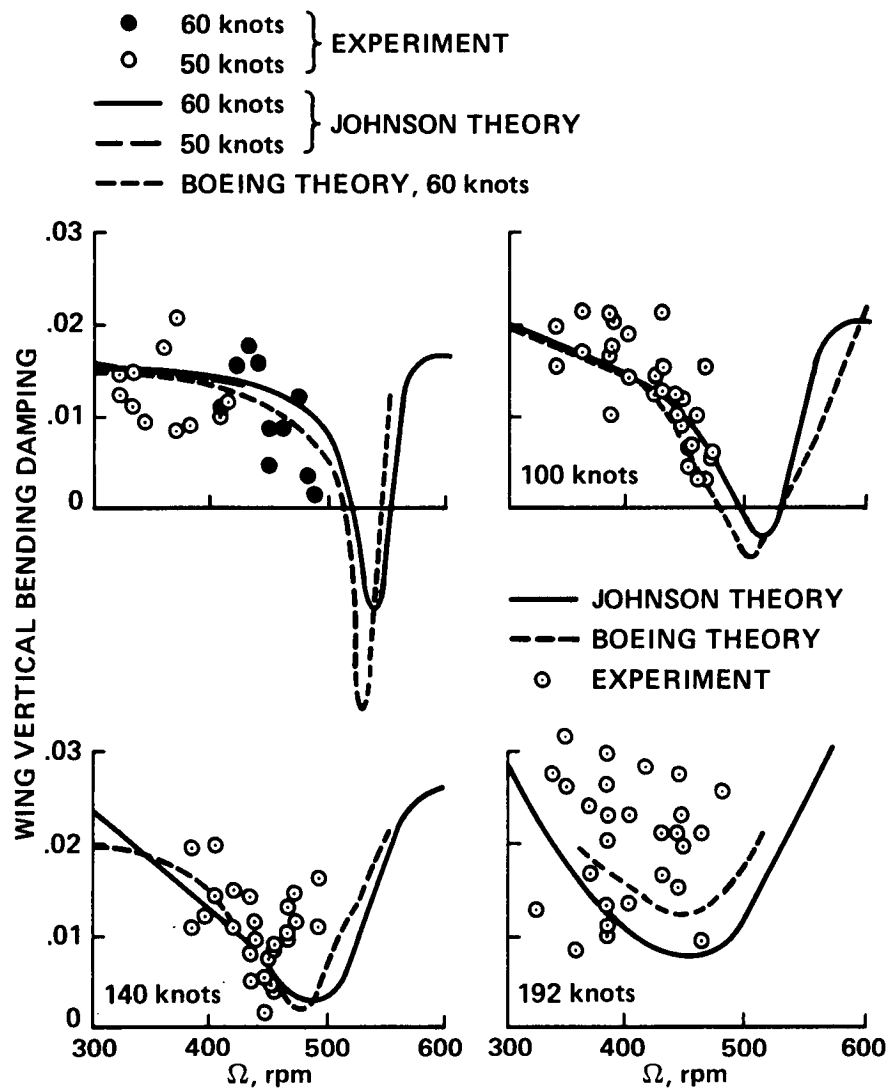


Figure 88.- Full-scale Boeing Vertol semispan rotor-pylon-wing model vertical wing bending mode experimental damping measurements compared with theory as a function of rotor speed for different tunnel velocities.

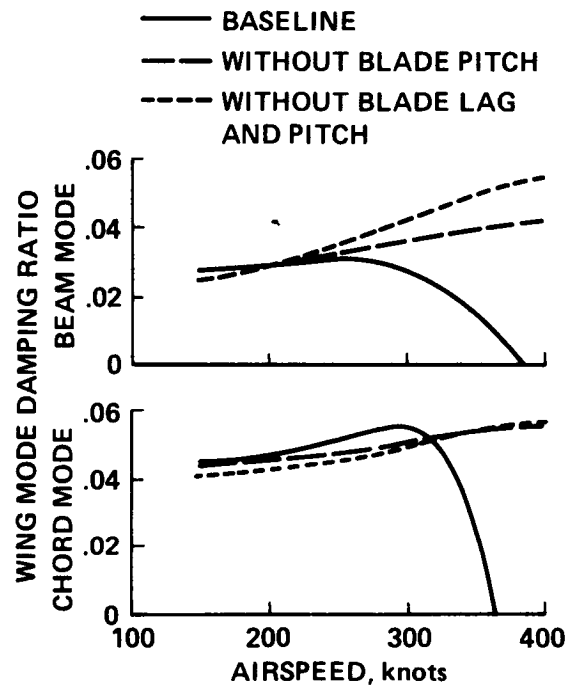


Figure 89.- Effects of rotor-blade pitch and lag motion on tilt-rotor wing bending mode damping in cruise flight.

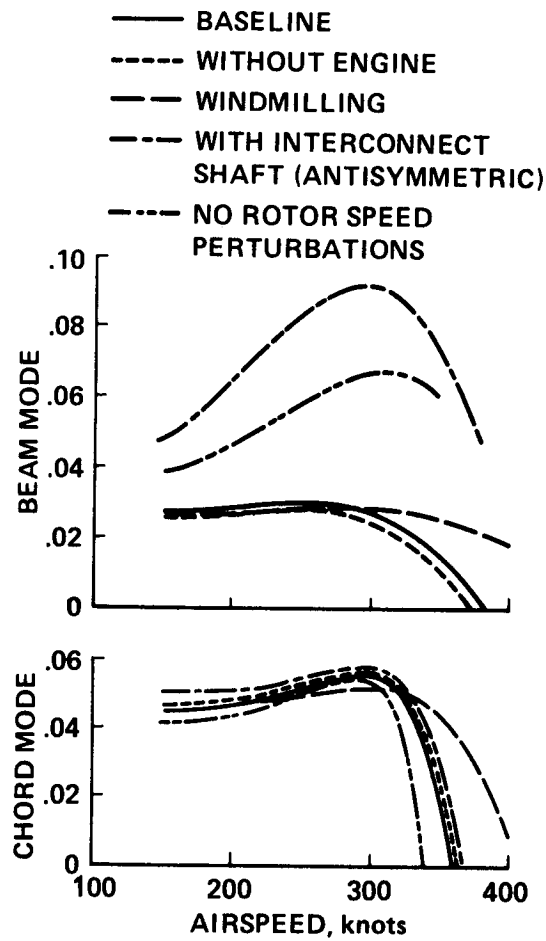


Figure 90.- Effects of rotor drive system dynamics and rotor-shaft interconnect on tilt-rotor wing bending-mode damping in cruise flight.

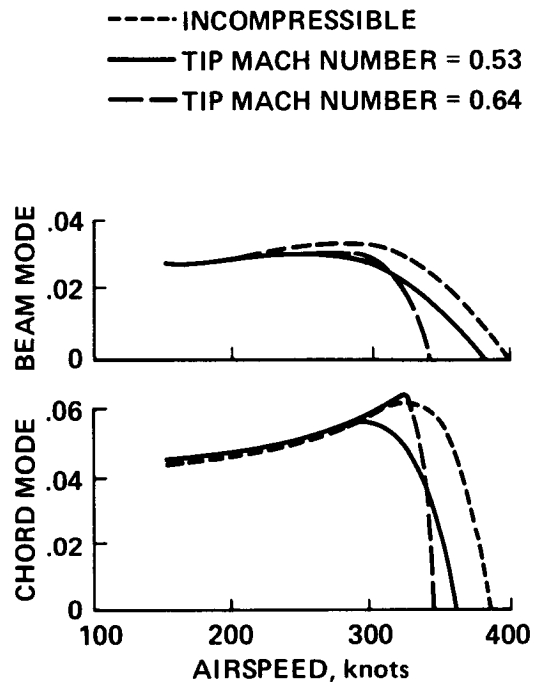


Figure 91.- Effects of compressible aerodynamics on tilt-rotor wing bending-mode damping in cruise flight.



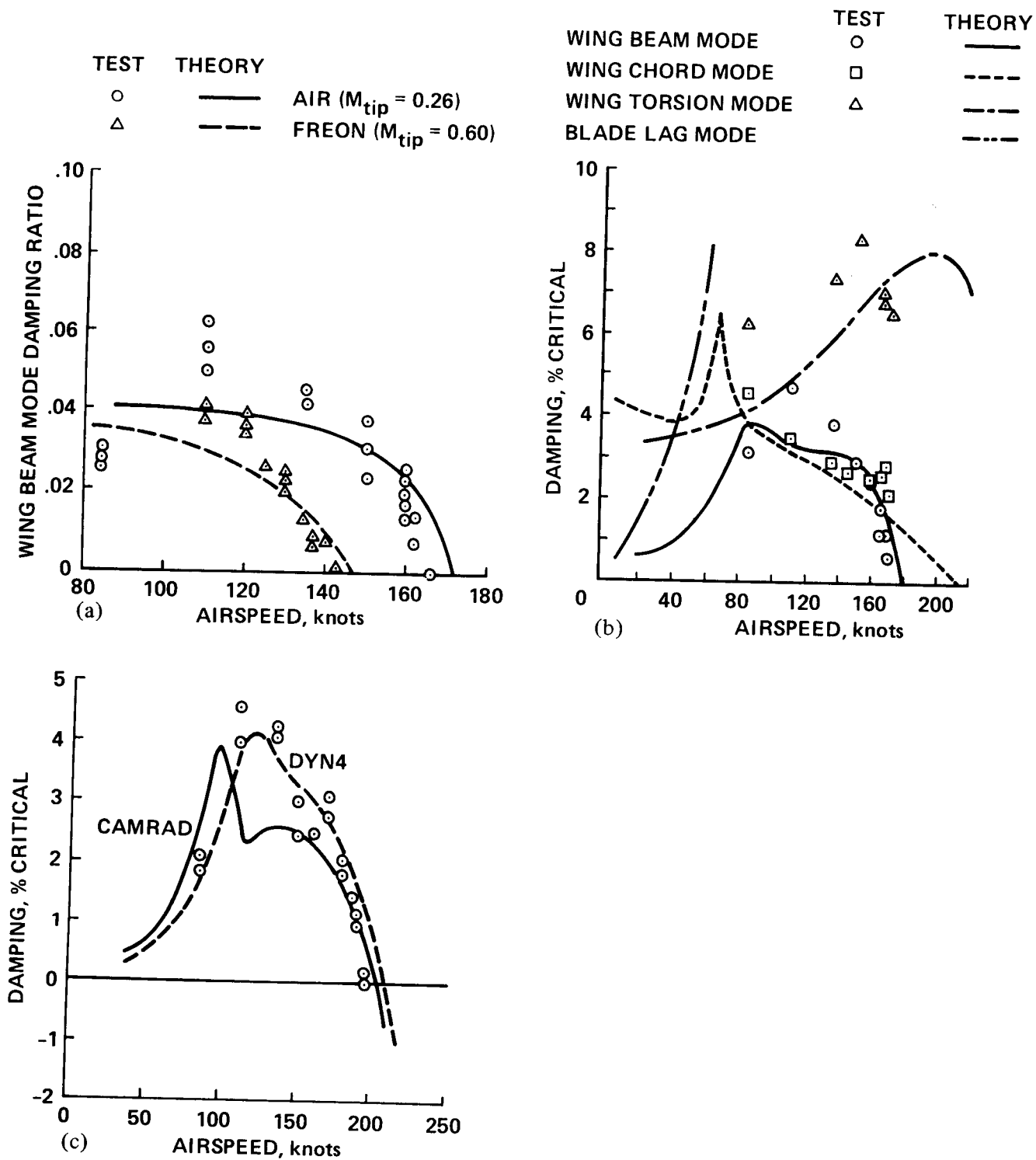


Figure 92.- Langley Transonic Dynamics Tunnel Model experimental stability measurements of small-scale V-22 tilt-rotor models compared with predictions of various theories. (a) CAMRAD. (b) PASTA. (c) CAMRAD and DYN4.

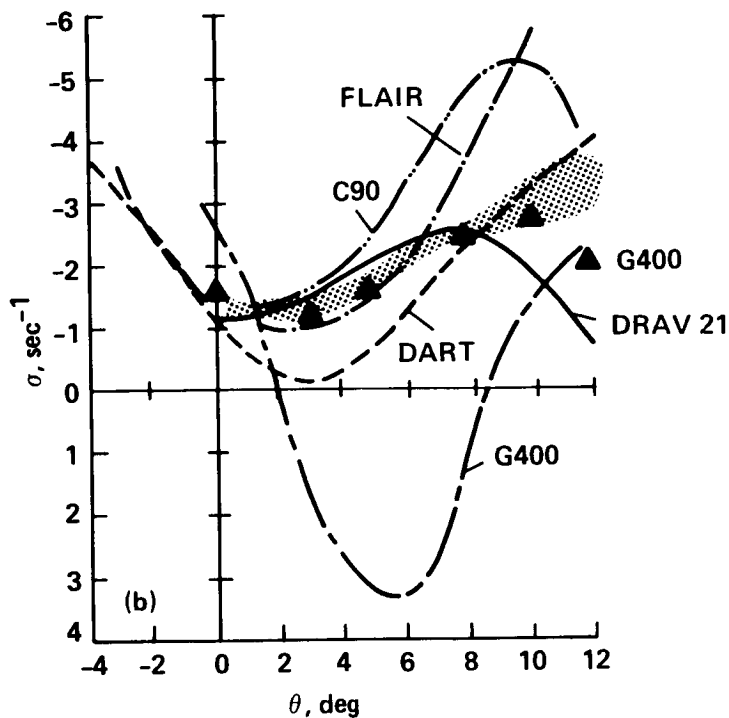
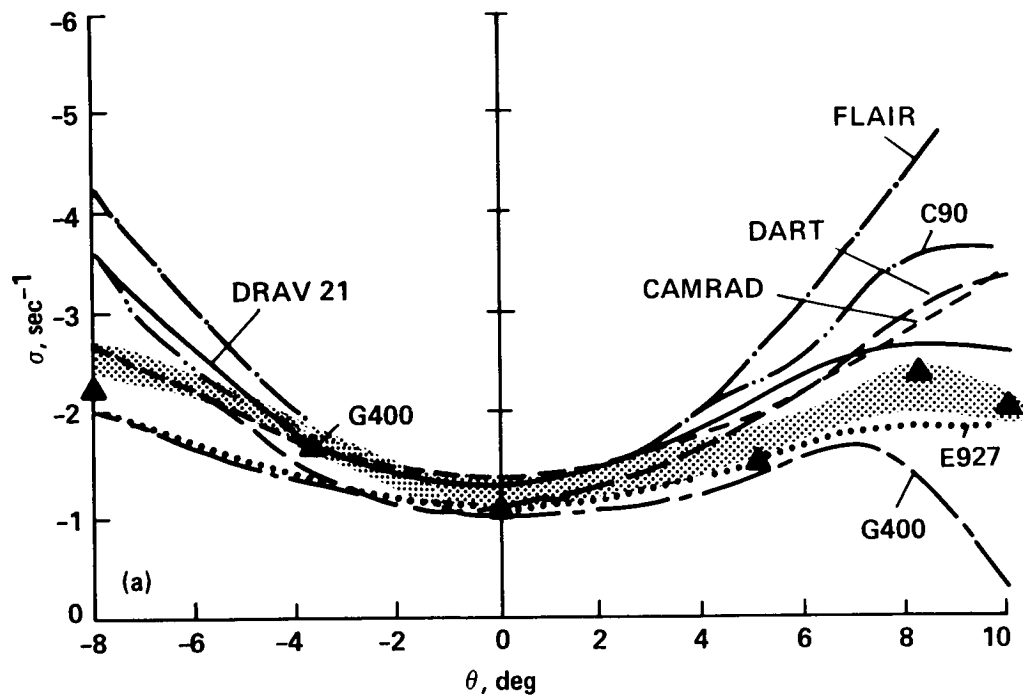


Figure 93.- Comparisons of lead-lag damping predicted by several aeroelastic stability analyses for a small-scale elastic blade flap-lag-torsion model in hover including experimental data; experimental data is shaded region. (a) No droop and stiff torsion flexure. (b)  $-5.0^\circ$  droop and soft torsion flexure.

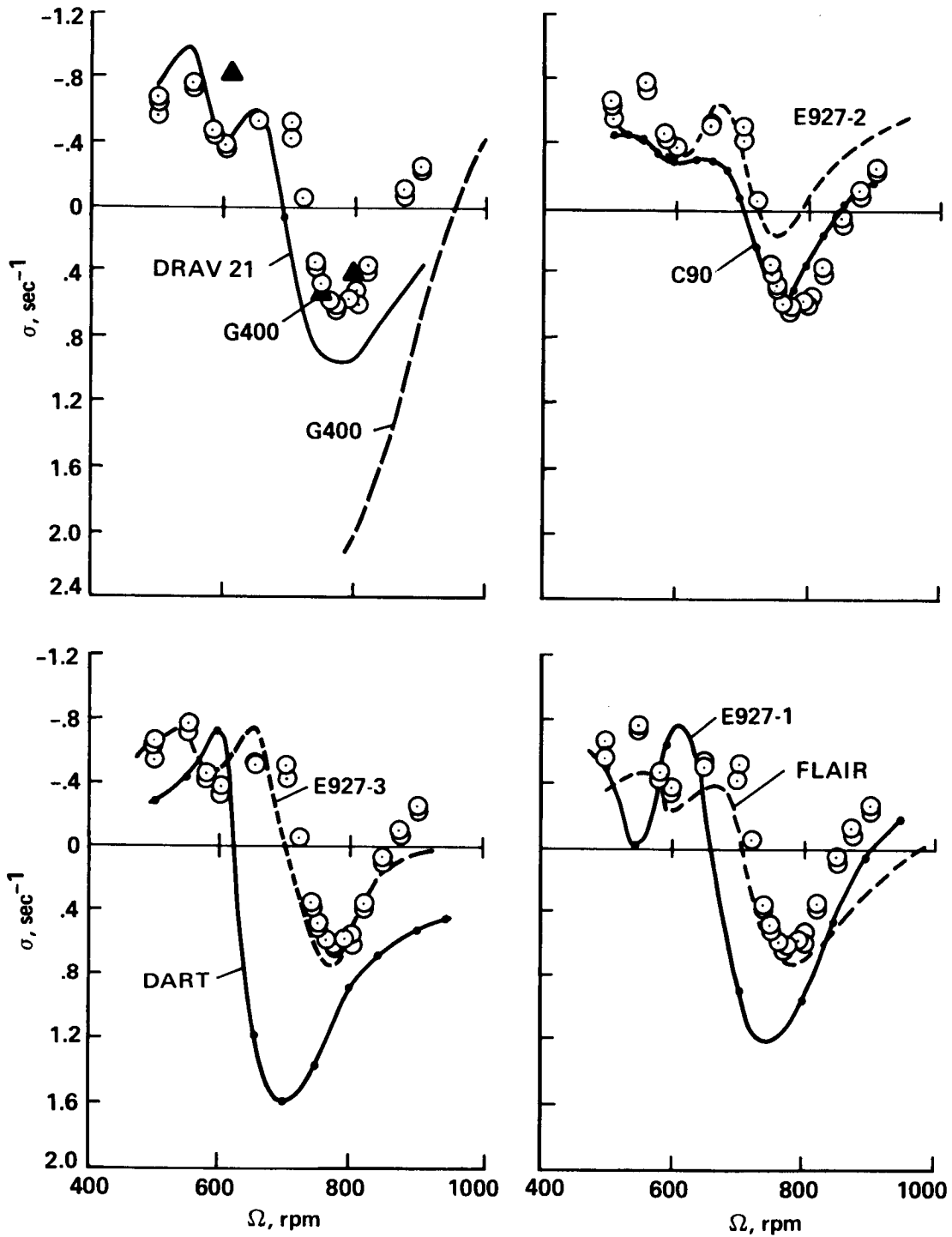


Figure 94.- Comparisons of regressing lead-lag damping predicted by several aeroelastic stability analyses for a coupled rotor-body model in hover including experimental data.

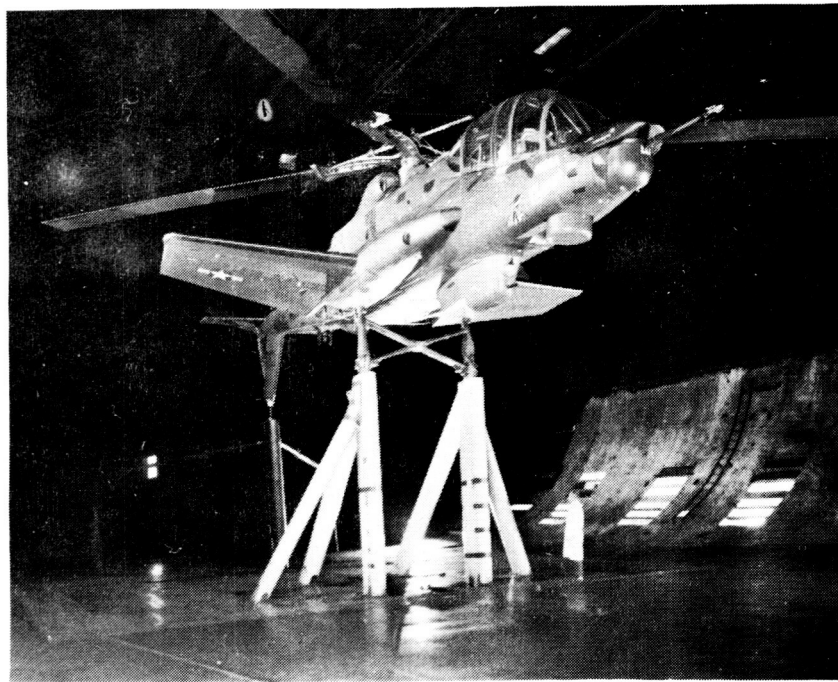


Figure 95.- Lockheed AH-56A Cheyenne installed in 40- by 80-Foot Wind Tunnel.

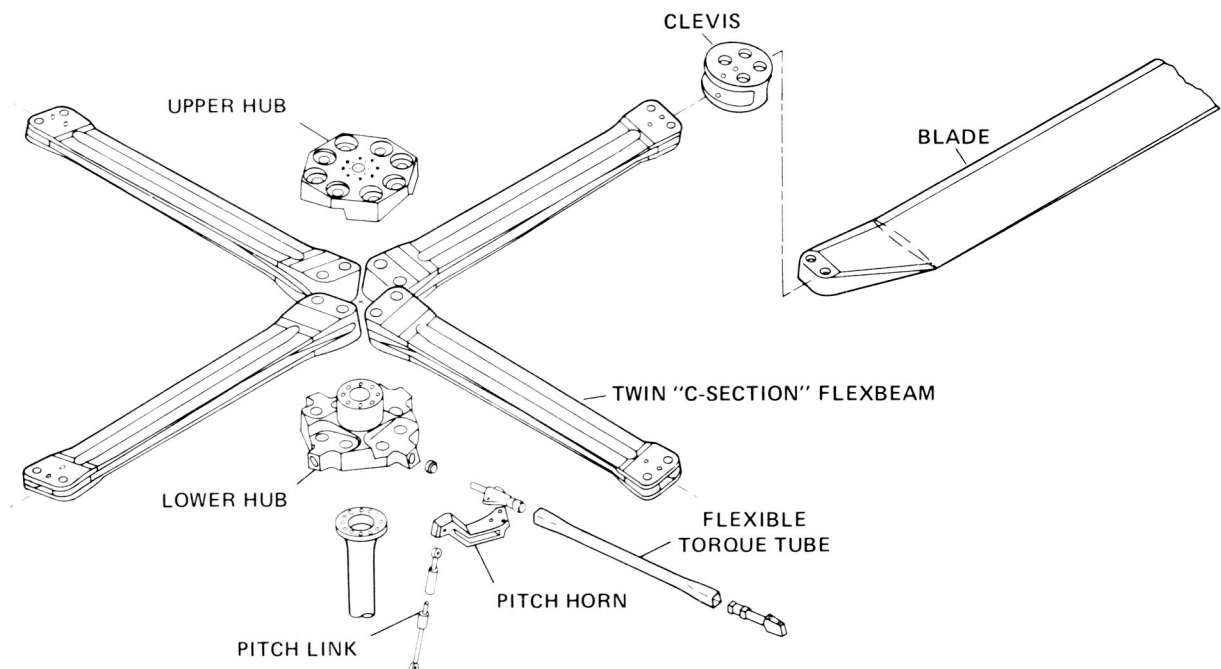
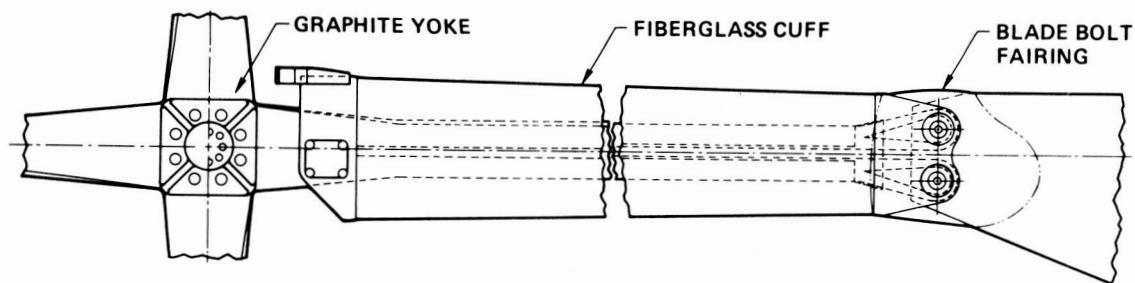


Figure 96.- Boeing Vertol bearingless main rotor (BMR).



ORIGINAL PAGE IS  
OF POOR QUALITY

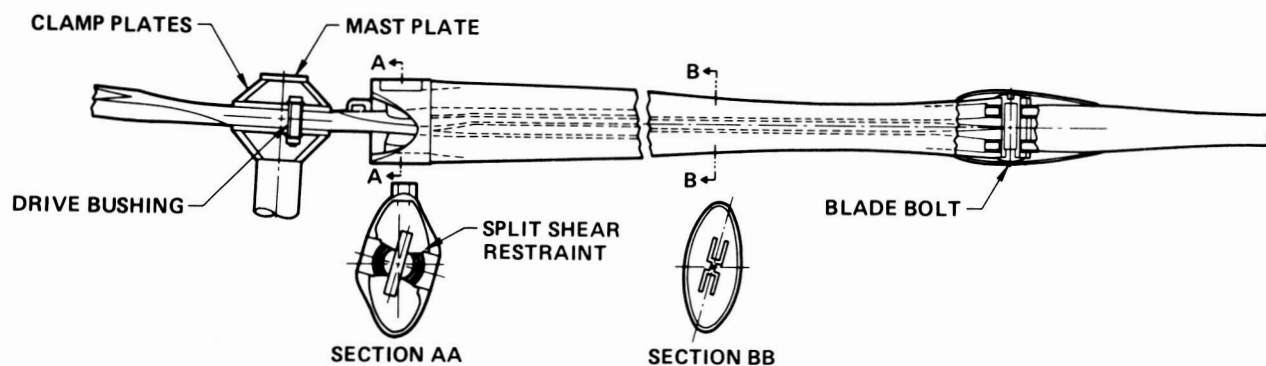


Figure 97.- A damperless bearingless-rotor hub design for the ITR/FRR rotor.

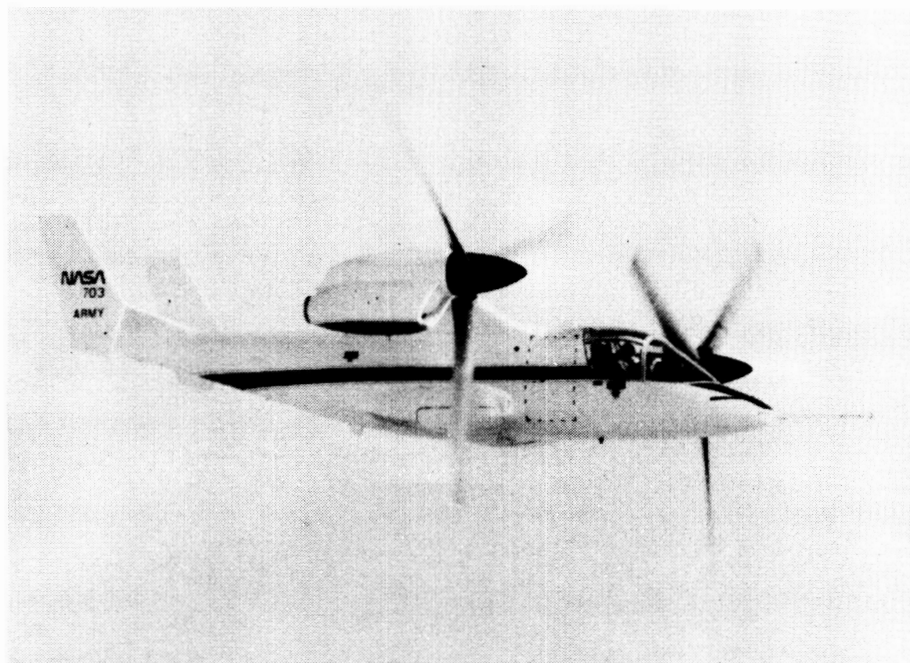


Figure 98.- Army/NASA-Bell XV-15 Tilt Rotor Research Aircraft in airplane configuration.

1. Report No. NASA CP-2495		2. Government Accession No.		3. Recipient's Catalog No.	
4. Title and Subtitle NASA/Army Rotorcraft Technology Volume I - Aerodynamics, and Dynamics and Aeroelasticity				5. Report Date February 1988	
				6. Performing Organization Code RJ	
7. Author(s)				8. Performing Organization Report No.	
				10. Work Unit No.	
9. Performing Organization Name and Address Office of Aeronautics and Space Technology National Aeronautics and Space Administration				11. Contract or Grant No.	
				13. Type of Report and Period Covered Conference Publication	
12. Sponsoring Agency Name and Address National Aeronautics and Space Administration Washington, DC 20546				14. Sponsoring Agency Code	
15. Supplementary Notes The conference was jointly sponsored by the National Aeronautics and Space Administration and the Department of the Army, with the participation of industry coordinated by the American Helicopter Society, Inc.					
16. Abstract The 1987 NASA/Army Rotorcraft Technology Conference was held at Ames Research Center, Moffett Field, California, March 17-19, 1987. The Conference Proceedings is a compilation of over 30 technical papers presented at this milestone event which reported on the advances in rotorcraft technical knowledge resulting from NASA, Army, and industry rotorcraft research programs over the last 5 to 10 years. The Conference brought together over 230 government, industry, and allied nation conferees to exchange technical information and hear invited technical papers by prominent NASA, Army, and industry researchers covering technology topics including aerodynamics, dynamics and aeroelasticity, propulsion and drive systems, flight dynamics and control, acoustics, systems integration, and research aircraft.					
17. Key Words (Suggested by Author(s)) helicopter                      flight dynamics rotor aerodynamics                      and control rotor dynamics propulsion acoustics				18. Distribution Statement  Unclassified - Unlimited  Subject Category 01	
19. Security Classif. (of this report) Unclassified		20. Security Classif. (of this page) Unclassified		21. No. of pages 536	
				22. Price A23	